DECAY AND PYRITISATION OF PLANTS

Fiona Brock

A dissertation submitted to the University of Bristol in accordance with the requirements of the degree of Doctor of Philosophy in the Faculty of Science

Department of Earth Sciences

October 2000

Word count (text only): 57,481

ABSTRACT

Plant tissues are susceptible to decay and are usually completely degraded, but under certain circumstances they can be preserved as organic fossils or by authigenic mineralisation. One of the most important minerals involved in the preservation of material in the plant fossil record is pyrite, FeS_2.

Model microbial decay experiments were used to investigate the geochemical and microbiological processes involved in the preservation of a range of plant tissues. Amorphous iron sulphide formed, lining the pith cell walls, within the middle lamella, at intercellular junctions, and partially infilling some cells, within 12 weeks in experiments in which *Platanus* and *Psilotum* twigs were decayed under open marine conditions. These results indicated that the initial processes involved in the pyritisation of plants may be rapid. A range of other conditions, including salinity, sulphate availability, iron source and nature of organic matter yielded no pyritisation within the plant material, indicating that this requires special conditions. Although pyritisation can be rapid enough to preserve cellular detail, relatively little plant material is preserved in pyrite in the fossil record.

Rapid mineralisation was accompanied by rapid bacterial decay of the plant material. Experimental observations on the decay of different plant tissues and types indicated that cellulose-based species are likely to be rapidly degraded and hence not preserved, but that heavily lignified tissues have a much higher preservation potential. Tissues with a composition between these extremes are likely to be preserved if they reach the depositional site intact, and the prevailing conditions facilitate pyrite formation.

Pyritised plant fossils from the Eocene London Clay of south-east England exhibit regions of exceptional cellular detail but very little organic matter is preserved. However, plant material from the Palaeocene Reading Beds yielded guaiacol lignin units which had not been significantly altered by diagenesis.

ACKNOWLEDGEMENTS

Firstly, I would like to thank my supervisors, Profs. Derek Briggs and John Parkes for their help and advice, and for being so supportive throughout this project.

This project was part of a NERC tied grant with the Dept. of Earth Sciences at the University of Wales, Cardiff. I would like to thank everyone involved in this project at Cardiff: Profs. Dianne Edwards and David Rickard, Dr Tim Jones who helped with fossil collections, Dr Ian Butler for valuable discussions on geochemistry, Dr Kevin Davies who carried out fossil identification and TEM sample preparation and analysis, and Tony Oldroyd and Mike Turner for their technical assistance. In particular, I would like to thank Dr Steve Grimes for all his help, hard work, and seemingly endless enthusiasm!

There are many other people at the University of Bristol to whom I am indebted for their help: the members of Geomicrobiology, especially Drs Ian Mather and Jens Sagemann; Prof. Richard Evershed and the members of the Environmental and Analytical Labs, School of Chemistry, in particular Jim Carter, Gordon Docherty and Zoe Crossman for help with pyrolysis-GC/MS, carbohydrate and lignin assays respectively; the staff of the micro-analytical lab, School of Chemistry for carrying out the elemental analysis; Dr Stuart Kearns for assistance with SEM analysis; Simon Powell for photographic work; Kim Goodman and Cheung Choi for help with ICP-AES; Pippa Hawes and Dr Sean Davies for help and advice on carbon mapping and X-ray analysis; Nick Wray at the university botanic garden for supplying much of the plant material.

Thanks go to Dr Nathalie Mahieu at Queen Mary & Westfield College, University of London who ran the ^{13}C solid state NMR samples and interpreted the results and Dr Pim van Bergen who helped with identification of pyrolysis-GC/MS data. Many thanks also to Tim Lawrence in the anatomy laboratory at Royal Kew Gardens for advice on tissue staining and the use of a microtome.

Special thanks to Ian Mather for the loan of his laptop computer, to Jo Lipscombe, who has always been there for a chat, lunch, a "quick" drink and who was a fantastic friend throughout this project, and to Duncan Kellett for his support and for putting up with me while I was writing up!

AUTHOR'S DECLARATION

I declare that the work in this dissertation was carried out in accordance with the Regulations of the University of Bristol. The work is original except where indicated by special reference in the text and no part of the dissertation has been submitted for any other degree.

Any views expressed in the dissertation are those of the author and in no way represent those of the University of Bristol.

The dissertation has not been presented to any other University for examination either in the United Kingdom or overseas.

SIGNED: F. Brock DATE: 13 March 2001

TABLE OF CONTENTS

LIST OF TABLES

LIST OF FIGURES

INTRODUCTION

Plant tissues are susceptible to decay and are usually completely degraded, but under certain conditions they can be preserved as organic fossils or by authigenic mineralisation (Schopf, 1975; Scott, 1990). Decay-resistant tissues such as leaf cuticles, seed coats or wood, can be preserved coalified (sometimes as compressions) or as fossil charcoal (fusain). Authigenic minerals can preserve a range of plant tissues as coats (2- or 3-dimensional internal moulds or external casts), infillings (permineralisations) or replacements (petrifactions) (Schopf, 1975; Scott, 1990). These modes of fossilisation are not mutually exclusive, and specimens may exhibit more than one type of preservation (Spicer, 1991). One of the most important minerals involved in plant fossilisation is pyrite (Scott, 1990), but the processes involved, the conditions required, and the biopolymers and tissues preserved are poorly understood, which limits our interpretation of the pyrite fossil record.

The majority of work on pyritised plant material has involved the study of polished sections (e.g. Collinson and Ribbins, 1977; Ribbins and Collinson, 1978; Poole, 1992, 1993a, 1996; Poole and Wilkinson, 1992, 1999, 2000), although some work has been undertaken using the SEM (e.g. Kenrick and Edwards, 1988).

Microbial decay experiments which promote authigenic mineralisation of organisms in the laboratory (e.g Briggs and Kear, 1993; Sagemann *et al.*, 1999) provide a new approach to the study of the preservation of organic tissues. Such experiments, combined with chemical studies of the decay of plant material and further investigations of pyritised plant fossils, allow a greater understanding of the processes

involved, and the biopolymers and tissues preserved, in the pyritisation of plant material.

Investigative aims

This work was undertaken as part of a comprehensive study of the fossilisation of plant material in pyrite which involved the analysis of the morphology and geochemistry of pyritised plants, microbial decay experiments to investigate the relationship between decay and pyritisation, and abiological experiments to study the mechanisms of pyrite formation within plant material in the laboratory.

Fossil plants from the Eocene of south-east England were chosen for this study for several reasons. The marine London Clay Formation is one of the world's most diverse and extensive fossil floras, containing a range of plant organs (including roots, stems, seeds and fruit) and is well documented (e.g. Collinson, 1983; Poole, 1992). Modern analogues of many of the fossil taxa have been identified and the pyritised specimens show a wide variation in the quality of preservation. Pyritised plant fossils from the deltaic Reading Beds allow the influence of depositional environment on the pyritisation process to be investigated. Both the London Clay and the Reading Beds are accessible, and are relatively recent to ensure only a modest diagenetic overprint.

There are three main aims of the work detailed here:

i) to study the formation of pyrite and its precursors within plant material in model microbial decay systems;

ii) to investigate the chemical changes in plant tissues during decay;

iii) to identify and determine the distribution of organic matter preserved within pyritised plant material.

Other closely related work was carried out in the Dept. of Earth Sciences at the University of Cardiff, and included:

i) the description and identification of plant species and pyrite textures within pyritised plant axes (twigs, stems and petioles) from the Eocene London Clay and Reading Beds. This allowed the development of a model to explain the formation of different pyrite textures in relation to plant tissues, decay, and the mineralisation sequence (Grimes *et al.*, 2001b);

ii) a series of abiological experiments undertaken to study the mechanism of pyrite formation within plant tissues. Amorphous FeS (FeSam) was seen to be the initial product to form within celery, chosen due to its relatively simple structure and wide vessels. Pyrite was later found nucleating on the inner walls of parenchyma cells, between cellulose microfibrils and in the middle lamella of cells. A dissolved species, FeSaq, was also detected, which may in part be responsible for the transport of iron and sulphur species into the plant (Grimes *et al.*, 2001a).

Clearly, the design and interpretation of such experiments requires an appreciation of the importance of the preservation of soft tissues, pyrite formation, the anatomy and biomolecular constituents of plant material, and the bacterial degradation of organic matter. These are all discussed in this introductory chapter.

Soft tissue preservation

Seilacher (1970) defined Konservat Lagerstätten as occurrences of extraordinarily preserved fossils, where the emphasis is on quality rather than quantity of preservation. The most important Konservat Lagerstätten are those preserving fossilised 'soft' tissues, those lacking any mineral component in life (Briggs, 1995b).

Soft tissues are a rich source of nutrients and can be rapidly decomposed. Their consumption by predators and scavengers, and decay

by micro-organisms, results in their preservation in the fossil record being rare. Where they are preserved, however, soft-bodied fossils provide a much more complete record of the diversity and palaeoecology of ancient communities than the shelly fossil record, they reveal the morphology of soft and lightly sclerotized animals, and they provide the only fossil evidence of many taxa. They also have the potential to provide insights into the factors controlling the formation of authigenic minerals within sediments (Briggs, 1991).

Seilacher (1970; see also Seilacher *et al.*, 1985) suggested that the preservation of soft tissues requires an exceptional combination of physical and chemical conditions, possibly including anoxia, stagnation, rapid burial, and cyanobacterial films. However, anoxia is ineffective as a long-term preservational agent as decomposition can be just as rapid under anoxic conditions as in oxic environments (e.g. Allison, 1988c; Canfield, 1989). Stagnation prevents disarticulation by inhibiting bioturbation and, in conjunction with anoxia, inhibits scavenging, promoting the preservation of hard parts but not soft parts (Allison, 1988b,c). Allison (1988b, c) showed that, while rapid burial may aid the preservation of articulated hard parts, it is rarely important in the preservation of soft tissues, although it may be important in establishing the required geochemical gradients. Cyanobacterial coatings are only found in shallow, well-lit environments, and have only been reported in a few localities (Allison 1988b,c). Their role in fossilisation is discussed by Wilby *et al.*, 1996b.

For more labile tissues to be preserved they must be replicated by authigenic minerals. This process must be rapid enough to avoid loss of morphological information by decay, but a fine balance is required as some decay is necessary to promote the conditions required for mineralisation (Allison, 1988a,b). For three-dimensional preservation,

mineralisation must also be rapid enough to prevent compaction of the organism. The preservational mineral of the biota is largely defined by the geochemistry of the depositional environment, but may be influenced by the original organic composition of the organisms which can lead to a geochemical taphonomic bias. Fossils associated with the earliest phase of mineralisation often show a higher level of preservation than those formed later, reflecting the degree of decay of the organism (Allison, 1988a)

The minerals involved in these fossilisation processes include silica, phosphates, carbonates, and pyrite (Schopf, 1975; Scott, 1990). Silica mineralisation is often the result of the release of hot silica-laden fluids during volcanic activity, where entire communities may be preserved almost intact, e.g. the Early Devonian Rhynie (Trewin, 1994, 1996). Preservation in silica has also been identified in some marine radiolarian cherts (Scott, 1990). Calcium carbonate is a common authigenic mineral in the preservation of plant material, especially wood. It is found in many environmental settings, including marine rocks, freshwater mudstones, siltstones and sandstones. Some plant tissues may be preserved in calcium carbonate in basaltic volcanic rocks (Scott, 1990), or within coal balls, which are calcium (or magnesium) carbonate concretions within coal beds. Calcium carbonate preservation may occur very early during diagenesis, and may be promoted by partial decay (Raiswell, 1971; 1976). The highest fidelity of soft tissue preservation is often in phosphates, which even preserve tissues of volatile composition (Briggs *et al.*, 1993; McCobb *et al.*, 2001). Despite being ubiquitous in marine environments, and commonly associated with fossil assemblages, pyrite is the least common replacement mineral. Where pyrite does preserve soft tissues, it is often associated with shelly fossils (e.g. Hudson, 1982) or refractory tissues (e.g. Kenrick and Edwards, 1988).

Pyritised soft tissues in the fossil record

Although pyrite is rarely associated with the preservation of soft tissues (Allison and Briggs, 1991), there are several examples of Konservat Lagerstätten where soft tissues are preserved in pyrite. The most notable of these are Beecher's Trilobite Bed in the Upper Ordovician of New York State (e.g. Briggs *et al.*, 1991) and the Lower Devonian Hunsrück Slate of western Germany (e.g. Stürmer *et al.*, 1980; Bartels and Brassel, 1990; Briggs *et al.*, 1996; Bartels *et al.*, 1998). Pyritised soft tissues are also sparsely found in the Middle Cambrian Burgess Shale of British Columbia (e.g. Conway Morris, 1986), and the Jurassic of La Voulte-sur-Rhône in France (Wilby *et al.*, 1996a).

The Eocene London Clay of south-east England is one of the best preserved and most diverse and extensive fossil plant assemblages in Europe (e.g. Collinson, 1983; Allison, 1988a). The plant material is preserved in apatite, calcite and pyrite. Pyritised plant fossils from the London Clay have been studied for many years, and are well documented in the literature (e.g. Bowerbank, 1840; Reid and Chandler, 1933; Chandler, 1964, 1978; Collinson, 1983 and Poole, 1992). Other pyritised plant fossils, in particular from the Devonian, have also been documented (e.g. Grierson, 1976; Edwards, 1980, 1981; Kenrick and Edwards, 1988; Kenrick *et al.*, 1991).

Pyritised plant material has been shown to be an important source of information regarding the structure and evolution of early land plants. Such fossils are the most common source of data of the 3D anatomy of Devonian vascular plants (Kenrick and Edwards, 1988; Kenrick *et al.*, 1991), facilitating the analysis and interpretation of cell wall ultrastructure, and providing a better understanding of pyrite formation. Studies of pyritised plant material from the Devonian allow analysis of the evolution of water-conducting tissues from in early land plants and

provide links between different species during a period of great diversification in vascular land plants (Kenrick and Edwards, 1988; Friedmann and Cook, 2000).

The distribution of pyrite in plant fossils may be interpreted in terms of the differential degradation of different types of cells and cell walls. For example, analysis of *Gosslingia breconensis* by Kenrick and Edwards (1988) indicated that lignified tissues remained coalified (organic), while other regions were pyritised. They proposed that the configuration of organic matter and pyrite could be explained in terms of relative rates of decay of cell contents, cellulose and lignin, combined with pyrite production. The evolution of more recalcitrant biomacromolecules than cellulose during the Devonian, such as lignin and cutin, would have required the evolution of new decomposers, in particular fungi. The presence of pyritised plant material throughout the Devonian, in particular during the time lag between the evolution of these new biomacromolecules and the organisms capable of degrading them, allows the possibility of tracking such evolutionary changes in decomposer organisms.

Pyrite formation

Pyrite is formed by the reaction of bacterially-produced hydrogen sulphide with reactive detrital iron minerals to form iron monosulphides which are then converted to pyrite. Difficulties in understanding the mechanisms of pyrite formation arise because hydrogen sulphide production by sulphate-reducing bacteria requires anaerobic and reducing conditions, and the conversion of iron monosulphide to pyrite is an oxidation reaction. Hence, the interpretations of the mechanisms of pyrite formation are equivocal.

Production of hydrogen sulphide by sulphate reducing bacteria

Sulphate reducing bacteria (SRB) in sediments reduce dissolved interstitial porewater sulphate to produce hydrogen sulphide, using organic matter as both an energy source and reducing agent. Bacterial sulphate reduction involves a complex series of individual steps (Jørgensen, 1982a), but the overall process can be summarised by:

$$2CH_2O + SO_4^{2-} \rightarrow H_2S + 2HCO_3^- \qquad \text{Eqn 1.1}$$

where CH_2O represents metabolisable organic matter (Westrich, 1983). Jørgensen (1982b) estimated that up to 50% of organic matter in coastal sediments is metabolised by SRB.

The SRB are obligate anaerobes, so conditions must be anoxic for bacterial sulphate reduction to take place. Anoxia is achieved through the action of aerobic bacteria living at the sediment-water interface. Oxygen reaches the sediment from the overlying waters via molecular diffusion, wave and current stirring, or bioturbational irrigation (Aller, 1980a; Berner, 1980). It is utilised in the bacterially-mediated conversion of organic matter to carbon dioxide. Rapid consumption of oxygen at the sediment-water interface leads to anoxia below a depth of a few mm or cm (Revsbech and Jørgensen, 1986). Thus, organic matter serves an important role in pyrite formation, not only a substrate for SRB, but also as an agent to produce anoxia for sulphate reduction.

The rate of sulphate reduction is controlled by sulphate concentrations only when levels are less than 3mM (Capone and Kiene, 1988). As most pyrite is formed where sulphate concentrations are much higher (Kaplan *et al.*, 1963), the effect of sulphate concentration on pyrite formation is relatively unimportant, except in micro-environments around decaying organisms. In normal marine conditions (i.e. where

bottom waters are oxygenated), the major factor controlling the rate of bacterial sulphate reduction is the amount and reactivity of available organic matter (Berner, 1984). However, the overall reactivity of organic matter decreases as the more reactive compounds are consumed and decomposition of the less reactive compounds, and those formed by ageing, is associated with lower rates of sulphate reduction (Berner, 1984).

In freshwater environments, where dissolved sulphate concentrations are, on average, several hundred-fold less than in seawater, sulphate concentrations are the major controlling factor, resulting in little pyrite formation and a build-up of organic matter (Berner, 1984). However, the small sulphate pool is rapidly turned over and SRB are adapted to very low (> 60μM) sulphate concentrations (Bak and Pfennig, 1991).

Berner (1984) described a crude correlation between sedimentation rate and organic matter and pyrite contents. Where sedimentation rates are low (for example, in pelagic regions) organic matter remains subject to oxic decay at the sediment-water interface and in the overlying water column for up to thousands of years, so little sulphate reduction occurs, resulting in little pyrite formation. Nutrient-rich waters lead to high production and sedimentation of organic matter which is rapidly buried. This results in elevated levels of reactive organic matter becoming available for sulphate reduction, even at depth, and hence high levels of hydrogen sulphide are produced, resulting in extensive pyrite formation.

Reaction of hydrogen sulphide with detrital iron minerals

Although up to 90% of bacterially-produced hydrogen sulphide is re-oxidised (Jørgensen, 1978), the remainder can react with detrital iron minerals in the sediment to produce a series of metastable iron

monosulphides such as mackinawite (FeS), amorphous FeS and greigite (Fe_3S_4) (Berner, 1970).

There are several mechanisms by which detrital iron minerals can react with hydrogen sulphide, all of which may be important (Canfield and Raiswell, 1991). Iron oxides may be reduced by hydrogen sulphide (Sørensen, 1982; Canfield, 1989b: Eqn. 1.2). Bacterially-mediated iron reduction may take place (e.g. Sørensen, 1982; Lovley and Philips, 1986a, b; Canfield, 1989b: Eqn. 1.3). Ferrous iron may also become available by the partial oxidation of iron sulphide minerals (Aller, 1980b; Giblin and Howarth, 1984: Eqn. 1.4)

$$2FeOOH + H_2S + 4H^+ \rightarrow 2Fe^{2+} + S^\circ + 4H_2O \qquad \text{Eqn 1.2}$$

$$4FeOOH + CH_2O + 8H^+ \rightarrow 4Fe^{2+} + CO_2 + 7H_2O \qquad \text{Eqn 1.3}$$

$$2FeS_2 + 7O_2 + 2H_2O \rightarrow 2Fe^{2+} + 4SO_4^{2-} + 4H^+ \qquad \text{Eqn 1.4}$$

There are effectively two main pools of sedimentary iron minerals: the oxides, which react rapidly with dissolved sulphide, and the iron-bearing silicates, which react much more slowly (Canfield, 1989b; Raiswell and Canfield, 1998). Canfield *et al.* (1992) defined the reactivities of iron minerals by estimating their half-life with respect to sulphidation (Table 1.1).

Regardless of the depositional environment, the amount of pyrite formed in a sediment is almost never limited by the total amount of iron present, but by its reactivity (Berner, 1984). (The exception is in highly calcareous sediments away from sources of terrigenous clays or silts, where sediments consist almost entirely of calcium carbonate from the skeletons of marine organisms, which contain insufficient iron to produce appreciable amounts of pyrite, even with high concentrations of organic matter and abundant hydrogen sulphide.) Raiswell and Canfield

(1998) suggested that the amount of reactive iron available probably limits pyrite formation in many of the most commonly studied sedimentary environments.

Iron mineral	Rate constant yr^{-1}	Half-life
ferrihydrite, $Fe_5HO_8.4H_2O$	2200	2.8 hr
lepidocrocite, γ-FeOOH	>85	< 3 days
goethite, α-FeOOH	22	11.5 days
haematite, α–Fe_2O_3	12	31 days
magnetite (uncoated), Fe_3O_4	$6.6x10^{-3}$	105 yrs
'reactive' silicates	$3.0x10^{-3}$	230 yrs
sheet silicates	$8.2x10^{-3}$	84000 yrs
ilmenite, garnet, augite, amphibole	$<< 8.2x10^{-3}$	>> 84000 yrs

Table 1.1. Rate constants and half-lives of sedimentary iron minerals with respect to their sulphidation (Canfield *et al.*, 1992).

In marine sediments with sulphate reduction, the presence or absence of dissolved sulphide is a sensitive indicator of the presence of reactive iron oxides (Canfield, 1989). Reactive iron oxides can effectively buffer the concentration of porewater sulphide to very low levels, even in the presence of active sulphate reduction. Accumulation of dissolved sulphide in sediments indicates that the reactive iron has been consumed and only less reactive iron minerals remain (Canfield, 1989), except in micro-environments associated with decaying carcasses where hydrogen sulphide concentrations may be high.

Transformation of iron monosulphides to pyrite

The importance of precursor iron monosulphides in pyrite formation was first recognised by Feld (1911) and Allen *et al.* (1912), but while metastable iron monosulphides transform to pyrite quite readily during

early diagenesis, the processes involved are still not properly understood. The range of geochemical environments in which pyrite is found, and its ubiquity in both modern sediments and ancient sedimentary rocks, suggest that there may be multiple, and possibly competing, pathways by which iron monosulphides are converted to pyrite.

Solid state oxidation of iron monosulphides (amorphous FeS and mackinawite) to pyrite via greigite (Fe_3S_4), with elemental sulphur (S°) as the oxidant, was first proposed by Berner (1970, 1984) and supported by Goldhaber and Kaplan (1974):

$$3FeS + S° \rightarrow Fe_3S_4 \qquad \text{Eqn 1.5}$$

$$Fe_3S_4 + 2S° \rightarrow 3FeS_2 \qquad \text{Eqn 1.6}$$

However, as the overall equation shows (Equation 1.7), insufficient elemental sulphur is produced to oxidise the iron monosulphides to pyrite completely, and thus a further oxidising agent is required (Berner, 1970):

$$18CH_2O + 9SO_4^{2-} + 6FeOOH \rightarrow 18HCO_3^- + 3FeS + 3FeS_2 + 12H_2O \qquad \text{Eqn 1.7}$$

Another possible mechanism, the "polysulphide pathway", was first suggested by Rickard (1975). He proposed that iron monosulphides reacted with an aqueous polysulphide species, and proceeded via either $FeSH^+$ or $Fe(SH)_2$:

$$FeS(s) + S^{2-}_x (aq) \rightarrow FeS_2 + S^{2-}_{(x-1)}(aq) \qquad \text{Eqn 1.8}$$

This pathway was also observed experimentally by Luther (1991) and Schoonen and Barnes (1991b), who assumed that the reaction proceeded by the addition of sulphur to the iron monosulphide. However, Wilkin and Barnes (1996) used S isotope ratios to show that the transformation of iron monosulphide to pyrite actually proceeds via the loss of ferrous iron from, and not the addition of sulphur to, the monosulphide:

$$2FeS(s) + 2H^+ \rightarrow FeS_2(s) + Fe^{2+} + H_2(g) \qquad \text{Eqn 1.9}$$

Difficulties detecting precursor iron monosulphides in many sediments (Morse and Cornwell, 1987), and considerable textural evidence (e.g. Rickard, 1994), suggest that there is at least one other pathway by which iron monosulphides are transformed into pyrite. The formation of pyrite via oxidation of iron monosulphide by hydrogen sulphide was proposed by Taylor *et al.* (1979) and Wächtershäuser (1988), and demonstrated in the laboratory at 100°C by Drobner *et al.* (1990), and at 25°C by Rickard (1997) :

$$FeS(S) + H_2S \rightarrow FeS_2(s) + H_2(g) \qquad \text{Eqn 1.10}$$

The mechanism and kinetics of this pathway were described in detail by Rickard (1997) and Rickard and Luther (1997), and it is particularly interesting for several reasons:

i) it competes with the solid state oxidation and polysulphide pathway and Rickard (1997) suggested that it would be favoured in strictly anoxic environments, while the other two pathways may prevail where molecular oxygen is present;

ii) it is by far the fastest of the pathways (Rickard *et al.*, 1995), although this is inconsistent with other experimental results (e.g. Berner, 1964,

1970; Roberts *et al.*, 1969; Taylor *et al.*, 1979a, b; Wilkin and Barnes, 1996, and references therein);

iii) it results in the production of hydrogen gas which Wächtershäuser (1988) proposed may have played an important role in the origin of primordial metabolic cycles and early ecosystems, the hydrogen providing an energy source for bacterial life.

In the laboratory, however, Benning *et al.* (2000) observed that, under reducing conditions with only hydrogen sulphide as a reactant, the formation of pyrite was inhibited over a range of pH and temperatures. They proposed that the overall rate of pyrite formation increases with increasing degree of oxidation, implying a requirement for an oxidised intermediate sulphur species (elemental sulphur or polysulphide) and/or surface oxidised monosulphides, thus ruling out the hydrogen sulphide oxidation pathway.

While it is generally accepted that sulphur species with oxidation states between those of sulphate and sulphur play an important role in pyrite formation (Benning *et al.*, 2000), Wilkin and Barnes (1996) suggested that O_2, H_2O_2, Fe(III), Mn(VI, III), nitrate, organic carbon and bicarbonate could all be important oxidants in the formation of pyrite in sedimentary environments.

Pyrite formation in euxinic sediments

Euxinic sediments are those deposited in hydrogen sulphide-rich bottom waters which are anoxic due to strong density stratification and stagnation, e.g. the Black Sea (Berner, 1984). Organic accumulation is high, leading to extensive sulphate reduction and a build-up of hydrogen sulphide in the bottom waters and underlying sediments (Sweeney and Kaplan, 1980). In euxinic environments, hydrogen sulphide can react with iron minerals before and after burial, and even during

sedimentation (e.g. Leventhal, 1983). Hence, the amount of pyrite formed depends on the amount and reactivity of iron minerals rather than the amount of locally deposited organic material.

Due to advection of hydrogen sulphide in the bottom waters, pyrite may form in the absence of local sulphate reduction, and without deposition of organic matter at the same location as the iron minerals. Thus, appreciable pyrite can build up even at low organic matter concentrations, where deposition rates are low (e.g. Raiswell, 1982; Berner, 1984; Raiswell and Berner, 1985). In euxinic as opposed to pelagic sediments, very slow deposition maximises the amount of pyrite formed, as the slower-reacting iron minerals have longer to react with the hydrogen sulphide available. This implies a mechanism of pyrite formation which proceeds under completely anoxic conditions.

Controls on the pyritisation of organisms

The pyritisation of decaying organisms is dependent on transport and nucleation processes (Schoonen and Barnes, 1991a; Raiswell, 1993; Grimes *et al.*, 2001a) and has been shown to require exceptional depositional conditions (Briggs *et al.*, 1991; Raiswell *et al.*, 1993).

Decaying organisms provide a locus for pyritisation due to the concentrations of metabolisable organic matter stimulating bacterial activity, resulting in the production of hydrogen sulphide (Raiswell *et al.*, 1993). However, plant cells contain insufficient metabolisable material to be able to completely infill the cell with pyrite (Grimes *et al.*, 2001a). The oxidation of iron monosulphide by hydrogen sulphide (Equation 1.4) results in the production of H_2, which can be used as an additional energy source for some bacteria (Widdel and Bak, 1992), forming the basis for autocatalytic pyrite formation. However, even if this does occur,

pyritisation of organic matter would still be controlled by the transport of iron and sulphur into the cell and pyrite nucleation.

The presence of a dissolved iron sulphide species, FeSaq, has been identified as a key component in pyrite formation (Rickard *et al.*, 1999; Buffle *et al.*, 1988; Davison *et al.*, 1999). Such a species would be able to move through the permeable parts of plant cells, possibly resulting in the pyritisation of plant material (Grimes *et al.*, 2001a).

Despite being energetically favoured, pyrite formation from aqueous solutions at ambient temperatures is inhibited by a reluctance of pyrite to nucleate (Schoonen and Barnes, 1991a). Various surfaces may enhance pyrite nucleation including FeSam (with or without surface O_2), S° and pyrite itself (Wilkin and Barnes, 1996; Graham and Ohmoto, 1994; Rickard and Luther, 1997). Enhanced precipitation has been observed on organic substrates such as bacterial cell walls (Donald and Southam, 1999), which may provide a further mechanism for the selective pyritisation of decaying organisms (Grimes *et al.*, 2001a).

The preservation of organisms by pyrite has been shown to require concentrations of dissolved iron within the surrounding sediment to be greater than the concentrations of dissolved sulphide at the decay site (Berner, 1980; Canfield and Raiswell, 1991). Raiswell *et al.* (1993) proposed a 3D model of diffusion-with-precipitation to explain the pyritisation of animal carcasses. This demonstrated that such pyritisation requires unusually high porewater dissolved iron to confine iron sulphide precipitation to the decay site. This model was applied to Beecher's Trilobite Bed (Raiswell *et al.*, 1993), where concentrations of iron reactive towards hydrogen sulphide were unusually high (Briggs *et al.*, 1991) and little organic matter was present in the surrounding sediments, resulting in limited sulphate reduction. The rarity of pyritised soft tissues shows how uncommon this combination of environmental conditions is.

Plant structure and anatomy

There are many differences in the chemistry and morphology of individual plant tissues and taxa. This is reflected in differences in decay susceptibility and preservation potential. Hence, some knowledge of plant biopolymers, the structure of plant cells and the internal organisation of plant stems is necessary to the understanding of the processes involved in decay and pyritisation of plant material.

Organic constituents of plant tissues

Plant tissues are composed of a range of chemically distinct substances, which play different roles in the structure and metabolism of the plant. These compounds vary in their resistance to decay, which affects the biodegradation of the plant tissues in which they occur.

Cellulose

Cellulose is the most abundant biomolecule occurring in nature (de Leeuw and Largeau, 1993). It is a linear polymer of up to 10,000 β-D-glucose monomeric units linked by glycosidic bonds (Figure 1.1). Numerous hydrogen bonds cross-link individual chains to form insoluble, non-hydrolysable fibrils. Cellulose can have crystalline or amorphous regions, and is found in all plant cell walls.

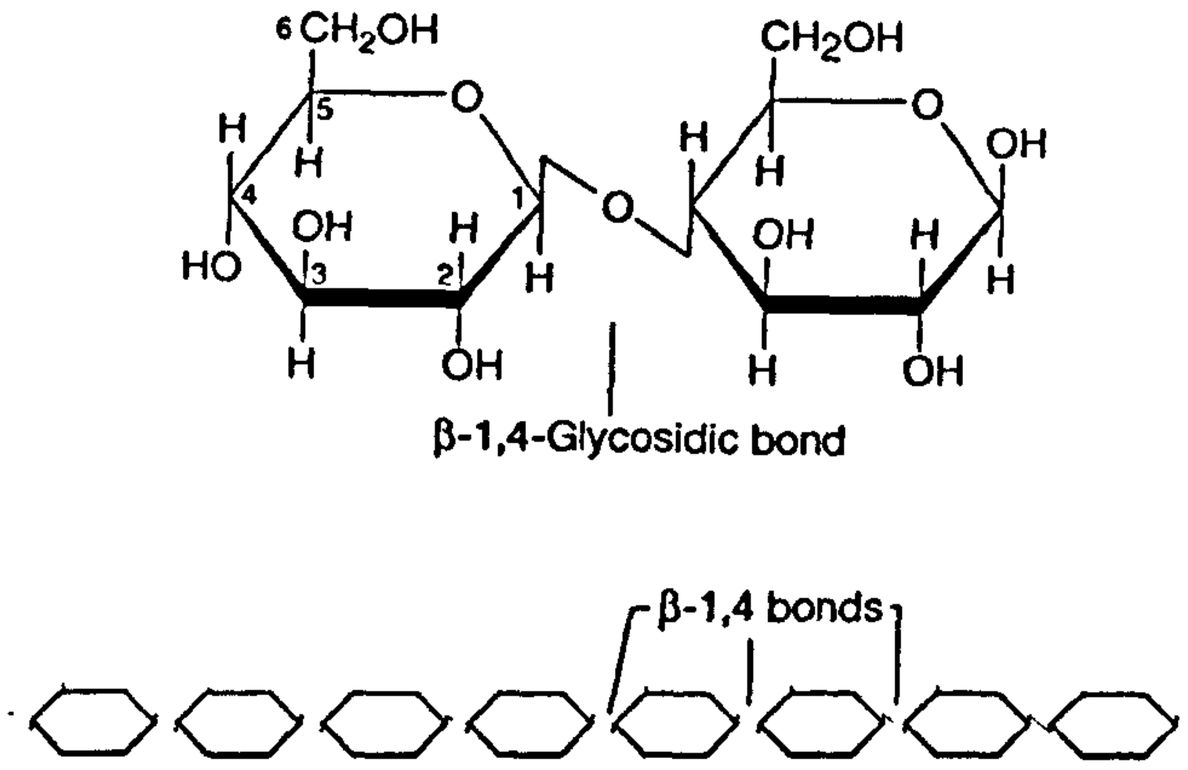

Figure 1.1. Formation of cellulose (Brock, 1997)

Hemicellulose

The term hemicellulose is used to define collectively a range of heteropolysaccharides composed of different sugars including glucoses, xylose, mannose, galactose and arabinose, and glucuronic acid and/or its 4-*O*-methyl ether (Galletti and Bocchini, 1995). These polysaccharides are branched and amorphous, and have different residues and linkages from those of cellulose. Hemicellulose polymers typically have only 50-200 monomeric units, and are more tightly packed and more soluble than cellulose (Galletti and Bocchini, 1995).

The composition of hemicellulose varies with tissue type. Hemicellulose is the only major source of the carbohydrates xylose and mannose, which form the backbone of the polysaccharide glucuronoxylan and glucomannan respectively. Angiosperms and gymnosperms have characteristically different levels of glucuronoxylan and glucomannan hemicellulose (Timell, 1957; Sjöström, 1981), and so xylose and mannose can be used as taxonomically diagnostic sugars (Cowie and Hedges, 1984).

Hemicellulose is present in all layers of plant cell walls, often closely associated with lignin.

Lignin

Lignin is the second most abundant organic compound on Earth (Phelps and Young, 1997), forming approximately 25% of the existing organic carbon within the plant kingdom (Ziomek and Williams, 1989), and up to 30% of woody plant tissues (Reid, 1995). Although lignin is known to be abundant in vascular land plants, there is some disagreement over whether it also occurs in other plants, such as mosses and algae (Lewis and Yamamoto, 1990).

Lignin is a very random and stable 3D polyphenolic macromolecule. It is formed by the oxidative condensation of 3 phenyl propanoid monomers (Figure 1.2), *p*-coumaryl, coniferyl and sinapyl alcohol (Goodwin and Mercer, 1972) which originate from the reduction of the corresponding *p*-coumaric, ferulic and sinapic acids (de Leeuw and Largeau, 1993). The phenyl moieties of these compounds differ in the hydroxy and methoxy substituents and are called *p*-hydroxyphenyl (H), guaiacyl (G) and syringyl (S) units respectively. The structure of lignin is uncertain, but it is thought to have a molecular mass of 600-1000kDa (de Leeuw and Largeau, 1993). It is held together by irregular C-C and diaryl ether linkages (Healy and Young, 1979) which impart a complex structure which is insoluble and lacks hydrolysable linkages.

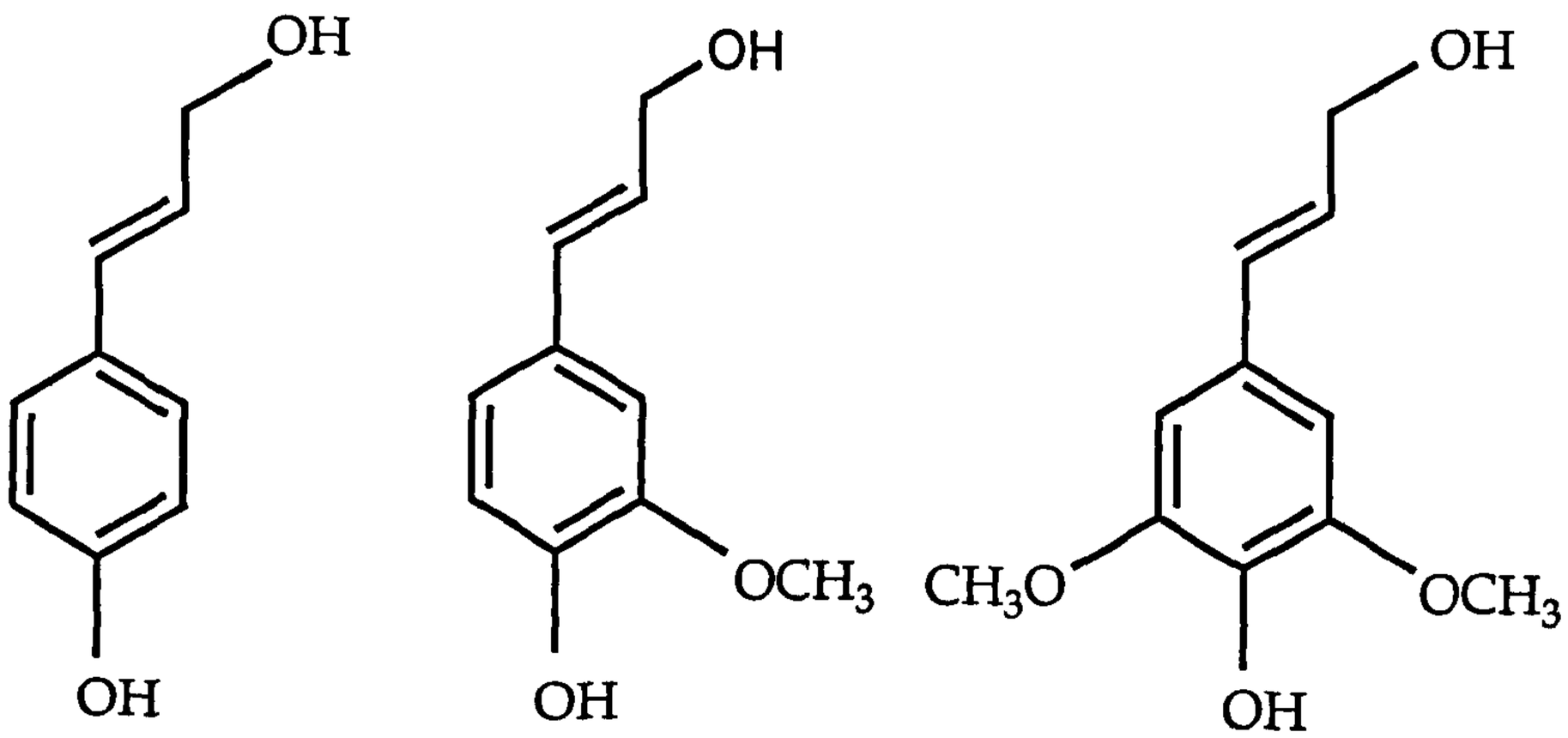

Figure 1.2. Structures of lignin precursors (a) *p*-coumaryl alcohol or *p*-hydroxyphenyl monomeric unit (H), (b) coniferyl alcohol or guaiacyl monomeric unit (G), (c) sinapyl alcohol or syringyl monomeric unit (S) (Galletti and Bocchini, 1995).

Lignin is composed of different combinations of the three monomers depending on the plant family and the morphological region of the tissues. In general, most gymnosperm lignin consists of guaiacyl units and woody angiosperms consist of equal amounts of guaiacyl and syringyl units. *p*-hydroxyphenyl units are only found in low concentrations in both gymnosperms and woody angiosperms, but are major constituents in grass lignin. There are, however, many exceptions to this generalisation (Sarkanen and Ludwig, 1971). Differences in lignin composition between samples of the same specimen and species are due to interspecific variations and variations within a single plant, e.g. normal and compression wood (Sarkanen and Ludwig, 1971).

Lignin is restricted to specialised tissues such as fibres and conducting tissues where it performs its numerous functions. It confers rigidity and mechanical strength on the plant, minimises water permeation between xylem cells, and protects the plant from microbial attack due to its complex refractory structure and strong bonds (Sarkanen and Ludwig, 1971; Kirk, 1984; Eriksson *et al.*, 1990). Lignin tissues also play an important role in the intricate internal transport of water, nutrients and metabolites within plants, and lignin is a permanent bonding agent between cells in woody parts, generating a composite structure with outstanding resistance to impact, compression and bending.

Pectins

Pectins are polysaccharides rich in galacturonan and contain a mix of sugars including rhamnose, arabinose and galactose. Many variations in pectin composition are known (BeMiller, 1986). Pectins are divided into two broad groups, pectic and pectinic acids.

Pectins are characteristic of the middle lamella and the primary cell walls of dicotyledons where they may be covalently linked to phenols,

cellulose and proteins. They are also found in the primary cell walls of monocotyledons, woody tissues and grasses, but to a lesser extent than in dicotyledons.

Tannins

Tannins are polyphenolic compounds which can be divided into three groups, condensed tannins (proanthocyanidin polymers), hydrolysable tannins and phlorotannins, the last being found only in brown algae (de Leeuw and Largeau, 1993). Condensed tannins are probably universal in the major gymnosperm groups and widespread among woody angiosperms (Foo and Porter, 1980; Shen *et al.*, 1986; Stafford, 1988). They are rare or lacking in non-woody angiosperms. Condensed tannins are usually associated with lignins in woody plants, and together provide structural rigidity (Stafford, 1988). They are also major constituents in many plants such as pine (e.g. Foo, 1982). Hydrolysable tannins are known in some higher plants, but are absent in many primitive vascular groups (Bate-Smith, 1984). Tannins exhibit anti-microbial properties because they are able to interact with proteins (de Leeuw and Largeau, 1993).

Other plant biomacromolecules

Starch is a major intracellular storage polysaccharide occurring in granular form within storage organelles called amyloplasts. Starch consists of glucose monomers forming two main polymers, amylose (amounting to 25% of total starch) and amylopectin. As well as storage, starch is also involved in osmoregulation and the lowering of the freezing-point of tissue water.

Triglycerides are another class of storage products, consisting of esters of glycerol and fatty acids in a 3:1 ratio.

Proteins are extremely abundant within plant cells. They consist of long polypeptide chains formed from amino acids. The number of possible amino acid combinations results in a huge variety of proteins. The polypeptide chains are either globular or fibrous. Globular proteins have highly folded chains, are usually water soluble, and form enzymes and storage proteins. Fibrous proteins are long, stringy molecules which are usually water-insoluble and have structural or protective functions.

Cutin, cutan are present in cuticles covering the aerial parts of plants which lack secondary thickening e.g. leaves, stalks and stems (Holloway, 1982a) where they are involved in preventing water-loss and attack from micro-organisms. Cutin is a macromolecular polyester, usually consisting of ω-hydroxy C_{16} and C_{18} fatty acid monomers. It is insoluble but hydrolysable. Cutan, an insoluble and non-hydrolysable biopolymer, was first identified in the cuticles of leaves and stems of higher plants by Nip *et al.* (1986a, b). More recent analysis has suggested that cutan may not be present in living species, but may form in fossils as part of diagenetic alterations (Mösle *et al.*, 1997; Collinson *et al.*, 1998).

Suberin, suberan are thought to play similar roles to cutin and cutan in regions of secondary growth. Suberin is a biopolyester with aliphatic and aromatic regions. Analysis of its composition has been limited, but it appears to be similar to cutin but with different fatty acid chain lengths (Holloway, 1984). It is found mainly in the walls of cork cells, providing a similar protective role in tissues with secondary growth to cutin, but is also present in the cell walls of specialised tissues such as bundle sheaths of grasses, and cell walls surrounding calcium oxalate crystals. Suberan is a non-hydrolysable polymethylenic macromolecule similar to cutan and found in suberised tissues in cork.

Other plant biomolecules include gums, rubbers, resins, and sporopollenin (for a full review, see de Leeuw and Largeau, 1993).

Structure of the plant cell wall

Plant cell walls consist of several layers. The primary cell wall is formed first and is composed mainly of cellulose microfibrils bound together with a hemicellulose matrix. Once the cell has stopped growing, the secondary cell wall may be deposited between the primary cell wall and the plasmalemma (the plasma membrane surrounding the contents of the cell). The secondary cell wall is usually much thicker than the primary cell wall, and generally consists of a cellulosic framework bound by hemicellulose with encrusting components such as terpenes, tannins, and lignin lying within the cellulose fibrils. The lignin and polysaccharides bind through covalent bonds to form a lignin-carbohydrate complex. Cross-linking of hemicellulose and lignin occurs through bridging units such as *p*-coumaric and ferulic acids via ether or ester bonds (de Leeuw and Largeau, 1993).

Where there are no secondary walls, the primary walls may be relatively thick. Within woody plants, the secondary cell wall is comprised of three distinct layers differing in the orientation of cellulose fibrils and degree of lignification (Barghoorn, 1952).

The walls of adjacent cells are "glued together" by the middle lamella, which is composed of pectic substances. The level of lignification of the middle lamella varies around the circumference of the cell; it is greatest at the corners of the cell and on the radial, as opposed to tangential, walls.

Pits present in the cell wall allow transport between adjacent cells. These are usually lined with an unlignified membrane.

Plant cell types

There are three basic types of cell and tissue within plant material (Mauseth, 1995; Raven *et al.*, 1999).

Parenchyma cells have only primary walls and these remain thin (Figure 1.3). Parenchyma tissues are comprised of a mass of parenchyma cells. These are the most common types of cells and tissues within plants. They have a range of functions in photosynthesis and short-range transport of materials between cells, and secretion of substances such as mucilages, resins and oils. Parenchyma cells are alive at maturity, with an active metabolism and water-permeable cell walls.

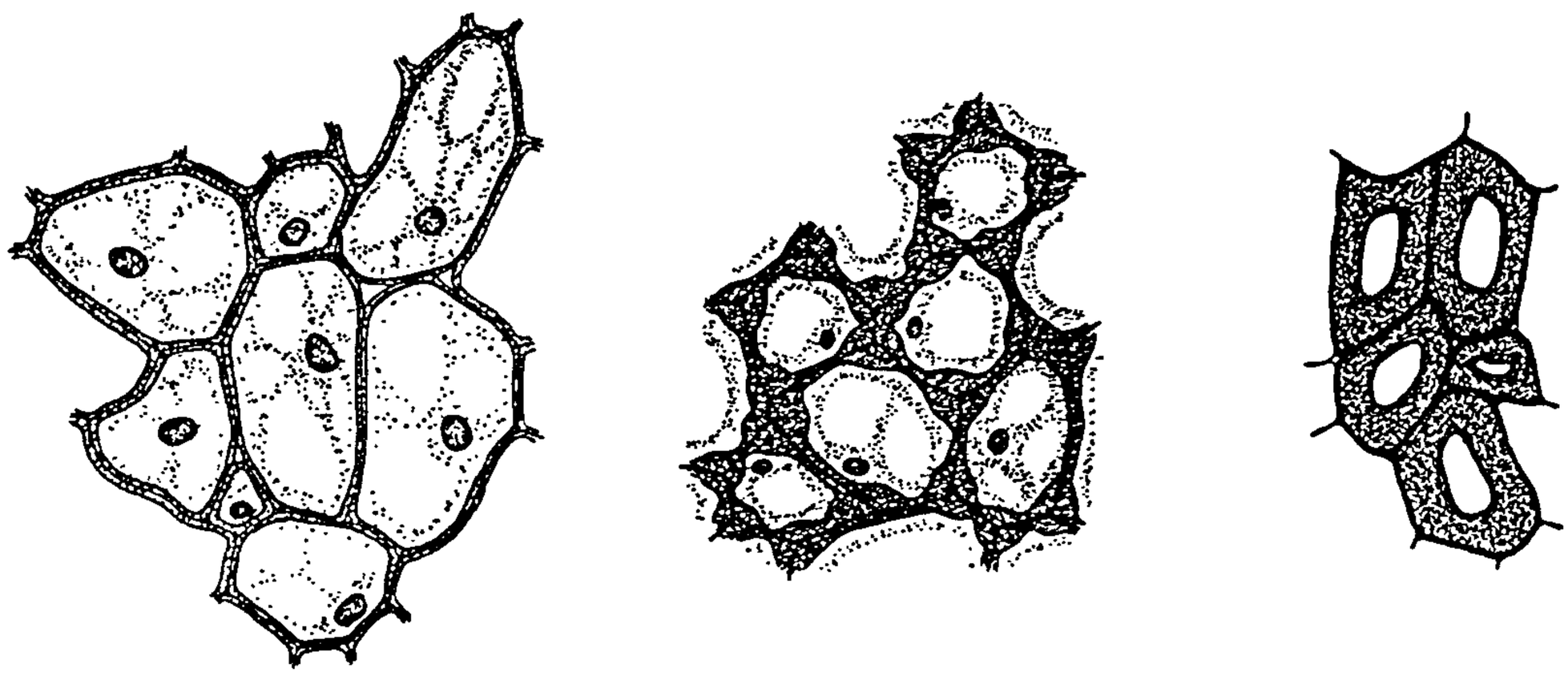

(a) (b) (c)

Figure 1.3. Cross sections of simple plant cells: a) parenchyma; b) collenchyma; c) sclerenchyma (Muller, 1979).

Collenchyma cells also have only a primary wall, but these are thickened in some areas, in particular the corners of the cells (Figure 1.3). These cells exhibit plasticity, and are present usually only in shoot tips and petioles where the cells elongate during growth. They are also alive at maturity.

The third basic type of cells and tissues is sclerenchyma (Figure 1.3). These cells have both a primary cell wall and a lignified secondary wall, and have elastic properties. They are usually found in mature tissues which have finished growing, and provide support within the plant.

Many sclerenchyma cells no longer have an active metabolism at maturity, and their cell walls are effectively impermeable to water. Sclerenchyma tissues are divided into conducting and mechanical sclerenchyma. The conducting cells form the plants xylem, and are divided into tracheids and vessel elements (see page 27). Mechanical sclerenchyma consists of long, flexible fibres which provide strength and elasticity, and short, often almost cuboid, sclereids which confer brittleness and inflexibility to string tissues such as fruit stones.

The internal organisation of plant stems

The structure of gymnosperm and angiosperm stems (Figure 1.4) is critical to the understanding of the experimental results and is therefore reviewed below. Further details can be found in standard treatments such as Mauseth (1995).

Non-woody stems

The outermost cells of herbaceous (non-woody) stems form the epidermis, a thin layer of parenchyma cells (e.g. Mauseth, 1995). Its role is to prevent desiccation of the plánt and act as a barrier against microbial invasion. The epidermis also prevents the plant from overheating in bright sunlight and protects the internal cells from abrasion by dust particles, passing animals, or simply rubbing against other plant stems and leaves.

A thin extracellular layer known as the cuticle covers the epidermis of most non-woody plant organs (e.g. Muller, 1979). The cuticle is thought to be consist of a mixture of cutin, pectins and waxes (de Leeuw and Largeau, 1993), and makes the outer wall of the plant impermeable to water. To allow the entry of carbon dioxide for photosynthesis, the

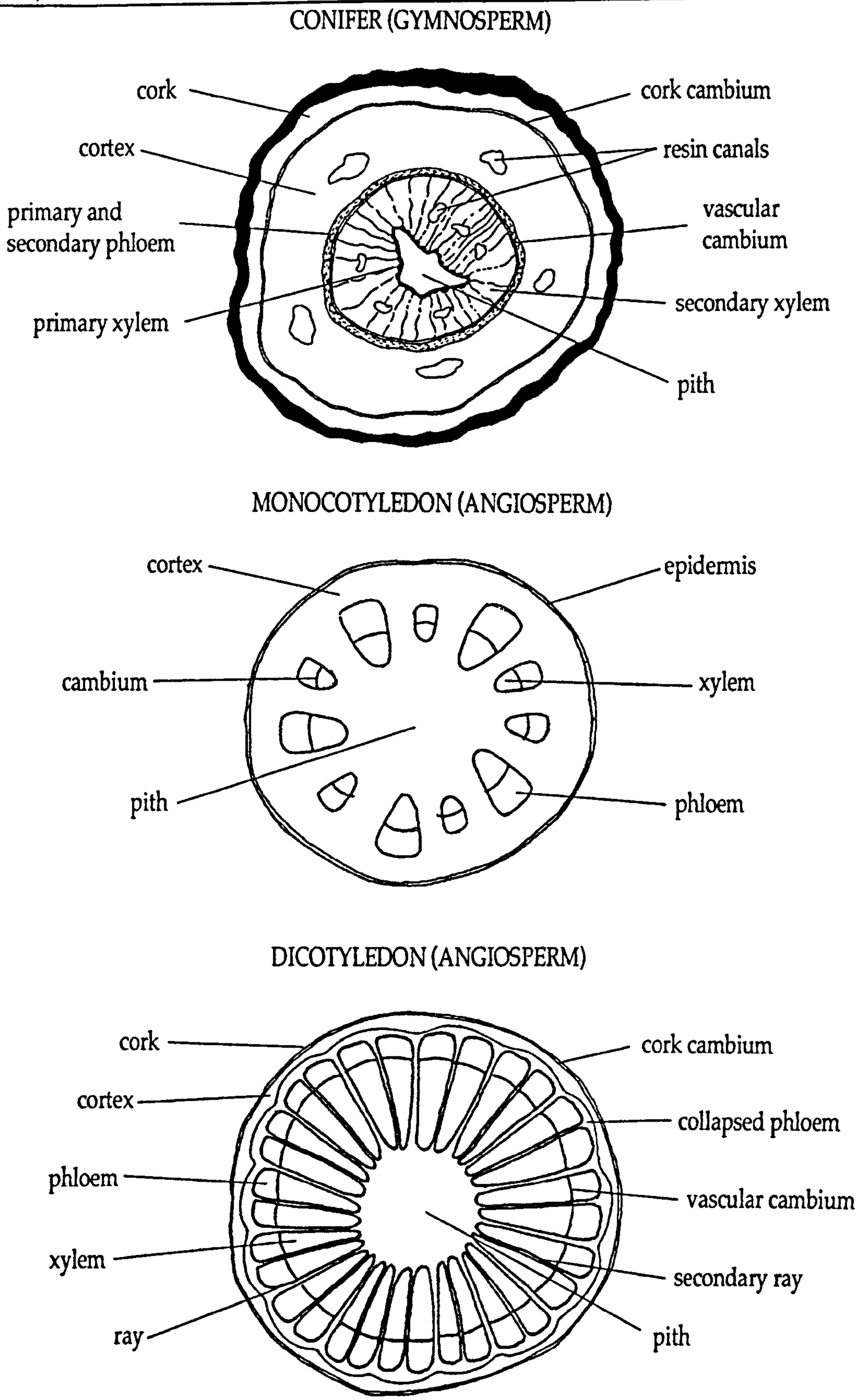

Figure 1.4. Generalised cross-sections of typical conifer, monocotyledon and dicotyledon stems (adapted from Bell & Woodcock, 1968; Mauseth, 1995)

epidermis of the leaves and thin stems contains stomata which can be opened during the daytime (Muller, 1979; Mauseth, 1995).

Lying interior to the epidermis is the cortex. In many plants this can be quite simple and homogeneous, being composed of photosynthetic parenchyma and sometimes collenchyma cells (Mauseth, 1995). In other species, however, the cortex can be very complex, containing specialised cells which secrete substances such as resin or mucilage. Some cortex cells contain silica deposits or large calcium oxalate crystals (Simon *et al.*, 1980). Within stems, the cells of the cortex are usually packed quite compactly.

Vascular tissues exist to provide transport within all but the simplest of organisms. Two types of vascular tissues occur in plants: xylem, which conducts water and minerals up along the roots and stem, and phloem, which distributes sugars and minerals throughout the plant (Simon *et al.*, 1980; Mauseth, 1995; Raven *et al.*, 1999).

Within the xylem, there are two types of conducting cells, tracheids and vessel elements (Figure 1.5), both of which can be referred to as tracheary elements (Mauseth, 1995; Raven *et al.*, 1999). As young parenchyma cells mature into tracheary elements they stop dividing and elongate into long, narrow cells. A secondary wall is deposited to strengthen the primary wall as the cells become sclerenchyma. The cells die and the protoplasm degenerates, leaving a hollow tubular cell (e.g. Simon *et al.*, 1980).

The secondary wall is impermeable to water, so areas of the permeable primary wall must remain uncovered to allow movement of water into and out of the cell (Mauseth, 1995). The simplest type of tracheary element has only a small amount of secondary wall which forms annual thickenings on the inside of the primary wall. These annular thickenings provide a large surface area for water movement in and out of the cell,

but give little strength to the prevent the cell walls from collapsing into the cell as water transfer occurs. Helical thickening occurs when the secondary wall exists as one or two helices interior to the primary wall.

Extra strength is provided in scalariform thickening due to the extensive secondary wall coverage of the primary wall (Mauseth, 1995). Pits are present where the secondary wall is absent to allow for movement of water. In tracheary elements with reticulate thickening, the secondary wall is deposited in the shape of a net.

The strongest and most derived tracheary elements have circular bordered pits. These are present where a secondary wall has been deposited within virtually all of the primary wall. The weakness in the wall caused by the presence of pits is reduced by a border of extra wall material around the pit.

The variation in secondary wall thickening in the different forms of tracheary elements provides selective advantages and disadvantages for each type under different conditions (Mauseth, 1995). Weaker tracheary elements with annular or helical thickenings have a large area available for water movement, but the cells are more likely to collapse. The stronger tracheary elements with scalariform or reticulate thickenings, or circular bordered pits, cannot conduct water as quickly, but are most important under dry conditions.

Tracheids obtain water form other tracheids below them and pass it on to others above them (Mauseth, 1995). To facilitate this transport, tracheids are positioned in groups, with some lying side by side, and the ends of others overlapping neighbouring cells (Figure 1.5). Pits of adjacent tracheids are aligned forming pit-pairs allowing water to pass from one cell to the next. The primary walls of the pits, and the middle lamella between them, form the water-permeable pit membrane.

Water moves through vessel elements with less friction than through tracheids. Vessel elements are individual cells which deposit regions of secondary cell wall before dying at maturity. However, during the final stages of cell differentiation, a large hole is digested through part of the primary wall, often removing the entire end wall of a vessel element forming a perforation plate. The perforations of adjacent vessel elements are aligned (Figure 1.5) forming vessels. The perforations are wide and have no pit membranes to offer any resistance, allowing water to flow along vessels with relatively little friction (Mauseth, 1995; Raven *et al.*, 1999).

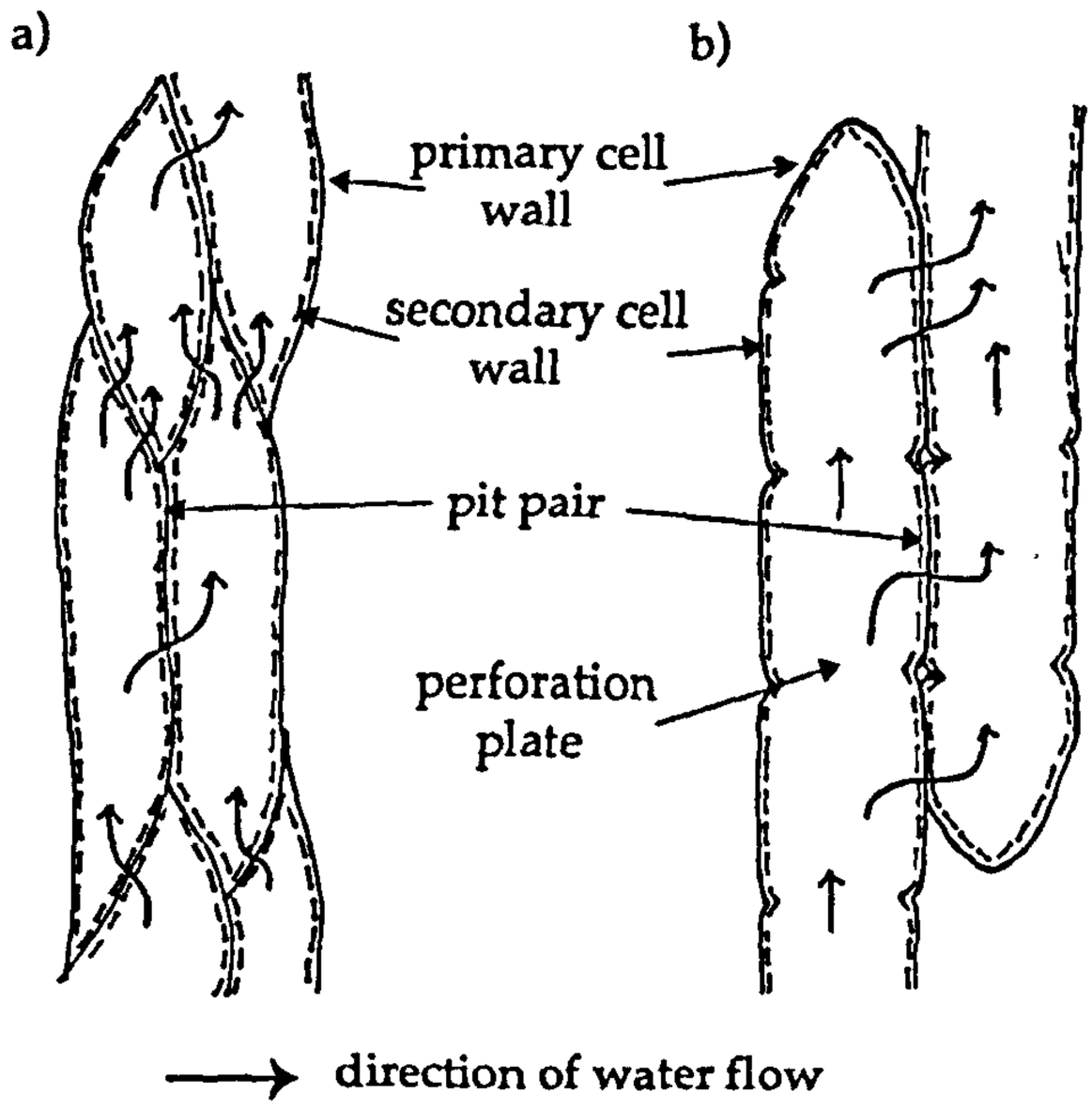

Figure 1.5. Movement of water through xylem: a) water passes between tracheids through pit-pairs; b) water moves between vessels though perforations and pit pairs (Mauseth, 1995).

Vessels can absorb water from parenchyma cells, tracheids, or other vessels, and pass it on upwards through the plant (Simon *et al.*, 1980; Mauseth, 1995). Pits are present in the side walls to allow for lateral

transfer, and all forms of thickening found in tracheids are also present in vessels. The length of vessels varies, from only a few cm long, to several metres, running from a root tip to a shoot tip.

Tracheids are present in all vascular plants, and are thought to have evolved 420 million years ago. Vessels evolved more recently, and are found almost exclusively in angiosperms (Mauseth, 1995).

There are two types of conducting cells within phloem: sieve cells and sieve tube members, either or both of which may be referred to as sieve elements (Mauseth, 1995; Raven *et al.*, 1999). Unlike xylem cells which die at maturity, phloem cells must remain alive to be able to conduct sugars and minerals. Phloem cells are parenchyma and have only a primary cell wall.

As immature sieve elements begin to mature, plasmodesmata in the cell walls begin to enlarge, forming sieve pores, which are found in clusters known as sieve areas (Muller, 1979; Mauseth, 1995). As the sieve elements differentiate, the plasma membrane which lined the plasmodesmata continues to line the sieve pore, the amount of cytoplasm within the pore increases, and rapid bulk movement of sugars and minerals between cells can begin. For this transport to happen, sieve pores of adjacent cells must be aligned.

The two types of sieve elements differ both in shape and location of sieve areas (Mauseth, 1995; Raven *et al.*, 1999). Sieve cells are elongated and spindle-shaped (like tracheids) with sieve areas distributed all over their surface. Sieve tube members are short and wide with particularly large sieve areas, known as sieve plates, on their usually flat end walls. These cells are stacked end to end with their sieve areas aligned to form sieve tubes. Sieve cells were the first phloem cells to evolve and are

found in older fossil plants and non-angiosperm vascular plants. Sieve tube members evolved later, and are only present in angiosperms.

Sieve elements are unusual as the cells remain alive even though their nuclei degenerate. The cytoplasm cannot carry out its complex metabolism without a nucleus, and the necessary control is provided by intimately associated cells: albuminous cells for sieve cells, and companion cells for sieve tube members (Raven *et al.*, 1999). These cells are often much smaller than the conducting cells, and contain a prominent nucleus and a dense cytoplasm packed with ribosomes. The walls between the conducting cells and their controlling cells have complex passages between them, consisting of sieve areas on one side and large plasmodesmata on the other.

Xylem and phloem occur together as vascular bundles in plant stems, located just interior to the cortex. In dicotyledons the vascular bundles form a ring surrounding a region of parenchyma cells called the pith. In monocotyledons, the vascular bundles are distributed as a complex network throughout the inner part of the stem, and are packed by parenchyma cells.

Woody stems

The tissues described above make up the primary stems of herbaceous plants, but additional tissues are present in woody species, namely wood (secondary xylem) and bark (secondary phloem and cork) (Mauseth, 1995). These secondary tissues are produced by the vascular and cork cambiums, and are present in all species of gymnosperms and some species of dicotyledons.

In non-woody stems, the cells in the centre of the vascular bundles ultimately stop dividing and differentiate into conducting tissues. However, in woody stems these cells continue to divide instead of

maturing, and some of the mature parenchyma cells between vascular bundles resume dividing, together forming a complete cylinder of vascular cambium within the stem.

The vascular cambium consists of two types of cells, fusiform initials and ray initials (e.g. Raven *et al.*, 1999). Fusiform initials are long tapered cells which produce the elongate cells of wood (tracheids, vessel elements and fibres) and secondary phloem (sieve cells, sieve tube members, companion cells and fibres). Ray initials are short and more or less cuboidal cells. They produce short storage xylem and phloem parenchyma and in gymnosperms, albuminous cells.

Ray and fusiform initials are organised in specific patterns (Mauseth, 1995; Raven *et al..*, 1999). Ray initials are typically grouped together in short vertical rows which may be one cell wide (uniseriate rays), two cells wide (biseriate rays) or many cells wide (multiseriate rays). Fusiform initials may occur in regular horizontal rows (storied cambium) or irregularly with no horizontal pattern (non-storied cambium).

All cells which are formed interior to the vascular cambium develop into secondary xylem cells. Wood may contain the same types of cells as seen in primary xylem (tracheids, vessel elements, fibres, sclereids and parenchyma) but no new cells. The only real differences between primary and secondary xylem are the origin and arrangement of the cells. The arrangement of secondary xylem reflects which initial cells they are formed from: fusiform initials produce an axial system, and ray initials result in a radial system (Mauseth, 1995).

The axial system is composed of tracheary elements (tracheids or vessels or both) which carry out the longitudinal conduction of water through wood. In many dicotyledons, the axial system also contains fibres providing strength and flexibility, and some immature cells may divide and differentiate into columns of xylem parenchyma. This parenchyma is

important as a temporary water reservoir. Dicotyledons can be described as hardwoods, due to the large amounts of fibres that they contain, whereas conifers with few or no fibres are known as softwoods.

The radial system is much simpler than the axial system. In angiosperms, the radial system consists only of parenchyma cells arranged in uni-, bi- and multiseriate masses called rays. These store carbohydrates and other nutrients during dormant periods and conduct material over short distances radially within wood. In gymnosperms, the xylem rays are almost exclusively uniseriate, and are only ever multiseriate if they contain a resin canal. Gymnosperms may also contain ray tracheids. These are horizontal, rectangular cells with secondary walls, circular bordered pits, and protoplasts which degenerate quickly once the secondary wall is completed.

Annual rings are formed in wood due to the activity of vascular cambium in plants living in regions with strong seasonal climatic variations (Muller, 1979; Mauseth, 1995). During times of stress, such as the winter cold or a summer drought, the vascular cambium becomes quiescent. Once this period of stress has ceased, the vascular cambium becomes very active and cell division begins. Spring or early wood contains a high proportion of wide vessels (or tracheids in gymnosperms) to provide good conduction as new leaves which have not yet developed a waterproof cuticle lose a lot of water. Later, once a cuticle has developed and transpiration (water loss) rates are lower, late (summer) wood with a lower proportion of wide vessels or tracheids is formed. At this stage the plant needs less water but more support, so the summer wood often contains numerous fibres (or narrow, thick-walled tracheids in gymnosperms). At the end of the growing season, the vascular cambium becomes dormant again. Annual rings are composed of a years growth of early and late wood.

Secondary phloem, like secondary xylem, also has axial and radial systems (Raven *et al.*, 1999). The axial system conducts sugars and minerals up and down the stem and consists of sieve tube members and companion cells in dicotyledons and sieve tubes in gymnosperms. Fibres and non-conducting parenchyma may also be present. Rays are formed from storage parenchyma.

The production and differentiation of secondary xylem cells results in the vascular cambium and secondary phloem being pushed outwards (Mauseth, 1995; Raven *et al.*, 1999). As the youngest, inner-most phloem cells form and mature, their diameter increases, resulting in increased pressure on the outermost tissues. The periphery cells of the plant such as the epidermis and cortex respond either by growing in circumference or being torn apart. As the circumference continues to stretch, some storage parenchyma cells become reactivated and undergo cell division, thus forming a new cambium, the cork cambium (phellogen).

The cork cambium is very different to the vascular cambium. The cells are all cuboidal. The inner cells usually remain as cork cambium, while the outer cells differentiate to form cork cells (phellem cells). A mature layer of parenchyma cells known as the phelloderm may also form inside the cork cambium. Together, the cork cells, cambium and phelloderm comprise the periderm (Raven *et al.*, 1999).

As cork cells mature they increase in volume. The thin primary walls become encrusted with suberin, making them waterproof and chemically inert (Mauseth, 1995; Raven *et al.*, 1999). The cells die, and the protoplasm breaks down leaving nothing digestible or nutritious for animals to eat. In some cells, a secondary cell wall may be deposited, and the cells mature into lignified sclereids, alternating with the cork cells, producing an impervious and tough layer.

This layer is so impermeable that the external tissues such as the epidermis, cortex, and older, secondary phloem, die due to a lack of water and nutrients. The periderm only provides temporary protection to the plant because the stem continues to grow interior to it, and it continues to get stretched. Unlike vascular cambium, the cork cambium only produces cells for a few weeks, after which all cells differentiate into cork cells and die. The layer of cork cells cannot expand much, so after several years, a new cork cambium must be produced, and eventually several layers of cork cells build up (Mauseth, 1995).

The outer bark is comprised of all tissues outside the innermost cork cambium. The inner bark consists of the secondary phloem between the vascular cambium and the innermost cork cambium (Mauseth, 1995).

Bacterial decay of organic matter

The decay of organic matter is the primary factor controlling pH, redox and dissolved porewater species, and therefore mineral paragenesis in sediments (Berner, 1981). The rate at which microbes metabolise, respire and multiply on organic matter is generally controlled by the quantity and availability of organic carbon, temperature, supply of oxidants such as oxygen, nitrate and sulphate, depositional setting and rate of burial (Allison and Briggs, 1991). There are many variations in depositional conditions which influence the bacterial decay of organic matter, including porosity, permeability, the presence of clays, pH, high salinity and the presence of toxic compounds.

Different organic compounds have different decay susceptibilities: volatile compounds are subject to rapid degradation and more refractory compounds, such as cellulose and lignin, degrade more slowly. The reactivity of organic matter also decreases as the more reactive compounds are consumed, and the less reactive compounds, and those

formed by ageing, bring about lower rates of bacterial activity (Berner, 1984). Westrich and Berner (1984) demonstrated that organic matter can be divided into essentially two fractions with very different rates of decay. Preservation of almost all organic material is less than 0.5% efficient in marine environments (Hedges and Keil, 1995), and the ultimate end products of bacterial decay are carbon dioxide and methane (Figure 1.6).

There are two major pathways by which organic compounds can be bacterially degraded: respiration, in which molecular oxygen or another oxidant acts as the terminal electron acceptor, and fermentation, where internally balanced oxidation-reduction occurs in the absence of any terminal electron acceptors (Brock, 1997).

On entry to an aqueous decay environment, organic matter is subjected to hydrolysis, which breaks down biopolymers into smaller units, usually monomers, by the addition of water. In aerobic respiration organic carbon combines with molecular oxygen, releasing carbon dioxide and water. However, if the supply of organic matter is greater than the supply of oxygen, oxygen becomes depleted, resulting in anoxia. Oxygen is rapidly consumed in most coastal and many freshwater sediments, and thus organic matter degradation is dominated by anaerobic processes (e.g. Jørgensen, 1982a; Wellsbury *et al.*, 1996)

Anaerobic bacterial communities operate as an obligatory interactive team, with different bacteria capable of breaking down and producing different compounds which can be metabolised by other species. Anaerobic bacteria use a range of inorganic substrates, e.g. nitrate, ferric iron and sulphate, as alternative electron acceptors. This produces broad depth stratification within the sediment, with the species liberating the greatest free energy highest in the sequence (Figure 1.7). Only when a species has been exhausted can the oxidations lower in the sequence occur. However, sediment heterogeneity and bioturbation can blur this

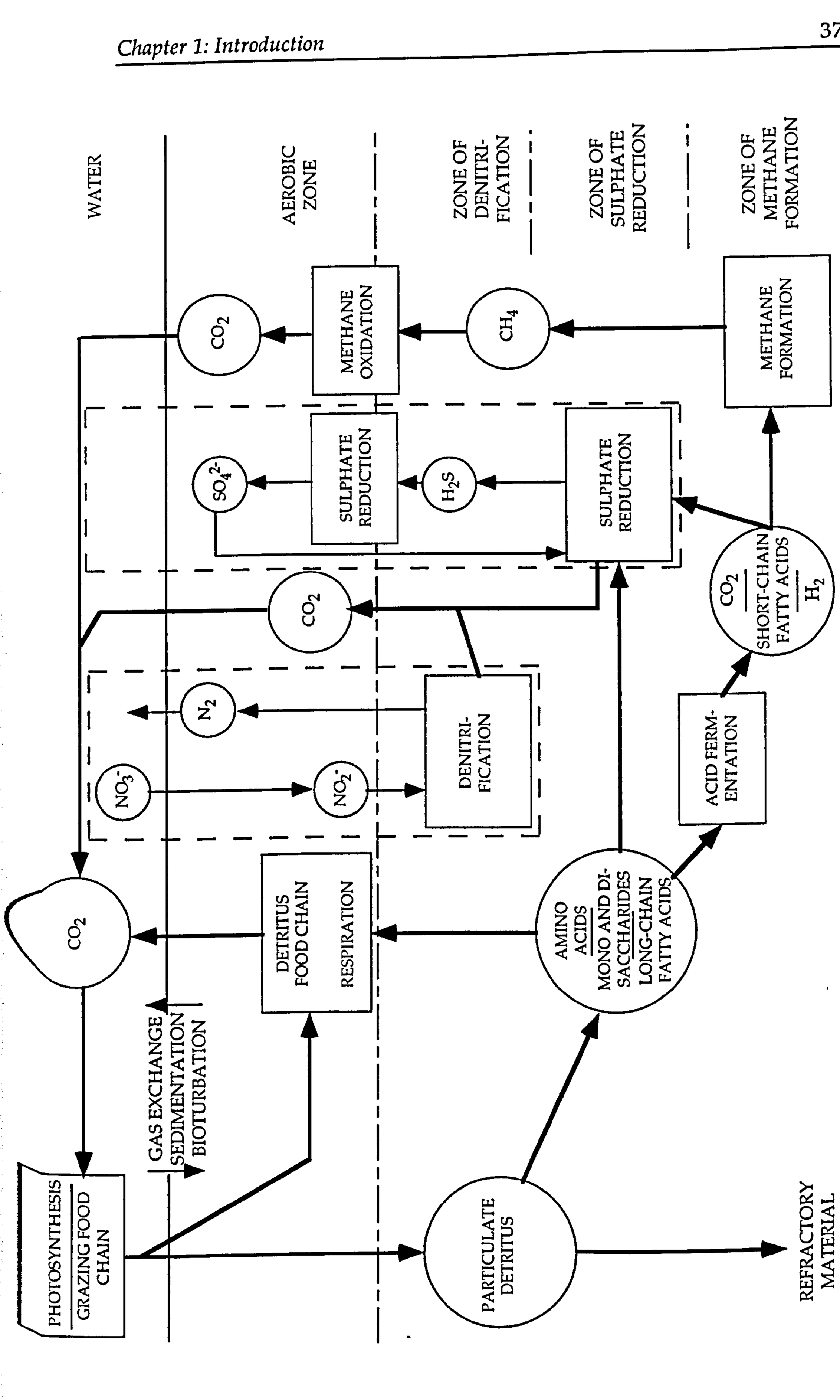

FIGURE 1.6. Transformations of organic carbon during anaerobic decomposition in a marine sediment. Pathways leading to the nitrogen and sulphur cycles are also indicated (Jorgensen, 1983).

Increasing free energy yield

AEROBIC DECAY

$$(CH_20)_{106}(NH_3)_{16}H_3PO_4 + 106\,O_2 \rightarrow 106CO_2 + 16NH_3 + H_3PO_4 + 106H_2O$$

ANAEROBIC DECAY

Manganese Reduction

$$(CH_20)_{106}(NH_3)_{16}H_3PO_4 + 212MnO_2 + 332CO_2 + 120H_2O \rightarrow 438HCO^-_3 + 16NH_4^+ + HPO^{2-}_4 + 212Mn_4^{2-}$$

Nitrate Reduction

$$(CH_20)_{106}(NH_3)_{16}H_3PO_4 + 84NO^-_3 \rightarrow 7.2CO_2 + 98.8HCO^-_3 + 16NH_4^+ + HPO^{2-}_4 + 42.4N_2 + 49H_2O$$

Iron Reduction

$$(CH_20)_{106}(NH_3)_{16}H_3PO_4 + 424Fe(OH)_3 + 756CO_2 \rightarrow 862\,HCO^-_3 + 16NH_4^+ + HPO^{2-}_4 + 424Fe^{2+} + 304H_2O$$

Sulphate Reduction

$$(CH_20)_{106}(NH_3)_{16}H_3PO_4 + 53SO^{2-}_4 \rightarrow 39CO_2 + 67HCO^-_3 + 16NH_4^+ + HPO^{2-}_4 + 53HS^- + 39H_2O$$

Carbonate Reduction (Methanogenesis)

$$(CH_20)_{106}(NH_3)_{16}H_3PO_4 + 14H_2O \rightarrow 39CO_2 + 14\,HCO^-_3 + 53CH4 + 16NH_4^+ + HPO^{2-}_4$$

Figure 1.7. Stratification of bacterial reduction zones in ideal sediments. After Redfield (1958); Allison and Briggs (1991)

theoretical sequence of microbial processes. Not all oxidants are present in all sediments and the relative amounts of oxidants vary, thus modifying the expected microbial depth profiles even further. For example, due to naturally occurring high levels of porewater sulphate, marine sediments are dominated by sulphate reduction, followed by methanogenesis, whilst low sulphate concentrations in freshwater systems result in anaerobic processes being dominated by methanogenesis (Malcolm and Stanley, 1982).

Iron and manganese metabolism and cycling

Bacteria have been isolated from marine and freshwater sediments that are capable of oxidising a range of organic substrates, including aromatic compounds, using ferric iron and Mn (IV) as terminal electron acceptors (Lovley and Phillips, 1986a; Lovley *et al.*, 1993; Nealson and Saffarini, 1994; Nealson and Little, 1997). Within sediments, these bacteria play an important role in the dissolution of insoluble iron (III) and manganese (IV), releasing soluble iron (II) and manganese (II) respectively. This can often result in the formation of Fe (II) and Mn (II) bearing minerals such as magnetite (Karlin *et al.*, 1987), siderite (Coleman *et al.*, 1993) and manganese (II) carbonates (Middelburg *et al.*, 1987). The mechanisms by which the reduction of Fe (III) and Mn (IV) take place are poorly understood (Lovley *et al.*, 1993), but direct contact is needed between the bacteria and the iron and manganese minerals (Nealson and Saffarini, 1994).

Ferric iron can also be reduced by reaction with hydrogen sulphide (Equation 1.2).

The sulphur cycle: the bacteria involved

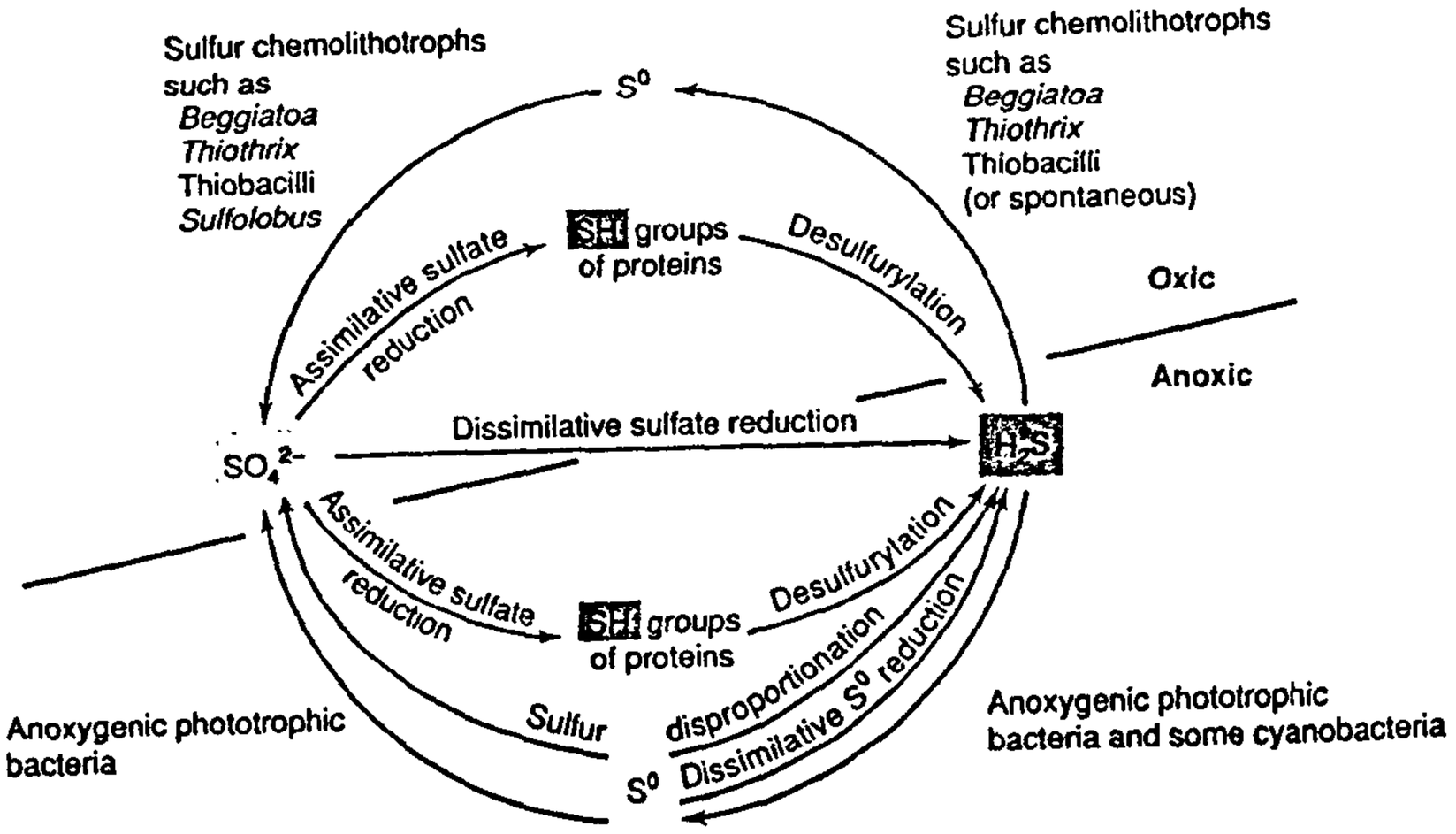

Figure 1.8. The sulphur redox cycle and the bacterial processes involved (Brock, 1997).

The sulphur cycle is complex, involving a variety of oxidation states. Although bacterial metabolism is involved in most aspects of the cycle (Figure 1.8), some transformations between states may take place chemically at significant rates as well. For example, sulphide speciation is pH-dependent, with the dominant species being S^{2-} at high pH, HS^- at neutral pH, and hydrogen sulphide, H_2S, at pH less than 6. Relative rates of chemical and bacterial sulphide oxidation vary depending on the environmental conditions. Jørgensen (1982a) showed that hydrogen sulphide oxidation took place entirely chemically in the euxinic Black Sea, but in a *Beggiatoa* mat on the mud surface of Danish Bay the residence time of sulphide was ca 0.6 seconds, and oxidation was almost exclusively bacterially-mediated. In a monomictic lake the sulphide residence time was 10-20 minutes, and bacteria were responsible for 30-50% of hydrogen sulphide oxidation.

The sulphur bacteria

The colourless sulphur bacteria have the potential to oxidise many reduced inorganic sulphur compounds, most commonly hydrogen sulphide (Eqn. 1.11), elemental sulphur (Eqn. 1.12), and thiosulphate, using oxygen or nitrate as electron acceptors (Jørgensen, 1982a).

$$H_2S + 2O_2 \rightarrow SO_4^{2-} + 2H^+ \qquad \text{Eqn. 1.11}$$

$$S^\circ + H_2O + 1.5O_2 \rightarrow SO_4^{2-} + 2H^+ \qquad \text{Eqn. 1.12}$$

$$HS^- + 1.5O_2 + H^+ \rightarrow S^\circ + H_2O \qquad \text{Eqn. 1.13}$$

The colourless sulphur bacteria exhibit a wide range of morphological, physiological and ecological types, including *Thiobacillus* and *Beggiatoa*, which utilises hydrogen sulphide. Many form mats or veils to reduce the chemical oxidation of hydrogen sulphide.

If light reaches the sulphide zone, photosynthetic bacteria can utilise hydrogen sulphide as an electron donor in anoxygenic photosynthesis. Purple and green sulphur bacteria can utilise acetate and pyruvate as a carbon source, and some species of purple sulphur bacteria may use several other organic compounds. Due to differences in sulphide tolerance, the purple sulphur bacteria often develop above the more hydrogen sulphide-tolerant green sulphur bacteria in a depth sequence (Brock, 1997).

The sulphate-reducing bacteria

Sulphate-reducing bacteria (SRB) are a heterogeneous assemblage of obligate anaerobes with the common ability to use sulphate as an electron acceptor. They exhibit a wide range of metabolic, physiological and morphological types and are widely distributed in aquatic and terrestrial environments. Anaerobic sulphate reduction is a particularly important

process in coastal and estuarine sediments, and in shallow water sediments it can be the dominant degradation process, accounting for up to 50% of organic matter degradation (Jørgensen, 1982b).

Sulphate is very stable chemically, and does not reduce spontaneously, except in very high temperature environments, where thermo-chemical sulphate reduction occurs. Its reduction by bacteria involves a number of intermediate steps, with hydrogen sulphide as the end product. In assimilatory sulphate reduction this hydrogen sulphide is incorporated into amino acids as organic sulphur. On death, desulfurylation returns this organic sulphur to hydrogen sulphide. In contrast, that formed by dissimilatory sulphate reduction is excreted into the environment where it plays an important biogeochemical role in several processes, including the formation of sedimentary metal sulphides (Brock, 1997).

Eighteen genera of dissimilatory sulphate reducers are currently recognised (Odom and Singleton Jr, 1993; Brock, 1997), which can be divided into two main groups. Group I, the non-acetate oxidisers, includes *Desulfovibrio*, *Desulfomonas* and *Desulfobulbus*.

$$2\,C_3H_6O_3 + 4H_2O \rightarrow 2CH_3COO^- + 2CO_2 + 4H_2 \qquad \text{Eqn 1.14}$$

These utilise lactate, formate, malate, pyruvate, hydrogen, ethanol and certain fatty acids as a carbon and energy source, reducing sulphate to hydrogen sulphide, and excreting acetate as an end-product (Equation 1.14). Some strains of *Desulfotomaculum* are also capable of utilising glucose, but this is generally rare. Group II consists of the acetate oxidisers, such as *Desulfobacter* and *Desulfococcus*. These specialise in the oxidation of fatty acids, especially acetate, and reduce sulphate to

sulphide releasing carbon dioxide: e.g.

$$CH_3COO^- + SO_4^{2-} + 3H^+ \rightarrow 2CO_2 + H_2S + 2H_2O \qquad \text{Eqn 1.15}$$

Parkes *et al.* (1989) observed that acetate is the main *in situ* substrate for sulphate reduction. Lovley *et al.* (1993) also observed that certain species of SRB are capable of enzymatically reducing iron (III) and uranium (VI), although insufficient energy is conserved in these reactions to support bacterial growth.

Some sulphate reducers are also capable of disproportionation. This involves splitting sulphur compounds of intermediate oxidation state into two new compounds, one more reduced and the other more oxidised than the original substrate e.g.

$$S_2O_3^{2-} + H_2O \rightarrow SO_4^{2-} + H_2S \qquad \text{Eqn 1.16}$$

$$4S^\circ + 4H_2O \rightarrow 3H_2S + SO_4^{2-} + 2H^+ \qquad \text{Eqn 1.17}$$

Experimental work has shown the importance of SRB in the precipitation of iron monosulphide (Herbert *et al.*, 1998) and its transformation to pyrite (Donald and Southam, 1999).

The sulphur-reducing bacteria

A variety of sulphur-reducing bacteria, generally distinct from the sulphate-reducing bacteria, can reduce elemental sulphur to hydrogen sulphide, and often use thiosulphate and sulphite. They cannot usually reduce sulphate to sulphide.

Methanogenesis

Seven major groups of methanogens have been recognised, including a total of 17 genera, which exhibit a variety of morphological types (Oremland, 1988; Brock, 1997). Most methanogens used carbon dioxide as a terminal electron acceptor and hydrogen as an electron donor: e.g.

$$4H_2 + CO_2 \rightarrow CH_4 + 2H_2O \qquad \text{Eqn 1.18}$$

The methanogens have to compete with other bacteria for many of their electron donors, especially H_2 and acetate. As long as sulphate is present within an environment, the SRB will generally be favoured in the competition with methanogens. Once sulphate is no longer present, methanogenesis will be the dominant terminal oxidising reaction. However, some 'non-competitive' substrates, such as methanol, methylated amines and certain organic sulphur compounds (Oremland, 1988; Whiticar, 1999), tend only to be used by methanogens, thus enabling methane formation to occur even in the presence of high sulphate concentrations.

Acetogenesis

The homoacetogens, like the methanogens, are carbon dioxide-reducers, producing acetate from carbon dioxide and hydrogen. The overall reaction is:

$$4H_2 + H^+ + 2HCO_3^- \rightarrow CH_3COO^- + 4H_2O \qquad \text{Eqn 1.19}$$

Carbon dioxide reduction releases more energy by methanogenesis than by acetogenesis. The homoacetogens are obligate anaerobes, and as well as growing autotrophically using hydrogen and carbon dioxide, they

can grow chemoorganotrophically by the fermentation of sugars and other organic compounds.

The homoacetogens do not form a taxonomically defined group, but include a range of widely differing organisms, such as gram positive *Clostridium aceticum* and gram negative *Acetobacteriam woodii*.

Fermentation

Fermentation is a decay process where the organic compound serves as both the electron donor and acceptor and occurs simultaneously to the above respiration processes. Fermentation results in the formation of both partially oxidised and partially reduced compounds from the original substrate. There are a number of different types of fermentation, none of which generates much energy, as energy generation is limited to substrate phosphorylation, i.e. no electron transport occurs as in respiration.

Even if a single fermentation reaction does not provide favourable energetics, the product may favour the process, in particular H_2, which can be used by another organism in a more energetically favourable reaction. This is an example of syntropy, or mutual feeding, where two organisms do something together which neither can do separately, e.g. the fermentation of ethanol to acetate and methane by an ethanol fermentor and a methanogen.

$$2CH_3CH_2OH + 2H_2O \rightarrow 4H_2 + 2CH_3COO^- + 2H^+ \quad \text{Eqn 1.20}$$

$$4H_2 + CO_2 \rightarrow CH_4 + 2H_2O \quad \text{Eqn 1.21}$$

The fermentation of ethanol (Equation 1.20) is energetically unfavourable, but results in the production of hydrogen which can be used in the energetically favourable reduction of carbon dioxide,

resulting in an overall energetically favourable process. This is known as interspecies H_2 transfer. Similarly, in the multi-stage break-down of polysaccharides such as cellulose to methane, any hydrogen produced by the fermentation of glucose is immediately consumed by methanogens, homoacetogens, and SRB.

Resistant plant biomacromolecules

Some macromolecules are more decay resistant and have a higher preservation potential than others. The preservation potential of many plant biomacromolecules is summarised in Table 1.2. However, the preservation potential of more readily decomposed tissues may be enhanced when they are incorporated into structural tissues. For example, recognisable traces of cellulose, which is readily degraded under normal circumstances, have been preserved when linked with lignin in the walls of fruits and seeds (van Bergen *et al.*, 1994b-d, 1995).

Resistant biomacromolecules can be divided into two groups, those which are highly aliphatic, and those with aromatic properties (van Bergen *et al.*, 1995). Highly aliphatic biomacromolecules are recognised in plant remains such as cuticles, bark, algal cell walls, pollen and spores (e.g. Nip *et al.*, 1986; Tegelaar, 1990; Collinson *et al.*, 1994), where their composition is similar to the original with only minor chemical alterations. Aromatic macromolecules are present in leaves, secondary wood, vascular tissues and stony fruit walls (e.g. Hedges *et al.*, 1985; Boon *et al.*, 1989; Haslam, 1989; Tegelaar, 1990), and can undergo significant transformations, including polymerisation, during diagenesis (van Bergen *et al.*, 1995; Briggs, 1999). Both the nature of the lithology and the amount of overburden influence the extent of diagenetic alteration of such compounds (van Bergen *et al.*, 1994c, d).

Biomacromolecule	Preservation potential
starch	-
fructans	-
cellulose	-/+
xylans (hemicellulose)	-/+
pectins	-/+
mannans (hemicellulose)	-/+
galactans (hemicellulose)	-/+
mucilages	+
gums	+
proteins	-/+
extensin (glycoproteins)	-/+
DNA, RNA	-
glycolipids	+/++
rubber, gutta, dolichols	+
resins, ambers	+/++
cutins, suberins	+/++
lignins	+++
tannins	+++/++++
sporopollenins	+++
cutan	++++
suberan	++++

Table 1.2 Inventory of presently known plant biomacromolecules and their potential for survival during sedimentation and diagenesis (adapted from Tegelaar *et al.*, 1989b). "Preservation potential" ranges from '-' (extensive degradation under any depositional conditions) to '++++' (little or no degradation under any depositional conditions).

Lignins are the most abundant biomacromolecules in extant vascular plants (van Bergen *et al.*, 1995). Chemically modified versions of lignin are preserved in fossil woods, seed coats and fruit walls (de Leeuw and Largeau, 1993; de Leeuw *et al.*, 1995). Lignin biomarkers have been found in 50 million year old Messel kerogen (Goth *et al.*, 1988) and buried

woods from Recent to Miocene sediments (Kagemori, 1969). Similar biomarkers have also been described from Carboniferous (Logan and Thomas, 1987) but chemical evidence for the preservation of lignin from this period is equivocal (van Bergen *et al.*, 1997a). Sigleo (1978) described wood polymers which had survived 200 million years of silicification and diagenesis in the Petrified Forest National Park of Arizona, USA. Several studies have shown that carbohydrates are present in fossil plant tissues (e.g. Wilson *et al.*, 1987; Hatcher *et al.*, 1989; Macko *et al.*, 1989).

Fossilised plant cuticles are well documented and are preserved due to the decay resistance of cutin, and possibly also cutan. The analysis of fossil and extant plant cuticles has been well documented (e.g. Nip *et al.*, 1986; van Bergen *et al.*, 1994b-d; Kerp, 1990; Mösle *et al.*, 1997; Collinson *et al.*, 1998; Briggs, 1999). The nature of cutan within extant plant species or as a diagenetic product has been discussed on page 22.

The relative decay susceptibilities of different plant tissues may also affect the mode of preservation (see page 5).

MICROBIAL DECAY EXPERIMENTS

Introduction

Fossil material provides only limited evidence for the processes involved in the authigenic mineralisation of organisms. This evidence cannot fully explain the dynamics of microbial activity and the timing or sequence of mineral growth involved in the preservation of the fossil organism. In addition, the information that it reveals regarding the conditions under which the organism was deposited and the decay processes prior to mineralisation is limited. Critical evidence may also be hidden by subsequent diagenesis (Briggs, 1995).

Laboratory experiments which attempt to reproduce the biogeochemical processes involved in soft tissue mineralisation are essential to understand the processes of, and controls on, fossilisation and the relative influence of biological and abiological reactions. They also allow a better assessment of preservational biases in the fossil record. For example, experiments can be used to study the role of different factors, such as oxygen availability, temperature, salinity and different types of microbial activity, in fossilisation.

Soft tissue preservation can be investigated successfully in the laboratory due to the speed with which it must occur to prevent loss of morphological detail - within days or weeks, rather than on a geological time scale. For example, calcium carbonate and calcium phosphate have been shown to precipitate in association with decaying shrimps within 2-4 weeks (e.g. Briggs and Kear, 1993, 1994; Sagemann *et al.*, 1999).

Fine scale chemical gradients are probably crucial in determining fossilisation, and these can be measured by using micro-electrodes (oxygen, nitrate, sulphide and pH; Revsbech and Jørgensen, 1983; Parkes

and Senior, 1988). Steep chemical gradients are created by the activity of a range of microbes involved in the decomposition of organic matter (Jørgensen, 1982, 1983; Herbert, 1992), and a recent study by Sagemann *et al.* (1999) has demonstrated that these occur around decaying organisms leading to fossilisation.

Experimental Aims

While many varied laboratory experiments have investigated the fossilisation of invertebrates (see Briggs, 1995, for a full review), those involving plant material are more limited, focusing on transport dynamics (e.g. Ferguson, 1985; Spicer, 1981, 1991) and the role of bacterial biofilms (Dunn *et al.*, 1997).

This study aimed to provide a greater understanding of the relationship between decay and the authigenic mineralisation processes involved in the pyritisation of vascular plants by studying the biogeochemical processes in the laboratory. Model microbial decay experiments were run to investigate the relative influences of biological and abiological controls on authigenic pyritisation. A range of destructive and non-destructive techniques were used to monitor the critical controls that determine the balance between decay and mineralisation. Micro-electrodes were used to monitor oxygen, pH and sulphide gradients on a mm-scale to detect distinct chemical conditions around the plant material with minimum disturbance to the decay environment. Microscopy (SEM, TEM and light microscopy of tissue-stained thin sections) was used to study the changes in tissue structure caused by decay of the plant material.

Experimental conditions were chosen to represent a range of environmental settings conducive to pyrite formation. Plant material to be decayed was chosen to represent a wide range of tissues and species,

including species which are pyritised in the fossil record. The majority of plant species identified from the Eocene London Clay are now found only in tropical regions (Collinson, 1983). Of the species still indigenous to the British Isles, the Platanaceae (plane) family, first identified in the London Clay by Poole (1992), was chosen as the main decay organism due to the availability of large amounts of fresh material. Five or six twigs were used to form a single layer of plant material covering the sediment layer, ensuring that all twigs were in contact with the sediment.

Canfield (1988) estimated that the iron oxide content of freshly-deposited fine-grained, siliclastic marine sediments is approximately 0.6-1.5% weight. However, it has been suggested that high iron concentrations are required for the pyritisation of carcasses (Raiswell *et al.*, 1993). This correlates with elevated iron levels which have been documented in beds yielding pyritised fossils, such as the Hunsrück Slate of Germany (2.66 ± 0.91% potential reactive iron in slates adjacent to the fossils: Briggs *et al.*, 1996) and Beecher's Trilobite Bed, New York State (2.78 ± 0.41% potentially reactive iron in the sediment: Briggs *et al.*, 1991). Amorphous iron oxyhydroxide (FeOOH) was chosen as the main iron source to be added to the sediment within the decay experiments as it is one of the detrital iron minerals most reactive to sulphide (Table 1.1: Canfield *et al.*, 1992).

Experiments were run to investigate different environmental conditions, and the influence of limiting factors on pyrite formation: in particular reactivity and availability of sulphate, iron and organic matter.

In natural environments, pyrite formation is limited by the rate of sulphate reduction only when sulphate concentrations are less than 3mM (Capone and Kiene, 1988). Although sulphate concentrations within the starting medium were much higher than this (ca 30mM), concentrations in the sediment may have been limiting. To overcome

this, a sulphate-containing agar layer was placed beneath the sediment to provide a steady supply of sulphate to the deepest sediments.

In most environments, the amount of pyrite formed in never limited by the total amount of iron present, but by its reactivity (Raiswell and Canfield, 1988). However, a diffusion-with-precipitation model has shown that high levels of dissolved porewater iron are required for the pyritisation of animal carcasses (Raiswell *et al.*, 1993), and unusually high levels often were identified in the Hunsrück Slate (Briggs *et al.*, 1996) and Beecher's Trilobite Bed (Briggs *et al.*, 1991). To investigate the influence of iron availability and reactivity, experiments were run with different concentrations of iron oxyhydroxide or different iron sources added to the sediment.

The major factor controlling the rate of bacterial sulphate reduction, and hence pyrite formation, in normal marine sediments is the amount and reactivity of organic matter deposited within the sediments (Berner, 1984). The influence of the amount of available organic matter on pyrite formation was investigated by varying the number of twigs decayed (including no twigs in one experiment), and by stimulating bacterial activity with yeast extract or by the addition of extra twigs or glucose solution during experiments. the reactivity of organic matter was studied by using different species of plant with different tissue composition and structural arrangement, and hence different decay susceptibilities.

Before deposition and mineralisation, much of the plant material within the pyrite fossil record may have been subjected to aerobic, especially fungal decay, which would have altered the amount and reactivity of available organic matter for bacterial respiration. This was studied by using twigs which had been subjected to decay by fungi indigenous to the twigs or by a fungal inoculum for 12 weeks.

In natural systems it is unlikely that plant material would have entered aqueous systems, and would immediately have become in contact with the sediment, and hence much of the bacterial population, without being buried. Decay experiments were run where the twigs were allowed to float and others where sedimentation was simulated with regular additions of sediment. Experiments were also run which combined floating twigs with sedimentation. Further experiments were carried out where the twigs were buried in the sediment.

The importance of the addition of bacterial inoculum and the dimensions of the decay vessels were also investigated.

Despite low levels or sulphate being present naturally in freshwater systems, pyritised plant fossils have been documented from freshwater environments (e.g. Kenrick and Edwards, 1988). Experiments were run to investigate the formation of pyrite in freshwater systems, using freshwater sediment, medium and bacterial inoculum. The effect of sulphate availability was investigated under freshwater conditions by placing a sulphate-containing agar layer beneath the sediment to provide a constant supply of sulphate.

Sealed marine and freshwater systems were run to investigate the importance of oxygen in pyrite formation. Sealing the systems not only affected the bacterial processes involved, but may also have influenced the mechanism of pyrite formation as the role of oxidants is though to be important in the transformation of iron monosulphide to pyrite (Wilkin and Barnes, 1996). Some of the conditions studied in the open systems, such as the effect of amount and reactivity of organic matter were also investigated under sealed conditions.

Abiological changes within the decay systems were studied by irradiating sealed marine systems. Sulphide was added to some of the marine systems before sealing and irradiation to stimulate the reducing

conditions created by bacterial decay, so that the direct and indirect effects of bacterial metabolism on mineral formation, particularly iron sulphides, could be investigated.

Experimental Methods

Procedure for decay experiments

Over 140 individual decay experiments, referred to as decay systems, were run. These were designed to investigate different environmental conditions and were all set-up, dismantled and analysed according to the basic protocol for open marine decay systems detailed below. Variations from the standard protocol, representing different experimental conditions, are detailed in Table 2.1.

Each set of experimental conditions was studied in two (or occasionally more) decay systems, referred to as replicates. These were set up at the same time as each other, with sediment from the same source, and medium and inoculum from the same batches. Each set of replicates was also set up simultaneously with (one or) two standard open marine systems (set up according to the basic protocol and referred to as standards) or, where relevant, controls which are detailed in Table 2.1, to allow the relative influence of the experimental conditions to be studied.

Each individual decay system has an identification number (i.d. no.), as listed in Table 2.1, to allow easy access of results and comparison between replicates, standards and/or controls.

Standard decay systems were run for either 5.4, 6, 12 or 14 weeks, after which they were sampled and dismantled. These arbitrary time periods were chosen following preliminary runs of standard open marine systems which indicated that oxygen began to penetrate the medium after 5.4 weeks when some sulphide was still present adjacent to the decaying twigs, and after 12 weeks, when all sulphide had been utilised and the

medium was no longer anoxic immediately above the sediment. Several decay systems had to be run for 14 weeks due to failure of the computer-run micro-electrode monitoring system. The duration of each decay system is listed in Table 2.1.

The individual decay systems and the month in which they were set-up in are listed in Appendix 1, so that any effects of seasonality, of either sediment and/or plant material, can be taken into consideration when analysing experimental results.

Basic protocol for open marine decay systems

Fresh anoxic sediment (10ml) from an estuarine site with local and overhanging plant growth (the banks of the River Wye, Chepstow, national grid reference ST535944), was transferred into a 100ml wide-necked screw-top glass jar using a cut-off 10ml syringe. Amorphous iron oxyhydroxide (FeOOH) was made by neutralising 0.4M ferric chloride solution to pH 7 with sodium hydroxide (Lovley and Phillips, 1986). The product was washed thoroughly with de-ionised water, dried on a Buchner filter funnel, and then centrifuged at 5500rpm for 10 minutes and any excess water removed, before being added to the sediment (1% wt of sediment). The sediment and iron oxyhydroxide were mixed thoroughly and spread into an even layer covering the base of the jar.

Five fresh, 1-2 year old, plane twigs (*Platanus acerifolia*), with no visible knots, decay or damage, were cut to 35-40mm lengths using a razor blade to ensure smooth, flat ends for later microscopy. The twigs were placed in a single layer and pressed slightly into the sediment, to prevent them from floating and to ensure contact with the sediment.

Yeast extract solution (7ml of 1.5% solution) was added to the jar as an extra energy source to encourage bacterial growth, followed by bacterial inoculum (10ml). The total volume of the jar was then made up to

Experimental conditions	Experimental details	Time period	I.D. no.
	1.Standard open marine conditions (*Platanus*)		
1a. Time series	Standard method: 1 jar dismantled per week for 12 weeks	1-12 weeks	1-12
1b. Extended time series	Standard method	12 weeks	13-15
		24 weeks	16-18
		36 weeks	19-21
1c. Experimental standards	Standard method	5.4 weeks	22
		6 weeks	23
		12 weeks	24-28
		14 weeks	29
	2. Effect of sulphate availability		
2. Effect of sulphate availability	5% agar layer (10ml) of 30mM sodium sulphate beneath sediment	12 weeks	30,31
	3a. Effect of iron availability		
3a-i. Amount of additional iron added	5% wt FeOOH mixed with sediment	12 weeks	32-35
	3% wt FeOOH mixed with sediment	12 weeks	36-39
	No iron source added to the sediment	5.4 weeks	40
		12 weeks	41
3a-ii. Location of iron source	3% wt FeOOH in a layer above sediment	12 weeks	42,43
	3b. Effect of iron reactivity		
3b. Different iron sources added to sediment	Haematite (1% wt of sediment) mixed with sediment in place of FeOOH	12 weeks	44,45
	Haematite (0.5% wt) and FeOOH (0.5% wt) mixed with sediment	12 weeks	46,47
	Ferric chloride (0.5% wt) and FeOOH (0.5% wt) mixed with sediment	12 weeks	48,49

Table 2.1. Experimental conditions and procedures for decay experiments

Experimental conditions	Experimental details	Time period	I.D. no.
	4a. Effect of amount of organic matter		
4a-i. Number of twigs decayed	Single *Platanus* twig added to open marine systems	12 weeks	50,51
		24 weeks	52,53
	Fifteen *Platanus* twigs added to open marine systems	12 weeks	54,55
		24 weeks	56,57
4a-ii. Additional plant material added	Six extra *Platanus* twigs added to open marine systems after 6 weeks	12 weeks	58,59
4a-iii. No plant material	No plant material in open marine system	14 weeks	60
4a-iv. No stimulation with yeast extract	No yeast extract added to open marine systems (total volume made up to 100ml with marine medium)	12 weeks	61, 62
4a-v. Effect of promotion of bacterial growth	20mM glucose added to open marine systems after 6 weeks	12 weeks	63,64
	4b. Effect of organic matter reactivity		
4b-i. Different species decayed for 6 weeks	*Apium* sp. (celery) (3.5g)	6 weeks	65
	Vitis vinifera (vine) (3.5g)	6 weeks	66
	Cyathea chinensis (fern) (3.5g)	6 weeks	67
4b-ii. Different species decayed for 12 weeks	*Vitis* sp. (vine) (five twigs)	12 weeks	68
	Equisetum sp. (horse-tail fern) (five twigs)	12 weeks	69
	Prunus sp. (cherry) (five twigs)	12 weeks	70
	Psilotum nudum (five twigs)	12 weeks	71
	Gingko biloba (five twigs)	12 weeks	72
	Sequoia sp. (redwood) (five twigs)	12 weeks	73

Table 2.1. Experimental conditions and procedures for decay experiments

Experimental conditions	Experimental details	Time period	I.D. no.
4b-iii Different species decayed for 14 weeks	*Apium* sp. (celery) (3.5g)	14 weeks	74
	Psilotum nudum (fresh, green material) (3.5g)	14 weeks	75
	Psilotum nudum (older, orange material) (3.5g)	14 weeks	76
	Vitis vinifera (vine) (3.5g)	14 weeks	77
	Cyathea chinensis (fern) (3.5g)	14 weeks	78
	Pinus sp. (pine) (3.5g)	14 weeks	79
	5. Effect of lowering pH		
5. Effect of lowering pH	i) $FeCl_3$ (1% wt) mixed with sediment in place of FeOOH	12 weeks	80,81
	ii) As above. pH maintained at 6.5-7.0 by addition of 50% HCl	12 weeks	82,83
	6. Effect of fungal decay prior to bacterial decay		
6a. Effect of decay by indigenous fungi	*Platanus* twigs were placed in a beaker with a small petri dish of water, and covered with cling film. The beaker was stored at 25°C, and the water kept topped up. This treatment was to promote growth of fungi endemic to the plant material. After 12 weeks, six twigs were transferred to standard marine decay systems.	12 weeks	84,85
6b. Effect of decay by fungal inoculum	*Platanus* twigs were buried in a mixture of woodchippings and soil with fungal growth (fungal inoculum) in a beaker fun. A small petri dish of water was placed on top of the mixture, and the beaker covered with cling film. The beaker was stored at 25°C, and the water kept topped up. After 12 weeks, six twigs were transferred to standard marine conditions	12 weeks	86,87

Table 2.1. Experimental conditions and procedures for decay experiments

Experimental conditions	Experimental details	Time period	I.D. no.
	7. Effect of twigs floating, sedimentation, and twigs being buried		
7a. Effect of twigs floating	Twigs were left to float or sink within the decay system in open marine systems	5.4 weeks	88
		12 weeks	89
7b. Effect of sedimentation	2ml of a marine medium/sediment mixture (1:1) was added to open marine systems once a week	5.4 weeks	90
		12 weeks	91
7c. Effect of twigs floating and sedimentation	Twigs were left to float or sink. 2ml of a marine medium/sediment mixture (1:1) was added to open marine systems once a week	5.4 weeks	92
		12 weeks	93
7d. Effect of burial of the decay organism	Twigs were buried in the sediment of open marine systems instead of being placed on top of it	5.4 weeks	94
		12 weeks	95
	8. Effect of decay by bacteria indigenous to the twigs		
8. Effect of indigenous bacteria population	No inoculum added to open marine systems (total volume made up to 100ml with marine medium)	12 weeks	96,97
	9. Effect of dimensions of decay vessel		
9. Influence of decay vessel	Standard open marine conditions in 100ml Duran bottle instead of jar	12 weeks	98,99

Table 2.1. Experimental conditions and procedures for decay experiments

Experimental conditions	Experimental details	Time period	I.D. no.
	10. Effect of open freshwater conditions		
10a.Open freshwater standards	Standard conditions with freshwater sediment (10ml), freshwater medium (Appendix 2). 1.5% (wt) FeOOH mixed with sediment	5.4 weeks 12 weeks	100 101-103
10c. Effect of closing freshwater systems	Freshwater jars were sealed with screw lids and incubated in anaerobic gas bags flushed with N_2/CO_2 (80:20) at 15°C	1 week 2 weeks 4 weeks 9 weeks 12 weeks	106,107 108,109 110,111 112,113 114,115
10b. Effect of sulphate availability in freshwater systems	As above, with 5% agar layer (10ml) containing 250µM sodium sulphate beneath sediment	12 weeks	104-105
	11. Effect of sealing marine systems		
11a.Standard marine sealed systems	Standard marine conditions, with six *Platanus* twigs, in a 100ml Duran bottle sealed with a PTFE bung and 'O'-ring sealed screw lid. Bottles were stored in clear anaerobic gas bags flushed with N_2/CO_2 (80:20) in the dark at 15°C	12 weeks 18 weeks 24 weeks	116,117 118,119 120,121
11b. Open systems as control	As a control, standard marine conditions set up as in 11a, but left open to the atmosphere	12 weeks 24 weeks	122,123 124,125

Table 2.1. Experimental conditions and procedures for decay experiments

Experimental conditions	Experimental details	Time period	I.D. no.
11c. Effect of adding plant material to anaerobic systems over time	i) Sealed standard marine bottles (as above) were opened after 12 weeks and six *Platanus* twigs added before resealing	24 weeks	126,127
	ii) As a control, sealed bottles were opened for the same time period as the above bottles, before resealing with no plant material added	24 weeks	128,129
11d. Effect of organic material reactivity in anaerobic systems	Six *Cyathea chinensis* twigs were decayed in standard marine sealed bottles	12 weeks 24 weeks	130,131
11e. Effect of sterile conditions	i) Sealed marine systems (as in 11a) were irradiated to 25kGy at a maximum temperature of 39.5°C (Isotron Ltd., Swindon)	12 weeks 24 weeks	132,133 134,135
	ii) Sealed marine systems (as in 11a) with 2mM sulphide were irradiated to 25kGy as above	12 weeks 24 weeks	136,137 138,139
11f. Effect of salinity in sealed systems (i.e. freshwater)	Sealed systems were set up as 11a, with freshwater sediment, freshwater medium (Appendix 2) and 1.5% (wt) FeOOH mixed with the sediment	12 weeks 24 weeks	140,141
11g. Effect of light on sealed freshwater systems	i) Freshwater sealed systems (as in 11f) were incubated under a Grow-lux light for 8 hours a day	9 weeks	142,143
	ii) Freshwater Duran bottle (as in 11f) was incubated in the dark	9 weeks	144,145

Table 2.1. Experimental conditions and procedures for decay experiments

100ml with Widdel's artificial marine salts (Appendix 2). An unlined polypropylene lid was screwed on to the jar loosely to minimise evaporation and prevent foreign bodies from entering the system, whilst allowing gaseous diffusion in and out of the jar. The jar was transferred to a waterbath at 15°C, and left in natural daylight.

At the end of the experiment, the jar was profiled using micro-electrodes, dismantled, and the medium, sediment, and twigs were analysed.

Chemical gradients within the system were monitored on a mm-scale using oxygen, pH and sulphide micro-electrodes (Diamond General, Ann Arbour, USA). The oxygen micro-electrode (768-20R, Diamond General) was attached to a chemical microsensor (product 1201, Diamond General), the needle combination pH micro-electrode (811, Diamond General) to a pH meter (Orion model 720A, Boston, MA), and the needle sulphide micro-electrode (663027, Diamond General) to a mV meter (Orion model 720A, Boston, MA). These meters were attached to a micro-manipulator (Marzhauser, Germany). The micromanipulator was controlled using a MC2000 multi-controller (Marzhauser, Germany) which was run by FVP software (Diamond General) on a MacQuadra 650 computer. Data were collected and stored using Workbench software (Strawberry Tree Inc., USA).

Once the micro-electrode measurements were taken, medium was removed from the just below the air-medium interface and just above the sediment-medium interface and stored for further analysis as follows:

- 1ml in 10% zinc acetate (250µl) at 4°C for sulphide analysis by the Cline method (page 66) and sulphate by ion-exchange chromatography (page 68);

- 1ml in 0.5M hydrochloric acid (5ml) at 4°C for analysis of dissolved Fe (II) by the Ferrozine method (page 67), and major elements (Al, Ca, Fe, Mg, Mn, P) by ICP-AES (page 69).

The twigs were removed from the sediment, rinsed in de-ionised water and wiped with a tissue to remove any salts or sediment from the cut surfaces. One twig was fixed in ethanol/acetic acid (3:1) and stored at 4°C for tissue-staining of thin sections with alcian blue (cellulose) and safranin (lignin) (page 72). If TEM analysis was required, a 2mm section was cut from the end of another twig, quartered, and stored in a small amount of medium from the decay system under nitrogen at 4°C before fixing (page 71). Remaining twigs were either frozen and then freeze-dried or fixed in ethanol/acetic acid (3:1) for 2-3 days before being taken through an alcohol dehydration series for SEM studies (page 70).

The sediment was removed and frozen immediately for analysis of total reduced inorganic sulphur (TRIS) (page 69).

Media preparation

See Appendix 2 for media compositions.

Anaerobic media were prepared for both bacterial cultures and decay experiments following a modified method of Widdel and Bak (1989).

The basic medium was made in modified 2l Duran flasks, autoclaved at 121°C and 15 psi for 45 minutes, and cooled under N_2/CO_2 (80:20). Once the medium was cool, additions were made from pre-prepared sterile anaerobic stock solutions (Appendix 2), and the pH adjusted to pH 7.5 using sterile 1M $NaCO_3$.

The medium was dispensed either aerobically into the pre-prepared decay experiment jars, or anaerobically into 50ml crimp vials (Phase Separations, Clwyd) *via* a sterile dispensing hood based on that of Widdel and Bak (1989). The headspace of the crimp vials was flushed

with N_2/CO_2 (80:20) and the vials crimp-sealed using sterile butyl septa (Phase Separations, Clwyd).

Calibration and use of micro-electrodes

Oxygen, pH and sulphide micro-electrodes were used simultaneously to profile individual decay systems, with the needles within 1mm of each other. The micromanipulator moved the micro-electrodes downwards by 1mm every 30 seconds. Data were recorded every 10 seconds, but only the last reading for each depth was accepted to allow for stabilisation of the micro-electrodes. The lowest point of the depth profiles was either directly above the twigs, or immediately above the sediment-medium interface, depending on the original position of the electrodes.

The oxygen needle micro-electrode (768-20R, Diamond General) with internal reference has a response time of ≤ 3 seconds at 90% oxygen saturation. The electrode was calibrated at 100% saturation using 100ml de-ionised water through which air was bubbled for 15 minutes, and at 0% saturation using 3% sodium sulphite solution. The percentage of oxygen saturation of the calibration solutions was checked using an OXI 92 oxygen meter with >99% accuracy (WTW, GMBH, Germany).

The oxygen micro-electrode was found to be sensitive to solutions with high sulphide content, resulting in steep increases in oxygen saturation up to 700%. As little or no sulphide will be present in oxic systems, oxygen saturation was reset to zero where sulphide was present to remove these false oxygen readings from any depth profiles.

The needle combination pH micro-electrode (811, Diamond General) has a response time of 10 seconds. The electrode was calibrated using standard pH 4, 7 and 10 solutions (Sigma Aldrich, Poole). Very occasionally the pH electrode was subject to electrical interference from the mini reference electrode used in conjunction with the sulphide

electrode. This caused the reading to be elevated by up to 0.9 pH units. Where such electrical interference was suspected, the pH of the medium was checked using pH paper, and the readings adjusted accordingly.

The needle sulphide micro-electrode (663-27, Diamond General) has a response time of 90% in <15 seconds at 0.001M, and a detection range of 0.1-0.00001M. The electrode was used in conjunction with a mini reference electrode (product 401, Diamond General). The micro-electrode was calibrated in sulphide standards made up in mineral salts medium and conducted under a constant stream of nitrogen at the temperature of the decay systems. The exact sulphide concentrations of the standards was determined by a colorimetric method after Cline (1969) (page 66). However, problems were encountered as correction for pH-dependence is made difficult due to the activity of the artificial seawater. Sulphide correction for pH is defined using Equation 2.1, based on the Davies equation (Kuhl and Jorgensen, 1992):

$$S_t = [S^{2-}] \times \left(1 + \frac{a(H^+)^2}{K_1' K_2'} + \frac{a(H^+)}{K_2'}\right) \quad \text{Eqn 2.1}$$

where K_1' and K_2' are the first and second dissociation constants of the sulphide equilibrium system respectively, $[S^{2-}]$ is the sulphide concentrations, and aH^+ is the hydrogen ion activity.

In normal sulphide solutions, the ionic activity of water is 1, but marine solutions have a slightly lower activity. This activity is extremely difficult to calculate, due to the number of, and differing concentrations of, ionic species within the medium. This is further complicated by the release of decay products, the exact identities and concentrations of which are not known. Several attempts were made to calculate sulphide concentrations accurately from the mV readings and correcting for pH-dependence, but the Cline method indicated that none of the methods

used was accurate enough. In later experiments, sulohide analysis of the medium was undertaken prior to micro-electrode profiling. If no sulphide was present, no sulphide micro-electrode data was collected. Selected sulphide (V) and pH data are presented in Appendix 3.

Determination of sulphide ion concentration

Sulphide was measured using a method after Cline (1969).

25µl of 10% zinc acetate solution was pipetted into seven 1.5ml Eppendorf tubes. A standard sulphide solution was made with 0.1875g washed and dried sodium sulphide in 250ml of de-oxygenated distilled water. 10µl, 25µl, 50µl, 100µl, 150µl and 200µl aliquots of this solution were added to the zinc acetate solution. One Eppendorf tube was left as the blank. 100µl of each sample to be analysed (previously fixed in zinc acetate solution) was pipetted into a separate Eppendorf tube.

Acidified ferrous chloride solution (60g per litre 50% HCl) and N,N-dimethyl-p-phenylene diamine solution (40g per litre 50% HCl) were mixed together in equal quantities. 100µl of this complex was pipetted into each Eppendorf tube.

The colour was left to develop for 50 minutes before the volume of each Eppendorf tube was made up to 1ml with distilled water (Table 2.2).

After a further 5 minutes, colour intensity was measured spectrophotometrically (Cecil CE292 Series 2 Digital Ultra-Violet Spectrophotometer) at 670nm. A plot of standard absorption (minus that of the blank) against sulphide molarity gives a linear response with the equation:

$$\text{molarity} = (\text{gradient} \times \text{absorption}) + \text{intercept}$$

This equation was used to determine sample molarity, and the results were corrected for dilution.

		ZnAc (µl)	complex (µl)	water (µl)
sulphide (µl)	0	25	100	875
	10	25	100	865
	25	25	100	850
	50	25	100	825
	100	25	100	775
	150	25	100	725
	200	25	100	675
sample (µl)	100	-	100	800

Table 2.2 . Proportions of sulphide solution, reagent and water required in the sulphide assay.

The precision of analysis of replicate standards was ±4% with an accuracy of ±5%.

Determination of Fe(II) in water by the Ferrozine method

Ferrous iron was measured using a method after Stookey (1970).

5ml of 0.5M HCl was transferred to six 13ml centrifuge tubes. Standard Fe(II) solution was made with 0.05g ferrous sulphate dissolved in 50ml of 1.2M HCl, and 0.05ml, 0.15ml, 0.30ml, 0.50ml and 0.80ml aliquots were added to the 5ml of 0.5M HCl. One centrifuge tube was left as the blank. The quantity in each tube was made up to 6ml with de-ionised water.

1ml of sample was pipetted into a centrifuge tube containing 5ml 0.5M HCl.

0.5ml of each sample and of each standard were transferred to 5ml Ferrozine solution (0.5g Ferrozine dissolved in 500ml of 50mM HEPES buffer at pH7.0) in separate centrifuge tubes. The colour was allowed to develop for 30 minutes before centrifuging at 2000 rpm for 10 minutes to settle any sediment particles.

Colour intensity was measured spectrophotometrically (Cecil CE292 Series 2 Digital Ultra-Violet Spectrophotometer) at 562 nm. A plot of standard absorption (minus that of the blank) against Fe(II) concentration should gives a linear response with the equation:

Fe (II) concentration = (gradient x absorption) + intercept

This equation was used to determine the concentration of Fe(II) in each sample.

The precision of analysis was ±0.004 for 95% confidence limits, with <1% error.

Determination of sulphate ion concentration

Sulphate analysis was performed by ion exchange chromatography (HPIC) (Dionex), with an eluent of 1.8mM Na_2CO_3 (Analar, BDH) and 1.7mM $NaHCO_3$ (Analar, BDH) in de-ionised water at an isocratic flow rate of 2ml/minute. Detection was by conductivity, after passing through a micro-membrane suppressor system with a 25mM H_2SO_4 regenerant. Quantification was performed by a Spectra-Physics SP4600 integrator.

Samples were centrifuged at 13,000rpm for 10 minutes to remove any particulate matter. Samples and standards (10µl) were diluted with de-ionised water (990µl) before being analysed. Sulphate concentrations were calculated by comparison of peak area with those of the standards, and corrected for dilution. The sulphate detection limit was <0.1mM, and analytical errors were usually <1%. Thiosulphate and sulphite were never detected.

Determination of major element ion (P, Al, Fe, Mn, Mg, Ca) concentration

Concentration of major element ions (P, Al, Fe, Mn, Mg, Ca) within aqueous medium was measured by ICP-AES using a Jobin-Yvon JY24 sequential ICP-AES.

Calibration solutions were made using 1,000ppm and 10,000ppm standard solutions of the individual ions (BDH, Lutterworth; Fisher Scientific, Loughborough).

Samples (1ml sample in 5ml 0.5M hydrochloric acid) were analysed with a flush time (uptake time) of 60 seconds. Three sequential readings were taken for each elemental ion with a reading time of 4 seconds each.

Concentrations were corrected for machine drift (checked regularly with a standard solution) and dilution factor.

Determination of total reduced inorganic sulphur (TRIS)

A sequential distillation was used to separate sediment sulphides into three fractions: acid volatile sulphide (AVS), pyritic sulphide, and elemental sulphur (Allen and Parkes, 1995).

The total sediment removed from each experimental jar was thawed and thoroughly vortexed with 10ml de-oxygenated, distilled water and transferred into a conical flask containing a magnetic stirrer. The flask was then attached to a 5-place, all-glass distillation rig. The flask headspace was flushed with oxygen-free nitrogen for 15 minutes at 80ml per minute before the addition of 6M HCl (2ml). The flask was heated to 80°C and distilled for 40 minutes. Liberated acid volatile sulphide was collected in a trap containing 10% zinc acetate solution (10ml).

The flask was allowed to cool and a fresh 10% zinc acetate (10ml) trap attached to the distillation rig. 95% ethanol (5ml), chromous chloride (25ml, made by passing 1M chromic chloride in 0.5M HCl through a

Jones reductor column containing 300g zinc, 300ml 2% mercuric chloride solution and 2ml concentrated nitric acid; Allen, 1996) and concentrated HCl (5ml) were added to the flask. This distillation was allowed to proceed for 40 minutes, and the pyritic sulphide fraction was collected. A fresh zinc acetate (10ml) trap was attached to the rig before the flask was then heated to 80°C for a further 40 minutes and the elemental sulphur fraction was trapped.

The sulphide in each fraction was measured spectrophotometrically (see sulphide assay, page 66), and the total reduced inorganic sulphur (TRIS) was calculated as the sum of all three fractions in each sample.

Not all sediments were analysed for TRIS. Sediments from some decay systems had been prepared for analysis of the iron minerals present by a digestion method and ICP-AES by freeze-drying and then drying at 200°C. The first samples analysed this way produced extremely variable results but the remaining samples were unsuitable for TRIS analysis due to being dried at such high temperatures.

SEM sample preparation

Fresh and decayed plant material were prepared for SEM analysis in two ways: by freeze-drying, using a Genevac SF50 dryer attached to a Genevac CVP100 pump, or by dehydration series (after Sagemann *et al.*, 1999). Plant material for dehydration was removed from the experimental system and fixed in 95% ethanol/acetic acid (3:1), before being taken through an ethanol dehydration series (15%, 30%, 50%, 70% for 30 minutes each). The twigs were then cut into ca 2mm thick sections using a razor blade and the sections were taken through a further ethanol dehydration series (95%, 100%, 100% for 1 hour each). The samples were then immersed in hexamethyldisilizane (HMDS) for a further hour.

Sections of plant material were mounted on aluminium stubs and coated with gold for secondary electron imaging, or carbon for backscatter imaging, on a Cambridge Stereoscan 250 Mk3 SEM. Minerals were identified using an Oxford Instruments PCXA energy-dispersive analyser (EDS), and digital images were taken and stored using a Mica slow scan digitising system.

The dehydration technique was preferred to freeze-drying as it ensured that as much sediment was washed off the plant material as possible. Some artefacts of freeze-drying could also be confused with morphological signs of decay, such as splitting of cell walls and pulling apart of cells.

Samples of some of the softer plant tissues, such as *Equisetum* and *Cyathea*, could not be analysed by SEM as they were very soft and tended to collapse when sectioned and mounted.

TEM sample preparation

On removal from the experimental system, a 2mm section from the cut end of a twig was quartered and fixed in glutaraldehyde/ paraformaldehyde in cacodylate buffer (see Appendix 4 for composition) at 4°C for 1 hour. The sections were then washed overnight in cacodylate buffer at 4°C to remove any remaining fixative. The sections were osmicated in osmium tetroxide in cacodylate buffer at 4°C for one hour, before being taken through a dehydration series of 50%, 70% and 90% ethanol for 15 minutes each at 4°C. Further dehydration was carried out in two consecutive solutions of 100% ethanol for 30 minutes at room temperature.

The sections were then infiltrated with a series of Spurrs (Agar Scientific, Essex) resin/ethanol mixtures for 1 hour each (see Table 2.3) before being left overnight in Spurrs resin.

Spurrs resin: ethanol
1 : 3
1 : 1
3 : 1

Table 2.3. Ratios of Spurrs resin and ethanol used in impregnation of plant samples for TEM analysis.

The sections were then embedded in 100% Spurrs resin which was polymerised at 60°C overnight. Sections were cut using a diamnond blade and floated onto 100 mesh copper grids (Agar Scientific, Essex) in water. Samples were analysed using a Jeol 1210 TEM.

Fungal material could not be analysed by TEM due to problems impregnating the material with resin, even with extended dehydration and impregnation times.

Thin section tissue staining

Twigs were removed from the decay systems and fixed in ethanol/acetic acid (3:1) for 3-4 days before being stored in 70% ethanol. Thin cross- and longitudinal sections (ca 10-20 microns thick) were cut using a Reichert sliding microtome.

The sections were washed thoroughly in distilled water before being stained in Safranin (1g Safranin (Fisher Scientific) in 100ml 50% alcohol) for up to 2 minutes. After rinsing in distilled water, the sections were stained in alcian blue (1g alcian blue powder (Fisher Scientific) in 100ml distilled water, with a few crystals of phenol and 3 drops of glacial acetic acid). The sections were then taken through an alcohol dehydration series (50%, 70%, 95% and 100% ethanol) before clearing in Histoclear (Fisher Scientific).

The thin sections were mounted in Euparol (Fisher Scientific) on a glass slide and a cover slip was placed on top. The slides were left to dry at 60°C for several days, but can take up to 6 months to dry fully.

The softness of some of the plant specimens such as *Cyathea*, especially after decay, prevented them from being sectioned without disintegrating, even with the use of a cold-stage attached to the microtome. *Equisetum* could not be sectioned, even when fresh, as the stems are hollow, surrounded by only a small ring of cells. Sections could not be prepared by embedding these species as the stains cannot be used on embedded material.

RESULTS

Geochemical results

The geochemical results of replicate decay systems are compared with each other and with corresponding standards or controls. The identity number of each individual experiment (as listed in Table 2.1) is included to allow cross referencing to the geochemical data presented in Appendices 4-7. TRIS values are discussed where data are available. Concentrations of dissolved species are presented in one of three forms:

i) as a single value, e.g. 12.2mM, corresponding to a concentration which is constant with depth in a single decay system;

ii) as two different values separated by a forward stroke, e.g. 12.2/13.3mM. These values correspond to the concentration just below the air-medium interface (e.g. 12.2mM) and that just above the sediment-medium interface (e.g. 13.3mM) in a single decay system;

iii) as two different values separated by a dash, e.g 12.2-13.3mM, corresponding to a range of concentrations for two or more decay systems.

Oxygen and pH depth profiles are presented in Appendix 5. Sulphate, sulphide and ferrous ion concentrations of the medium and sedimentary TRIS data are presented in Appendix 6, and all ICP-AES data (concentrations of P, Al, Fe, Mn, Mg and Ca) in Appendix 7.

1a. Standard marine open time series

Marine, open decay systems were studied over 12 weeks. One jar was dismantled and analysed every week.

The medium was made anaerobically, but dispensed aerobically, and the lid of the jar was left open to allow gaseous diffusion. Despite this, the medium was anoxic below the top 3mm of the water column after week 1, and below only 1mm after week 2 (Figure 2.1a). Oxygen began to penetrate the system after week 3, with the medium anoxic below 3mm after week 3, and 4mm after week 4. Oxygen continued to penetrate the medium, and after week 5 a region of constant saturation appeared 5mm below the surface in the oxygen depth profile (Figure 2.1a). Oxygen saturation of the medium increased over the course of the time series, and after week 12 only the lowest 5mm of the medium was anoxic (Figure 2.1a).

The starting pH of the medium was 7.5, but after week one the pH had become more alkaline, at pH 7.9 (Figure 2.1a). These systems were not sampled mid-week, but preliminary experiments (data not included) showed that within the first week the pH of the medium initially decreased to ca pH 6.5 before becoming alkaline again . The pH continued to rise over time with little depth variation, reaching pH 8.8 after week 3, and peaking at ca 9.8 after week 6 (Figure 2.1a). The pH of the medium then decreased with time, reaching ca pH 8.6 adjacent to the twigs after week 12 (Figure 2.1b). (The unusual pH gradient at week 12 is likely to have been caused by a piece of surface film from the medium that

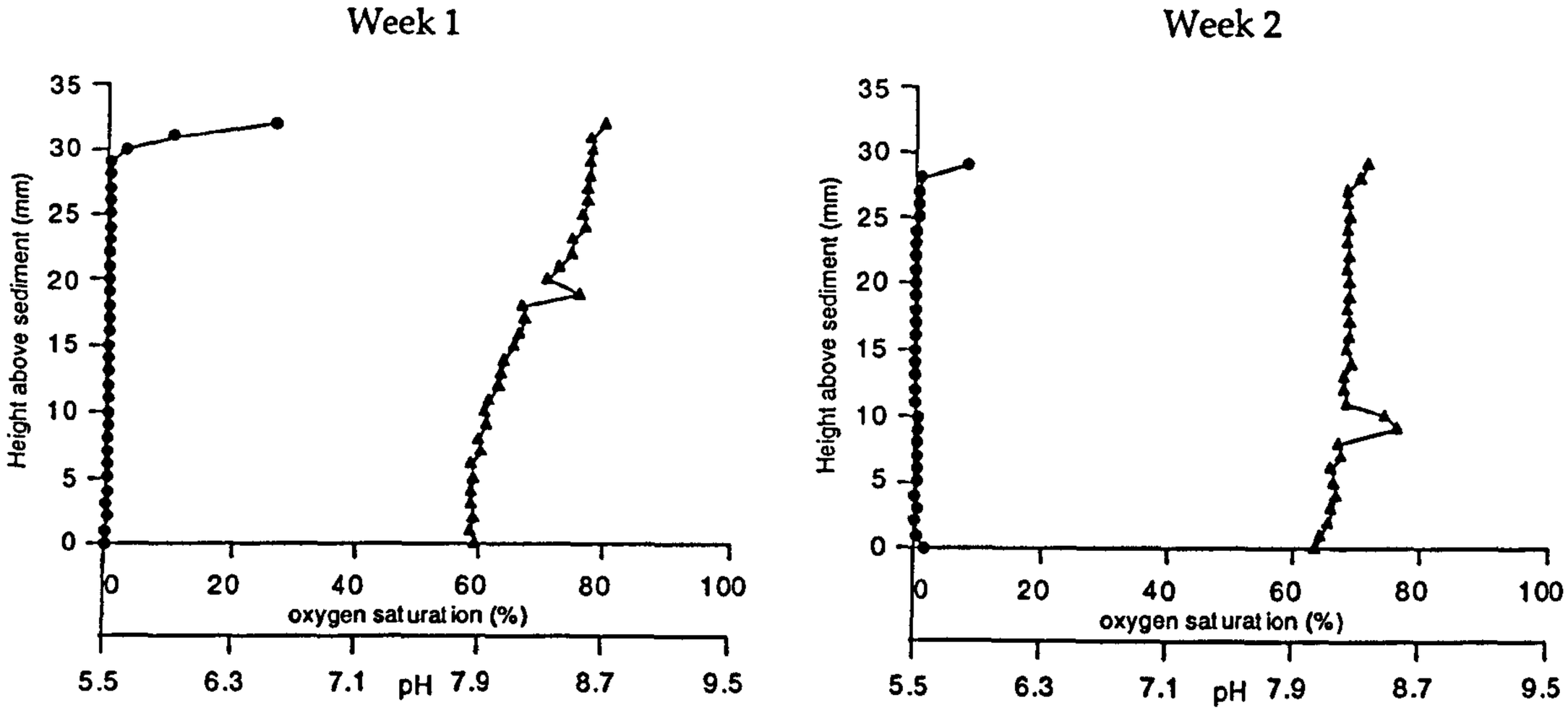

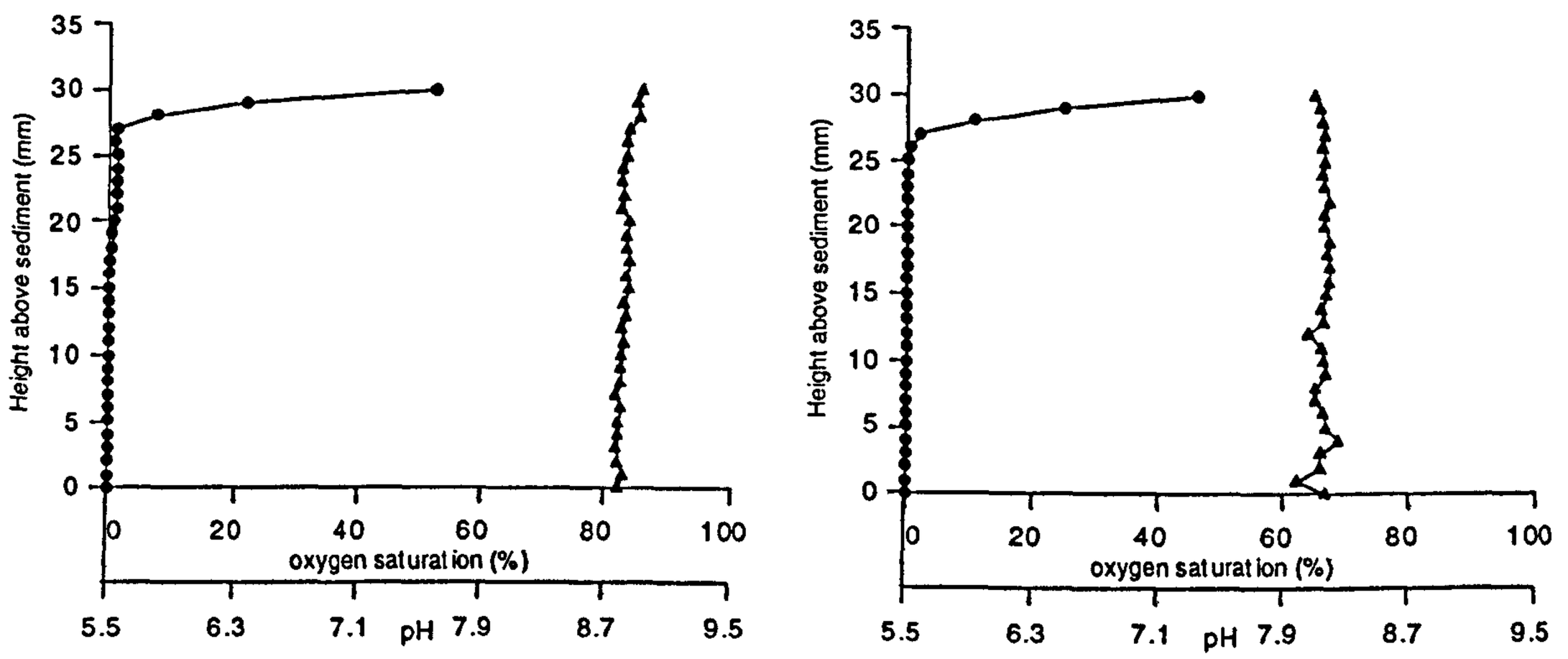

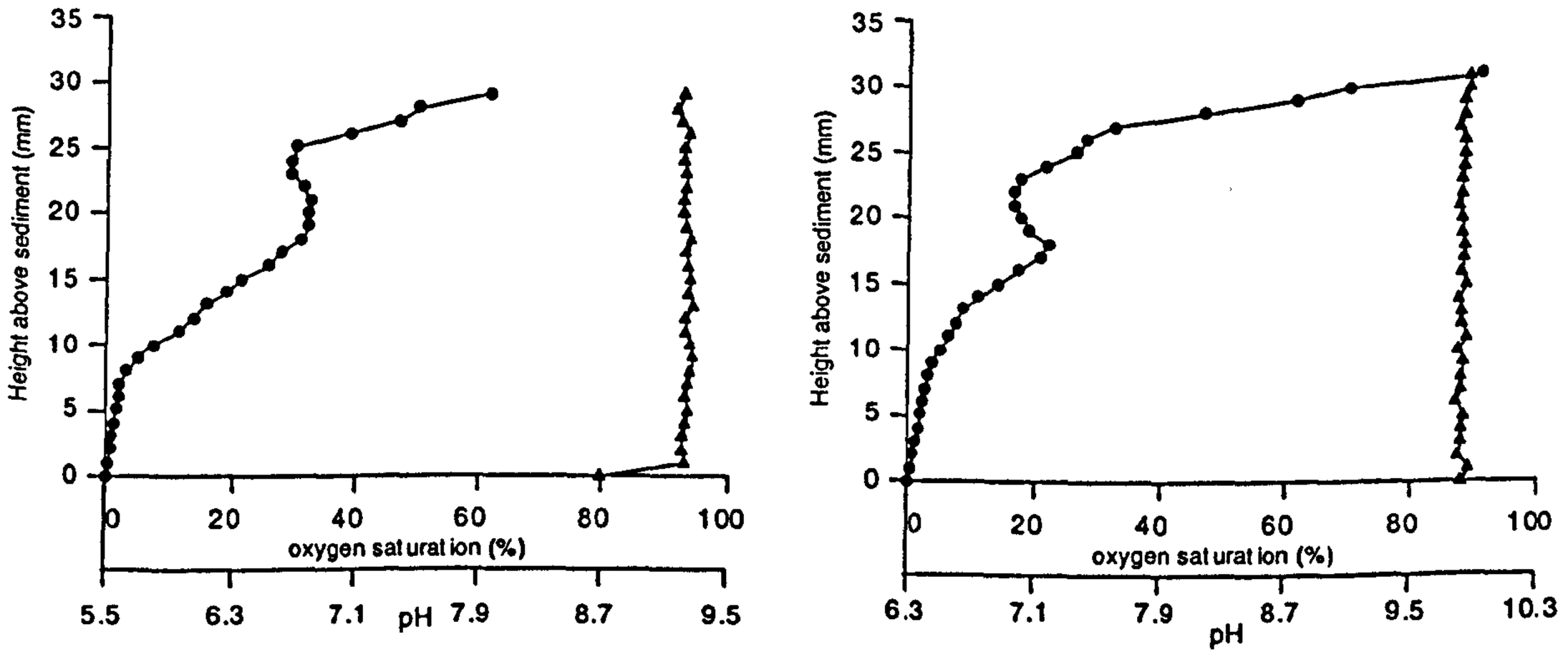

Figure 2.1a. Oxygen and pH depth profiles for weeks 1 to 6 of the standard open marine time series. Infilled circles represent oxygen data points. Infilled triangles represent pH data points. The highest data points above the sediment represent the air-medium interface.

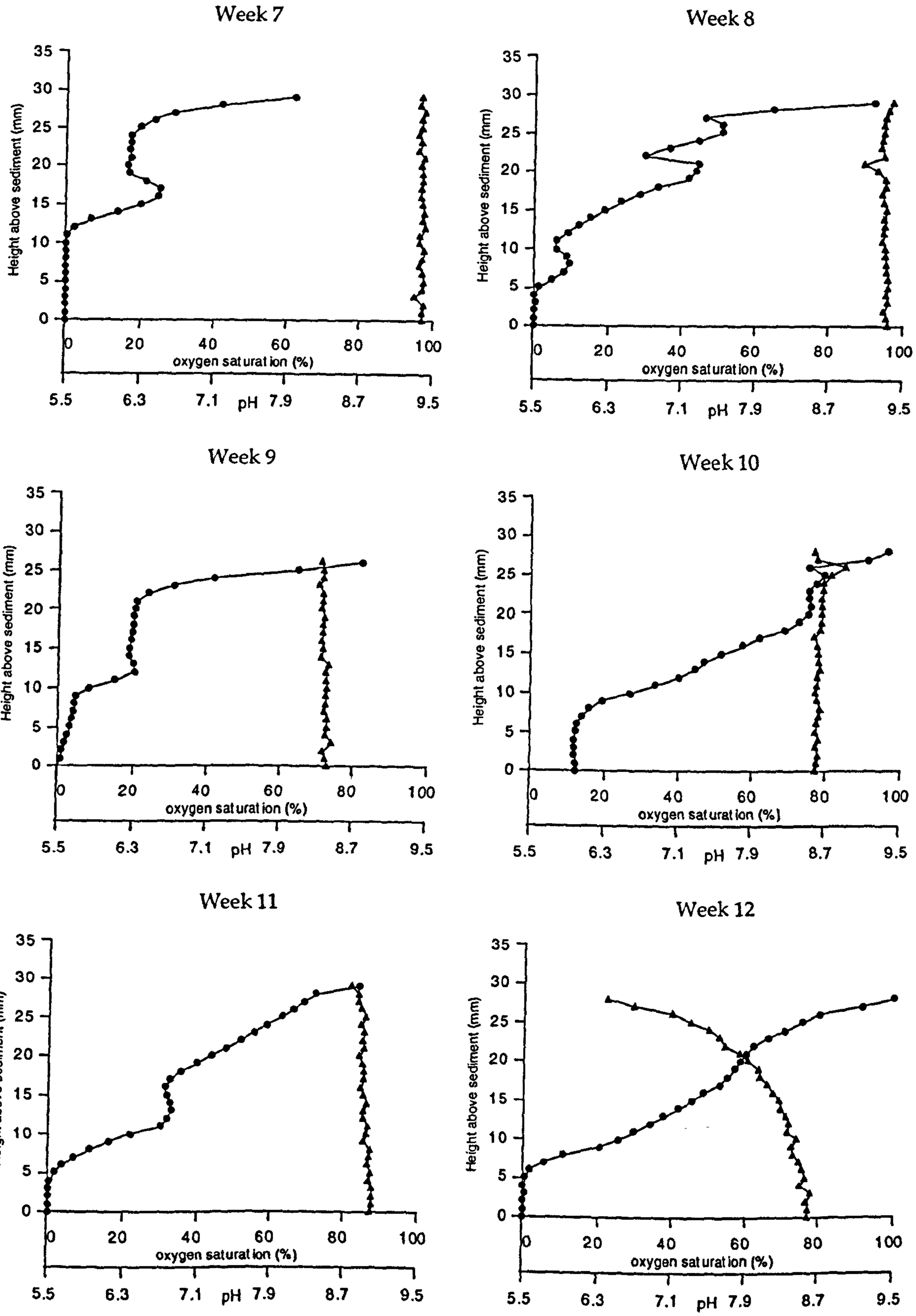

Figure 2.1b. Oxygen and pH depth profiles for weeks 1 to 6 of the standard open marine time series. Infilled circles represent oxygen data points. Infilled triangles represent pH data points. The highest data points above the sediment represent the air-medium interface.

became attached to the micro-electrode. This was removed during profiling, and the pH adjacent to the twigs is thought to be accurate).

Sulphate concentrations within the medium decreased rapidly from the starting concentration of 29.5mM to 23.0/22.1mM during week 1. Sulphate levels decreased more steadily during weeks 2 (18.7/17.4mM), 3 (16.4/16.7mM) and 4 (16.4/14.7mM), and then remained almost constant for the duration of the time series (18.6/14.2mM after week 12).

No sulphide was present in the starting medium, but sulphide was detected after week 1 (0.06/0.15mM), and at higher concentrations after week 2 (0.22/0.40mM). These results show a steep gradient, with sulphide concentrations much greater adjacent to the sediment than at the air-medium interface. Sulphide levels decreased during weeks 3 and 4, and only traces were detected after weeks 5-7 (≤ 0.03mM). No sulphide was detected after week 8.

Ferrous iron was not present in the starting medium, but up to 0.2mM was detected after week 1. Some ferrous iron was still present adjacent to the sediment after week 2 (≤ 0.05mM). Only occasional traces of ferrous iron (≤ 0.02mM) were detected between weeks 3 and 12.

Phosphorus levels within the medium decreased by almost 50% from 1.44mM to 0.78/0.89mM during week 1. Concentrations continued to decrease more steadily over the course of the time series, reaching 0.12/0.11mM after week 12.

Iron and manganese were not present in the starting medium, but 0.14/0.25mM and 0.03/0.01mM respectively were detected after week 1. Neither element was detected for the rest of the time series.

Concentrations of calcium within the medium increased greatly during week 1 from 1.0mM to 3.4/3.5mM, and then decreased steadily with time for the remaining 11 weeks to reach 2.0mM. Magnesium

concentrations also increased from 15.1mM to 16.0/16.8mM during week 1, and then decreased steadily to reach 12.1/12.0mM after week 12.

Aluminium (0.02mM) was present in the starting medium, but was not detected again at any point during the 12 weeks.

Increases in all forms of sedimentary sulphur (AVS, pyritic and elemental) occurred during weeks 1 and 2, with the total TRIS doubling in week 1 and again in week 2 (Table 2.4).

Time (weeks)	AVS (M)	Pyritic S (M)	S° (M)	TRIS (M)
0	0	0.6	0.1	0.7
1	0.2	0.8	0.3	1.3
2	1.2	1.5	0.4	3.0
3	0.9	1.4	0.9	3.2
4	1.0	1.5	0.4	2.8
5	1.2	1.6	0.4	3.3
6	1.3	1.7	0.5	3.5
7	1.1	1.6	0.4	3.1
8	1.1	1.7	1.0	3.7
9	1.8	1.6	1.1	4.6
10	1.3	1.7	0.5	3.4
11	1.3	1.0	0.9	3.1
12	1.0	1.5	0.9	3.4

Table 2.4. Sedimentary sulphur data for open marine decay systems from 0-12 weeks.

Levels increased slightly after week 3 and then remained constant, until increasing after week 8 and further after week 9. TRIS levels decreased after week 10 and remained constant for the rest of the time series. After week 2 pyritic sulphur and AVS concentrations remained constant, until after week 11 when pyritic sulphur decreased, and after week 12 when AVS levels deceased. Elemental sulphur levels continued

to increase after AVS and pyritic sulphur concentrations had stabilised, reaching 0.9M after week 4. Levels then decreased by week 5 and remained constant until week 9 when values increased further. Elemental sulphur concentrations remained constant at this concentration until the end of the time series, with the exception of week 10, when levels dropped substantially (Table 2.4). Pyritic sulphur was the largest of the sedimentary sulphur pools at all stages of the time series (Table 2.4). A plot of ln (rate), i.e. ln (TRIS), against time is presented in Figure 2.2.

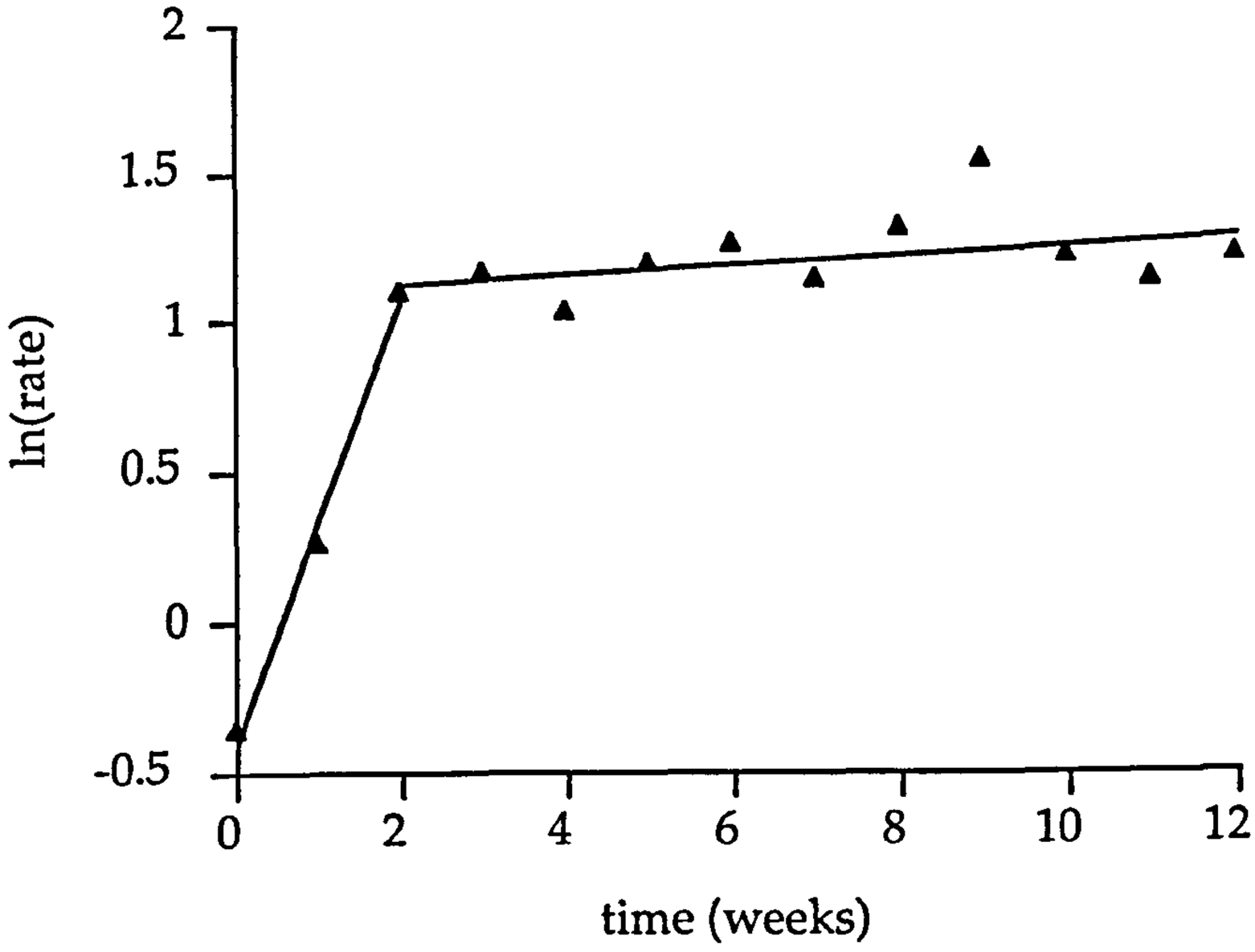

Figure 2.2. Plot of ln (rate), i.e. ln (TRIS), against time for the open marine time series.

After week 1, EDS analysis of the cut surfaces of the plant material indicated that some iron and sulphur were present, in particular associated with bacteria, but no crystals were visible. Silicon, calcium, potassium and chloride peaks were also present, but no individual crystals of these elements were observed. Iron and silicon were detected

by EDS over much of the surface of the plant material after week 2, but no crystals were observed, and no sulphide appeared to be associated with the iron. A suite of elements was detected by EDS across the plant material surface after week 4. Iron was present, which occurred with and without sulphur, or associated with silicon and aluminium, and occasionally potassium. Mixtures of any of the following elements were also present: silicon, iron, potassium, phosphorus, magnesium, sulphur, calcium, titanium. Crystals were rarely evident, even at high magnifications and using backscatter imaging. Those that were observed were small and usually amorphous. Some large crystals almost entirely infilled pith, and sometimes xylem, cells. These yielded EDS peaks of either silicon or calcium.

1b. Effect of extended incubation times on open marine systems

Although decay intensity decreased substantially and oxygen penetrated much of the medium after 12 weeks, open marine systems were incubated for 12 weeks (13, 14, 16), 24 weeks (16, 17, 18) and 36 weeks (19, 20, 21) to investigate the effects of extended incubation periods.

Oxygen saturation of the medium increased with time, reaching up to 58% adjacent to the twigs after week 24 but did not increase further. After 12 weeks, the pH of the medium was ca 8.8-8.9, but it decreased to pH 8.6 after 24 weeks, and reached pH 8.7 after 36 weeks.

After an initial decrease during the first 12 weeks to 13.9-17.3mM, sulphate concentrations increased with time, reaching similar, or slightly higher, concentrations to the starting medium (ca 29.5mM), or possibly slightly higher, after 36 weeks (27.1-33.4mM). No sulphide was detected at any point, and low levels of ferrous iron (0.01mM) were only detected after 36 weeks.

Phosphorus concentrations remain constant with time (Table 2.5). Magnesium and calcium concentrations followed similar patterns, decreasing by 24 weeks, and then increasing again by 36 weeks (Table 2.5). No aluminium, iron or manganese was detected at any point.

Time	P (mM)	Ca (mM)	Mg (mM)
12 weeks (13-15)	0.05-0.24	≤ 0.2	13.0-15.3
24 weeks (16-18)	≤ 0.11	0	6.0-7.2
36 weeks (19-21)	0.04-0.10	2.0-2.4	12.5-14.7

Table 2.5. Phosphorus, calcium and magnesium concentrations after 12, 24 and 36 weeks.

There are no TRIS data for this extended time series. However, the sediment, which had been black after 12 weeks indicating the presence of AVS, turned brown beneath the twigs at 24 weeks and was completely brown after 36 weeks. EDS analysis of the plant material revealed the presence of similar elements at 12, 24 and 36 weeks to those in the time series at 12 weeks (pages 79-80). However, backscatter SEM analysis allowed some precipitates to be observed through the bacterial glycocalyx covering the cell. In particular FeSam and calcium were evident along pith cell walls (Figure 2.3A). This FeSam occurred at the end of only one twig of fifteen after 12 weeks, and was not observed in any twigs after 24 or 36 weeks.

1c. Standard marine open systems

Open marine systems were run as standards for every experiment investigating the effects of different environmental conditions, and were used to study the reproducibility of the decay systems. Eight standard marine open systems were incubated for different time periods: one for

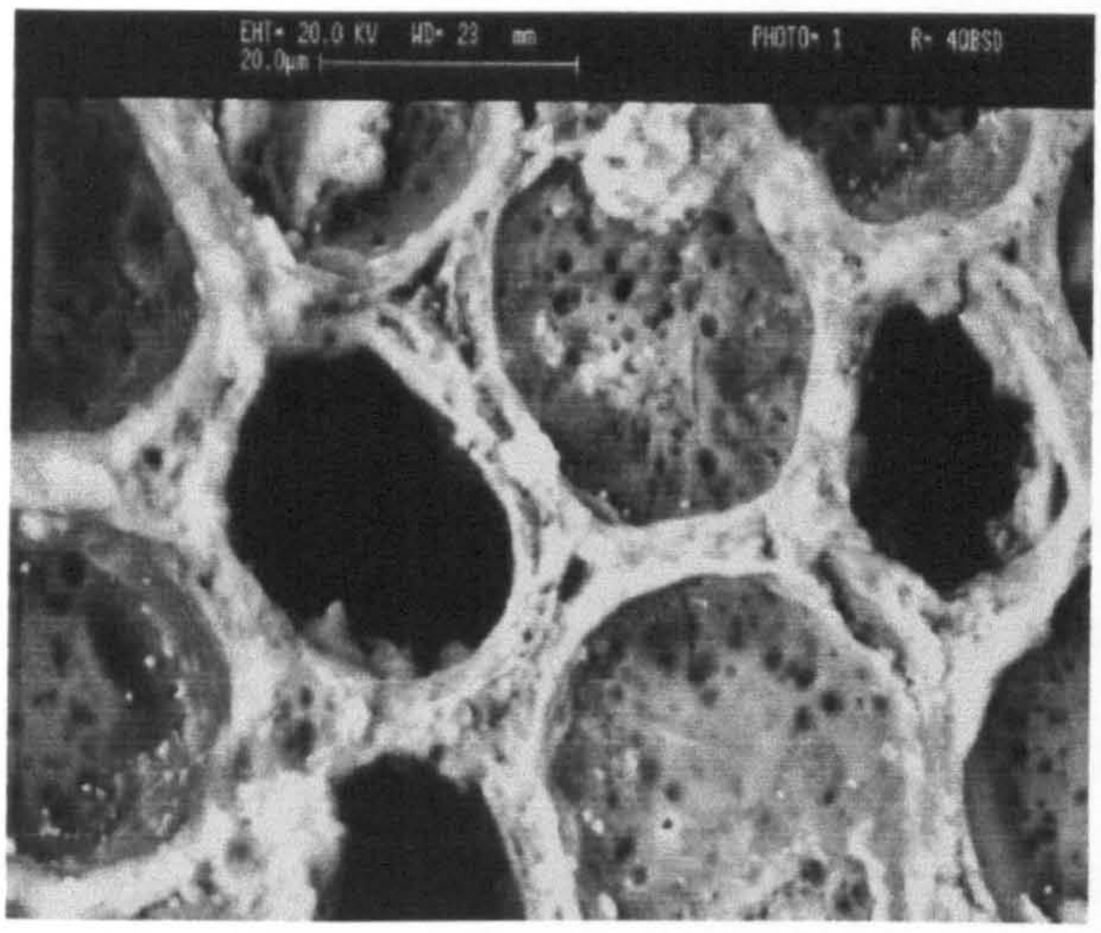

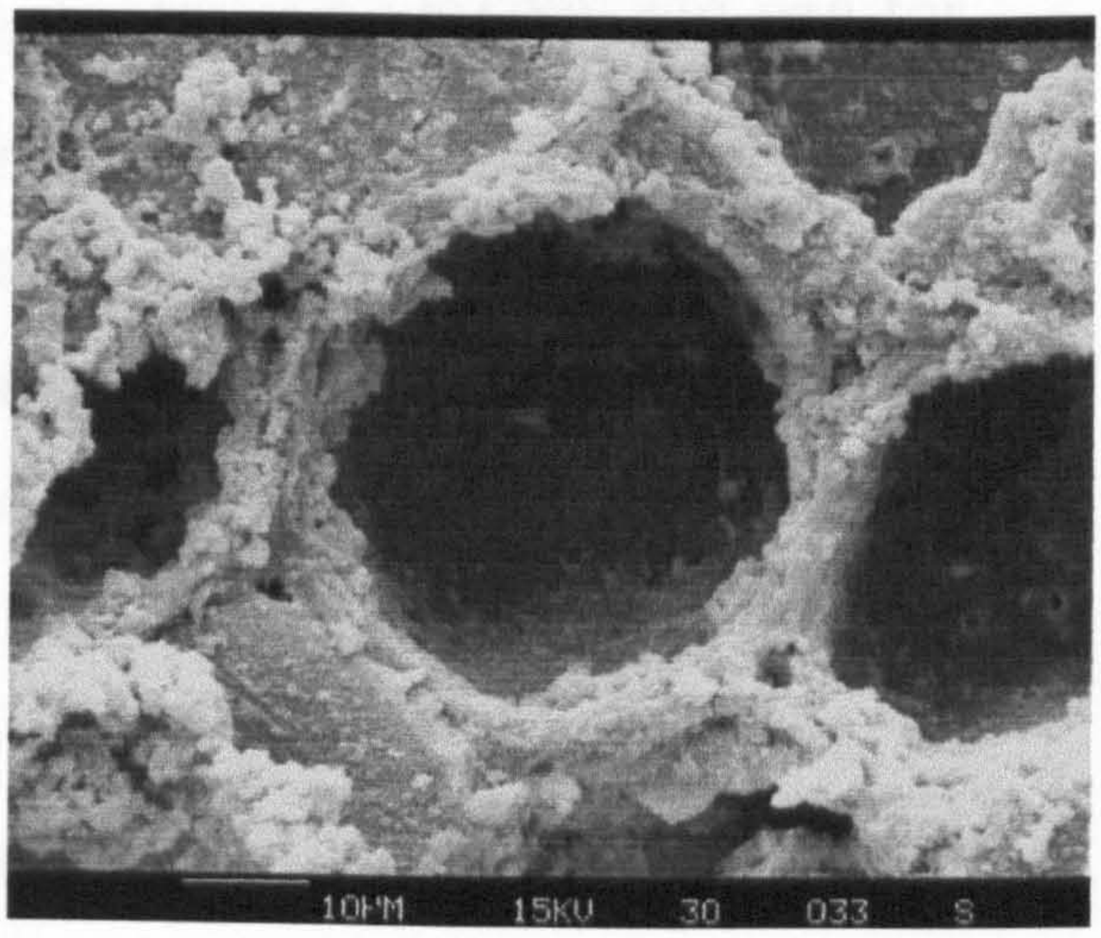

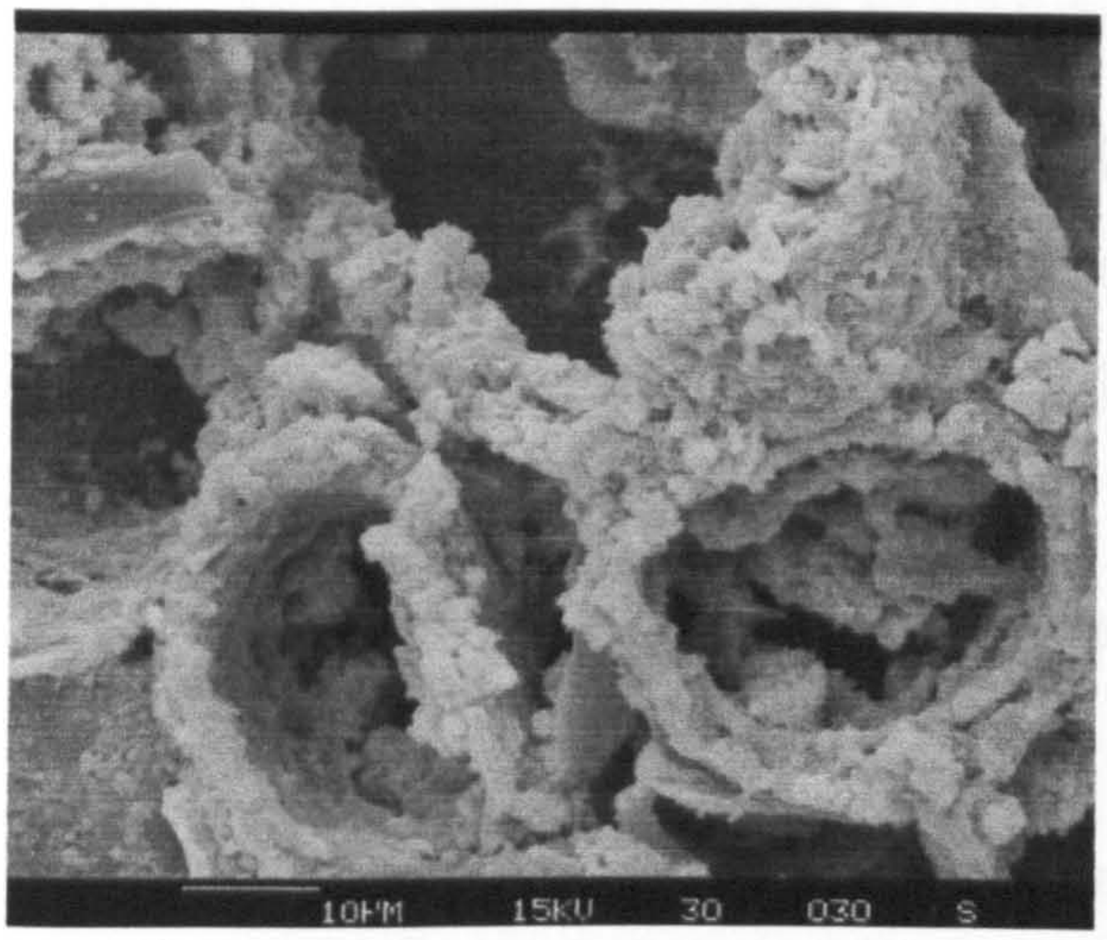

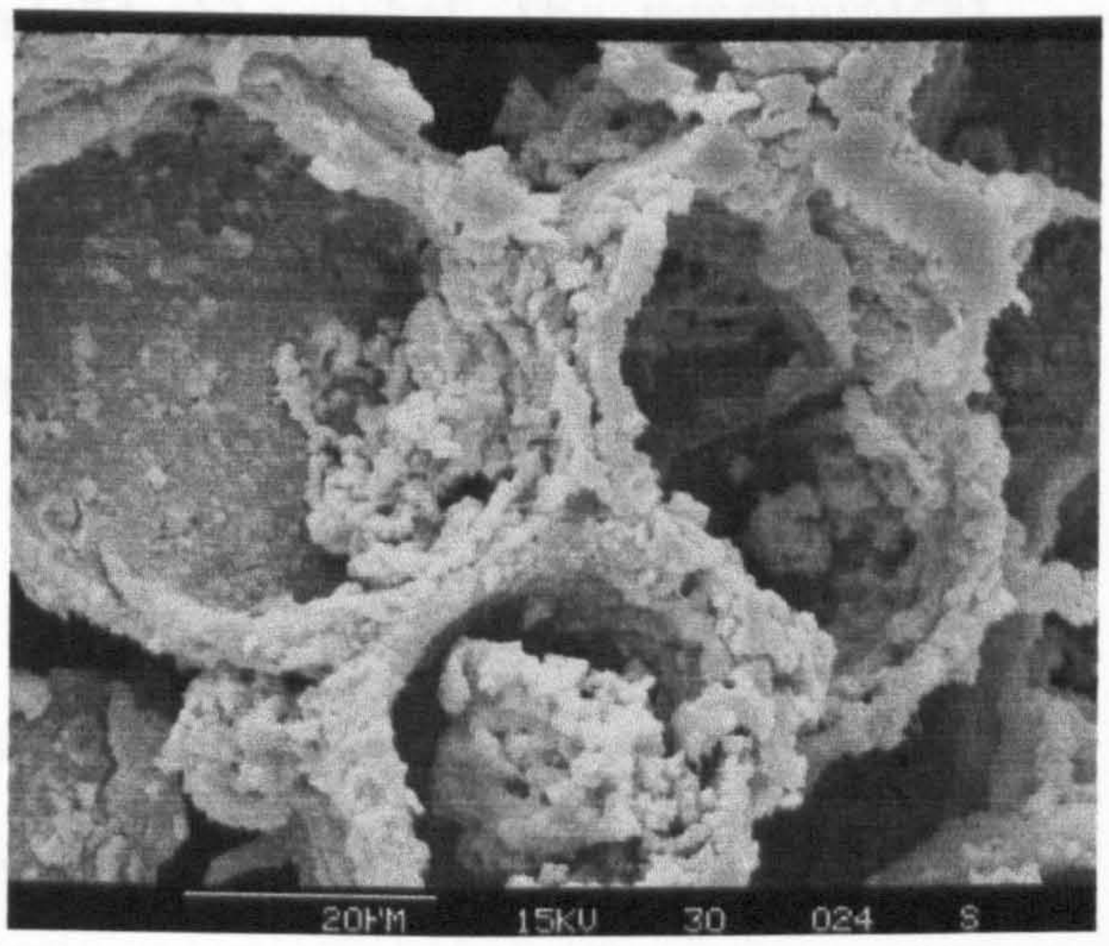

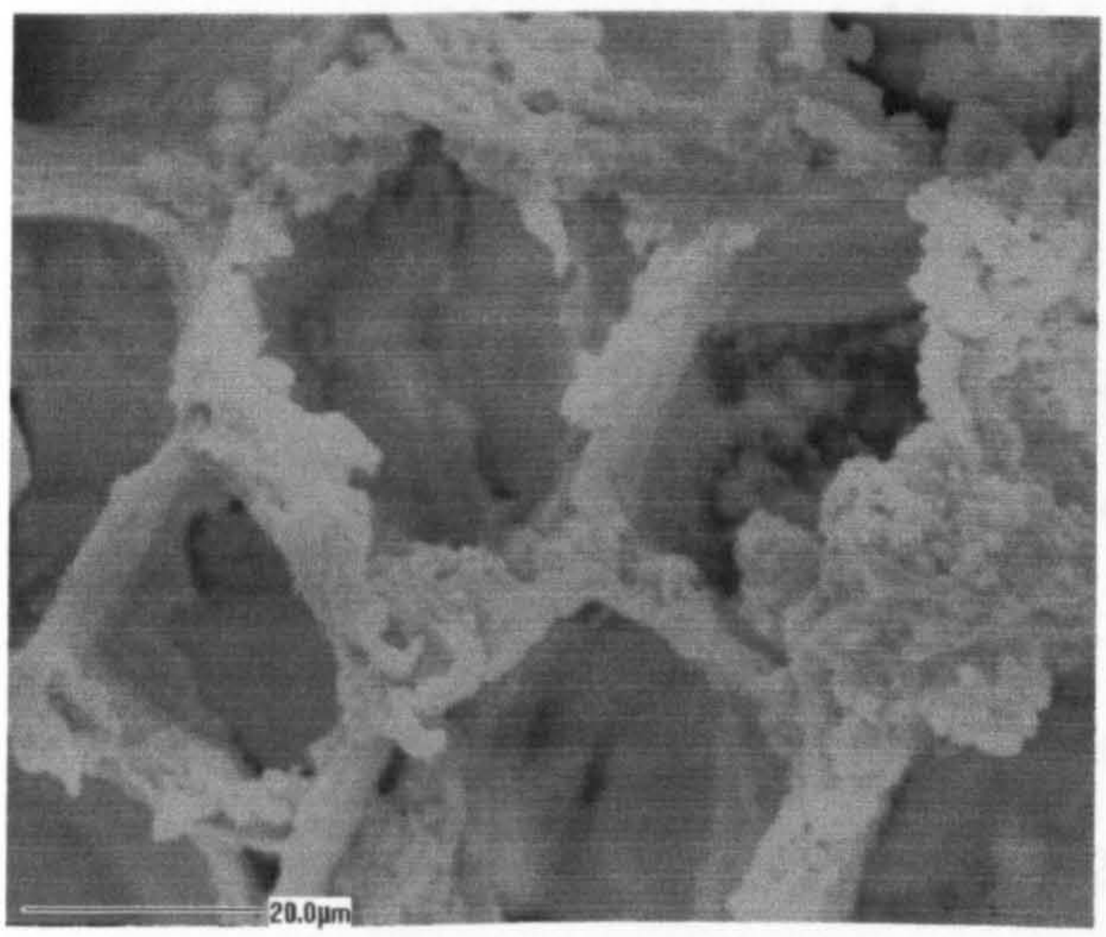

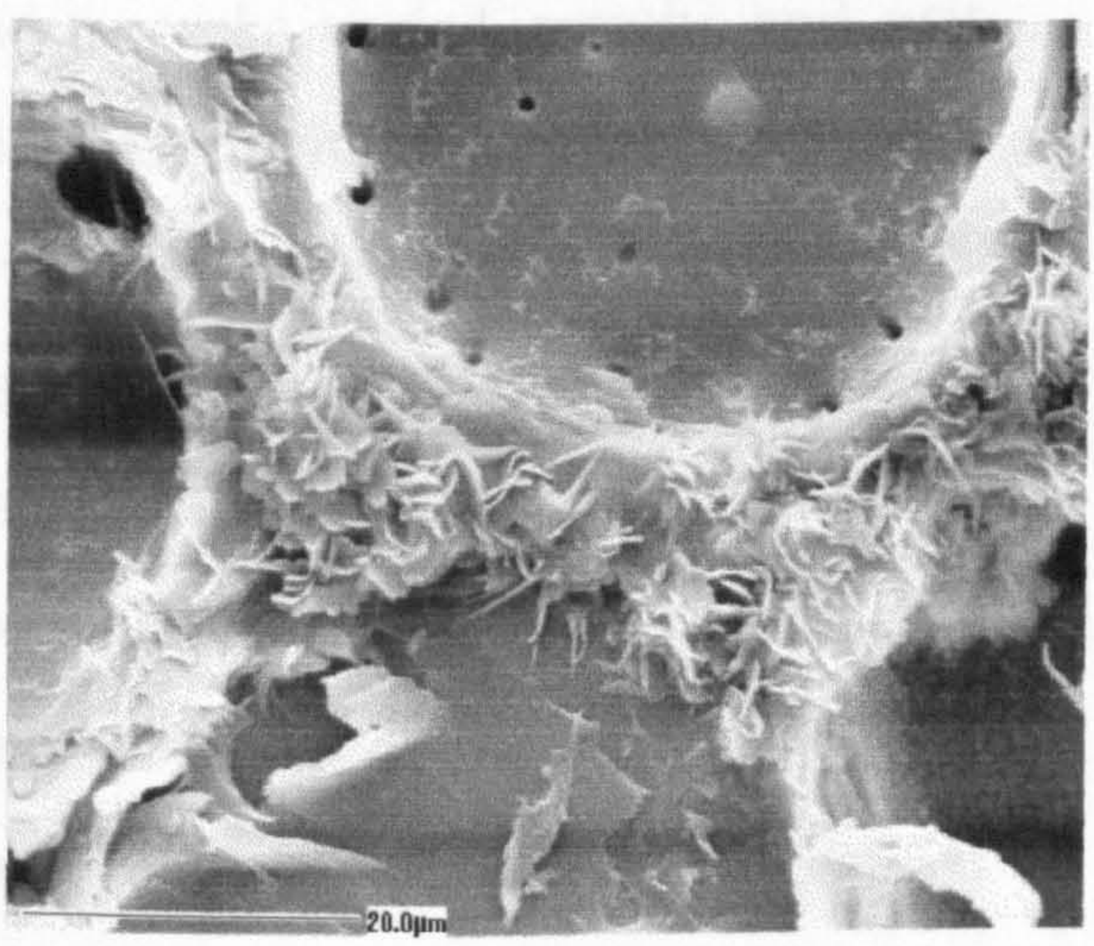

Figure 2.3. A: FeSam and calcium crystals growing on *Platanus* pith parenchyma cell walls, seen beneath a bacterial film using backscatter imaging. B, C, D: FeSam growing on *Platanus* pith parenchyma cell walls, at cell walls junctions, and beginning to infill cells. E: FeSam growing on *Psilotum* parenchyma cell walls and at cell wall junctions. F: Clay minerals (Si/Al/Fe) growing within *Platanus* pith cells in material which had been subjected to 12 weeks of fungal decay.

5.4 weeks (22), one for 6 weeks (23), five for 12 weeks (24-28), and one for 14 weeks (29). Several of these were replicates, having been set up at the same time as each other, with sediment from the same source, and medium and inoculum from the same batches: systems 22 and 24; systems 23 and 29; systems 25 and 26; and systems 27 and 28 (Table 2.6).

These eight standard systems could be compared with the time series systems after 6 and 12 weeks (systems 6 and 12 respectively) and the 12-week systems in the extended time series (systems 13-15).

In general, these standard systems behaved as the time series, with the exception of systems 22 (5.4 weeks) and 24 (12 weeks). The geochemical data for all the standards, including the times series systems after 6 and 12, weeks and the extended time series after 12 weeks (13-15) are presented in Table 2.6. Oxygen and pH depth profiles are presented in Figures 2.4a-b.

The oxygen depth profiles varied between systems not only in the amount of oxygen saturation, but also in the presence or absence of a region of constant saturation just below the air-medium interface (Figure 2.4a-b). The pH of all systems incubated for 12 to 14 weeks was pH 8.6-8.9 (Table 2.6). However, the pH at 5.4 and 6 weeks varied greatly, and was especially high in system 6. The pH decreased with time in systems 6 to 12 and 23 to 29, but increased from pH 8.3-8.4 to pH 8.6-8.7 in systems 19 and 21. Frequent monitoring of systems 22 and 24 (every 2-3 days) showed that the pH rose slowly and steadily from the starting value of pH 7.5 to the final value of pH 8.6-8.7 after 12 weeks, instead of increasing and then decreasing, as seen in the other systems.

Sulphate concentrations after 12 or 14 weeks fall into two ranges, 14-19mM and 21-23mM. The lowest concentrations overall (13.3/14.1mM) are in system 24. Sulphate concentrations decreased with time. Sulphide was present in system 22 after 5.4 weeks (0.03/0.31mM) but only traces

Time (weeks)	5.4	12	6	12	6	14	12	12	12	12	12	12	12
I.D. number	22	24	6	12	23	29	13	14	15	25	26	27	28
pH	8.3-8.4	8.6-8.7	9.8	8.6-8.7	8.9	8.6	8.8-8.9	8.8-8.9	8.8-8.9	8.8-8.9	8.8-8.9	8.6	8.6
SO_4^{2-} (mM)	14.2/13.9	**13.3/14.1**	15.3/15.7	18.6/14.2	22.6/22.4	21.5/21.0	15.6/15.6	13.9/17.3	15.5/14.8	21.4/21.2	22.5/21.0	15.8/15.9	18.7/18.0
S^{2-} (mM)	**0.03/0.31**	0	0.01/0.02	0	0	0/0.01	0	0	0	0	0/0.01	0.02/0	0/0.04
Fe^{2+} (mM)	0.04/0.04	0.02/0.03	0.02/0.01	0	0/0.03	0	0	0	0	0.02/0.02	0.03/0.04	0	0
P (mM)	**0.34/0.56**	**0.67/0.71**	0.54/0.57	0.12/0.11	0.18/0.27	0.07/0.08	0.24/0.20	0.05/0.19	0.14/0.14	0.13/0	0.20/0.20	0.20/0.21	0.15/0.16
Al (mM)	**0.06/0**	0	0	0	0	0	0	0/0.01	0	0	0	0	0
Fe (mM)	**0.19/0.05**	0	0	0	0	0	0.01/0	0/0.01	0	0	0	0	0
Mn (mM)	**0.0/0.03**	0	0	0	0	0	0.01/0	0/0.01	0	0	0	0	0
Mg (mM)	11.7/12.2	11.3/13.0	14.9/14.9	12.1/12.0	**12.9/13.1**	**5.7/6.0**	15.3/14.4	14.5/13.0	14.2/14.4	12.7/13.0	13.1/13.4	10.1/10.7	10.0/10.3
Ca (mM)	2.1/2.0	0.01/1.1	2.3/2.3	2.0/2.0	0.7/0.8	0	0.2/0	0/0.2	0	1.6/0	1.9/1.9	0.2/0.3	0
AVS (M)	-	-	1.3	1.0	-	-	-	-	-	1.3	0.5	1.4	1.1
Pyritic S (M)	-	-	**1.7**	**1.5**	-	-	-	-	-	**1.0**	**1.4**	**2.0**	**2.2**
S° (M)	-	-	0.5	**0.9**	-	-	-	-	-	0.6	0.3	0.3	0.3
TRIS (M)	-	-	3.5	3.4	-	-	-	-	-	2.9	2.2	3.7	3.6

Table 2.6. Medium and sedimentary compositions for standard open marine systems after 5.4, 6, 12 and 14 weeks. These systems were all run as controls for the other experimental conditions. Decay systems are grouped togther in the table with replicates set up at the same time using the same batches of inoculum and medium, and sub-samples from the same sediment sample. Two values are given for each of the medium concentrations: the first is the concentration from just below the air-medium interface and the second was sampled from just above the sediment-medium interface. Numbers in bold indicate concentrations significantly different from those in other standards.

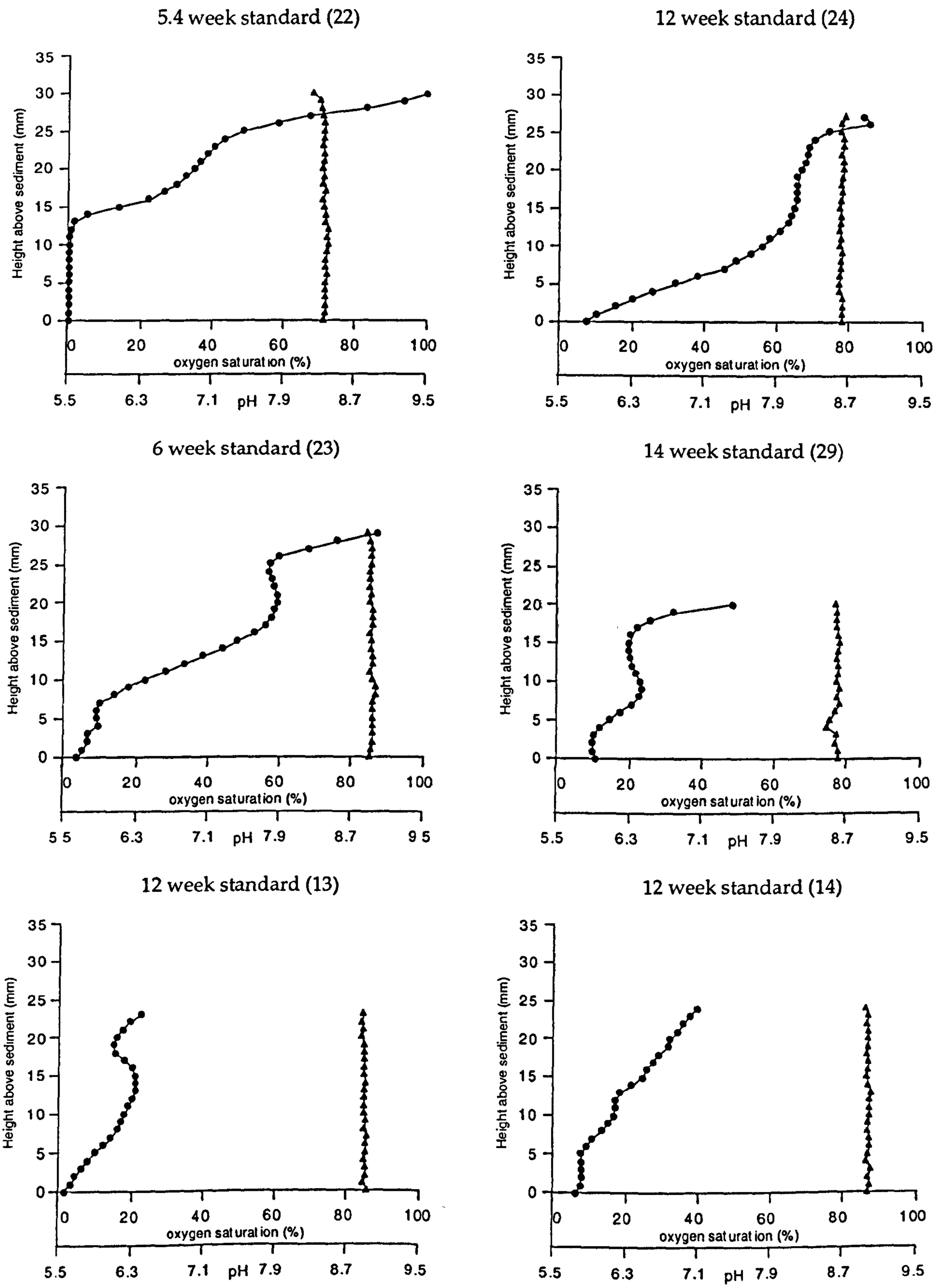

Figure 2.4a. Oxygen and pH depth profiles for standard open marine decay systems. Infilled circles represent oxygen data points. Infilled triangles represent pH data points. The highest data points above the sediment represent the air-medium interface.

12 week standard (15)

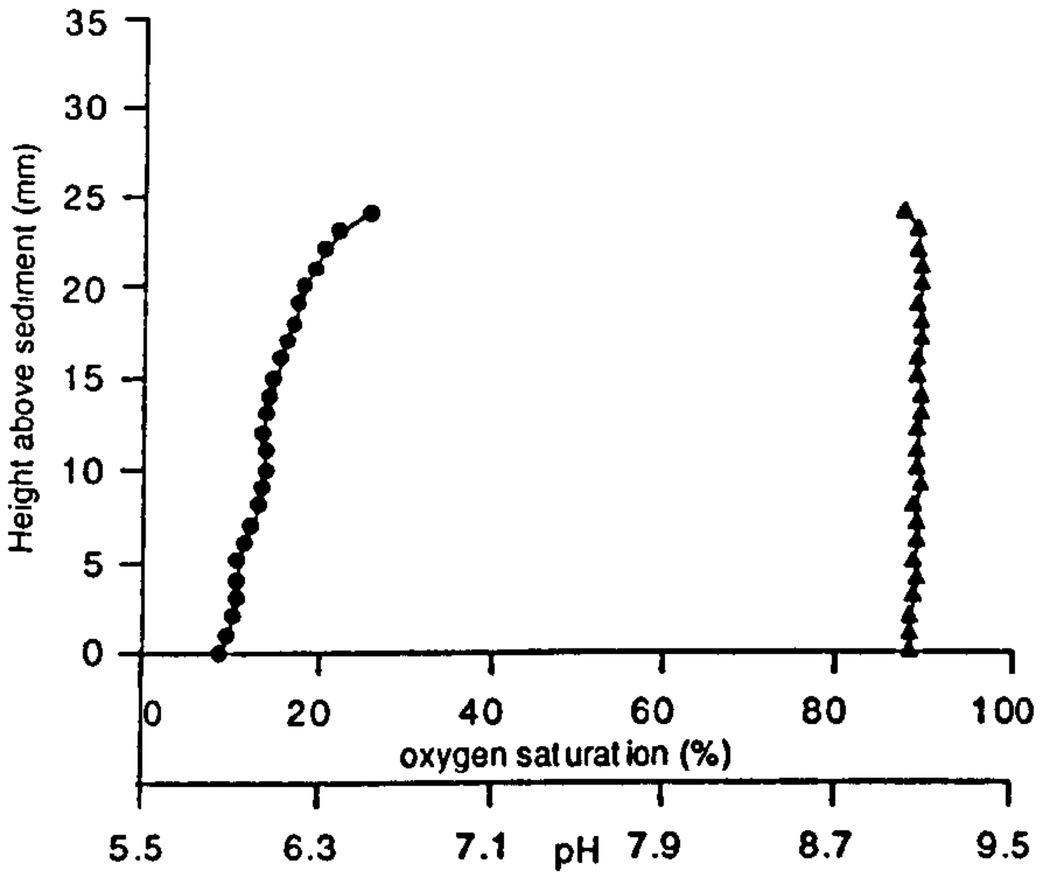

12 week standard (25)

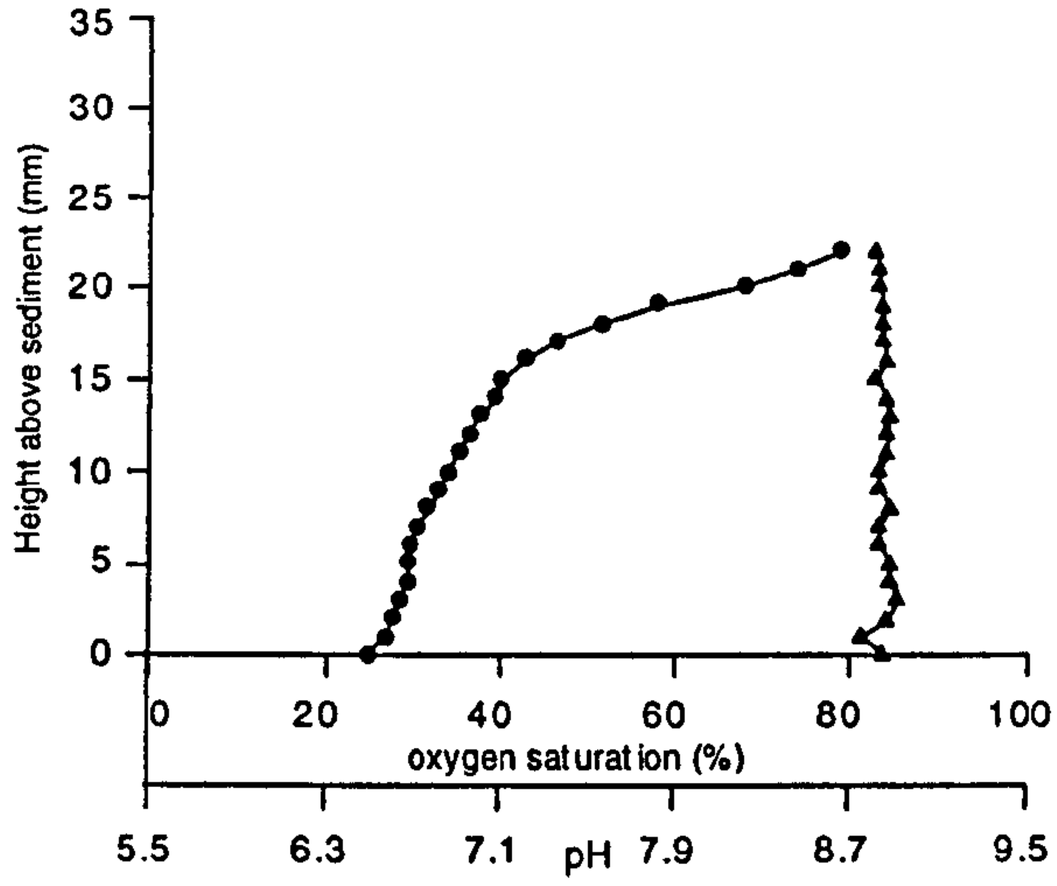

12 week standard (26)

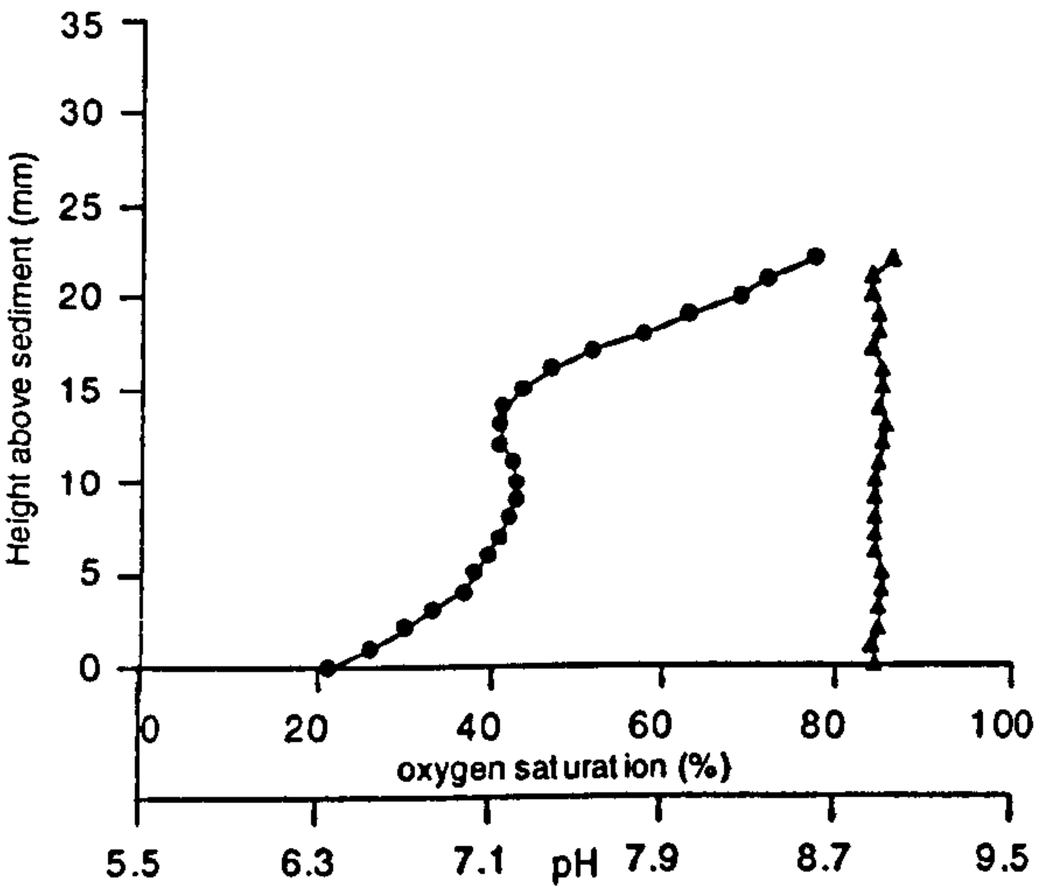

12 week standard (27)

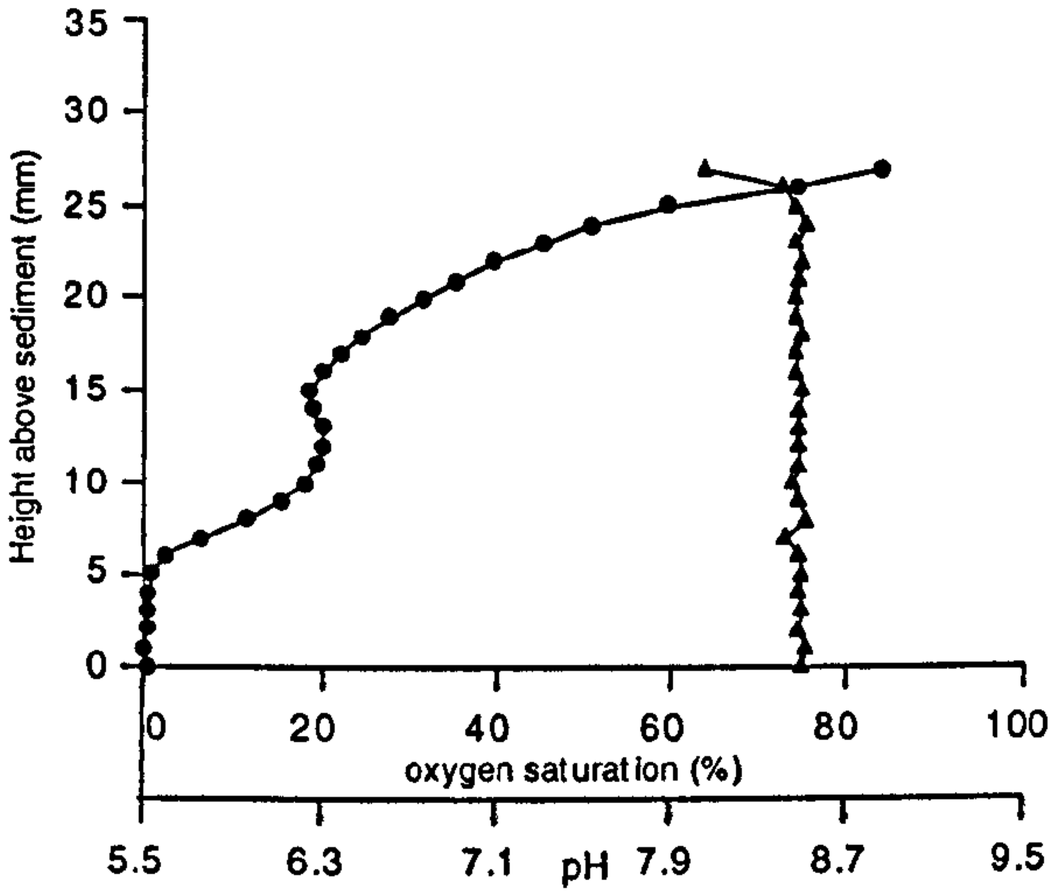

12 week standard (28)

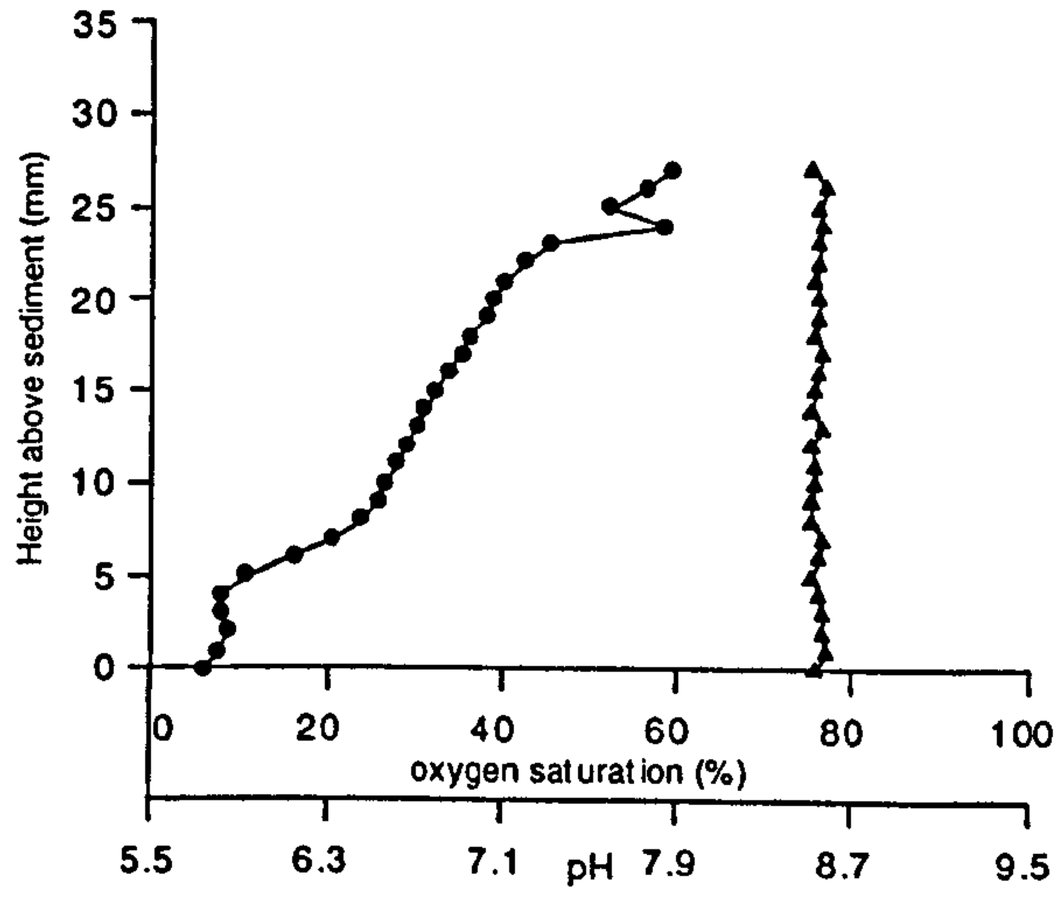

Figure 2.4b. Oxygen and pH depth profiles for standard open marine decay systems. Infilled circles represent oxygen data points. Infilled triangles represent pH data points. The highest data points above the sediment represent the air-medium interface.

of sulphide (≤ 0.02mM) were present after 6, 12 or 24. The maximum concentration of ferrous iron detected at any time was 0.04mM, and concentrations decreased slightly with time.

After 12 weeks phosphorus concentrations were similar in all systems (0-0.27mM), except for system 24, which had a much higher concentration (0.67/0.71mM). Levels of phosphorus decreased with time, from system 6 after 6 weeks to system 12 after 12 weeks, and after 6 weeks in system 23 to system 29 after 14 weeks, but decreased between 5.4 weeks and 12 weeks in systems 22 and 24 respectively. Magnesium concentrations ranged from 10.0mM to 15.3mM after 12 weeks, but after 14 weeks concentrations were much lower (5.7/6.0mM) in system 29. Magnesium levels decreased with time, but much more significantly in systems 23 to 29 than in the other systems. Calcium concentrations were 0.7-2.3mM after 5.4 and 6 weeks, but were slightly lower (0 and 2.0mM) after 12 and 14 weeks. Aluminium, iron and manganese were rarely detected, except in system 22 after 5.4 weeks.

TRIS data were not available for all standards. The largest sedimentary sulphur pool was always the pyritic pool (1.0-2.2M). AVS levels ranged between 1.0 and 1.4mM (except for system 26 with only 0.5M) and elemental sulphur concentrations were 0.3-0.6M (except for system 12 with 0.9M). TRIS levels were 3.4-3.7M for systems 6, 12, 27, 28, and slightly lower for systems 25 and 26 at 2.2M and 2.9M respectively. Unfortunately, no TRIS data are available for systems 13, 14, 15, 22, 23, 24 and 29.

Most standards displayed a similar suite of elements within the plant material to those observed in the time series, except for systems 22 and 24. Unlike the suite of elements which were detected on the cut surfaces of the plant material of the time series after only 4 weeks and in varying amounts in all other standards, small crystals of FeS were present within

the plant material after 5.4 weeks in standard 19. It was uncertain whether this was just sediment attached to the twig, or mineral growth on the plant material. After 12 weeks, however, considerable crystal growth was present infilling pith cells, at cell walls and cell wall junctions at the end of one twig (Figures 2.3B-D). EDS revealed this to be Fe and S only; comparison of EDS peaks with iron sulphide standards indicated that it was amorphous iron monosulphide, FeSam. Debye-Scherrer XRD analysis of this material was difficult due to the small amount of mineral in relation to large amounts of organic material, but it indicated the presence of mackinawite and possibly small amounts of pyrite. This precipitate was firmly attached to the plant material (it could not be scraped out of the cell) and was found in similar locations to that in fossils from the Eocene London Clay (see Chapter 4; Grimes et al., 2001b). Mineralisation occurred in only one end section out of 5 twigs.

2. Effect of sulphate availability in open marine systems

Pyrite formation is limited by the rate of sulphate reduction where sulphate concentrations are less than 3mM (Capone and Kiene, 1988). Although the medium of the standards was shown not to be sulphate-limiting, sulphate may have been limiting within the sediments, especially with depth. To try to overcome this, a sulphate agar layer was placed beneath the sediment in two open marine decay systems to release sulphate into the sediment over the course of 12 weeks. Comparison with the standards (25, 26) was complicated by differences in the chemistry of the duplicate agar layer systems (30, 31).

One of the sulphate agar systems (31) remained anoxic below 4mm of the medium. Oxygen saturation was similar in the other sulphate agar systems (30) and in the standards at 21-25% adjacent to the twigs. The pH of one of the sulphate agar layer systems (30) was identical to that of the

standards at pH 8.8-9.0; the pH of the other sulphate agar layer system (31) was slightly less alkaline, at pH 8.6-8.5.

Control jars, containing only medium above the agar layer, indicated that sulphate was released from the agar for up to 10 weeks. Despite this, the sulphate concentrations of the sediment-agar layer systems (15.1/14.1mM in system 30, 9.9/8.4mM in system 31) were lower than those of the standards after 12 weeks (21.0-22.5mM). Only traces of sulphide (≤0.01mM) were detected in the standards (30, 31) and one of the agar layer systems (30), but up to 0.5mM sulphide was present in the other agar layer system (31). Similar trace levels of ferrous iron (≤ 0.05mM) were detected in both the standards and the sulphate agar layer systems.

There were no apparent differences in the concentrations of phosphorus, aluminium, iron, manganese, magnesium and calcium between the medium of the standards and that of the sulphate agar layer jars.

Despite differences in the TRIS values for the duplicate standards (25, 26), the concentration of all forms of sedimentary sulphur were greater in the sulphate agar layer systems than in the standards (Table 2.7). A black ring was evident in the agar layers on dismantling the sulphate agar layer systems.

Decay system	AVS (M)	Pyritic S (M)	S° (M)	TRIS (M)
Standard (25)	1.3	1.0	0.6	2.9
Standard (26)	0.5	1.4	0.3	2.2
+ SO_4^{2-} (30)	1.6	1.8	0.7	4.1
+ SO_4^{2-} (31)	1.1	1.5	0.8	3.4

Table 2.7. Sedimentary sulphur data for open marine standard systems and systems with additional sulphate.

EDS analysis of the plant material showed similar elements present in both the sulphate agar layer systems and the standards. Silicon was the dominant element detected, associated with some aluminium, potassium, and traces of iron. No sulphur was detected.

3a. Effect of iron availability in open marine systems

Amount of iron available

Additional amorphous iron oxyhydroxide was added to decay systems as elevated iron concentrations have been associated with the pyritisation of organisms (Briggs *et al.*, 1991; Raiswell *et al.*, 1993; Briggs *et al.*, 1996). The amount of total iron mixed with the sediment was increased to 3% and 5% and incubated for 12 weeks. Standards with 1% FeOOH (25, 26) were compared with 3% FeOOH (36, 37) and 5% FeOOH (32, 33). These conditions were repeated, and standards with 1% FeOOH (27, 28) were compared with 3% FeOOH (38, 39) and 5% FeOOH (34, 35). Standards with 1% FeOOH were compared with systems with no added FeOOH at 5.4 weeks (22 and 40 respectively) and 12 weeks (24 and 41 respectively).

Oxygen saturation varied greatly depending on the mount of iron available (Figure 2.5). The most oxygen saturation was observed in the

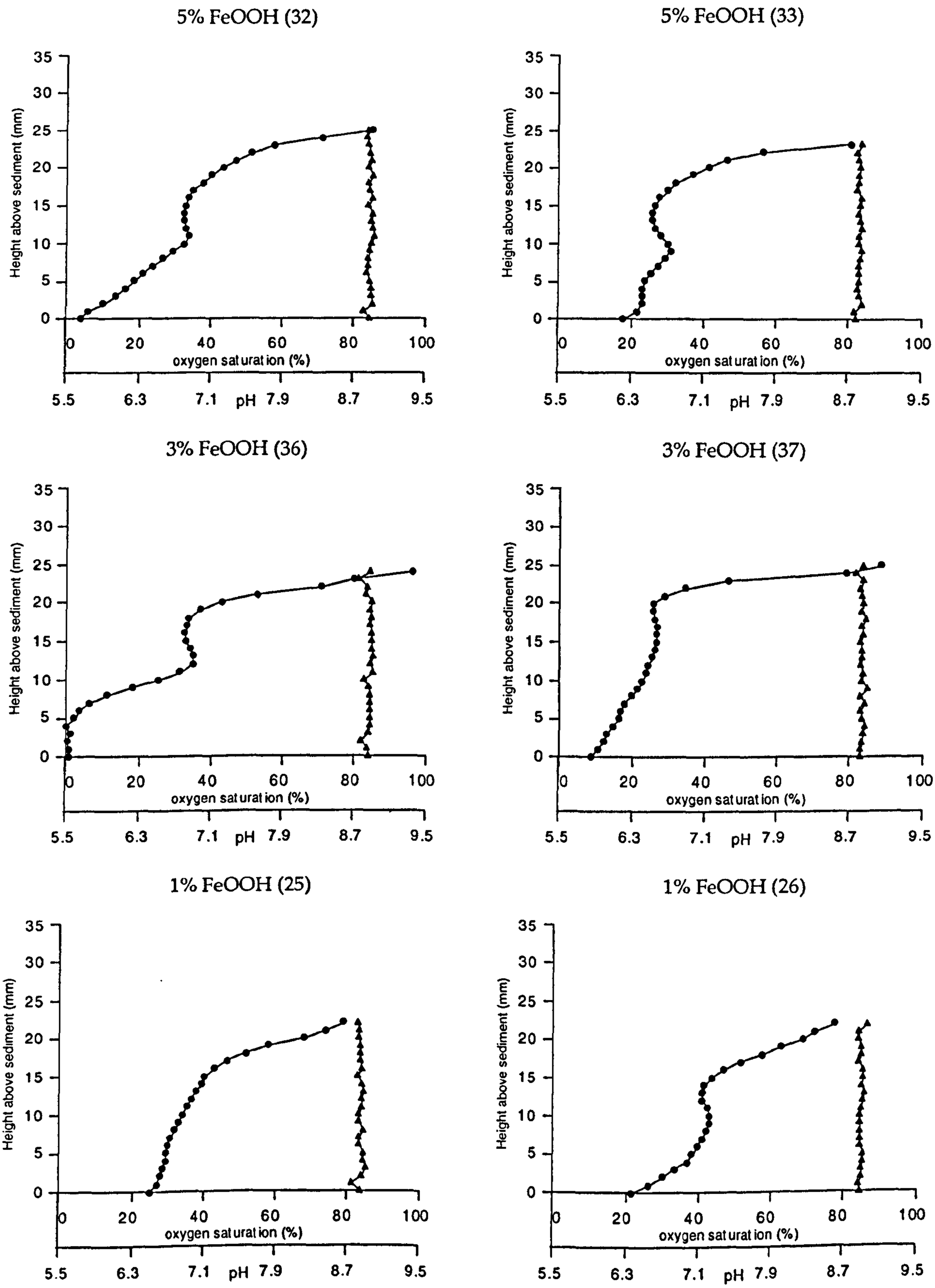

Figure 2.5. Oxygen and pH depth profiles for open marine decay systems with 5%, 3% and 1% iron oxyhydroxide. Infilled circles represent oxygen data points. Infilled triangles represent pH data points. The highest data points above the sediment represent the air-medium interface.

systems with 1% FeOOH, and the least in the 3% FeOOH systems. The pH of the medium did not appear to be affected by the amount of available iron.

The amount of iron present affected the sulphate concentration of the medium, which reflected trends seen in the oxygen saturation of the systems (Table 2.8). Highest sulphate concentrations were present with 1% FeOOH; lowest sulphate concentrations were detected with 3% FeOOH. Only trace levels of sulphide and ferrous iron were detected in any of the systems and thus appeared not to be affected by the amount of available iron. None of the ICP-AES monitored elements (P, Al, Fe, Mn, Mg, Ca) was influenced by the iron availability.

FeOOH	I.D. no.	SO_4^{2-} (mM)	AVS (M)	Pyritic S (M)	S° (M)	TRIS (M)
5%	32	15.1/15.1	-	-	-	-
5%	33	15.3/13.4	2.2	1.2	0.6	4.0
3%	36	12.4/12.2	1.9	0.9	0.7	3.5
3%	37	12.2/11.9	2.8	1.8	0.5	5.1
1%	25	21.4/21.2	1.3	1.0	0.6	2.9
1%	26	22.5/21.0	0.5	1.4	0.3	2.2
5%	34	15.1/17.4	1.3	1.8	0.6	3.6
5%	35	13.4/12.5	1.2	1.6	0.4	3.2
3%	38	11.3/8.0	1.4	1.7	0.5	3.7
3%	39	10.4/14.2	1.0	1.1	0.7	2.8
1%	27	15.8/15.9	1.4	2.0	0.3	3.7
1%	28	18.7/18.0	1.1	2.2	0.3	3.6
1%*	22	14.2/13.9	-	-	-	-
0%*	40	10.6/14.9	-	-	-	-
1%	24	13.3/14.1	-	-	-	-
0%	41	15.2/11.4	-	-	-	-

Table 2.8. Sulphate and sedimentary sulphur concentrations for open marine decay systems with different iron concentrations after 12 weeks (or 5.4 weeks *). (No TRIS data are available for systems with 0% FeOOH).

TRIS data (Table 2.8) are difficult to interpret due to differences between replicate systems, but in general higher TRIS concentrations are detected in systems with lower sulphate concentrations, and vice versa.

The range of elements detected by EDS within the plant material was unaffected by the amount of iron present within the systems, and was similar to that described for the open marine time series. Although increased TRIS levels were detected for some of the systems with increased iron in the sediment, no iron sulphides were observed within the plant material.

Location of available iron source

The rate and intensity of decay by bacterial iron (III) reduction, and hence the concentration of available dissolved iron, may be affected by the position of the available iron within the sediment. 3% iron oxyhydroxide was concentrated in a layer above the sediment in two decay systems (42, 43) as opposed to being mixed with it (36, 37).

This appeared to affect only the sulphate concentrations of the medium and the sedimentary TRIS values. Sulphate concentrations were higher with a layer of FeOOH above the sediment (15.8-18.2mM compared with 11.9-12.4mM). TRIS data (Table 2.9) differed greatly between the duplicate mixed iron/sediment systems (36, 37): the total concentrations for system 36 were lower than the layered iron systems, and those for system 37 were higher.

The position of the iron oxyhydroxide within the sediment did not affect the formation of minerals within the plant material. The main peak observed by EDS was silicon, associated with traces of iron, aluminium and potassium.

Decay system	AVS (M)	Pyritic S (M)	S° (M)	TRIS (M)
Layer of FeOOH (42)	2.0	1.7	0.9	4.6
Layer of FeOOH (43)	1.8	1.8	0.4	4.7
Mixed FeOOH (36)	1.9	0.9	0.7	3.5
Mixed FeOOH (37)	2.8	1.8	0.5	5.1

Table 2.9. Sedimentary sulphur data for open marine systems with mixed and layered 3% FeOOH.

3b. Effect of iron reactivity in open marine systems

The amount of pyrite formed in most sediments is almost never limited by the amount of available iron, but by its reactivity (Raiswell and Canfield, 1988). To investigate the effect of the reactivity of the iron source within decay experiments, standards containing 1% FeOOH mixed with the sediment (25, 26) were compared after 12 weeks with systems containing different iron sources: 1% haematite (44, 45), 0.5% haematite and 0.5% FeOOH (46, 47), and 0.5% ferric chloride and 0.5% FeOOH (48, 49).

Oxygen saturation varied slightly depending on the iron source (Figure 2.6a,b). Least oxygen penetrated the haematite systems: the medium was still anoxic at the base of one system (45) and oxygen saturation reached 11% adjacent to the twigs in the other one (44). Oxygen saturation was greatest in the 1% FeOOH systems. The mixed iron source systems showed similar oxygen saturations to each other The pH was also affected slightly by the iron source. The pH of the haematite/iron oxyhydroxide systems was the same as the standards, at pH 8.8-9.0. The pH of the ferric chloride/FeOOH systems was 0.3-0.4 pH units lower than the standards at pH 8.5-8.7, and the haematite systems were a further 0.1 units lower still at pH 8.5.

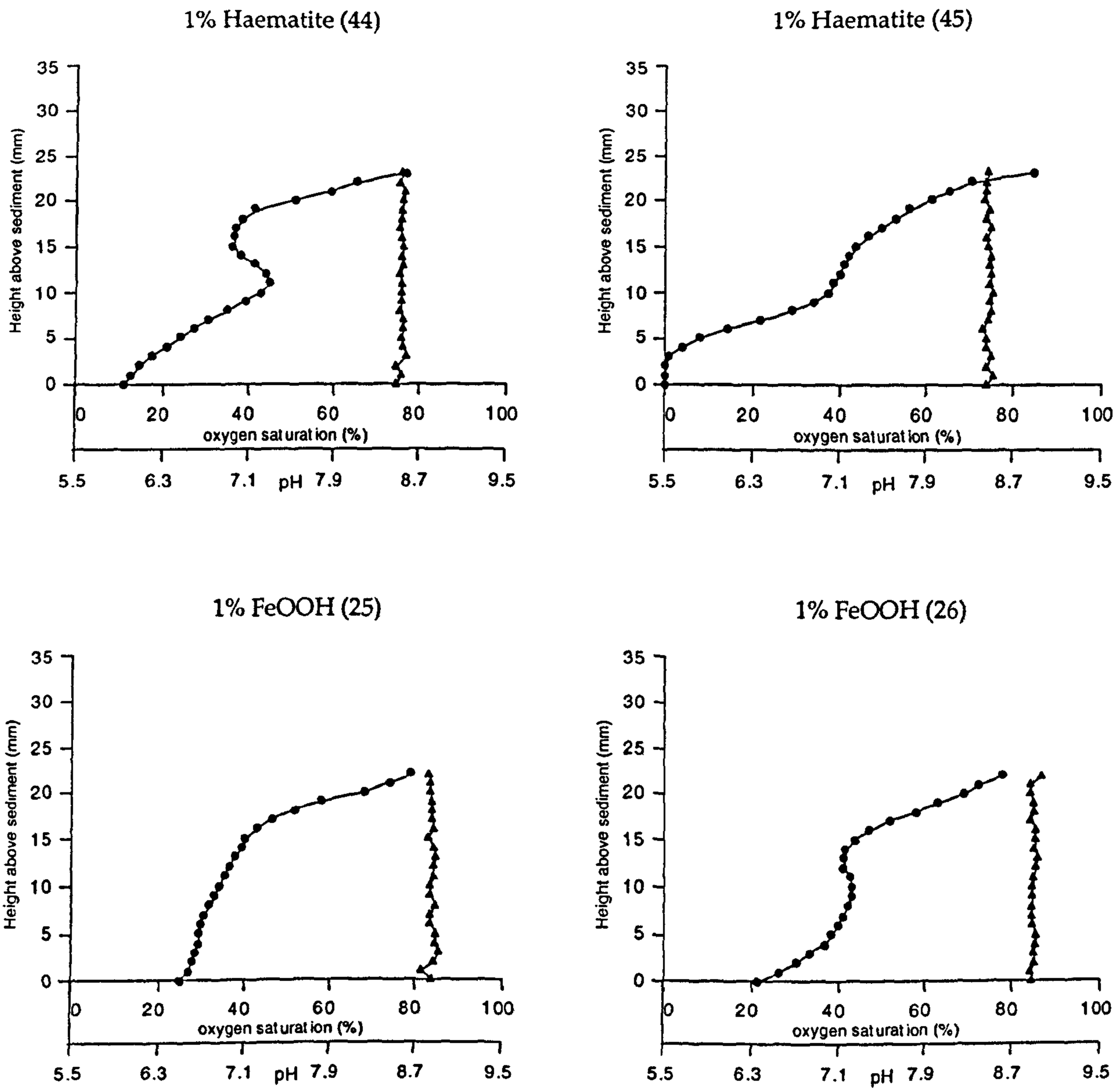

Figure 2.6a. Oxygen and pH depth profiles for 1% haematite and 1% FeOOH open marine systems after 12 weeks. Infilled circles represent oxygen data points. Infilled triangles represent pH data points. The highest data points above the sediment represent the air-medium interface.

Sulphate concentrations were unaffected by the iron source, except for the ferric chloride/iron oxyhydroxide system, where sulphate levels were

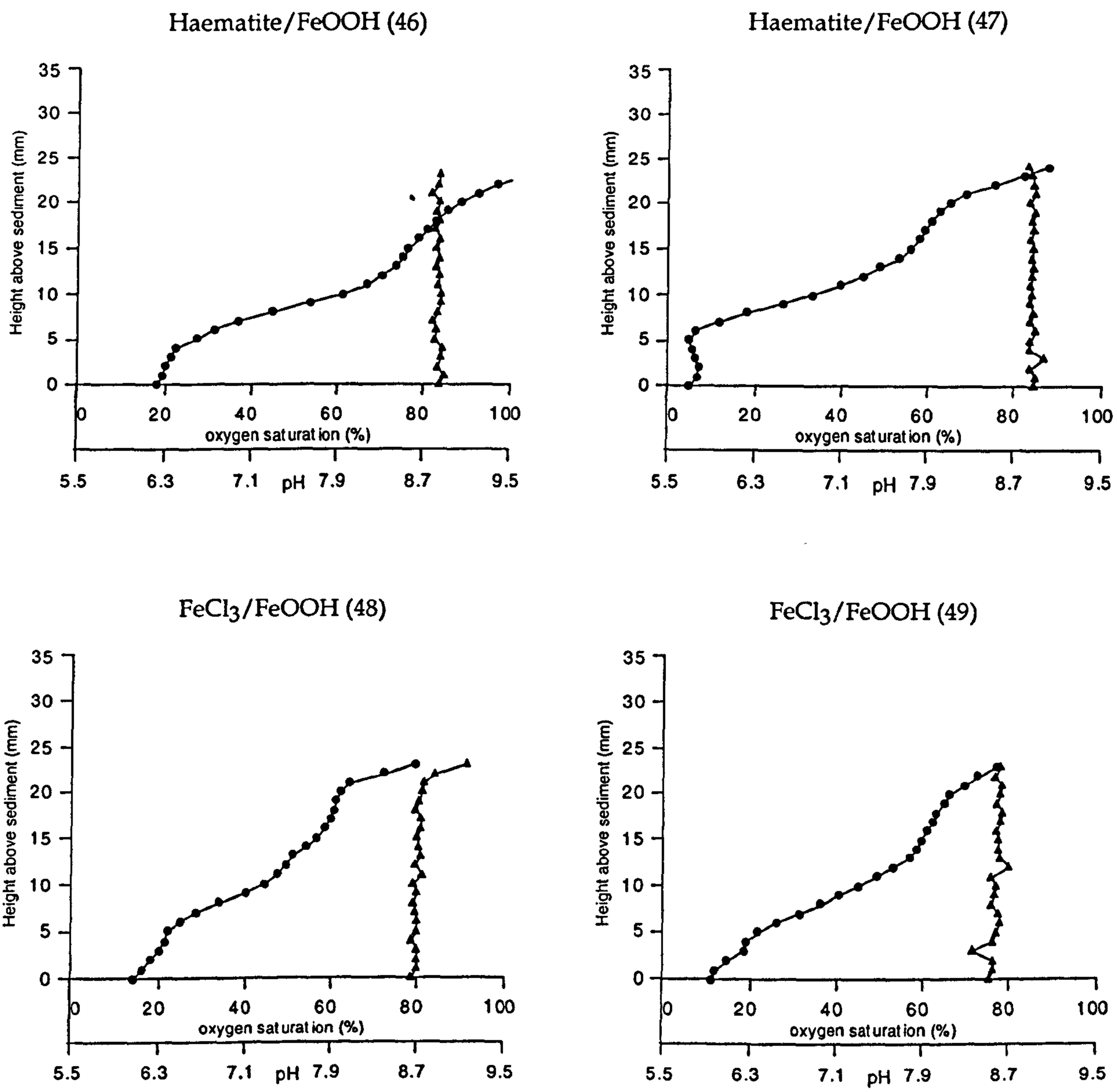

Figure 2.6b. Oxygen and pH depth profiles for haematite/FeOOH and ferric chloride/FeOOH open marine systems after 12 weeks. Infilled circles represent oxygen data points. Infilled triangles represent pH data points. The highest data points above the sediment represent the air-medium interface.

lower than in the standards (15.7-17.8mM compared with 19.7-22.5mM). Sulphide was not detected in any of these systems. Ferrous iron levels

were slightly higher in the iron oxyhydroxide standards (0.02-0.04mM) than in the other iron systems (≤ 0.02mM).

The concentrations of phosphorus, calcium and magnesium are unaffected by the iron source. Iron, manganese and aluminium were not detected by ICP-AES in any of these systems.

TRIS results varied between all duplicates, and no trends are evident (Table 2.10).

Decay system	AVS (M)	Pyritic S (M)	S° (M)	TRIS (M)
FeOOH (25)	1.3	1.0	0.6	2.9
FeOOH (26)	0.5	1.4	0.3	2.2
Fe_2O_3 (44)	1.7	1.6	0.4	3.6
Fe_2O_3 (45)	1.3	1.1	0.4	2.8
Fe_2O_3/FeOOH (46)	-	-	-	-
Fe_2O_3/FeOOH (47)	1.2	1.3	0.6	3.1
$FeCl_3$/FeOOH (48)	2.6	2.3	0.5	5.3
$FeCl_3$/FeOOH (49)	1.4	1.3	0.4	3.1

Table 2.10. Sedimentary sulphur data for open marine decay systems with different iron sources.

EDS analysis of the plant material did not distinguish any differences between samples from the different iron source systems. The main peak was silicon, associated with iron and traces of aluminium and potassium. The haematite systems also had high chloride peaks.

4a. Effect of amount of organic matter in open marine systems

Pyrite formation in normal marine environments is limited by the availability and reactivity of organic matter (Berner, 1984). The influence of the availability of organic matter in the open marine decay systems

was investigated by varying the number of twigs added to the systems, and by adding extra plant material or glucose during the course of the experiments. The effect of using yeast extract to stimulate bacterial activity was also studied.

Number of twigs available

Open marine systems with five plane twigs (25, 26) were compared with systems containing a single twig (50, 51) and fifteen twigs (54, 55) after 12 weeks. Single twig systems (52, 53) were also compared with fifteen twig systems (56, 57) after 24 weeks. No five-twig standards were run for 24 weeks.

Oxygen saturation of the different systems varied greatly depending on the amount of twigs present. After 12 weeks, oxygen saturation had reached 43-45% adjacent to the sediment in the single twig systems and 21-24% in the five-twig standards. Where there were fifteen twigs, ca 15mm of the medium above the sediment remained anoxic. After 24 weeks, oxygen saturation had increased to 53-60% adjacent to the sediment in the single twig systems, but anoxia was maintained at the very base of the medium in the systems containing fifteen twigs.

After 12 weeks, the pH of the medium in the system with fifteen twigs (pH 8.4-8.5) was lower than that of the five-twig standards (pH 8.8-8.9), which was slightly lower than in the single twig systems (pH 8.7-8.9). The pH decreased in the single twig systems to pH 7.9-8.3 (52, 53) after 24 weeks, but the pH of the fifteen twig systems remained constant at pH 8.4-8.5 (56, 57).

After 12 weeks, sulphate concentrations were greatest where only a single twig was present (25.3-27.0mM), and were considerably lower with fifteen twigs (4.5-10.2mM) than in the five-twig standard systems (21.0-22.5mM). There was a very slight increase in sulphate concentration in

both the single and fifteen twig systems between 12 and 24 weeks reaching 25.5-27.7mM and 10.8-13.7mM respectively, although this increase may have been a result of evaporation of medium.

Sulphide was only detected in the fifteen twig systems, and the concentration decreased between 12 and 24 weeks, from 0.03-0.05mM to 0.01-0.02mM. Ferrous iron was present in the five-twig standards (0.02-0.04mM) and the fifteen twig systems (0.03-0.05mM) at 12 weeks. In the systems with fifteen twigs, sulphide concentration was higher than that of ferrous iron, but this was reversed in the five-twig standards systems, where Fe (II) levels were higher than sulphide levels. Ferrous iron was also present in the fifteen twig systems after 24 weeks, at 0.01-0.02mM.

After 12 weeks, the highest phosphorus and calcium concentrations occurred in the fifteen twig systems, at 0.37-0.46mM and 2.3-2.6mM respectively. The lowest were in the single twig systems (0.10-0.11mM and 1.3-1.4mM respectively). After 24 weeks, the phosphorus and calcium concentrations of both systems had decreased to 0.04-0.10mM and 0.04mM respectively in the single twig systems, and 0.10-0.30mM and 0.1-1.9mM respectively in the fifteen twig systems. Concentrations of magnesium were unaffected by the amount of plant material, ranging from 12.0-12.9mM, and increased slightly between 12 and 24 weeks, reacting a maximum of 15.9mM. Aluminium, iron and manganese were not detected in any system at either 12 or 24 weeks.

After 12 weeks, there was very little difference in the amount of TRIS in fresh sediment and in that of the one twig systems (Table 2.11). The total sediment TRIS was considerably higher in the fifteen-twig systems than in the five-twig standard sediment, in particular with regard to AVS (Table 2.11). The total TRIS in these fifteen twig systems was among the highest in the decay systems (Table 2.11).

After 24 weeks, all forms of sediment sulphur had decreased in both the single and fifteen twig systems. Where there was only one twig, the TRIS values were lower than in the fresh sediment at the start of the experiment. In the systems with fifteen twigs, the TRIS levels were higher after 12 weeks than those of the five-twig standard systems. While AVS levels dropped substantially, elemental sulphur levels decreased only slightly, and the pyritic fraction was almost unchanged.

Although increasing the amount of organic material resulted in an increase in TRIS, the amount of TRIS produced was not directly proportional to the number of twigs available. In the single twig systems, each twig resulted in the production of 0.41 ± 0.25M TRIS, but in the five-twig standards each twig only contributed towards 0.38 ± 0.07M TRIS, and in the fifteen-twig systems, only 0.25 ± 0.003M TRIS was formed per twig.

Decay system	AVS (M)	Pyritic S (M)	S° (M)	TRIS (M)
Time 0				
Fresh sediment	0.04	0.36	0.24	0.64
12 weeks				
Single twig (50)	0.1	0.4	0.3	0.8
Single twig (51)	0.4	0.6	0.3	1.3
Five twigs (25)	1.3	1.0	0.6	2.9
Five twigs (26)	0.5	1.4	0.3	2.2
Fifteen twigs (54)	2.3	1.6	0.4	4.3
Fifteen twigs (55)	2.2	1.3	0.9	4.4
24 weeks				
Single twig (52)	0	0.3	0.1	0.4
Single twig (53)	0.1	0.2	0.1	0.4
Fifteen twigs (56)	1.6	1.9	0.2	3.7
Fifteen twigs (57)	1.4	1.2	0.4	2.9

Table 2.11. Sedimentary sulphur data for single-, five- (i.e. standard) and fifteen-twig open marine systems after 12 and 24 weeks.

EDS analysis of the twigs from both the single and fifteen twig systems after 12 weeks detected silicon and calcium, but no iron or sulphur. No change was evident between 12 and 24 weeks.

Effect of adding extra plant material after 6 weeks

Six extra twigs were added to marine, open decay systems after 6 weeks, and dismantled after a further 6 weeks (58, 59). The chemistry of these systems was compared with that of the 12 week system from the time series (12).

Where extra plant material was added to the decay systems anoxia was sustained in the lowest 20mm of the medium, compared with only 5mm in the standard systems. The pH of the medium was unaffected by the addition of fresh twigs (pH 8.6-8.7).

Sulphate concentrations were lower with added plant material (12.2-13.5mM) than in the standard (18.6/14.2mM). No sulphide or ferrous iron was detected in either system after 12 weeks.

Despite considerable differences between the phosphorus concentrations of the systems with added twigs (0.24-0.46mM), levels were much higher than in the standard medium (0.12/0.11mM). Calcium levels were also higher with additional plant material (2.5-2.7mM compared with 2.0mM), but magnesium levels were unaffected, at 11.9-13.2mM. Aluminium, iron and manganese were not detected in either system after 12 weeks.

There were considerable differences between the TRIS values for the duplicate systems with added twigs (Table 2.12). Levels of AVS in system 59 were almost double that of the sediment from system 58 (2.1M compared with 1.2mM), but both systems contained considerably more AVS than the standard (1.0M). Concentrations of pyritic, elemental and total sulphur of system 59 were higher than those in the standards, but

concentrations of pyritic, elemental and total sulphur of system 58 were lower than in the standard (Table 2.12).

Decay system	AVS (M)	Pyritic S (M)	S° (M)	TRIS (M)
Standard (12)	1.0	1.5	0.9	3.4
Extra twigs (58)	1.2	1.6	0.9	3.8
Extra twigs (59)	2.1	0.8	0.5	3.3

Table 2.12. Sedimentary sulphur data for a standard system and open marine systems with extra twigs added after 6 weeks.

No plant material present

One open marine system containing no plant material (60) was compared with one standard system (29). Both were incubated for 14 weeks.

Levels of oxygen saturation were much lower where plant material was present, reaching only 11% saturation adjacent to the sediment, compared with 58% where there were no twigs. The pH of the medium was less alkaline where there was no plant material (pH 8.4) compared to pH 8.6.

Where there were no twigs present, sulphate levels (27.4/28.9mM) were almost unchanged from the starting medium (ca 29.5mM). Sulphate concentrations were much lower in the standard (21.0/21.5mM). Sulphide and ferrous iron were not detected in either system.

Phosphorus concentrations in the system with no plant material (0.1/-0.14mM) were double those of the standard (0.07/0.08mM). Magnesium levels were also higher when no plant material was present

(7.2/7.6mM compared with 5.7/6.0mM). Calcium, aluminium, iron and manganese were not detected in either system.

No TRIS data are available for either the system with no plant material or the standard with twigs.

Effect of stimulating bacterial activity with yeast extract

Standard marine, open systems were incubated for 12 weeks with (27, 28) and without (61, 62) added yeast extract.

Oxygen levels, pH ranges (pH 8.6-87.) and concentrations of sulphate (15.8-21.7mM), sulphide (≤ 0.05mM) and ferrous iron (0mM) were not affected by the presence or absence of yeast extract.

Magnesium levels were slightly lower with added yeast extract (11.3-12.6mM compared to 10.1-10.7mM). Traces of calcium (≤ 0.3mM) were present in the systems with yeast extract, but none was detected in the systems without. Concentrations of phosphorus (0.13-0.21mM) were not affected by the presence of yeast extract. Aluminium, iron and manganese were not detected in any of the decay systems.

TRIS was higher with yeast extract (3.6-3.7M compared with 2.3-3.2M). Concentrations of elemental sulphur were identical in both systems (0.3M), but the pyritic sulphur fraction was much larger with yeast extract (2.0-2.2M compared with 1.2-1.7M). The wide range of AVS concentrations in duplicate systems (1.1-1.4mM with yeast extract compared with 0.8-1.3M without yeast extract) made it impossible to identify any trends.

EDS analysis revealed a similar suite of minerals both in systems with and without added yeast extract to those described for the standard open marine time series.

Effect of promoting bacterial activity by the addition of glucose solution

Glucose (20mM) was added to open marine systems after 6 weeks and then incubated for a further 6 weeks before being analysed (63, 64). These systems were compared to a standard system after 12 weeks (12).

Less oxygen penetrated the systems with added glucose: anoxia was sustained in the lowest 10mm of the medium of the glucose systems, compared with only 5mm in the standard. The pH of the glucose medium was slightly more alkaline at pH 8.7-8.8 than that of the standard (pH 8.6 adjacent to the twigs and sediment).

Much less sulphate was present in the glucose systems (7.1-10.7mM) compared to the standards (18.6/14.2mM). No sulphide or ferrous iron was detected in either system.

Phosphorus levels differed considerably between the two glucose systems (0.38/0.41mM and 0.27mM) but were still higher than in the standard (0.12/0.11). Calcium concentrations were similar with or without the added glucose, at 1.7-2.1mM. Magnesium concentrations were slightly higher with glucose (12.1-12.8mM) compared with 12.0mM in the standard. Aluminium, iron and manganese were not detected either in systems with or without glucose.

Sedimentary TRIS values for the glucose systems were amongst the highest in any of the decay systems (4.2-4.4M). AVS levels were much higher in the glucose systems 2.1M and 1.6M than in the standard (1.0mM). Pyritic sulphur concentrations were slightly higher in the glucose systems (1.6-1.9M) than in the standard (1.5M). Concentrations of elemental sulphur were slightly lower with added glucose than in the standard (0.7M and 0.9M respectively).

EDS analysis of the plant material revealed similar suites of elements in the glucose to those in the standard (described in the time series).

Despite the extra iron sulphides in the sediment, none was seen within the plant material.

4b. Effect of reactivity of organic matter (different plant species) in open marine systems

The effect of the reactivity of organic matter on the formation of pyrite was investigated by decaying a range of plant species with different compositional tissues and structural organisations. Different plant species were decayed under open, marine conditions and incubated for three different time periods.

6 week decay systems

Plane (23), celery (65), vine (66) and *Cyathea* (67) were decayed for 6 weeks.

Oxygen and pH depth profiles are presented in Figure 2.7. Oxygen saturation adjacent to the twigs was as follows, in descending order: celery > plane > vine > *Cyathea*. All four systems had similar pH, at 8.8-8.9 (Figure 2.7).

Sulphate levels in descending order were: plane (22.6/22.4mM) > vine (20.8/21.4mM) > celery (19.2/19.1mM) > *Cyathea* (14.8mM). Sulphide was only detected at the sediment-medium interface in the *Cyathea* system (0.03mM). Low concentrations of ferrous iron (≤ 0.12mM) were present in all the systems.

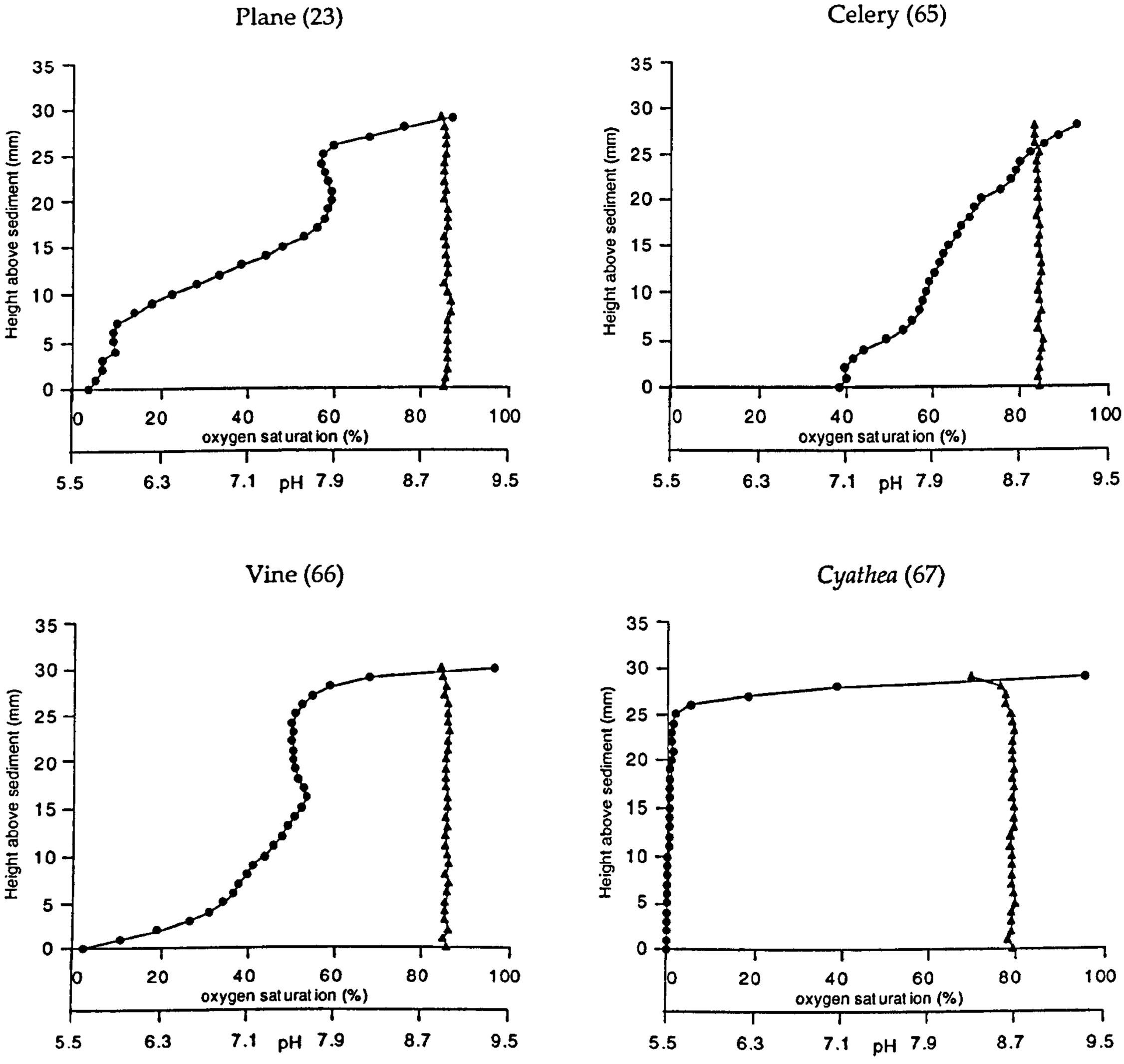

Figure 2.7. Oxygen and pH depth profiles for open marine systems containing different plant species decayed for 6 weeks. Infilled circles represent oxygen data points. Infilled triangles represent pH data points. The highest data points above the sediment represent the air-medium interface.

There were differences in phosphorus, calcium and magnesium concentrations between different plant species (Table 2.13) but no aluminium, iron or manganese was detected in any of these systems.

Decay system	P (mM)	Ca (mM)	Mg (mM)
Plane (23)	0.18/0.27	0.7/0.8	12.9/13.1
Celery (65)	0.35/0.40	1.5/1.3	11.8/12.2
Vine (66)	0.18/0.16	1.0/1.9	11.5/12.0
Cyathea (67)	1.12/1.18	0.6/0.5	13.0/14.0

Table 2.13. Phosphorus, calcium and magnesium concentrations in plane, celery, vine and *Cyathea* open marine systems after 6 week.

EDS analysis of the decayed vine after 6 weeks indicated the presence of silicon in association with aluminium, iron and potassium. The plane twigs contained lots of sodium chloride crystals, and a similar suite of elements to those seen in the vine. The *Cyathea* was too soft to be sectioned and analysed. Very little remained of the celery, and there was no structural support to allow the material to be sectioned or prepared for SEM analysis. No TRIS data are available.

12 week decay systems

Plane (24), vine (68), *Equisetum* (69), cherry (70), *Psilotum* (71), *Ginkgo* (72) and *Sequoia* (73) were decayed for 12 weeks.

Comparison of the total oxygen saturation of the decay systems run for 12 weeks is difficult due to the differences in gradient and form of the oxygen depth profiles (Figure 2.8: plane is included in Figure 2.4a).

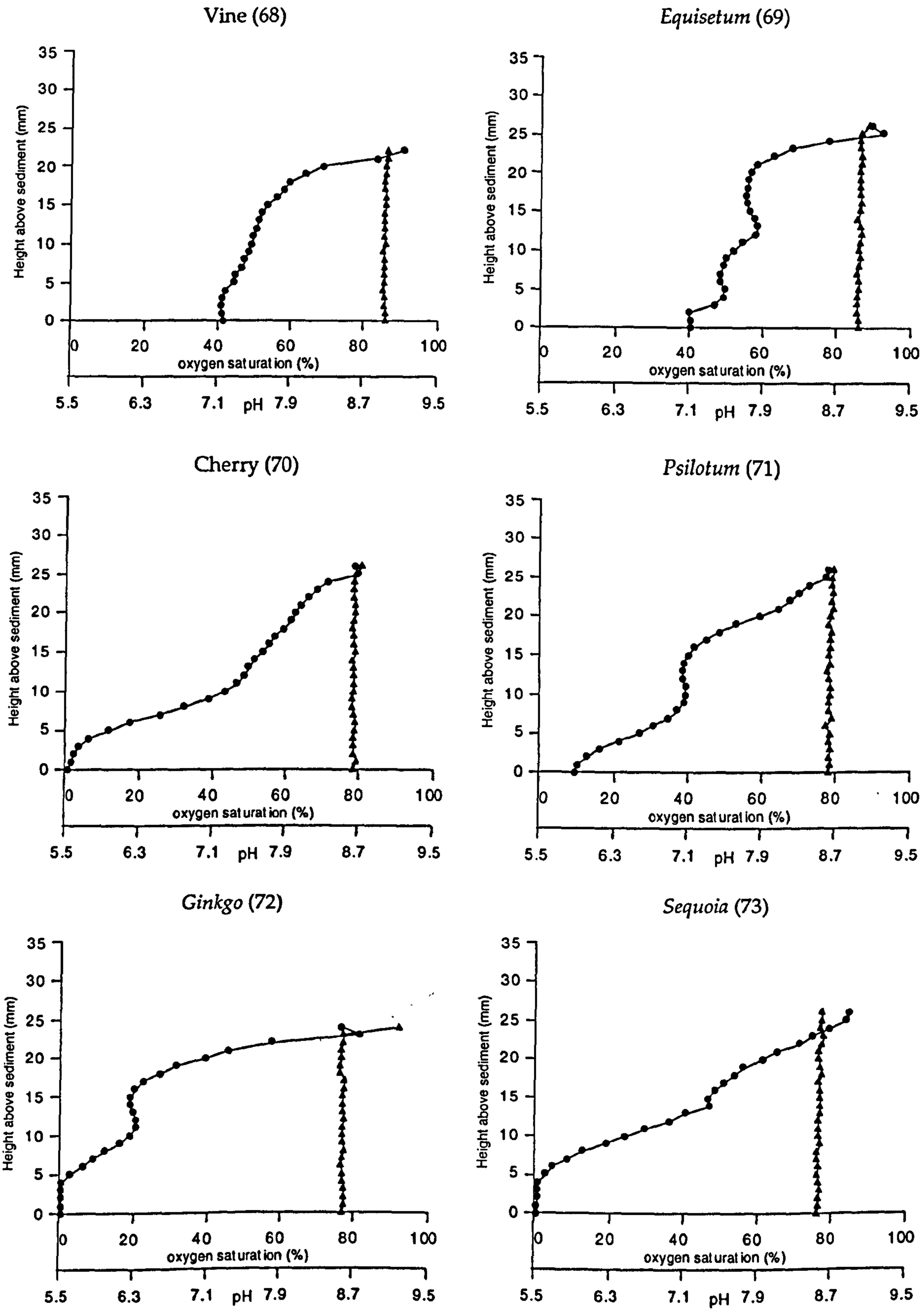

Figure 2.8. Oxygen and pH depth profiles for open marine systems containing different plant species decayed for 12 weeks. Infilled circles represent oxygen data points. Infilled triangles represent pH data points. The highest data points above the sediment represent the air-medium interface.

However, the percentage oxygen saturation adjacent to the twigs and sediment, in decreasing order, was: *Equisetum* > vine > plane > cherry > *Sequoia* > *Psilotum* > *Ginkgo*. The pH of the medium was ca 8.6-8.7 for all plant species, except for the *Equisetum* and vine systems which were slightly more alkaline at pH 8.8-8.9 (Figure 2.8).

Sulphate levels, in descending order, were as follows: vine (14.4/14.9mM) > plane (13.3/14.1mM) > cherry (12.3/13.0mM) > *Equisetum* (11.1/11.2mM) > *Sequoia* (10.0/9.5mM) > *Psilotum* (5.9/7.9mM). *Ginkgo* could not be placed in this sequence due to the steep sulphate gradient within the system (15.8/8.1mM). No sulphide was detected in any of these systems. Traces of ferrous iron (≤ 0.03mM) were found in all systems, except for 0.06mM of ferrous iron just above the sediment-medium interface of the *Sequoia* system.

Concentrations of ICP-AES monitored elements are presented in Table 2.14.

No TRIS data are available for these systems. The FeSam found in the plane system (24) was described earlier (pages 87-88) but no FeSam was detected in the systems containing the other species. EDS analysis of the decayed vine showed that sodium chloride crystals were present. Cherry, *Ginkgo*, *Psilotum* and *Sequoia* all contained similar suites of elements to those described in the marine time series. The *Equisetum* could not be analysed by SEM due to the softness of the decayed tissues.

Decay system	P (mM)	Ca (mM)	Mg (mM)	Al (mM)	Fe (mM)	Mn (mM)
Plane	0.67	0.01	11.3	0	0	0
(24)	0.71	1.1	13.0	0	0	0
Vine	0.37	2.4	15.2	0	0	0
(68)	0.32	2.5	16.0	0.11	0	0.02
Equisetum	0.62	2.0	12.7	0.23	0.26	0.30
(69)	0.52	2.0	12.5	0.23	0.21	0.24
Cherry	0.78	1.8	13.7	0.04	0.20	0.19
(70)	0.80	0	11.1	0	0	0
Psilotum	0.59	3.0	13.5	0.11	0.11	0.13
(71)	0.67	3.0	13.7	0.14	0.17	0.19
Ginkgo	0.29	2.1	14.1	0.09	0	0.01
(72)	0.28	2.1	14.0	0.09	0	0.01
Sequoia	0.42	2.6	15.3	0.10	0	0.02
(73)	0.96	0	13.1	0	0	0

Table 2.14. ICP-AES data for open marine systems containing different plant species incubated for 12 weeks. Two concentrations are given for each element: the upper on is the concentration just below the air-medium interface, the lower one is the concentration just above the sediment-medium interface.

14 week decay systems

Plane (29), celery (74), newer, green *Psilotum* (75), older, orange/brown *Psilotum* (76), vine (77), *Cyathea* (78) and pine (79) were decayed for 14 weeks.

Oxygen and pH depth profiles for celery, new and old *Psilotum*, *Cyathea*, vine, and pine after 14 weeks of decay are presented in Figure 2.9 (the plane depth profile is presented in Figure 2.4a). Oxygen saturation adjacent to the twigs, in descending order, was as follows: celery > vine >

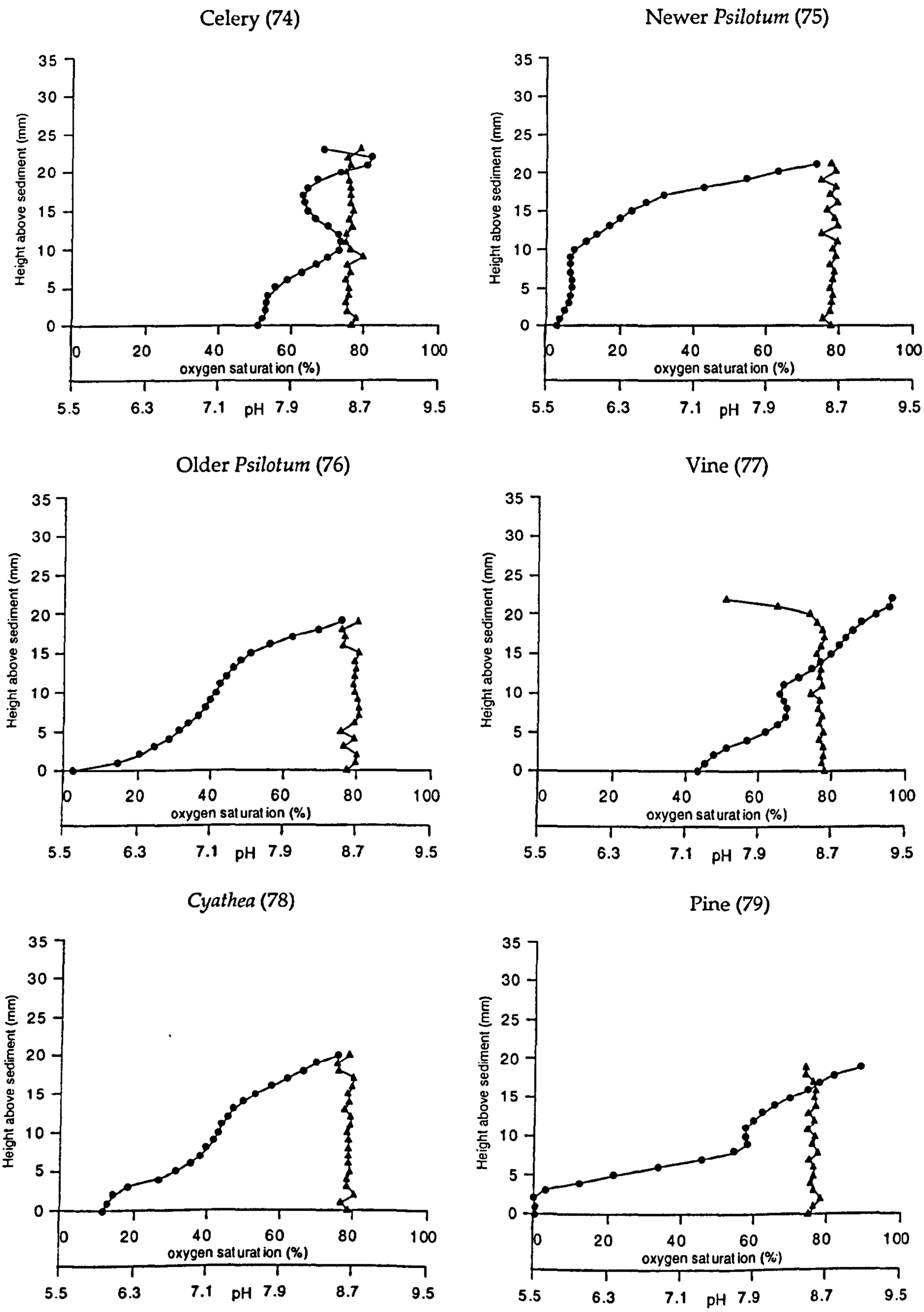

Figure 2.9. Oxygen and pH depth profiles for open marine systems containing different plant species decayed for 14 weeks. Infilled circles represent oxygen data points. Infilled triangles represent pH data points. The highest data points above the sediment represent the air-medium interface.

plane, *Cyathea* > newer Psilotum > older *Psilotum* > pine. The pH of all these systems was pH 8.5-8.6 (Figure 2.9).

Sulphate levels in descending order were: celery (22.4/23.4mM) > vine (22.6/22.4mM) > plane (21.5/21.0mM) > newer *Psilotum* (19.4mM) > pine (18.1/17.9mM) > *Cyathea* (16.9/16.5mM) > older *Psilotum* (16.1/16.0mM). Low levels of sulphide (≤ 0.08mM) were detected at the sediment-medium interface in both of the *Psilotum* systems and the *Cyathea* system. Traces of ferrous iron (≤ 0.06mM) were present in all systems except for celery (0mM), and at the sediment-medium interface of the newer and older *Psilotum* systems (0.26mM and 0.11mM respectively).

Concentrations of phosphorus, calcium, magnesium, iron, aluminium and manganese for these 14-week decay systems are presented in Table 2.15.

Decay system	P (mM)	Ca (mM)	Mg (mM)	Al (mM)	Fe (mM)	Mn (mM)
Plane (29)	0.07	0	5.7	0	0	0
	0.08	0	6.0	0	0	0
Celery (74)	0.23	0.8	7.4	0.01	0	0
	0.27	0.8	7.2	0	0.01	0
Newer *Psilotum* (75)	0.22	0	6.6	0	0	0
	0.32	1.3	7.0	0.11	0.14	0
Older *Psilotum* (76)	0.09	0.7	7.5	0	0	0
	0.14	0.7	6.8	0	0	0
Vine (77)	0.33	0.8	7.2	0	0	0
	0.37	0.8	7.0	0.02	0.03	0
Cyathea (78)	0.27	0	6.6	0	0	0
	0.26	0.2	6.4	0	0	0
Pine (79)	0.28	0	6.9	0	0	0
	0.27	0	7.3	0	0	0

Table 2.15. ICP-AES data for systems containing different plant species decayed for 14 weeks. Two concentrations are given for each element: the

upper one is the concentration just below the air-medium interface, the lower one is the concentration just above the sediment-medium interface.

EDS analysis detected FeSam in the parenchyma cells of one end of one the older *Psilotum* twigs (Figure 2.3E). This material occurred in a similar location to that in the plane described previously (page 85) but was more amorphous in appearance. The mineralisation did not extend to any depth within the twig. No FeSam was detected by EDS in any of the other plant species studied after 14 weeks. The older *Psilotum* twigs also contained some calcium and silicon. The decayed newer *Psilotum* and vine contained very little mineral content, except for sodium chloride crystals. The pine and plane twigs contained a suite of elements, including calcium, chloride, sodium, aluminium and silicon. No iron or sulphur were detected in either species. The celery and *Cyathea* were too soft to section.

Geochemical changes between 6 and 14 weeks

The celery, vine, *Cyathea* and plane systems decayed for 14 weeks were replicates of those decayed for only 6 weeks. For all four species, oxygen saturation increased, and the pH became less alkaline. Sulphate concentrations decreased in the celery, vine and *Cyathea* systems, but increased in the plane system. Phosphorus concentrations decreased with time for all species except for vine. Magnesium concentrations decreased substantially, and calcium levels also decreased.

5. Effect of pH in open marine systems

Pyrite forms readily under normal marine conditions which have a pH range of 6-9 (Stumm and Morgan, 1981). Pyrite formation has been

reported in the laboratory between pH 5.5-8 (e.g. Berner, 1969; Luther, 1991; Rickard, 1994; Wilkin and Barnes, 1996). However, the pH of the time series and many of the open marine standards was observed to reach more alkaline pH (up to pH 9.8 in system 6), and so decay experiments were run with ferric chloride (1%) (80, 81) as the iron source instead of the iron oxyhydroxide used in standard marine open systems (25, 26) in an attempt to reduce the pH. Both the ferric chloride and iron oxyhydroxide systems were analysed after 12 weeks.

The amount of oxygen in the ferric chloride systems differed between the two systems, remaining anoxic at the base of one (80) but reaching 10% saturation adjacent to the sediment in the other (81). Oxygen saturation was higher in the standards, reaching 21-24% at the base of the medium. The pH of the ferric chloride systems was only ca 0.3 pH units less alkaline than that of the standards, at pH 8.6 compared with pH 8.8-8.9.

Sulphate concentrations were much lower in the ferric chloride systems (13.1-14.6mM) than the iron oxyhydroxide systems (21.0-22.5mM). Sulphide was not detected in the systems with either ferric chloride or iron oxyhydroxide. Trace levels of ferrous iron were slightly higher in the standards than in the systems with ferric chloride (0.02-0.04mM compared to 0.01-0.02mM).

Phosphorus and magnesium levels were unaffected by the different iron sources (0-0.20mM and 12.7-13.6mM respectively) but calcium concentrations in the ferric chloride systems (3.1-3.4mM) were double those of the standards (0-1.9mM). Aluminium, iron and manganese were not detected in the systems with either iron source.

TRIS levels of the ferric chloride systems were considerably higher than those of the iron oxyhydroxide standards, and were amongst the highest seen in any decay systems (Table 2.16). Concentrations of all

forms of sedimentary sulphur were greater in the systems with ferric chloride than in the systems with iron oxyhydroxide (Table 2.16).

Decay system	AVS (M)	Pyritic S (M)	S° (M)	TRIS (M)
$FeCl_3$ (80)	1.8	1.9	1.0	4.7
$FeCl_3$ (81)	2.1	1.7	1.0	4.8
Standard (25)	1.3	1.0	0.6	2.9
Standard (26)	0.5	1.4	0.3	2.2

Table 2.16. Sedimentary sulphur data for open marine decay systems incubated with 1% ferric chloride and 1% iron oxyhydroxide.

EDS analysis of the cut ends of the twigs did not detect any different elements within the plant material between the ferric chloride systems, the standards, and the open marine time series systems after 12 weeks. Despite the high TRIS in the sediment of the ferric chloride systems, none was detected within the plant material.

To try to reduce the pH of the open marine systems further, the ferric chloride systems were repeated and the pH was lowered to ca pH 6.5 by titration with hydrochloric acid every 2-3 days (82, 83). These systems were compared with a standard (12) after 12 weeks.

Reducing the pH resulted in anoxia only in the lowest 1mm of the medium, compared with 5mm in the standard. Despite the acid titrations, the pH of the ferric chloride systems tended to stabilise at pH 7.5-8.0 within 1-2 days after the addition of hydrochloric acid. After 12 weeks, the pH was 8.0, only 0.6 units less alkaline than the standard (pH 8.6).

The sulphate concentrations of the ferric chloride/acid systems were the lowest in any of the decay systems, at only 2.1-3.2mM after 12 weeks compared with 18.6/14.2mM in the standard. No sulphide or ferrous iron was detected with ferric chloride/acid or in the standard.

Phosphorus and magnesium concentrations were slightly lower in the standards, but calcium levels were much higher in the ferric chloride/acid systems (Table 2.17). Concentrations of iron, aluminium and manganese were all less than 0.1mM (Table 2.17).

Decay system	P (mM)	Ca (mM)	Mg (mM)	Al (mM)	Fe (mM)	Mn (mM)
$FeCl_3$ / HCl (82)	0.95	10.6	16.3	0	0	0.06
	0.87	9.3	14.2	0	0	0.05
$FeCl_3$ / HCl (83)	0.33	8.8	14.6	0	0	0
	0.30	8.7	14.2	0	0	0
Standard (12)	0.12	2.0	12.1	0	0	0
	0.11	2.0	12.0	0	0	0

Table 2.17. ICP-AES data for open marine systems with ferric chloride / acid and a standard open marine system after 12 weeks. Two concentrations are given for each element: the upper one is the concentration just below the air-medium interface, the lower one is the concentration just above the sediment-medium interface.

Despite the low sulphate concentrations, sedimentary TRIS levels in the ferric chloride/acid systems were only slightly higher than those of the standard (3.7-3.8M compared with 3.4M). AVS levels were higher in the ferric chloride systems, at 1.5-1.7M compared with 1.0M. However, a grey/black suspension persisted throughout the medium of the ferric chloride/acid system after week 1.

EDS analysis observed silicon, calcium, aluminium, potassium and traces of iron, but no sulphur, within the plant material from the ferric chloride/acid systems as well as the standard. No crystals were observed.

6. Effect of fungal decay prior to bacterial decay in open marine systems

Much of the plant material which has been preserved in the pyrite fossil record may have undergone decay to some extent before fossilised. This decay would have removed some of the more readily metabolisable organic material from the plant axes, which may have affected the bacterial, and hence geochemical, processes which would have occurred later in the fossilisation process. To investigate the effect of decay prior to entry into the aqueous decay systems, plant material was subjected to fungal decay by indigenous bacteria (84, 85) or fungal inoculum (86, 87) for 12 weeks before being transferred to open marine decay systems. After 12 weeks, these systems were compared with standard marine open systems (27, 28).

Although fungal decay prior to bacterial decay of the twigs affected the geochemistry of the systems, the source of the fungal degraders (fungi indigenous to the twigs, or present within wood chippings) did not influence the geochemistry of the systems.

After 12 weeks, more oxygen had penetrated the fungal systems, reaching 14-42% adjacent to the twigs, than the standard systems, with only 0-6% saturation (Figure 2.10). The pH of the fungal systems was much lower than that of the standards, at ca 6.8-7.0 compared with pH 8.4-8.5 (Figure 2.10).

Sulphate concentrations were higher in the fungal systems (18.5-23.7mM) than in the standards (15.8-18.7mM). No sulphide or ferrous iron was detected in the fungal systems or the standards.

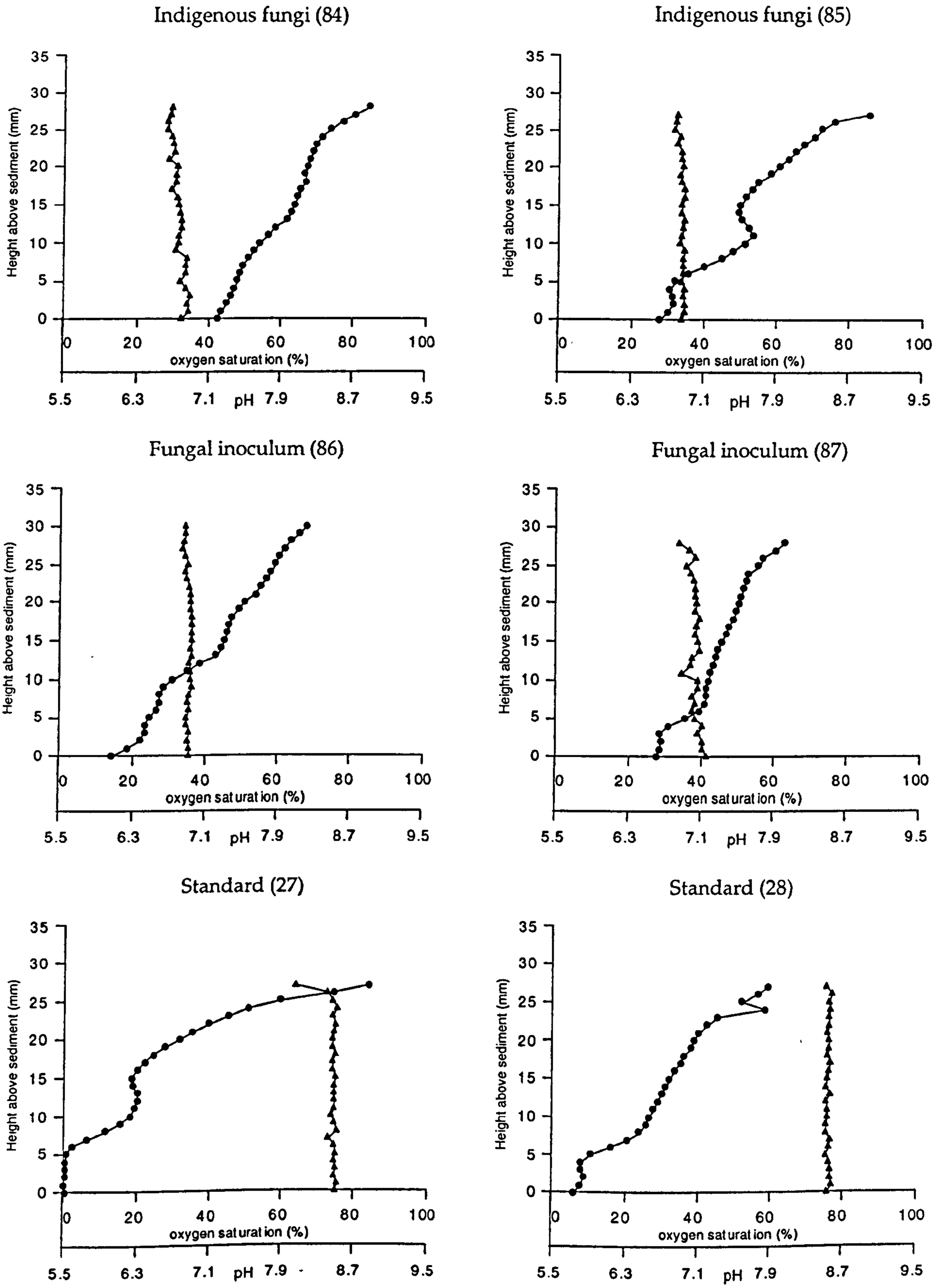

Figure 2.11. Oxygen and pH depth profiles for open marine systems containing fungal-decayed plant material and standard decay systems incubated for 12 weeks. Infilled circles represent oxygen data points. Infilled triangles represent pH data points. The highest data points above the sediment represent the air-medium interface.

Phosphorus concentrations within the medium were significantly higher in the fungal systems than the standards (0.26-0.77mM compared with 0.16-0.21mM). Calcium and magnesium levels were also higher in the fungal systems (0.5-1.2mM compared with ≤ 0.3mM, and 10.7-12.0 compared with 10.0-10.7mM, respectively). Aluminium, iron and manganese were not detected in the fungal systems or the standards.

AVS, pyritic sulphur and TRIS were much lower in the fungal systems than in the standards, but elemental sulphur levels were higher (Table 2.18).

Decay system	AVS (M)	Pyritic S (M)	S° (M)	TRIS (M)
Fungal decay (84)	0.1	1.1	0.3	1.5
Fungal decay (85)	0.2	1.1	0.3	1.6
Fungal decay (86)	0.3	1.3	0.5	2.0
Fungal decay (87)	0.2	1.1	0.4	1.6
Standard (27)	1.4	2.0	0.3	3.7
Standard (28)	1.1	2.2	0.3	3.6

Table 2.18. Sedimentary sulphur data for fungal decay open marine systems and standards after 12 weeks.

After 12 weeks in the aqueous decay systems, clay minerals had formed along the walls of the pith cells on the cut surface of the plant material, and attached to the pith cell walls at depths of up to 3mm within the twigs (Figure 2.3F). These were identified by EDS peaks for Si and Al in combination with Fe, K and Mg.

7a. Effect of floating of twigs in open marine systems

To reproduce a more natural decay situation, twigs were allowed to float in open marine systems instead of in being pressed into contact with

the sediment. These systems were incubated for 5.4 weeks (88) and 12 weeks (89) and were compared with standards after 5.4 weeks (22) and 12 weeks (24).

There was very little difference in the chemistry of the floating systems and that of the standards. After 5.4 weeks the floating system was anoxic higher above the sediments than in the standards, but after 12 weeks more oxygen had penetrated the floating system reaching 11% saturation adjacent to the twigs compared with 8% in the standard. The pH of the medium was slightly higher in the standard after 5.4 weeks (pH 8.3-8.4 compared with pH 8.1), and had increased more steeply by 12 weeks than that of the floating system (pH 8.6 compared to pH 8.4).

Sulphate levels were slightly higher in the system with the floating twigs (16.3/14.7mM after 5.4 weeks and 15.7/15.9mM after 12 weeks) than in the standards (14.2/13.9mM after 5.4 weeks and 13.3/14.1mM after 12 weeks). Sulphide levels were higher than the standard after 5.4 weeks (0.25/0.53mM compared to 0.03/0.31mM), but zero within both systems after 12 weeks. Traces of ferrous iron ($\leq$ 0.04mM) were detected in both systems.

The phosphorus concentrations of the medium were higher in the floating system after 5.4 weeks (Table 2.19). Phosphorus levels decreased considerably in the floating system by 12 weeks, but increased in the standards with time. As a result phosphorus concentrations were higher in the standard than in the floating system. Calcium levels decreased with time in both systems, and were higher in the floating systems after both 5.4 and 12 weeks (Table 2.19). Aluminium, iron, manganese and magnesium concentrations were greater in the floating systems after both 5.4 and 12 weeks (Table 2.19).

Despite being allowed to float, all the twigs had sunk to the sediment surface within the first week.

No TRIS data are available for these systems. EDS detected some iron associated with sulphur after 5.4 weeks in the floating system, but no crystals were detected. Calcium, silicon and chloride were also detected. After 12 weeks the same elements were detected, but still no crystals were seen.

Decay system	P (mM)	Ca (mM)	Mg (mM)	Al (mM)	Fe (mM)	Mn (mM)
Floating	0.53	3.0	12.6	0.33	0.53	0.09
(5.4 weeks: 88)	0.59	2.9	12.6	0.25	0.47	0.07
Floating	0.20	2.4	14.3	0.08	0	0.02
(12 weeks: 89)	0.20	2.7	14.6	0.13	0	0.02
Standard	0.34	2.1	11.7	0.06	0.19	0.05
(5.4 weeks: 22)	0.56	2.0	12.2	0	0.05	0.03
Standard	0.67	0.01	11.3	0	0	0
(12 weeks: 24)	0.71	1.1	13.0	0	0	0

Table 2.19. ICP-AES data for open marine systems where twigs were allowed to float, and in standards where the twigs were pushed into the sediment after 12 weeks. Two concentrations are given for each element: the upper one is the concentration just below the air-medium interface, the lower one is the concentration just above the sediment-medium interface.

7b. Effect of sedimentation in open marine systems

A sediment/medium (1:1) mixture (2ml) was added to open marine systems weekly to simulate sedimentation. These systems were studied after 5.4 weeks (90) and 12 weeks (91). These were compared with standards at 5.4 weeks (22) and 12 weeks (24).

After 5.4 weeks, oxygen had penetrated throughout the medium, reaching 9% saturation adjacent to the sediment, increasing to 56% after

12 weeks in the sedimentation systems. The standards remained anoxic adjacent to the twigs, even after 12 weeks. The pH of the medium in the sedimentation systems was similar to that of the standards, at pH 8.2-8.4 compared to pH 8.1 after 5.4 weeks, and pH 8.4-8.5 compared to pH 8.6 after 12 weeks.

Despite weekly additions of sulphate to the medium in the sedimentation systems, sulphate concentrations were lower than in the standards after both 5.4 weeks (13.7/12.9mM compared with 14.2/13.9mM) and 12 weeks (12.2/13.1mM compared with 13.3/14.1mM). Traces of sulphide and ferrous iron were not detected in the replicate sedimentation systems after either 5.4 or 12 weeks. Sulphide and ferrous iron were present in the standard after 5.4 weeks (0.03/0.31mM and 0.04mM respectively), but not after 12 weeks.

Phosphorus concentrations were similar in the sedimentation systems and the standards after 5.4 and 12 weeks, increasing with time in both systems (Table 2.20). Calcium levels were lower in the sedimentation systems after 5.4 and 12 weeks (Table 2.20). Calcium concentrations decreased in both the standards and the sedimentation systems with time. Magnesium levels were considerably higher than in the standard after 5.4 weeks, and concentrations had increased in both systems after 12 weeks (Table 2.20). Iron and manganese levels were similar under both conditions after 5.4 and 12 weeks (Table 2.20). Low levels of aluminium ($\leq$ 0.13mM) were present in the sedimentation systems, but only at the air-medium interface of the standard after 5.4 weeks.

No TRIS data are available for these systems. Unlike the standards where FeSam was detected, none was present in the twigs from the sedimentation systems. Calcium and silicon were detected in the twigs from the sedimentation systems after both 5.4 and 12 weeks.

Decay system	P (mM)	Ca (mM)	Mg (mM)	Fe (mM)	Mn (mM)	Al (mM)
Sedimentation	0.50	2.5	14.4	0.18	0.03	0.04
(5.4 weeks: 90)	0.46	2.3	13.2	0.22	0.03	0.09
Sedimentation	0.60	2.1	16.3	0	0.02	0.13
(12 weeks: 91)	0.59	2.1	16.5	0	0.02	0.13
Standard	0.34	2.1	11.7	0.19	0.05	0.06
(5.4 weeks: 22)	0.56	2.0	12.2	0.05	0.03	0
Standard	0.67	0.01	11.3	0	0	0
(12 weeks: 24)	0.71	1.1	13.0	0	0	0

Table 2.20. ICP-AES data for open marine sedimentation systems and standards after 5.4 and 12 weeks. Two concentrations are given for each element: the upper one is the concentration just below the air-medium interface, the lower one is the concentration just above the medium-sediment interface.

7c. Effect of floating of twigs with sedimentation in open marine systems

Twigs were left to float in systems with sedimentation and dismantled after 5.4 weeks (92) and 12 weeks (93). These were compared with standards at 5.4 weeks (22) and 12 weeks (24).

After 5.4 weeks, the floating/sedimentation system was anoxic for most of the medium, as was the standard. After 12 weeks, oxygen saturation had reached 46% adjacent to the twigs in the floating/sedimentation system, in contrast with the standard which was still anoxic. The pH of the floating/sedimentation systems were only slightly less alkaline than the standards after 5.4 and 12 weeks.

Sulphate concentrations were much lower in the floating/ sedimentation systems than in the standards (22, 24), the systems where the twigs were allowed to float without sedimentation (88, 89) and where sedimentation took place when the twigs were in contact with the

sediment (90, 91) (Table 2.21). Traces of sulphide and ferrous iron are present after 5.4 weeks in both the standard (0.03/0.31mM) and floating/sedimentation system (0.04/0.07mM), but were not detected in either after 12 weeks.

Decay system	Sulphate (mM)
Floating (5.4 weeks: 88)	16.3/14.7
Floating (12 weeks: 89)	15.7/15.9
Sedimentation (5.4 weeks: 90)	13.7/12.9
Sedimentation (12 weeks: 91)	12.2/13.1
Floating/Sed. (5.4 weeks: 92)	7.5/12.6
Floating/Sed. (12 weeks: 93)	7.9/9.1
Standard (5.4 weeks: 22)	14.2/13.9
Standard (12 weeks: 24)	13.3/14.1

Table 2.21. Sulphate concentrations for floating, sedimentation, and floating / sedimentation open marine systems and standards after 5.4 weeks and 12 weeks.

Phosphorus, magnesium and calcium levels were much higher than in the standards (Table 2.22). Phosphorus and magnesium concentrations increased between 5.4 weeks and 12 weeks, while calcium levels decreased. Concentrations of aluminium, iron and manganese were much higher than the standards after 5.4 weeks, but none was detected after 12 weeks (Table 2.22).

Although the twigs were free to float within the medium, they had all sunk to the sediment surface within the first week. No TRIS data are available for the floating/sedimentation systems or the standards. EDS analysis of the plant material revealed a wide range of elements present in the plant material of the floating/sedimentation systems, including

calcium, silicon, magnesium, phosphorus and chloride. No iron or sulphide was present after 5.4 or 12 weeks.

Decay system	P (mM)	Mg (mM)	Ca (mM)	Al (mM)	Fe (mM)	Mn (mM)
Floating/sed.	0	13.5	2.6	0.34	0.54	0.10
(5.4 weeks: 92)	0.12	12.7	2.9	0.36	0.61	0.09
Floating/sed.	0.36	14.0	1.9	0	0	0
(12 weeks: 93)	0.42	13.9	1.9	0	0	0
Standard	0.34	11.7	2.1	0.06	0.19	0.05
(5.4 weeks: 22)	0.56	12.2	2.0	0	0.05	0.03
Standard	0.67	11.3	0.01	0	0	0
(12 weeks: 24)	0.71	13.0	1.1	0	0	0

Table 2.22. ICP-AES data for floating/sedimentation open marine systems and standards after 5.4 and 12 weeks. Two concentrations are given for each element: the upper one is the concentration just below the air-medium interface, the lower one is the concentration just above the medium-sediment interface.

7d. Effect of burial of twigs in open marine systems

Twigs were buried in the sediment of open marine systems which were incubated for 5.4 weeks (94) and 12 weeks (95). These were compared with standards dismantled after 5.4 weeks (22) and 12 weeks (24).

There were considerable differences between the buried twig systems and the standards. Less oxygen had penetrated the burial system after 5.4 weeks but both burial system and standard were still anoxic at the sediment-medium interface. After 12 weeks oxygen saturation in both the burial system and the standard was 8-9% adjacent to the sediment. The pH of the burial system was slightly less alkaline than that of the

standard after 5.4 weeks (pH 8.2 compared with pH 8.3-8.4) and 12 weeks (pH 8.4 compared with pH 8.6-8.7).

Sulphate concentrations were much lower in the buried twig system than the standard after 5.4 weeks (8.0/9.6mM compared to 14.2/13.9mM), but levels increased with time in the burial system so that concentrations were similar under both conditions after 12 weeks (12.6-14.3mM). After 5.4 weeks 0.25mM sulphide was present just above the sediment-medium interface of the buried twig system, compared with 0.03mM just below the air-medium interface and 0.31mM just above the sediment-medium interface in the standard. No sulphide was present in either system after 12 weeks. Ferrous iron was present in the buried twig system (0.13/0.01mM) and the standard (0.04mM) after 5.4 weeks. After 12 weeks, only traces (≤ 0.03mM) were detected in either system.

Phosphorus levels were higher in the burial systems after 5.4 weeks. Between 5.4 weeks and 12 weeks phosphorus concentrations decreased drastically in the burial systems but increased in the standards, so that concentrations were much greater in the standards after 12 weeks (Table 2.23). Concentrations of magnesium were slightly higher than the standard after 5.4 weeks, but were similar after 12 weeks (Table 2.23). Calcium levels were much higher in the burial systems after 5.4 and 12 weeks, decreasing with time in both the burial systems and the standards (Table 2.23). Aluminium, iron and manganese levels were higher in the burial systems after 5.4 weeks, but only traces of all three were present in either system after 12 weeks (Table 2.23).

Decay system	P (mM)	Mg (mM)	Ca (mM)	Al (mM)	Fe (mM)	Mn (mM)
Buried twigs	0.67	12.8	2.5	0.23	0.45	0.08
(5.4 weeks: 94)	0.59	12.4	2.4	0.14	0.42	0.05
Buried twigs	0.14	12.5	1.9	0	0	0
(12 weeks: 95)	0.10	12.4	2.0	0	0	0
Standard	0.34	11.7	2.1	0.06	0.19	0.05
(5.4 weeks: 22)	0.56	12.2	2.0	0	0.05	0.03
Standard	0.67	11.3	0.01	0	0	0
(12 weeks: 24)	0.71	13.0	1.1	0	0	0

Table 2.23. ICP-AES data for buried twig open marine systems and standards after 5.4 and 12 weeks. Two concentrations are given for each element: the upper one is the concentration just below the air-medium interface, the lower one is the concentration just above the medium-sediment interface.

No TRIS data are available for the floating/sedimentation systems or the standards. EDS analysis of the plant material revealed silicon, calcium, iron and some potassium in the buried twigs after 5.4 weeks. After 12 weeks large silicon and calcium crystals were observed. Some iron and sulphur was detected, although no crystals were observed, and aluminium and titanium were also present.

8. Decay by the indigenous bacterial population of the sediment in open marine systems (no added inoculum)

A bacterial inoculum was added to the majority of the standard decay systems to promote bacterial activity within the experiments. To investigate the effect of this inoculum, open marine systems were incubated for 12 weeks with only the indigenous bacterial population in the sediment (25, 26). These systems were compared with others set up

with the same sediment and medium and which contained bacterial inoculum(96, 97).

Without the presence of bacterial inoculum, oxygen saturation reached 22-25%adjacent to the twigs after 12 weeks. Of the systems with inoculum, the oxygen saturation of one was similar to that in the systems without (27% in system 25), while the other had much less oxygen (4% in system 26). The pH of the decay systems without inoculum was ca 0.2 pH units more alkaline than those with inoculum (pH 8.8-8.9 compared to pH 8.6-8.7).

Sulphate concentrations were much higher without added inoculum (21.0-22.5mM) than with inoculum (15.4-17.0mM). No sulphide was detected in either system, and traces of ferrous iron (≤ 0.03mM) were present in both systems.

Phosphorus (≤ 0.22mM), magnesium (11.5-13.4mM) and calcium (≤ 1.9mM) concentrations were unaffected by the presence of inoculum. No aluminium, iron or manganese were present with or without inoculum.

TRIS data are presented in Table 2.24. However, values varied too much between duplicate pairs for any trends to be identified, although as sulphate was higher without inoculum, TRIS should have been lower.

Decay system	AVS (M)	Pyritic S (M)	S° (M)	TRIS (M)
- inoculum (25)	1.3	1.0	0.6	2.9
- inoculum (26)	0.5	1.4	0.3	2.2
+ inoculum (96)	2.3	1.0	0.7	3.9
+ inoculum (97)	1.2	0.9	0.8	2.9

Table 2.24. Sedimentary sulphur concentrations for open marine systems with and without bacterial inoculum after 12 weeks.

EDS analysis of the plant material detected the same range of elements as in the standard open marine time series, both with and without inoculum.

9. Influence of dimensions and headspace of reaction vessel (Duran bottle vs. Jar) in open marine systems

Most of the decay experiments were run in screw-top jars, but the sealed systems had to be run in Duran bottles which could be sealed more effectively. Open marine systems were run as controls for the sealed systems in Duran bottles, and the influence of the dimensions of the decay vessels was investigated to try to explain any anomalies between the open jar systems and the open Durans. Open marine systems were run in with internal dimensions of 55mm x 120mm, a 30mm diameter opening, and a 55mm deep headspace (98, 99), and in screw-top glass jars with internal dimensions of 65mm x 70mm, a 60 mm diameter opening, and a 15mm headspace depth (25, 26).

The dimensions of the reaction vessel had little effect of the chemistry of the decay systems, except for oxygen saturation (Figure 2.11) and sulphate concentrations (Table 2.25). Oxygen saturation reached 21-24% adjacent to the twigs in the jars, but the Durans remained anoxic adjacent to the sediment.

TRIS data (Table 2.25) differed between replicate systems. Except for one of the Duran systems (98), sulphate concentrations were consistent with the TRIS levels i.e. the lowest sulphate concentrations were for the system with the highest TRIS and vice versa.

Decay vessel	SO_4^{2-} (mM)	AVS (M)	Pyritic S (M)	S° (M)	TRIS (M)
Duran (98)	19.4/19.0	0.6	0.8	0.6	2.1
Duran (99)	16.0/16.3	0.8	1.6	0.7	3.1
Jar (25)	21.4/21.2	1.3	1.0	0.6	2.9
Jar (26)	22.5/21.0	0.5	1.4	0.3	2.2

Table 2.25. Sulphate and sedimentary sulphur concentrations for open marine systems run in Duran bottles and glass jars after 12 weeks.

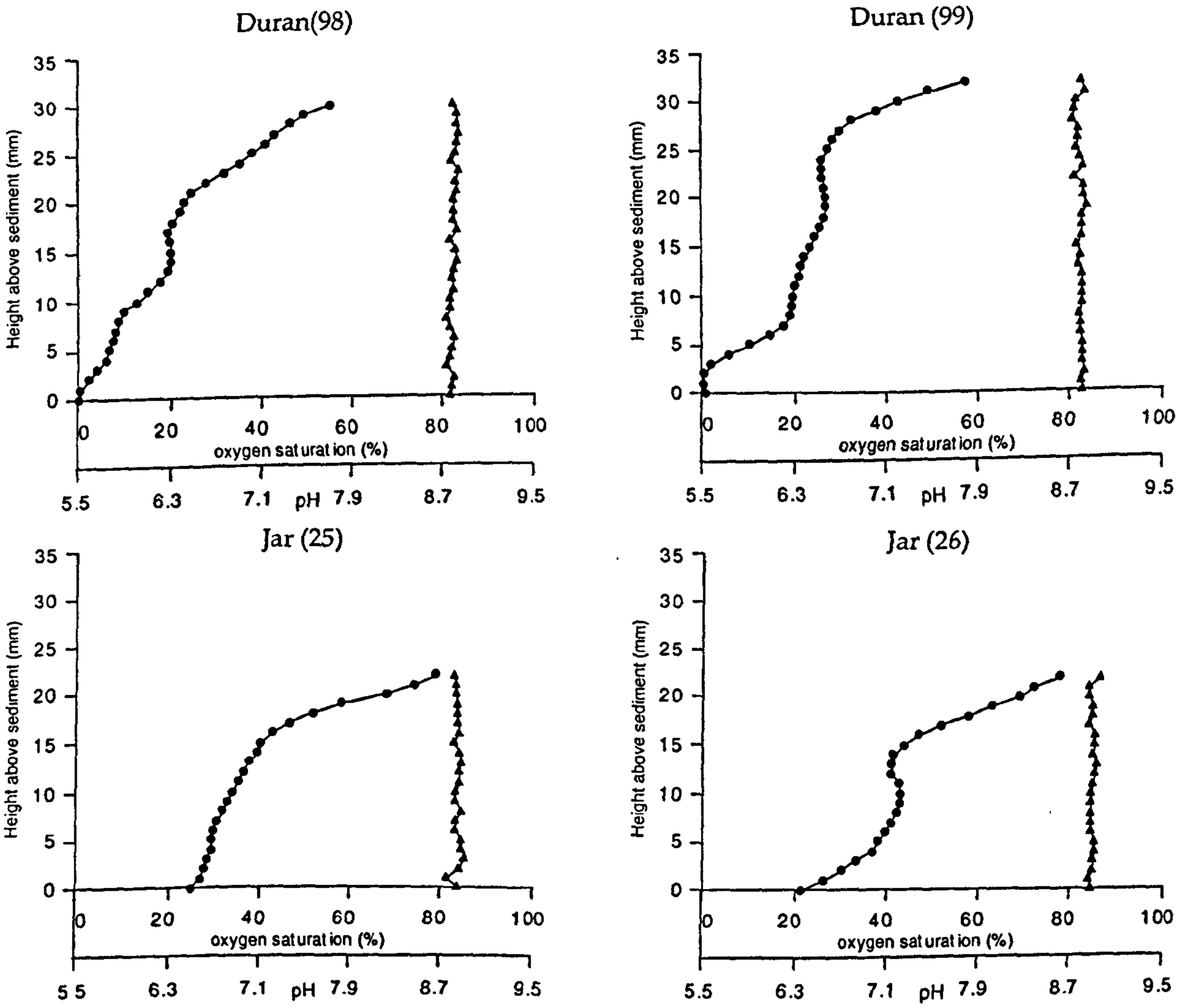

Figure 2.11. Oxygen and pH depth profiles for open marine decay systems in Duran bottles and glass jars. Infilled circles represent oxygen data points and infilled triangles represent pH data points. The highest data points above the sediment represent the air-medium interface.

10a. Effect of salinity: open freshwater systems

Although sulphate reduction is limited under freshwater conditions with low sulphate concentrations and most pyrite fossil beds were deposited under marine conditions, some pyritised plants from freshwater beds have been reported (e.g. Kenrick and Edwards, 1988). Freshwater decay experiments were run to investigate the decay processes which dominate under freshwater conditions. These systems were investigated twice, after 5.4 weeks (100) and 12 weeks (101) and, in a later experimental run, after 12 weeks (102, 103). The starting conditions in these freshwater systems were quite different to those of the marine systems as the sediment, medium and inoculum compositions were different. This must have influenced the development of the decay systems. The two sets of freshwater decay systems resulted in very different chemistries, probably reflecting the different sediment sources, and systems 100 and 101 are therefore treated separately to systems 102 and 103.

After 5.4 weeks, the medium of system 100 was anoxic below 7mm. After 12 weeks system 101 was also anoxic below 7mm (Figure 2.12). After 5.4 weeks the pH was constant with depth at ca 8.5. After 12 weeks, a gradient had formed, ranging from pH 7.6 at the medium surface to pH 6.0 adjacent to the sediment (Figure 2.12).

No sulphate was present in the starting medium and none was detected after 5.4 or 12 weeks. Sulphide levels were 0.28/0.08mM after 5.4 weeks, but had decreased to 0.08/0.06mM after 12 weeks. Ferrous iron levels dropped from 2.4/2.3mM after 5.4 weeks to 1.7mM after 12 weeks.

Phosphorus concentrations increased from 5.4 weeks to 12 weeks (0.53/0.46mM to 0.63/0.66mM) as did calcium levels (16.3/14.0mM to 22.4/21.2mM). Iron levels decreased slightly with time, from 1.79/1.64mM to 1.72/1.46mM, and magnesium levels remained constant

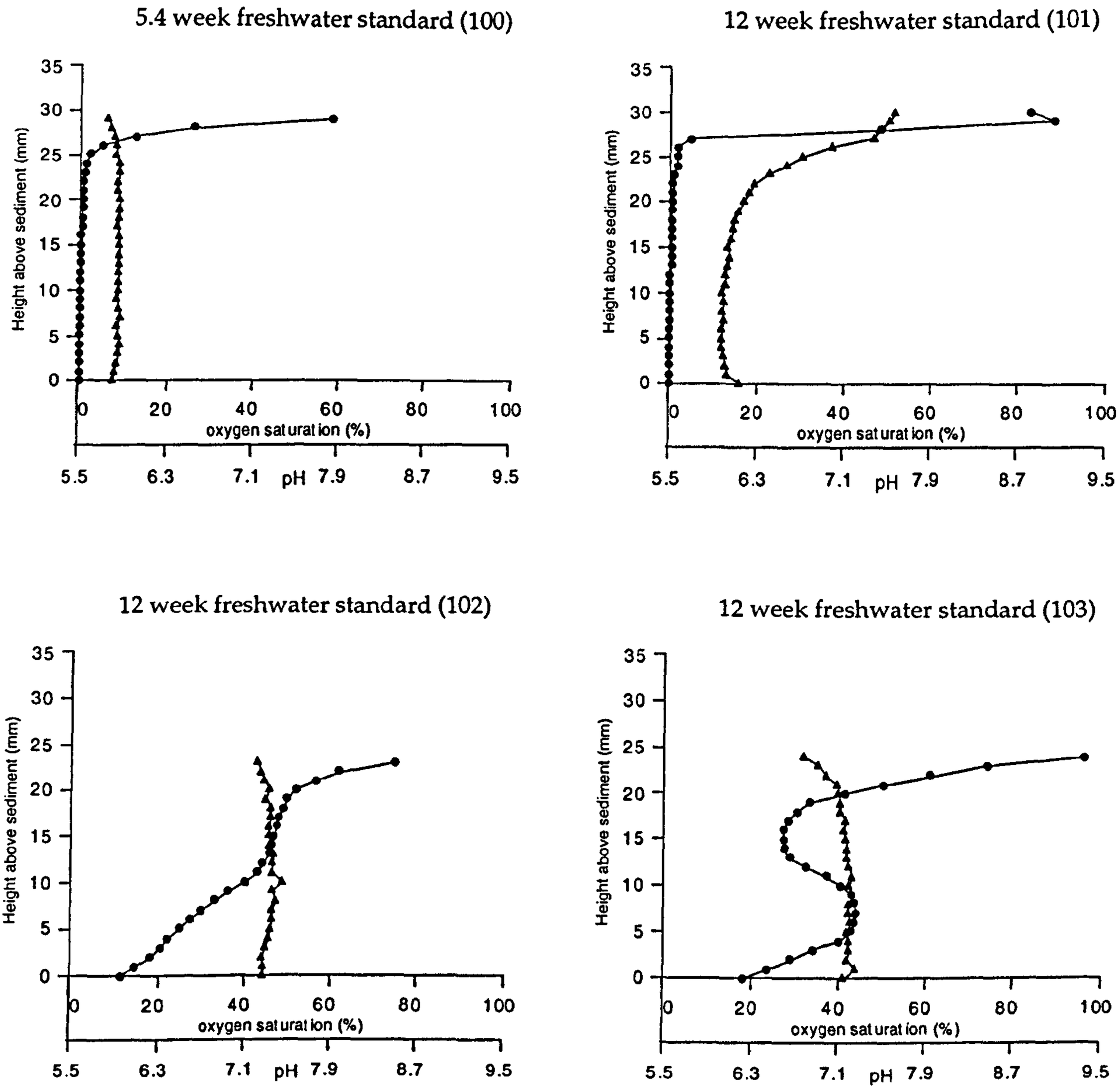

Figure 2.12. Oxygen and pH depth profiles for open freshwater decay systems. Infilled circles represent oxygen data points. Infilled triangles represent pH data points. The highest data points above the sediment represent the air-medium interface.

at 4.2-5.3mM. Low levels of manganese were detected after 5.4 weeks (0.11/0.10mM), but none remained after 12 weeks. Aluminium was not detected at either stage of the experiment, except for 0.04mM just below the air-medium interface in the standard after 12 weeks.

Very few crystals were observed within the plant material by EDS. The only elements which were identified were calcium and silicon. Very few crystals were seen, and those that were filled entire cells and consisted of either calcium or silicon, but not mixtures of the two.

The chemistry of freshwater open systems 102 and 103 differed substantially from that of system 101 after 12 weeks.

Oxygen saturation of systems 102 and 103 reached 4-26% adjacent to the twigs, and the pH of the medium was ca 7.2 after 12 weeks (Figure 2.12).

Sulphide was not detected, but 1.3mM of sulphate and 0.02mM of ferrous iron were present in the medium of both replicate systems.

Calcium (1.4-1.7mM) and magnesium (0.6-0.7mM) concentrations were lower than in the other freshwater systems. Iron (0.8mM) was only detected at the sediment-medium interface of system 103. Phosphorus, aluminium and manganese were not detected in either of the replicate freshwater systems.

As in the other freshwater systems (100, 101), EDS detected only calcium and silicon in the plant material.

10b. Effect of sulphate availability in open freshwater systems

A sulphate agar layer was placed beneath the sediment to release low levels of sulphate into the deeper sediments of freshwater open systems (104, 105). The systems were dismantled after 12 weeks, and compared with standards (102, 103).

Oxygen saturation was considerably greater with the added sulphate agar layer, reaching 78-84% saturation adjacent to the twigs compared with only 4-26% oxygen in the standards. The presence of extra sulphate

also forced the pH more alkaline by up to 1 pH unit (pH 7.9-8.2 compared with pH 7.1-7.3).

Sulphate concentrations with and without the sulphate layer were identical (1.2-1.3mM). No sulphide was detected in either the sulphate agar layer systems or the standards. Trace levels of ferrous iron (≤ 0.02mM) were detected under both experimental conditions.

Calcium concentrations were slightly elevated with the presence of the sulphate agar layer (1.9-2.1mM compared with 1.4-1.7mM). Magnesium levels were very slightly reduced with the presence of the sulphate agar layer (0.6mM compared with 0.6-0.7mM). Iron was only detected just below the air-medium interface of one standard freshwater system (0.8mM in system 103). Traces of manganese (≤ 0.01mM) were detected with or without the sulphate agar layer. Neither phosphorus nor aluminium were detected in either the systems with or without additional sulphate.

Despite the identical sulphate concentrations, the replicate sulphate agar layer systems had differing TRIS values, as do the two standards, making interpretation of the results difficult (Table 2.26). Levels of all sedimentary sulphur pools were low (≤ 1.0M).

Decay system	AVS (M)	Pyritic S (M)	S° (M)	TRIS (M)
+ sulphate (104)	0.1	0.1	0.2	0.4
+ sulphate (105)	0.3	0.3	0.4	1.0
Standard (102)	0.3	0.5	0.2	0.9
Standard (103)	0.2	0.3	0.1	0.6

Table 2.26. Sedimentary sulphur data for open freshwater systems with and without a sulphate agar layer after 12 weeks.

EDS analysis of the plant material from the freshwater systems with a sulphate agar layer revealed only small crystals of calcium and silicon.

11. Closed freshwater time series

Closed freshwater systems were run to investigate the processes taking place when the systems were kept anoxic, and were analysed after 1 week (106, 107), 2 weeks (108, 109), 4 weeks (110, 111), 9 weeks (112, 113) and 12 weeks (114, 115).

The closed freshwater systems provided very little information due to large variations in medium chemistry, both over time and between replicates. This may have been due to the fact that some of the systems were not completely sealed, allowing some gaseous diffusion into and out of the system. In comparison with the open freshwater system at 12 weeks (101), the pH of the closed system was ca 1.5 pH units more alkaline adjacent to the twigs (pH 7.1 and pH 7.6 in the closed systems compared with pH 6.0-6.1 in the open system). Iron, magnesium and calcium levels were all considerably lower in the closed systems, and sulphide levels were also slightly lower (Table 2.27). Otherwise, the chemistry of the closed and open systems after 12 weeks was similar .

Decay system	Fe (II) (mM)	Fe (mM)	Mg (mM)	Ca (mM)	S^{2-} (mM)
Closed	0.35	0.36	3.3	6.3	0
(114)	0.29	0.38	3.5	6.8	0.01
Closed	0.67	0.21	1.6	6.5	0
(115)	0.68	0	0.3	5.8	0
Open	1.7	1.72	5.3	22.4	0.08
(85)	1.7	1.46	4.2	21.2	0.06

Table 2.27. Iron, magnesium, calcium and sulphide concentrations for closed and open freshwater systems after 12 weeks. Two values are given

for each ion or element for each decay system: the upper one is the concentration of the species just below the air-medium interface, the lower one is the concentration just above the sediment-medium interface.

12a. Effect of sealing marine systems

Sealed marine experiments were run to investigate the processes which occurred when oxygen could not enter the decay systems. This was expected to influence the bacterial processes involved and the mechanisms of pyrite formation.

Sealed marine Durans were incubated for 12 weeks (116, 117), 18 weeks (118, 119) and 24 weeks (120, 121). Open marine Durans were run as controls for 12 weeks (122, 123) and 24 weeks (124, 125).

All sealed marine systems were anoxic. After 12 weeks one of the open systems was anoxic immediately adjacent to the sediment (122) whereas the oxygen saturation had reached 2.5% adjacent to the sediment in the other system (123) (Figure 2.13a). After 24 weeks both open systems were anoxic adjacent to the sediment (124, 125) (Figure 2.13b).

After 12 weeks, the sealed systems had a pH of ca 7.2, in comparison with pH 9.0 in the open systems (Figure 2.13a). The pH of the sealed systems decreased to ca 6.7 after 18 weeks and remained constant. The pH of the open systems also decreased, reaching pH 8.6 (124) and pH 8.4 (125) after 24 weeks (Figure 2.13b).

Sulphate was not detected in any of the closed systems, but was present at concentrations of 11.7-12.8mM after 12 weeks in the open systems, decreasing slightly with time to 6.9-10.3mM. Sulphide levels reached 4.3-7.7mM in the closed systems after 12 weeks, compared with traces of less than 1mM in the open systems. Sulphide concentrations decreased from 0.37-1.30mM after 12 weeks to 0.04-0.19mM after 24 weeks

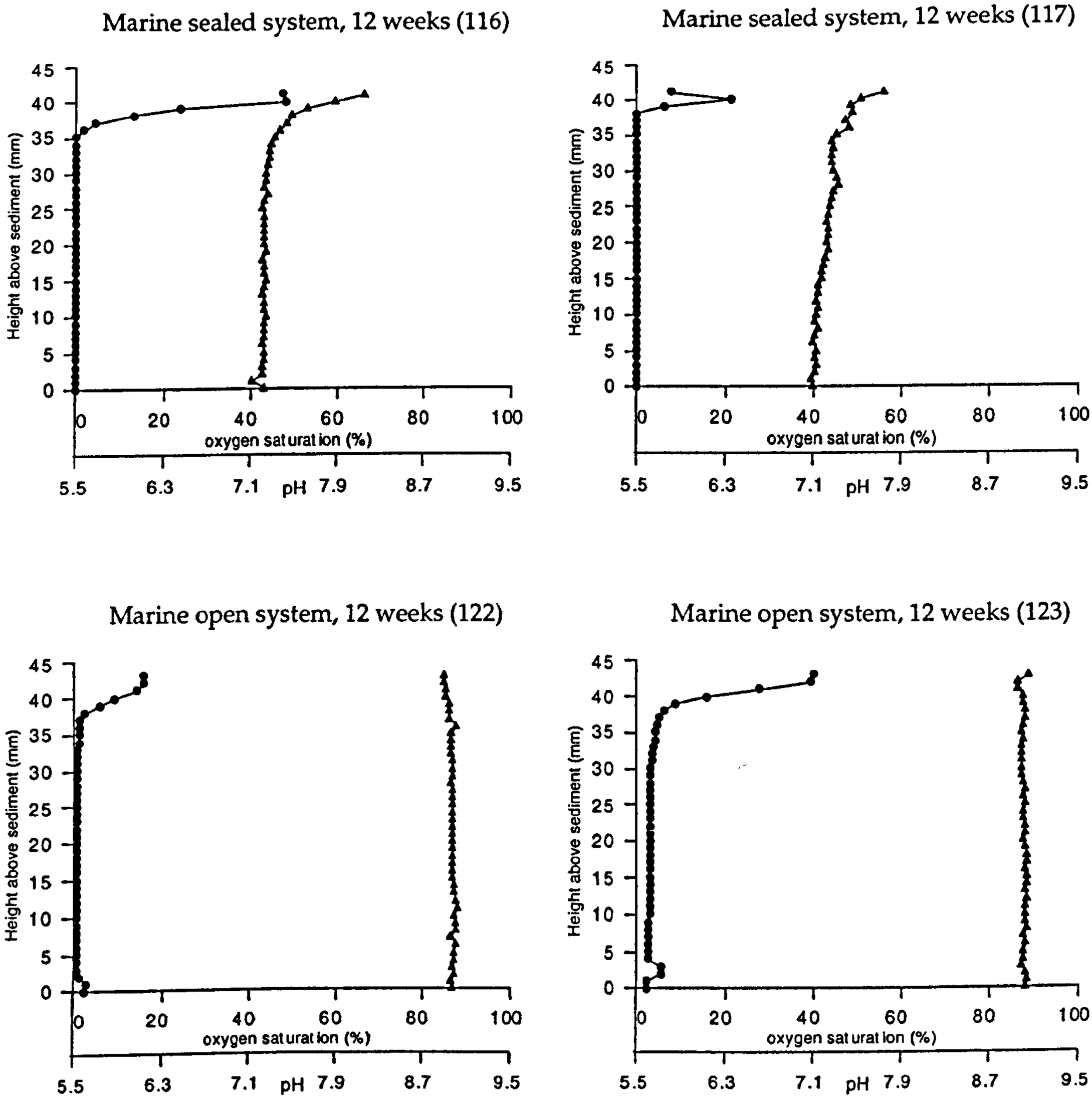

Figure 2.13a. Oxygen and pH depth profiles for sealed and open marine systems after 12 weeks. Infilled circles represent oxygen data points and infilled triangles represent pH data points. The highest data points above the sediment represent the air-medium interface.

in the open systems, and from 4.3-7.7mM after 12 weeks to 0.2-3.5mM in the sealed systems. Ferrous iron was not detected in either the open or sealed systems.

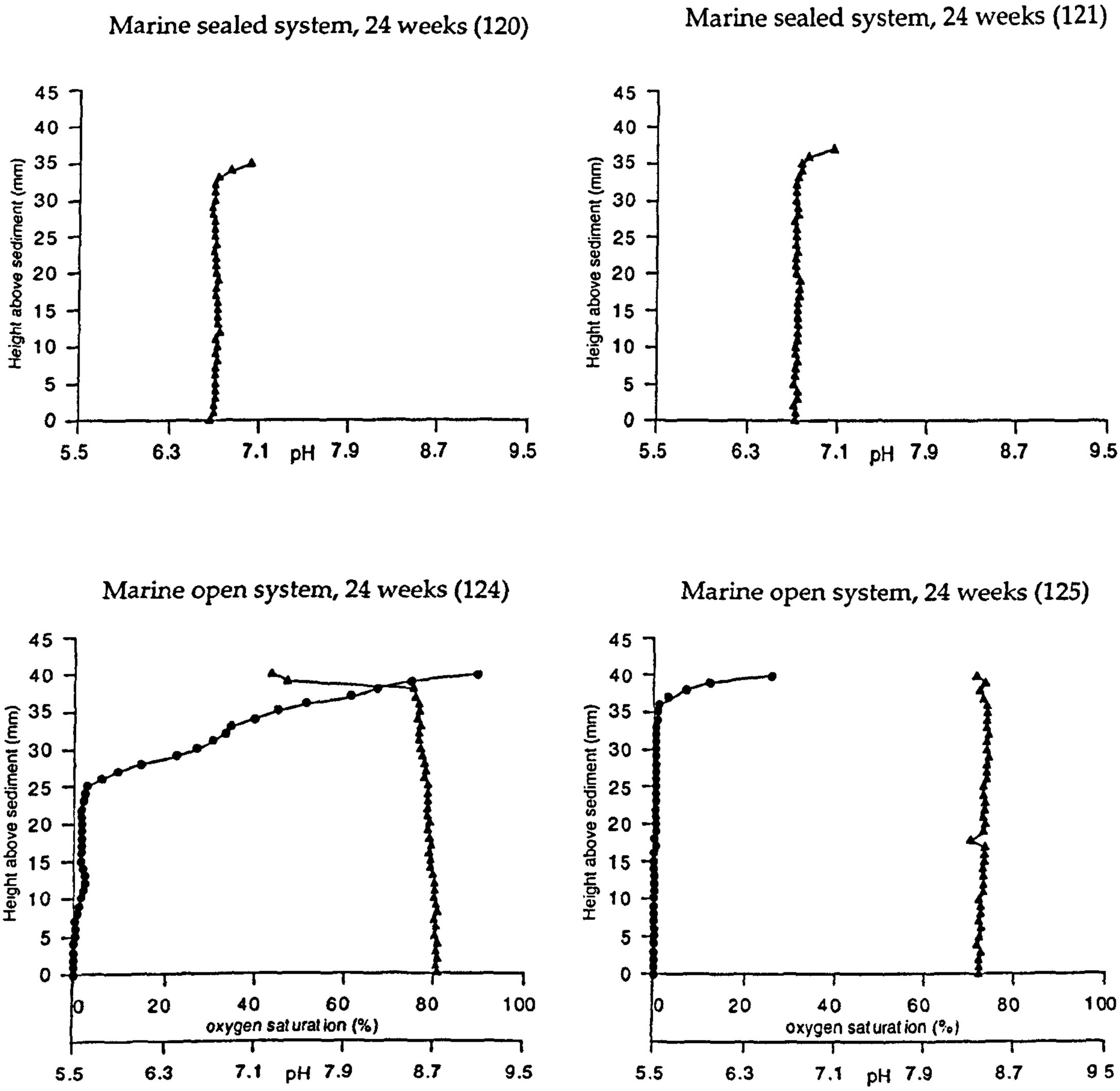

Figure 2.13b. Oxygen and pH depth profiles for sealed and open marine systems after 24 weeks. Infilled circles represent oxygen data points and infilled triangles represent pH data points. The highest data points above the sediment represent the air-medium interface.

Phosphorus levels were high in the sealed systems after 12 weeks, at 1.84-1.99mM. Concentrations of phosphorus decreased between 12 and 18 weeks (1.42-1.57mM), and then remained constant in the sealed systems (1.57-1.73mM after 24 weeks). Phosphorus levels in the open systems

appeared unchanged with time (0.22-0.47mM). Calcium levels were similar in both open and sealed systems after 12 weeks at 1.7-2.0mM and 1.6-2.3mM respectively, and had decreased to less than 0.05mM in both after 24 weeks. Magnesium levels were slightly higher in the sealed systems than the open ones after 12 weeks (14.9-15.6mM and 12.2-13.7mM respectively) and remained constant with time. Low levels of manganese (≤ 0.07mM) were detected at 12, 18 and 24 weeks in the sealed systems, but not in the open ones. Traces of aluminium (≤ 0.03mM) were detected in both the open and sealed systems. Iron was not present in the open systems and was only detected in the sealed systems after 24 weeks (≤ 0.02mM).

A build-up of gas in the closed systems increased the pressure in the Durans so that the 'O'-ring sealed stoppers were pushed upwards, and were only held in place by the screw-lids. On removal of the lids after 12 weeks, the release of gas, in particular from the sediment, forced much of the sediment and occasionally some of the twigs upwards into the water column. This gas was identified as mainly methane by gas chromatography. The pressure of the closed systems increased with time.

No TRIS data are available for any of the sealed systems. The sediment was dark grey in the sealed systems and black in the open systems. Silicon, calcium and possibly some phosphorus were detected by EDS in the surface of the twigs from the sealed systems. A suite of elements including calcium, silicon and magnesium were detected on the surface of the twigs in the open systems, but no iron or sulphide was present. These minerals did not change with time in either the open or sealed systems with time.

12b. Organic matter availability in sealed marine systems: effect of adding extra plant material

Sealed marine systems were opened and additional plant material was added to continue the production of decay products and to introduce a small amount of oxidant to aid in the transformation of iron monosulphide to pyrite.

Two sealed marine systems were opened briefly after 12 weeks and six additional *Platanus* twigs added. The systems were resealed and left for a further 12 weeks (126, 127). Replicate systems were opened for the same time period and resealed without any plant material being added as a control (128, 129). These systems were compared with standard sealed marine systems (120, 121) after 24 weeks.

The only difference observed between the systems with added plant material, the controls, and sealed standards was in the phosphorus concentration. Phosphorus levels were highest with the added plant material (2.00-2.32mM) and were slightly higher in the opened controls (1.62-1.72mM) than in the sealed standards (1.57-1.64mM).

Silicon and aluminium, along with some magnesium, chloride and calcium, was detected on the surface of the twigs that had been in the system since the start of the experiment. Low levels of phosphorus, magnesium and some iron were detected on the surfaces of the additional twigs.

12c. Effect of organic material reactivity in sealed marine systems

The reactivity of organic matter was investigated in open marine systems using a range of different plant species with different structures and compositional tissues. To investigate this effect under sealed marine systems, the fern *Cyathea* was chosen as a decay organism due to its cellulose-based composition in comparison with the lignified woody

angiosperm, plane. Six *Cyathea* twigs were decayed in sealed marine systems for 12 weeks (130, 131) and 24 weeks, instead of plane (116,117). However, the mass of plane twigs and *Cyathea* twigs differs considerably, and so less organic matter was effectively available in the *Cyathea* systems than in the plane ones.

The difference in plant material did not affect the chemistry of the system greatly. After 12 weeks, all systems were anoxic. The pH of the *Cyathea* systems (pH 6.5-6.7) was ca 0.5 pH units lower than that of the plane systems (pH 7.1-7.3).

Sulphate was not present in either system after 12 weeks. Sulphide levels ranged from 4.3-7.7mM and ferrous iron concentrations were ≤0.02mM in both the *Cyathea* and plane systems.

Phosphorus levels were lower tin the *Cyathea* systems than in the plane systems (1.49-1.67mM compared with 1.84-1.99mM), and calcium levels were higher (2.6-2.9mM compared with 1.6-2.3mM). Manganese and magnesium levels appeared unaffected by the difference in organic matter, at ≤ 0.04mM and 13.9-15.6mM respectively. Traces of aluminium were present in both systems (≤ 0.08mM for *Cyathea* and ≤ 0.02mM for plane). Iron were not detected in either system.

There was a substantial build-up of pressure in the *Cyathea* systems which caused mixing of the sediment and twigs with the medium on opening after 12 weeks. The pressure increased with time, and forced the bottom out of one of the *Cyathea* systems intended for dismantling after 24 weeks after only 14 weeks. The other *Cyathea* system was dismantled shortly afterwards to prevent another explosion, but was not analysed.

No EDS data are available for the *Cyathea* twigs as the plant material was too soft to section and mount for SEM analysis.

12d. Abiological changes in sealed marine systems

Effect of sterilisation

Sealed marine systems were irradiated to investigate the abiological changes within the aqueous systems. These systems were analysed after 12 weeks (132, 133) and 24 weeks (134, 135), and compared with standard sealed marine systems (116, 117 after 12 weeks; 120, 121 after 24 weeks).

All sealed systems were anoxic. The pH of the sterile systems was unchanged from the starting pH (7.5) after 12 weeks, compared with a slight decrease in pH to 7.2 in the non-sterile standards. After 24 weeks the sterile systems were still slightly alkaline at pH 7.1-7.2, compared with the standards at pH 6.7.

Sulphate levels were unchanged from the starting medium (ca 29.5mM) in the sterile systems (27.3-36.2mM), but none was present in the non-sterile standards after either 12 or 24 weeks. Sulphide was not present in the sterile systems, but was detected in the non-sterile standards (4.3-7.7mM after 12 weeks, 0.2-3.5mM after 24 weeks). Only traces of ferrous iron ($\leq$ 0.04mM) were detected in the sterile and non-sterile systems.

Phosphorus concentrations were much lower in the sterile systems than the non-sterile standards after 12 weeks (0.86-0.99mM and 1.84-1.99mM respectively) and decreased with time under both sterile and non-sterile conditions to 0.72-0.78mM and 1.57-1.73mM respectively. Calcium levels were slightly lower in the sterile systems (1.6-2.3mM compared with 2.9-3.4mM) and decreased with time to $\leq$ 0.3mM in both systems. Magnesium concentrations were similar in the sterile and non-sterile systems at 12.5-1.6mM and were unchanged with time. Manganese concentrations were $\leq$ 0.08mM in the sterile and non-sterile systems after 12 and 24 weeks. Iron and aluminium were not detected in either system at any stage.

After both 12 and 24 weeks the irradiated sediment retained its fresh brown colour compared to the non-sterile sediment which had turned black. There was no build-up of gas developed in the sterile systems. After 12 weeks the only crystals observed on the surface of the plant material from the sterilised systems were sodium chloride, which were found mainly on the pith cell walls. After 24 weeks silicon and low levels of aluminium and iron were also detected throughout the plant material, although no crystals were observed.

Effect of sterilisation of sealed marine systems with added sulphide

Sulphide (2mM) was added to marine systems before sealing and irradiating to stimulate the reducing-conditions produced by bacterial decay, allowing the biological and abiological effects on iron sulphide formation to be investigated. Sealed irradiated marine systems containing sulphide (2mM) were dismantled after 12 weeks (136, 137) and 24 weeks (138, 139) and were compared with sterile systems without added sulphide (132, 133 after 12 weeks; 134, 135 after 24 weeks).

All the irradiated systems were anoxic. After 12 weeks the sulphide sterilised systems had pH gradients ranging from pH 7.7-7.9 at the air-medium interface to 7.3-7.4 adjacent to the sediment compared with a constant pH of 7.5 in the sterile systems without sulphide. After 24 weeks the pH of the sulphide systems was constant with depth at ca 7.2-7.3, compared with 7.1-7.2 in the sterile systems without sulphide.

Sulphate concentrations were slightly lower in the sulphide systems (19.9-27.6mM) than in the sterile systems without sulphide (27.3-36.9mM) but remained constant in both with time. No sulphide was detected after 12 or 24 weeks either with or without sulphide. Up to 0.05mM ferrous iron was present in the sulphide sterile systems, compared with ≤ 0.04mM in the sterile systems without sulphide.

Phosphorus levels were unaffected by the presence of sulphide, at 0.86-0.88mM after 12 weeks, decreasing slightly to 0.68-0.80mM after 24 weeks. Magnesium (11.5-12.3mM) and calcium (1.4-2.5mM) levels were slightly lower in the sterilised systems with sulphide compared to the sterile systems without sulphide (12.8-13.9mM and 2.9-3.4mM respectively) after 12 weeks. The magnesium levels remained constant with time, as in the sterile systems without sulphide, but calcium concentrations dropped to ≤ 0.3mM in both the sterile and non-sterile systems after 24 weeks. Manganese levels were identical in both systems, at ≤ 0.09mM. A maximum of 0.05mM iron was detected in the sulphide sterile systems, compared with ≤ 0.02mM in the sterile systems without sulphide. Aluminium was only detected at the sediment-medium interface of one sulphide sterile system after 12 weeks (0.06mM).

After 12 and 24 weeks the sediment retained its fresh brown colour. There was no build up of gas. EDS analysis was the same as for the sterile systems without sulphide.

12d. Effect of salinity: sealed freshwater systems

Sealed freshwater systems were incubated for 12 weeks (140, 141) and 24 weeks to investigate the effect of prolonged anoxia on the bacterial and geochemical processes within freshwater systems.

The sealed freshwater systems were anoxic after 12 weeks, with a pH of 6.8-6.9. No sulphate was present, and only traces of sulphide (0.1mM) and ferrous iron (<1mM) were detected. The concentrations of phosphorus (0.98-1.60mM), aluminium (≤ 0.13mM), iron (0.40-0.98mM), magnesium (2.2-3.2mM) and calcium (4.1-5.9mM) differed considerably between the duplicate freshwater systems.

As with the *Cyathea* marine systems, there was an intense build-up of pressure within the sealed freshwater systems within 12 weeks. Those

intended for dismantling after 24 weeks were dismantled at the same time as the *Cyathea* system exploded (14 weeks) to prevent similar explosions and were not analysed.

No TRIS data are available for the sealed freshwater systems.

Only crystals containing calcium and silicon were observed within the plant material from the sealed freshwater systems. These crystals were mainly distributed within the pith parenchyma cells.

12e. Effect of light on sealed freshwater systems

To investigate whether photosynthesis was taking place within the decay systems, sealed freshwater systems were kept under a Grow-Lux light for 8 hours a day for 9 weeks (142, 143) and compared with identical decay systems which had been kept in the dark (144, 145). As this was to check to photosynthesis, only oxygen, pH and sulphide were measured. No differences were observed between the light and dark decay systems.

Morphological Results

Fresh *Platanus* material is presented in Figures 2.14A-C. Figure 2.14A shows a cross-section of a plane stem. In the centre of the twig is the pith parenchyma (P). Exterior to this lies the xylem (X), through which run the rays (R). The vascular cambium (VC) is a thin layer of parenchyma cells located between the xylem and the phloem (Ph). Exterior to the phloem lies the bark (B). The structure of plant stems has been discussed previously in Chapter 1 (pages 25-34).

Figure 2.14B shows pith parenchyma cells with intact cell walls, little or no intercellular spaces, and amyloplasts (starch storage organelles, Am) filling the cells. Figure 2.14C shows rays (R) running through the xylem, which consists of wide vessels (V), fibres and tracheids.

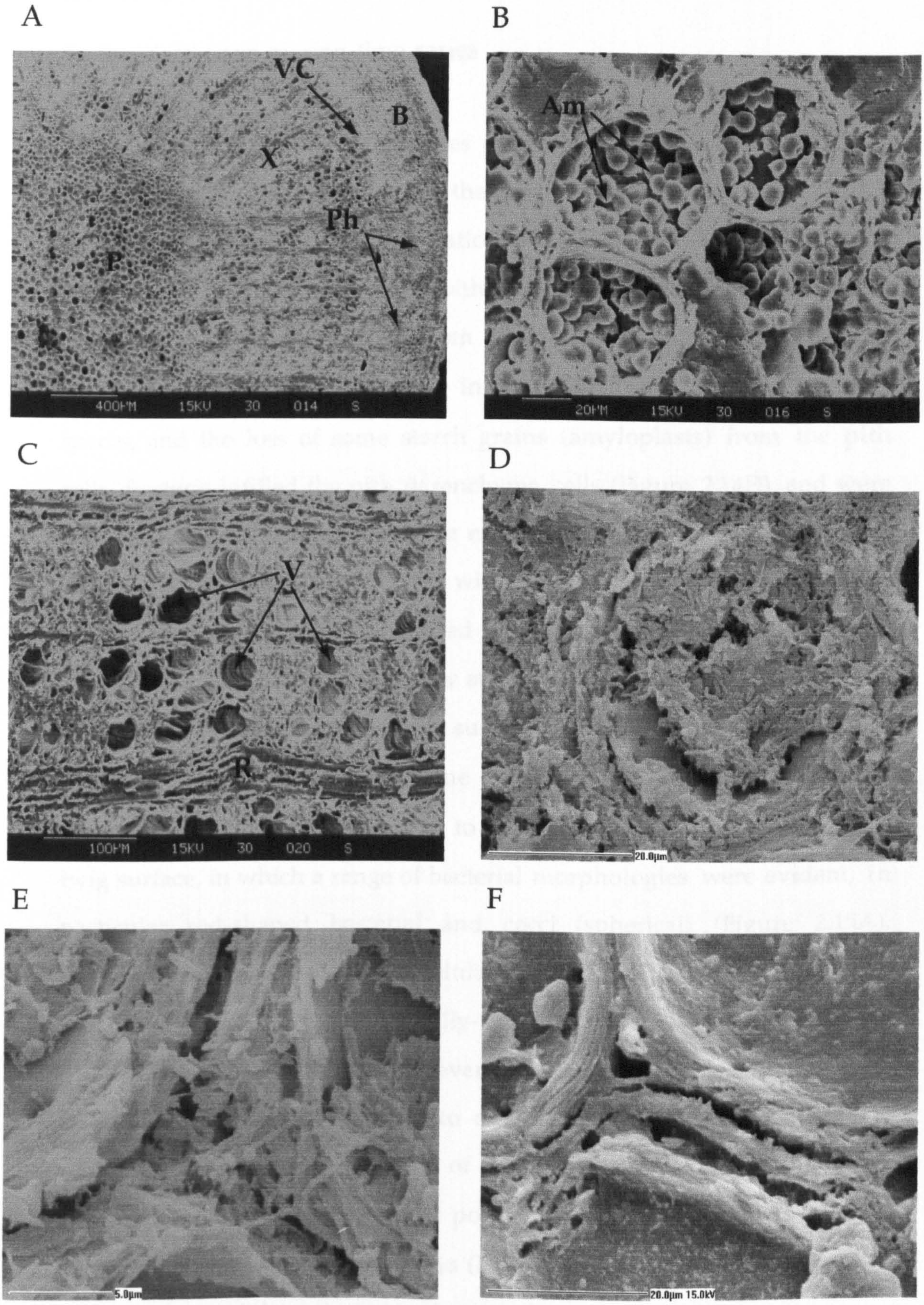

Figure 2.14. A: Cross section of fresh *Platanus* stem (P: pith; X: xylem; B: bark; VC: vascular cambium; Ph: phloem). B: Pith cells in fresh *Platanus* containing amyloplasts (Am). C: Xylem in fresh *Platanus*, including rays (R) and vessels (V). D: Bacteria infilling pith parenchyma cell after 1-2 weeks incubation in open marine systems. E: Enlargement of intercellular spaces and bacterial attack after 1 week of decay. F: "Layering" of pith parenchyma cell wall after 1 week of decay under open marine conditions.

1a. Standard open marine time series

SEM analysis

SEM analysis of the cut surfaces of the plant material showed that decay was well under way within the first week of the experiment. This was evidenced by the partial separation of the bark and the phloem from the central tissues (xylem and pith) along the line of the vascular cambium, by the pulling apart from each other of some pith cell walls which also resulted in the increase in the area of some pith intercellular spaces, and the loss of some starch grains (amyloplasts) from the pith cells. Bacteria infilled the pith parenchyma cells (Figure 2.14D), and were present along the cell walls and at enlarged intercellular spaces (Figure 2.14E). Bacteria were less common within the xylem than in the pith, but where they were present they tended to be concentrated along the rays.

After the second week, very few starch granules remained within the open pith parenchyma cells on the surface of the twig. The pith cell walls had pulled apart further, and some walls appeared flaky and "layered" (Figure 2.14F). Bacteria had begun to form a thick mat over parts of the twig surface, in which a range of bacterial morphologies were evident, in particular rod-shaped bacterial and cocci (spherical) (Figure 2.15A). Bacteria were common at intercellular junctions (Figure 2.15B). Strands and films, presumed to be bacterially-produced, formed across part of the pith surface, and the films often covered cell walls and lined cells (Figure 2.15C). The phloem had begun to disintegrate due to bacterial attack, resulting in increased separation of the bark from the rest of the twig. The xylem became more densely populated with bacteria, which were heavily concentrated along the rays (Figure 2.15D). Bacteria also began to colonise some of the xylem vessels.

After week 3, almost the entire pith was covered with a mat of bacteria, so that the cell walls and the contents of the cells were largely

A

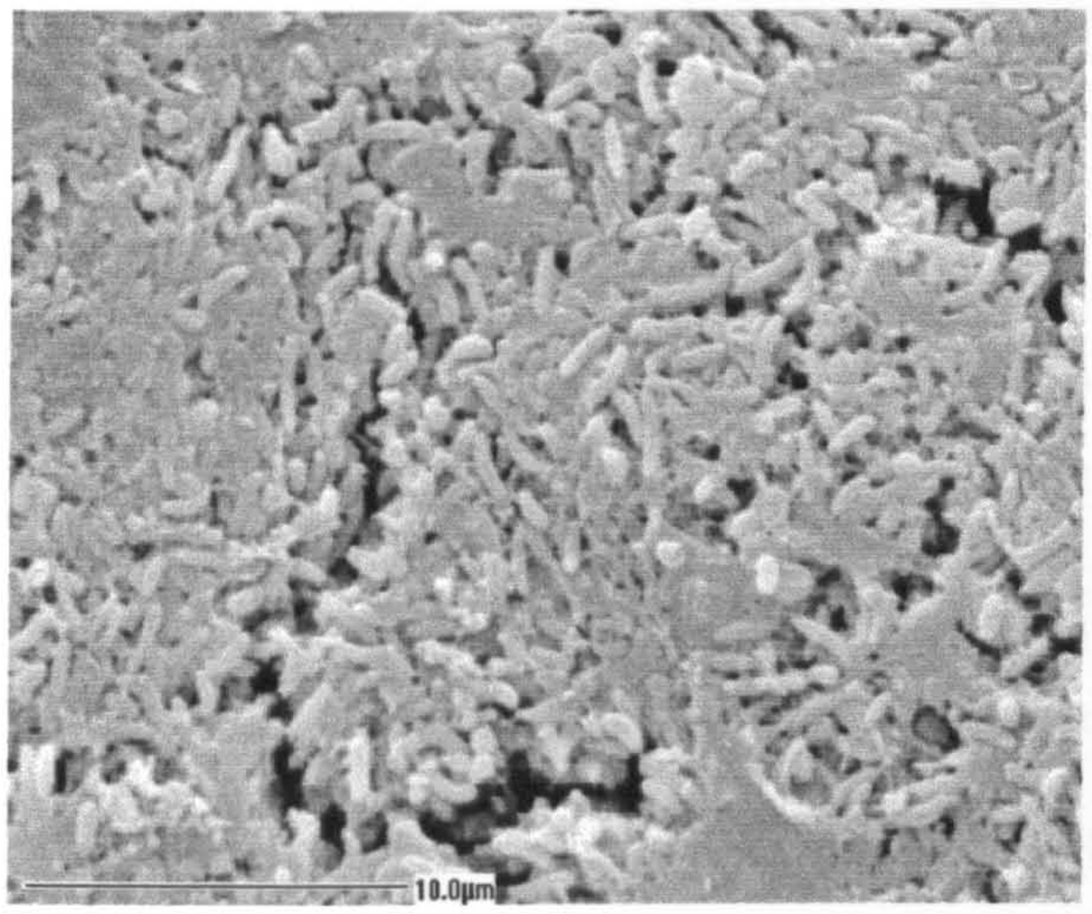

B

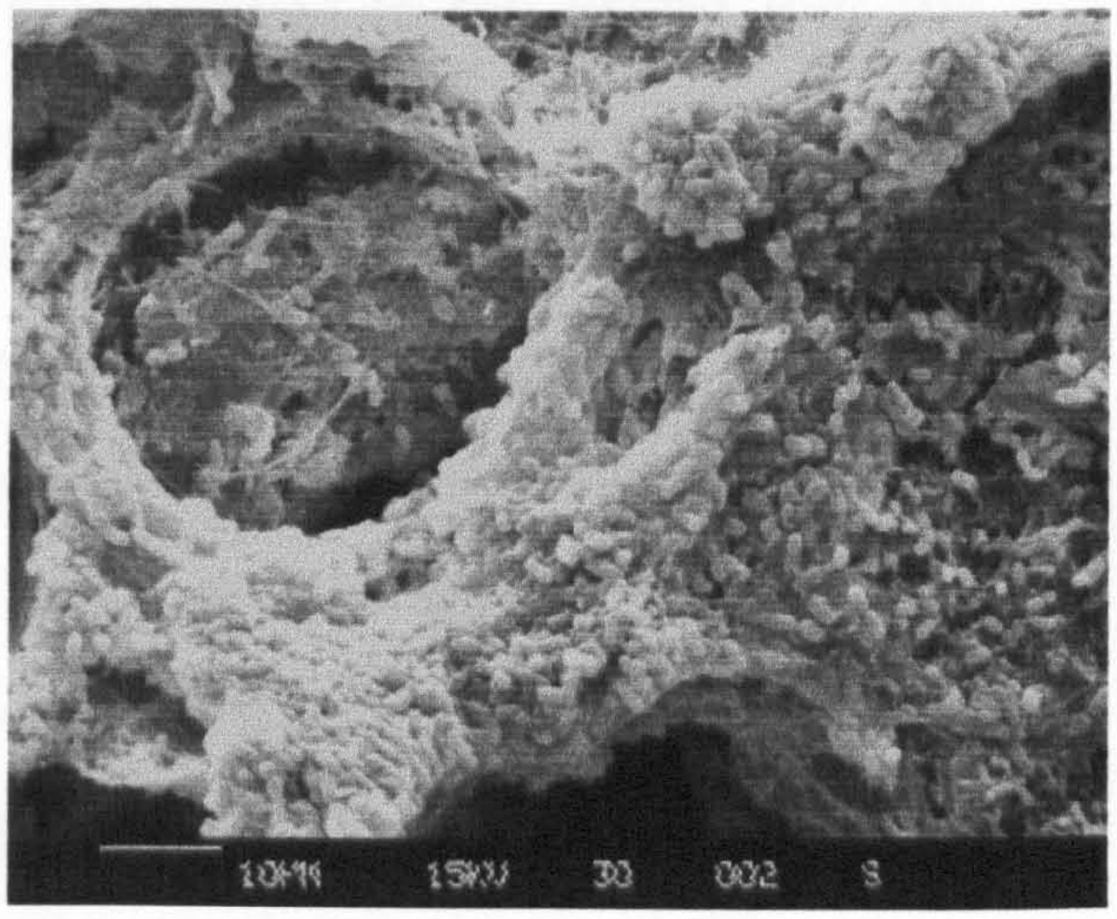

C

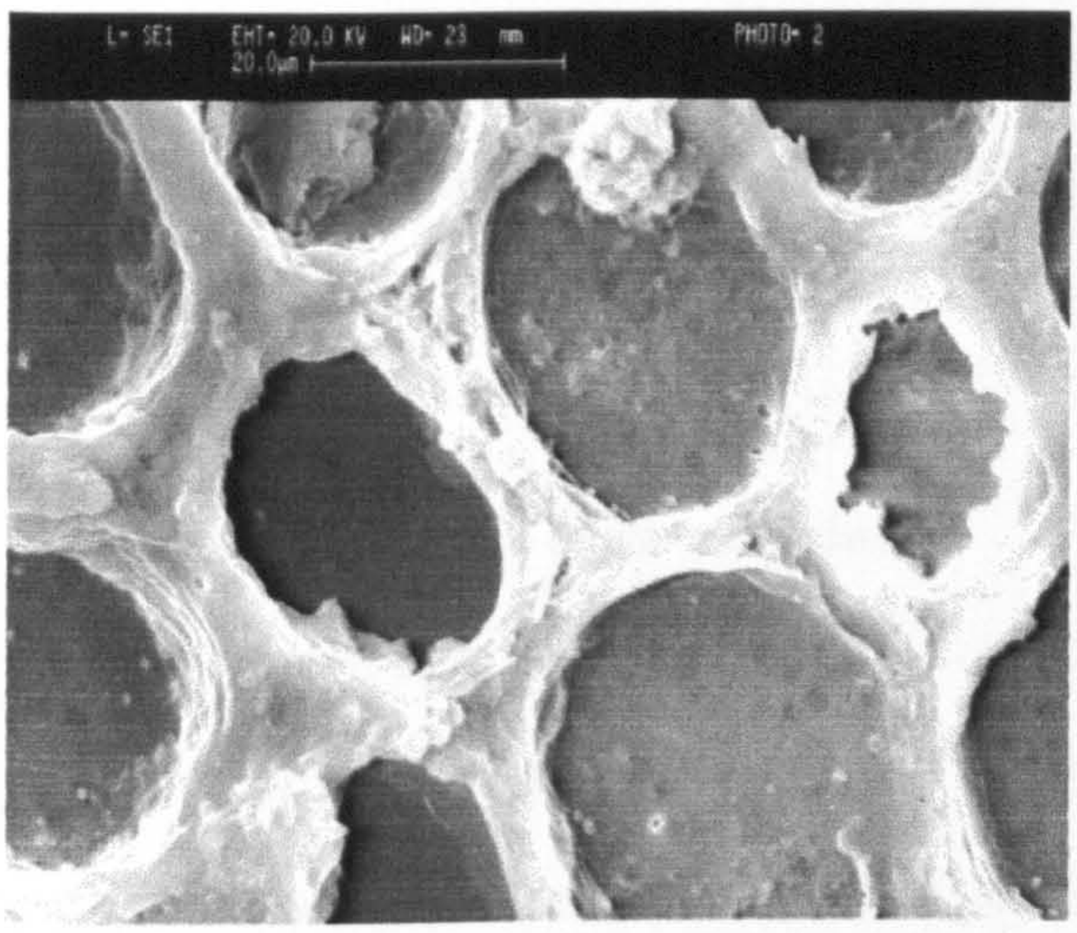

D

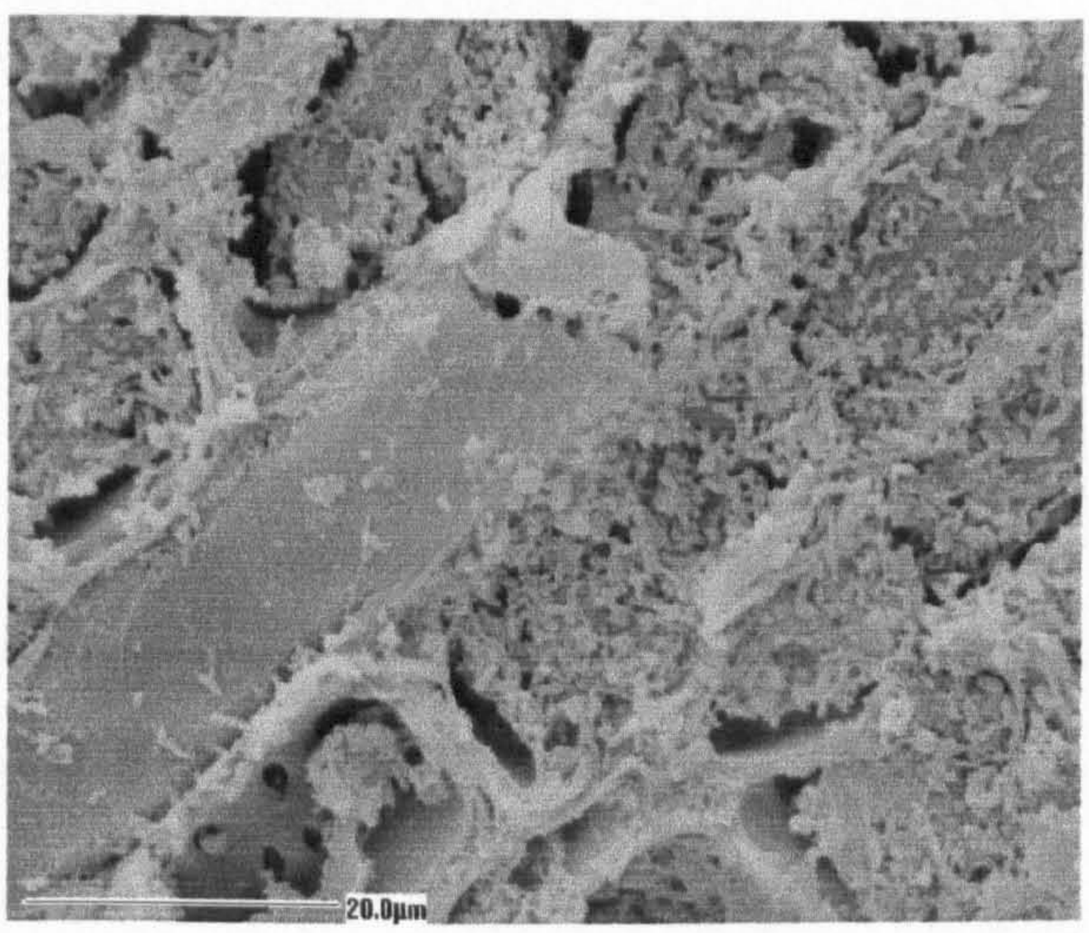

E

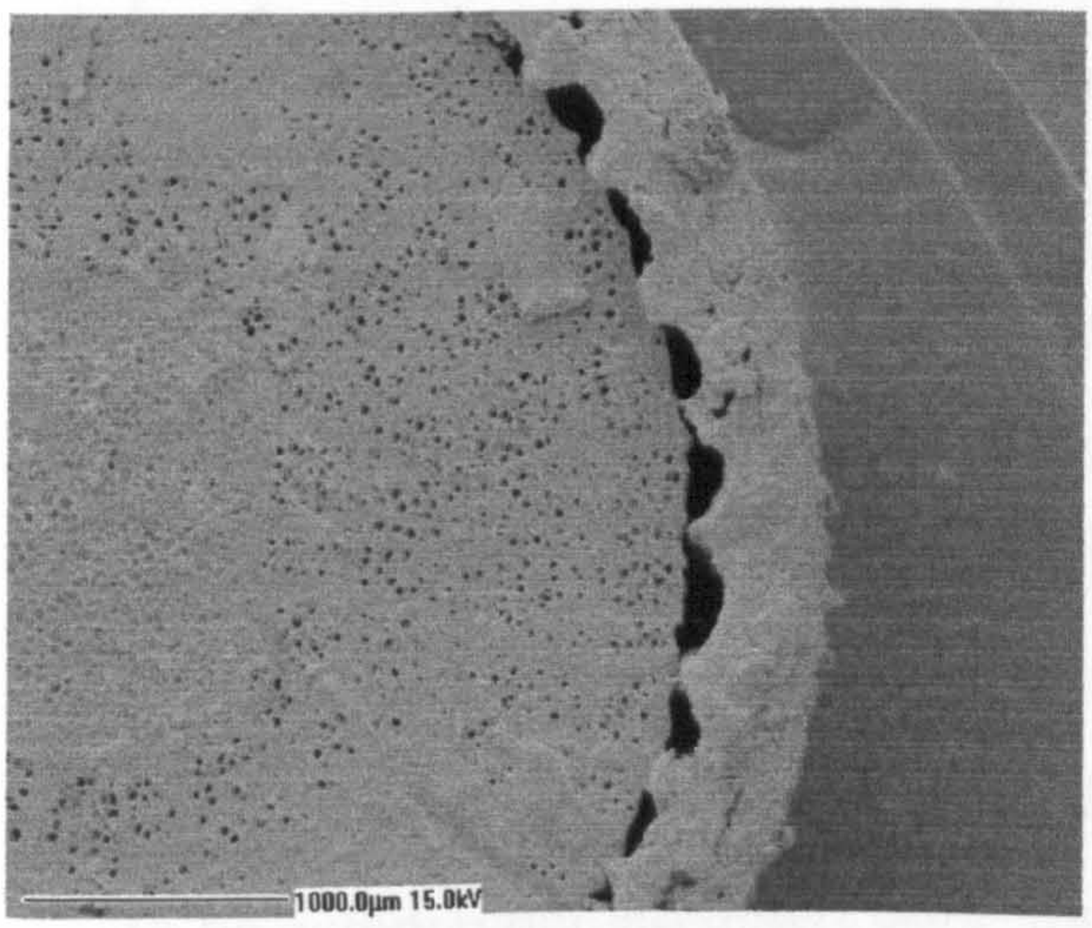

F

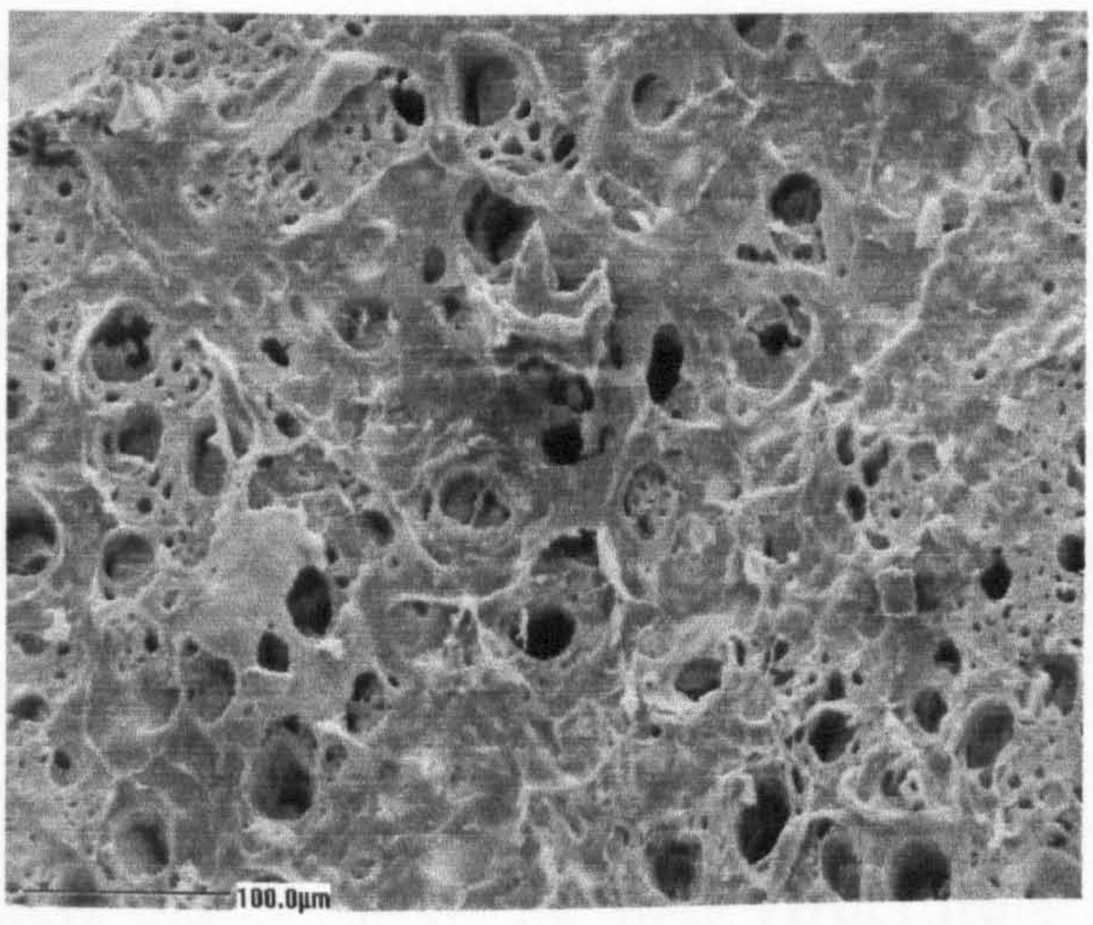

Figure 2.15. A: Mat of bacteria covering surface of *Platanus* twig after 2 weeks of decay. B: Bacteria infilling pith parenchyma cell and massing on cell walls and at intercellular junctions after 2-3 weeks of decay. C: Bacterially-produced film covering pith parenchyma cell walls and lining cells after 2-3 weeks of decay. D: Bacteria attacking xylem ray cells after 2-3 weeks of decay. E: Degradation of the phloem, resulting in the bark separating from the xylem after 3-4 weeks of decay. F: Bacterial film covering region of xylem, leaving larger vessels uncovered after 4 weeks of decay.

obscured. In most places the phloem had decayed to the extent that the bark had separated entirely from the xylem and pith tissues (Figure 2.15E). However, at a depth of ca 2mm within the twig, there were no signs of decay, and no bacteria were present.

After week 4, the bacterial mat and films extended from the pith to cover much of the xylem as well. Most of the cells were obscured, although some xylem vessels remained uncovered and empty of bacteria (Figure 2.15F). In a few pith cells which were not entirely infilled with bacteria or covered by a bacterial mat or film, bacteria were evident concentrated around the pits between adjacent cells (Figure 2.16A). However, no bacteria were evident at depths of 2mm or more below the cut surface of the twig.

Tissue-stained thin sections

These sections are only 1-2 cells thick, allowing the changes in cellular contents and structure to be observed. Alcian blue stains the cellulosic tissues blues. Safranin stains phenolic tissues red, and can be used as a proxy for lignin in fresh material. Both cross-sections and longitudinal sections were prepared and examined under light microscopy.

The tissue-stained thin sections indicated that plasmolysis, loss of cellular contents and flaking and pulling apart of cell walls all occurred within the first week of the twigs being subjected to bacterial decay. Within the first week, the intensity of the blue stain in the pith and the ray cells had decreased, and continued to decrease with further decay. The large blue-stained parenchyma cells of the phloem were the first tissues to be extensively decayed, with the cells losing much of their structure and the walls splitting apart from each other. The decay of these cells continued with time, and after week 6 extensive degradation resulted in

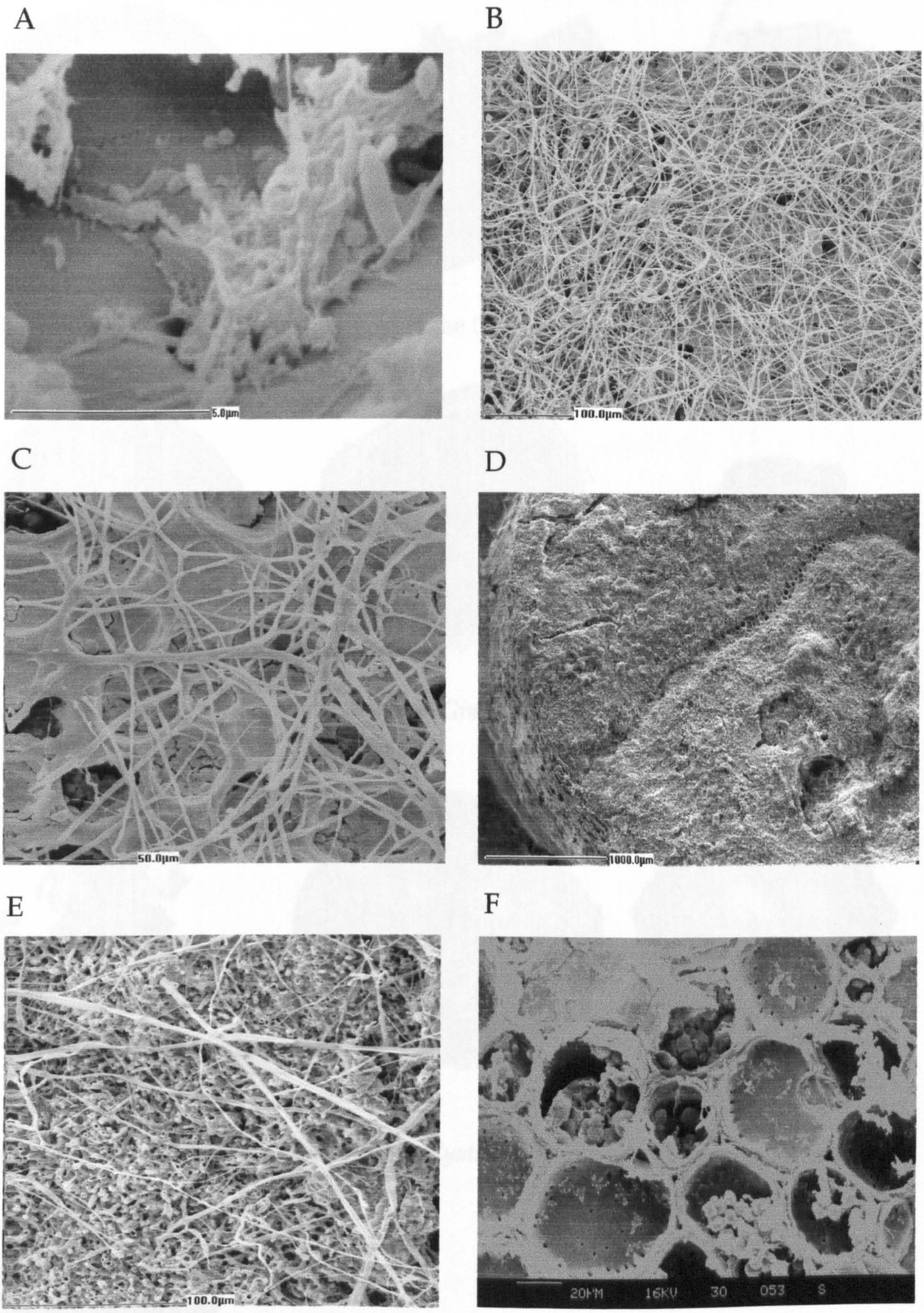

Figure 2.16. A: Bacteria surrounding a pit in the wall of a *Platanus* pith parenchyma cell after 4 weeks of bacterial decay. B, C: Fungal hyphae covering the surface of a *Platanus* twig after 12 weeks of decay by fungi indigenous to the twig. D, E: Fungal hyphae covering the surface of a *Platanus* twig after 12 weeks of decay by a fungal inoculum. F: Sterilised *Platanus* pith parenchyma cells containing starch grains after 12 weeks in a sealed marine decay system.

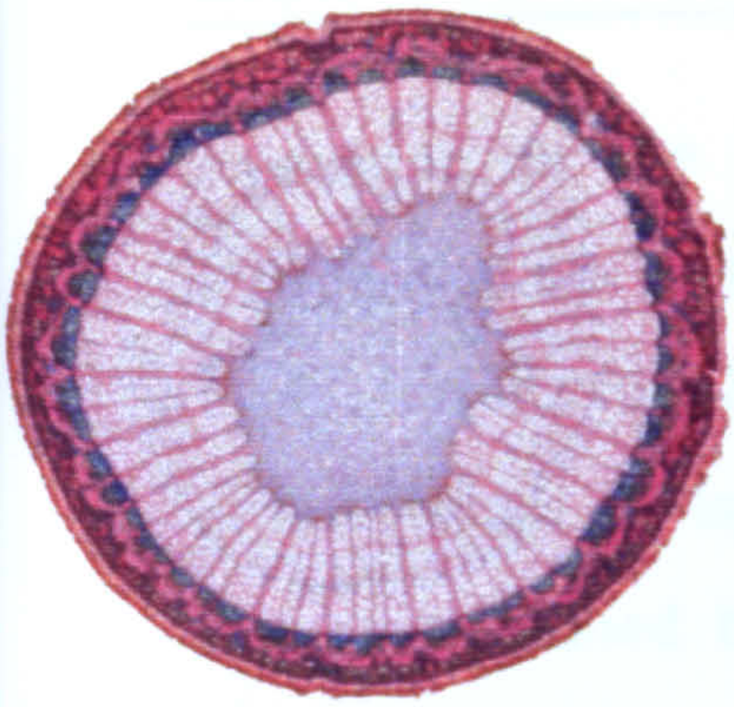

Fresh plane (*Platanus* sp.)

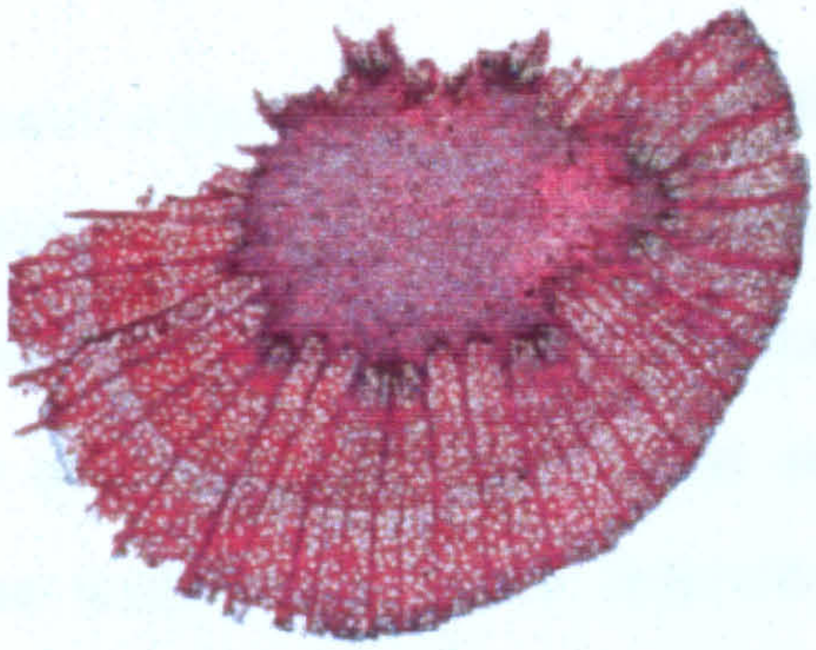

Decayed plane (12 weeks)

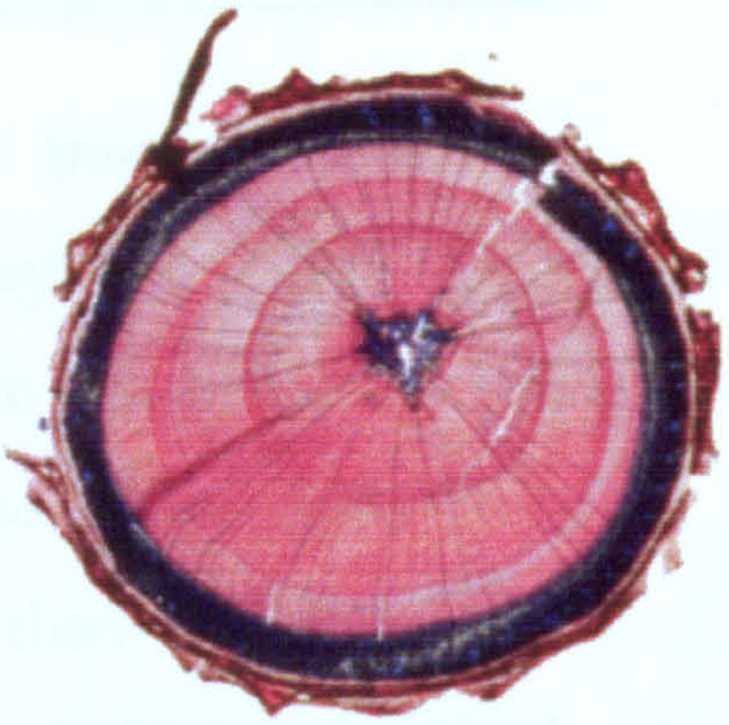

Fresh redwood (*Sequoia* sp.)

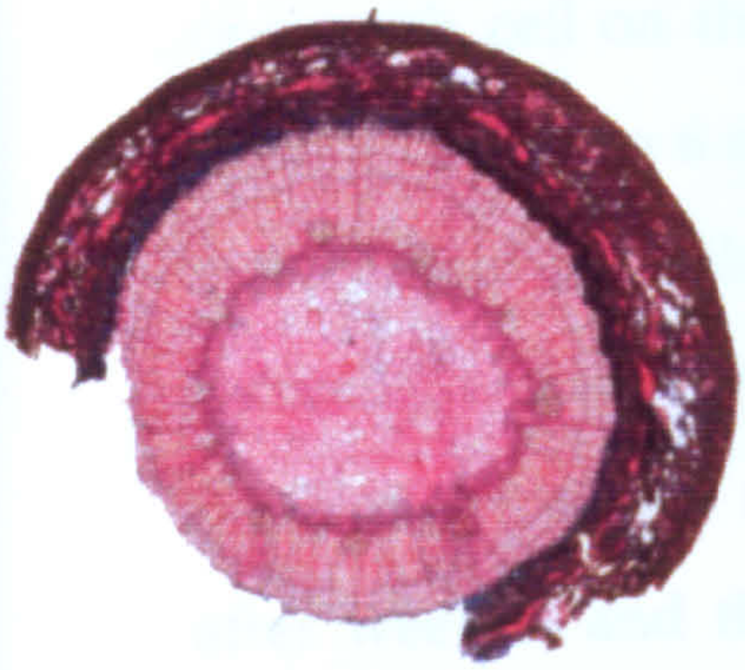

Fresh cherry (*Prunus* sp.)

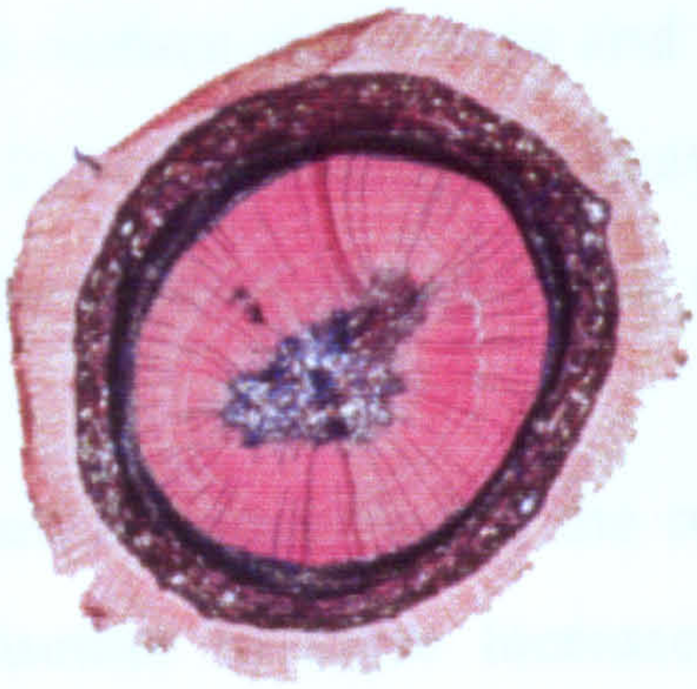

Fresh *Ginkgo*

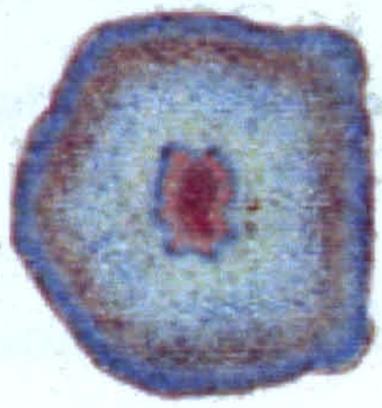

Fresh *Psilotum*

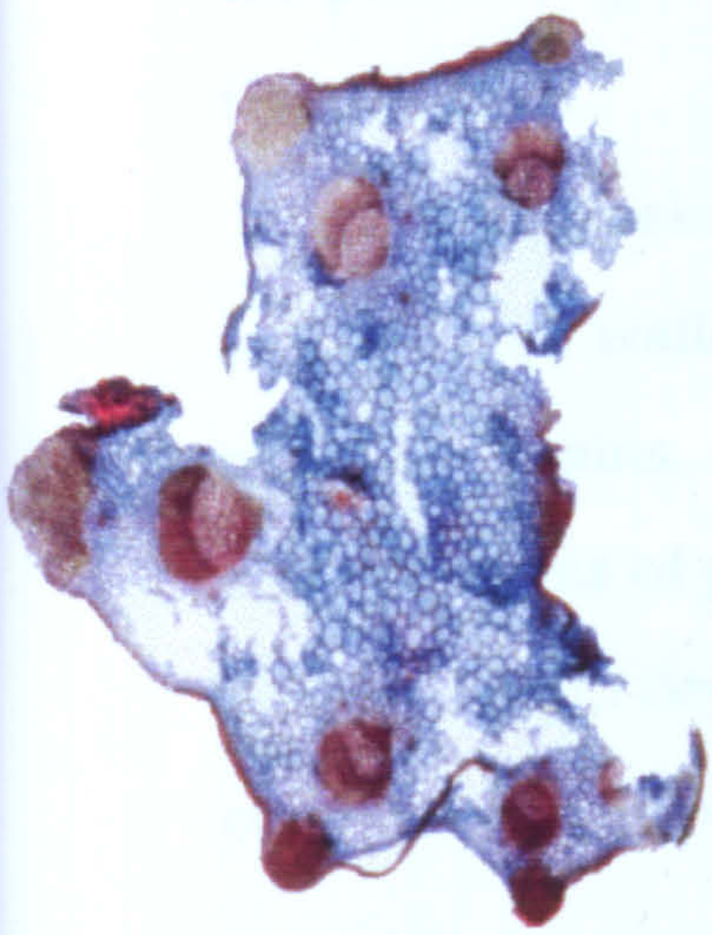

Fresh celery (*Apium* sp.)

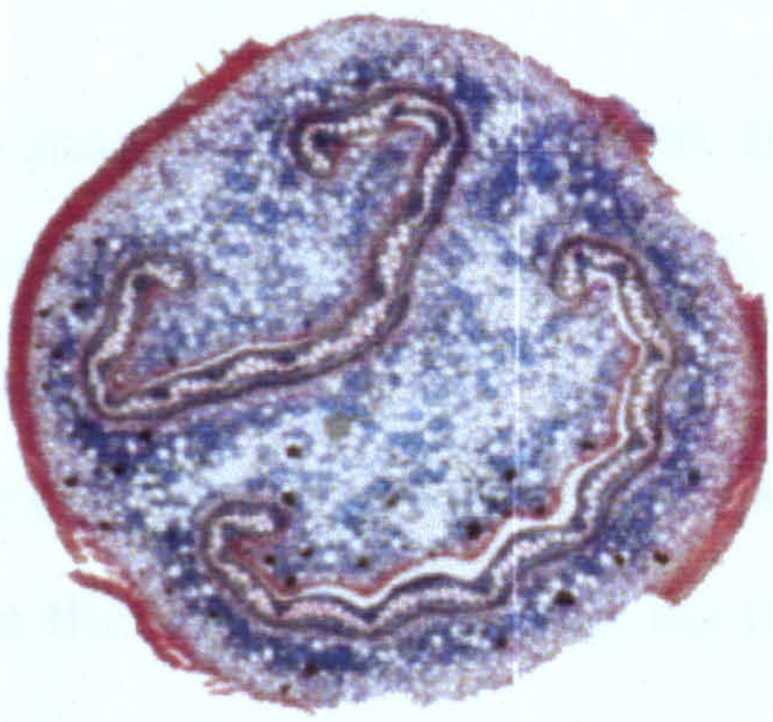

Fresh *Cyathea*

Fresh vine (*Vitis* sp.)

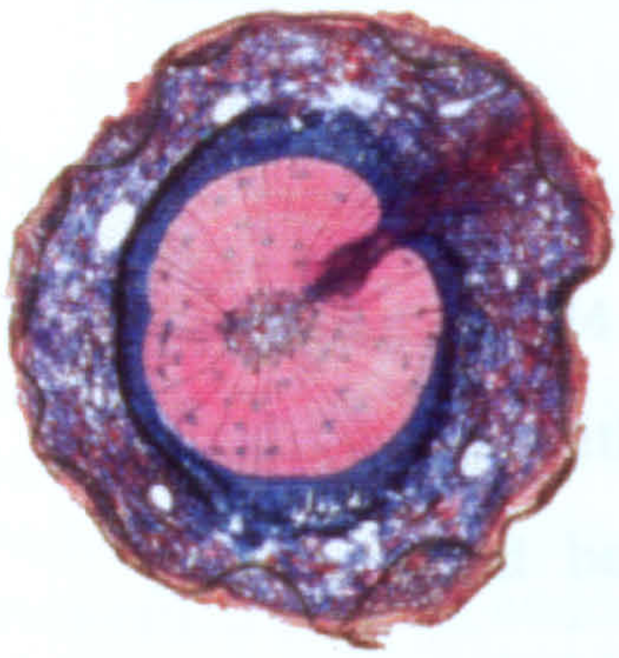

Fresh pine (*Pinus* sp.)

— 1mm

Figure 2.17. Tissue stained thin cross-sections of plant material. Alcian blue stains cellulose. Safranin (red) stains for lignin. Refer to Figure 1.4 for identification of specific tissues.

separation of the heavily-lignified bark from the inner tissues on sectioning (as seen in Figure 2.17 after 12 weeks of decay).

Within the first 2 weeks of decay, most of the starch grains had left the pith cells and a wispy material appeared within some of the pith. This substance stained blue with much more intensity than cellulose and appeared in more cells as decay proceeded. After week 12 longitudinal sections indicated the presence of this wispy material in almost every open pith cell on the cut surface of the twig and occasionally in several (usually between 6 and 12) longitudinally-adjacent pith cells. The ray cells also contain a similar blue-stained material, the concentration of which increases with decay.

Globules which stained red appeared in the centre of some pith cells after week 5, and the number of these increased with time. As decay increased, the intensity of the red stain taken up by the cell walls across the pith and xylem increased, resulting in very red sections after week 12 (Figure 2.17).

After 12 weeks, the majority of pith cells on the surface of the twigs had split cell walls, were pulling apart from each other, and were empty of starch grains. Although the number of cells affected by decay (e.g. showing signs of plasmolysis, splitting cell walls, loss of starch grains etc.) increased with depth in the twigs with decay, no trends in depth of decay could be identified.

1b. Effect of extended incubation on standard open marine systems

TEM analysis

TEM analysis of material from standard marine open systems incubated for 24 and 36 weeks indicated increased numbers of bacteria were present within the top 2mm of the twigs, but that little or no decay had occurred beneath this point. Although the number of bacteria

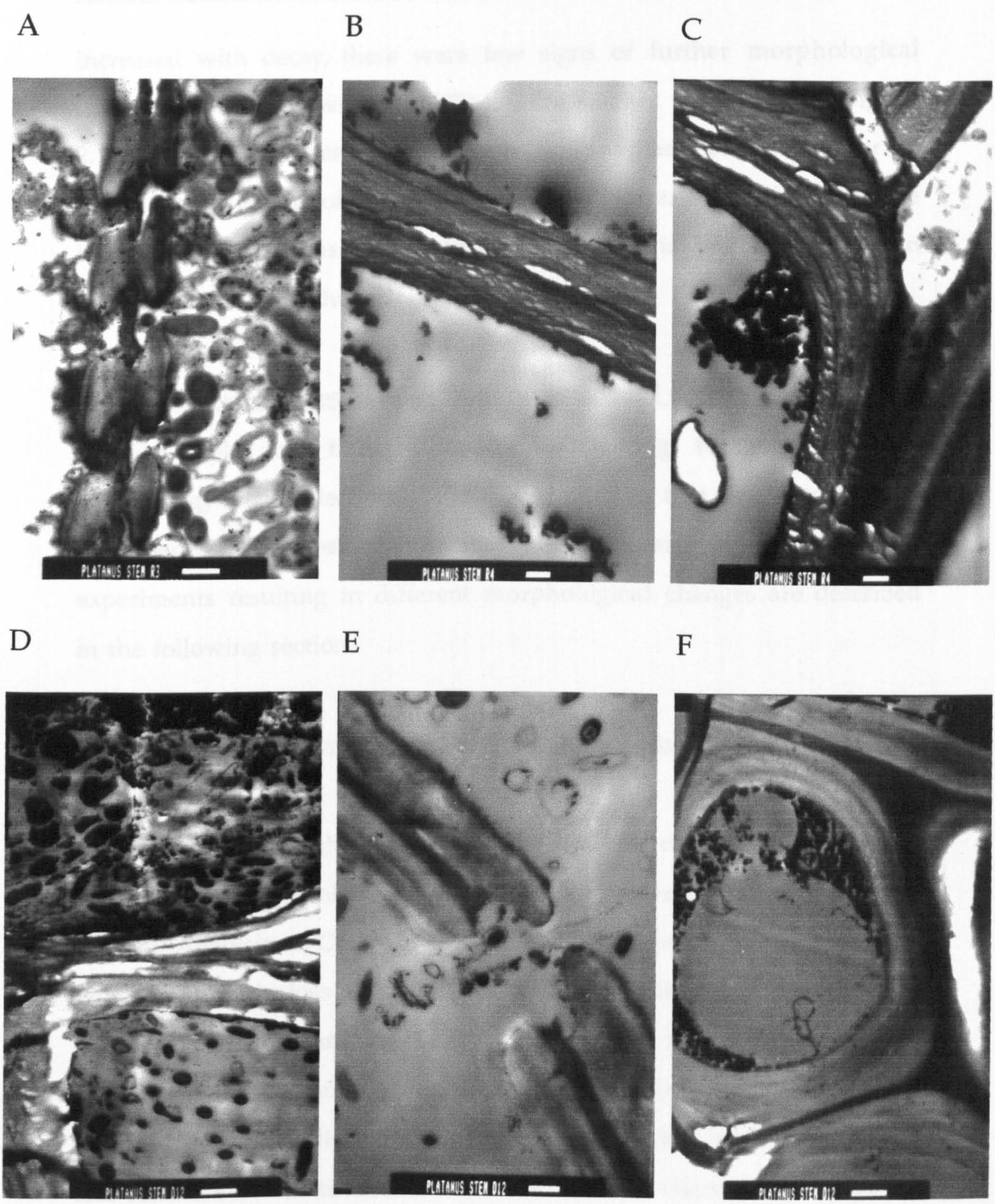

Figure 2.18. TEM images of *Platanus* twigs after 12 weeks incubation in decay systems. Scale bar represents 1 micron in all images. A: Bacteria present in pith parenchyma cells of a twig from an open marine system after 12 weeks decay. B, C: Deterioration of cell walls, with splitting along the middle lamella and enlargement of intercellular spaces after 12 weeks decay in open marine systems. D: Degradation of cell wall in association with bacteria in the pith of a *Platanus* twig from a sealed marine system. E: Loss of pit membrane after 12 weeks decay in a sealed marine system. F: Plasmolysis in a pith cell of a twig from a sealed sterilised marine system.

increased with decay, there were few signs of further morphological changes to those observed by SEM. TEM images presented in Figure 2.18A-C show the presence of bacteria within plane pith cells after 12 weeks, the layering of pith cell walls, and increases in space at the intercellular junctions. Interestingly, few bacteria were observed in association with the changes in cell wall structure.

Morphological changes in twigs from non-standard decay systems

SEM, TEM and thin section tissue staining revealed that the morphology of the decayed plane was similar to that described for the time series in almost every other decay experiment. Hence, only experiments resulting in different morphological changes are described in the following section.

Effect of reactivity of organic material: different plant species

SEM analysis

SEM analysis of the decayed *Equisetum* and celery specimens was impossible due loss of most of the material, even after only 6 weeks (celery). Analysis of *Cyathea* was also hindered due to extensive decay which resulted in loss of tissues and structural definition. The vine and all the *Psilotum* samples had lost most of their cellulosic pith parenchyma tissues, and only consisted of the vascular tissues and cortex of the vine, and the lignified outer tissues (epidermis and some cortex) and central vascular tissues in *Psilotum*. *Sequoia*, cherry and *Ginkgo* all showed similar loss of starch grains from the pith cells, and pulling apart and flaking of the pith cell walls to that described for the decayed plane of the marine time series. The surfaces of these three samples were often obscured by sediment attached to the specimens which had not been removed during SEM preparation by freeze-drying. The pine twigs which

had been incubated in the decay systems for 14 weeks showed the least signs of decay of any of the species. Some pith cells still contained starch grains, and most of the cellulosic parenchyma tissues were intact.

Tissue stained thin sections

Stained cross-sections of plane, *Sequoia*, cherry, *Ginkgo*, *Psilotum*, celery, *Cyathea*, vine and pine are presented in Figure 2.17. The more heavily lignified species, *Sequoia*, cherry and *Ginkgo* all contain relatively low concentrations of cellulose, and that which is present is usually closely associated with lignin. The fresh pine is heavily lignified and has a large area of cellulosic phloem, but the rest of the cellulose is associated with lignin, imparting resistance to decay. Only the phloem of the *Ginkgo* and the pine is highly cellulosic with little lignin to offer protection against decay. The tissues stained thin sections of the decayed *Sequoia*, cherry, *Ginkgo* and pine all indicated similar levels of decay to the plane of the time series after 12 weeks. Much of the cellulose had decomposed, and the bark of the *Ginkgo* and the pine separated readily from the central tissues on sectioning due to the loss of the phloem. The intensity of the red stain increased for these species with decay.

Fresh *Psilotum*, celery, *Cyathea* and vine all contain much higher proportions of cellulose than the pine, plane, cherry, *Sequoia* and *Ginkgo* (Figure 2.17). The least structural support is provided within the celery, which contains small lignified vascular bundles distributed throughout the pith. Decayed samples of these species could not be sectioned due to extensive decay of the cellulosic regions of these tissues. After only 6 weeks of decay, only the vascular bundles and a few strands of fibres remained of the celery. The *Cyathea.*, *Psilotum* and vine had all lost a lot of structural definition and were very soft.

Effect of fungal decay prior to entry into aqueous bacterial decay systems

SEM analysis

After the initial 12 weeks of fungal decay, the twigs were subject to SEM analysis. Fungal hyphae were observed in the xylem of the twigs which had been decayed by indigenous fungi (Figure 2.16B). The pith cells of these twigs appeared relatively unaffected by the fungi, with starch grains still present and cell walls still intact (Figure 2.16C).

The twigs which had been degraded by a fungal inoculum had been subject to much more decay. In most cases, the entire cut surfaces of the twig were covered with a hyphal mat, with very little cellular detail visible from beneath it (Figure 2.16D-E). Fungal hyphae extended to depths of at least 5mm within the twig, and some pith cells within the twigs no longer contained any starch grains.

It was impossible to tell whether 12 weeks of bacterial decay had further altered the plant material as the fungal hyphae covered much of the plant surfaces, obscuring the cells beneath.

Effect of sealing marine systems

TEM analysis

TEM analysis revealed the break down of *Platanus* pith parenchyma cell walls in cells containing bacteria after 12 weeks of decay (Figure 2.18D). Bacteria were also seen in association with decayed pit membranes (Figure 2.18E)

Effect of adding plant material to sealed marine systems

SEM analysis

On removal of the plant material which had been added to sealed marine systems after 12 weeks and then incubated for a further 12 weeks, the twigs looked very similar to fresh plane material, although some loss

of starch grains had occurred, and several pith cell walls appeared to be pulling apart from each other. The original twigs appeared similar to those which had been in the sealed controls for 24 weeks.

Effect of abiological changes: sterilisation of sealed marine systems

SEM analysis

SEM analysis of the plant material from the sealed sterilised marine systems, both with and without sulphide, revealed no signs of bacterial decay and no bacteria were observed. Many pith cells still contained starch grains (Figure 2.16F). Some pith cell walls appeared slightly layered, but were not pulling apart from one another (Figure 2.16F). The bark of the sterilised sections was still attached to the rest of the twig, and the phloem cells remained intact.

TEM analysis

TEM analysis of the material from the sterilised systems showed little sign of decay, although there were some signs of cytoplasmic degeneration. No bacteria were observed within the plant. Cell walls were still intact, but plasmolysis (shrinkage of the protoplasm away from the cell wall) had occurred in many cells (Figure 2.18F) due to osmosis while the twigs had been in the medium.

Tissue stained thin sections

Tissue stained thin sections revealed that most pith cells still contained starch grains and that most cell walls were intact, although some plasmolysis had occurred. The alcian blue revealed that cellulose was still present throughout the twig, and the bark was still attached to the rest of the twig. Some wispy material was present in the pith and ray cells which stained blue intensely, as described in time series. This

material was also in seen in adjacent pith cells in the longitudinal sections, infilling up to 20 cells in a row longitudinally. Some red globules were also present in a few pith cells, both on the surface of the material and with depth.

Discussion

Open marine decay systems (12 weeks)

The twigs and organic matter present within the sediment would have initially been subjected to hydrolysis and aerobic decay within the aqueous decay systems. However, due to the initial low oxygen concentrations and the intensity of microbial activity, the demand for oxygen was greater than that which could enter by diffusion, and the system became anoxic beneath the top few mm of the medium. Subsequently, bacterial degradation of metabolisable organic matter proceeded by anaerobic respiration. Soluble, and hence reduced, iron and manganese were not present in the starting medium, but were detected by ICP-AES after week 1, and probably reflect the anaerobic respiration of iron and manganese oxides. At the same time, sulphate concentrations decreased demonstrating active bacterial sulphate reduction began to dominate the anaerobic processes.

The bacterially-produced hydrogen sulphide (Equation 1.1) reacted with iron present in the sediment to form iron sulphides. This was evidenced by an increase in all forms of sedimentary sulphur and thus TRIS, and the sediment turning black (Table 2.4).

Anoxic conditions were maintained up to a few mm below the air-medium interface (Figure 2.1), demonstrating that decay reactions continued after weeks 2 and 3. Constant levels of TRIS and sulphate, and the low sulphide levels indicated that most of the bacterially produced

sulphide was being re-oxidised to sulphate rather than precipitating with sedimentary iron.

The region of constant or slightly increasing oxygen saturation below about 5mm from the air-medium interface after week 5 was puzzling, but may have been due to oxygenic photosynthesis. The position of photosynthetic activity probably reflects the availability of light within the medium; the amount of light reaching the rest of the medium was reduced due to the presence of the jar lid and the waterbath.

The decay intensity of the systems decreased with time, presumably as the most readily metabolisable and accessible plant tissues, yeast extract and sedimentary organic matter were utilised. This decrease in decay intensity resulted in steady increase in oxygen penetration (Figure 2.2). After 12 weeks, the decay intensity was still sufficient to sustain anoxia in the 5mm of medium directly above the twigs and the sediment.

After week 8, oxygen had penetrated the system to 5mm above the sediment, corresponding with a slower anaerobic decay rate. This oxygen, as well as other oxidised species such as ferric ions, allowed iron sulphides to be oxidised (Equations 2.2-2.4), as evidenced by the slight increase in sulphate concentrations after week 12 and slight decreases in pyrite and AVS after weeks 11 and 12:

$$FeS_2 + 14Fe^{3+} + 8H_2O \rightarrow 15Fe^{2+} + 2SO_4^{2-} + 16H^+ \quad \text{Eqn 2.2}$$

$$4Fe^{2+} + O_2 + 10H_2O \rightarrow 4Fe(OH)_3 + 8H^+ \quad \text{Eqn 2.3}$$

$$FeS_2 + 15O_2 + 14H_2O \rightarrow 4Fe(OH)_3 + 8H_2SO_4 \quad \text{Eqn 2.4}$$

Several processes control the pH of the medium during the decay experiments. The initial drop in pH to 6.5 during the first week (unpublished data) is due to production of organic acids, carbon dioxide, phosphoric acid and hydrogen sulphide during decay. Removal of

weakly acidic hydrogen sulphide by precipitation as iron sulphides, and production of ammonia during decay, forced the pH slightly more alkaline than the starting value by the end of week 1. The continued increase in TRIS concentrations during week 2 resulted in the further increase in pH to 8.0-8.1.

Ben-Yaakov (1973) proposed that the upper pH limit of marine systems is pH 8.3, and that this level is controlled by the precipitation of iron sulphides and the hydrolysis of calcium carbonates. The pH of the experimental decay systems continued to rise past this level after production of iron sulphides had ceased. The pH reached a maximum of 9.8 after week 6, indicating that other factors were controlling the pH.

The removal of carbon dioxide from the system by oxygenic photosynthesis may have been partly responsible for the pH increase after week 5 , but it is surprising that the region of constant oxygen saturation in the depth profiles was not reflected in the pH profiles. The increased alkalinity of the marine open systems was probably caused by the release of carbon dioxide from the buffer solution added to the original medium.

The decrease in pH observed during the last 5 weeks of the time series (from pH 9.8 to pH 8.6) was probably due to the release of hydrogen ions from the oxidation of iron sulphides (Equations 2.2-2.4).

During the course of the time series, the pH of the medium was buffered by calcium phosphate (Equations 2.5 and 2.6 depending on the pH) and calcium carbonate (Equation 2.7), which was reflected in the calcium and phosphate concentrations of the medium.

$$Ca_3(PO_4)_2\,(s) + 2H^+ \text{ --> } 3Ca^{2+} + 2HPO_4^{2-} \qquad \text{Eqn 2.5}$$

$$Ca_3(PO_4)_2\,(s) + 4H^+ \text{ --> } 3Ca^{2+} + 2H_2PO_4^{2-} \qquad \text{Eqn 2.6}$$

$$Ca^{2+} + 2HCO_3^- \text{ <==> } CaCO_3\,(s) + H_2CO_3 \qquad \text{Eqn 2.7}$$

The solubility of calcium carbonate depends on the partial pressure of carbon dioxide: any process adding carbon dioxide to the system (as in aerobic, and many anaerobic, decay processes) leads to the dissolution of calcium carbonate and the release of aqueous calcium species. This process is partly responsible for the initial decrease in pH in the experimental decay systems.

Carbonates are somewhat soluble in solutions containing no carbon dioxide (Equation 2.8).

$$CaCO_3 + H_2O \text{ <==> } Ca^{2+} + HCO_3^- + OH^- \qquad \text{Eqn. 2.8.}$$

This reaction does not proceed far in the forward direction, but far enough to make water in contact with carbonates appreciably basic (Krauskopf and Bird, 1995).

Phosphorus occurs in the decay systems in the form of aqueous phosphate. $H_3PO_4^-$ is the dominant form in acidic solutions, HPO_4^{2-} dominates in alkaline solution, and PO_4^{3-} is dominant only above pH 12.4 (Krauskopf and Bird, 1995). However, the latter is the chief form of phosphate which reacts with cations, in particular calcium and iron. After manganese reduction had taken place, the reduced manganese may have reacted with bicarbonate ions released during decay to form manganese carbonate. Magnesium ions also react with bicarbonate, forming magnesium carbonate, which may then proceed to form $CaMg(CO_3)_2$.

The plot of ln (rate), i.e. ln (TRIS), against time (Figure 2.2) indicates that the decomposition of organic matter within the systems fits the 2G model described by Westrich and Berner (1984). This indicates that decay proceeded by the successive first order (exponential) decay of two reactive pools of organic material that had different decomposition reactivities to.

It is likely that the most reactive organic matter contained highly decay-susceptible compounds, and was rapidly consumed within the first 2 to 3 weeks of the experiment, whilst the second group consisted of more recalcitrant compounds, such as lignin, which were decayed much more slowly.

The amorphous material covering much of the plant surface and often associated with bacteria appears to be a mixture of clay minerals, calcium and phosphate minerals, and possibly some iron sulphide, which may nucleate on the bacteria, as observed by Donald and Southam (1999). Beveridge and Fyfe (1985) observed that metals may bind to the anionic carboxyl or phosphoryl groups within the bacterial cell wall, either as soluble aquo-ions or hydrous cationic species such as $(Fe(H_2O)_5(OH))^{2+}$ or $(Fe(H_2O)_4(OH)_2)^{+}$, before reacting with sulphide. This could explain the areas of bacteria which have EDS readings for iron.

Beveridge and Fyfe (1985) proposed that in this way bacterial cells may provide a reactive interface where metals become sufficiently concentrated to exceed the solubility product of the corresponding metal sulphide. There is also experimental evidence to suggest that metals complexed to bacteria are more reactive towards sulphide than in a strictly inorganic environment (Trudinger, 1976; Mohaghegi *et al.*, 1984). Hence, there may be some areas where small amounts of FeS nucleate on bacterial surfaces.

The Si/Al/Fe mixtures are most likely to be clay minerals, possibly with limonitic characteristics, as described in association with bacteria by Ferris *et al.* (1987) and Konhauser *et al.*, (1993).

The large calcium crystals observed in some pith cells may be calcium oxalate or possibly calcium carbonate. The latter may have been formed during mineralisation within the decay systems, but both may be storage products within the original plant material. There are two functions for

calcium storage within plants: to reduce the amount of calcium within the cytoplasm (calcium regulates enzyme activity) or to make plants unpalatable for animals to eat (Mauseth, 1995).

Chloride was occasionally detected by EDS on plant cell walls; it is probably caused by precipitation from the marine medium on the plant material.

Effect of extended incubation

Where marine open systems were left to run for longer than 12 weeks, the rate and intensity of decay was seen to decrease. As decay slowed down more oxygen entered the medium, reaching 58% saturation adjacent to the twigs after 24 weeks. As the system was now oxic, it is clear that decay had extensively slowed, probably limited by a lack of metabolisable organic material. The oxygen saturation remained constant between 24 and 36 weeks; although more oxygen penetration had probably occurred, some oxygen was utilised in the re-oxidation of iron sulphides in the sediment and sulphide in the medium. This re-oxidation caused the change in colouration from black back to brown and the increase in sulphate levels. The decrease in pH from 8.8-8.9 after week 12 to pH 8.6-8.7 after weeks 24 and 36 may be due to the release of hydrogen ions in the oxidation of sedimentary sulphides (Equation 2.4).

Standard open marine systems

With the exception of systems 22 (5.4 weeks) and 24 (12 weeks), the standards behaved similarly to the open marine time series (see Figures 2.2 and 2.4, Table 2.6), and their geochemistry can be explained by the same processes. Any differences between these standards are most likely due to natural variations in sediment, inoculum and plant material. Different processes must have dominated systems 22 and 24 to explain

their geochemistry and possibly also the nucleation of FeSam within the plant material.

The geochemistry of systems 22 and 24 indicate that the initial decay intensity of these systems was much higher than that of the other standards, but that the rate of decay had decreased more after 12 weeks, resulting in greater oxygen penetration of the systems. High initial decay intensity explains the continued presence of sulphide and ferrous iron in system 22 after 5.4 weeks when only traces were detected in the other systems. This also explains the low levels of oxygen saturation and slightly lower sulphate concentrations in system 24 after 12 weeks than in the other standards (13.1/14.1mM compared with 14-23mM).

Intense decay would have resulted in elevated production of acidic decay products such as carbon dioxide and organic acids which may have counter-balanced the diffusion of carbon dioxide out of the system witnessed in the other decay systems. Hence the pH rose steadily (after an initial decrease to pH 6.5) within the first week, reaching the final pH of 8.6 after 12 weeks, instead of increasing and then decreasing. The constant increase in pH in systems 22 and 24 also indicate that sulphide oxidation did not occur in these systems. These results also indicate that the pH of these systems is significant in the formation of amorphous FeS within the plant material.

The low sulphate concentrations, and the formation of FeSam within the plant material suggest that sedimentary TRIS levels may have been elevated, but there is no data to support this. It is impossible to estimate the sedimentary TRIS concentrations purely from the amount of sulphate utilised as the other systems suggest that organic sulphur and porewater sulphate may contribute significantly to iron monosulphide formation.

Effect of sulphate availability

In natural environments, pyrite formation is only limited by the rate of sulphate reduction when concentrations of sulphate are less than 3mM (Capone and Kiene, 1988). In marine environments, sulphate concentrations are usually much higher than this, and so rate of sulphate reduction is not usually a limiting factor in pyrite formation in surface sediments. However, deeper sediments may be sulphate limiting, and so a sulphate agar layer was placed underneath the sediment of marine open systems to provide a source of sulphate. Any sulphide produced by sulphate reduction deeper in the sediments was able to precipitate with ferrous iron out of contact with potential oxidants in the medium, resulting in higher TRIS levels than in the standard systems (3.4-4.1M compared to 2.2-2.9M) and lower sulphate concentrations (8.4-15.1mM compared with 21.0-22.5mM). Despite the increased TRIS concentrations (Table 2.7), no iron sulphides were detected within the plant material, indicating that further controls are involved in the pyritisation of organic matter. This is discussed further in the conclusion section to this chapter.

The black ring observed within the agar layer on dismantling the system was formed by diffusion of ferrous iron and sulphide into the agar where they precipitated to form iron monosulphide (AVS). The ring formation is an example of a Liesegang ring which are seen in artificial gel systems (Wimpenny, 1992).

Effect of iron availability: amount of iron oxyhydroxide added to sediment

The amount of pyrite formed in a sediment is almost never limited by the total amount of iron present, but by its reactivity (Raiswell and Canfield, 1988). Although iron monosulphide and pyrite were formed in

the sediments of the standard open marine systems, additional iron was mixed with the sediments of some systems, as Raiswell *et al* (1993) suggested that high concentrations of reactive iron are required for the pyritisation of carcasses. This correlates with data from the Hunsrück Slate of Germany and Beecher's Trilobite Bed (Briggs *et al.*, 1991; Briggs *et al.*, 1996).

Comparison of the systems with 1%, 3% and 5% FeOOH indicated that the most oxygen penetrated the systems with 1% iron, and the least penetrated the systems with 3% iron (Figure 2.5). The highest sulphate concentrations were present in the 1% systems, and the lowest in the 3% iron systems (Table 2.8). The 5% iron oxyhydroxide systems had intermediate concentrations of oxygen and sulphate.

The oxygen saturation, sulphate concentrations and TRIS levels are difficult to interpret. Concentrations of different species vary between replicates, and it is unclear why the 3% FeOOH systems should behave so differently to the 1% and 5% FeOOH systems. It is therefore assumed that the non-reproducibility of these systems and the confusing results are due to heterogeneous mixing of the amorphous iron oxyhydroxide within the sediment. Such heterogeneous mixing would presumably also occur in nature.

Effect of iron availability: location of iron source

Where iron oxyhydroxide (3%) was present as a layer above the sediment, it was effectively more concentrated than in the systems where the iron was mixed in with the sediment. Hence, decay proceeded via iron reduction for longer, less sulphate reduction took place, sulphate levels were less depleted and less precipitation of iron sulphides occurred (Table 2.9). After 12 weeks the ferrous iron concentrations of both systems were identical, indicating effective oxidation of the excess iron (II).

Effect of iron reactivity

As the reactivity of iron is more important that its total concentration (Raiswell and Canfield, 1988), haematite and haematite /iron oxyhydroxide and ferric chloride/iron oxyhydroxide mixtures were used as alternative iron sources (1%) to iron oxyhydroxide.

The different iron sources did not affect the geochemistry of the decay systems greatly. The ferric chloride/iron oxyhydroxide systems had a lower pH than the standards (pH 8.5-8.7 compared with pH 8.8-9.0) due to the formation of iron oxide complexes and the release of hydrogen ions (Figure 2.6a). The less alkaline pH of the haematite systems (pH 8.5) may have been due to hydrolysis of the anhydrous haematite.

The sulphate levels of the ferric chloride/iron oxyhydroxide system were the lowest of these systems (15.7-17.8mM compared with 19.7-22.5mM) and these corresponded with elevated TRIS concentrations (Table 2.10). This may have been due to the availability of the soluble ferric ions, which may have precipitated as oxides and sunk to the sediment surface where they would have formed a concentrated area of ferric iron for iron (III) reducers. This would have resulted in elevated levels of iron reduction, and hence greater precipitation of iron sulphides, but this would not result in elevated sulphate reduction. It is possible that the combination of the iron sources and the ferrous iron generated in the sediment via bacterial Fe (III) reduction may generate hydrogen which may stimulate bacterial sulphate reduction.

The variation of TRIS between the replicates may reflect the heterogeneous distribution of the added iron within the sediment, and therefore the effect of iron reactivity on sulphide production could not be determined.

Effect of organic matter availability: amount of twigs added to decay systems

In most normal marine systems, i.e. those with oxygenated bottom waters, pyrite formation is limited by the reactivity and availability of organic matter (Berner, 1984).

Although an unknown quantity of organic matter was present within the sediment, the influence of organic matter availability on pyrite formation is demonstrated well by comparisons of the single twig and fifteen twig decay systems. With less metabolisable organic matter available in the single-twig systems, little sulphate reduction took place. Oxygen entered the system early on during the experiment due to the low decay intensity, and any sulphide produced was re-oxidised to sulphate instead of precipitating as iron sulphides. Hence, sedimentary TRIS levels were similar to those in the fresh sediment after 12 weeks.

Between 12 and 24 weeks, more oxygen diffused in the decay systems, and some of the remaining sedimentary sulphides were oxidised. This resulted in a slight increase in sulphate concentration and a slight decrease in alkalinity (from pH 8.4-8.5 to pH 7.9-8.3) due to the release of hydrogen ions (Equation 2.2-2.4). The TRIS concentrations after 24 weeks were lower than in the fresh sediment (Table 2.11).

In contrast, in the fifteen twig systems, where much more metabolisable organic matter was available, decay was sustained for longer, resulting in prolonged anoxia and sulphate reduction. The sulphide formed was trapped by ferrous iron, resulting in low sulphate concentrations, and elevated TRIS (and in particular AVS) concentrations compared to the standards, although no iron sulphide was detected in any of the plant material (Table 2.11).

The greater decay intensity produced higher levels of acidic decay products such as carbon dioxide and phosphate, which resulted in less

alkaline pH (pH 8.4-8.5 compared with pH 8.7-8.9) and higher phosphate concentrations (0.37-0.46mM compared with 0.10-0.11mM) than the single twig systems after 12 weeks. The increased production of carbon dioxide resulted in additional dissolution of calcium carbonate and hence elevated calcium concentrations.

These results demonstrate that the standard open marine systems were organic matter limited (rather than iron limited) with respect to iron sulphide and pyrite formation. However, although increased amounts of organic matter resulted in elevated TRIS production, the increase in TRIS was not directly proportional to the increase in twig number. Both these results and the lack of iron sulphides within the plant material despite the elevated TRIS of the fifteen-twig systems indicates that other factors are responsible for the pyritisation of organic matter than just pyrite formation.

Effect of organic matter availability: additional twigs added to standard decay systems after 6 weeks

The addition of extra plant material (six plane twigs) to standard open marine systems after 6 weeks provided a further energy source for anaerobic bacterial respiration, causing decay to be sustained for longer. This was evidenced by prolonged anoxia, lower sulphate concentrations and elevated levels of sedimentary iron sulphides (Table 2.12). This was in marked contrast to the situation under standard conditions where sulphide oxidation occurred by week 12.

The pH of the system was unaffected by the addition of extra twigs (pH 8.6-8.7), but calcium and phosphate concentrations were elevated. The additional decay resulted in the release of additional phosphate and carbon dioxide, which in turn was responsible for the dissolution of calcium carbonate and hence calcium levels increased. The overall pH

was not affected by the addition of twigs due to buffering by calcium carbonates, bicarbonates and phosphates.

Effect of organic matter availability: no twigs added to an open marine decay system

Where no plant material was present in the decay systems, only decay of sedimentary organic carbon occurred. This was limited, as 58% oxygen was present adjacent to the sediment, and little sulphate reduction would have occurred resulting in the sulphate concentrations being almost unchanged from starting levels at 27.4/28.9mM. These results demonstrate that the twigs in standard conditions directly stimulated bacterial decay, including sulphate reduction, and associated chemical changes.

However, the pH of the medium still became more alkaline with time reaching pH 8.4, only 0.2 units less alkaline than the standard, indicating that major changes driving the systems alkaline were not directly related to elevated decay in the open marine systems. This pH change was probably caused by the diffusion of carbon dioxide out of the systems which had been added with the buffer at the start of the experiment. The 0.2 pH unit difference in alkalinity of the system with no twigs and the standard may have been caused by the production of ammonium by decay in the standard.

Phosphate concentration of the system with no twigs was double that of the standard, indicating that the decay of plant material is not a substantial source of phosphate. Magnesium concentrations are also higher in the absence of plant material. No calcium was detected in either the system without twigs or the standard, although 1mM was present in the starting medium and must have precipitated, probably as

phosphate due to the lack of decay and hence lack of carbonate production.

Effect of organic matter availability: addition of yeast extract to open marine systems

Yeast extract (0.1 g/l) was added to all decay systems to stimulate bacterial activity. Its influence was investigated by running two open marine systems without yeast extract. The presence of yeast extract did not affect oxygen, sulphate or ferrous iron concentrations or pH of the decay systems, but less TRIS, in particular pyritic sulphur, was produced in the absence of yeast extract (2.3-3.2M TRIS compared with 3.6-3.7M with yeast extract). The TRIS results do not correlate with the sulphate concentrations, and hence the effect of yeast extract is difficult to determine. These results and the low concentrations of yeast extract added to most of the decay systems indicate that yeast extract was probably more important to ensure the presence of trace organics such as vitamins, co-factors and proteins, rather than as a quantitatively important source of organic carbon.

Effect of organic matter availability: effect of promoting bacterial activity with glucose

The addition of glucose (20mM) to the decay systems after 6 weeks of incubation stimulated bacterial activity due to the addition of an extra energy source. This prolonged activity, resulting in less oxygen saturation of the system, more sulphate reduction and more sulphide being trapped by ferrous iron to form iron sulphides, and hence low sulphate concentrations and high TRIS. Despite the elevated TRIS concentrations (amongst the highest seen, at 4.2-4.4M) no iron sulphides were detected within the plant material, indicating the importance of other factors such

as transport and nucleation in the pyritisation of organic matter. This is discussed further in the conclusion section to this chapter.

The pH of the glucose systems was slightly more alkaline than those without glucose (by 0.1 pH unit), which may be due to the elevated production of iron sulphides and the removal of hydrogen sulphide from the systems.

Phosphate concentrations of the glucose systems were more than double those of the standards (0.21-0.41mM compared with 0.12/0.11mM). This may be due to less iron being available to form iron phosphates resulting from the high levels of iron sulphide precipitation.

Effect of organic matter reactivity: different plant species decayed for 6 weeks

Plane, celery, vine and *Cyathea* (3.5g each) were decayed for 6 week in open marine systems. Oxygen saturation adjacent to the twigs in descending order was: celery > plane > vine > *Cyathea* (Figure 2.7). Sulphate concentrations in descending order were: plane > vine > celery > *Cyathea*. No TRIS data are available. The *Cyathea* sustained decay for longest, hence the most sulphate was utilised by sulphate reduction and the most sulphide was trapped by iron, forming iron sulphides. As decay was still continuing at a relatively high intensity after 6 weeks, little oxygen remained in the system. Rate and intensity of decay was lower in the pine and plane systems after 6 weeks, resulting in less sulphate reduction and/or more sulphide oxidation, and higher oxygen saturation in these systems. The tissue-stained thin section of celery (Figure 2.17) indicates that celery is mainly cellulose-based and is therefore highly susceptible to decay. Thus, initial decay was rapid, but intensity soon decreased when most of the organic matter was degraded (as evidenced by only fibres remaining after 6 weeks decay), resulting in most of the

sulphide produced being re-oxidised and little further sulphate reduction continuing and high oxygen saturation.

The variations in phosphate and calcium concentrations (Table 2.13) between these four systems cannot entirely be explained due to pH, as all systems had a pH of 8.8-8.9.

The four species can be placed in descending order of decay susceptibility after 6 weeks as follows: celery > plane > vine > *Cyathea*.

Effect of organic matter reactivity: different plant species decayed for 12 weeks

Plane, vine, *Equisetum*, *Sequoia*, *Ginkgo*, *Psilotum* and cherry (six twigs of each) were decayed in open marine systems for 12 weeks. Oxygen saturation adjacent to the twigs in descending order was: *Equisetum* > vine > plane > cherry > *Sequoia* > *Psilotum* > *Ginkgo* (Figure 2.8). Sulphate concentrations in descending order were: vine > plane > cherry > *Equisetum* > *Sequoia* > *Psilotum*. *Ginkgo* could not be placed in this sequence due to a large sulphate gradient.

The same explanations for oxygen saturation and sulphate concentration as for 6 week decay systems can be applied to the species decayed for 12 weeks. Like the celery, *Equisetum* is highly decay susceptible, especially as the stems are mainly hollow, and the remaining tissues are cellulose-dominated. The species can be put in descending order of decay susceptibility as follows: *Equisetum* > vine > plane > cherry > *Sequoia* > *Psilotum* > *Ginkgo*.

The pH of all systems was 8.8-8.9 except for the *Equisetum* and vine systems, which had a pH of 8.6-8.7 (Figure 2.8). This less alkaline pH may have been due to the production of higher concentrations of acidic decay products such as carbon dioxide and organic acids and/or lower concentrations of iron sulphides being formed.

Effect of organic matter reactivity: different plant species decayed for 14 weeks

Pine, plane, vine, older and newer *Psilotum*, *Cyathea* and celery (3.5g of each) were decayed for 14 weeks in open marine decay systems.

Oxygen saturation adjacent to the twigs in descending order was: celery > vine > plane, *Cyathea* > newer *Psilotum* > older *Psilotum* > pine (Figure 2.9). Sulphate concentrations in descending order were: celery > vine > plane > newer *Psilotum* > pine > *Cyathea* > older *Psilotum*.

The explanations used in the 6 week and 12 week decay systems to place the plant species in order of decay susceptibility are blurred slightly after 14 weeks, and it is harder to define an exact sequence. This may be due to the changes in rates and intensities of decay of the different species over longer incubation periods, resulting in variations in oxygen saturation and sulphide oxidation However, it is still clear that celery is the most decayed species, followed by vine. Plane, pine, older and newer *Psilotum* and *Cyathea* have all undergone similar amounts of decay.

Effect of pH

The pH of the open marine systems was reduced in several experiments following the high pH of many of the standard systems, in particular within the time series after week 6 (pH 9.8), as pyrite forms naturally at slightly less alkaline pH (Stumm and Morgan, 1981).

The availability of soluble ferric chloride for bacterial iron reduction was probably much more than insoluble ferric sources and may have resulted in greater production of ferrous ions. Higher ferrous production would trap more of the sulphide production during sulphate reduction as iron sulphides, instead of it being re-oxidised to sulphide. This is reflected in the high TRIS (in particular AVS) and low sulphate concentrations (Table 2.16). Once decay intensity began to decrease, any

oxygen entering the system would have rapidly re-oxidised the ferrous iron within the medium, and hence less oxygen was seen penetrating the medium than in the standard systems.

The pH of the medium was only 0.3 units less alkaline than that of the standards (pH 8.6 compared to pH 8.8-8.9), possibly due to the release of hydrogen ions during the formation of iron (hydr)oxides from soluble ferrous chloride. The high concentration of calcium ions within the medium is difficult to explain, but may have been released during buffering of the medium by calcium carbonates and bicarbonates. It is somewhat surprising that this increase in calcium is not associated with elevated phosphate concentrations.

The geochemistry of ferric chloride systems which were titrated with hydrochloric acid was very different to those systems to which acid was not added. Despite the addition of the concentrated acid, pH stabilised at 7.5-8.0 within 2-3 days of titration, reflecting the buffer capacity of the medium. As in the ferric chloride systems without additional acid, bacterial iron reduction probably produced more ferrous ions than in the standards containing insoluble iron (III) sources. However, the iron sulphides formed in the acid-titrated systems were not present within the sediment (as evidenced by TRIS concentrations of 3.7-3.8M, which were only slightly higher than the standard at 3.4M) but remained as a grey/black suspension within the medium. This is presumably due to the formation of a soluble iron sulphide complex caused by variations in the pH (6.5-8.0). It is unclear why the particles failed to coalesce, and the chemical composition of this complex is unknown.

Effect of fungal decay prior to entry into the aqueous bacterial decay systems

It is possible that much of the plant material preserved in pyrite fossil beds may have been subject to decay, in particular fungal decay, prior to entry into the depositional environment. To investigate the influence of this decay, twigs were subject to decay by fungi indigenous to the twigs or a fungal inoculum for 12 weeks before being placed in open marine decay systems.

The source of fungi did not influence the subsequent development of the geochemistry of the aqueous decay systems. After 12 weeks under open marine conditions, both oxygen saturation (Figure 2.11) and sulphate concentrations were higher than in the standard experiments, indicating that the fungi had already removed much of the readily available organic matter within the twigs. As a result of this, less iron sulphides were formed, as evidenced by the low sedimentary TRIS data (Table 2.18).

It is unclear why the pH of the fungal systems was weakly acidic (pH 6.8-7.0), as opposed to the alkaline open marine systems (pH 8.4-8.5). As the open marine system with no twigs was more alkaline after 12 weeks of decay, this low pH cannot have been caused by the lack of degradable organic matter. The pH must be influenced by the presence of fungi, which may possibly be producing acidic polymers. The high concentrations of phosphates (0.26-0.77mM compared with 0.16-0.21 in the standards) may reflect the dissolution of calcium phosphates under acidic conditions.

Silicon, iron and aluminium containing clay minerals were observed under SEM forming on the cell walls of the plant material, even at depths of up to 3mm. Similar crystals were not detected in plant material from any other decay systems, suggesting that the way the fungi had

degraded or altered the chemical structure of the cell walls may have provided a surface which enhanced the effectiveness of clay mineral nucleation. Clay minerals were not seen to nucleate on the fungi.

Effect of twigs being allowed to float in open marine systems

Less decay took place in open marine systems where the plane twigs were allowed to float instead of being pressed into the sediment, as the twigs were not in direct contact with the sediment and associated high bacterial population. Even after the first week, when the twigs had sunk to the sediment surface, they did not lie flat on the sediment, and several cut ends lay facing upwards into the medium. After 5.4 weeks, decay intensity was great enough to prevent much oxygen penetrating the system, but after 12 weeks, oxygen saturation was higher than in the standard. It in unclear why phosphate and calcium concentrations were lower in the burial systems than in the standards after 12 weeks.

Effect of sedimentation in open marine systems

A 1:1 mixture of sediment and marine medium (2ml) was added to two open marine decay systems to simulate sedimentation in the natural environment.

After 5.4 weeks and 12 weeks, more oxygen had penetrated the sedimentation system than the standard, possibly due to less decay being sustained after this period or aeration due to the addition of the sediment slurry. However, despite the addition of sulphate-, calcium- and phosphate-containing medium, concentrations of phosphate were similar to those in the standard, and sulphate and calcium levels were lower than in the standard. The sedimentation resulted in the twigs being partly buried, bringing the open surfaces of the twig in close contact with sedimentary bacteria, allowing bacterially-produced sulphide to

precipitate with iron out of contact with potential oxidisers in the medium. This precipitation resulted in greater formation of iron sulphide, hence no iron or sulphide was detected in the medium, unlike in the standard, and sulphate concentrations were lower. It is unclear why the phosphate and calcium levels were the same, and lower, respectively, than the standard, although it is likely that there was some co-precipitation.

Effect of sedimentation in open marine systems where twigs are free to float

Twigs were allowed to float in open marine systems with sedimentation for 5.4 and 12 weeks. After 5.4 weeks, oxygen saturation was the same in the floating/sedimentation systems as in the standard, indicating the same intensity of decay. Despite the twigs floating and being out of contact with sedimentary bacteria, they sunk within the first week, and then became covered by sediment. Bacterially-produced sulphide would have been trapped by iron within the sediment, instead of being oxidised in the medium, and hence sulphate concentrations were much lower than in the standard (Table 2.21). Concentrations of phosphate, magnesium and calcium were much higher in the floating/sedimentation system than in the standard after 5.4 weeks, presumably due to the addition of these species in the extra medium and sediment, but it is unclear why the geochemistry of the sedimentation and the floating/ sedimentation systems were dissimilar to each other.

After 12 weeks, oxygen saturation was much higher in the floating / sedimentation systems than the standards. This suggests that decay intensity was lower than in the standard system, but it is unclear why. The decrease in calcium concentrations over time (Table 2.22) must have been due to precipitation of calcium, although it is uncertain why this

occurred. Elevated iron sulphide formation within the floating/sedimentation systems would have resulted in the formation of lower concentrations of iron phosphates. Phosphate concentrations were unaffected with time, but may precipitate as calcium phosphate instead of iron phosphates.

Effect of burial of twigs

Twigs were buried in the sediment of open marine decay systems, allowing them to be in close contact with the sediment bacteria and sources of iron. Sulphide produced by sulphate reduction within the sediment was also kept away from potential oxidisers in the medium, and hence trapped as iron sulphides. Some sulphide and iron had diffused into the medium, possibly due to bacterial reduction of sedimentary organic matter near the surface of the sediment. Due to the proximity of the plant material to the bacteria, and hence the amount of organic material available for decomposition, decay was sustained for longer, resulting in lower oxygen saturation of the burial system than the corresponding standard. The pH was slightly less alkaline in the burial systems (pH 8.4 compared with pH 8.6-8.7 after 12 weeks), possibly due to the production of higher levels of acidic decay products. It is unclear why the concentrations of phosphate and calcium were so much higher than in the standard, although some phosphates may have been released from iron phosphates due to iron sulphide formation.

After 12 weeks incubation, the geochemistry of the system with the buried twigs and the standard were very similar, except for much lower phosphate concentrations and slightly lower pH (Table 2.23). These similarities are likely to be due to similar levels of decay in both systems over 12 weeks, but it is unclear why the phosphate concentrations are so different.

Effect of decay by bacteria indigenous to the sediment instead of a bacterial inoculum

A marine bacterial inoculum (which had been enriched under anoxic conditions) was included in standard open marine decay systems. To investigate the influence of this inoculum, two decay systems were run without inoculum, relying only on the bacteria indigenous to the sediment.

Without the inoculum decay was less intense because less bacteria were present within the system. Oxygen saturation was unaffected by the addition of the inoculum as decay was still sustained both with and without inoculum. Sulphate levels were much higher without inoculum (21.0-22.5mM compared with 15.4-17.0mM). The bacterial inoculum contained large numbers of sulphate reducing bacteria, and hence without this inoculum less sulphate reduction took place, resulting in the higher sulphate concentrations, and lower TRIS levels (Table 2.24).

The pH of the systems without inoculum was 0.2 units more alkaline than those with inoculum. This may have been caused by the lower levels of production of acidic decay products to counterbalance the effect of the removal of carbon dioxide from the buffer from the system.

Effect of reaction vessel of open marine decay systems

Open marine decay systems were incubated in 100ml Duran bottles and jars. After 12 weeks, oxygen saturation was much higher in the jars than in the Duran bottles (Figure 2.11). This was probably due to different shapes of vessels, in particular the wider neck opening of the jars. There was also a shorter distance between the air-medium and medium-sediment interfaces within the jars than the Duran bottles, which would have allowed oxygen to reach the sediment much more rapidly in the

jars. This is reflected in the higher sulphate concentrations within the jars, which were probably a result of more aerobic decay, less sulphate reduction and higher levels of sulphide oxidation, while more sulphide was trapped by iron within the Durans. The large differences in TRIS between duplicates (Table 2.25) make it difficult to prove that more iron sulphide precipitation occurred in the Durans. These differences may have been caused by heterogeneous mixing of iron oxyhydroxide within the sediment.

Open freshwater decay systems

The open freshwater systems behaved very differently to the open marine systems due to differences in sediment, medium and inoculum, which result in the dominance of different bacterial processes. Sulphate concentrations are naturally low in freshwater environments and degradation processes are dominated by aerobic degradation and when oxygen levels decrease fermentation and, finally anaerobic methanogenesis.

The low pH of the freshwater systems (pH 6.0-7.2 in standard open freshwater systems after 12 weeks: Figure 2.12) was probably due to the initial formation of fermentation products such as organic acids and carbon dioxide under anaerobic conditions with limited sulphate. As oxygen was rapidly consumed creating anoxic conditions (Figure 2.12). The production of fermentation products such as carbon dioxide must have balanced the loss of carbon dioxide from the system which results in the alkalinity of the marine open systems. In addition, there was a very limited sulphate reduction which would normally result in increased pH.

Some of the fermentation products would have been used by the iron-reducing bacteria, resulting in the elevated concentrations of ferrous

iron (1.7mM in system 85, 0.02mM in systems 86 and 87) in the medium after 12 weeks. Although there was no sulphate in the starting medium, up to 0.08mM sulphide was detected in system 85 after 12 weeks. Presumably the majority of this was from the reduction of any sulphate in the sediment or from desulfurylation of the twigs and sedimentary organic matter during decay. The brown colouration of the sediment, and the low TRIS values for systems 86 and 87 (<1M) indicate that in the absence of sulphate, little or no iron sulphides were precipitated, despite the higher iron content in freshwater systems (1.5% FeOOH).

The increase in calcium and phosphate concentrations from 5.4 weeks to 12 weeks was due to the dissolution of calcium phosphate, carbonate and bicarbonate due to the production of carbon dioxide and the acidic pH. Levels of calcium and phosphate were lower in the less acidic systems due to less dissolution of phosphates, carbonates and bicarbonates. The slight decrease in ferrous iron concentrations from 5.4 weeks to 12 weeks (1.79/1.64mM - 1.72/1.46mM) may have been due to formation of iron phosphates.

The differences between system 85 and systems 86 must have been due to differences in the composition of, and concentrations of organic matter, the two different sediment sources.

Effect of sulphate availability within open freshwater systems

In freshwater environments, sulphate concentrations are much lower than 3mM, the concentration below which Capone and Kiene (1988) proposed that sulphate reduction, and hence pyrite formation was sulphate limited. However, SRB can adapt to very low (< 60μM) sulphate concentrations in freshwater sediments (Bak and Pfennig, 1991), and the small sulphate pool could be turned over rapidly.

Despite the low numbers of SRB present in the freshwater inoculum (and presumably also in the sediment), some sulphate reduction was stimulated by sulphate addition, evidenced by the identical sulphate concentrations present in the freshwater sulphate systems with and without sulphate agar layers (1.2-1.3mM). This demonstrated that the additional sulphate had been reduced. Additional sulphate reduction would have reduced fermentation processes, consumed organic acids from the remaining fermentation and, with along with the precipitation of iron sulphides, all of these processes would account for the increase in alkalinity (Ben-Yaakov, 1973)

The variations in sedimentary sulphur concentrations observed between the two freshwater systems with sulphate agar layers (Table 2.26) may have been caused by differences in the low levels of sulphate released from the agar layer and numbers of active sulphate reducing bacteria. Heterogeneous mixing of the iron within the sediments may also have affected the results.

Sealed marine decay systems

In the sealed marine systems, any oxygen within the medium would have been rapidly utilised (as in the open systems), leading to bacterial sulphate reduction and iron (III) reduction. After 12 weeks, all the sulphate had been reduced, and much of the sulphide produced had reacted with ferrous iron to form iron sulphides, turning the sediment black. In the open systems, a significant amount of the sulphide produced was been re-oxidised to sulphate, but this could not happen in the sealed systems, resulting in 4.3-7.7mM of sulphide and no sulphate remaining, compared with < 1mM sulphide and 11.7-12.8mM sulphate in the open systems. Once the available sulphate and iron had been utilised,

anaerobic decay would have proceeded by fermentation and methanogenesis.

The presence of sulphide after 12 weeks in the absence of ferrous iron indicated that iron was limiting within the sealed marine systems. However, sulphide levels had decreased even further after 24 weeks in the sealed systems (0.2-3.5mM) demonstrating relatively slow reaction kinetics between the hydrogen sulphide and the added FeOOH and/or different iron sources found naturally within the sediment (Canfield *et al.*, 1992). Although no TRIS data are available for the sealed system sediments, much more sulphate had been removed from the medium of sealed systems than the open ones, which would have resulted in very high sedimentary iron sulphide concentrations. Despite this, no iron sulphides were detected within the plant material, indicating that there are other controls involved in the pyritisation of plant material. This is discussed further in the summary discussion and conclusion.

The decrease in pH from the starting value of 7.5 to 7.2 after 12 weeks, and 6.7 after 24 weeks (Figure 2.13), was due to the build-up of decay products, in particular carbon dioxide, which would normally diffuse out of the open systems, and which resulted in the build-up of pressure which the sealed systems. The alkaline pH in the open systems (pH 9.0 after 12 weeks) compared with the lower pH of the sealed systems supports the hypothesis that the high pH of the open systems was caused by the removal of carbon dioxide present in the initial buffer solution from the medium, which could not leave the sealed systems.

The high phosphorus concentration of the sealed systems may have been due to the high levels of iron sulphide formed, which would have left less iron available to react with phosphates. The high phosphate concentrations may also have been affected by the acidity of the medium. At acidic pHs, the dominant phosphate is $H_2PO_4^-$, which is much less

reactive than PO_4^{3-}, the more common phosphate under alkaline conditions (Krauskopf and Bird, 1995). This may have resulted in the formation of less iron phosphates within the sediment and hence higher concentrations of phosphate.

Effect of adding plant material to sealed marine systems

Additional plant material was added to the sealed marine systems to allow continued production of decay products and to introduce a small amount of oxidant to assist the conversion of iron monosulphides into pyrite (Wilkin and Barnes, 1996).

The opening of sealed systems, and the addition of six extra twigs appeared only to affect the phosphate concentrations of the medium. SEM analysis of the added twigs indicated that they had been subjected to little or no decay. As seen in the sealed marine systems, all the sulphate and ferrous iron had been utilised after 12 weeks, the point at which the extra twigs were added. In the absence of sulphate reduction, decay may have proceeded slowly by methanogenesis, but few methanogens would have been present in the original inoculum which had been designed to culture sulphate-reducing bacteria, and the high sulphide concentrations (4.3-7.7mM) present in the medium after 12 weeks may have been toxic to many bacteria, inhibiting decay (Brown *et al.*, 1973).

However, opening the sealed systems would have released some of the carbon dioxide which had built-up as a result of decay, and thus would have resulted in the pH of these systems becoming slightly more alkaline. The identical pHs of the opened systems (ca pH 6.7), with or without additional twigs, and the sealed systems after 24 weeks indicate that decay had continued, resulting in the production of carbon dioxide and organic acids, which had restored the acidity of the medium.

The increase in phosphate concentration of the medium with the addition of twigs cannot be explained. Even if this increase is caused by the release of phosphoric acids by decay, this does not explain why concentrations were higher in the opened systems than the sealed ones.

Effect of organic matter reactivity (different plant species) in sealed marine systems

The more acidic pH of the *Cyathea* systems (6.5-6.7 compared to 7.1-7.3 of the plane systems) and the greater build-up of gas indicated that the *Cyathea* contained much more available, metabolisable organic matter than the plane twigs. This is despite a lower mass of *Cyathea* twigs being decayed than that of plane, as the same number of twigs were placed in each system, but *Cyathea* is lighter than plane. This supports the contention that the build-up of decay products is controlling pH in these systems and producing lower pH.

Effect of sterilisation of sealed marine systems

After twelve weeks incubation of sterilised marine sealed systems, no sulphate reduction had taken place. Thus, the initial concentrations of sulphate remained in the medium (27.3-36.2mM) and no sulphide was present. Traces of ferrous iron (≤ 0.04mM) were detected, which may either have diffused out of the sediment or have been formed by iron (III) reduction during the 12 hours between the systems being set-up and irradiated. The brown colouration of the sterile sediment indicated that little or no iron sulphide formed abiologically.

The pH was unchanged from the starting value of 7.5 after 12 weeks, but had decreased to pH 7.1-7.2 after 24 weeks. This was probably due to slow chemical equilibration of the systems, indicating that overall the abiological changes in the systems were small compared to the

biologically-induced pH changes seen in both the open and sealed systems.

The decrease in phosphate and calcium concentrations during the whole of the experiment indicate the precipitation of calcium phosphate and possibly also iron phosphate.

The SEM and tissue-stained thin sections of the irradiated plant material showed some alterations which had previously been taken as indications of decay, such as splitting and pulling apart of cell wall. These changes may have been caused by the irradiation process, or may be artifacts of water-logging or osmotic shock, or of the freeze-drying process. But the presence of many starch grains in the sterile material indicates that these are being decayed in the twigs in the non-sterile systems, and are not being physically removed from the pith cells during the time in the aqueous systems or in the SEM preparations.

Effect of sterilisation of sealed marine systems with added sulphide

Sulphide (2mM) was added to marine systems before sealing and irradiating to simulate reducing conditions created by bacterial decay so that the direct and indirect effects of bacterial metabolism on mineral formation, in particular iron sulphide, could be recognised.

As in the sterilised systems without added sulphide, no decay was evident with the addition of sulphide. The slight decrease observed in sulphate concentration (19.9-27.6mM, compared to ca 29.5mM in the initial medium) may have been due to sulphate reduction prior to irradiating the systems. The removal of sulphide from the system indicated that iron sulphide formation took place by reduction of iron oxyhydroxides by hydrogen sulphide (Equation 1.2). Only 1.57mM of iron was added to the sediments of these systems, but there was probably enough additional iron already present in the sediment to allow all the

sulphide to precipitate with iron. Despite this, the sediment was still brown. The reaction of hydrogen sulphide with sedimentary iron may have been responsible for the pH gradient within these systems, which ranged from pH 7.7-7.9 at the air-medium interface to 7.3-7.4 adjacent to the sediment after 12 weeks.

Closed and sealed freshwater decay systems

The results of the closed freshwater time series are too varied to allow interpretation. This may have been due to the systems being incompletely sealed, allowing some carbon dioxide and other gases to escape from some systems but not others. It is unlikely that any oxygen would have entered these systems as they were kept in anaerobic gas bags flushed with nitrogen/carbon dioxide.

The slightly acidic pH of the sealed freshwater systems (pH6.8-6.9) probably reflects a combination of fermentation, ferric iron reduction and restricted sulphate reduction. Methanogenesis may well have developed, including acetate and H_2/CO_2 pathways, which would have limited the pH decrease by removing some of the acidic decay products from the systems. In contrast, the conditions in the open and closed freshwater systems were probably insufficiently reducing for methane formation.

The greater build-up of pressure and the slightly lower pH of the freshwater sealed systems compared to the marine sealed systems does not necessarily suggest that the rate or intensity of decay was greater in the freshwater systems, but that more gaseous products were formed in the dominant decay processes.

Morphological discussion

It is difficult to detect the extent of decay of much of the plant material in the biological decay systems. Many differences were observed between fresh and decayed plane material, such as loss of starch grains, splitting, "layering" and pulling apart of cell walls (e.g. Figure 2.14E), plasmolysis (Figure 2.18F) and increase in the size of intercellular junction (Figure 2.14E). It is impossible to determine how much of this was caused by decay, and how much was caused by osmotic shock or water-logging within the decay systems, or are effects of irradiation. However, the chemical gradients formed in the systems and the increasing numbers of bacteria, and formation of biofilms and glycocalyx with increasing incubation periods indicates that decay was occurring.

The observation of intact cell walls and starch grains, and the lack of intercellular spaces in the fresh plant material indicate that the effects were not artifacts of freeze-drying or dehydration in the SEM preparation. The presence of starch grains in the twigs from the abiological systems shows that these were mostly decayed in the decay systems, and were not falling out of the cells in the decay systems or during preparation for microscopic analysis.

Because of these factors, it is impossible to determine from SEM and TEM analysis whether plane twigs were more decayed in any particular decay systems than in others.

The tissue-stained thin sections show the loss of cellulose (a decrease in intensity of blue stained cell walls) with decay, and also the chemical alteration of lignin, as evidenced by the increased intensity of the red stain. The decay-susceptibility of cellulose-based tissues is evident, due to the softness of the remaining celery, *Psilotum*, *Cyathea* and *Equisetum* tissues after decay, which retain little or no structure and cannot be sectioned due to their softness. The vine, which had a large region of

cellulosic pith parenchyma at the interior of the stem, had undergone extensive decay of the pith, but the outer tissues (xylem and bark), were still intact. The more heavily lignified species - plane, *Sequoia*, *Ginkgo* and cherry - underwent some decay, as evidenced by the loss of blue-stained cellulose and increase in red-stain intensity of the lignin, but were still almost intact, except for the phloem, after up to 14 weeks of decay.

Both the tissue-staining and SEM analysis revealed that the phloem was the most readily-degraded part of the plant for all species, especially the woody ones. The phloem was particularly susceptible to decay not only because of its unlignified parenchyma cells, but also because of its contents of dissolved sugars and other nutrients which it transports throughout the plant. The extensive decay of the phloem resulted in the separation of the heavily-lignified and decay-resistant bark separating from the inner tissues of the plane twigs after approximately 6 weeks of decay.

The identity of the intensely-stained blue wispy material within the parenchyma cells of the stained sections is uncertain, but its presence in the irradiated twigs suggests that it may be a product of chemical alteration of the plant material, although not necessarily decay. The dark red globules observed in some pith cells may be tannins and/or other decay products released from the cell walls during decay which have coalesced in the centre of the cells.

Due to the huge variations in cellular structure within individual twigs and twigs from the same decay systems, it is impossible to quantify the extent of decay of the plant material from different decay systems, or to identify trends with time or decay, although the extent of decay does increase with time.

SEM analysis of the plant material which had been subjected to fungal decay revealed that the fungi colonised the surface of the twigs in a different manner to the bacteria. The fungi indigenous to the twigs were often concentrated over the xylem, while the bacteria primarily colonised the pith, phloem and rays. The fungi present in the inoculum reproduced quickly enough to completely cover the surface of the twigs within 12 weeks. The fungi would have preferentially colonised the xylem, despite the heavily lignified walls and lack of nutrients, because the long vessels allowed the fungal hyphae to penetrate within the twig, and access metabolisable organic material at depths in the twig. After 12 weeks of fungal decay, much of the surface-accessible metabolisable organic material had been utilised, leaving few energy sources for bacterial respiration, and hence slow bacterial population growth and little sign of bacteria on the specimens after 12 weeks.

Summary discussion and conclusions

The four major environmental conditions under which decay experiments were carried out (open marine, open freshwater, sealed marine, sealed freshwater) and the abiological (sterile) systems were dominated by different bacterial processes, which in turn affected the geochemistry of the systems.

The open marine systems were dominated by sulphate reduction and, to varying extents, iron (III) reduction. The pH of these systems was forced alkaline by the removal of weakly acidic hydrogen sulphide by precipitation as iron sulphides (Ben-Yaakov, 1973), but the upper limit of the pH was controlled by the diffusion of carbon dioxide which had been added to the systems with the buffer. The pH usually reached a maximum after 6 weeks of decay, after which it became slightly less alkaline, due to the oxidation of iron sulphides, stabilising at pH 8.6-8.8

after 12 weeks. Exceptions to this were standards 22 and 24, in which FeSam nucleated, the pH of which rose steadily for 5.4 and 12 weeks respectively, presumably due to the production of high levels of acidic decay products such as carbon dioxide and organic acids, which outweighed the effect of the loss of carbon dioxide. FeSam only formed in plant material in open marine systems, and then only sporadically.

Fermentation was a dominant process in the open freshwater and sealed marine systems. In the open freshwater systems, this was due to the low concentrations of sulphate, although ferric reduction would have occurred. The low pH (6.0-7.2 after 12 weeks) was due to the production of acidic fermentation products, which would have outweighed the loss of carbon dioxide added with the buffer, plus only limited sulphate reduction occurred. The sealed marine systems were dominated by fermentation, once all the sulphate and ferric iron had been utilised. The low pH values (7.2 after 12 weeks, 6.7 after 24 weeks in standards) were due to production of acidic decay products, and because the carbon dioxide originally added to the system could not escape from the sealed vessels.

The sealed freshwater systems may have been dominated by methanogenesis, which would have utilised H_2/CO_2 and acetate produced by fermentation. The removal of these acidic decay products and the production of methane limited the decrease in pH.

In the abiological (sterile) systems, where no decay occurred, the pH of the system remained constant for 12 weeks, and only decreased after 24 weeks, indicating that chemical equilibrium was approached very slowly, and had a very small influence on the system compared to that of biological processes in the non-sterile systems.

The different bacterial processes and the changes in the pH influenced mineral precipitation. Calcium, phosphate and magnesium

concentrations in the medium were influenced by the pH of the systems and buffering. Acidic conditions, and the production of carbon dioxide, resulted in the dissolution of calcium phosphate, carbonate and/or bicarbonate. Alkaline conditions resulted in the precipitation of these minerals. Phosphate concentrations also depended on the amount of iron available to form iron phosphates. Bacterial processes influence inorganic reactions in a number of ways, including precipitation and dissolution in the medium via changes in the redox of the system and metal ions are absorbed into bacterial surfaces e.g. $(Fe(H_2O)_5(OH))^{2+}$, as reported by Beveridge and Fyfe (1985). This was confirmed by the lack of mineralisation or concentration of elements in the sterile controls.

It is difficult to place the individual plant species in an order of decay susceptibility, due to changes in decay rate and intensity with time, differences in structure as evidenced by tissue-stained thin sections, and variation in the amount of plant tissues in different experiments (either 5 twigs or 3.5g of plant material). However, taking these factors into consideration, as well as evidence of fluctuation in oxygen saturation, sulphate concentrations and pH, it is clear the *Equisetum* and celery are the most readily degraded followed by vine and then plane. The decay susceptibilities of the remaining species (*Ginkgo, Sequoia,* cherry, *Psilotum, Cyathea* and pine) cannot be ranked.

Amorphous iron sulphide, FeSam, was observed on the pith parenchyma cell walls, in the middle lamella and at the cell wall junctions of plant material (plane or *Psilotum*) from only 4 of a total 145 individual decay systems studied, and resulted in infilling of several pith cells in one of these four systems. All four of these systems were open marine systems, indicating that extreme conditions may not be required for pyritisation of plants to occur. The sealed systems failed to yield iron sulphides within the plant material, indicating the requirement of an

oxidant, possibly molecular oxygen, in the transformation of iron sulphide to pyrite, as proposed by Wilkin and Barnes (1996). The rare occurrences of the amorphous iron sulphide within the twigs reflects the rarity of the pyritisation of plant material in the fossil record.

The formation of this iron monosulphide was rapid: individual crystals were evident after only 5.4 weeks, and cells were partially infilled in one systems after 12 weeks. Amorphous iron monosulphide only ever formed in small areas on the surface of a twig, and never on more than one twig from each experimental system. This mineralisation presumably occurred only in discrete micro-environments around the decaying plant material, the precise conditions of which could not be measured due to the micro-scale and not being able to access individual or even groups of cells. These precise conditions could not be replicated exactly due to heterogeneity beyond the experimental controls. This included seasonal and sampling changes in sediment mineral and organic matter composition, the batch variation in bacterial inoculum, seasonal changes in the twigs affecting their susceptibility to decay, and probably also the heterogeneous distribution of added iron sources.

The formation of amorphous iron sulphide lining the cell wall, along the middle lamella, and at intercellular spaces is in similar locations to that of FeSam and pyrite in celery in abiological experiments (Grimes *et al.*, 2001a) and in the London Clay pyrite plant fossil record. This suggests that the mechanisms involved in the microbial decay systems are similar to those in the London Clay.

Even when elevated TRIS levels (including pyrite) were produced in systems with additional organic matter (including glucose), extra available sulphate, increased sedimentary iron, or the presence of ferric iron as an iron source in open marine systems, no iron sulphides precipitated within the plant material. This indicates that the formation

of iron monosulphide and pyrite was not the main control on pyritisation of the plant material, and that additional controls are required for the preservation of plants. These controls could include nucleation and transport processes.

Although pyrite exhibits a reluctance to nucleate (Schoonen and Barnes, 1991), iron monosulphides and pyrite have been reported to nucleate on organic surfaces such as bacterial cell walls (Donald and Southam, 1999) and on, and within the cell walls of celery (Grimes *et al.*, 2001a). However, the medium geochemistry indicates that calcium carbonate, calcium phosphate and iron phosphates formed in some of the decay systems, but none of these minerals were seen to precipitate on the plant surface. Clay minerals nucleated in the pith cell walls in twigs which had been subjected to fungal decay, but in this case the fungi may have been responsible for altering the chemical composition of the cell walls and/or the production of metabolites or extracellular compounds which may have enhanced the nucleation potential of the clay minerals.

The rate of pyrite formation is transport-rate controlled rather than chemical reaction-rate controlled (Raiswell, 1993). Transport processes are critical in the pyritisation of organic matter (Grimes *et al.*, 2001a). Raiswell *et al.* (1993) proposed a diffusion-with-precipitation model for pyrite formation. This model predicted that for a decaying organism to be preserved in pyrite the sulphide produced by bacterial sulphate reduction must be trapped within the carcass and prevented from diffusing out in the surrounding sediment. High iron porewater concentrations probably provide the mechanism to trap the sulphide at the site of decay.

Briggs *et* al. (1991) and Raiswell *et al.* (1993) applied this model to Beecher's Trilobite Bed in the Ordovician of New York State, where organic matter concentrations in the sediment surrounding the organisms were low, confining sulphate reduction to carcasses. They

proposed that high concentrations of porewater iron trapped the sulphide produced within the decaying organisms. Pyrite concentrations of the surrounding sediment were low. However, organic matter would have been required to reduce ferric iron to produce the high porewater concentrations of iron and for even higher levels of sulphate reduction to produce the sulphide needed to pyritise the organism. Hence, sedimentary organic matter concentrations may have been high during deposition in Beecher's Bed, and this model cannot be effectively applied to the microbial decay systems in this investigation.

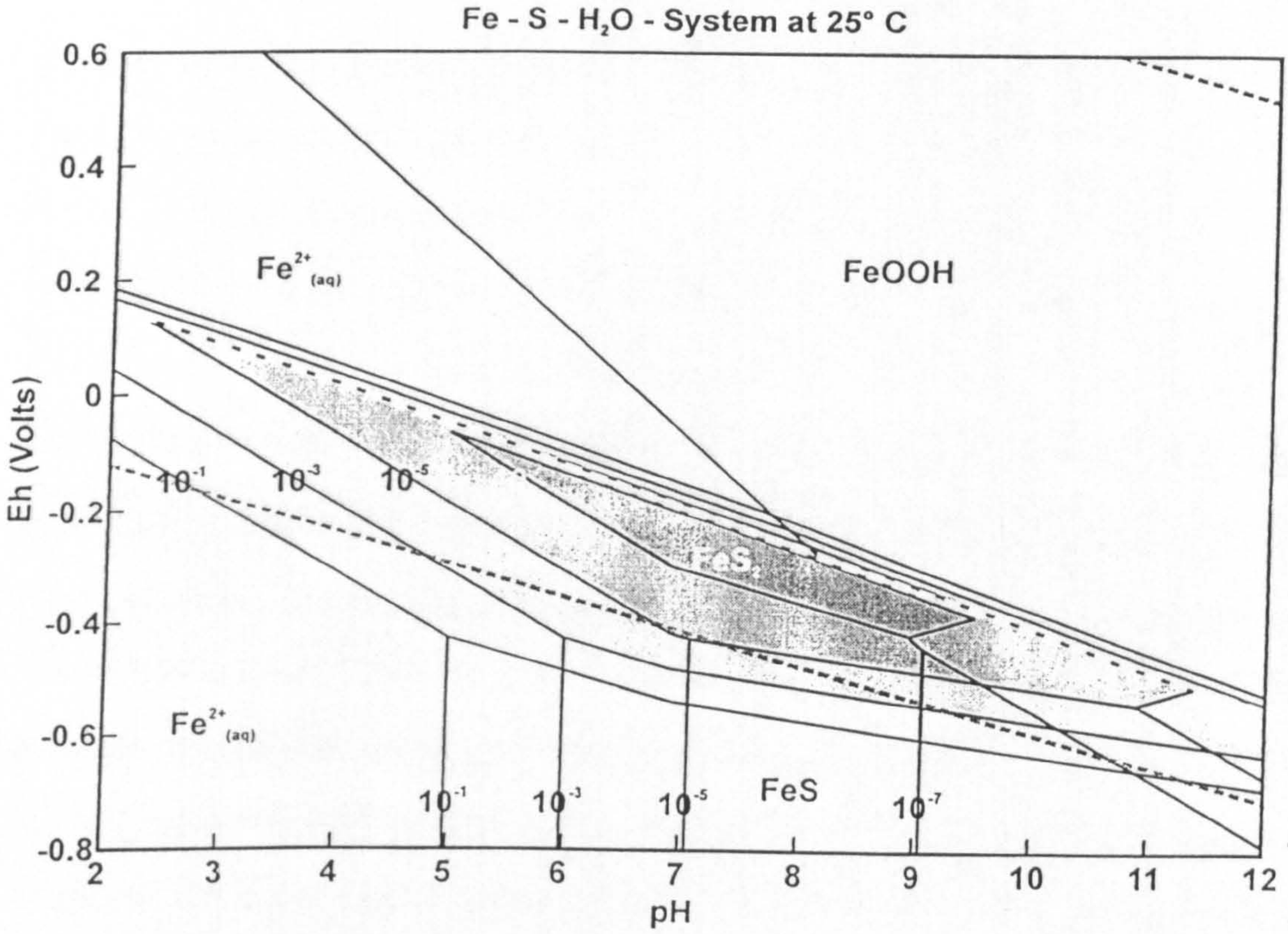

Figure 2.19. Fe-S-H_2O system at 25°C (Grimes *et al.*, 2001b).

The high pH of some of the decay systems (reaching a maximum of pH 9.8 in the open marine system after 6 weeks) may have been a significant controlling factor in the formation of iron sulphides, in particular pyrite, in the decay experiments. Such high pHs lie above the

stability zone for pyrite formation (Figure 2.19), but the steady increase in pH of the systems in which amorphous FeS formed, to a maximum of pH 8.6 after 12 weeks may have provided more favourable conditions for pyrite (and iron monosulphide) formation.

ORGANIC DECAY OF PLANT MATERIAL

Introduction

The processes involved in the biodegradation of plant tissues vary greatly, depending on the type of plants, the microbial processes involved, and the environmental conditions.

Microbial activity and resulting organic matter breakdown are normally most rapid in moist, warm, highly aerobic environments (Barghoorn, 1952). The presence of oxygen is a major factor influencing the rate of decay, especially as the majority of wood-decaying organisms are obligate aerobes (Nicholas, 1973).

In terrestrial environments, most wood and plant material is degraded by fungi and, to a lesser extent, bacteria. The only organisms capable of extensively biodegrading lignin are the Basidiomycetes (Reid, 1995). The white rots are capable of decomposing both lignin and cellulose completely. Brown rots primarily attack cellulose and hemicellulose, modifying the lignin and leaving a brown, brittle residue (Levy, 1987; Reid, 1995). Soil fungi belonging to Ascomycetes and Fungi imperfecti also attack lignin and cellulose (Levy, 1987).

In freshwater and coastal marine sediments, where molecular oxygen is absent or present in very low concentrations (Berner, 1976), bacteria are thought to be responsible for the majority of wood decomposition (Sen and Basak, 1957; Boutelje and Goransson, 1975; Greaves, 1971; Nicholas, 1973; Benner *et al.*, 1984b). The bacterial decomposition of organic matter in general has already been discussed at length in Chapter 1.

As well as the presence of oxygen and decomposing organisms, other factors influencing decay processes include the moisture content of the

material, pH, temperature, burial, and the presence, movement or accumulation of nutrients (Levy, 1987).

Microbial degradation of organic matter can proceed by the use of extracellular enzymes such as cellulase. The degradation of cellulose by soil fungi is catalysed by three types of cellulase enzymes: C_1 enzymes, C_x or β-1-4 glucanase enzymes, and β-glucosidase enzymes, each of which catalyze various conversions of cellulose (Atlas and Bartha, 1987)

It is a common assumption that under anaerobic conditions lignin is only degraded slowly (Benner *et al.*, 1984a) if at all (Hackett *et al.*, 1977; Zeikus, 1980; Crawford, 1981). Ziomek and Williams (1989), however, showed that sulphate-reducing bacteria are capable of breaking down lignin compounds, although not completely to carbon dioxide.

Different plant biopolymers and tissues have different decay susceptibilities, ranging from readily-degradable hemicellulose to recalcitrant lignin, as discussed in Chapter 1. Carbohydrates have been shown to be decomposed preferentially over lignin (e.g. Hatcher *et al.*, 1982, 1983a, b; Hedges *et al.*, 1985; Spiker and Hatcher, 1987). However, the structural organisation of the plant, and the association between different biopolymers and tissues, may alter the preservation potential of individual tissues (van Bergen *et al.*, 1995). Lignin is known to inhibit the decay of associated polysaccharides (Barghoorn, 1952; Sen and Basak, 1957; Nicholas, 1973), possibly by shielding them from extra-cellular hydrolytic enzymes (Kirk, 1973; Schmidt, 1980; Crawford, 1981; Melillo *et al.*, 1982). For example, pectin is readily degraded within pit membranes (e.g. Highly and Lutz, 1970), but becomes much more resistant to decay when associated with lignin in the middle lamella (Wilcox, 1973; Panshin and de Zeeuw, 1980).

Gymnosperm wood is more resistant to decomposition than angiosperm wood (e.g. Kohara, 1956; Nicholas, 1973; Hedges *et al.*, 1985).

This is thought to be due more to differences in tissue structure than dissimilarities in the chemical composition of the lignin and polysaccharides in the two taxonomic groups (Wilcox, 1973).

Experimental aims

This work was an investigation into the effect of bacterial decay on a range of plant species, and its aim was three-fold:

i) to study the change in chemical composition of the plant material caused by decay;

ii) to identify the tissues and species that are preferentially degraded or preserved;

iii) to investigate the rate of decay of different tissues and species.

Fresh samples of six different plant species (Table 3.1) were comprehensively analysed by elemental analysis, carbohydrate and lignin assays, pyrolysis-GC/MS and solid-state ^{13}C NMR. The results were compared with those from samples of the same species which had been subjected to bacterial decay for either 6 or 14 weeks.

Plant	Taxonomic group	Species
Plane	woody angiosperm	*Platanus acerifolia*
Vine	woody angiosperm	*Vitis vinifera*
Celery	non-woody angiosperm	*Apium* sp.
Pine	gymnosperm	*Pinus* sp.
Cyathea	fern	*Cyathea chinensis*
Psilotum	Psilotophyta	*Psilotum nudum*

Table 3.1. Plant species of which fresh and decayed samples were analysed.

Plane, vine and pine were chosen as decay organisms as they are modern representatives of species identified from the Eocene London Clay (e.g. Collinson, 1983; Poole, 1996; Poole and Wilkinson, 2000; this study). Ferns are also common in the London Clay (e.g. Collinson, 1983; Ribbins and Collinson, 1978), and *Cyathea* was chosen as a representative species. *Psilotum* was chosen as it is the extant vascular plant with the earliest fossil representatives, and has the simplest structure of all vascular plants (Mauseth, 1995). Fresher, green *Psilotum* and older, orange/brown *Psilotum* were decayed and analysed separately to investigate any changes in decay caused by ageing and maturing of the plant material. Celery was chosen for comparison with the results of abiological experiments to investigate the mechanisms of pyrite formation within plants (page 3; Grimes *et al.*, 2001a). Celery was chosen for those experiments due to its relatively simple structure and wide, open vessels.

Experimental methods

Decay of plant material

Plant material (3.5g of each species) was decayed for 14 weeks in individual aqueous microbial decay systems as described in Chapter 2. Samples of plane and *Cyathea* were also decayed for 6 weeks. The geochemistry of the decay systems, and the morphological changes caused by decay of the plant material, are described on page 145-158.

The individual analyses carried out on each species are listed in Table 3.2. Not all analyses were carried out for all species if insufficient plant material was available.

Sample	CHN	Carb.	Lignin	Pyrol.	NMR
Fresh celery	•	•	•	•	x
Decayed celery (6 wks)	•	x	x	x	x
Decayed celery (14 wks)	•	•	x	•	x
Fresh newer *Psilotum*	•	•	•	•	x
Decayed newer *Psilotum*	•	•	x	•	x
Fresh older*Psilotum*	•	•	x	•	•
Decayed older *Psilotum*	•	•	x	•	•
Fresh vine	•	•	•	•	•
Decayed vine	•	•	•	•	•
Fresh *Cyathea*	•	•	•	•	•
Decayed *Cyathea* (6 wks)	•	•	x	•	•
Decayed *Cyathea* (14 wks)	•	•	•	•	•
Fresh pine	•	•	x	•	•
Decayed pine	•	•	x	•	•
Fresh plane	•	•	•	•	•
Decayed plane (6 wks)	•	•	x	•	•
Decayed plane (14 wks)	•	•	•	•	•

Table 3.2. Analyses carried out on fresh and decayed plant samples. Pyrol. represents pyrolysis-GC/MS. All decayed samples were decayed for 14 weeks unless otherwise stated. • represents analysis undertaken. x indicates insufficient sample for analysis.

Sample Preparation

On removal from the decay systems, the twigs were freeze-dried using a Genevac SF50 dryer attached to a Genevac CVP100 pump. They were then finely ground with a pestle and mortar and stored frozen prior to analysis.

Alditol assay for carbohydrate analysis

Finely ground plant material (10mg) was weighed into a Young's tube. 72% sulphuric acid (100µl) was added to the plant material and the tube evacuated. The contents of the tube were kept at room temperature with regular vortexing for one hour.

The mixture was then diluted with double-distilled di-chloro-methane (DCM)-extracted water (900µl) and heated at 100°C under vacuum for 2 hours. After cooling, the mixture was made neutral with respect to ammonia by the addition of 18M ammonia solution (300µl) and then filtered through DCM-extracted cotton wool into a 4ml vial. Pentaerythritol solution (20mg/ml) was added as an internal standard (10µl), and a 400µl aliquot of the mixture transferred to a culture tube.

Sodium borahydrate (2ml) was added to the mixture, which was then incubated at 40°C for 90 minutes. The mixture was decomposed by the addition of glacial acetic acid (200µl) and then acetylated with 1-methylimidazole (200µl) and acetic anhydride (1ml). After mixing, the mixture was left for 10 minutes. Excess acetic anhydride was decomposed by the addition of double-distilled DCM-extracted water (6ml).

After cooling, diethyl ether (2ml) was added with thorough vortexing. The ether was removed and placed in a separate 8ml vial. This extraction was repeated a further 3 times. The ether was evaporated and the remaining syrup re-dissolved in double-distilled DCM-extracted water. The solvent extraction was repeated, and the diethyl ether passed through a magnesium sulphate column on removal from the mixture.

The sample (1µl) was analysed using a Hewlett Packard 5890 gas chromatograph fitted with a flame ionisation detector. Analysis was carried out using a 60m BPX-70 column with an on-column injector. The carrier gas was hydrogen with a head pressure of 10psi. The column temperature was programmed at 50°C for 1 minute before being ramped

to 200°C at a rate of 20°C per minute and then further to 230°C at 4°C per minute. This final temperature was held for 22 minutes.

Lignin analysis

The copper oxide oxidation products of lignin were analysed according to the method of Hedges and Ertel (1982).

Finely-ground plant material (50mg) was weighed into a large vial and 2:1 chloroform:methanol (10ml) added. The mixture was ultrasonicated for 20 minutes, before the solvent was removed and centrifuged at 3000rpm for 10 minutes. This lipid extraction of the plant material was repeated twice more, and the combined remaining plant material left to air-dry.

A sub-sample of the extracted plant material (25mg) was placed in a Teflon beaker within a mini-bomb (Parr Instruments Co., Illinois, USA) with copper oxide (1.0g), iron ammonium sulphate hexa-hydrate (100mg) and 2M sodium hydroxide solution (7ml). The headspace of the mini-bomb was purged with nitrogen before sealing. The mini-bomb was then heated at 170°C for 3 hours, before being cooled rapidly in a stream of cool air.

Ethyl vanillin in pyridine (0.333µg/µl) was added (20µl) to the cooled mixture as an internal standard. The mixture was washed into a centrifuge tube with 1M sodium hydroxide solution and centrifuged at 1200rpm for 10 minutes.

The supernatant was removed and kept, and the residue washed with 1M sodium hydroxide (20ml). This mixture was ultrasonicated for 10 minutes and then centrifuged at 1200rpm for 10 minutes. The residue was then washed with further 1M sodium hydroxide solution (20ml) and ultrasonicated and centrifuged as before.

The combined supernatants were acidified to pH 1 with 6M hydrochloric acid. This mixture was extracted 3 times with ethyl ether (20ml) which had been treated with a saturated aqueous solution of $Fe(NH_4)_2(SO_4)_2.6H_20$ to remove peroxides.

The combined ether extracts were passed through an anhydrous sodium sulphate column. The ethyl ether was then reduced to 1-2ml volume by vacuum rotorevaporation. The remaining sample was passed through a fresh anhydrous sodium sulphate column before the ether was removed under nitrogen. The sample could be stored dry at 4°C at this point.

BSTFA and 1% TMCS (50µl) and pyridine (50µl) were added to the dry oxidation product. The mixture was heated at 80°C for 15 minutes. Any solvent was removed under nitrogen and the remaining syrup dissolved in dichloromethane and the sample was analysed immediately for characteristic lignin phenolic compounds (see below) by gas chromatography.

Samples were analysed on a Hewlett Packard 5890 series II gas chromatograph fitted with a flame ionisation detector using a Chrompack CPSIL5 column with an on-column injector. The carrier gas was hydrogen with a headspace pressure of 10psi. The column temperature was kept at 50°C for 2 minutes and then ramped to 300°C at a rate of 4°C per minute. The column was maintained at this temperature for a further 20 minutes.

Sample peaks were identified by GC-MS using a Carlo Erba 5160 gas chromatograph with an on-column injector directly coupled to a Finnegan MAT 4500 Quadrupole mass spectrometer. Compounds were separated using a Chrompack CPSIL-5cb column (50m x 0.32mm internal diameter, with a 0.4µm film thickness) with a helium flow and a

headspace pressure of 8psi. The source temperature was 170°C. The mass spectrometer was operated at 50-650 scan range at 1 scan per second.

Cupric oxide oxidation of lignified plant material produces characteristic phenolic products which can be assigned to four structural families. The syringyl, vanillyl (i.e. guaiacyl) and *p*-hydroxyphenyl families are each composed of an aldehyde, a ketone, and a carboxylic acid. The cinnamyl family is comprised of two phenols with *trans*-propenoic acid substitution (Hedges and Ertel, 1982).

The major phenolic products (syringyl, vanillyl and cinnamyl families) are unique to vascular plants and occur in patterns which allow different taxonomic (i.e. gymnosperm versus angiosperm) and tissue (i.e. woody versus non-woody) types to be distinguished (Hedges and Mann, 1979a; Sarkanen and Ludwig, 1971). With rare exceptions for the cinnamyl phenols either all or none of the members of any family are produced by CuO oxidation.

The relative abundances of aldehyde and acidic phenols and the ratios of different phenolic families (S/V, P/V) can provide information regarding the taxonomic affinity of the plane (e.g. S/V > O for all angiosperms; Hedges and Mann, 1979), and the decay of the material e.g. the vanillyl acid/aldehyde ratio, (Ad/Al)v, is elevated with fungal degradation (Hedges *et al.*, 1988c). These ratios are presented in Table 3.3 and are discussed further in the discussion section of this chapter.

CHN elemental analysis

Carbon, nitrogen and hydrogen were measured using a Carlo-Erba EA1108 elemental analyser. Carbonate levels were analysed using a Coulomat 702 (Strohlein Instruments). Total organic carbon was calculated by subtracting the carbonate value from the overall carbon concentration. All samples were analysed twice and the mean result

Ratio 1:	S/V:	$\frac{\text{(syringic acid + syringaldehyde + acetosyringone)}}{\text{(vanillic acid + vanillin + acetovanillone)}}$
Ratio 2:	P/V:	$\frac{\text{(}p\text{-hydroxybenzoic acid + }p\text{-hydroxybenzaldehyde + }p\text{-hydroxyacetophenone)}}{\text{(vanillic acid + vanillin + acetovanillone)}}$
Ratio 3:	(Ad/Al)v:	$\frac{\text{vanillic acid}}{\text{acetovanillone}}$
Ratio 4:	(Ad/Al)s:	$\frac{\text{syringic acid}}{\text{syringaldehyde}}$

Table 3.3. Lignin phenolic compositional ratios (Hedges and Mann, 1979)).

calculated. This analysis was carried out by the staff of the micro-analytical laboratory at the School of Chemistry, University of Bristol.

^{13}C Solid State NMR

Finely ground freeze-dried plant material was packed into a cylindrical Zirconia rotor (internal dimensions 5.6mm x 17mm) which was sealed with a Kel-F cap. The samples were run on a Bruker MSL 300 spectrometer operating at 75.5 MHz for ^{13}C. The contact time for each sample was 1ms and the relaxation delay was 0.5-2.0s depending on the sample. Two experiments were performed for each sample:

i) cross-polarisation/magic angle spinning (CP/MAS) with total suppression of side-bands (TOSS);

ii) non-quarternary suppression (NQS) with TOSS, often referred to in the literature as dipolar dephasing (DD).

The spectra were divided into 7 chemical shift regions (Kolodziejski *et al.*, 1982) (Table 3.4). More specific individual peaks are assigned in the results section.

By assuming that the NMR spectrum is representative of all the carbon in the samples, the proportions of carbon in each functional group can be calculated as mg C per g of material.

Beyer (1996) proposed a method for estimating the total amounts of proteins, lipids, lignins and polysaccharides in any given sample. This is done by combining the amounts of each of the seven functional groups into 4 categories, 0-45ppm, 45-110ppm, 110-160ppm and 160-220ppm, and making the following assumptions:

i) 100% of the lipids contribute to the 0-45ppm signals;

ii) 100% of the polysaccharides contribute to the 45-110ppm signals;

iii) 40% of the proteins contribute to the 0-45ppm signals;

iv) 25% of the proteins contribute to the 45-110ppm signals;

Chemical shift	Functional group	C atoms
0-45ppm	alkyls	includes CH_2 and CH_3 in aliphatic alkanes, fatty acids and waxes
45-65ppm	N-alkyls	methoxyl C of lignin and hemicellulose and/or N-substituted aliphatic C in amino acids (if lost in DD, most likely N-alkyl)
65-92ppm	O-alkyls	often interpreted as the "carbohydrate band"
92-110ppm	acetals	de-oxygenated C, e.g. acetal, anomeric C of polysaccarides
110-140ppm	aromatics	C or H substituted aromatic C
140-160ppm	phenolics	aromatic bonded to OH groups, probably includes N-substituted aromatic C (aromatic NH_2 groups)
160-220ppm	carboxyls	carbonyl C, carboxyl groups in aliphatic acids and benze-carboxylic acids, C in amide and ester structures, C=O groups of quinones

Table 3.4. Identification of compounds contributing to different chemical shift regions in ^{13}C NMR spectra of plant material.(Kolodziejski *et al.*, 1982)

v) 5% of the proteins contribute to the 110-160ppm signals;

vi) 30% of the proteins contribute to the 160-220ppm signals;

vii) 44% of the lignins contribute to the 45-110ppm signals;

viii) 56% of the lignins contribute to the 110-160ppm signals.

Pyrolysis-GC/MS

Freeze-dried, finely ground plant material (ca 10mg) was placed in a 18ml vial. Chloroform/methanol (2:1, 5ml) was added, and the mixture was ultrasonicated for 10 minutes. The solvent was removed, and the extraction repeated a further 4 times.

The extracted sample was pyrolysed at 610°C for 10 seconds using a CDS pyroprobe 1000 with an interface temperature of 250°C. This was linked to a Carlo-Erba 4130 gas chromatograph directly coupled to a Finnegan MAT 4500 quadrupole mass spectrometer via a heated transfer line.

Compounds were separated using a Chrompack CPSIL-5cb column (50m x 0.32mm internal diameter, with a 0.4µm film thickness). The source temperature was 170°C. The oven temperature was held at 35° for 5 minutes before being ramped to 310°C at a rate of 4°C per minute. This temperature was held for 15 minutes.

The mass spectrometer was operated at 35-500 scan range at 1 scan per second. Electron ionisation was carried out at 70eV with 300µAmp emission.

This method is not quanititative.

Results

Alditol assay for carbohydrates

The gas chromatographs produced for each fresh or decayed plant sample are presented in Figure 3.1. The major sugar peaks are identified

in Table 3.5. The yields of each individual sugar were calculated in mg carbohydrate per g sample by comparing the relative peak areas with that of the internal standard and are presented in Table 3.6.

Peak no.	Sugar
1.	rhamnose
2.	fucose
3.	ribose
4.	arabinose
5.	xylose
6.	mannose
7.	galactose
8.	glucose
I.S.	internal standard

Table 3.5. Identification of peaks of sugars in samples of fresh and decayed plant material.

Glucose was the dominant sugar in the fresh and decayed samples for all species, ranging from 53.3% of the total sugars in fresh celery to 71.9% in fresh pine, and reaching 88.6% in fresh *Cyathea*. Either mannose or xylose, both of which are present in hemicellulose in different proportions depending on the taxonomic affinity of the species, was the second most abundant sugar within fresh or decayed samples, except for pine, where arabinose, a constituent of pectin, was present in greater concentrations. Ribose, fucose and rhamnose each comprised less than 2% of the total sugars in both the fresh and decayed samples of all plant species studied.

There was no unique sequence for the relative degradation of the individual sugars between the different species, even for species from the same taxonomic group (vine and plane). However, xylose was the least degraded sugar for celery, older *Psilotum*, vine and plane, and was one of

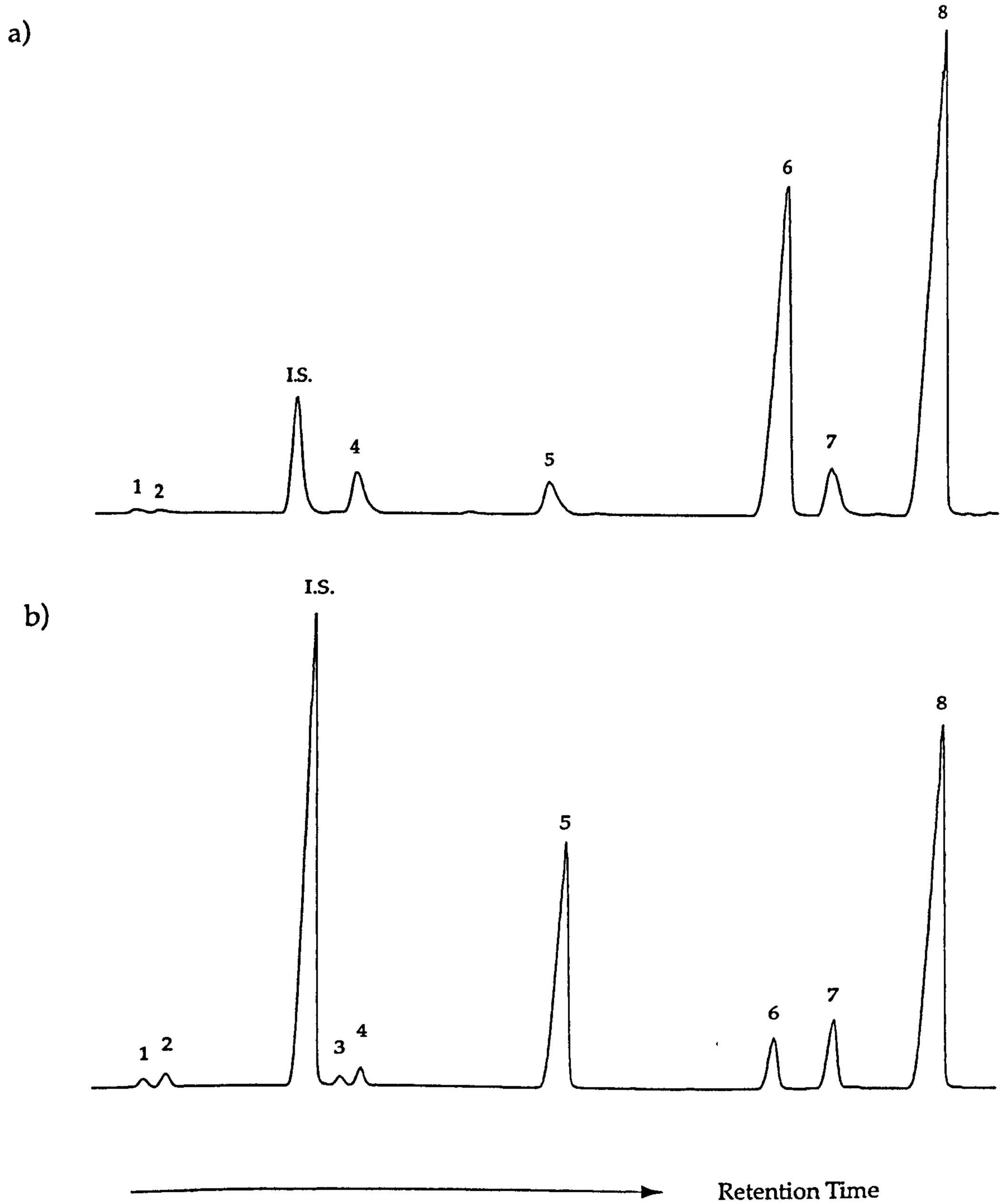

Figure 3.1a. Gas chromatographs of sugars present in a) fresh celery and b) celery decayed for 14 weeks

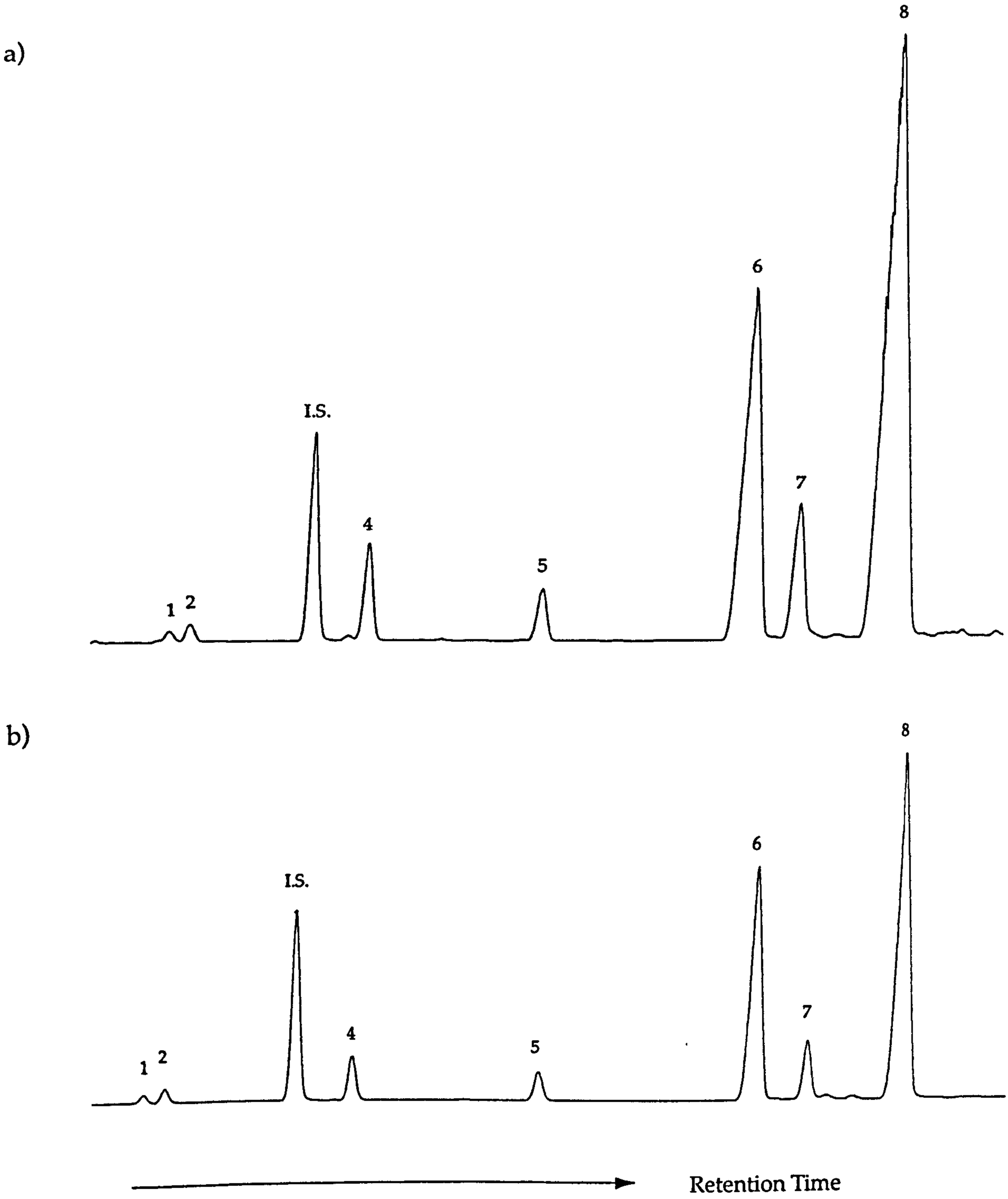

Figure 3.1b. Gas chromatographs of sugars present in a) fresh newer *Psilotum* and b) newer *Psilotum* decayed for 14 weeks

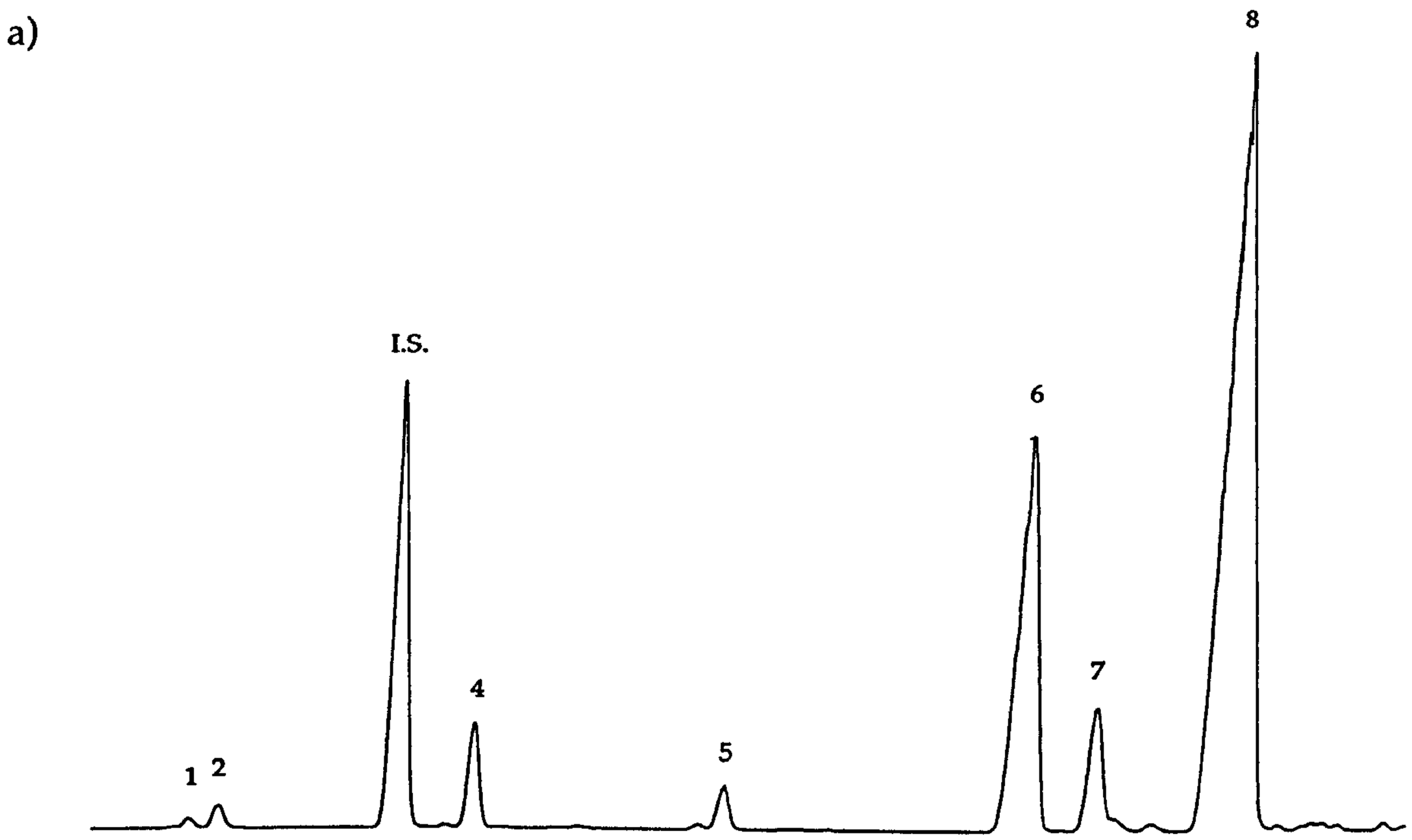

Figure 3.1c. Gas chromatographs of sugars present in a) fresh older *Psilotum* and b) older *Psilotum* decayed for 14 weeks

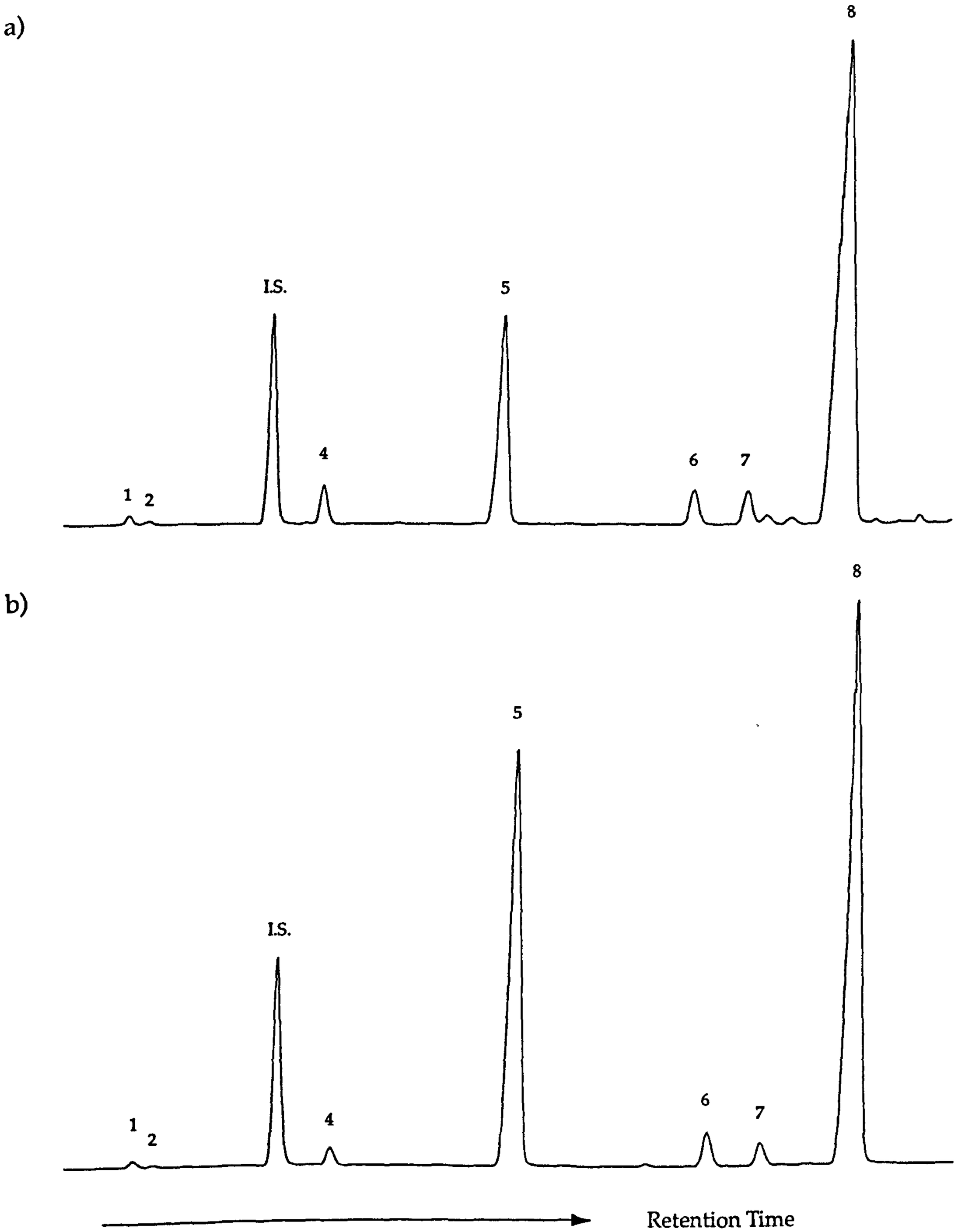

Figure 3.1d. Gas chromatographs of sugars present in a) fresh vine and b) vine decayed for 14 weeks

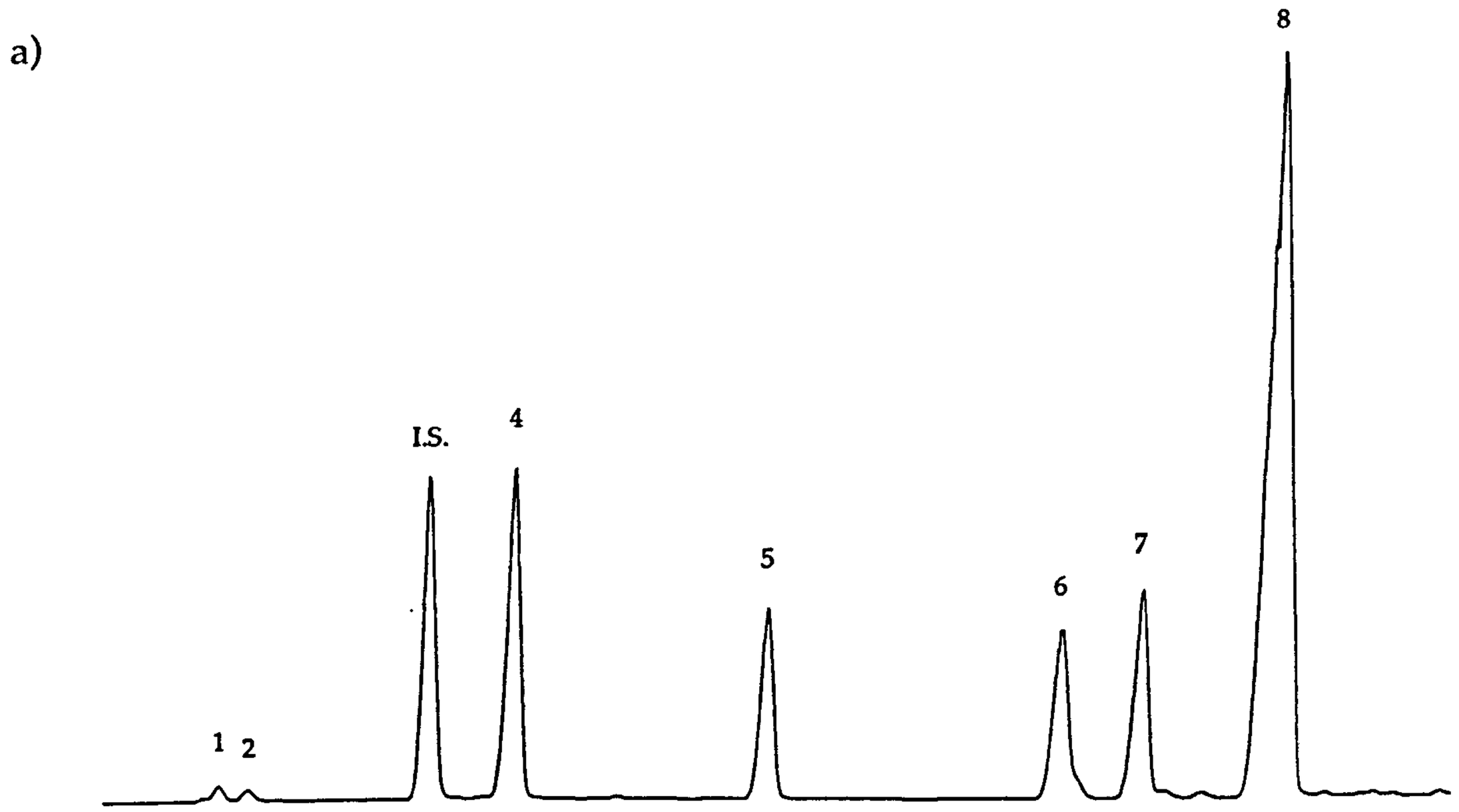

Figure 3.1e. Gas chromatographs of sugars present in a) fresh pine and b) pine decayed for 14 weeks

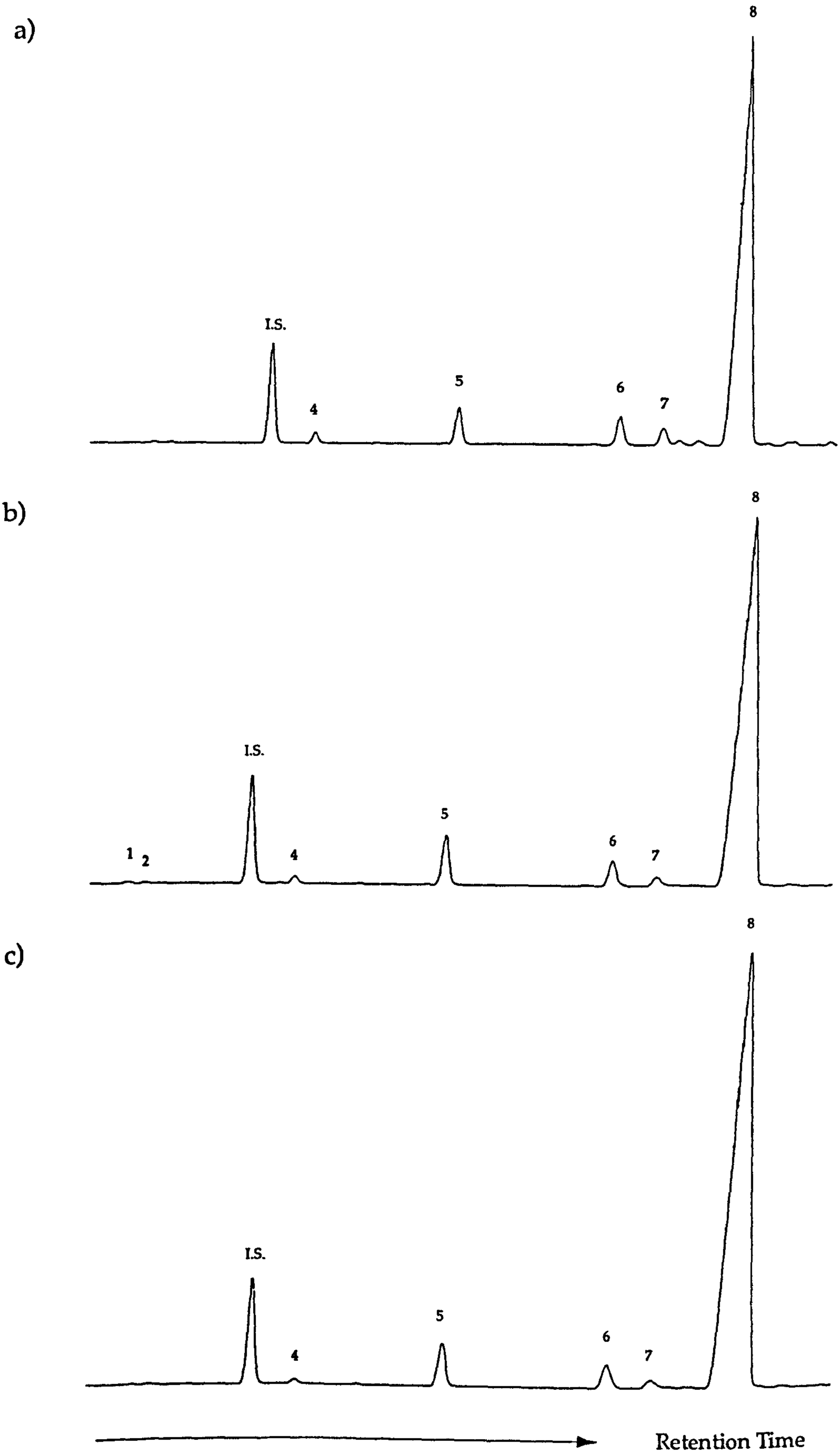

Figure 3.1f. Gas chromatographs of sugars present in a) fresh *Cyathea,* b) *Cyathea* decayed for 6 weeks and c) *Cyathea* decayed for 14 weeks

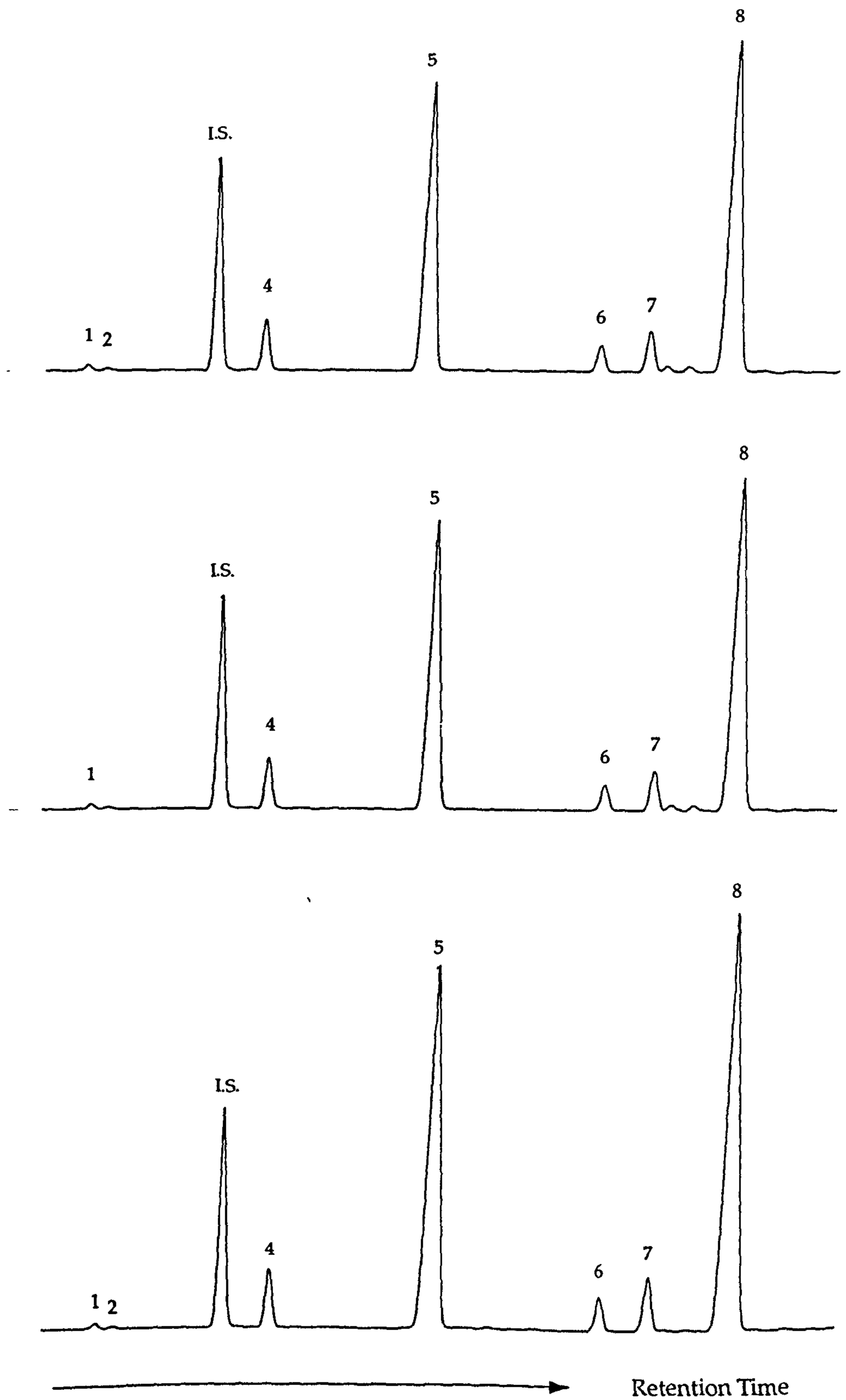

Figure 3.1g. Gas chromatographs of sugars present in a) fresh plane, b) plane decayed for 6 weeks and c) plane decayed for 14 weeks

Plant sample	GLU	XYL	MAN	ARA	GAL	FUC	RIB	RHA	TOTAL
	mg C per g								mg C / g
Fresh celery	1178.8	74.0	753.3	86.6	100.9	7.2	3.6	8.5	2212.9
Decayed celery (14 weeks)	186.9	107.8	18.6	5.3	24.5	4.3	2.9	2.8	353.1
(% change with 14 weeks decay)	-84.1%	+45.6%	-97.5%	-93.9%	-75.8%	-40.2%	-20.5%	-66.9%	-84.0%
Fresh newer *Psilotum*	1339.5	51.9	606.3	90.9	158.3	17.4	4.1	11.3	2676.6
Decayed newer *Psilotum* (14 weeks)	525.6	31.7	334.0	46.3	63.4	14.2	0	10.0	1025.2
(% change with 14 weeks decay)	-60.8%	-38.9%	-44.9%	-49.0%	-59.9%	-18.5%	-100%	-11.4%	-61.7%
Fresh older *Psilotum*	705.8	17.4	260.5	39.5	65.5	9.6	1.5	4.2	1104.0
Decayed older *Psilotum* (14 weeks)	400.9	36.1	227.1	70.6	65.7	14.7	2.4	5.6	823.1
(% change with 14 weeks decay)	-43.2%	+108.2%	-12.8%	+78.8%	+0.3%	+52.4%	+62.1%	+34.9%	-25.4%
Fresh vine	926.1	239.5	37.3	35.7	37.6	3.3	0	8.2	1287.7
Decayed vine (14 weeks)	839.5	558.9	37.0	17.8	24.2	0	0	6.9	1484.3
(% change with 14 weeks decay)	-9.3%	+133.4%	-0.7%	-50.2%	-35.6%	-100%	-	-16.5%	+15.3%
Fresh *Cyathea*	1706.1	79.6	70.9	22.3	42.7	0	0	3.3	1924.9
Decayed *Cyathea* (6 weeks)	1719.5	103.5	59.7	15.2	24.6	3.2	2.0	4.0	1931.7
(% change with 6 weeks decay)	+0.8%	+29.9%	-15.8%	-31.8%	-42.4%	+100%	+100%	+22.1%	+0.4%
Decayed *Cyathea* (14 weeks)	2239.5	93.2	60.5	9.8	18.6	2.3	0	2.4	2426.3
(% change with 14 weeks decay)	+31.3%	+17.0%	-14.7%	-56.1%	-56.5%	+100%	-	-26.7%	+26.0%
Fresh pine	842.4	128.9	14.0	231.9	153.9	6.5	0	10.8	1388.4
Decayed pine (14 weeks)	402.8	117.7	76.1	282.6	141.4	3.9	0	3.5	1028.0
(% change with 14 weeks decay)	-52.2%	-8.7%	+442.2%	+21.9%	-8.2%	-40.2%	-	-67.5%	-26.0%
Fresh plane	1219.7	568.8	79.1	76.6	102.1	3.9	1.6	9.6	2061.4
Decayed plane (6 weeks)	503.1	393.9	27.3	48.4	42.8	1.9	0	5.1	1022.5
(% change with 6 weeks decay)	-58.8%	-30.7%	-65.4%	-36.9%	-58.1%	-52.8%	-100%	-46.2%	-50.4%
Decayed plane (14 weeks)	656.1	559.4	33.4	52.8	51.8	2.1	0	5.0	1360.6
(% change with 14 weeks decay)	-46.2%	-1.7%	-57.8%	-31.5%	-49.3%	-47.2%	-100%	-47.2%	-34.0

Table 3.6. Relative concentrations of individual sugars present in fresh and decayed plant material and their relative changes with decay. GLU: glucose; XYL: xylose; MAN: mannose; ARA: arabinose; GAL: galactose; FUC: fucose; RIB: ribose; RHA: rhamnose

the least degraded sugars for pine, newer *Psilotum*, and *Cyathea*. Relative concentrations of xylose increased with decay for celery, older *Psilotum*, vine and *Cyathea*.

The total amount of carbohydrates present decreased after 14 weeks of decay, for all species except for vine and *Cyathea*. The relative decreases (or increases) in the total concentrations of carbohydrates in the decayed samples allow the species to be put in the following sequence of decreasing decay after 14 weeks: celery > newer *Psilotum* > plane > pine > older *Psilotum* > vine > *Cyathea*.

The individual sugars can be assigned to the three main polysaccharide tissues (Hedges *et al.*, 1985). Xylose and mannose are the major constituents of hemicelluloses (Timell, 1957; Sjöström, 1981), and glucose is the predominant sugar in α-cellulose (Timell, 1957). Arabinose, galactose, fucose and rhamnose (and galacturonic acid, which was not analysed) are found in pectins (Aspinall, 1970). Ribose is present in RNA. The sum of the total sugars for each tissue in each sample is presented in Table 3.7.

There are no trends in decay susceptibilities of the three polysaccharide tissues between plant species.

Lignin assay

Gas chromatograms of lignin phenolic components are presented in Figure 3.2. The major lignin phenolic peaks are identified in Table 3.8. Ferulic acid peaks were very small and could not be identified confidently.

Sample	Cellulose	Hemicellulose	Pectin
Fresh celery	1178.8	827.4	203.2
Decayed celery	186.9	126.3	36.8
change with decay	-84.1%	-84.7%	-81.9%
Fresh Newer *Psilotum*	1339.5	658.3	277.9
Decayed Newer *Psilotum*	525.6	365.7	133.9
change with decay	-60.8%	-44.4%	-51.8%
Fresh Older *Psilotum*	705.8	277.9	118.8
Decayed Older *Psilotum*	400.89	263.2	156.6
change with decay	-43.2%	-5.3%	+31.%
Fresh vine	926.1	276.8	84.8
Decayed vine	839.5	595.9	48.9
change with decay	-9.3%	+115%	-42.4%
Fresh *Cyathea*	1706.1	150.5	68.3
Decayed *Cyathea* (6 wks)	1719.5	163.2	47.0
change with decay	+0.8%	+8.4%	-31.2%
Decayed *Cyathea* (14 wks)	2239.5	153.7	33.1
change with decay	+31.3%	+2.1%	-51.6%
Fresh pine	842.4	142.9	403.2
Decayed pine	402.8	193.8	431.4
change with decay	-52.2%	+35.6%	+7.0%
Fresh plane	1219.7	647.8	192.2
Decayed plane (6 wks)	503.1	421.3	98.2
change with decay	-58.8%	-35.0%	-48.9%
Decayed plane (14 wks)	656.1	592.7	111.6
change with decay	-46.2%	-8.5%	-41.9%

Table 3.7. Changes in relative concentrations of cellulose, hemicellulose and pectin with decay.

Peak no.	Phenolic compound	Family
1.	*p*-hydroxybenzaldehyde	*p*-hydroxyphenyl
2.	*p*-hydroxyacetophenone	*p*-hydroxyphenyl
3.	vanillin	vanillyl (guaiacyl)
4.	ethyl vanillin	internal standard
5.	acetovanillone	vanillyl (guaiacyl)
6.	*p*-hydroxybenzoic acid	*p*-hydroxyphenyl
7.	syringaldehyde	syringyl
8.	acetosyringone	syringyl
9.	vanillic acid	vanillyl (guaiacyl)
10.	syringic acid	syringyl
11.	*p*-coumaric acid	cinnamyl

Table 3.8. Identification of peaks of major lignin phenols in samples of fresh and decayed plant material.

The fresh and decayed samples of each species yielded the expected characteristic phenolic families according to Sarkanen and Ludwig (1973), Erickson and Miksche (1974) and Logan and Thomas (1985). The woody angiosperms (vine and plane) contained vanillyl (guaiacyl) and syringyl units. All other species were vanillyl (guaiacyl) dominated. Traces of *p*-hydroxyphenyls were present in all fresh and decayed samples.

The total amounts of each phenolic compound for each sample are presented in Table 3.9. The relative concentrations of total lignin (the sum of all seven of the main phenolic compounds) increased with decay for celery, newer *Psilotum*, vine and plane, but decreased for *Cyathea*.

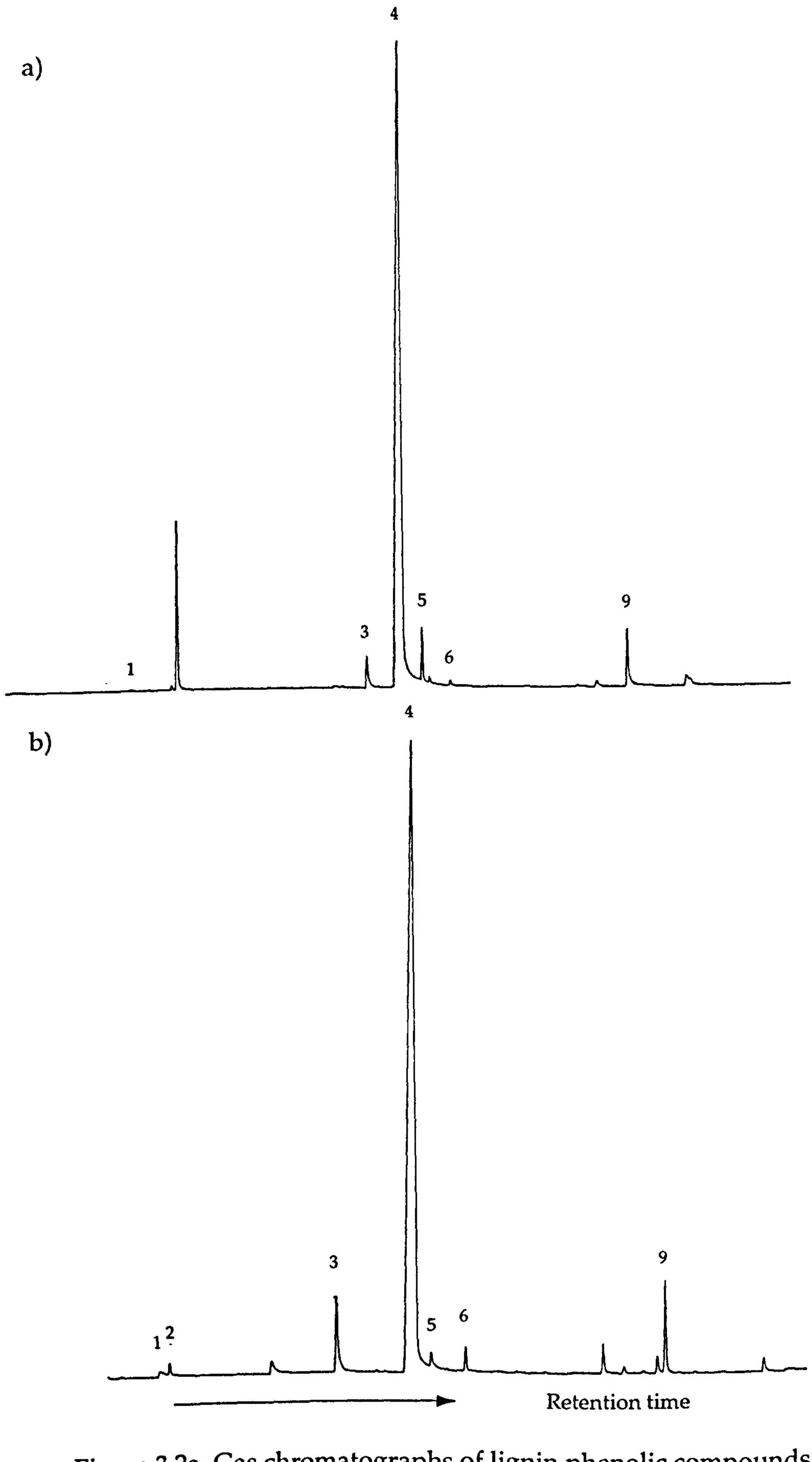

Figure 3.2a. Gas chromatographs of lignin phenolic compounds for a) fresh celery and b) fresh newer *Psilotum*

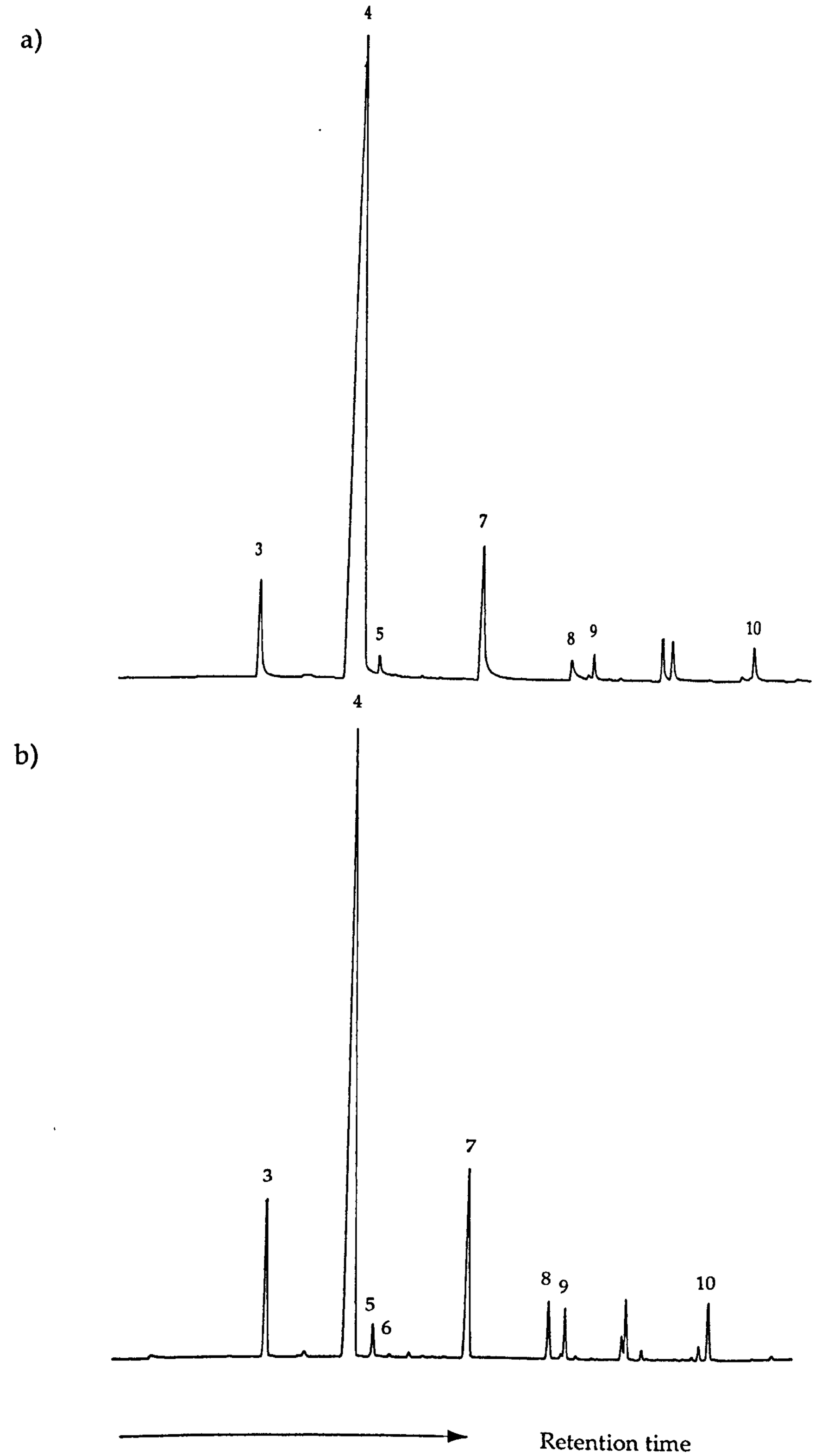

Figure 3.2b. Gas chromatographs of lignin phenolic compounds for a) fresh vine and b) vine decayed for 14 weeks

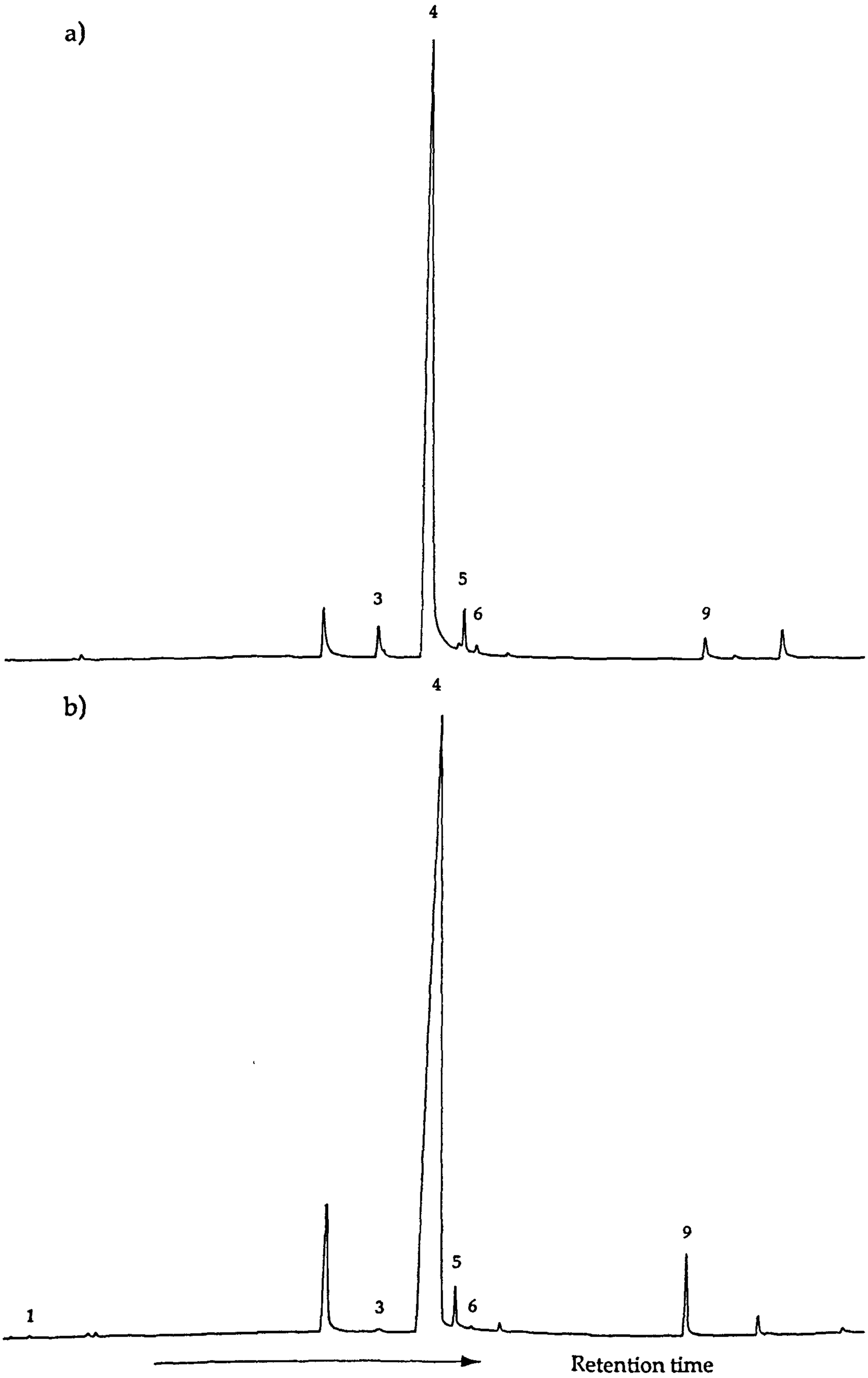

Figure 3.2c. Gas chromatographs of lignin phenolic compounds for a) fresh *Cyathea* and b) *Cyathea* decayed for 14 weeks

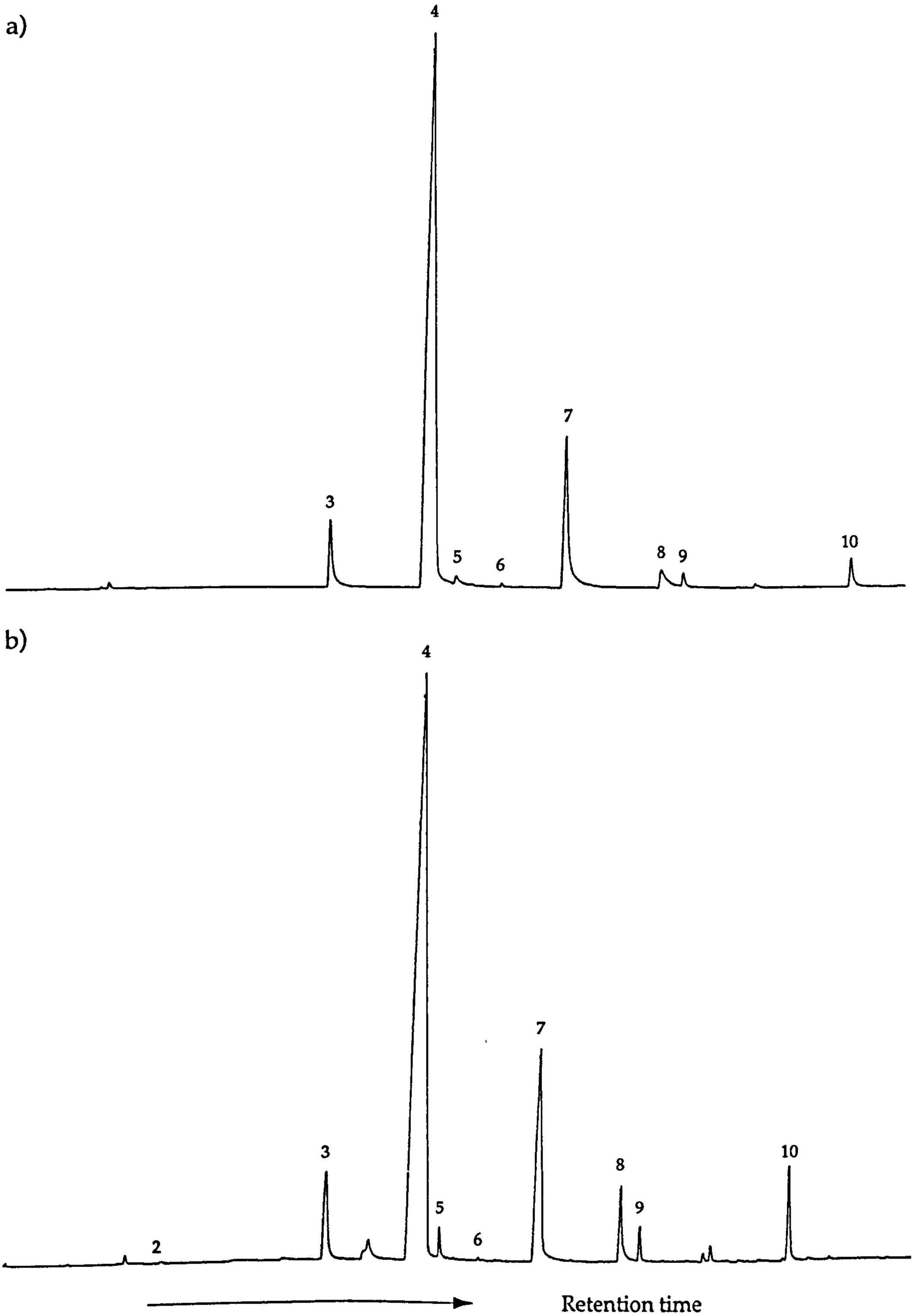

Figure 3.2d. Gas chromatographs of lignin phenolic compounds for a) fresh plane and b) plane decayed for 14 weeks

	Alp	Kp	Alv	Kv	Adp	Als	Ks	Adv	Ads	Adc	TOTAL
Fresh celery	1.0%	0%	25.8%	32.1%	2.6%	0%	0%	38.6%	0%	0%	95277
Fresh newer *Psilotum*	21.7%	12.5%	41.9%	7.1%	4.7%	0%	0%	6.5%	0%	5.7%	118066
Fresh vine	0.1%	0%%	28.6%	6.8%	0.3%	43.3%	7.3%	5.5%	7.6%	0.4%	205990
Decayed vine (14 weeks)	0%	0%	31.8%	5.3%	0%	45.4%	9.6%	8.0%	0%	0%	369463
Fresh *Cyathea*	0%	0%	29.3%	45.6%	2.9%	0%	0%	22.2%	0%	0%	81307
Decayed *Cyathea* (14 weeks)	1.6%	0%	3.9%	36.9%	4.6%	0%	0%	53.0%	0%	0%	57048
Fresh plane	0.4%	0%	19.1%	4.2%	0.5%	55.1%	9.0%	3.4%	7.3%	0.3%	317917
Decayed plane (14 weeks)	0.1%	0.3%	17.3%	3.2%	0.2%	52.7%	11.2%	3.5%	11.1%	0.5%	37764

Table 3.9. Percentage yields of lignin phenolic units from fresh and decayed plant material. Alp: *p*-hydroxybenzaldehyde; Kp: *p*-hydroxyacetophenone; Alv: vanillin; Kv: acetovanillone; Adp: *p*-hydroxybenzoic acid; Als: syringaldehyde; Ks: acetosyringone; Adv: vanillic acid; Ads: syringic acid; Adc: *p*-coumaric acid; TOTAL: relative peak areas for all peaks for each sample.

The phenolic compositional ratios for each fresh and decayed sample were calculated as in Table 3.3. and are presented in Table 3.10.

Sample	P/V	S/V	(Ad/Al)v	(Ad/Al)s
Fresh celery	0.04	-	1.5	-
Fresh new *Psilotum*	0.70	-	0.16	-
Fresh vine	0.01	1.4	0.19	0.17
Decayed vine	0	1.2	0.25	0
Fresh *Cyathea*	0.03	-	0.76	-
Decayed *Cyathea*	0.08	-	13.6	-
Fresh plane	0.04	2.7	0.18	0.13
Decayed plane	0.02	3.1	0.20	0.21

Table 3.10. Lignin phenol compositional ratios for fresh and decayed plant material.

Elemental analysis

The total organic carbon for each species ranged from 34.2% for fresh celery, to 48.2% in fresh pine. The C/N ratios of the fresh material varied greatly for each species, with the lowest ratio of 29.1 for celery and the highest of 253 for *Cyathea*. Trends in C/N ratios varied with decay between different plant species (Figure 3.3).

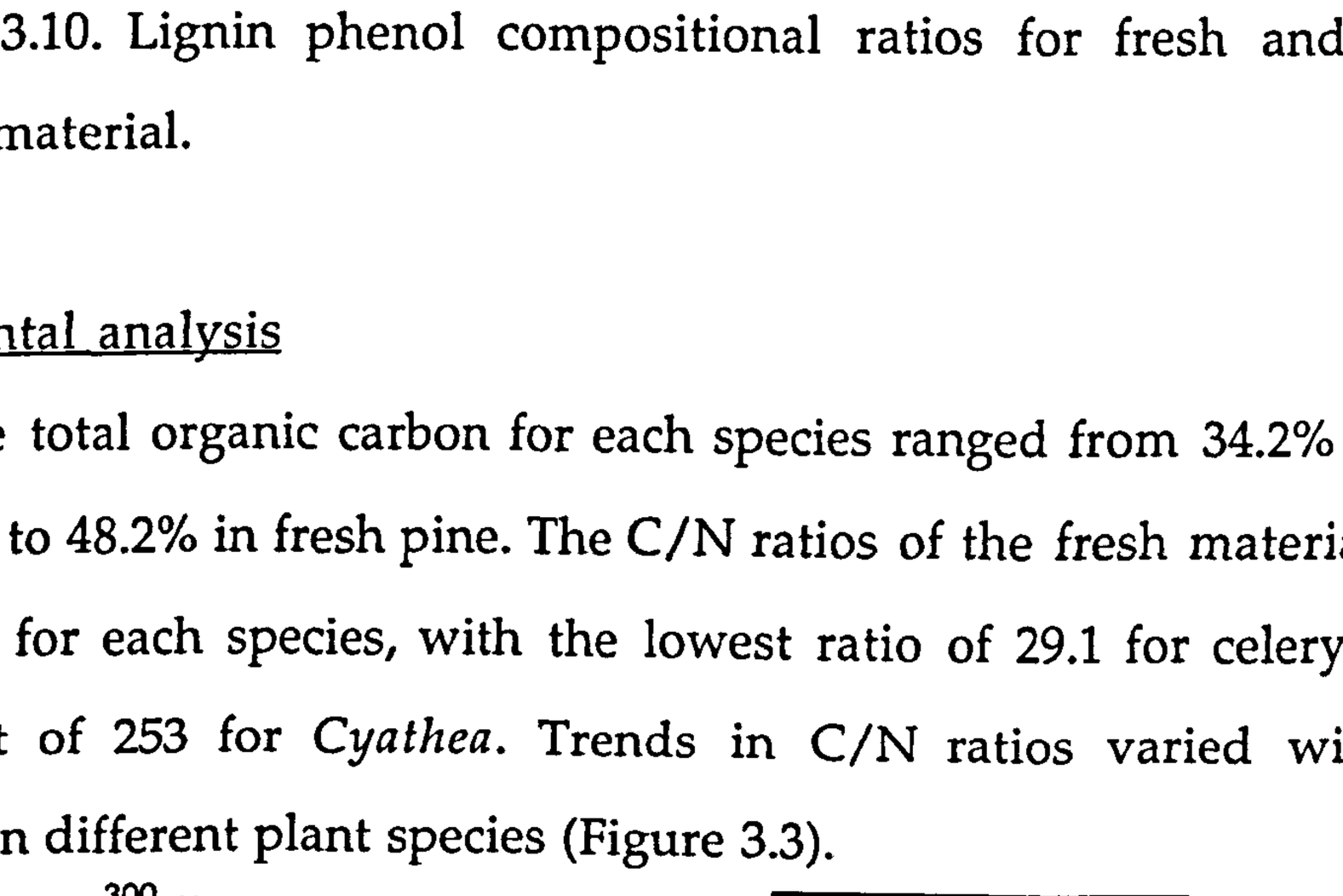

Figure 3.3 Changes in C/N ratios with decay for different plant species.

Pyrolysis-GC/MS

Pyrograms for all fresh and decayed samples are presented in Figure 3.4. Peaks were identified by comparison with retention times and mass spectra in the following literature: Faix *et al.*, 1990, 1991; Ralph and Hatfield, 1991; Galletti and Bocchini, 1995. Pyrolysis products identified are listed in Table 3.11.

The pyrolysis products can be ascribed to lignins, polysaccharides, and, occasionally, proteins. Lignin pyrolysis products are easily identifiable due to highly diagnostic mass spectra containing an intense molecular ion peak along with characteristic fragments. Guaiacyl, syringyl and *p*-hydroxyphenyl moieties are retained in most lignin pyrolysates. Polysaccharide pyrolysis products are considerably harder to identify unequivocally by mass spectrometry due to their facile fragmentation which produces many low molecular weight ions. Molecular ions are often absent or present only at very low intensity. Identification is further confused by the production of numerous structural and positional isomers. Typical polysaccharide pyrolysates include furans, pyrans and cyclopentenes, and key masses are m/z 43 ($C_2H_3O^+$), m/z 55 ($C_3H_3O^+$), m/z 57 ($C_3H_5O^+$), m/z 60 ($C_2H_4O_2^+$) and m/z 73 ($C_3H_5O_2^+$) (Faix *et al.*, 1991).

Peak no.	Compound name	Origin
1.	3-hydroxypropanal	PS
2.	pyruvic acid methyl acid	PS
3.	3-furaldehyde	PS
4.	2,4-pentadienal	PS
5.	2-furaldehyde	PS
6.	1-acetoxypropan-2-one	PS
7.	2-hydroxymethylfuran	PS
8.	(5H)-furan-2-one	PS
9.	2-methyl-2-cyclopenten-1-one	PS
10.	2-acetylfuran	PS
11.	2,3-dihydro-5-methylfuran-2-one	PS

Peak no.	Compound name	Origin
12.	4-(hydroxymethyl)tetrahydropyran-3-one	PS
13.	2,3-dihydroxyhex-1-ene-4-one	
14.	5-methyl-2-furfuraldehyde	PS
15.	4-hydroxy-5,6-dihydro-(2H)-pyran-2-one	PS
16*.	phenol	L-H
17.	3-hydroxy-2-methyl-2-cyclopenten-1-one	PS
18.	2,4-dihydropyran-3-one	PS
19.	2-methoxytoluene	
20.	2,3-dimethylcyclopenten-1-one	PS
21.	2-hydroxy-3-methyl-2-cyclopenten-1-one	PS
22.	2-methylphenol	L-H
23*.	4-methylphenol	L-H
24.	3-methylphenol	L-H
25.	2-(propan-2-one)tetrahydrofuran	PS
26.	guaiacol	L-G
27.	a dimethyldihydropyranone?	PS
28.	3,5-dihydroxy-2-methyl-5,6-dihydro-4H-pyran-4-one	PS
29.	2,4-dimethylphenol	L-H
30.	5-hydroxymethyl-2-tetrahydrofuraldehyde-3-one	PS
31.	4-methylguaiacol	L-G
32.	catechol	
33.	5-hydroxymethyl-2-furfuraldehyde	PS
34*.	4-vinylphenol	L-H
35.	3-methoxycatechol	
36.	3-methylcatechol	
37.	4-ethylguaiacol	L-G
38.	4-methylcatechol	
39.	indole	P
40.	4-vinylguaiacol	L-G
41.	2,6-dimethoxyphenol	L-S
42.	eugenol	L-G
43.	4-propylguaiacol	L-G
44.	1,4-dihydroxy-3-methoxybenzene?	
45.	vanillin	L-G
46.	*cis* *i*isoeugenol	L-G
47.	4-hydroxyacetophenone	L-H
48.	2,6-dimethoxy-4-methylphenol	L-S
49.	homovanillin	L-G

Peak no.	Compound name	Origin
50.	*trans* isoeugenol	L-G
51.	acetovanillone	L-G
52.	4-ethyl-2,6-dimethoxyphenol	L-S
53.	guaiacylacetone	L-G
54.	2,6-dimethoxy-4-vinylphenol	L-S
55.	propiovanillone	L-G
56.	4-allyl-2,6-dimethoxyphenol	L-S
57.	syringaldehyde	L-S
58.	*cis* 2,6-dimethoxy-4-propenylphenol	L-S
59.	dihydroconiferyl alcohol	L-G
60.	*cis* coniferyl alcohol	L-G
61.	*trans* 2,6-dimethoxy-4-propenylphenol	L-S
62.	acetosyringone	L-S
63.	*trans* coniferaldehyde	L-G
64.	*trans* coniferyl alcohol	L-G
65.	syringylacetone	L-S
66.	dihydrosinapyl alcohol	L-S
67.	cis sinapyl alcohol	L-S
68.	*trans* sinapaldehyde	L-S
69.	*trans* sinapyl alcohol	L-S

Table 3.11. Major compounds identified in the pyrolysates of fresh and decayed plant material. Peak numbers refer to peaks on the pyrograms, Figure 3.4. Origin: L, lignin; PS, polysaccharide; P, protein; H, *p*-hydroxyphenyl; G, guaiacyl; S, syringyl. *: may also be ascribed to proteins (Tsuge and Matsubara, 1985).

The most abundant pyrolysis products for the fresh and decayed samples reflected the taxonomic group of the plant. Pyrolysates of pine, *Cyathea*, and both newer and older *Psilotum* were dominated by guaiacyl units, in particular guaiacol (26), 4-vinyl guaiacol (40) and *trans* isoeugenol (50) (Figures 3.4a-d). 4-methylguaiacol (31) was significant in the pine and *Cyathea* pyrolysates (Figures 3.4a, b) and 4-ethylguaiacol (37)

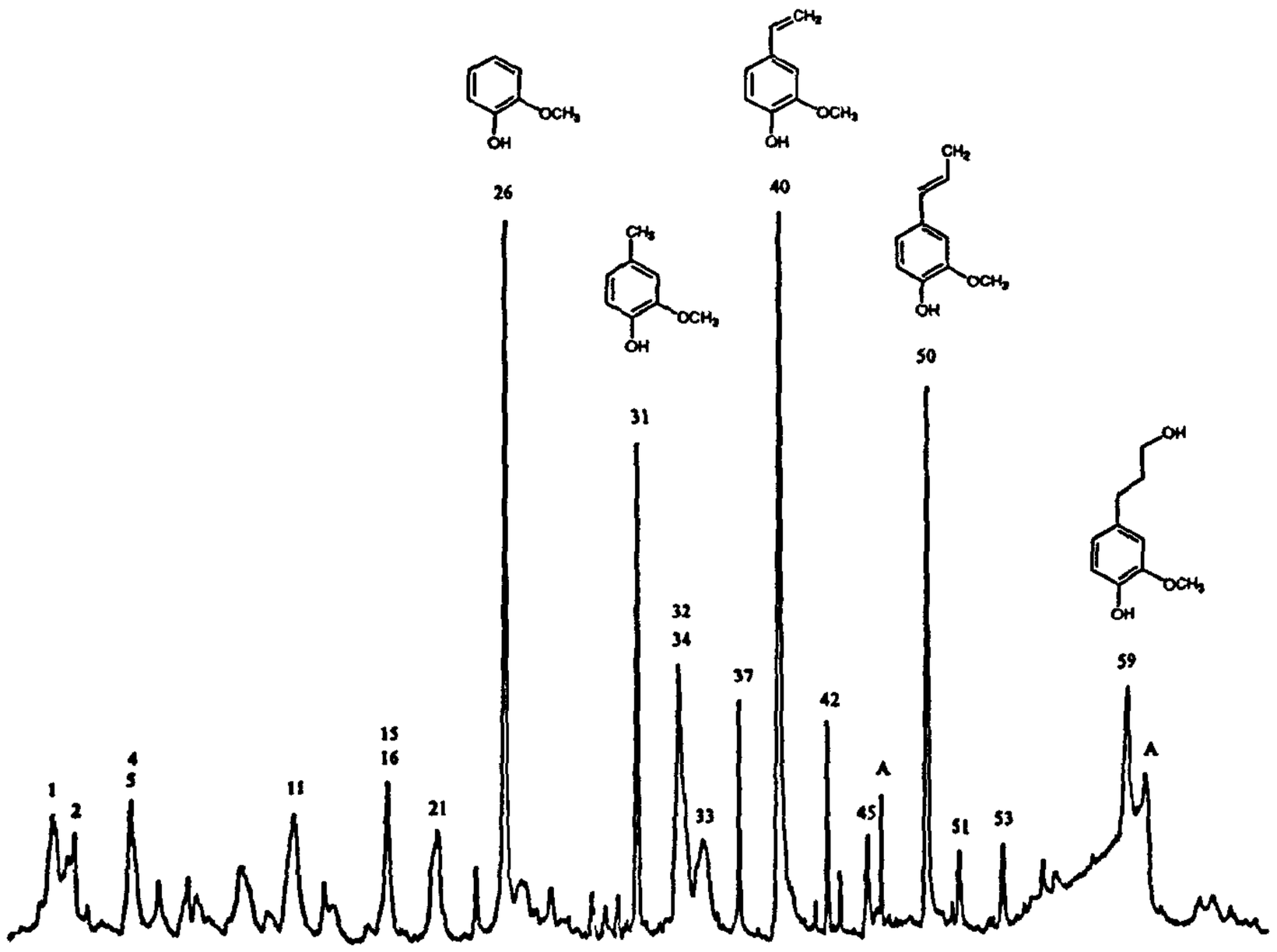

Figure 3.4a. Pyrolysis-GC/MS traces for a) fresh pine and b) pine decayed for 14 weeks. (A: anhydrosugars).

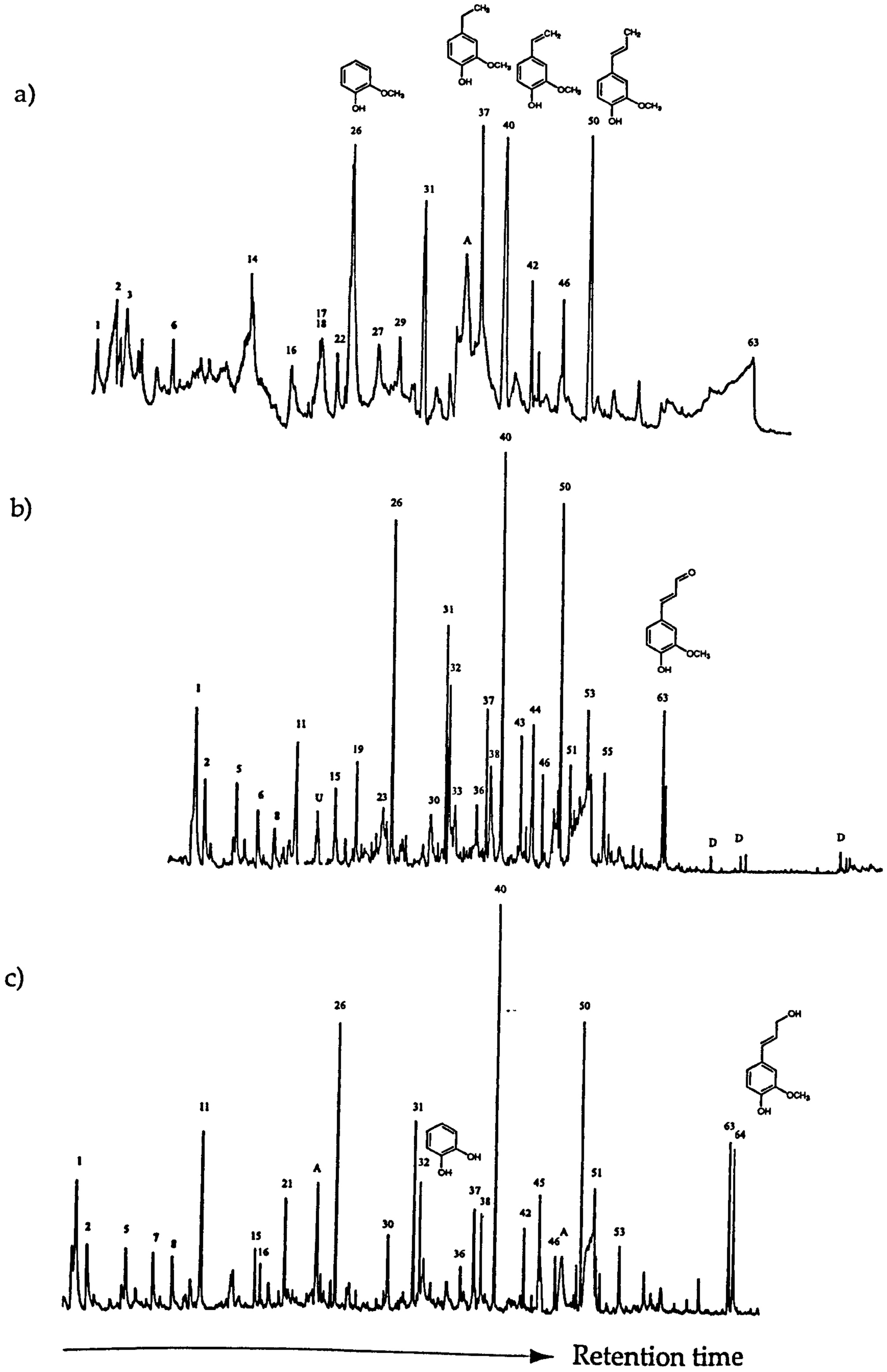

Figure 3.4b. Pyrolysis-GC/MS traces for a) fresh *Cyathea*, b) *Cyathea* decayed for 6 weeks and c) *Cyathea* decayed for 14 weeks. (A: anhydrosugars; D: Dimers).

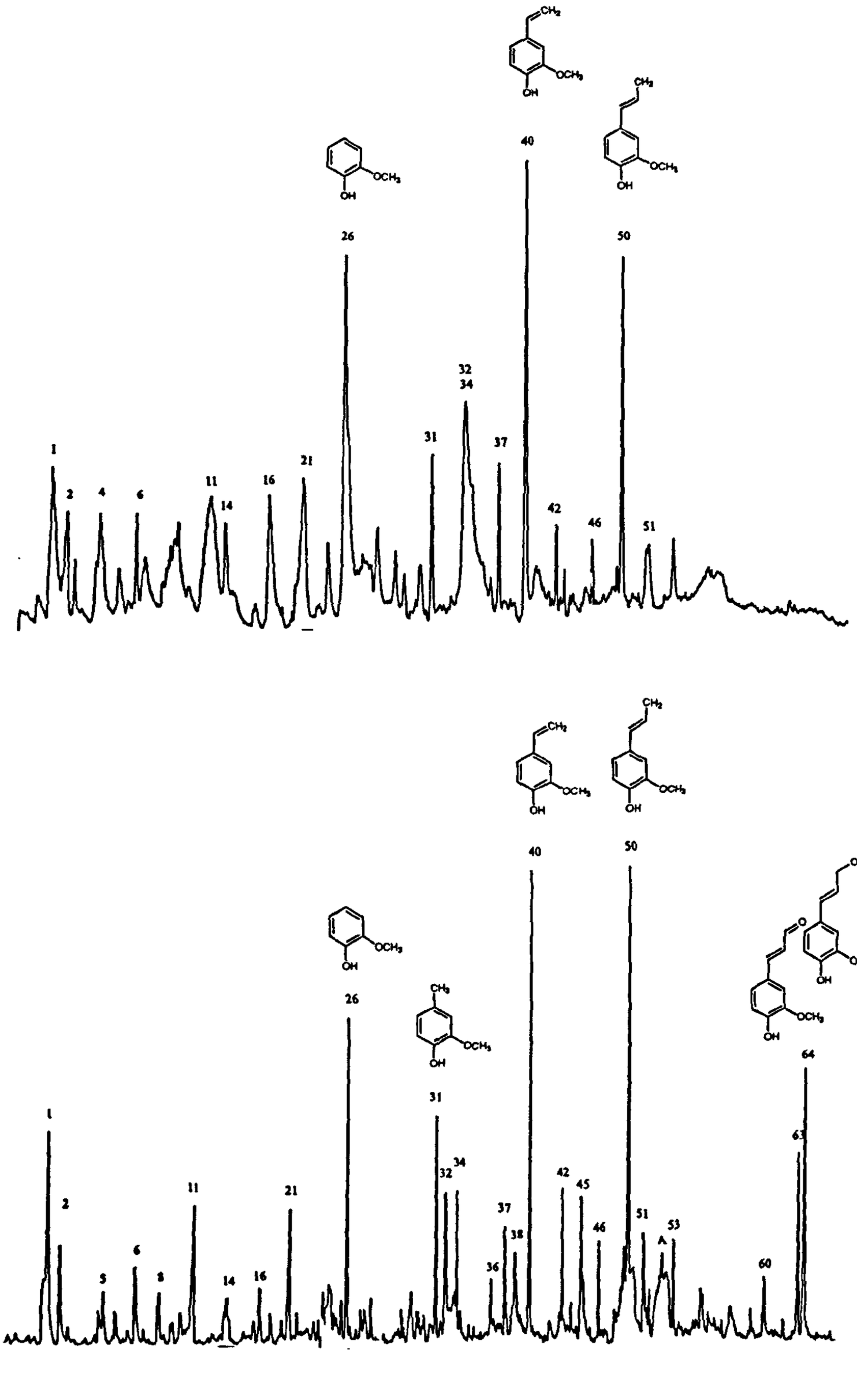

Figure 3.4c. Pyrolysis-GC/MS traces for a) fresh newer *Psilotum* and b) newer *Psilotum* decayed for 14 weeks. (A: anhydrosugars).

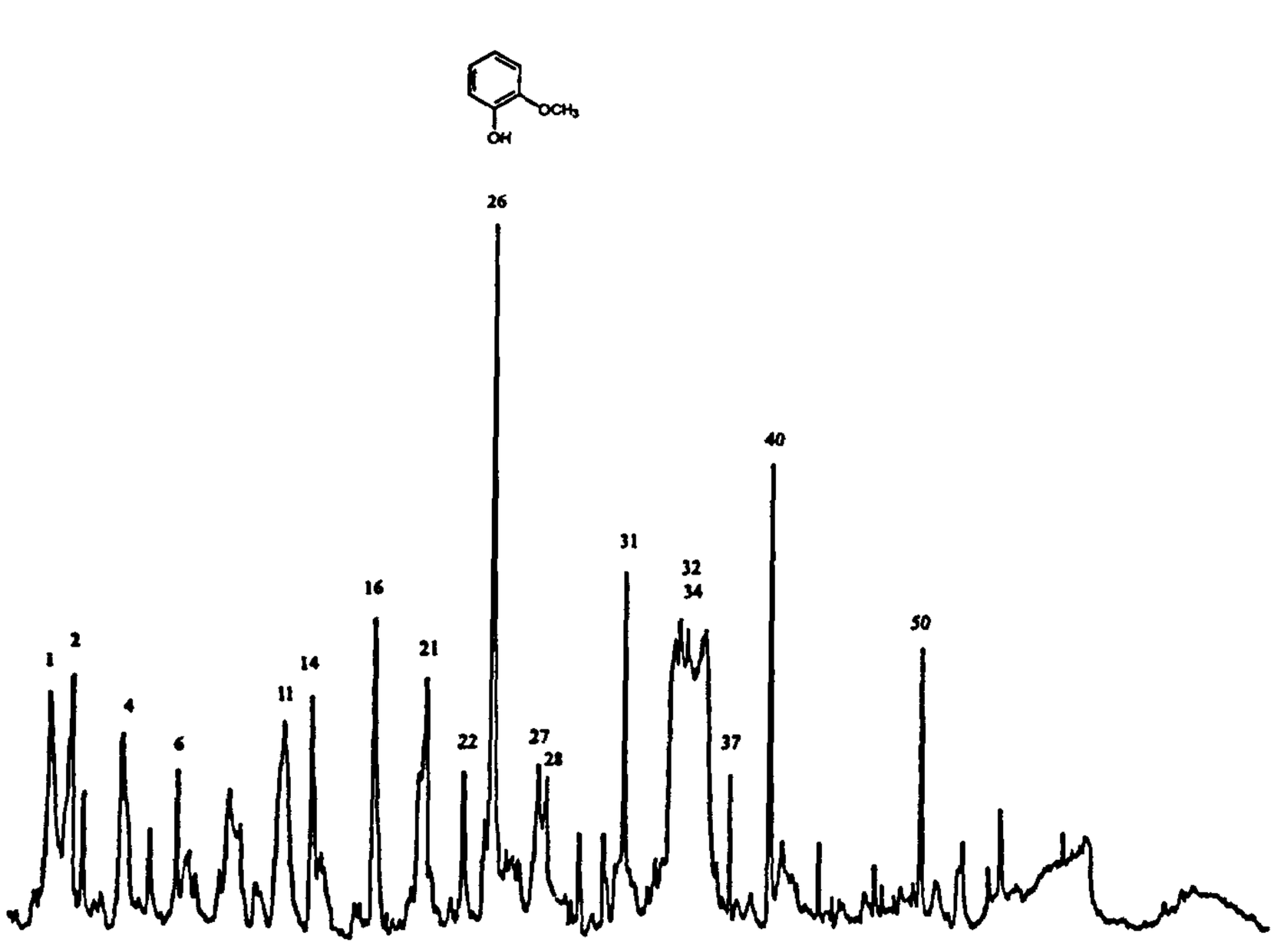

Figure 3.4d. Pyrolysis-GC/MS traces for a) fresh older *Psilotum* and b) older *Psilotum* decayed for 14 weeks.

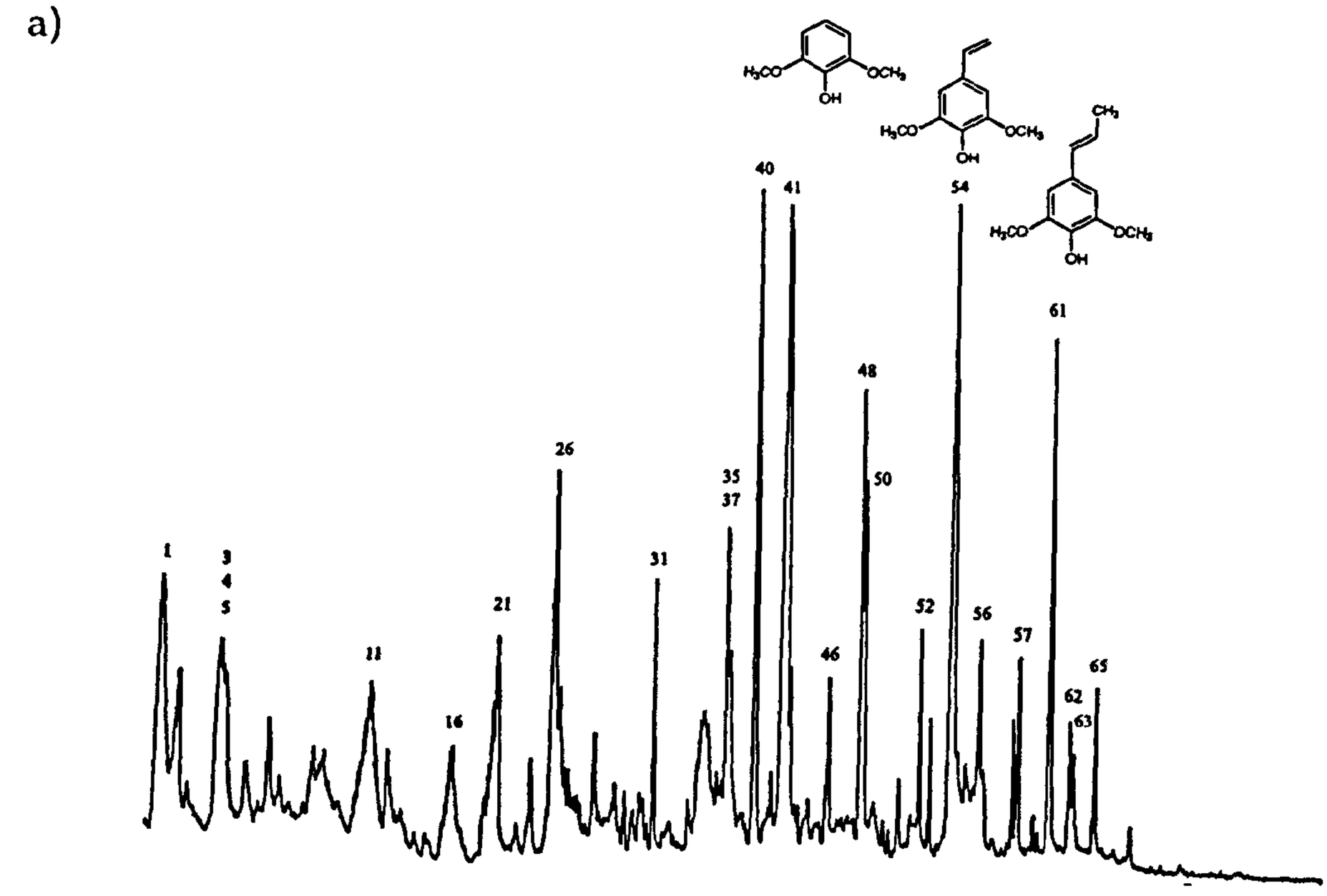

Figure 3.4e. Pyrolysis-GC/MS traces for a) fresh vine and b) vine decayed for 14 weeks. (A: anhydrosugars).

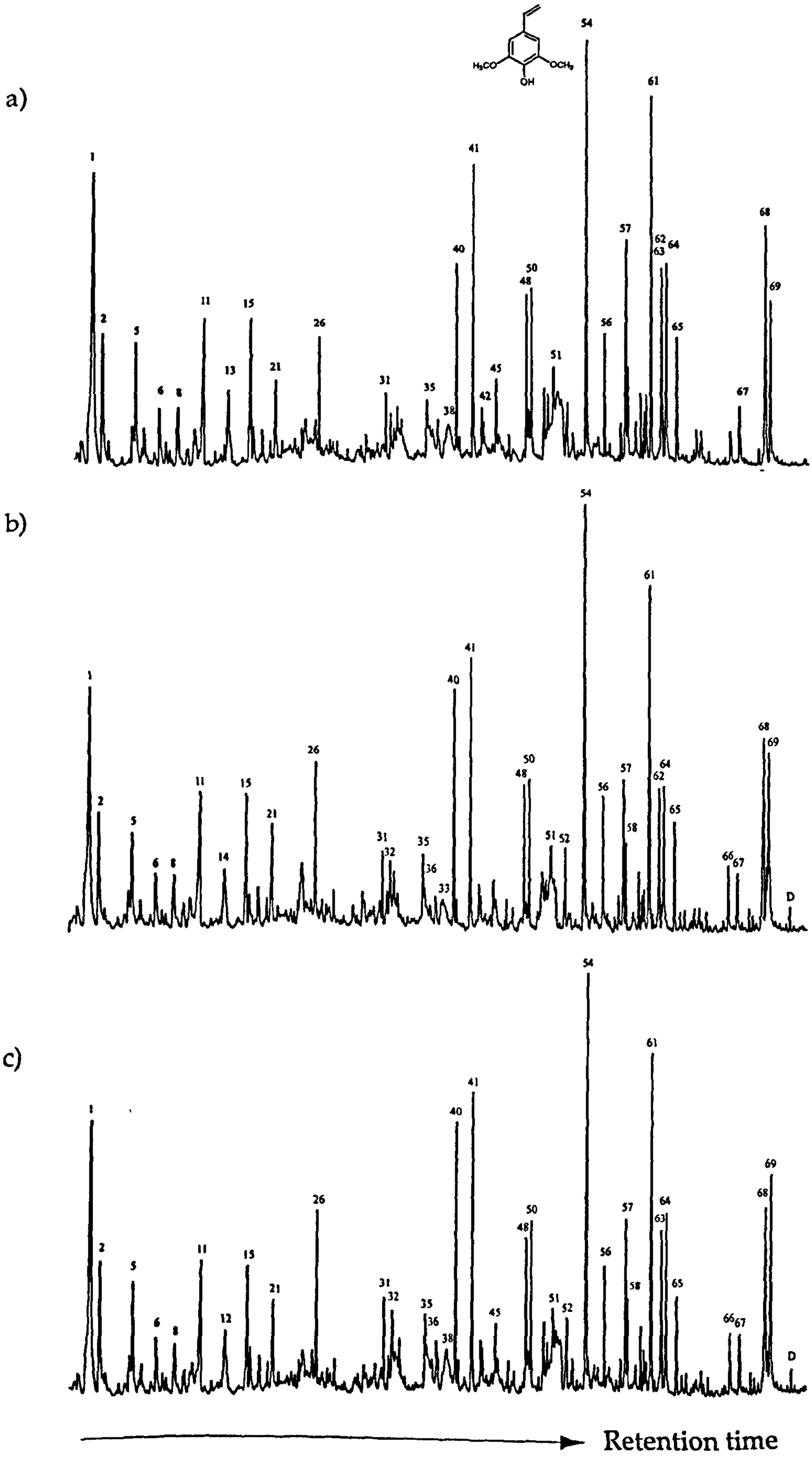

Figure 3.4f. Pyrolysis-GC/MS traces for a) fresh plane, b) plane decayed for 6 weeks and c) plane decayed for 14 weeks. (D: Dimers).

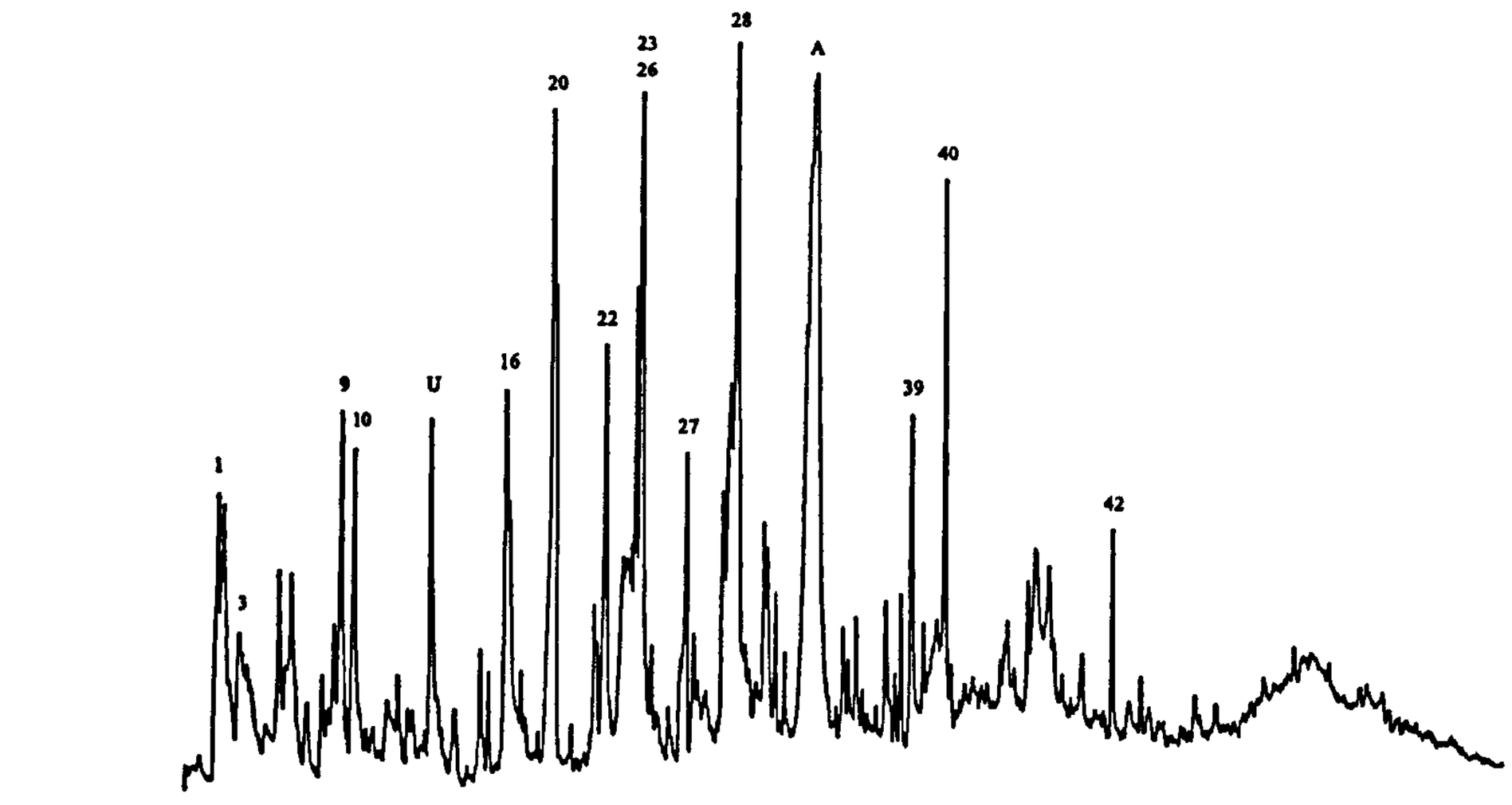

Figure 3.4g. Pyrolysis-GC/MS traces for a) fresh celery and b) celery decayed for 14 weeks. (A: anhydrosugars; U: unknown).

was also dominant amongst the *Cyathea* pyrolysates. The pyrolysates of the woody angiosperms, vine and plane, were syringyl-dominated (Figure 3.4e,f): the most abundant pyrolysis products were 2,6-dimethoxyphenol (41), 2, 6-dimethoxy-4-vinylphenol (54) and *trans* 2,6-dimethoxy-4-propenylphenol (61). The polysaccharide 3-hydroxypropanol (1) and 4-vinylguaiacol (40) were also significant pyrolysis products of fresh and decayed vine and plane (Figures 3.4e,f). Celery (Figure 3.4g), a non-woody angiosperm, yielded a very different suite of pyrolysates to the other species, consisting mainly of polysaccharides (20, 23, 28), although guaiacol (26) and 4-vinylguaiacol (40) were also abundant in the fresh material.

The relative abundances of the dominant pyrolysis products in the pyrolysates of the fresh material were significantly altered following 14 weeks of decay, and other pyrolysis products were more dominant in some of the decayed samples. Celery was most affected, with strongly contrasting pyrograms for fresh and decayed material (Figures 3.4g), whilst the pyrolysis products of decayed plane were very similar to those of the fresh material.

One of the main differences between the pyrolysates of the fresh and the decayed samples for many species was the presence of catechol (1,2-benzendiol, 32) and 3- and 4-methylcatechol (36, 38). All three of these products were present in the pyrolysates of the decayed *Cyathea* but not in those of the fresh material (Figures 3.4b). Small amounts of catechol were detected in a double peak with 4-vinylphenol (34) in the pyrolysates of the fresh pine and both the fresh *Psilotum* samples (Figures 3.4a, c, d). In the pyrolysates of the decayed pine and *Psilotum* material there was better resolution of catechol (32) and 4-vinylphenol (34), with significant peaks for both, as well as 3- (36) and 4-methylcatechol (38) (Figures 3.4a, c, d), which was not present in the pyrolysates of the fresh material.

Catechol and 3- and 4-methylcatechol were not detected in the pyrolysates of the fresh celery (Figure 3.4g) or the fresh vine (Figure 3.4e). Catechol was detected, however, in the pyrolysate of decayed celery (Figure 3.4g) and catechol and 3-methylcatechol were present in the pyrolysate of the decayed vine (Figure 3.4e). 4-methylcatechol (38) was present in the pyrolysate of fresh plane, and in the pyrolysates of the decayed plane after 6 and 14 weeks, along with catechol and 3-methylcatechol (Figures 3.4f)

The pyrograms of the decayed material showed more pyrolysis products in total than those of the fresh material in all species except celery. The pyrolysates of decayed celery (Figure 3.4g) gained polysaccharide pyrolysis products (in particular 11, 21, 25 and anhydrosugars (A)), but lost most of the lignin units such as guaiacol (26) 4-vinylguaiacol (40) and eugenol (42) as well as the protein, indole (39). The pyrolysates of both newer and older *Psilotum*, vine and *Cyathea* all increased in vanillin (45) (Figures 3.4c, d, b). The pyrolysates of the older *Psilotum* and vine both gained in eugenol (42). Acetovanillone (51) and guaiacylacetone (53) increased in the pyrolysates of the pine and older *Psilotum* (Figures 3.4a, d); the newer *Psilotum* showed increased levels of guaiacylacetone (Figure 3.4c), and the pyrolysates of *Cyathea* increased in acetovanillone (Figures 3.4b). The pyrolysates of the woody angiosperms, vine and plane, both increased in the syringyl unit 4-ethyl-2,6-dimethoxyphenol (52) (Figures 3.4e, f).

The pyrolysates of almost all samples show some loss of polysaccharide products but anhydrosugars increased with decay in the pyrolysates of celery, pine, *Cyathea* and vine. Late-eluting pyrolysis products such as *trans* coniferaldehyde (63) and *trans* coniferyl alcohol (64), which are rarely detected in the pyrolysates of fresh material, often appeared in decayed material, sometimes as significant peaks, as in the newer *Psilotum* sample (Figure 3.4c). Such peaks appeared in all samples

except for plane, where they were detected in the pyrolysates of the fresh material (Figure 3.4f), and celery (Figure 3.4g).

Late-eluting lignin dimers (x) were present in the pyrolysates of decayed material of all species except celery and vine.

^{13}C Solid State NMR

Individual peaks in ^{13}C solid state NMR CP/MAS and NQS spectra were assigned to specific carbon atoms as listed in Table 3.12. Guaiacyl, syringyl and cellulose units are illustrated in Figure 3.5 to identify the individual carbon atoms within them. ^{13}C solid state NMR CP/MAS and NQS spectra are presented in Figure 3.6.

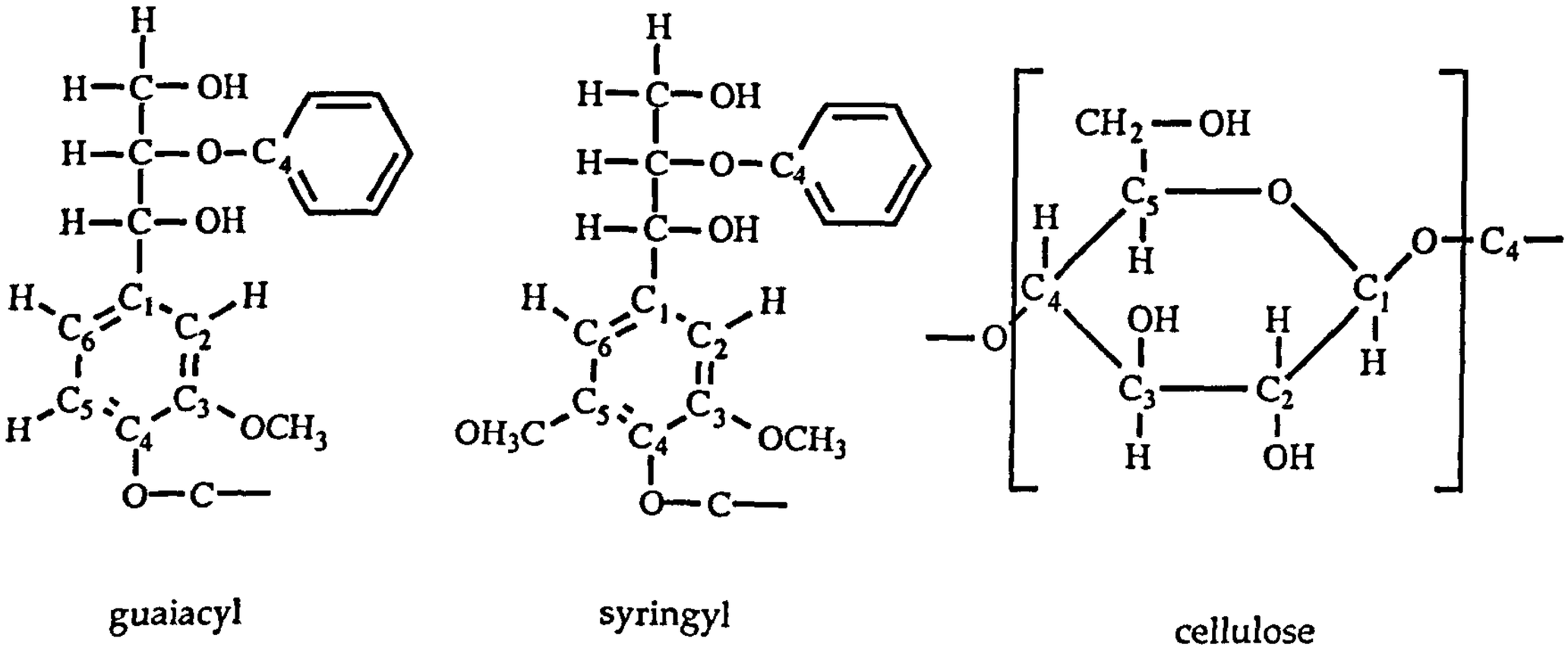

Figure 3.5. Numbered carbon atoms for guaiacyl, syringyl and cellulose units (Baldock and Preston, 1995)

Chemical shift (ppm)	Functional group (Carbon atom)
15 ppm	terminal methyl of long chains
22ppm	methyl C of hemicellulose acetyl groups
30 & 33ppm	alkyl C in long chain polymethylene, $(CH_2)_n$, type structure (e.g. fatty acids, waxes, resins)
56 & 63ppm	methoxyl C or, if the peaks disappear in the NQS spectrum, C adjacent to the amine group in amino acids
62ppm	non-crystalline C6 of cellulose
65ppm	crystalline C6 of cellulose
72-75ppm	C2, C3, C5 in cellulose and hemicellulose
84, 89ppm	non crystalline C4 in cellulose and hemicellulose
100-108ppm	syringyl C2 and C6 of lignin
103-105ppm	de-oxygenated anomeric C1 in hemicellulose; if signal remains in NQS, assignable to flavanoid and tannin
115-120ppm	guaiacyl C2, C5, C6 of lignin
133ppm	guaiacyl and syringyl C1 and phenolic C4 of lignin
144ppm	condensed tannins
148ppm	guaiacyl C3 of lignin
153ppm	phenolic guaiacyl C4, syringyl C3 and C5
173ppm	carboxyl C in hemicellulose acetate

Table 3.12. Assignment of specific ^{13}C solid state NMR peaks to cellulose and lignin carbon atoms (Kolodziejski *et al.*, 1982; Baldock *et al*, 1990).

The proportions of carbon in each functional group for each species are presented in mg C per g sample (assuming that the NMR spectra are representative of all the carbon in the sample) in Table 3.13.

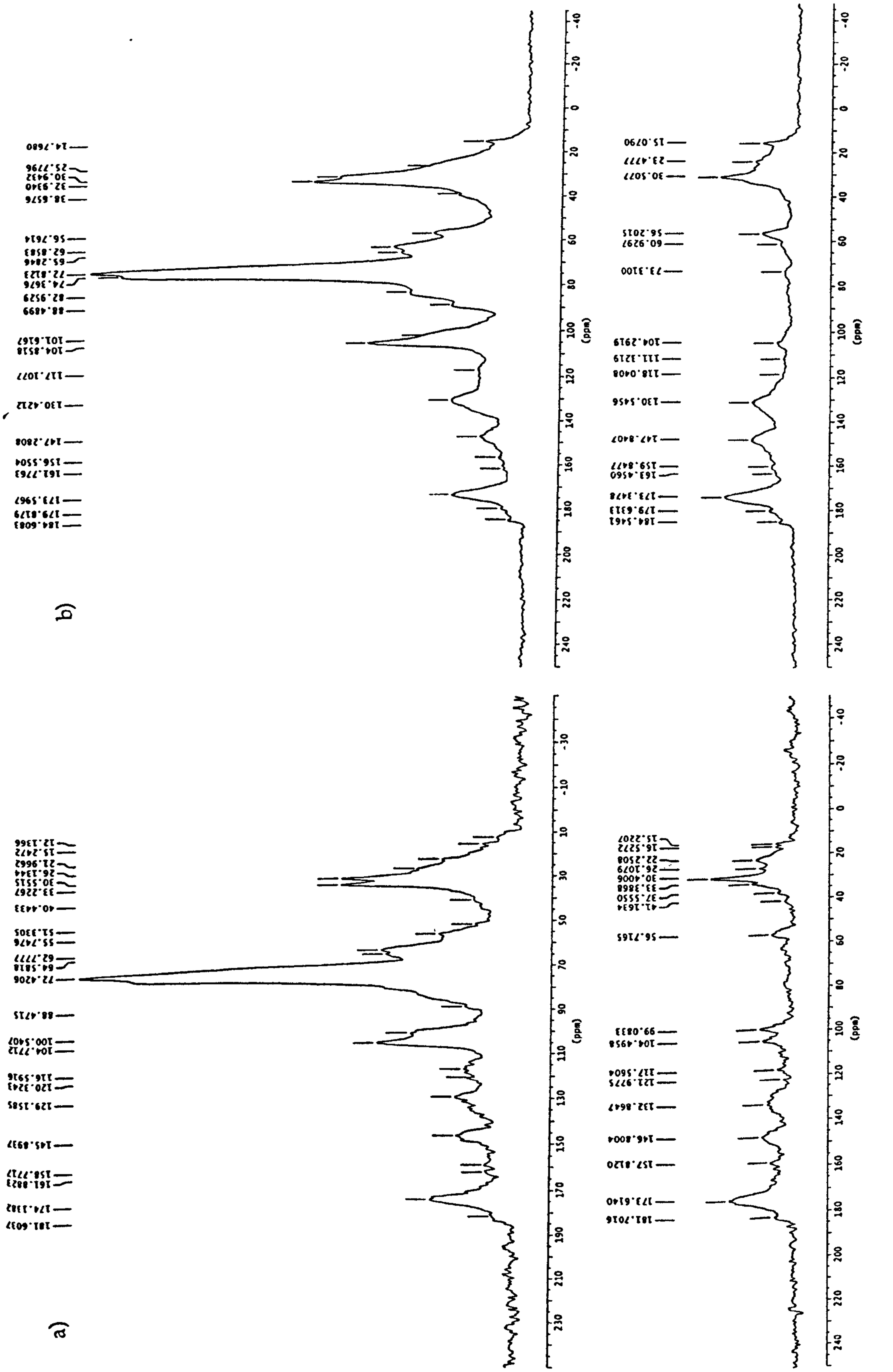

Figure 3.5a. ^{13}C NMR CP/MAS and NQS spectra for a) fresh older *Psilotum* and b) older *Psilotum* after 14 weeks decay.

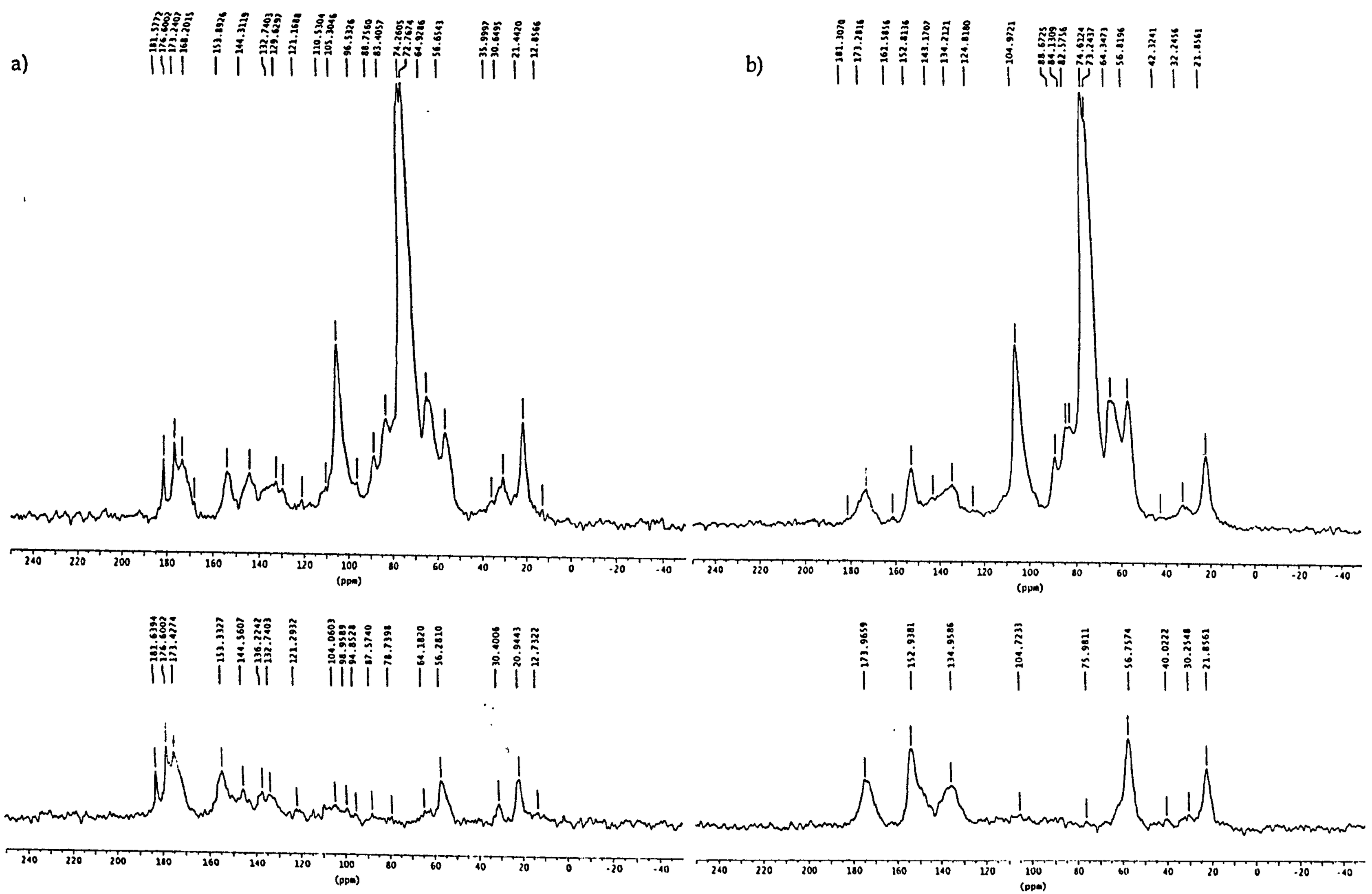

Figure 3.5b. ^{13}C NMR CP/MAS and NQS spectra for a) fresh vine and b) vine after 14 weeks decay.

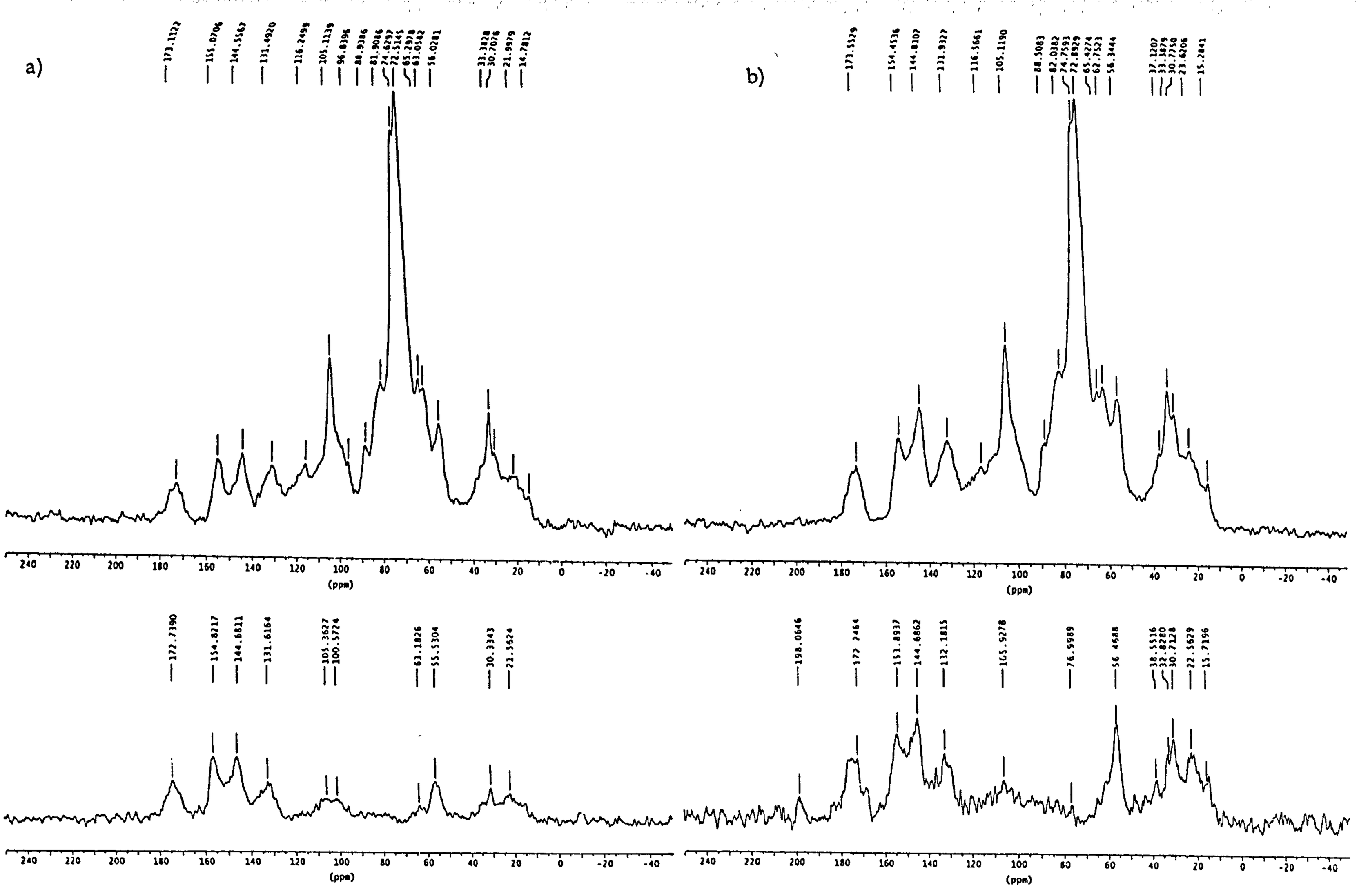

Figure 3.5c. ^{13}C NMR CP/MAS and NQS spectra for a) fresh pine and b) pine after 14 weeks decay.

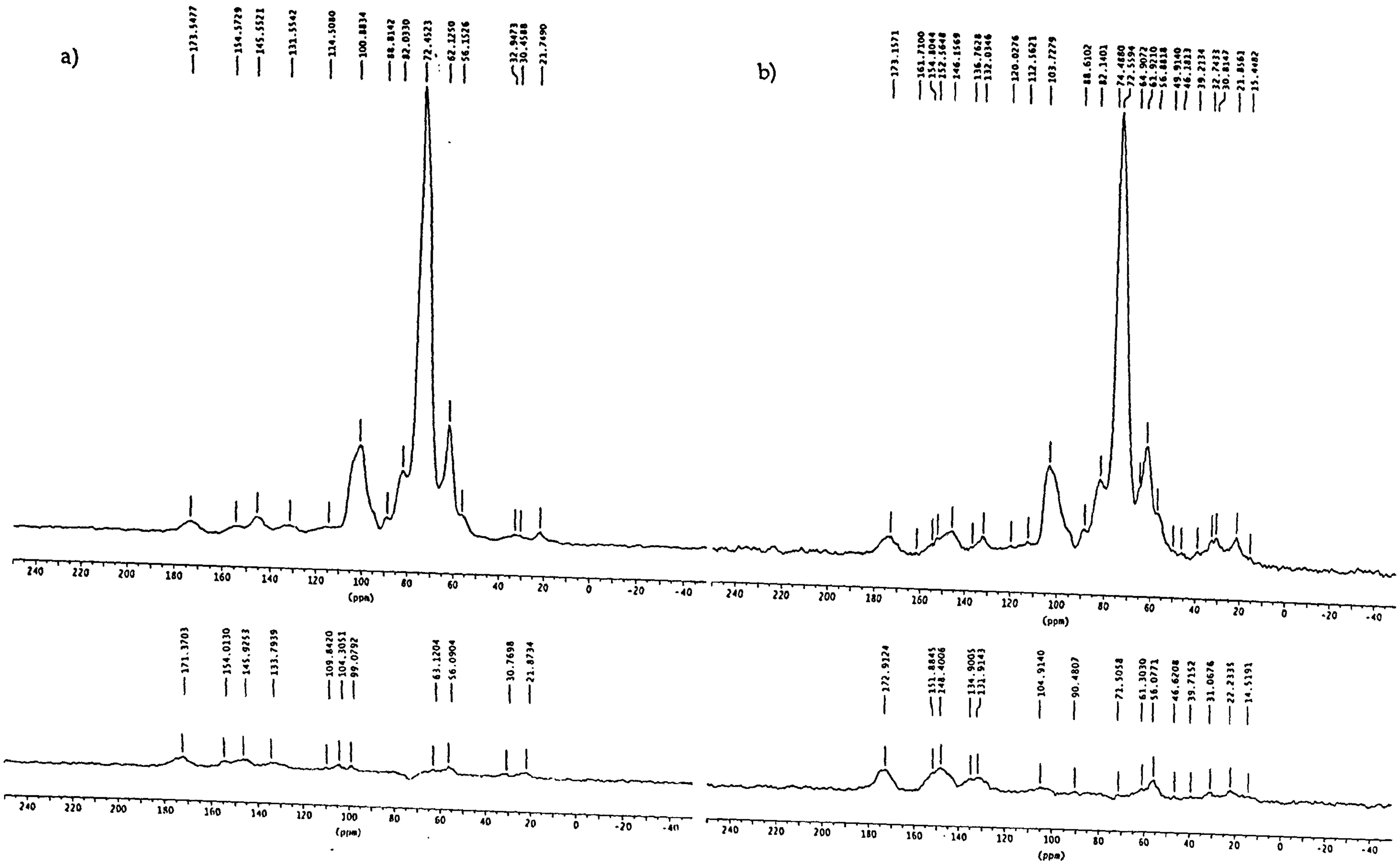

Figure 3.5d. ^{13}C NMR CP/MAS and NQS spectra for a) fresh *Cyathea* and b) *Cyathea* after 6 weeks decay.

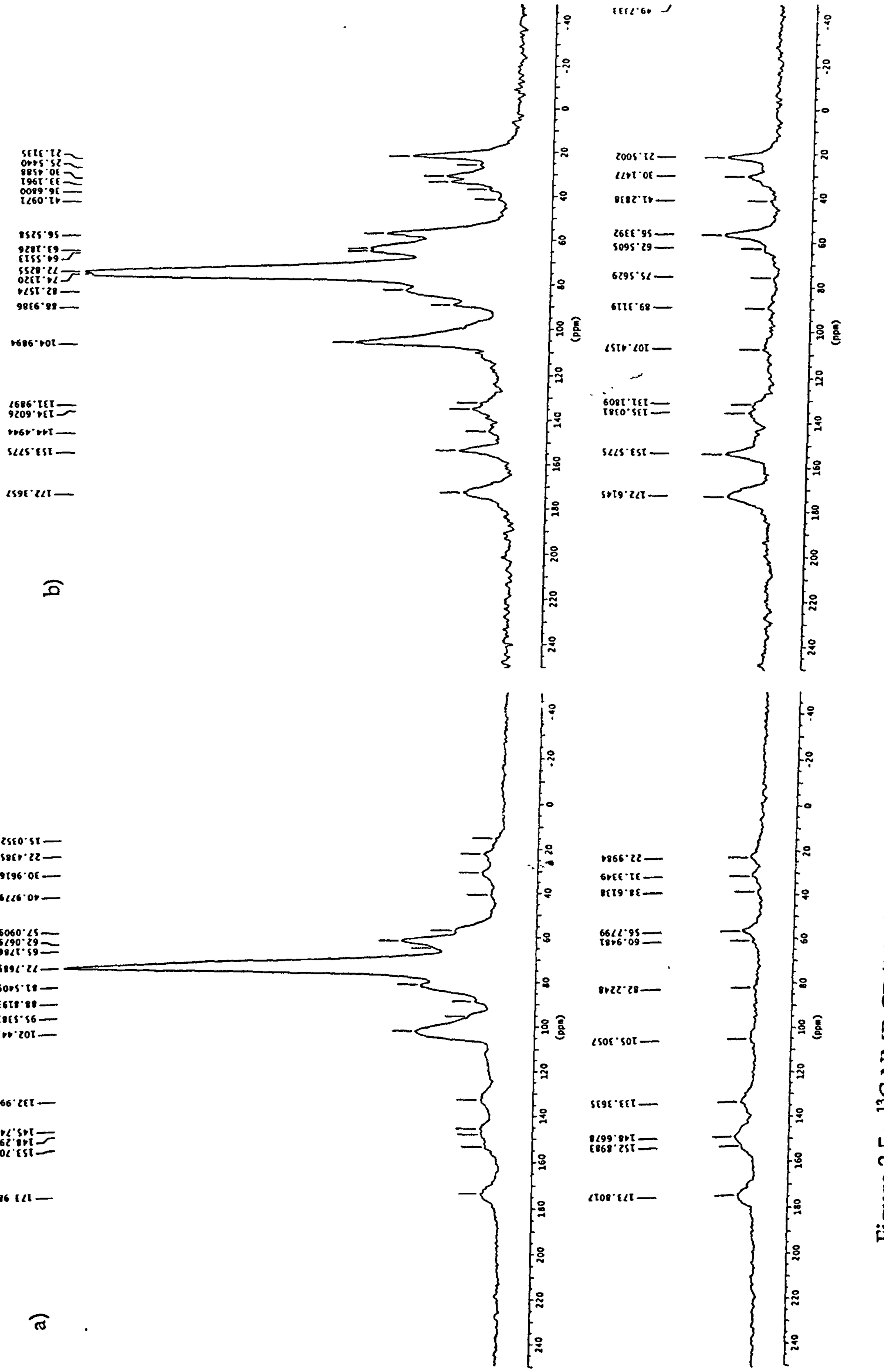

Figure 3.5e. ^{13}C NMR CP/MAS and NQS spectra for a) *Cyathea* after 14 weeks decay and b) fresh plane.

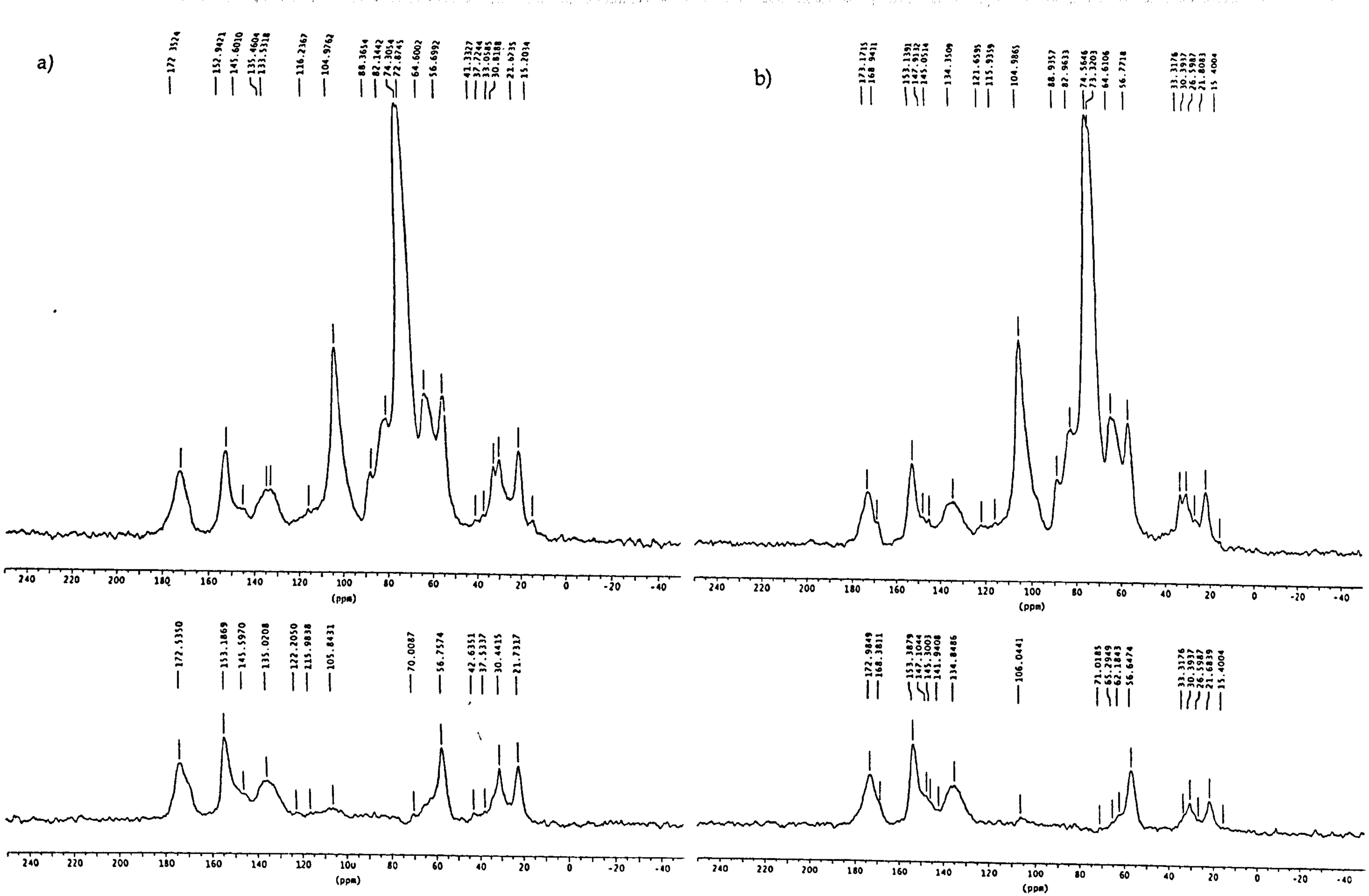

Figure 3.5f. ^{13}C NMR CP/MAS and NQS spectra for a) plane after 6 weeks decay and b) plane after 14 weeks decay.

	alkyl	N-alkyl	O-alkyl	acetal	aromatic	phenolic	carboxyl
	mg C / g of material						
Fresh older *Psilotum*	85.9	58.2	159.9	49.7	44.4	26.2	35.7
Decayed older *Psilotum*	89.8	50.0	142.8	42.1	46.5	19.5	21.2
Fresh vine	36.8	53.9	174.7	49.3	25.9	22.2	26.1
Decayed vine	28.2	67.7	169.2	49.0	31.9	19.9	18.1
Fresh *Cyathea*	11.1	55.2	241.8	60.7	16.0	13.5	7.8
Decayed *Cyathea* (6 wks)	28.6	64.2	210.2	52.9	21.1	17.6	6.4
Decayed *Cyathea* (14 wks)	25.3	56.8	208.1	50.5	22.5	14.0	6.8
Fresh pine	62.5	68.9	193.9	58.1	50.0	33.7	14.8
Decayed pine	67.9	56.3	150.1	44.8	53.0	45.2	20.7
Fresh plane	55.8	79.5	193.7	56.5	31.5	21.3	19.5
Decayed plane (6 wks)	51.4	73.5	173.6	58.1	33.8	26.0	23.6
Decayed plane (14 wks)	37.8	69.8	182.1	63.3	36.0	25.2	17.6

Table 3.13. Proportions of carbon in each functional group of fresh and decayed plant material (14 weeks decay unless stated otherwise).

Alkyls

Concentrations of alkyls, the CH_2 and CH_3 groups in aliphatic alkanes, including waxes and fatty acids, ranged from 11.1mg C/g of fresh *Cyathea* to 85.9mg C/g in fresh material of older *Psilotum*.

The fresh pine and plane contained similar amounts of alkyls (62.5mg C/g and 55.8mg C/g respectively), but they consisted mainly of CH_2 groups in long chains (probably in waxes) in pine (30/33ppm) and methyl groups in plane (22ppm). The concentration of alkyls increased with decay in the pine, but decreased with decay in the plane, especially between 6 and 14 weeks.

Like the pine, the *Psilotum* contained more CH_2 alkyls, and the concentrations of these, especially at 33ppm, increased slightly with decay. The vine and *Cyathea* samples contained the lowest concentrations of alkyls of all the species studied. In vines these were mainly CH_2 alkyls, and concentrations, in particular at 33ppm, decreased with decay. It is difficult to identify which alkyls were present in the fresh *Cyathea*, but the concentrations of both CH_2 and CH_3 alkyls increased with decay between 0 and 6 weeks and 0 and 14 weeks.

N-alkyls

The fresh samples all contained similar concentrations of N-alkyls, ranging from 53.9mg C/g in fresh vine to 79.5mg C/g in fresh plane. Most of these N-alkyls were from lignin and hemicellulose; only some were from proteinaceous material. Total concentrations of N-alkyls decreased with decay in *Psilotum*, pine and plane, but increased with decay in vine and *Cyathea*. There was a slight increase in the 56ppm peak for vine, pine, and *Cyathea* with decay.

O-alkyls

The O-alkyls are known as the "carbohydrate band", reflecting hemicellulose and cellulose carbons (see Table 3.12: the O-alkyl band is 65-92ppm). These were the predominate functional group in all fresh and decayed samples. Concentrations decreased with decay in all species.

Acetals

All fresh species had similar concentrations of acetals, ranging from 49.3mg C/g for vine to 60.7mg C/g for *Cyathea*. Concentrations of alkyls decreased with decay for older *Psilotum*, *Cyathea* and pine, increased for plane, and remained constant for vine. Some tannins were detected in the acetal band in the older *Psilotum*. In the *Cyathea* and plane samples, the peaks at 100ppm and 105ppm increased with decay, indicating a relative increase in cellulose (C1).

Aromatic and phenolics

Concentrations of aromatics were low in fresh *Cyathea* and vine (16.0 and 25.9mg C/g respectively) and highest in pine (50.0mg C/g). Concentrations of phenolics were low for all fresh samples, ranging from 13.5mg C/g in *Cyathea* to 33.7mg C/g in pine. Relative concentrations of aromatics increased for all species, as did the phenolics in *Cyathea*, pine and plane. Relative phenolic concentrations decreased for older *Psilotum* and vine.

The pine samples contained the largest amount of guaiacyl lignin. Condensed tannins (the peak at 144ppm) increased with decomposition. The older *Psilotum* also contained a lot of condensed tannins. The fresh and decayed samples of vine and plane both contained syringyl and guaiacyl lignin units. The peak at 145ppm decreased with decay in both the vine and older *Psilotum* samples. There was a strong increase in the

relative intensity of the 153ppm peak (phenolic guaiacyl C4 and syringyl C3 and C5 carbons) with decomposition in the plane samples. The low relative concentrations of aromatics and phenolics in fresh and decayed *Cyathea* indicate low concentrations of lignins.

Carboxyls

The relative concentration of carboxyls in fresh samples varied greatly, ranging from 7.8mg C/g in *Cyathea* to 35.7mg C/g for older *Psilotum*. Relative concentrations of carboxyls decreased slightly with decomposition for all species, although there was an initial increase in the plane after 6 weeks followed by a decrease after 14 weeks.

The origin of the sharp peak at 181ppm present in vine, and at lower intensity in the older *Psilotum* was puzzling; it may be due to fatty acids rather than hemicellulose.

The estimated total amounts of proteins, polysaccharides, lipids and lignin present in each fresh and decayed sample are presented in Table 3.14.

In fresh and decayed samples of all species studied, polysaccharides were the dominant functional group, and concentrations were particularly high for *Cyathea* (Table 3.14). Lipids were present in the lowest concentrations in fresh and decayed samples of all the species.

In older *Psilotum*, vine and *Cyathea* the most decay susceptible biomacromolecules were proteins and polysaccharides, and lipids were the most decay resistant. Polysaccharides were the most decay susceptible group in the pine material, where proteins were the most decay resistant. Lipids were the most decay susceptible biomolecules in plane, where lignins and proteins were the most resistant to decay.

Sample	proteins	polysac.	lipids	lignins
	mg C / g material			
Fresh older *Psilotum*	119.2	188.4	37.0	115.4
Decayed Older *Psilotum* (14 wks)	70.7	168.8	60.8	111.6
% change with decay	-40.7%	-10.4%	+64.3%	-3.3%
Fresh vine	86.9	222.7	1.2	78.2
Decayed vine (14 wks)	60.4	233.1	3.4	87.1
% change with decay	-30.5%	+4.7%	+183%	+11.4%
Fresh *Cyathea*	26.1	329.3	0.4	50.2
Decayed *Cyathea* (6 wks)	21.3	292.7	19.8	67.2
% change with decay	-18.4%	-11.1%	+4850%	+33.9%
Decayed *Cyathea* (14 wks)	22.6	282.1	16.0	63.2
% change with decay	-13.4%	-3.6%	+3900%	+25.9%
Fresh pine	49.3	245.3	42.2	145.2
Decayed pine (14 wks)	69.2	160.1	39.6	169.2
% change with decay	+40.4%	-34.7%	-6.2%	+16.5%
Fresh plane	65.0	275.2	29.1	88.6
Decayed plane (6 wks)	78.6	242.4	19.1	99.8
% change with decay	+20.9%	-11.9%	-34.4%	+12.6%
Decayed plane (14 wks)	58.7	255.4	13.8	104.1
% change with decay	-9.7%	-7.2%	-52.6%	+17.5%

Table 3.14. Estimated total amounts of proteins, polysaccharides, lipids and lignins for fresh and decayed plant material determined by ^{13}C solid state NMR.

Discussion

Carbohydrates

Carbohydrates were the largest group of polymers within the fresh and decayed samples of pine, vine, plane, older *Psilotum* and *Cyathea*. The tissue stained thin sections (Figure 2.17) show that this was also true for celery.

The results of the carbohydrate assay and the solid state ^{13}C NMR indicate that carbohydrates were degraded in preference to other bio-macromolecules, in particular lignin. This is in agreement with Spiker and Hatcher (1987), who reported a linear correlation between carbon content and stable carbon isotope composition in modern and ancient buried wood. They proposed that this was due to the loss of carbohydrates and selective preservation of lignin-like molecular substances during early diagenesis. Hedges *et al.* (1985) also reported the preferential degradation of carbohydrates in buried wood.

No overall trends in relative rates of decay of the polysaccharide tissues cellulose, hemicellulose or pectin were observed. The sequence observed for both newer and older *Psilotum*, pine and plane, where cellulose was the most degraded and hemicellulose the least degraded, is the same as that observed by Boutelje and Goransson (1975) in the selective degradation of submerged pine needles. None of the species in this study reflected the decay sequences observed by Hedges *et al.* (1985) in buried woods (pectin > α-cellulose > hemicellulose) or Hoffman (1981), who noted equal degradation of α-cellulose and hemicellulose in waterlogged oak woods. These variations in selective degradation may reflect the influence of tissue structure, decay environment, decomposer organisms, and time periods involved in the decomposition of plant material.

The presence and arrangement of associated lignin may be a major factor in the differences in decay susceptibilities of different polysaccharides. For example, pectin is readily degraded although it may be preserved when associated with lignin (as described in the introduction to this chapter). Conversely, the greatest decay of pectins was observed in vine and *Cyathea* which ^{13}C NMR showed to be the least

lignified of the species studied (except for celery, which was not analysed by ^{13}C NMR).

Relative proportions of most individual sugars (i.e. the percentage mass of the total plant sample) decreased with decay, except for the relative proportions of xylose. The increase in xylose in most species suggests that it was the least degraded of the individual sugars. This is in contrast to the sequence of sugar stabilities observed in buried woods by Hedges *et al.* (1985) i.e. in order of decreasing stability, arabinose, galactose, fucose, rhamnose > glucose > mannose > xylose > ribose. None of the plant species in this study demonstrated this sequence, possibly due to the wide range of tissue structures and taxonomic groups studied and differences in decomposer micro-organisms, decay environments and time-scales involved between the two studies. However, it is still puzzling that this study identified xylose, which Hedges *et al.* (1985) found to be one of the most degraded sugars, as one of the most decay resistant. This may be due to structural changes similar to those in pectins: the xylose backbone of hemicellulose may likewise have been protected in the fresh material, but may have been made more accessible to the carbohydrate assay following decay.

The unexpected increase in anhydrosugars in the pyrolysates of decayed pine, *Cyathea*, vine and celery (Figures 3.4a, b, e, g) may likewise be explained by considering the structure of cellulose and other polysaccharides in the plant material. Cleavage of the hydrogen-bonds holding together the cellulose crystalline framework, and a rapid decrease in polymerisation caused by the cleavage of glycosidic bonds within individual cellulose chains, result in the greater abundance of some anhydrosugars in the pyrolysates of decayed material (Stout *et al.*, 1988 and references therein).

Lignin

The increase in relative proportions of lignin in all the decayed versus fresh samples, except *Cyathea*, revealed by the lignin assay indicates the preferential loss of non-lignin biomacromolecules during degradation (Hedges *et al.*, 1985). This is supported by ^{13}C NMR evidence which shows that polysaccharides, and sometimes lipids and proteins, were degraded in preference to lignin in vine, pine, plane, older *Psilotum*, and *Cyathea*. Nonetheless, pyrolysis-GC/MS and the lignin assays provide evidence that some lignin degradation occurred in only 14 weeks in all the species studied.

Guaiacyl (vanillyl) lignin units

Although low levels of catechol (1,2-benzendiol) and 3- and 4-methylcatechols may be present in fresh plant material, they can also be products of guaiacyl lignin degradation. In fresh material catechol and 4-methylcatechol may be present in tannins or as original structural moieties of lignin, but in degraded plant material catechol becomes prominent and 3-methylcatechol is observed to elute before 4-methylcatechol (Galletti, 1991; Galletti and Reeves, 1992). These catechols are formed by the demethylation of methoxy groups in guaiacyl units, and are important indicators of decay in buried and archaeological wood (Hatcher, 1988; Hatcher *et al.*, 1989; van Bergen *et al.*, 2000). The increased yields of catechol and 4-methylcatechol, and the presence of 3-methylcatechol in the degraded plant material in this study indicate that some decomposition of lignin has occurred in all species, except possibly for plane.

P/V ratios from the lignin assay decreased with decay for newer *Psilotum*, vine and plane, remained constant for celery, and increased for *Cyathea*. The increase in P/V for *Cyathea* may be due to the production of

p-hydroxyl phenols by demethoxylation of vanillyl compounds, as reported in buried woods (Hedges *et al.*, 1985). The reason for the decreases in P/V in the other plant species is unclear.

Syringyl lignin units

Demethylation of syringyl units in angiosperm woods is reflected in prominent 3-methoxycatechol peaks in pyrolysates of decayed plant material (van Bergen *et al.*, 2000). The abundance of this compound is similar in both the fresh and decayed vine and plane material, indicating that little or no degradation of the syringyl lignin units has taken place.

S/V ratios from the lignin assays are only relevant to the woody angiosperms (vine and plane) where syringyl phenols are present. Hedges *et al.* (1985) reported a decrease in S/V ratios in buried wood, and proposed that this was evidence for preferential degradation of syringyl units. The S/V ratio decreased with decay for vine, suggesting that syringyl units were degraded preferentially to guaiacyl units, but the S/V ratio for plane increased with decay. The reason for this contrast is unclear.

Other evidence for modification of lignin

The increase in methylphenols with decay, as seen in the pyrolysates of older *Psilotum*, pine and plane, provides evidence of microbially-induced lignin modification (Stout *et al.*, 1988).

Decay of plant material normally results in the loss of sinapyl and coniferyl alcohols due to the dehydration of the side-chains of methoxyphenols (van der Hage *et al.*, 1993; van der Heijden and Boon, 1994). However, these compounds, and other late-eluting pyrolysis products such as *trans* coniferaldehyde, were often present in the pyrolysates of decayed material but not in the corresponding fresh

material. Ralph and Hatfield (1991) suggested that this may be due to contamination of the insert of the pyroprobe. However, more refined pyrolysis techniques were used for the analyses carried out in the present investigation, and contamination is unlikely to be the cause of the lack of these pyrolysis products. The appearance of such late-eluting compounds (as well as lignin dimers in the pyrolysates of all decayed material except vine and celery) suggests a change in the biomolecular structure of the plant material. It is uncertain how the structure is altered during decay, but changes similar to those described for xylose in the carbohydrate assay may result in these late-eluting compounds being more accessible to pyrolysis-GC/MS in decayed material.

Acid/aldehyde ratios for both syringyl and vanillyl phenolic families characteristically lie between 0.1 and 0.2 for fresh woods of all types (Hedges, 1975; Hedges *et al.*, 1982, 1985, 1986, 1988c; Ertel and Hedges, 1984). The acid/aldehyde ratios of all the woody tissues studied here lie between these limits, but non-woody *Cyathea* and celery have much higher Ad/Al ratios. However, vanillic acid has been shown to be ester-bound to polysaccharides in some non-woody vascular plant tissues (Whitehead *et al.*, 1981; Yamamoto *et al.*, 1989), and this can result in high (Ad/Al)v ratios in fresh samples (Goñi, 1992) as seen in the *Cyathea* and celery samples.

(Ad/Al)v ratios increased with decay in all samples. These ratios have been shown to increase with fungal decay due to the oxidation of lignin side-chains (Hedges *et al.*, 1988) but these experiments are the first demonstrate elevated (Ad/Al)v ratios in bacterially-degraded plant samples. This is at odds with the view of Benner *et al.* (1991), who argued that bacteria degrade lignin side-chains and ring structures at similar rates, resulting in no change in the (Ad/Al)v ratios.

(Ad/Al)s ratios are thought to behave in the same manner as (Ad/Al)v ratios. In this study the (Ad/Al)s ratios increased with decay in plane, but decreased with decay for vine.

Proteins

^{13}C NMR showed that proteins were highly susceptible to decay in older *Psilotum* and vine, were readily degraded in *Cyathea* and plane, but were the most decay resistant group of biomacromolecules in pine. The variation in decay susceptibility of proteins may be related to their distribution within the plant structure.

C/N ratios are a good indicator of decay of plant tissues (Taylor *et al.*, 1989). Preferential degradation of organic nitrogen compounds such as proteins by deamination results in an initial increase in C/N ratio (Biddanda and Riemann, 1992) as occurred in vine, pine, plane and the newer *Psilotum* (Figure 3.1).

For tissues with low-lignin content such as those of *Cyathea* and celery (as indicated by tissue-stained thin sections and ^{13}C NMR), the C/N ratio expresses the carbohydrate/protein ratio as opposed to the (carbohydrate and lignin)/protein ratio (Gloaguen and Touffet, 1982). The extremely high C/N ratio obtained for fresh *Cyathea* was confirmed by ^{13}C NMR which showed that *Cyathea* is composed of 81.1% polysaccharides and only 6.4% protein.

Lignin is known to inhibit the decay of associated polysaccharides (as discussed in the Introduction to this chapter). With little or no lignin to protect the carbohydrates and low levels of protein rapid degradation may explain the decrease in C/N exhibited by *Cyathea* and celery. Alternatively, the ratios for *Cyathea* and celery may have risen early in decay and then dropped again by the 6 week sampling point. However, C/N ratios decrease after prolonged periods of decay (Benner *et al.*, 1991;

Rice and Tenore, 1981, and references therein). The increase in *Cyathea* C/N ratios between 6 and 14 weeks is anomalous, but may reflect the fact that, in the absence of lignin, carbohydrate decay is faster than that of protein.

Other biomacromolecules

^{13}C NMR showed that the relative proportions of lipids varied greatly between species, with very low levels in fresh *Cyathea* and vine (0.4-1.4 mg C/g), and much higher levels in fresh older *Psilotum*, plane and pine (29.1mg C/g). Lipids were highly resistant to decay in older *Psilotum*, vine and *Cyathea*, but were much more readily degraded in pine and plane.

Tannins, especially condensed tannins, were shown by ^{13}C NMR and pyrolysis-GC/MS to be present in older *Psilotum* and pine, and relative abundances of these increased with decomposition. Goodwin and Mercer (1972) observed that tannins often accumulate in dead or dying cells and Almendros *et al.* (2000) proposed that the selective preservation of tannins may control the decomposition of other plant biomacromolecules, resulting in differences in degradation between species.

Almendros *et al.* (2000) suggested that the alkyl fraction in the spectra of ^{13}C NMR contains suberin and cutin and other highly decay resistant biopolymers present in waxes which accumulate in humic substances formed by extensive decay of organic matter. The decay-resistance of these compounds explains the relative increase in alkyl abundances with decay in older *Psilotum*. and pine. The relative decrease of alkyls with decay in the plane samples, and the high proportion of methyl groups within the plane alkyl fraction indicate that cutin and suberin are present in very low concentrations, if at all, in fresh plane.

Conclusions

These experiments demonstrate that decay of organic plant material is rapid, with extensive degradation of carbohydrates and, in some species, protein, in preference to lignin and other decay resistant biomolecules such as tannins, suberin and cutin. However, degradation of lignin did occur under essentially anaerobic conditions within 14 weeks in all species except plane.

Celery was one of the most decay susceptible plants, being composed essentially of cellulose, leaving only a few strands of fibres after 6 weeks, whereas pine and plane were much more decay resistant. However, no clear sequence of decreasing decay resistant (increasing decay susceptibility) of the species studied emerged from the experimental results. This is due to differences in the structure of the different species, and in the constituent biopolymers and the associations between them.

Of the six species studied, celery, vine and *Cyathea* were the most degraded, resulting in a visible loss of structure (as described in Chapter 2) and a large decrease in the relative concentrations of carbohydrates. Celery and *Cyathea* are cellulose-dominated, with little lignin to provide structural protection either on a stem-wide scale (i.e. lignified tissues are distributed almost randomly throughout the stems) or on a biopolymer-scale (i.e. there is little lignin to protect the carbohydrates in a cellular level). Although the pith of fresh vine is cellulose-dominated and is readily decayed, the outer tissues, including the lignified cortex and epidermis, impart a level of decay-resistance. Nonetheless, these lignified tissues were partially decayed within 14 weeks, as evidenced by the appearance of catechol and 3- and 4-methylcatechol in the pyrolysate of the decayed vine formed by degradation of guaiacol units.

Tissue-stained thin sections (Figure 2.17) indicate that plane and pine are much more heavily lignified than celery, vine and *Cyathea*, with no

large areas of unprotected cellulose and these species are consequently more decay-resistant. Fresh plane does not have particularly high levels of lignin relative to those in other species, it does not contain tannins, and only contains low levels of suberin, cutin and phenolics, as revealed by solid state ^{13}C NMR. Little lignin degradation occurred in the plane (evidenced by no increase in catechol and the methylcatechols in the pyrolysates of the decayed material compared to the fresh). In the absence of decay-resistant biopolymers such as tannins, the distribution of lignin throughout the plant, and in particular in the pith, must have imparted the high preservation potential.

Pine and *Psilotum* contain the highest concentrations of decay-resistant polymers, in particular tannins, as well as suberin and cutin in waxes. The tissue stained thin section of pine (Figure 2.17) revealed only small regions of cellulose-dominated tissues (the phloem). In contrast, large areas of cellulose-based tissues are evident in the *Psilotum* species, which would suggest a higher susceptibility to decay than was indicated by the chemical data within this chapter for the decayed *Psilotum*. This is particularly interesting due to the presence of relatively high levels of decay-resistant biopolymers such as tannins, suberin and cutin in *Psilotum*, which is the earliest known extant vascular plant.

It is difficult to identify any differences between the newer green stems of the *Psilotum* and the older brown ones, partly due to insufficient decayed material being available for lignin assays and ^{13}C NMR analysis. However, the fresh older *Psilotum* contained lower relative concentrations of carbohydrates, which may indicate more lignified, and hence more decay-resistant, tissues. C/N ratios and pyrolysis-GC/MS data was similar for both the newer and older *Psilotum* samples.

Fresh pine has a very different composition to that of the other species studied, with high levels of protein and arabinose but relatively low

concentrations of hemicellulose (evidenced by the low levels of xylose and mannose). Gymnosperm wood has been reported to be more resistant to decomposition than angiosperm wood (e.g. Kohara, 1956; Nicholas, 1973; Hedges et al., 1985). This has previously been attributed to differences in tissue structure and the presence of substances such as tannins rather than chemical dissimilarities in lignins and polysaccharides from the two wood types (Wilcox, 1973). The results of this study allow the decay resistance of pine to be attributed to its substantially different chemical composition.

The relationships between the chemical data in this chapter and the geochemical data from the microbial decay systems are discussed in Chapter 5.

PRESERVATION OF ORGANIC MATTER IN PYRITISED PLANT FOSSILS

Introduction

The organic plant fossil record is the result of the selective preservation of tissues which contain resistant biomacromolecules, such as cutan in cuticles, algaenan in algal cell walls, sporopollenin in spore and pollen walls, and lignin in seed coats and woody tissues (van Bergen *et al.*, 1995). These constituent biomacromolecules vary in composition (as discussed in Chapter 1), susceptibility to decay, and behaviour during diagenesis. Such variations in preservation potential can lead to a potential bias in the fossil record both within and between tissues (e.g. Tegelaar *et al.*, 1991; van Bergen *et al.*, 1994). These biomacromolecular substances also make the major contribution to kerogen, coals and lignite (e.g. Tegelaar *et al.*, 1989; de Leeuw and Largeau, 1993).

The distribution of minerals and preserved organics within fossil material can be interpreted in terms of different degradation histories of different cells and tissues (e.g. Kenrick and Edwards, 1988) and this is related to their biomolecular composition. Thus, type and style of preservation can be used as a proxy for determining the original biomacromolecular composition of fossilised material (e.g. Kenrick and Edwards, 1988; Grimes *et al.*, 2001b) as discussed in Chapter 1.

Experimental Aims

The aim of this work was to investigate the distribution of pyrite and organic material within pyritised plant material, to determine whether any organic matter had survived and if so identify, as far as possible, the chemical composition of this matter.

Experimental methods

Source of fossil material

Fossil twigs were collected from two fossil beds in the Tertiary of south-east England.

The Eocene London Clay

The Eocene London Clay is a sequence of marine silty clays, clay- and sandy silts, and subordinate sands reaching a thickness of up to 165m (Allison, 1988a; see also King, (1984) for a comprehensive stratigraphic sequence). The assemblage contains a diverse range of plant macrofossils which may have originated from inshore mangrove swamps (Collinson, 1983) or may have been transported from much further inland by mass rafting down rivers into the sea (Poole, 1992b) before being deposited in the grey plastic clay offshore. Fossil material which had been washed out of the clay by wave action was collected from the beaches at Warden Point and Minster on the Isle of Sheppey, Kent (NGR TM955738-TM024717).

The Palaeocene Reading Beds

The foreshore outcrop of the Reading Beds in West Sussex consists mainly of clays, but includes a lignite bed which is richly fossiliferous (Bone, 1986). Most of the nearest living relatives of the plant material previously studied from this site are aquatics or marginal aquatics, which were deposited in fluvial and partly deltaic sediments (Bone, 1986). Pyritised axes from the lignite bed were collected from the beach at Felpham (national grid reference SZ942989-950993), although the best preserved samples are often found within clay nodules. This site has since been converted into sea defences.

Preparation of fossil specimens

One hundred and twenty pyritised fossil twigs were sectioned, polished and identified at Cardiff University (Grimes et al., 2001b, unpublished data). Of the specimens studied, 86.3% were identified as dicotyledons, 1.7% as monocotyledons, and 8.5% as gymnosperms (Davies, Grimes and Edwards, unpublished data). These ratios are similar to those recorded by Chandler (1964), Scott and de Klerk (1974) and Poole (1992), although some ferns were also identified in some of these studies.

Eight specimens in which SEM analysis revealed regions of exceptional cellular preservation and organic material were chosen for analysis of their organic content. These samples are listed in Table 4.1. Specimens which were also studied by Grimes *et al.* (2001b) are now housed in the National Museum of Wales, Cardiff, and their repository numbers are included in Table 4.1.

Specimen	Source	Form genus	Repository No.
Conifer stem 1	LC	*Pityoxylon*	-
Conifer stem 2	LC	*Pityoxylon*	-
Conifer stem 3	RB	*Pityoxylon*	-
Dicot. stem 1	LC	*Platininium*	-
Dicot. stem 2	LC	*Vitaceoxylon*	NMW00.13G.4
Dicot. stem 3	LC	unidentified	-
Dicot. root 1	LC	unidentified	-
Dicot. root 2	LC	unidentified	NMW00.13G.5

Table 4.1. Identification and source of pyritised plant axes analysed for organic matter content. LC, London Clay; RB, Reading Beds.

The plant axes used were identified where possible, and were assigned their form genus. *Pityoxylon* is the form genus for modern pine,

Platininium is the form genus for modern plane, and *Vitaceoxylon* the form genus for vine.

Elemental Analysis

The outer surfaces of the fossil samples were removed with a saw. The remaining fossils were rinsed with de-ionised water and allowed to air dry. They were then ground to a fine powder using a 28-6750 type freezer mill (Glen Creston Ltd., Middlesex). The powdered fossil material was analysed for total carbon, nitrogen and hydrogen using a Carlo-Erba EA1108 elemental analyser. Carbonate levels were analysed using a Coulomat 702 (Strohlein Instruments). Total organic carbon was calculated by subtracting the carbonate value from the overall carbon concentration All samples were analysed twice and the mean result was calculated for each.

Carbon Mapping

Fossil specimens were fractured using a clamp vice to reveal the structure and composition in cross-section. The fracture sections were mounted on aluminium stubs with silver DAG (Acheson Colloids Co., Plymouth). Uncoated samples were mapped for carbon, iron, sulphur and oxygen using a Jeol 5600LV SEM. X-ray microanalysis was carried out using Oxford Link Isis, with a range of 20keV.

Problems were encountered mapping the fossil samples due to interference from surface topography. Polishing the sections was not a solution as the polishing processes plucked out small sections of organic matter or microcrystalline pyrite.

Pyrolysis-GC/MS

Fossil material was ground to a fine powder as above.

Powdered material (50-60mg) was placed in a Pyrex centrifuge tube and treated with 3M HCl (1ml). The mixture was ultrasonicated for 1 minute before being left to stand for 1 hour at room temperature. The mixture was then brought to the boil and kept at this temperature (ca 120°C) for minute before being centrifuged at 3500rpm for 5 minutes. The supernatant was removed and the residue rinsed with double-distilled water. The sample was centrifuged at 3500rpm for 5 minutes and the supernatant removed. The sample was rinsed and centrifuged again until neutrality of the rinsing water was reached. The samples were left to air-dry and stored under nitrogen to prevent pyrite decay.

The sample was pyrolysed at 610°C for 10 seconds using a CDS pyroprobe 1000 with an interface temperature of 250°C. This was linked to a Carlo-Erba 4130 gas chromatograph directly coupled to a Finnegan MAT 4500 quadrupole mass spectrometer via a heated transfer line.

Compounds were separated using a Chrompack CPSIL-2cb column (50m x 0.32mm internal diameter, with a 0.4µm film thickness). The source temperature was 170°C. The carrier gas was hydrogen, with a headspace pressure of 8psi. The column temperature was held at 35°C for 5 minutes before being ramped to 320°C at a rate of 4°C a minute. The column was maintained at this temperature for a further 15 minutes.

The mass spectrometer was operated at 35-500 scan range at 1 scan per second. Electron ionisation was carried out at 70eV with 300µAmp emission.

This method is not quantitative.

Results

Elemental analysis

Carbon, hydrogen and nitrogen analyses of fossil plant samples are presented in Table 4.2. The pyritised plant fossils contained low proportions of organic matter, and carbon levels ranged from 1.16% to 3.68%. C/N ratios varied: two of the three conifer stems and one of the dicotyledon roots had much higher ratio (>30) than the other specimens (18.9-21.6%).

Specimen	Source	C (%)	H (%)	N (%)	C/N
Conifer stem 1	LC	1.54	0.43	0.04	38.5
Conifer stem 2	LC	1.54	0.28	0.05	30.8
Conifer stem 3	RB	3.68	0.55	0.17	21.6
Dicot. stem 1	LC	1.32	0.28	0.07	18.9
Dicot. stem 2	LC	1.16	0.38	0.06	19.3
Dicot. stem 3	LC	1.56	0.40	0.08	19.5
Dicot. root 1	LC	2.12	0.28	0.07	30.3
Dicot. root 2	LC	2.08	0.54	0.11	18.9

Table 4.2. C, H, N elemental data for pyritised fossil plants from the London Clay and Reading Beds.

Carbon mapping

It was very difficult to produce and carbon maps of the fossil material, partly due to the topographical variations of the samples, and partly due to the low concentrations of carbon present. Figure 4.1a shows a region of pith parenchyma from the *Vitaceoxylon* stem with pyrite framboids within the cells. X-ray analysis of this region revealed that substantial levels of carbon ware present and the sulphur, iron and carbon maps (Figure 4.1b) show the organic carbon distribution is mainly in the cell wall.

A

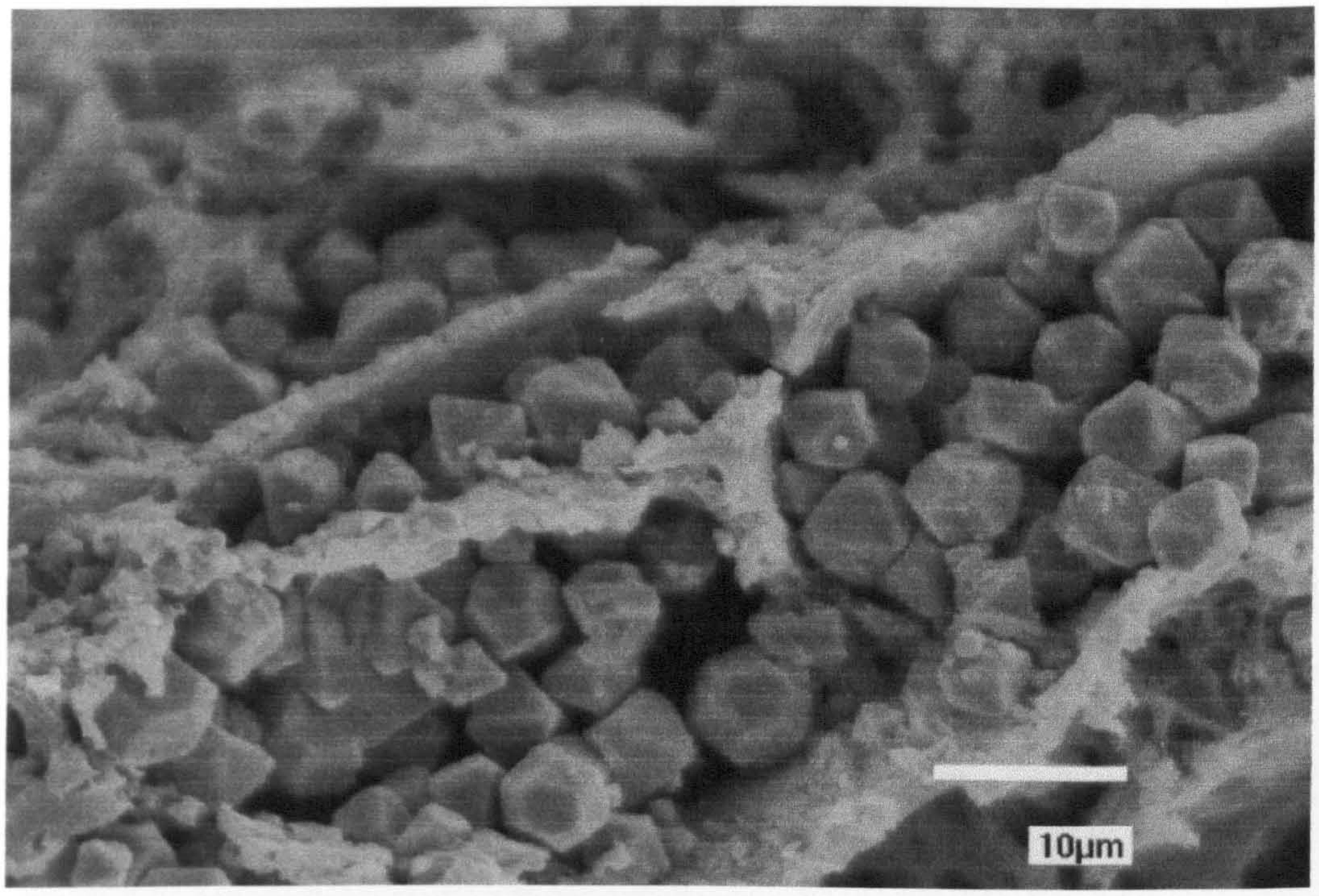

B

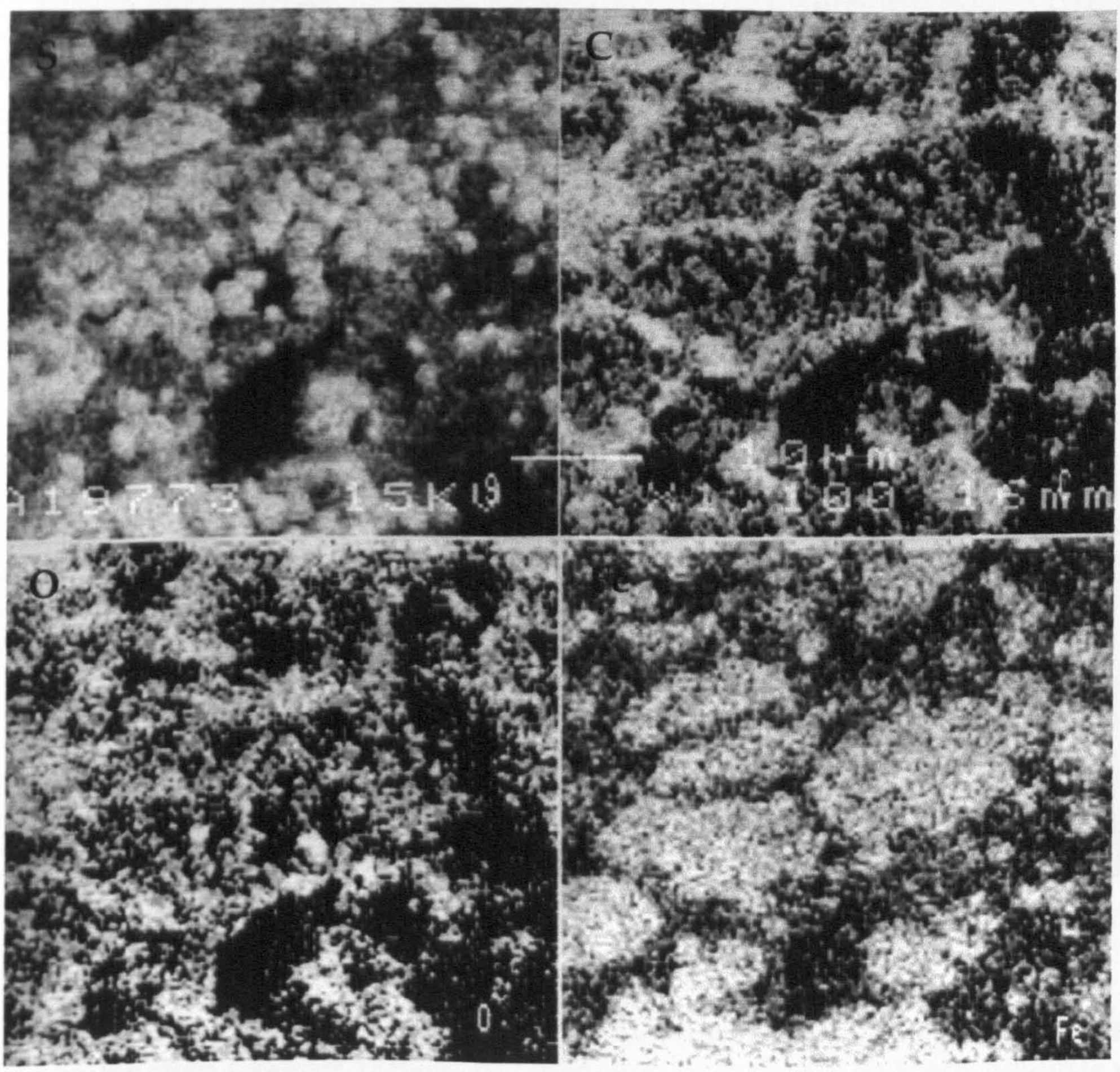

Figure 4.1. A: Region of pith parenchyma of *Vitaceoxylon* stem from the London Clay, with pyrite framboids and octahedra within the cells. B: Sulphur, carbon, oxygen and iron maps of the same region of pith parenchyma. Carbon and oxygen are mainly distributed within in the cell walls with pyrite infilling the cells.

A

B

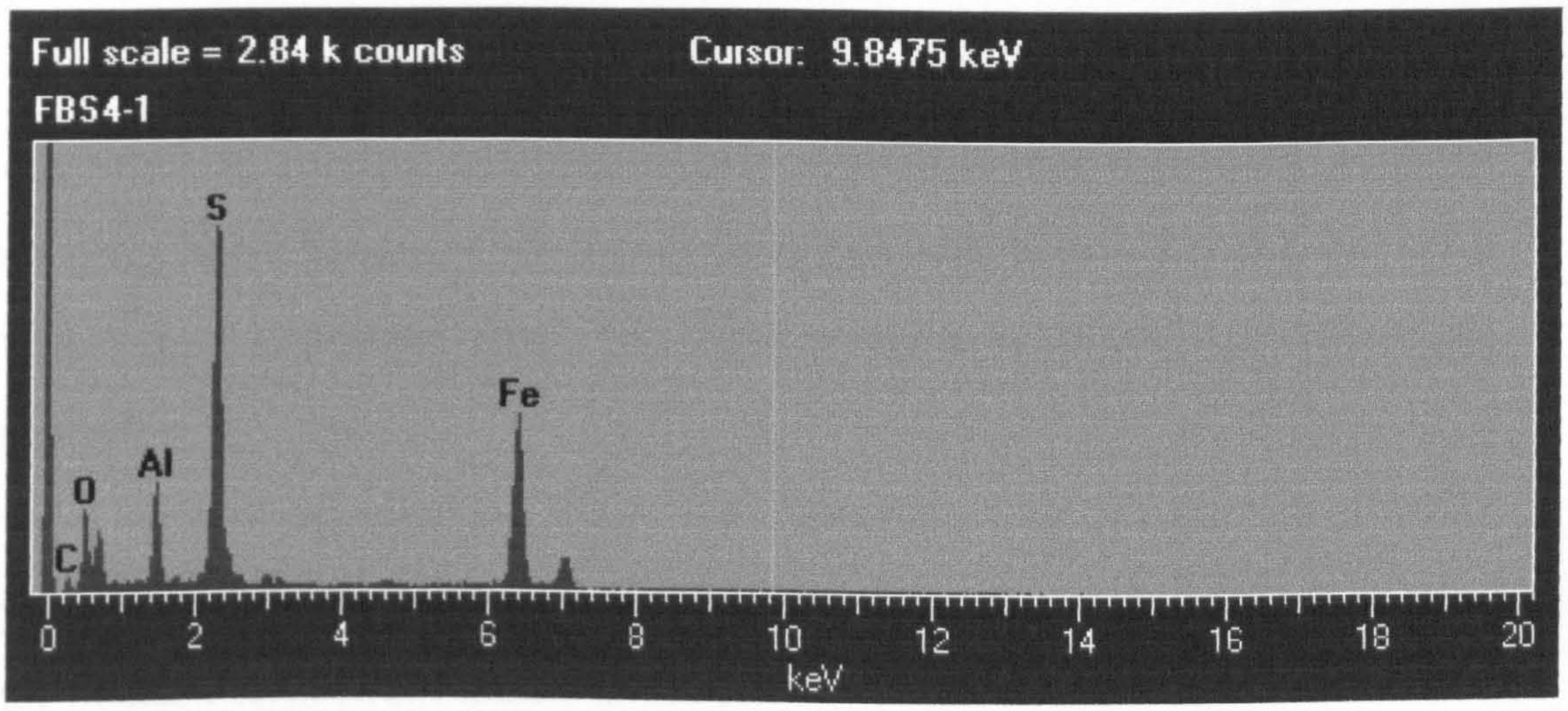

Figure 4.2. A: Pyritised xylem vessels with detail of bordered pits and rays in a conifer stem (conifer 1) from the Eocene London Clay. B: X-ray analysis reveals that, despite the exceptional preservational detail, very little carbon is present.

The area mapped in Figure 4.1 is unusual among these samples; rarely was sufficient carbon detected by X-ray analysis to allow maps to be produced. X-ray analysis of regions of exceptional pyritisation, for example the xylem of conifer 1 from the London Clay (Figure 4.2a) in which individual bordered pits are preserved, revealed that little carbon was present (Figure 4.2b).

Pyrolysis-GC/MS

The pyrolysates of the fossil plant material varied greatly. Pyrograms of the conifer from the Reading Beds and conifer 2 from the London Clay are presented in Figures 4.3a and 4.3b respectively.

The pyrolysate of the conifer from the Reading Beds (Figure 4.3a) contained diagnostic guaiacyl lignin pyrolysis products such as guaiacol, 4-ethyl-guaiacol, 4-vinyl-guaiacol and *trans* isoeugenol. Catechol was also present. Some sulphur compounds that formed during the pyrolysis of pyrite are also evident.

The pyrolysate of the London Clay conifer 2 (Figure 4.3b) was dominated by sulphur compounds and contaminants including adipates and phthalates. Traces of the lignin unit guaiacol were detected, but only in very low concentrations. No other diagnostic plant markers were detected.

All seven specimens from the London Clay produced similar pyrolysates. Traces of guaiacol were detected in all pyrolysates, except for that of the *Platininium* stem.

Discussion

The fossil samples contained low levels of organic carbon. Pyrolysis-GC/MS revealed that the majority of this organic material for all but the conifer stem from the Reading Beds represented contaminants, probably

1. *thiophene*
2. 2-methylthiophene
3. 3-methylthiophene
4. phenol
5. guaiacol
6. 4-methylguaiacol
7. catechol
8. unknown
9. unknown
10. 4-ethylguaiacol
11. 4-vinylguaiacol
12. *cis* isoeugenol
13. unknown
14. homovanillin
15. *trans* isoeugenol
16. S_8
17. phthalate (contaminant)

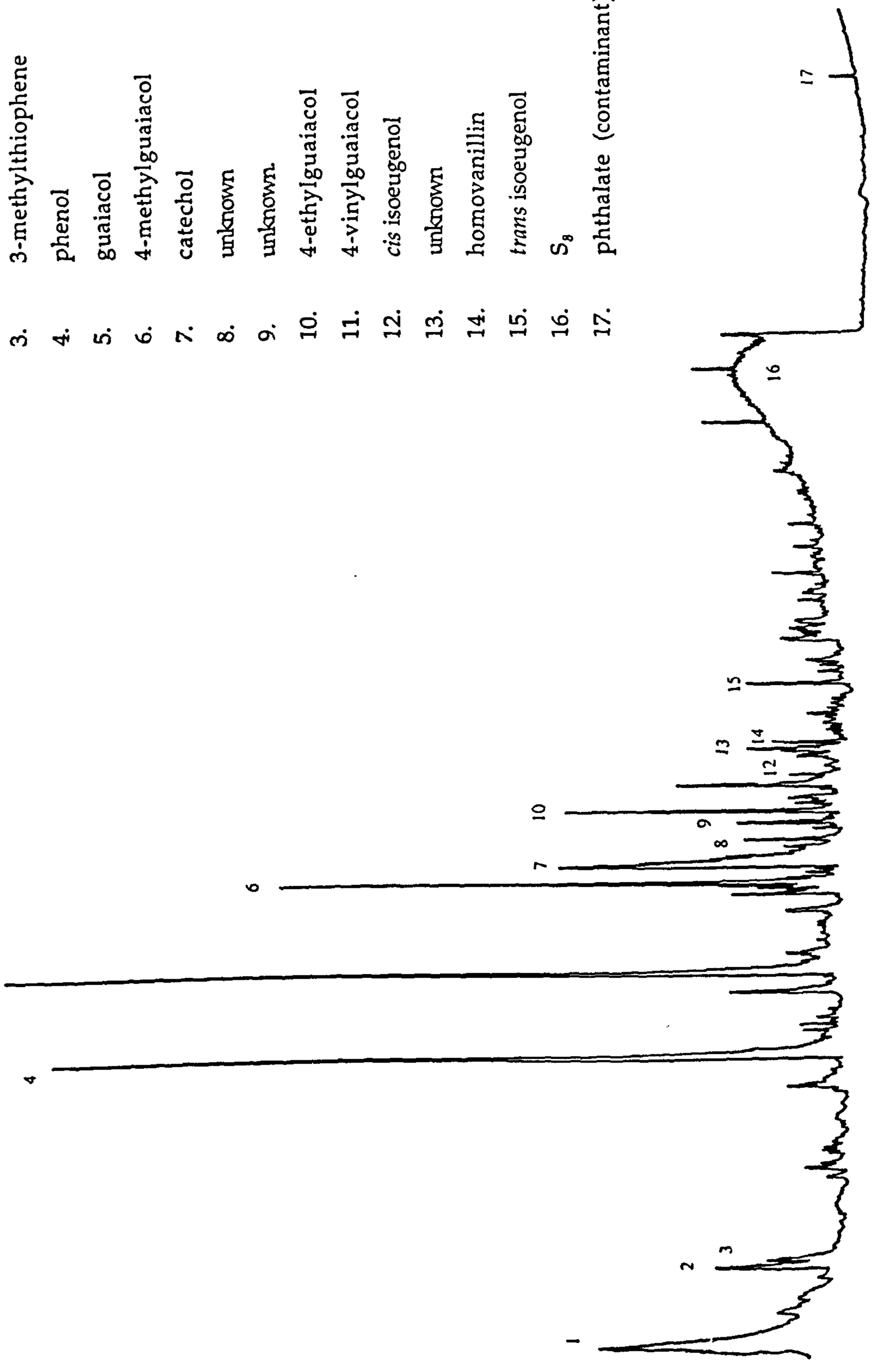

Figure 4.3a. Pyrolysis-GC/MS trace of pyritised conifer stem from the Palaeocene Reading Beds.

1. Thiophene
2. 2-methylthiophene
3. 3-methylthiophene
4. ?methylfuran (contaminant)
5. C2 alkyl benzene (styrene)
6. phenol
7. C3 alkyl benzene
8. guaiacol
9. C4 alkyl benzene
10. benzoic acid
11. unknown
12. unknown
13. unknown (methylated diacid?)
14. contaminant
15. methyl benzothiophene
16. long chain substituted C3 alkyl benzene
17. S8
18. C21 alkane
19. C18 alkane
20. phthalate (contaminant)

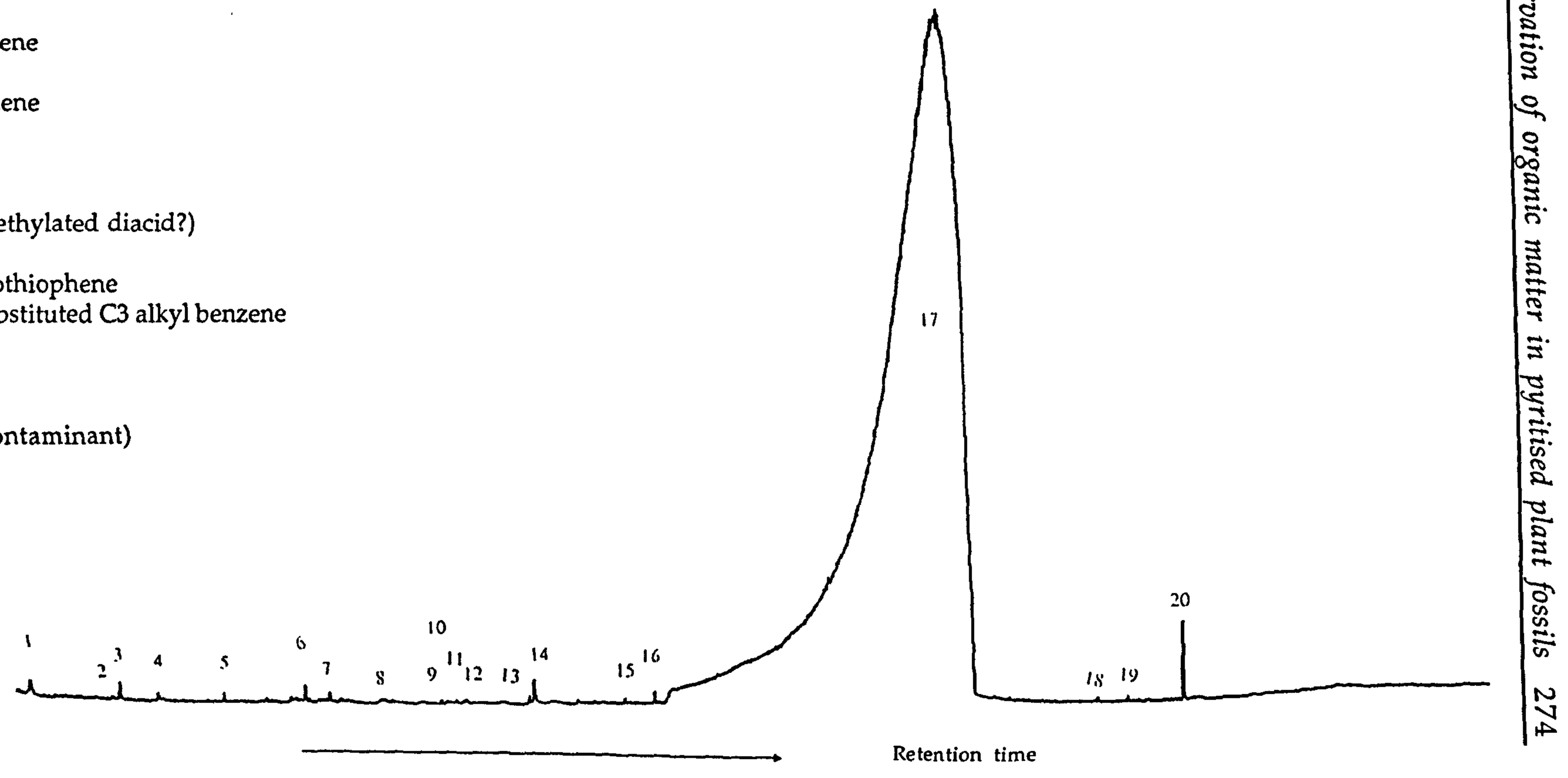

Figure 4.3b. Pyrolysis-GC/MS trace of pyritised conifer stem from the Eocene London Clay.

from the plastic bags which the samples had been stored in after collection. Despite cleaning the samples prior to analysis, these contaminants were the major organic components.

The conifer from the Reading Beds contained higher concentrations of organic carbon than the samples from the London Clay. Diagnostic lignin markers were present, and catechol, which indicates that the plant material had decayed to some extent prior to fossilisation.

The combination of carbon mapping and pyrolysis-GC/MS revealed that carbon was not equally distributed throughout the plant material: while high levels of carbon were seen within the pith cell walls of *Vitaceoxylon*, only low levels of plant biomarkers were detected by pyrolysis-GC/MS, suggesting that carbon was only present in the walls of a small number of cells. The carbon within this specimen was associated with a unique combination of framboidal and octahedral pyrite, with no microcrystalline pyrite (Grimes *et al.*, 2001b).

Conclusions

Elemental analysis, pyrolysis-GC/MS and carbon mapping and X-ray analysis indicate that very little organic matter is preserved in the seven London Clay samples which were analysed. Some carbon was observed in cell walls of the pith of *Vitaceoxylon*, but this fossil contained the lowest organic carbon composition of the fossils studied, and negligible levels of compounds that could be ascribed to plants. This suggests that organic carbon was only preserved in a very small area within the fossil, and this was confirmed by the X-ray analysis and carbon maps.

The fossil conifer from the Reading Beds contains much more elemental carbon than the London Clay fossils. Its distribution could not be mapped, however, for topographic reasons and because the fossil material was very soft and tended to crumble when sectioned. The

diagnostic lignin guaiacol markers present are highly-decay resistant and are characteristic of conifers (Sarkanen and Ludwig, 1973). The presence of catechol in the pyrolysate indicates that some decay of the material may have taken place prior to mineralisation, although in the absence of methylcatechols, the catechol may have been present in the fresh material, possibly in tannins or as original lignin moieties (see Chapter 2).

Despite the differences in preservation between the fossil conifer stem from the Reading Beds and the seven fossilised axes from the London Clay, the sample is too small for any conclusions to be drawn on the influence of the depositional environment on the pyritisation processes and organics preserved. Very few fossils with any cellular detail were collected from the Reading Beds: such specimens are rare and no further collections could be undertaken due to the construction of sea defences over the fossil bed.

The low levels of organic preservation in the fossils from the Reading Beds and the London Clay contrast markedly with pyritised plant axes from the Devonian Brecon Beacons in which lignified tissues such as cell walls and xylem thickenings are coalified (e.g. *Gosslingia breconensis*, reported by Kenrick and Edwards, 1988). The differences in preservation of organic matter may be caused by many factors, including the depositional environment, and the microbiological processes involved. The intensity of microbiological activity would have influenced the rate of decay and mineralisation. The nature of the decomposing organisms may also have been important in the preservation of these lignified tissues. As discussed in Chapter 1, the Devonian was a period of evolution both of decay-resistant plant biopolymers and the organisms capable of decomposing them. The preservation of coalified organic material in the Devonian fossils may reflect an absence of decomposers

capable of degrading this material, while suitable decomposers had evolved by the Eocene. If this is the case, these plant specimens lived in a time after the evolution of new decay-resistant tissues such as lignin prior to the evolution of organisms capable of degrading them.

Although very little organic material is preserved in the fossilised plant material studied from the London Clay and the Reading Beds, the quality of cellular detail preserved, e.g. bordered pits in the walls of xylem vessels in Conifer 2 (Figure 4.2) indicates that mineralisation must have been rapid to avoid loss of detail. This is consistent with experiments discussed in Chapter 2 and documented by Grimes *et al.* (2001a), and is discussed further in Chapter 5. For further details on the pyrite textures observed in the London Clay fossils, and possible mechanisms for their formation, see Grimes *et al.*, 2001b.

SUMMARY DISCUSSION AND FUTURE WORK

Under most normal environmental conditions, plant material is degraded and ultimately recycled, and hence leaves no fossil record. However, under exceptional conditions, plant tissues can be preserved. One mode of plant tissue preservation involves replication and/or replacement by authigenic minerals, such as pyrite. The mechanisms of the pyritisation of plant material, including the microbial and geochemical processes involved and the tissues which are preserved (either in their original or an altered state), were poorly understood. This work investigated the processes involved in the formation of pyrite and its precursors in plant material, the fine scale geochemical changes and the alteration of biopolymers during the microbial decay of a range of plant species, and the preservation of organic matter in the pyrite fossil record of the Tertiary of south-east England.

Microbial decay experiments

The formation of amorphous FeS within the cells of plane and *Psilotum* under experimental conditions showed that, although not extensive, mineralisation was rapid: FeS crystals were formed in under 5.4 weeks, and pith parenchyma cells were lined and occasionally partially infilled within 12 weeks. This rapid mineralisation coincided with rapid microbial decay. This suggests that the initial stages of the preservation of plants in pyrite occurred on a short-term, rather than geological-time scale. While the initial stages in pyritisation may be short, as evidenced by the partial infilling of pith parenchyma cells in 12 weeks (Figure 2.3B-D) the complete process may take much longer,

depending on the time required for the transformation of iron monosulphides into pyrite.

The amorphous iron monosulphide formed in similar locations to those observed in the fossil specimens from the London Clay, and in experiments on celery by Grimes *et al.* (2001a). Mineral growth was observed in the experiments lining the interior walls of pith parenchyma, within the middle lamella, and at the cell wall junctions between pith cells. This distribution of iron monosulphide would have provided a template to preserve cellular structure before morphological details were lost by decay. However, to protect against compaction prior to complete infilling of the plant material, the templates in the fossil plants must have been composed of pyrite.

Despite the range of experimental conditions investigated, including factors known to limit pyrite formation such as sulphate concentration, and iron and organic matter availability and reactivity, only 4 decay systems out of a total 145 resulted in the nucleation of amorphous FeS within the pith parenchyma cells of twigs. These four systems were all set-up under "standard", non-extreme conditions with active microbial decay, reasonable amounts of organic matter and open, marine conditions. This suggests that these conditions are essential for the pyritisation of organic matter in the natural environment. The fact that iron sulphides never formed within the plant material in any of the sealed anaerobic decay systems may have important implications for models of pyrite formation which require anoxia (e.g. the H_2S pathway, Rickard (1997)), and supports theories which suggest that oxidants are required (e.g. Wilkin and Barnes, 1996). The lack of pyrite formation in the freshwater systems is anomalous in the light of occurrences of pyritised plant material in what were thought to be freshwater

environments in the fossil record (e.g. Kenrick and Edwards, 1988). This implies a source of sulphate which was not present in the experiments.

The geochemistry of the four standard systems in which FeSam nucleated within the plant material was similar after 12 or 14 weeks, but no TRIS data are available for the sediments of any of these systems. It should be remembered that amorphous iron sulphides formed in the twigs from only 2 of 9 replicate standard systems which were incubated for 12 or 14 weeks. Hence, the lack of nucleation of amorphous iron sulphide in different plant species such as pine or *Cyathea*, which were decayed under the same conditions but in only one system each, does not necessarily indicate that these species cannot be preserved in pyrite. In addition, the relatively limited occurrence of pyritisation in these experiments is consistent with the limited pyritised plant fossil record.

Even where high concentrations of TRIS formed (with fifteen twigs, added glucose, extra sulphate, increased sedimentary iron, or the presence of ferric iron) no FeSam was observed with the twigs from these systems. This indicates that there are additional controls on the preservation of plant material by pyrite other than the limiting factors of sulphate, iron and organic matter availability and reactivity.

Pyrite is reluctant to nucleate (Schoonen and Barnes, 1991a), but this has been shown to occur on organic surfaces such as bacterial cell walls (Donald and Southam, 1999), on and within the cell walls of celery (Grimes *et al.*, 2001a) and on pyrite itself (e.g. Schoonen and Barnes, 1991a; Butler *et al.*, 2000).

Transport processes are also critical to the pyritisation of organisms (Raiswell, 1993; Grimes *et al.*, 2001a). Grimes *et al.* (2001a) reported the presence of an aqueous species, FeSaq, within their abiological experiments on the pyritisation of celery. Such a species may have a vital role in the transport of iron and sulphur into decaying organisms prior

to pyritisation, and would allow plant material to be infiltrated with iron and sulphur through pits, decayed walls, and along vessels and tracheids. The importance of such an aqueous species is highlighted by the complete infilling of cells which were originally lined with pyrite in the fossil record; FeSaq would have been able to reach, and precipitate within, small gaps in the pyrite.

Grimes *et al.* (2001b) proposed that the formation of different pyrite textures in plant material from the London Clay resulted from constantly evolving micro-environments (e.g. pH, Eh, S^{2-}, Fe^{2+}), possibly within individual cells, and the gradual closing of the system. Laboratory experiments have shown that even very small changes in Eh and pH can effect the formation of pyrite, which may explain the lack of iron sulphide and pyrite within plant material from most of the decay systems. The high pH achieved in many of the decay systems (up to pH 9.8) is out of the stability range for pyrite formation (Figure 2.19), preventing the preservation of the plant material by pyrite. The gradual rise in pH to a maximum of pH 8.6 in systems 22 and 24 in which FeSam formed in the plant material, may be significant.

Other factors which may have influenced the formation of iron monosulphide or pyrite in the twigs from the decay systems include the amount of organic matter available, and the scale of the experiments. Raiswell *et al.* (1993) proposed a diffusion-with-precipitation model for the pyritisation of decaying carcasses. They proposed that high levels of metabolisable organic matter within the carcass required high porewater iron concentrations to confine the sulphide within the carcass by precipitation, instead of allowing it to diffuse out. This model was applied to Beecher's Trilobite Bed (Ordovician, New York State; Briggs *et al.*, 1991) where levels of sedimentary iron were unusually high and sedimentary organic matter concentrations low. However, the

concentrations of sedimentary organic matter at the time of deposition are unknown, and high levels of organic carbon would have been required both for the reduction of ferric iron to produce the porewater ferrous iron, and the reduction of sulphate to produce sulphide.

Although chemical analysis of the plant material in the experiments indicated that decay had taken place to varying extents in all species, there was no morphological evidence for decay below the cut surface of the plant twigs. Precipitation and nucleation of iron sulphides in the twigs may have been inhibited by either the absence of the required sulphide within the twigs, or by a lack of alteration of the structure of the cell walls to provide a surface with enhanced nucleation potential.

The finite scale of the decay experiments may also have prevented the extensive formation of pyrite within the plant material. The individual jars had a limited constant volume, and hence limited chemical reservoir, with no through-flux or new inputs, as would occur in the natural environment. The time scale on which the experiments were run may also have been limiting, especially as pyrite is a slow-forming mineral.

The formation of clay minerals within the fungal-degraded twigs (Figure 2.16) may have been influenced by the low pH (pH 6.8-7.0) of the systems, but may also have been promoted by the chemical alteration of the cellular material by the fungi.

<u>Chemistry of organic decay</u>

One of the aims of this investigation was to produce a model to predict the types of plant tissues of species which would be susceptible to preservation in pyrite. The results of the chemical analyses of plant material decayed under aqueous marine conditions for up to 14 weeks indicate that, while it is possible to make some generalisations about

which tissues may be preserved and end-member plant species with very different preservation potentials, a complete model would be difficult to formulate. For example, highly cellulosic tissues or species, such as celery, are highly susceptible to decay and are unlikely to be preserved. In contrast, heavily lignified tissues, and species containing other decay-resistant biopolymers such as tannins, cutin and suberin, are more likely to be preserved. However, the differing combinations of constituent biopolymers, and the variations in structural arrangement of these macromolecules, makes predicting the preservation potential of species which lie between the highly cellulosic and heavily-lignified extremes difficult.

Cyathea, pine, plane and vine were all chosen for these experiments as they are modern analogues of plants identified in the London Clay (e.g. Collinson and Ribbins, 1977; Poole, 1992, 1996; Poole and Wilkinson, 2000). Tissue-stained thin sections (Figure 2.17) and chemical analysis indicates that these species differ greatly from each other. Hence, conditions in the London Clay must have been such that a variety of tissue compositions could be preserved.

Comparison of the relative proportions of taxonomic groups identified in the London Clay does not help in the formulation of a model to predict decay resistance and preservation potential. The 120 fossils collected for this study from the London Clay consisted of 86.3% dicotyledons, 1.7% monocotyledons and 8.5% gymnosperms. Poole (1992) reported 58.1% dicotyledons, 8.65% gymnosperms, 1.25% ferns, 32% unidentified axes, and 0% monocotyledons in a study of 2000 plant axes from the London Clay. The low numbers of monocotyledons and ferns do not necessarily indicate a high decay susceptibility, although these taxonomic groups are more cellulose-based with less structural protection from lignified tissues than the dicotyledons and

gymnosperms. The monocotyledons and ferns may have simply been less common in the Tertiary of south-east England. They do not tend to form twigs, but rather small length, small diameter axes which would have been subjected to sorting and mechanical damage during transport to the deposition site or sorting during fossil collection. The catchment area for the London Clay was large, and transport from the site of the main plant body to the deposition site may have involved long journeys along rivers (Poole, 1992). Monocots and ferns may have been more susceptible to fragmentation and aerobic decay during these transport processes than the dicots and gymnosperms.

SEM and optical microscopy of the decayed twigs (Chapter 2) revealed that one of the most decay-susceptible tissues was the phloem, which had cellulose walls and contained nutrients and sugars. The extensive degradation of the phloem tissues resulted in the separation of the bark from the xylem and pith after only a few weeks of decay. The lack of phloem and bark in any of the London Clay fossils indicates that similar decay processes occurred in these axes prior to fossilisation, but it is impossible to determine whether decay occurred prior to arrival at the depositional site, during transport, or after deposition. As the bark of a plant is formed to protect against abrasion as well as microbial attack, it is unlikely that abrasion during transport would have resulted in the complete loss of the bark without any decay in the adjacent phloem.

Preservation of organic material in pyritised fossil plants

The fossilised plants from the London Clay and the Reading Beds were found to consist almost entirely of pyrite, with very little organic matter. One exception to this was a conifer stem from the Reading Beds in which pyrolysis-GC/MS revealed lignin units such as guaiacol, 4-vinyl guaiacol, *trans* isoeugenol and homovanillin. This specimen reflects the

decay-resistance of lignin and shows that original decay-resistant organic material can be preserved without significant diagenetic alteration. Syringyl lignin is absent in gymnosperms such as conifers; it has not been lost during decay.

It is unclear whether the survival of lignin in this conifer from the Reading Beds is an extremely rare occurrence, or is due to the depositional environment. Interpreting the preservation of organic matter in pyrite is problematic due to the small amount of fossils with good morphological preservation and/or which contain organic matter. In the case of the Reading Beds, further investigation is prevented as sea defences have been erected on the site.

The distribution of carbon within the cell walls of the *Vitaceoxylon* stem from the London Clay is rare within the sample in general, and is associated with a unique combination of framboids and octahedra and a lack of microcrystalline pyrite. This suggests that exceptional conditions prevailed in a small region of this particular stem, as observed in the microbial decay experiments. These small areas of organic carbon also indicate that similar localised regions of organic preservation may exist within other fossil specimens.

The low levels of organic matter in the Tertiary pyritised twigs are in contrast with pyritised axes from the Devonian (Kenrick and Edwards. 1988; Kenrick *et al.*, 1991) which contain much more coalified organic matter. It is thought that lignified tissues are preserved coalified, while more decay-susceptible tissues with high cellulose content were replaced by pyrite. This difference in preservational style may reflect differences in the depositional environment (especially as these specimens are from freshwater beds), but may be due to preservation during a period between the evolution of lignin and decomposer organisms capable of degrading it.

The presence of pyritised fungi in the pyritised axes from the London Clay indicate that some decay of the plant material had occurred prior to deposition at the fossil bed. Bacterial decay also occurred, but bacteria have a much lower preservation potential than fungi and were not observed.

General conclusions

This work has demonstrated that the initial stages of pyritisation of plant material can be extremely rapid, even if complete preservation in pyrite requires a much longer time period. The formation of pyrite precursors is also associated with rapid microbial decay and "non-extreme" open marine conditions and controls. The rare occurrence of FeSam within the plant material suggests a combination of exceptional conditions and controls operating in a micro-scale, possibly within the decaying plant. The difficulty in replicating these conditions, even under near-identical starting environments and diagenetic conditions, reflects the rarity of pyritisation of plant material within the fossil record. As pyritisation can occur rapidly within the laboratory, this should enable further investigation on controls on pyritisation.

Plant tissues and species which are almost exclusively comprised of cellulose are highly susceptible to decay and are unlikely to be preserved, and heavily lignified tissues have a high preservation potential. The variety of species preserved in the London Clay with a wide range of biopolymeric composition and tissue structure, however, indicate that any species lying within these extremes of preservation potential may be pyritised as long as they reached the deposition site relatively intact and prevailing conditions facilitate pyritisation. Nonetheless, almost all of the organic matter in the twigs has degraded. Only guaiacol lignin was

detected in the fossil samples, indicating that the lignin had not been significantly altered diagenetically.

Future work

Although this study has investigated a wide range of controls on the pyritisation of plant material, there are several areas which would benefit from further study.

1. Experimental conditions

Many different environmental conditions were investigated in the microbial decay experiments. If any of these conditions were repeated, or further conditions investigated, more detailed analysis of the sediment should be carried out. Special consideration should be given to the amount and bioavailability of organic matter in the sediment, organic and inorganic sulphur and sedimentary porewater sulphate concentrations, and the mineral component of the sediment.

The influence of the carbon dioxide which was added to the medium with the sodium bicarbonate buffer also needs to be investigated further. The presence of carbon dioxide greatly influenced the pH of the medium, and this in turn may have affected the ability of pyrite to nucleate.

However, more detailed insights into the mechanisms of pyrite formation within plant material may require chemical gradients, pH etc. to be monitored on a much smaller scale than possible in these experiments, possibly on a cellular scale. However, it is uncertain how this would be achieved effectively using existing techniques.

2. Rates of reaction of microbial decay experiments

If studies of decay conditions other than open marine systems were repeated in more detail, for example as a time series, with weekly

analysis of systems over a 12-week period, TRIS data could be used to calculate decay constants and rates of reaction for the decay of organic material under different conditions. This would allow comparisons to be made between rates of sulphate reduction and/or decomposition of different types of organic matter with published experimental work, such as the decay of plankton by Westrich & Berner (1984). For such calculations to be carried out accurately, the porosity of the sediment should also be analysed.

3. Range of plant species studied

To aid in the formulation of a model to predict the preservation of plant material in pyrite, a much wider range of species need to be analysed. Enough fresh and decayed plant material is required to ensure that all analyses are undertaken for all species, and that replicate analysis from the same twigs can be carried out to allow for intraspecies variations. This may also overcome the limited likelihood of pyritisation even under initially identical experimental conditions.

4. Fossil material

To allow further investigation of the preservation of organic matter in pyritised plant fossils, more fossil specimens, in particular from freshwater sites, need to be studied. Such an investigation is hindered by the burial of the Reading Bed under sea defences, and so different fossil sources need to be located. In addition, a greater understanding of the processes by which the plant material was transported to the deposition site and the associated decay and mechanical alteration is required.

REFERENCES

ALLEN, E.T., CRENSHAW, J.L., JOHNSTON, J. & LARSEN, E.S. (1912) Mineral sulphides of iron. *American Journal of Science*, **33**, 169-236.

ALLEN, R.E. & PARKES, R.J. (1995) Digestion procedures for determining reduced sulfur species in bacterial cultures and in ancient and Recent sediments. In: *Geochemical Transformations of Sedimentary Sulfur* (Ed. by V. Schoonen), pp. 243-257. American Chemical Series.

ALLER, R.C. (1980a) Diagenetic processes near the sediment-water interface of Long Island Sound. II Fe and Mn. *Advances in Geophysics*, **90**, 79-95.

ALLER, R.C. (1980b) Quantifying solute distributions in the bioturbated zone of marine sediments by defining an average microenvironment. *Geochimica et Cosmochimica Acta*, **44**, 1955-1965.

ALLISON, P.A. (1988a) Konservat-Lagerstätten: cause and classification. *Paleobiology*, **14**, 331-344.

ALLISON, P.A. (1988b) The role of anoxia in the decay and mineralization of proteinaceous macro-fossils. *Paleobiology*, **14**, 139-154.

ALLISON, P.A. (1988c) Taphonomy of the Eocene London Clay biota. *Palaeontology*, **31**, 1079-1100.

ALLISON, P.A. & BRIGGS, D.E.G. (1991) Taphonomy of non-mineralized tissues. In: *Taphonomy: Releasing the Data Locked in the Fossil Record, 9, Topics in Geobiology* (Ed. by P.A. Allison & D.E.G. Briggs). Plenum Press, New York.

ALMENDROS, G., DORADO, J., GONZALEZ-VILA, F.J., BLANCO, M.J. & LANKES, U. (2000) ^{13}C NMR assessment of decomposition patterns during composting of forest and shrub biomass. *Soil Biology & Biochemistry*, **32**, 793-804.

ASPINALL, G.O. (1970) Pectins, plant gums, and other plant polysaccharides. In: *The Carbohydrates, IIB* (Ed. by W. Pigman & D. Horton), pp. 515-536. Academic Press.

ATLAS, R.M. & BARTHA, R. (1987). *Microbial Ecology: Fundamentals and Applications*. Benjamin Cummings Publishing.

BAK, F. & PFENNIG, N. (1991) Microbial sulfate reduction in littoral sediment of Lake Constance. *FEMS Microbiology Ecology*, **85**, 31-42.

BARGHOORN, E.L. (1952) Degradation of plant tissues in organic sediments. *Journal Of Sedimentary Petrology*, **22**, 34-41.

BARTELS, C., BRIGGS, D.E.G. & BRASSEL, G. (1998) *The Fossils of the Hunsrück Slate: Marine Life in the Devonian*. Cambridge University Press.

BARTELS, C. & BRASSEL, G. (1990) *Fossilien im Hunsruckschiefer - Dokumente des Meereslebens in Devon: Idar-Oberstein, Museum Idar-Oberstein*.

BATE-SMITH, E.C. (1984) Age and distribution of galloyl esters, iridoids and certain other repellents in plants. *Phytochemistry*, **23**, 945-950.

BELL, P. & WOODCOCK, C. (1968) *The Diversity of Green Plants*. Edward Arnold Publishers Ltd.

BEMILLER, J.N. (1986) An Introduction to Pectins: Structure and Properties. In: *ACS Symposium Series*, pp. 2-12. American Chemical Society, Washington D.C.

BEN-YAAKOV, S. (1973) pH Buffering of pore water of Recent anoxic marine sediments. *Limnology & Oceanography*, **18**, 86-94.

BENNER, R., FOGEL, M.L. & SPRAGUE, E.K. (1991) Diagenesis of belowground biomass of *Spartina alterniflora* in salt-marsh sediments. *Limnology & Oceanography*, **36**, 1358-1374.

BENNER, R., MACCUBBIN, A.E. & HODSON, R.E. (1984a) Anaerobic biodegradation of the lignin and polysaccharide components of lignocellulose and synthetic lignin by sediment microflora. *Applied and Environmental Microbiology*, **47**, 998-1004.

BENNER, R., NEWELL, S.Y., MACCUBBIN, A.E. & HODSON, R.E. (1984b) Relative contributions of bacteria and fungi to rates of degradation of lignocellulose detritus in salt-marsh sediments. *Applied and Environmental Microbiology*, **48**, 36-40.

BENNER, R., WELIKY, K. & HEDGES, J.I. (1990) Early diagenesis of mangrove leaves in a tropical estuary: Molecular-level analyses of neutral sugars and lignin-derived phenols. *Geochimica et Cosmochimica Acta*, **54**, 1991-2001.

BENNING, L.G., WILKIN, R.T. & BARNES, H.L. (2000) Reaction pathways in the Fe-S system below 100°C. *Chemical Geology*, **167**, 25-51.

BERNER, R.A. (1964). Distribution and diagenesis of sulfur in some sediments from the Gulf of California. *Marine Geology*, **1**, 117-140.

BERNER, R.A. (1967) Thermodynamic stability of sedimentary iron sulphides. *American Journal of Science*, **265**, 773-785.

BERNER, R.A. (1969) The synthesis of framboidal pyrite. *Economic Geology*, **64**, 383-384.

BERNER, R.A. (1970) Sedimentary pyrite formation. *American Journal of Science*, **268**, 1-23.

BERNER, R.A. (1976) The benthic boundary layer from the viewpoint of a geochemist. In: *The Benthic Boundary Layer* (Ed. by I. N. McCave), pp. 81-94. Plenum Press.

BERNER, R.A. (1980) *Early Diagenesis: A Theoretical Approach*. Princeton.

BERNER, R.A. (1981) Authigenic mineral formation resulting from organic matter decomposition in modern sediments. *Fortschr. Miner.*, **59**, 117-135.

BERNER, R.A. (1984) Sedimentary pyrite formation: An update. *Geochimica et Cosmochimica Acta*, **48**, 605-615.

BEYER, L., CORDSON, E., BLUME, H.P., SCHLEUSS, U., VOGT, B. & WU, Q. (1995) Soil organic matter in urbic anthrosols in the city of Kiel, NW-

Germany, as revealed by wet chemistry and CPMAS ^{13}C-NMR spectroscopy of whole soil samples. *Soil Technology*, **9**, 121-132.

BIDDANDA, B. & RIEMANN, F. (1992) Detrital carbon and nitrogen relations, examined with degrading cellulose. *Marine Ecology*, **13**, 271-283.

BONE, D.A. (1986) The stratigraphy of the Reading Beds (Palaeocene), at Felpham, West Sussex. *Tertiary Research*, **8**, 17-32.

BOON, J.J., STOUT, S.A., GENUIT, W. & SPACKMAN, W. (1989) Molecular paleobotany of Nyssa endocarps. *Acta Botanica Neerlandia*, **38**, 391-404.

BOUTELJE, J.B. & GORANSSON, B. (1975) Decay in wood constructions below the ground water table. *Swedish Journal of Agricultural Research*, **5**, 113-123.

BOWERBANK, J.S. (1840) *A History of the Fossil Fruits and Seeds of the London Clay*. John Van Vorst, London.

BRIGGS, D.E.G. (1995a) Experimental taphonomy. *Palaios*, **10**, 539,550.

BRIGGS, D.E.G. (1995b) Preservation of soft-tissue in the fossil record. *Ecologae Geologicae Helvitiae*, **88**, 623-626.

BRIGGS, D.E.G. (1999) Molecular taphonomy of animal and plant cuticles: selective preservation and diagenesis. *Philosophical Transactions of the Royal Society of London B*, **354**, 7-17.

BRIGGS, D.E.G., BOTTRELL, S.H. & RAISWELL, R. (1991) Pyritization of soft-bodied fossils: Beecher's Trilobite Bed, Upper Ordovician, New York State. *Geology*, **19**, 1221-1224.

BRIGGS, D.E.G. & EGLINTON, G. (1994) Chemical traces of ancient life. *Chemistry in Britain*, **31**, 907-912.

BRIGGS, D.E.G., EVERSHED, R.P. & LOCKHEART, M.J. (2000) The biomolecular paleontology of continental fossil. *Palaeobiology*, **26**, in press

BRIGGS, D.E.G. & KEAR, A.J. (1993) Fossilization of soft tissue in the laboratory. *Science*, **259**, 1439-1442.

BRIGGS, D.E.G. & KEAR, A.J. (1994) Decay and mineralization of shrimps. *Palaios*, **9**, 431-456.

BRIGGS, D.E.G., KEAR, A.J., MARTILL, D.M. & WILBY, P.R. (1993) Phosphatization of soft-tissue in experiments and fossils. *Journal of the Geological Society of London*, **150**, 1035-1038.

BRIGGS, D.E.G., RAISWELL, R., BOTTRELL, S.H., HATFIELD, D. & BARTELS, C. (1996) Controls on the pyritization of exceptionally preserved fossils: an analysis of the Lower Devonian Hunsrück Slate of Germany. *American Journal of Science*, **296**, 633-663.

BROCK, T.D. (1997) *Microbiology of Micro-organisms*. Prentice Hall International.

BROWN, D.E., GROVES, G.R. & MILLER, J.D.A. (1973) pH and Eh control of cultures of sulphate-reducing bacteria. *Journal of Applied Chemical Biotechnology*, **23**, 141-149.

BUFFLE, J., DE VITRE, R., PERRET, D. & LEPPARD, G.G. (1988) Combining field measurements for the speciation in non-perturbable water samples. In: *Metal Speciation: Theory, Analysis and Application* (Ed. by J. R. Kramer & H. E. Allen), pp. 99-124. Lewis Publishers Inc.

CANFIELD, D.E. (1989a) Reactive iron in marine sediments. *Geochimica et Cosmochimica Acta*, **53**, 619-632.

CANFIELD, D.E. (1989b) Sulfate reduction and oxic respiration in marine sediments: Implications for organic carbon preservation in euxinic environments. *Deep Sea Research*, **36**, 121-138.

CANFIELD, D.E. & RAISWELL, R. (1991) Pyrite Formation and fossil preservation. In: *Taphonomy: Releasing the Data Locked in the Fossil Record, 9, Topics in Geobiology* (Ed. by P. A. Allison, D.E.G. Briggs), pp. 337-387. Plenum Press, New York.

CANFIELD, D.E., RAISWELL, R. & BOTTRELL, S. (1992) The reactivity of sedimentary iron minerals toward sulfide. *American Journal of Science*, **292**, 659-683.

CAPONE, D.G. & KIENE, R.P. (1988) Comparison of microbial dynamics in marine and freshwater sediments: Contrasts in anaerobic carbon catabolism. *Limnology & Oceanography*, **33**, 725-749.

CHANDLER, M.E.J. (1964) *The Lower Tertiary Floras of Southern England IV. A survey of findings in the light of recent botanical observations.* British Museum (Natural History), London.

CLINE, J.D. (1969) Spectrophotometric determination of hydrogen sulphide in natural waters. *Limnology & Oceanography*, **14**, 454-458.

COLEMAN, M.L., HEDRICK, D.B., LOVLEY, D.R., WHITE, D.C. & PYE, K. (1993) Reduction of Fe(III) in sediments by sulphate-reducing bacteria. *Nature*, **361**, 436-438.

COLLINSON, M.E. (1983) *Fossil plants of the London Clay.* London University Press.

COLLINSON, M.E., MÖSLE, B., FINCH, P., SCOTT, A.C. & WILSON, R. (1988) The preservation of plant cuticle in the fossil record: a chemical and microscopical investigation. *Ancient Biomolecules*, **2**, 251-265.

COLLINSON, M.E. & RIBBINS, M.M. (1977) Pyritised fern rachides in the London Clay. *Tertiary Research*, **1**, 109-113.

COLLINSON, M.E., VAN BERGEN, P.F., SCOTT, A.C. & DE LEEUW, J.W. (1994) The oil-generating potential of plants from coal and coal-bearing strata through time: A review with new evidence from Carboniferous plants. In: *Coal and Coal-bearing strata as Oil-prone Source Rocks?, 77, Geol. Soc. Special Publications* (Ed. by A. C. Scott & A. J. Fleet), pp. 31-70.

CONWAY MORRIS, S. (1986) The community structure of the Middle Cambrian Phyllopod Bed (Burgess Shale). *Palaeontology*, **29**, 423-467.

COWIE, G.L. & HEDGES, J.I. (1984) Carbohydrate sources in a coastal marine environment. *Geochimica et Cosmochimica Acta*, **48**, 2075-2087.

CRAWFORD, R.L. (1981) *Lignin Biodegradation and Transformation.* Wiley.

DAVISON, W., PHILLIPS, N. & TABNER, B.J. (1999) Soluble iron sulphide species in natural waters: Reappraisal of their stoichiometry and stability constants. *Aquatic Science*, **61**, 23-43.

DE LEEUW, J.W., FREWIN, N.L., VAN BERGEN, P.F., SINNINGHE DAMSTE, J.S. & COLLINSON, M.E. (1995) Organic carbon as a palaeoenvironmental indicator in the marine realm. In: *Marine palaeoenvironmental analysis from fossil, 83, Geological Society Special Publication* (Ed. by D. W. J. Bosence & P. A. Allison), pp. 43-71.

DE LEEUW, J.W. & LARGEAU, C. (1993) A review of macromolecular organic compounds that comprise living organisms and their role in kerogen, coal and petroleum formation. In: *Organic geochemistry* (Ed. by M. H. Engel & S. A. Macko), pp. 23-67. Plenum Press, New York.

DONALD, R. & SOUTHAM, G. (1999) Low temperature anaerobic bacterial diagenesis of ferrous monosulfide to pyrite. *Geochimica et Cosmochimica Acta*, **63**, 2019-2023.

DROBNER, E., HUBER, H., WACHTERSHAUSER, G., ROSE, D. & STETTER, K.O. (1990) Pyrite formation linked with hydrogen evolution under anaerobic conditions. *Nature*, **346**, 742-744.

DUNN, K.A., MCLEAN, R.J.C., UPCHURCH JR., G.R. & FOLK, R.L. (1997) Enhancement of leaf fossilization potential by bacterial biofilms. *Geology*, **25**, 1119-1122.

EDWARDS, D. (1980) Studies on Lower Devonian petrifactions from Britain. 1. Pyritised axes of *Hostinella* from the Brecon Beacons Quarry, Powys, South Wales. *Review of Palaeobotany and Palynology*, **29**, 189-200.

EDWARDS, D. (1981) Studies on Lower Devonian petrifactions from Britain. 2. *Sennicaulis*, a new form genus for sterile axes based on pyrite and limonitic petrifactions from the Senni Beds. *Review of Palaeobotany and Palynology*, **32**, 207-226.

ERICKSON, M. & MIKSCHE, G.E. (1974) Charakterisierung der Lignine von Pteridophyten durch oxidativen Abbau. *Holzforschung*, **28**, 157-159.

ERIKSSON, K.-E.L., BLANCHETTE, R.A. & ANDER, P. (1990) *Microbial and Enzymatic Degradation of Wood and Wood Components*. Springer-Verlag.

ERTEL, J.R. & HEDGES, J.I. (1984) The lignin component of humic substances: Distribution among soil and sedimentary humic, fluvic, and base-insoluble fractions. *Geochimica et Cosmochimica Acta*, 2065-2074.

FAIX, O., FORTMANN, I., BREMER, J. & MEIER, D. (1991) Thermal degradation products of wood. A collection of electron-impact (EI) mass spectra of polysaccharide derived products. *Holz als Roh- und Werkstoff*, **49**, 299-304.

FAIX, O., MEIER, D. & FORTMANN, I. (1990) Thermal degradation products of wood: A collection of electron-impact (EI) mass spectra of monomeric lignin derived products. *Holz als Roh- und Werkstoff*, **48**, 351-354.

FELD, W. (1911) Über die Bildung von Eisenbisulfid (FeS_2) in Lösungen und die Entstehung der natürlichn Pyritlager. *Zeitschr. für angew. Chemie*, **24**, 97-103.

FERGUSON, D.K. (1985) The origin of leaf assemblages - New light on an old problem. *Review of Palaeobotany and Palynology*, **46**, 117-188.

FERRIS, F.G., FYFE, W.S. & BEVERIDGE, T.J. (1987) Bacteria as nucleation sites for authigenic minerals in a metal-contaminated lake sediment. *Chemical Geology*, **63**, 225-232.

FERRIS, F.G., SCHULTZE, S., WITTEN, T.C., FYFE, W.S. & BEVERIDGE, T.J. (1989) Metal interactions with microbial biofilms in acidic and neutral pH environments. *Applied and Environmental Microbiology*, **55**, 1249-1257.

FOO, L.Y. (1982) Polymeric proanthocyanidins of *Photinia glabrescens*, modification of molecular weight and nature of products from hydrogenolysis. *Phytochemistry*, **21**, 1747-1746.

FOO, L.Y. & PORTER, L.J. (1980) The phytochemistry of proanthocyanidin polymers. *Phytochemistry*, **19**, 1747-1754.

FRIEDMANN, W.E. & COOK, M.E. (2000) The origin and early evolution of tracheids in vascular plants: integration of palaeobotanical and neobotanical data. *Philosophical Transactions of the Royal Society Bulletin*, **355**, 857-868.

GALLETTI, G.C. (1991) Py-GC ion trap detection of sorghum grain polyphenols (*syn*. vegetable tannins): preliminary results. *Preparations American Chemical Society Division of Fuel Chemistry*, **36**, 691-697.

GALLETTI, G.C. & BOCCHINI, P. (1995) Pyrolysis/gas chromatography/mass spectroscopy of lignocellulose. *Rapid Communications in Mass Spectroscopy*, **9**, 815-826.

GALLETTI, G.C. & REEVES, J.B. (1992) Pyrolysis/gas chromatography/ion trap detection of polyphenols (vegetable tannins): preliminary results. *Organic Mass Spectrometry*, **27**, 226-230.

GIBLIN, A.E. & HOWARTH, R.W. (1984) Porewater evidence for a dynamic sedimentary iron cycle. *Limnology & Oceanography*, **29**, 47-63.

GLOAGUEN, J.C. & TOUFFET, J. (1982) Evolution du rapport C/N dans les feuilles et au cours de la composition des litieres sous climat atlantique. Le hetre et quelques coniferes. *Annales Sciences Forestieres*, **39**, 219-230.

GOLDHABER, M.B. & KAPLAN, I.R. (1974) The Sulfur Cycle. In: *The Sea, 5* (Ed. by E. D. Goldberg), pp. 569-655.

GONI, M.A. (1992) The use of CuO reaction products for the characterisation of organic matter in the marine environment. PhD thesis, University of Washington.

GONI, M.A. & HEDGES, J.I. (1990) Cutin-derived CuO reaction products from purified cuticles and tree leaves. *Geochimica et Cosmochimica Acta*, **54**, 3065-3072.

GONI, M.A. & HEDGES, J.I. (1992) Lignin dimers: Structures, distribution, and potential geochemical applications. *Geochimica et Cosmochimica Acta*, **56**, 4025-4043.

GONI, M.A., NELSON, B., BLANCHETTE, R.A. & HEDGES, J.I. (1993) Fungal decomposition of wood lignins: Geochemical perspectives from CuO-derived phenolic dimers and monomers. *Geochimica et Cosmochimica Acta*, **57**, 3985-4002.

GOODWIN, T.W. & MERCER, E.I. (1972) *Introduction to Plant Biochemistry*. Pergamon Press, Oxford.

GOTH, K., DE LEEUW, J.W., PUTTMANN, W. & TEGELAAR, E.W. (1988) Origin of Messel Oil Shale Kerogen. *Nature*, **336**, 759-761.

GRAHAM, U.M. & OHMOTO, H. (1994) Experimental study of the formation mechanism of hydrothermal pyrite. *Geochimica et Cosmochimica Acta*, **58**, 2187-2202.

GREAVES, H. (1971) The bacterial factor in wood decay. *Wood Science and Technology*, **5**, 6-16.

GRIERSON, J.D. (1976) *Leclercqia complexa* (Lycopsida, Middle Devonian): its anatomy, and the interpretation of pyrite petrifactions. *American Journal of Botany*, **63**, 1184-1202.

GRIMES, S.T., BROCK, F.,RICKARD, D., DAVIES, K.L., EDWARDS, D., BRIGGS, D.E.G. & PARKES, R.J. (2001a) Understanding fossilization: Experimental pyritization of plants. *Geology*, **29**, 123-126.

GRIMES, S.T., DAVIES, K.L., BUTLER, I.B., BROCK, F., EDWARDS, D., RICKARD, D., BRIGGS, D.E.G. & PARKES, R.J. (2001b). Fossil plants from the Eocene London Clay: The use of pyrite textures to determine the mechanism of pyritisation. In review

HACKETT, W.F., CONNORS, W.J., KIRK, T.K. & ZEIKUS, J.G. (1977) Microbial decomposition of synthetic ^{14}C-labeled lignins in nature: lignin biodegradation in a variety of natural materials. *Applied Environmental Microbiology*, **33**, 43-51.

HASLAM, E. (1989) *Plant Polyphenols. Vegetable Tannins Revisited*. Cambridge University Press.

HATCHER, P.G. (1988) Dipolar-dephasing C-13 NMR-studies of decomposed wood and coalified xylem tissue - evidence for chemical structural-changes associated with defunctionalization of lignin structural units during coalification. *Energy Fuels*, **2**, 48-58.

HATCHER, P.G., BREGER, I.A., MACIEL, G.E. & SZEVERENYI, N.M. (1983a) Chemical structures in coal: Geochemical evidence for the presence of mixed structural components. In: *Proceedings of the 1983 International Conference on Coal Science*, pp. 310-313.

HATCHER, P.G., BREGER, I.A., SZEVERENYI, N. & MACIEL, G.E. (1982) Nuclear magnetic resonance studies of ancient buried wood - II. Observations on the origin of coal from lignite to bitumous coal. *Organic Geochemistry*, **4**, 9-18.

HATCHER, P.G., LERCH III, H.E. & VERHEYEN, T.V. (1989) Organic geochemical studies of the transformation of gymnospermous xylem

during peatification and coalification to subbitumous coal. *International Journal of Coal Geology*, **13**, 65-97.

HATCHER, P.G., SPIKER, E.C. & SZEVERENYI, N.M. (1983b) Selective preservation: The origin of petroleum-forming aquatic kerogen. *Nature*, **305**, 498-501.

HEALY, J., J.B. & YOUNG, L.Y. (1979) Anaerobic biodegradation of eleven aromatic compounds to methane. *Applied and Environmental Microbiology*, **38**, 84-89.

HEDGES, J.I., CLARK, W.A. & COWIE, G.L. (1988) Fluxes and reactivities of organic matter in a coastal marine bay. *Limnology & Oceanography*, **33**, 1137-1152.

HEDGES, J.I., CLARK, W.A., QUAY, P.D., RICHEY, J.E., DEVOL, A.H. & SANTOS, U.D.M. (1986) Composition and fluxes of particulate organic matter in the Amazon River. *Limnology & Oceanography*, **31**, 717-738.

HEDGES, J.I. & ERTEL, J.R. (1982) Characterization of lignin by gas capillary chromatography of cupric oxide oxidation products. *Analytical Chemistry*, **54**, 174-178.

HEDGES, J.I. & KEIL, R.G. (1995) Marine chemistry discussion paper: Sedimentary organic matter preservation: an assessment and speculative synthesis. *Marine Chemistry*(4), 81-115.

HEDGES, J.I. & MANN, D.C. (1979a) The characterization of plant tissues by their lignin oxidation products. *Geochimica et Cosmochimica Acta*, **43**, 1803-1807.

HEDGES, J.I. & MANN, D.C. (1979b) The lignin geochemistry of marine sediments from the southern Washington coast. *Geochimica et Cosmochimica Acta*, **43**, 1809-1818.

HEDGES, J.L., COWIE, G.L., ERTEL, J.R., BARBOUR, R.J. & HATCHER, P.G. (1985) Degradation of carbohydrates and lignins in buried woods. *Geochimica et Cosmochimica Acta*, **49**, 701-711.

HERBERT JR, R.B., BENNER, S.G., PRATT, A.R. & BLOWES, D.W. (1998) Surface chemistry and morphology of poorly crystalline iron sulfides precipitated in media containing sulfate-reducing bacteria. *Chemical Geology*, **144**, 87-97.

HETHERINGTON, S. & ANDERSON, J.M. (1998) Simplified procedure for the characterisation of plant lignins by alkaline CuO oxidation. *Soil Biology and Biochemistry*, **30**, 1477-1480.

HIGHLEY, T.L. & LUTZ, J.F. (1970) Bacterial attack in water-stored bolts. *For. Prod. J.*, **20**, 43-44.

HOFFMANN, P. (1981) Chemical wood analysis as a means of characterising archaeological wood. In: *ProceedCOM Water Logged Wood Working Group Conference* (Ed. by D. W. Grattan), pp. 73-83, Ottawa.

HOLLOWAY, P.J. (1982) Structure and histochemistry of plant cuticular membranes: An overview. In: *The Plant Cuticle, Linnean Society Symposium Series* (Ed. by D. F. Cutler, K. L. Alvin & C. E. Price), pp. 1-32. Academic Press, London.

HOLLOWAY, P.J. (1984) Cutins and suberins, the polymeric plant lipids. In: *CRC Handbook of Chromatography, Lipids, 1* (Ed. by H. K. Mangold), pp. 321-346. CRC Press, Florida.

HUDSON, J.D. (1982) Pyrite in ammonite-bearing shales from the Jurassic of England and Germany. *Sedimentology*, 639-667.

JØRGENSEN, B.B. (1978) A comparison of methods for the quantification of bacterial sulphate reduction in coastal marine sediments III: Estimation from chemical and bacteriological field data. *Geomicrobiology Journal*, **1**, 49-64.

JØRGENSEN, B.B. (1982a) Ecology of the bacteria of the sulphur cycle with special reference to anoxic-oxic interface environments. *Philosophical Transactions of the Royal Society of London*, **298**, 543-561.

JØRGENSEN, B.B. (1982b) Mineralization of organic matter in the sea bed - the role of sulphate reduction. *Nature*, **296**, 643-645.

JØRGENSEN, B.B. (1983) Processes at the sediment-water interface. In: *The major biogeochemical cycles and their interactions* (Ed. by B. Bolin & R. B. Cook).

KAGEMORI, N. (1969) Chemical composition of fossil woods collected from the Cenozoic strata around Osaka. *Journal of the Geological Society of Japan*, **75**, 43-50.

KAPLAN, I.R., EMERY, K.O. & RITTENBERG, S.C. (1963) The distribution and isotopic abundance of sulfur in recent marine sediments off southern California. *Geochimica et Cosmochimica Acta*, **27**, 297-331.

KARLIN, R., LYLE, M. & HEATH, G.R. (1987) Authigenic magnetite formation in suboxic marine sediments. *Nature*, **326**, 490-493.

KENRICK, P. & EDWARDS, D. (1988) The anatomy of Lower Devonian *Gosslingia breconensis* Heard based on pyritized axes, with some comments on the permineralization process. *Botanical Journal of the Linnean Society*, **97**, 95-123.

KENRICK, P., EDWARDS, D. & DALES, R.C. (1991) Novel ultrastructure in water-conducting cells of the Lower Devonian plant *Sennicaulis hippocrepiformis*. *Palaeontology*, **34**(4), 751-766.

KERP, H. (1990) The study of fossil Gymnosperms by means of cuticular analysis. *Palaios*, **5**, 548-569.

KING, C. (1984) The stratigraphy of the London Clay formation and Virginia Water Formation in the coastal sections of the Isle of Sheppey (Kent, England). *Tertiary Research*, **5**, 121-160.

KIRK, T.K. (1973) The chemistry and biochemistry of decay. In: *Wood deterioration and its prevention by preservation treatments* (Ed. by D. D. Nicholas), pp. 149-182. Syracuse University Press, New York.

KIRK, T.K. (1984) Degradation of lignin. In: *Biochemistry of Microbial Degradation* (Ed. by D. T. Gibson), pp. 399-473. Marcel Dekker.

KOHARA, J. (1956) Studies of Japanese old timbers-XX Chemical analyses of unearthed woods. *Mokuzai Gakkashi*, **19**, 195-200.

KOLODZIEJSKI, W., FRYE, J.S. & MACIEL, G.E. (1982) Carbon-13 Nuclear Magnetic Resonance spectrometry with cross polarization and magic-angle spinning for analysis of Lodgepole Pine Wood. *Analytical Chemistry*, **54**, 1419-1424.

KONHAUSER, K.O., FYFE, W.S., FERRIS, F.G. & BEVERIDGE, T.J. (1993) Metal sorption and mineral precipitation by bacteria in two Amazonian river systems: Rio Solimoes and Rio Negro, Brazil. *Geology*, **21**, 1103-1106.

KRAUSKOPF, K.B. & BIRD, D., K,. (1995) *Introduction to geochemistry*. WCB McGraw-Hill.

KUHL, M. & JORGENSEN, B.B. (1992) Microsensor measurements of sulphate reduction and sulfide oxidation in compact microbial communities of aerobic biofilms. *Applied and Environmental Microbiology*, **58**, 1164-1174.

LEVENTHAL, J.S. (1983) An interpretation of carbon and sulfur relationships in Black Sea sediments as indictors of environments of deposition. *Geochimica et Cosmochimica Acta*, **47**, 133-138.

LEVY, J.F. (1987) The natural history of the degradation of wood., *Philosophical Transactions of the Royal Society*, **321**, 423-433.

LEWIS, N.G. & YAMAMOTO, E. (1990) Lignin: occurrence, biogenesis and biodegradation. *Annual Review of Plant Physiology and Plant Molecular Biology*, **41**, 455-96.

LOGAN, K.J. & THOMAS, B.A. (1985) Distribution of lignin derivatives in plants. *New Phytologist*, **99**, 571-85.

LOGAN, K.J. & THOMAS, B.A. (1987) The distribution of lignin derivatives in fossil plants. *New Phytologist*, **105**, 157-173.

LOVLEY, D.R. (1997) Microbial Fe(III) reduction in subsurface environments. *FEMS Microbiology Reviews*, **20**, 305-313.

LOVLEY, D.R. & PHILLIPS, E.J. (1986a) Availability of ferric iron for microbial reduction in bottom sediments of the freshwater tidal Potomac River. *Applied and Environmental Microbiology*, **52**, 7511-7517.

LOVLEY, D.R. & PHILLIPS, E.J.P. (1986b) Organic matter mineralization with reduction of ferric iron in anaerobic sediments. *Applied and Environmental Microbiology*, **52**, 683-689.

LOVLEY, D.R., RODEN, E.E., PHILLIPS, E.J.P. & WOODWARD, J.C. (1993) Enzymatic iron and uranium reduction by sulfate-reducing bacteria. *Marine Geology*, **113**, 41-53.

LUTHER III, G.W. (1991) Pyrite synthesis via polysulfide compounds. *Geochimica et Cosmochimica Acta*, **55**, 2839-2849.

MACKO, S.A., HELLEUR, R., HARTLEY, G. & JACKMAN, P. (1989) Diagenesis of organic matter - A study using stable isotopes of individual carbohydrates. *Organic Geochemistry*, **16**, 1129-1137.

MALCOLM, S.J. & STANLEY, S.O. (1982) The sediment environment. In: *Sediment Microbiology* (Ed. by D. B. Nedwell & C. M. Brown), pp. 1-14. Academic Press, London.

MAUSETH, J.D. (1995) *Botany: An introduction to plant biology*. Saunders College Publishing.

MELILLO, J.M., ABER, J.D. & MURATORE, J.F. (1982) Nitrogen and lignin control of hardwood leaf litter decomposition dynamics. *Ecology*, **63**, 621-626.

MIDDELBURG, J.J., DE LANGE, G.J. & VAN DER WEIJDEN, C.H. (1987) Manganese solubility control in marine pore waters. *Geochimica et Cosmochimica Acta*, **51**, 759-763.

MORSE, J.W. & CORNWELL, J.C. (1987) Analysis and distribution of iron sulfide minerals in recent anoxic marine-sediments. *Marine Chemistry*, **22**, 55-69.

MORSE, J.W., MILLERO, F.J., CORNWELL, J.C. & RICKARD, D. (1987) The chemistry of the hydrogen sulphide and iron sulphide systems in natural waters. *Earth-Science Reviews*, **24**, 1-42.

MORSE, J.W. & WANG, Q. (1997) Pyrite formation under conditions approximating those in anoxic sediments: II. Influence of precursor iron minerals and organic matter. *Marine Chemistry*, **57**, 187-193.

MÖSLE, B., FINCH, P., COLLINSON, M.E. & SCOTT, A.C. (1997) Comparison of modern and fossil plant cuticles by selective chemical extraction monitored by flash pyrolysis-gas chromatography-mass spectrometry and electron microscopy. *Journal of Analytical and Applied Pyrolysis*, **40**, 585-597.

MULLER, P.J. (1977) C/N ratios in Pacific deep-sea sediments: Effect of inorganic ammonium and organic nitrogen compounds sorbed by clays. *Geochimica et Cosmochimica Acta*, **41**, 765-776.

MULLER, W.H. (1979) *Botany: a functional approach*. Macmillan Publishing Co.

NEALSON, K.H. & LITTLE, B. (1997) Breathing manganese and iron: Solid-state respiration. In: *Advances in applied microbiology*, **45**. Academic Press.

NEALSON, K.H. & SAFFARINI, D. (1994) Iron and manganese in anaerobic respiration: Environmental significance, physiology, and regulation. *Annual Review of Microbiology*, **48**, 311-43.

NICHOLAS, D.D. (1973) *Wood deterioration and its prevention by preservation treatments*. Syracuse University Press, New York.

NIP, M., TEGELAAR, E.W., BRINKHUIS, H., DE LEEUW, J.W., SCHENCK, P.A. & HOLLOWAY, P.J. (1986a) Analysis of modern and fossil plant cuticles by Curie point Py-GC and Curie point Py-GC-MS: Recognition of a new, highly aliphatic and resistant biopolymer. *Organic Geochemistry*, **10**, 769-778.

NIP, M., TEGELAAR, E.W., DE LEEUW, J.W., SCHENCK, P.A. & HOLLOWAY, P.J. (1986b) A new non-saponifiable highly aliphatic and resistant biopolymer in plant cuticles. Evidence from pyrolysis and $^{1}3$C-NMR analysis of present-day and fossil plants. *Naturewissenschaften*, **73**, 579-585.

ODOM, J.M. & SINGLETON JR, R. (1993) *The Sulphate-Reducing Bacteria: Contemporary Perspectives*. Springer-Verlag, New York.

OREMLAND, R.S. (1988) Biogeochemistry of methanogenic bacteria. In: *Biology of Anaerobic Microorganisms* (Ed. by A. J. B. Zehnder), pp. 641-705. John Wiley, New York.

PANSHIN, A.J. & DE ZEEUW, C. (1980)*Textbook of Wood Technology*. McGraw-Hill.

PARKES, R.J., GIBSON, G.R., MUELLER-HARVEY, I., BUCKINGHAM, W.J. & HERBERT, R.A. (1989) Determination of the substrates for sulphate-reducing bacteria within marine and estuarine sediments with different rates of sulphate reduction. *Journal of General Microbiology*, **135**, 175-187.

PARKES, R.J. & SENIOR, E. (1988) Multistage Chemostats and Other Models for Studying Anoxic Ecosystems. In: *CRC Handbook of Laboratory Model Systems for Microbial Ecosystems, 1* (Ed. by J. W. T. Wimpenny), pp. 51-72. CRC Press Inc., Florida.

PHELPS, C.D. & YOUNG, L.Y. (1997) Microbial metabolism of the plant phenolic compounds ferulic and syringic acids under three anaerobic conditions. *Microbial Ecology*, **33**, 206-215.

POOLE, I. (1992) Pyritized twigs from the London Clay, Eocene, of Great Britain. *Tertiary Research*, **13**, 71-85.

POOLE, I. (1993) A Dipterocarpaceous Twig from the Eocene London Clay Formation of Southeast England. *Palaeontology*, **49**, 155-163.

POOLE, I. (1994) "Twig" -wood anatomical characters as palaeoecological indicators. *Review of Palaeobotany and Palynology*, **81**, 33-52.

POOLE, I. (1996) Conifer twigs from the London Clay (Eocene) of Southeast England. *Review of Palaeobotany and Palynology*, **94**, 25-37.

POOLE, I. & WILKINSON, H.P. (1992) Two sapindaceous woods from the London Clay (Eocene) of southeast England. *Review of Palaeobotany and Palynology*, **75**, 65-75.

POOLE, I. & WILKINSON, H.P. (1999) A celastraceous twig from the Eocene London Clay of south-east England. *Botanical Journal of the Linnean Society*, **129**, 165-176.

POOLE, I. & WILKINSON, H.P. (2000) Two early Eocene vines from south-east England. *Botanical Journal of the Linnean Society*, **133**, 1-26.

RAISWELL, R. (1971) The growth of Cambrian and Liassic concretions. *Sedimentology*, **17**, 147-171.

RAISWELL, R. (1976) The microbiological formation of carbonate concretions in the Upper Lias of N.E. England. *Chemical Geology*, **18**, 227-244.

RAISWELL, R. (1982) Pyrite texture, isotopic composition and the availability of iron. *American Journal of Science*, **282**, 1244-1263.

RAISWELL, R. (1993) Kinetic controls on depth variations in localised pyrite formation. *Chemical Geology*, **107**, 467-469.

RAISWELL, R. & BERNER, R.A. (1985) Pyrite formation in euxinic and semi-euxinic sediments. *American Journal of Science*, **285**, 710-724.

RAISWELL, R. & CANFIELD, D.E. (1998) Sources of iron for pyrite formation in marine sediments. *American Journal of Science*, **298**, 219-245.

RAISWELL, T., WHALER, K., DEAN, S., COLEMAN, M.L. & BRIGGS, D.E.G. (1993) A simple three-dimensional model of diffusion-with-precipitation applied to localised pyrite formation in framboids, fossils and detrital iron minerals. *Marine Geology*, **113**, 89-100.

RALPH, J. & HATFIELD, R.D. (1991) Pyrolysis-GC-MS characterization of forage materials. *Journal of Agriculture and Food Chemistry.*, **39**, 1426-1437.

RAVEN, P.H., EVERT, R.F. & EICHHORN, S.E. (1999) *Biology of Plants* W.H. Freeman & Co.

REDFIELD, A.C. (1958) The biological control of chemical factors in the environment. *American Scientist*, **46**, 206-220.

REID, E.M. & CHANDLER, M.E.J. (1933) *The Flora of the London Clay*. British Museum (Natural History), London.

REID, I.D. (1995) Biodegradation of lignin. *Canadian Journal of Botany*, **73** (suppl.1), S1011-1018.

REVSBECH, N.P. & JORGENSEN, B.B. (1986) Microelectrodes: their use in microbial ecology. In: *Advances in Microbial Ecology*, *9* (Ed. by K. C. Marshall), pp. 293-354. Plenum Press.

REVSBECH, N.P., JORGENSEN, B.B., BLACKBURN, T.H. & COHEN, Y. (1983) Microelectrode studies of the photosynthesis and O_2, H_2S, and pH profiles of a microbial mat. *Limnology & Oceanography*, **28**, 1062-1074.

RIBBINS, M.M. & COLLINSON, M.E. (1978) Further notes on pyritised fern rachides from the London Clay. *Tertiary Research*, **2**, 47-50.

RICE, D.L. & TENORE, K.R. (1981) Dynamics of carbon and nitrogen during the decomposition of detritus derived from estuarine macrophytes. *Estuarine, Coastal and Shelf Science*, **13**, 681-690.

RICKARD, D. (1994) A new sedimentary pyrite formation model. *Mineralogical Magazine*, **58A**, 772-773.

RICKARD, D. (1995) Kinetics of FeS precipitation: part 1. Competing reaction mechanisms. *Geochimica et Cosmochimica Acta*, **59**, 4367-4379.

RICKARD, D. (1997) Kinetics of pyrite formation by the H_2S oxidation of iron (ii) monosulfide in aqueous solutions between 25 and 125°C: The rate equation. *Geochimica et Cosmochimica Acta*, **61**, 115-134.

RICKARD, D. & LUTHER, G.W. (1997) Kinetics of pyrite formation by the H_2S oxidation of iron (ii) monosulfide in aqueous solutions between 25 and 125°C: The mechanism. *Geochimica et Cosmochimica Acta*, **61**, 135-147.

RICKARD, D., SCHOONEN, M.A.A. & LUTHER, G.W. (1995) Chemistry of iron sulfides in sedimentary environments. In: *Geochemical Transformations Of Sedimentary Sulfur*, **612**, (Ed. by M. a. S.

Vairaramurthy, M.), pp. 168-193. American Chemical Society Symposium Series.

RICKARD, D.T. (1975) Kinetics and Mechanism of pyrite formation at low temperatures. *American Journal of Science*, **275**, 636-652.

RICKARD, D.T., OLDROYD, A. & CRAMP, A. (1999) Voltametric evidence for soluble FeS complexes in anoxic estuarine muds. *Estuaries*, **22**, 693-701.

ROBERTS, W.M.B., WALKER, A.L. & BUCHANAN, A.S. (1969) The chemistry of pyrite formation in aqueous solutions and its relation to the depositional environment. *Mineralium Deposita*, **4**, 18-29.

SAGEMANN, J., BALE, S.J., BRIGGS, D.E.G. & PARKES, R.J. (1999) Controls on the formation of authigenic minerals in association with decaying organic matter: An experimental approach. *Geochimica et Cosmochimica Acta*, **63**, 1083-1095.

SARKANEN, K.V. & LUDWIG, C.H. (1971) *Lignins*. Wiley Interscience.

SCHMIDT, O. (1980) Laboratory experiments on the bacterial activity towards the woody cell wall. In: *Biodeterioration* (Ed. by T. A. Oxley, G. Becker & D. Allsopp). Pitman Publ. Ltd.

SCHOONEN, M.A.A. & BARNES, H.L. (1991a) Reactions forming pyrite and marcasite from solution: I. Nucleation of FeS_2 below 100°C. *Geochimica et Cosmochimica Acta*, **55**, 1495-1504.

SCHOONEN, M.A.A. & BARNES, H.L. (1991b) Reactions forming pyrite and marcasite from solution: II. Via FeS precursors below 100°C. *Geochimica et Cosmochimica Acta*, **55**, 1505-1514.

SCHOPF, J.M. (1975) Modes of fossil preservation. *Review of Palaeobotany & Palynology*, **20**, 27-53.

SCOTT, A.C. (1990) Anatomical preservation of fossil plants. In: *Palaeobiology: A Synthesis* (Ed. by D. E. G. Briggs & P. R. Crowther), pp. 263-266. Blackwell Science.

SCOTT, A.C. & DE KLERK, R. (1974) A preliminary study of London Clay pyritised "twigs" from the Isle of Sheppey. *Tertiary Times*, **2**, 73-82.

SEILACHER, A. (1970) Begriff and bedeutung der Fossil-Lagerstatten. *Neues Jarhbuch für Geologie und Palaontologie Abhandlungen*, **1970**, 34-39.

SEILACHER, A., REIF, W.-E. & WESTPHAL, F. (1985) Sedimentological, ecological and temporal patterns of *Fossil-Lagerstätten*. *Philosophical Transactions of the Royal Society of London*, **311B**, 5-23.

SEN, J. & BASAK, R.K. (1957) The chemistry of ancient buried wood. *Geol. Foren. Fohandl.*, **79**, 737-758.

SHEN, Z., HASLAM, E., FALSHAW, C.P. & BEGLEY, M.J. (1986) Procyanidins and polyphenols of *Larix gmelini* bark. *Phytochemistry*, **25**, 2629-2635.

SIGLEO, S.C. (1978) Degraded lignin compounds identified in silicified wood 200 million years old. *Science*, **200**, 1054-1056.

SIMON, E.W., DORMER, K.J. & HARTSHORNE, J.N. (1980)*Lowson's Botnay*, Fakenham Press

SJÖSTRÖM, E. (1981) *Wood chemistry: Fundamentals and applications.* Academic Press.

SØRENSEN, J. (1982) Reduction of ferric iron in anaerobic, marine sediment and interaction with reduction of nitrate and sulfate. *Applied Environmental Microbiology*, **43**, 319-324.

SØRENSEN, J. & JØRGENSEN, B.B. (1987) Early diagenesis in sediments from Danish coastal waters: Microbial activity and Mn-Fe-S geochemistry. *Geochimica et Cosmochimica Acta*, **51**, 1583-1590.

SPICER, R.A. (1991) Plant taphonomic processes. In: *Taphonomy: Releasing the Data Locked in the Fossil Record, 9, Topics in Geobiology* (Ed. by P. A. Allison and D.E.G. Briggs). Plenum Press, New York.

SPIKER, E.C. & HATCHER, P.G. (1987) The effects of early diagenesis on the chemical and stable carbon isotopic composition of wood. *Geochimica et Cosmochimica Acta*, **51**, 1385-1391.

STAFFORD, H.A. (1988) Proanthocyanidins and the lignin connection. *Phytochemistry*, **27**, 1-6.

STOOKEY, L.L. (1970) Ferrozine - a new spectrophotometric reagent for iron. *Analytical Chemistry*, **42**, 779-781.

STOUT, S.A., BOON, J.J. & SPACKMAN, W. (1988) Molecular aspects of the peatification and early coalification of angiosperm and gymnosperm woods. *Geochimica et Cosmochimica Acta*, **52**, 405-414.

STUMM, W. & MORGAN, J.J. (1981) *Aquatic Chemistry*. Wiley-Interscience, New York.

STURMER, W., SCHAARSCHMIDT, F. & MITTMEYER, H.-G. (1980) *Veresteinertes Leben im Rontgenlicht: Kleine Senckenberg Reihe.*

SWEENEY, R.E. & KAPLAN, I.R. (1980) Stable isotope composition of dissolved sulfate and hydrogen sulfide in the Black Sea. *Marine Chemistry*, **9**, 145-152.

TAYLOR, B.R., PARKINSON, D. & PARSONS, W.F.J. (1989) Nitrogen and lignin content as predictors of litter decay rates: A microcosm test. *Ecology*, **70**, 97-104.

TAYLOR, P., RUMMERY, T.E. & D.G., O. (1979a) On the conversion of mackinawite to greigite. *Journal of Inorganic and Nuclear Chemistry*, **41**, 595-596.

TAYLOR, P., RUMMERY, T.E. & OWEN, D.G. (1979b) Reactions of iron monosulfide solids with aqueous hydrogen sulphide up to 160oC. *Journal of Inorganic and Nuclear Chemistry*, **41**, 1683-1687.

TEGELAAR, E.W. (1990) Resistant biomacromolecules in morphologically characterized constituents of kerogen: A key to the relationship between biomass and fossil fuels. PhD thesis, University of Utrecht.

TEGELAAR, E.W., DE LEEUW, J.W., DERENNE, S. & LARGEAU, C. (1989a) A reappraisal of kerogen formation. *Geochimica et Cosmochimica Acta*, **53**, 3103-3106.

TEGELAAR, E.W., DE LEEUW, J.W., LARGEAU, C.D., S., SCHULTEN, H.-R., MULLER, R., BOON, J.J., NIP, M. & SPRENKELS, J.C.M. (1989b) Scope and

limitations of several pyrolysis methods in the structural elucidation of a macromolecular plant constituent in the leaf cuticle of *Agave americana* L. *Journal of Analytical and Applied Pyrolysis*, **15**, 29-54.

TEGELAAR, E.W., KERP, H., VISSCHER, H., SCHENCK, P.A. & DE LEEUW, J.W. (1991) Bias of the paleobotanical record as a consequence of variations in the chemical composition of higher vascular plant cuticles. *Paleobiology*, **17**, 133-144.

TIMELL, T.E. (1957) Carbohydrate composition of ten North American species of wood. *Tappi*, **40**, 568-572.

TREWIN, N.H. (1994) Depositional environment and preservation of biota in the Lower Devonian hot-springs of Rhynie, Aberdeenshire, Scotland. *Transactions of the Royal Society of Edinburgh: Earth Sciences*, **84**, 433-422.

TREWIN, N.H. (1996) The Rhynie Cherts: an early Devonian ecosystem preserved by hydrothermal activity. In: *Evolution of Hydrothermal Ecosystems of Earth (and Mars?)* (Ed. by G. R. Bock & J. A. Goode), pp. 131-145. Wiley, Chichester.

TSUGE, S. & MATSUBARA, H. (1985) High-resolution pyrolysis-gas chromatography of proteins and related materials. *Journal of Analytical and Applied Pyrolysis*, **8**, 49-64.

VAN BERGEN, P.F., A.C., S., BARRIES, P.J., DE LEEUW, J.W. & COLLINSON, M.E. (1994a) The chemical composition of Upper Carboniferous Pteridosperm cuticles. *Organic Geochemistry*, **21**, 107-112.

VAN BERGEN, P.F., BLAND, H.A., HORTON, M.C. & EVERSHED, R.P. (1997) Chemical and morphological changes in ancient seeds and fruits during preservation by desiccation. *Geochimica et Cosmochimica Acta*, **61**, 1919-1930.

VAN BERGEN, P.F., COLLINSON, M.E., BRIGGS, D.E.G., DE LEEUW, J.W., SCOTT, A.C., EVERSHED, R.P. & FINCH, P. (1995) Resistant biomacromolecules in the fossil record. *Acta botanica Neerlandica*, **44**, 319-342.

VAN BERGEN, P.F., COLLINSON, M.E., HATCHER, P.G. & DE LEEUW, J.W. (1994b) Lithological control on the state of preservation of fossil seed coats of water plants. *Organic Geochemistry*, **22**, 683-702.

VAN BERGEN, P.F., COLLINSON, M.E., SINNINGHE DAMSTE, J.S. & DE LEEUW, J.W. (1994c) Chemical and microscopical characterization of inner seed coats of fossil water plants. *Geochimica et Cosmochimica Acta*, **58**, 231-239.

VAN BERGEN, P.F., GONI, M., COLLINSON, M.E., BARRIE, P.J., SINNINGHE DAMSTE, J.S. & DE LEEUW, J.W. (1994d) Chemical and microscopic characterization of outer seed coats of fossil and extant water plants. *Geochimica et Cosmochimica Acta*, **58**, 3823-3844.

VAN BERGEN, P.F., POOLE, I., OGILVIE, T.M.A., CAPLE, C. & EVERSHED, R.P. (2000) Evidence for demelthylation of syringyl moieties in archaeological wood using pyrolysis-gas chromatography/mass spectrometry. *Rapid Communications in Mass Spectrometry*, **14**, 71-79.

VAN DER HAGE, E.R.E., MULDER, M.M. & BOON, J.J. (1993) Structural characterization and Curie-point pyrolysis-mass spectrometry and Curie-point pyrolysis-gas chromatography/mass spectrometry. *Journal of Analytical and Applied Pyrolysis*, **25**, 149-183.

VAN DER HEIJDEN, E. & BOON, J.J. (1994) A combined pyrolysis mass spectrometric and light microscopic study of peatified *Calluna* wood isolated from raised bog peat deposits. *Organic Geochemistry*, **22**, 903-919.

WÄCHTERSHÄUSER, G. (1988) Before enzymes and templates: theory of surface metabolism. *Microbiological Reviews*, **52**, 452-484.

WÄCHTERSHÄUSER, G. (1993) The cradle chemistry of life: on the origin of natural products in a pyrite-pulled chemoautotrophic origin of life. *Pure and Applied Chemistry*, **65**, 1343-1348.

WANG, Q. & MORSE, J.W. (1995) Laboratory simulation of pyrite formation in anoxic sediments. In: *Geochemical Transformation of Sedimentary Sulfur* (Ed. by V. Schoonen), pp. 206-223. American Chemical Society.

WANG, Q. & MORSE, J.W. (1996) Pyrite formation under conditions approximating those in anoxic sediments: I. pathway and morphology. *Marine Chemistry*, **52**, 99-121.

WELLSBURY, P., HERBERT, R.A. & PARKES, R.J. (1996) Bacterial activity and production in near-surface estuarine and freshwater sediments. *FEMS Microbiology Ecology*.**19**, 203-214

WESTRICH, J.T. (1983) The consequences and controls of bacterial sulphate reduction in marine sediments. Yale University.

WHITEHEAD, D.C., DIBB, H. & HARTLEY, R.D. (1981) Extractant pH and the release of phenolic compounds from soils, plant roots and leaf litter. *Soil Biology and Biochemistry*, **13**, 343-348.

WHITICAR, M.J. (1999) Carbon and hydrogen isotope systematics of bacterial formation and oxidation of methane. *Chemical Geology*, **161**, 291-314.

WIDDEL, F. & BAK, F. (1992) Gram-negative mesophilic sulfate-reducing bacteria. In: *The Prokaryotes*, pp. 3352-3378. New York.

WILBY, P.R., BRIGGS, D.E.G., BERNIER, P. & GAILLARD, C. (1996a) The role of microbial mats in the fossilization of soft-tissues. *Geology*, **24**, 787-790.

WILBY, P.R., BRIGGS, D.E.G. & RIOU, B. (1996b) Mineralization of soft-bodied invertebrates in a Jurassic metalliferous deposit. *Geology*, **24**, 847-850.

WILCOX, W.W. (1973) Degradation in relation to wood structure. In: *Wood deterioration and its prevention by preservative treatments* (Ed. by D. D. Nicholas), pp. 107-148. Syracuse University Press, New York.

WILKIN, R.T. & BARNES, H.L. (1996) Pyrite formation by reactions of iron monosulfides with dissolved inorganic and organic sulfur species. *Geochimica et Cosmochimica Acta*, **60**, 4167-4179.

WILSON, M.A., VERHEYEN, T.V., VASSALLO, A.M., HILL, R.S. & PERRY, G.J. (1987) Selective loss of carbohydrates from plant remains during coalification. *Organic Geochemistry*, **11**, 265-271.

WIMPENNY, J.W.T. (1992) Microbial systems; Patterns in time and space. In: *Advances in Microbial Ecology, 12* (Ed. by K. C. Marshall), pp. 469-522. Plenum Press, New York.

YAMAMOTO, E., BOKELMAN, G.H. & LEWIS, N.G. (1989) Phenylpropanoid metabolism in cell walls. In: *Plant Cell Wall Polymers, 399, American Chemical Society Symposium Series* (Ed. by N. G. Lewis & M. G. Paice), pp. 68-88.

ZEIKUS, J.G. (1980) Fate of lignin and related aromatic substances in anaerobic environments. In: *Lignin biodeterioration, 1* (Ed. by T. K. Kirk), pp. 101-109.

ZIOMEK, E. & WILLIAMS, R.E. (1989) Modification of lignins by growing cells of the sulphate-reducing anaerobe *Desulfovibrio desulfuricans*. *Applied and Environmental Microbiology*, **55**, 2262-2266.

Experimental conditions	time	Start month	i.d. no.
Standard marine conditions	1 wk	March	1
	2 wks	March	2
	3 wks	March	3
	4 wks	March	4
	5 wks	March	5
	6 wks	March	6
	7 wks	March	7
	8 wks	March	8
	9 wks	March	9
	10 wks	March	10
	11 wks	March	11
	12 wks	March	12
	12 wks	May	13
	12 wks	May	14
	12 wks	May	15
	24 wks	May	16
	24 wks	May	17
	24 wks	May	18
	36 wks	May	19
	36 wks	May	20
	36 wks	May	21
	5.4 wks	July	22
	6 wks	July	23
	12 wks	July	24
(no inoculum)	12 wks	November	25
(no inoculum)	12 wks	November	26
	12 wks	February	27
	12 wks	February	28
	14 wks	July	29
Sulphate availability	12 wks	November	30
	12 wks	November	31
Iron availability: 5% FeOOH	12 wks	November	32
	12 wks	November	33
	12 wks	February	34
	12 wks	February	35
Iron availability: 3% FeOOH (mixed)	12 wks	November	36
	12 wks	November	37
	12 wks	February	38
	12 wks	February	39
Iron availability: 0% FeOOH	5.4 wks	July	40
	12 wks	July	41
Iron availability: 3% FeOOH (layer)	12 wks	November	42
	12 wks	November	43
Iron source: 1% haematite	12 wks	November	44
	12 wks	November	45
Iron source: 0.5% haematite/ 0.5% FeOOH	12 wks	November	46
	12 wks	November	47
Iron source: 0.5% $FeCl_3$ / 0.5% FeOOH	12 wks	November	48
	12 wks	November	49

Experimental conditions	time	Start month	i.d. no.
Organic matter: single twig	12 wks	November	50
	12 wks	November	51
	24 wks	November	52
	24 wks	November	53
Organic matter: fifteen twigs	12 wks	November	54
	12 wks	November	55
	24 wks	November	56
	24 wks	November	57
Six extra twigs added after 6 weeks	12 wks	March	58
	12 wks	March	59
No plant material	14 wks	July	60
No added yeast extract	12 wks	February	61
	12 wks	February	62
Added glucose	12 wks	March	63
	12 wks	March	64
Celery	6 wks	July	65
Vitis vinifera	6 wks	July	66
Cyathea chinensis	6 wks	July	67
Vine	12 wks	July	68
Equisetum sp.	12 wks	July	69
Cherry	12 wks	July	70
Psilotum nudum	12 wks	July	71
Ginkgo biloba	12 wks	July	72
Sequoia sp.	12 wks	July	73
Celery	14 wks	July	74
Psilotum (newer, green material)	14 wks	July	75
Psilotum (older, orange/brown)	14 wks	July	76
Vitis vinifera	14 wks	July	77
Cyathea chinensis	14 wks	July	78
Pine	14 wks	July	79
pH: 1% $FeCl_3$ as iron source	12 wks	November	80
	12 wks	November	81
pH: $FeCl_3$ and 50% HCl added	12 wks	March	82
	12 wks	March	83
Fungal decay : indigenous fungi	12 wks	February	84
	12 wks	February	85
Fungal decay: fungal inoculum	12 wks	February	86
	12 wks	February	87
Twigs floating	5.4 wks	July	88
	12 wks	July	89
Sedimentation	5.4 wks	July	90
	12.wks	July	91
Twigs floating /sedimentation	5.4 wks	July	92
	12 wks	July	93
Burial	5.4 wks	July	94
	12 wks	July	95
Comparisons with no inoculum	12 wks	November	96
	12 wks	November	97
Standard marine systems: Duran bottle	12 wks	November	98
	12 wks	November	99

Experimental conditions	time	Start month	i.d. no.
Freshwater standards	5.4 wks	July	100
	12 wks	July	101
	12 wks	November	102
	12 wks	November	103
Freshwater with sulphate agar layer	12 wks	November	104
	12 wks	November	105
Closed freshwater systems	1 wk	July	106
	1 wk	July	107
	2 wks	July	108
	2 wks	July	109
	4 wks	July	110
	4 wks	July	111
	9 wks	July	112
	9 wks	July	113
	12 wks	July	114
	12 wks	July	115
Sealed marine standards	12 wks	March	116
	12 wks	March	117
	18 wks	March	118
	18 wks	March	119
	24 wks	March	120
	24 wks	March	121
Open marine standards: Durans	12 wks	March	122
	12 wks	March	123
	24 wks	March	124
	24 wks	March	125
Twigs added to sealed marine standards	24 wks	March	126
	24 wks	March	127
Sealed marine standards opened briefly	24 wks	March	128
	24 wks	March	129
Cyathea chinensis in sealed systems	12 wks	March	130
	12 wks	March	131
Sterilised sealed marine systems	12 wks	March	132
	12 wks	March	133
	24 wks	March	134
	24 wks	March	135
Sterilised systems with sulphide	12 wks	March	136
	12 wks	March	137
	24 wks	March	138
	24 wks	March	139
Sealed freshwater systems	12 wks	March	140
	12 wks	March	141
Effect of light (freshwater)	9 wks	March	142
	9 wks	March	143
Effect of dark (freshwater)	9 wks	March	144
	9 wks	March	145

APPENDIX TWO:

MEDIA RECIPES

The media used in both the inoculum and the decay experiments was based on Widdels Medium (Widdel and Bak, 1992)

Compound	Marine (g/l)	Freshwater (g/l)
sodium sulphate	4.0	0
potassium dihydrogen phosphate	0.2	0.2
ammonium chloride	0.25	0.25
sodium chloride	20.0	1.0
magnesium chloride	3.0	0.4
potassium chloride	0.5	0.5
calcium chloride	0.15	0.1
rezasurin[1]	1ml	1ml
sterile additions		
vitamin solution	3ml	3ml
selenite/tungstate solution	2ml	2ml
trace element solution	2ml	2ml
sodium sulphide[1]	3ml	3ml
sodium bicarbonate solution	30ml	30ml

1: present only in inoculum, not decay experiment medium

Combined vitamin solutions

Vitamin A:	4-aminobenzoic acid	4.0mg
	D(+) Biotin	1.0mg
	thiamine-HCl	10.0mg
	distilled water	100ml

The solution was filter sterilised (0.2µm filter) and stored wrapped in foil at 4°C.

Vitamin B:	folic acid	2.0mg
	pyridoxine-HCl	10.0mg
	riboflavin	5.0mg
	nicotinic acid	5.0mg
	DL calcium pantothenate	5.0mg
	lipoic acid	5.0mg
	distilled water	100ml

The solution was filter sterilised (0.2µm filter) and stored wrapped in foil at 4°C.

Vitamin B12:	cyanocobalamine	5.0mg
	distilled water	100ml

The solution was autoclaved at 121°C and 15 atm. for 10 minutes and stored wrapped in foil at 4°C.

Combined vitamin solution was made by mixing all three vitamin solutions.

Selenite/tungstate solution (per l)

sodium hydroxide	0.5g
$NaSeO_3.5H_2O$	3.0mg
$NaWO_4.2H_2O$	4.0mg

The solution was autoclaved at 121°C and 15 atm.

Trace element solution (per l)

$FeCl_2.4H_2O$	1.5g in 10ml 25% HCl
$CoCl_2.6H_2O$	0.19g
$MnCl_2.4H_2O$	0.10g
$ZnCl_2$	0.07g
H_3BO_3	0.062g
$Na_2MoO_4.2H_2O$	0.036g
$NiCl_2.6H_2O$	0.024g
$CuCl_2.2H_2O$	0.017g

The solution was autoclaved at 121°C and 15 atm.

Sulphide solution

$Na_2S.9H_2O$	12.0g

Washed crystals were dissolved in 100ml water and autoclaved at 121°C and 15 atm.

Bicarbonate solution

Standard (for inoculum): 84.0g/ $NaHCO_3$ bubbled through with CO_2 and autoclaved at 121°C and 15 atm.

Low buffer (decay experiment medium): 0.005% of normal buffer.

APPENDIX THREE:
TEM BUFFER RECIPE

Buffer solution for TEM sample preparation was prepared as follows:

Paraformaldehyde (0.5g), sucrose (3.42g) and calcium chloride (0.11g) were added to cacodylate buffer (ca 40ml) at pH 6.9 and dissolved with slight heat. After cooling at 4°C, 25% glutaraldehyde (4ml) was added to the buffer, and the total volume made up to 50ml with cacodylate buffer.

APPENDICES 4-7

CHAPTER 2 EXPERIMENTAL DATA

APPENDIX 4: SELECTED SULPHIDE & pH DATA

APPENDIX 5: OXYGEN & pH DEPTH PROFILES

APPENDIX 6: MEDIUM SULPHATE, SULPHIDE AND FERROUS IRON DATA, SEDIMENTARY SULPHIDE CONCENTRATIONS

APPENDIX 7: MAJOR ELEMENT ION MEDIUM CONCENTRATIONS (P, Al, Fe, Mg, Ca, Mn)

Experimental conditions	time	Air-medium interface		Mid-depth values		Medium-sediment interface		i.d. no.
		sulphide (V)	pH	sulphide (V)	pH	sulphide (V)	pH	
Standard marine conditions	1 wk	-0.116	8.699	-0.190	8.149	-0.243	7.887	1
	2 wks	-0.181	8.360	-0.276	8.260	-0.355	8.042	2
	3 wks	-0.113	8.937	-0.261	8.860	-0.428	8.789	3
	4 wks	-	-	-	-	-	-	4
	5 wks	-0.164	9.212	-0.170	9.253	-0.387	8.700	5
	6 wks	-0.134	9.869	-0.151	9.853	-0.285	9.834	6
	7 wks	-0.134	9.869	-0.168	9.402	-0.265	9.396	7
	8 wks	-0.110	9.387	-0.123	9.297	-0.170	9.343	8
	9 wks	-	-	-	-	-	-	9
	10 wks	-	-	-	-	-	-	10
	11 wks	-	-	-	-	-	-	11
	12 wks	-	-	-	-	-	-	12
	12 wks	-0.218	8.890	-0.159	8.901	-0.164	8.934	13
	12 wks	-0.115	8.946	-0.131	8.992	-0.134	8.978	14
	12 wks	-0.128	9.019	-0.141	9.069	-0.141	9.038	15
	24 wks	-	-	-	-	-	-	16
	24 wks	-	-	-	-	-	-	17
	24 wks	-	-	-	-	-	-	18
	36 wks	-	-	-	-	-	-	19
	36 wks	-	-	-	-	-	-	20
	36 wks	-	-	-	-	-	-	21
	5.4 wks	-0.190	8.229	-0.221	8.362	-0.563	8.352	22
	6 wks	-0.238	8.883	-0.251	8.925	-0.256	8.917	23
	12 wks	-0.314	8.661	-0.304	8.611	-0.365	8.625	24
(no inoculum)	12 wks	-	-	-	-	-	-	25
(no inoculum)	12 wks	-	-	-	-	-	-	26
	12 wks	-	-	-	-	-	-	27
	12 wks	-	-	-	-	-	-	28
	14 wks	-	-	-	-	-	-	29

Experimental conditions	time	Air-medium interface		Mid-depth values		Medium-sediment interface		i.d. no.
		sulphide (V)	pH	sulphide (V)	pH	sulphide (V)	pH	
Sulphate availability	12 wks	-	-	-	-	-	-	30
	12 wks	-	-	-	-	-	-	31
Iron availability: 5% FeOOH	12 wks	-	-	-	-	-	-	32
	12 wks	-	-	-	-	-	-	33
	12 wks	-	-	-	-	-	-	34
	12 wks	-	-	-	-	-	-	35
Iron availability: 3% FeOOH (mixed)	12 wks	-	-	-	-	-	-	36
	12 wks	-	-	-	-	-	-	37
	12 wks	-	-	-	-	-	-	38
	12 wks	-	-	-	-	-	-	39
Iron availability: 0% FeOOH	5.4 wks	-0.199	8.170	-0.484	8.239	-0.565	8.230	40
	12 wks	-0.309	8.597	-0.285	8.566	-0.282	8.550	41
Iron availability: 3% FeOOH (layer)	12 wks	-	-	-	-	-	-	42
	12 wks	-	-	-	-	-	-	43
Iron source: 1% haematite	12 wks	-	-	-	-	-	-	44
	12 wks	-	-	-	-	-	-	45
Iron source: 0.5% haematite/ 0.5% FeOOH	12 wks	-	-	-	-	-	-	46
	12 wks	-	-	-	-	-	-	47
Iron source: 0.5% FeCl3 / 0.5% FeOOH	12 wks	-	-	-	-	-	-	48
	12 wks	-	-	-	-	-	-	49
Organic matter: single twig	12 wks	-	-	-	-	-	-	50
	12 wks	-	-	-	-	-	-	51
	24 wks	-	-	-	-	-	-	52
	24 wks	-	-	-	-	-	-	53
Organic matter: fifteen twigs	12 wks	-	-	-	-	-	-	54
	12 wks	-	-	-	-	-	-	55
	24 wks	-	-	-	-	-	-	56
	24 wks	-	-	-	-	-	-	57
Six extra twigs added after 6 weeks	12 wks	-	-	-	-	-	-	58
	12 wks	-	-	-	-	-	-	59
No plant material	14 wks	-	-	-	-	-	-	60

Experimental conditions	time	Air-medium interface		Mid-depth values		Medium-sediment interface		i.d. no.
		sulphide (V)	pH	sulphide (V)	pH	sulphide (V)	pH	
No added yeast extract	12 wks	-	-	-	-	-	-	61
	12 wks	-	-	-	-	-	-	62
Added glucose	12 wks	-	-	-	-	-	-	63
	12 wks	-	-	-	-	-	-	64
Celery	6 wks	-0.101	8.832	-0.101	8.881	-0.103	8.882	65
Vitis vinifera	6 wks	-0.097	8.868	-0.106	8.924	-0.122	8.934	66
Cyathea chinensis	6 wks	-0.085	8.285	-0.347	8.671	-0.498	8.685	67
Vine	12 wks	-0.261	6.257	-0.256	8.939	-0.258	8.943	68
Equisetum sp.	12 wks	-0.260	9.064	-0.261	8.964	-0.261	8.950	69
Cherry	12 wks	-0.309	8.680	-0.268	8.616	-0.298	8.636	70
Psilotum nudum	12 wks	-0.265	8.596	-0.268	8.576	-0.595	8.556	71
Ginkgo biloba	12 wks	-0.313	8.726	-0.289	8.650	-0.525	8.646	72
Sequoia sp.	12 wks	-0.267	9.193	-0.309	8.596	-0.598	8.588	73
Celery	14 wks	-	-	-	-	-	-	74
Psilotum (newer, green material)	14 wks	-	-	-	-	-	-	75
Psilotum (older, orange/brown)	14 wks	-	-	-	-	-	-	76
Vitis vinifera	14 wks	-	-	-	-	-	-	77
Cyathea chinensis	14 wks	-	-	-	-	-	-	78
Pine	14 wks	-	-	-	-	-	-	79
pH: 1% FeCl3 as iron source	12 wks	-	-	-	-	-	-	80
	12 wks	-	-	-	-	-	-	81
pH: FeCl3 and 50% HCl added	12 wks	-	-	-	-	-	-	82
	12 wks	-	-	-	-	-	-	83
Fungal decay : indigenous fungi	12 wks	-	-	-	-	-	-	84
	12 wks	-	-	-	-	-	-	85
Fungal decay: fungal inoculum	12 wks	-	-	-	-	-	-	86
	12 wks	-	-	-	-	-	-	87
Twigs floating	5.4 wks	-0.202	8.276	-0.556	8.161	-0.557	8.115	88
	12 wks	-0.301	8.415	-0.272	8.408	-0.451	8.411	89

Experimental conditions	time	Air-medium interface		Mid-depth values		Medium-sediment interface		i.d. no.
		sulphide (V)	pH	sulphide (V)	pH	sulphide (V)	pH	
Sedimentation	5.4 wks	-0.222	8.349	-0.230	8.257	-0.247	8.268	90
	12 wks	-0.281	8.501	-0.277	8.454	-0.269	8.438	91
Twigs floating /sedimentation	5.4 wks	-0.225	8.431	-0.507	8.423	-0.553	8.392	92
	12 wks	-0.261	8.460	-0.259	8.435	-0.259	8.395	93
Burial	5.4 wks	-0.246	8.674	-0.486	8.208	-0.568	8.210	94
	12 wks	-0.301	8.595	-0.228	8.420	-0.431	8.401	95
Comparisons with no inoculum	12 wks	-	-	-	-	-	-	96
	12 wks	-	-	-	-	-	-	97
Standard marine systems: Duran bottle	12 wks	-	-	-	-	-	-	98
	12 wks	-	-	-	-	-	-	99
Freshwater standards	5.4 wks	-0.114	5.751	-0.398	5.867	-0.420	5.816	100
	12 wks	-0.310	7.570	-0.451	6.038	-0.463	6.142	101
	12 wks	-	-	-	-	-	-	102
	12 wks	-	-	-	-	-	-	103
Freshwater with sulphate agar layer	12 wks	-	-	-	-	-	-	104
	12 wks	-	-	-	-	-	-	105
Closed freshwater systems	1 wk	-0.098	6.499	-0.252	5.646	-0.392	5.573	106
	1 wk	-0.116	6.257	-0.109	5.966	-0.149	5.930	107
	2 wks	-0.238	7.226	-0.358	6.713	-0.375	6.050	108
	2 wks	-	-	-	-	-	-	109
	4 wks	-0.185	6.621	-0.139	6.354	-0.148	6.388	110
	4 wks	-0.083	6.453	-0.326	5.791	-0.316	5.761	111
	9 wks	-0.181	7.143	-0.165	6.774	-0.158	6.829	112
	9 wks	-0.224	6.164	-0.362	5.711	-0.399	5.725	113
	12 wks	-0.319	7.735	-0.457	7.582	-0.476	7.559	114
	12 wks	-0.400	7.129	-0.452	7.117	-0.462	7.087	115

Experimental conditions	time	Air-medium interface		Mid-depth values		Medium-sediment interface		i.d. no.
		sulphide (V)	pH	sulphide (V)	pH	sulphide (V)	pH	
Sealed marine standards	12 wks	-0.555	8.15	-0.576	7.231	-0.579	7.224	116
	12 wks	-0.579	7.747	-0.593	7.243	-0.592	7.108	117
	18 wks	-0.515	7.433	-0.484	6.748	-0.487	6.724	118
	18 wks	-0.440	7.573	-0.465	6.864	-0.463	6.814	119
	24 wks	-0.374	7.019	-0.427	6.725	-0.425	6.676	120
	24 wks	-0.485	7.073	-0.475	6.766	-0.475	6.736	121
Open marine standards: Durans	12 wks	-0.528	8.895	-0.599	8.986	-0.610	8.981	122
	12 wks	-0.579	9.016	-0.576	9.026	-0.605	9.029	123
	24 wks	-0.103	7.247	-0.114	8.664	-0.257	8.746	124
	24 wks	-0.209	8.355	-0.466	8.437	-0.476	8.396	125
Twigs added to sealed marine standards	24 wks	-0.311	6.789	-0.403	6.725	-0.408	6.697	126
	24 wks	-0.366	6.851	-0.386	6.815	-0.389	6.749	127
Sealed marine standards opened briefly	24 wks	-0.420	6.964	-0.440	6.816	-0.446	6.778	128
	24 wks	-0.443	7.138	-0.453	6.857	-0.457	6.764	129
Cyathea chinensis in sealed systems	12 wks	-0.519	6.631	-0.569	6.537	-0.569	6.473	130
	12 wks	-0.559	6.700	-0.576	6.631	-0.577	6.595	131
Sterilised sealed marine systems	12 wks	-0.267	7.750	-0.278	7.493	-0.278	7.530	132
	12 wks	-0.222	6.506	-0.238	7.495	-0.246	7.455	133
	24 wks	-0.377	7.480	-0.393	7.120	-0.400	7.133	134
	24 wks	-0.117	7.716	-0.121	7.258	-0.126	7.261	135
Sterilised systems with sulphide	12 wks	-0.188	7.873	-0.217	7.383	-0.228	7.301	136
	12 wks	-0.211	7.718	-0.227	7.474	-0.230	7.066	137
	24 wks	-0.292	8.596	-0.385	7.294	-0.392	7.296	138
	24 wks	-0.122	7.634	-0.134	7.215	-0.140	7.150	139
Sealed freshwater systems	12 wks	-0.272	7.628	-0.452	6.800	-0.459	6.802	140
	12 wks	-0.436	6.865	-0.451	6.813	-0.462	6.874	141
Effect of light (freshwater)	9 wks	-	-	-	-	-	-	142
	9 wks	-	-	-	-	-	-	143
Effect of dark (freshwater)	9 wks	-	-	-	-	-	-	144
	9 wks	-	-	-	-	-	-	145

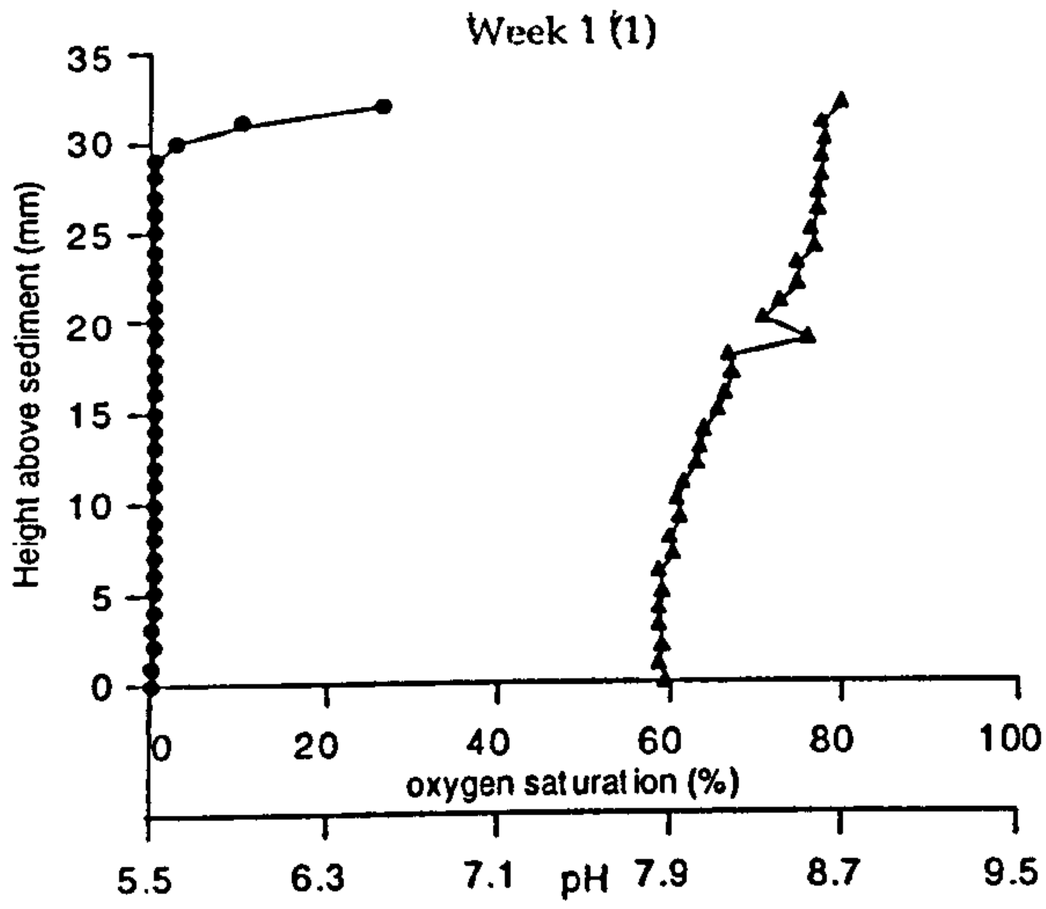

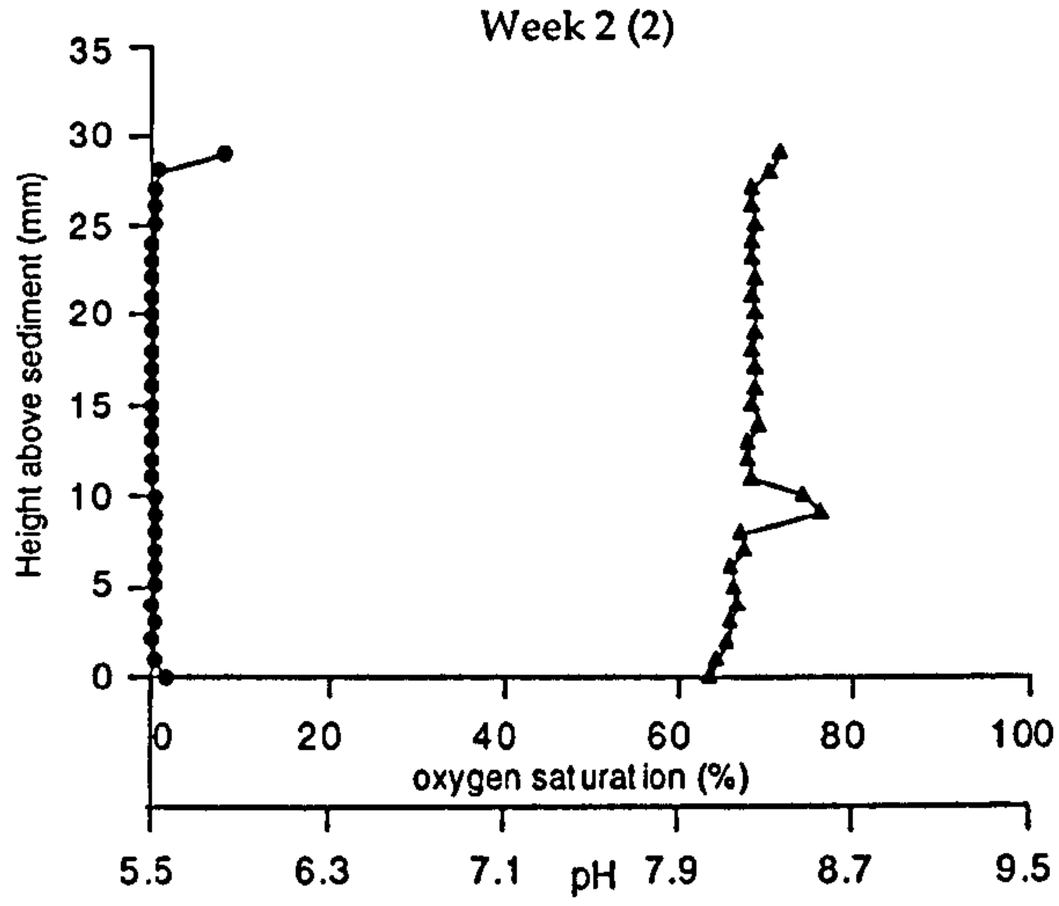

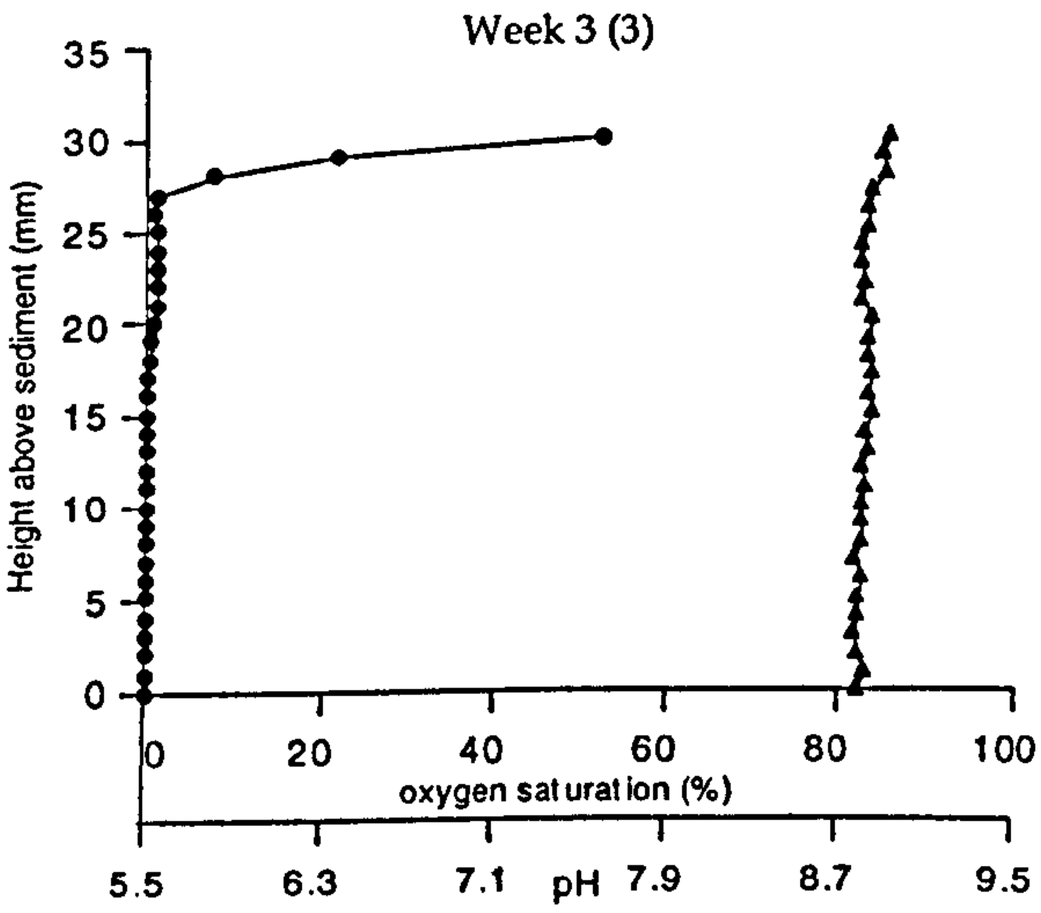

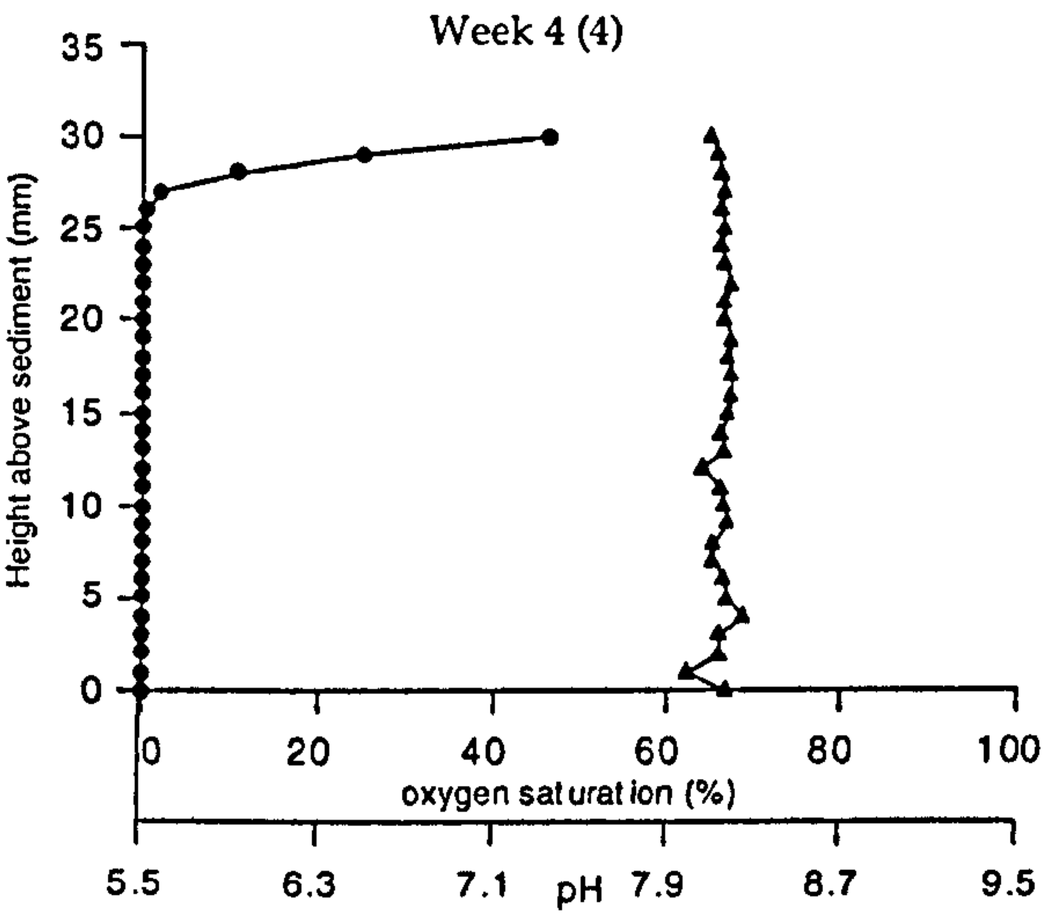

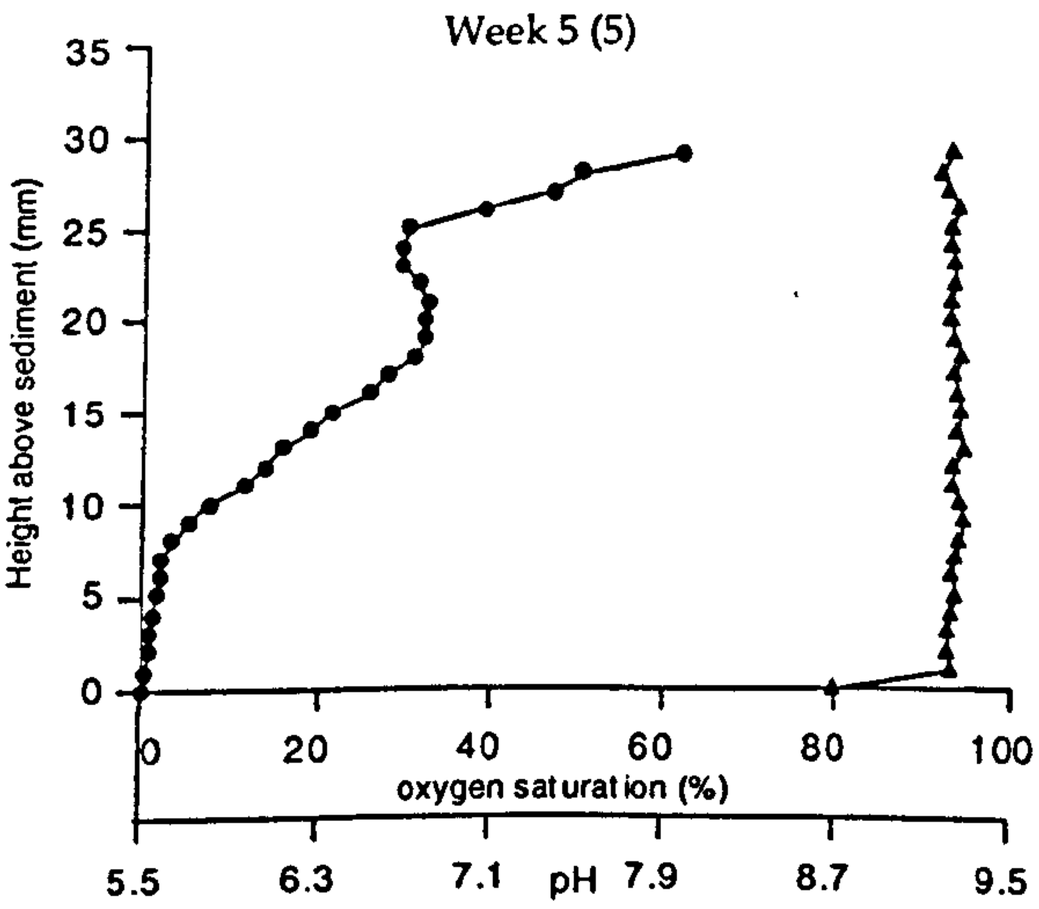

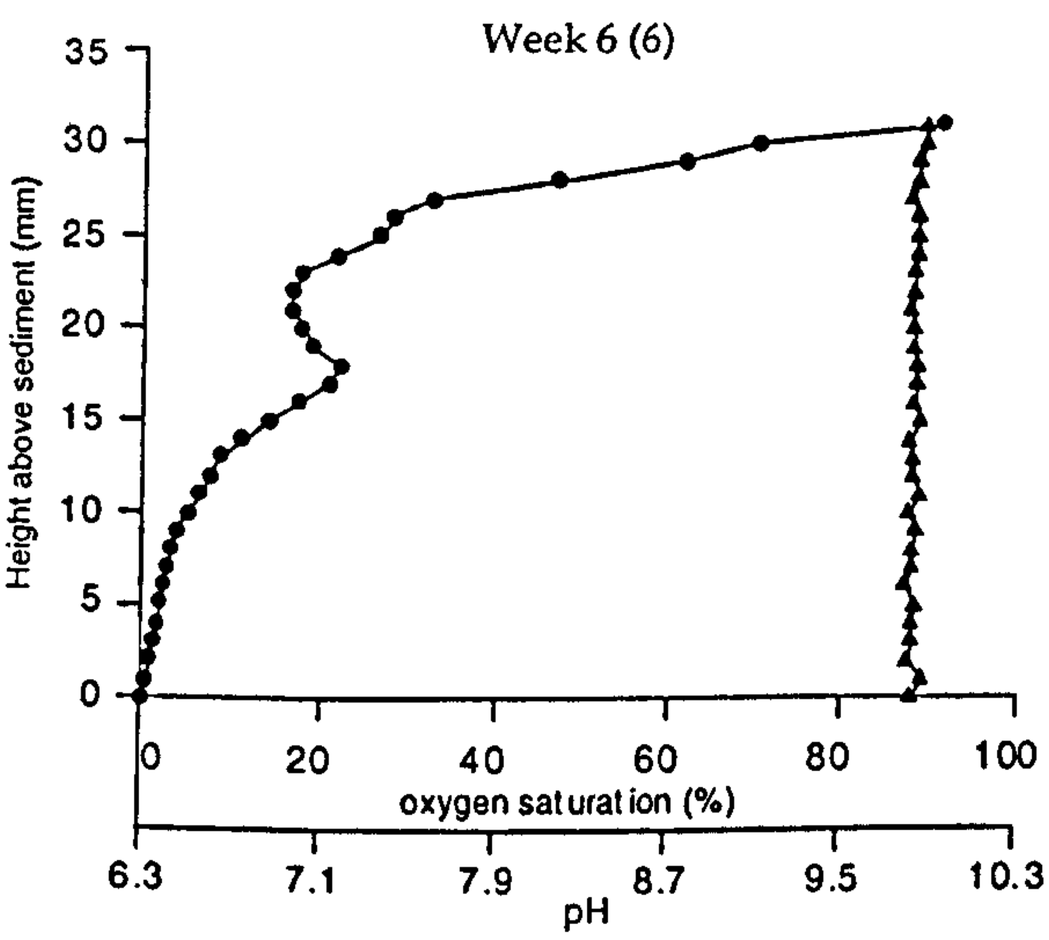

Oxygen and pH depth profiles for weeks 1 to 6 of the standard open marine time series. Infilled circles represent oxygen data points. Infilled triangles represent pH data points. The highest data points above the sediment represent the air-medium interface.

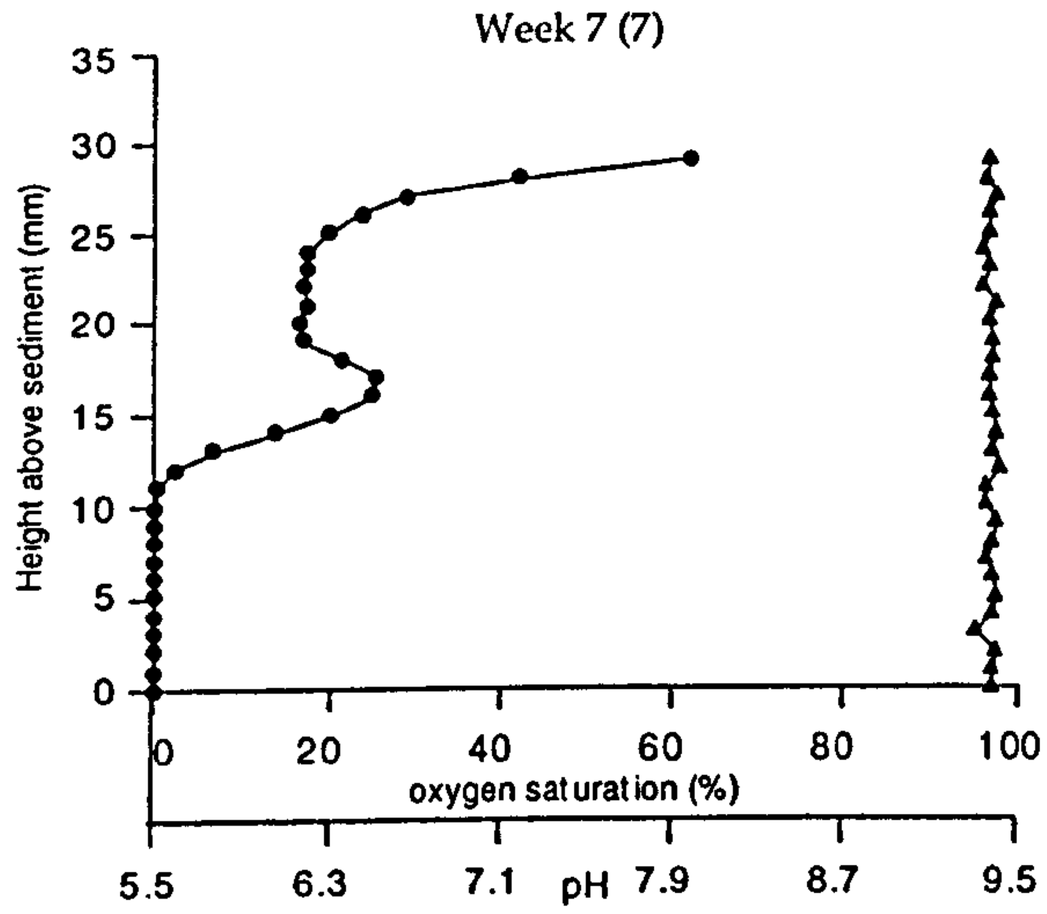

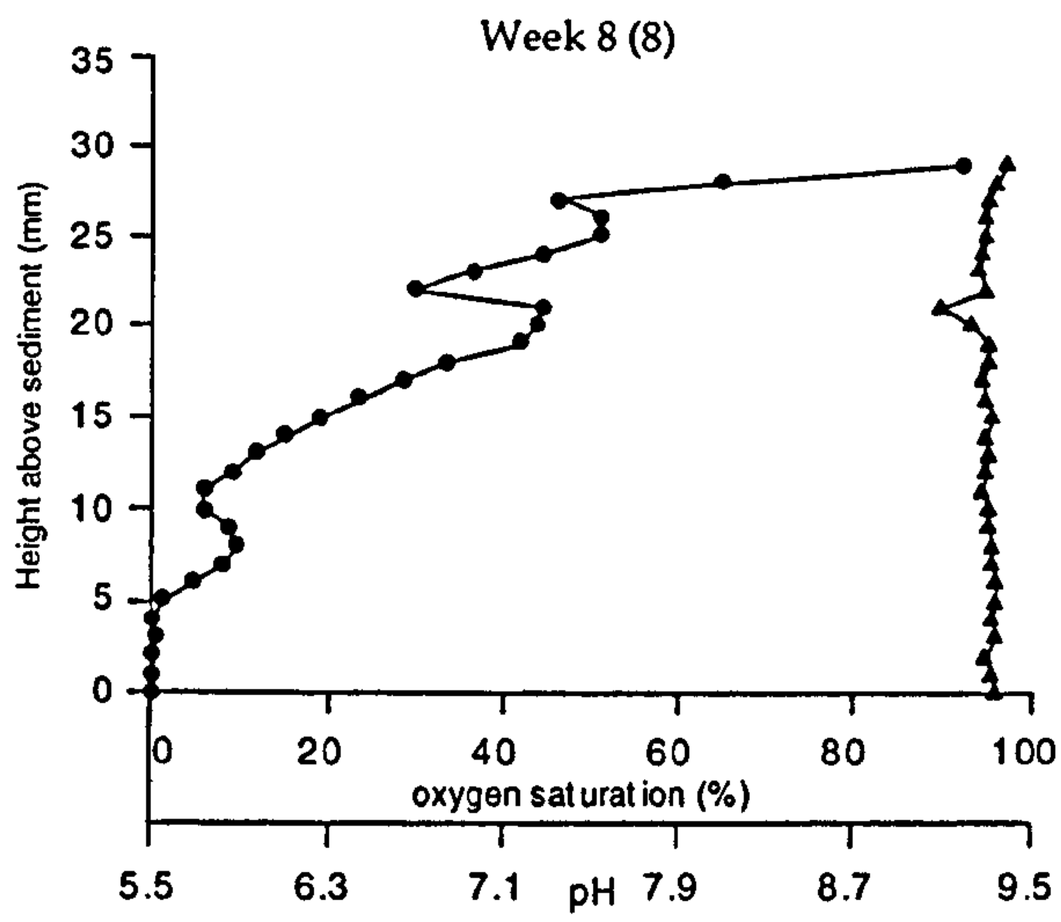

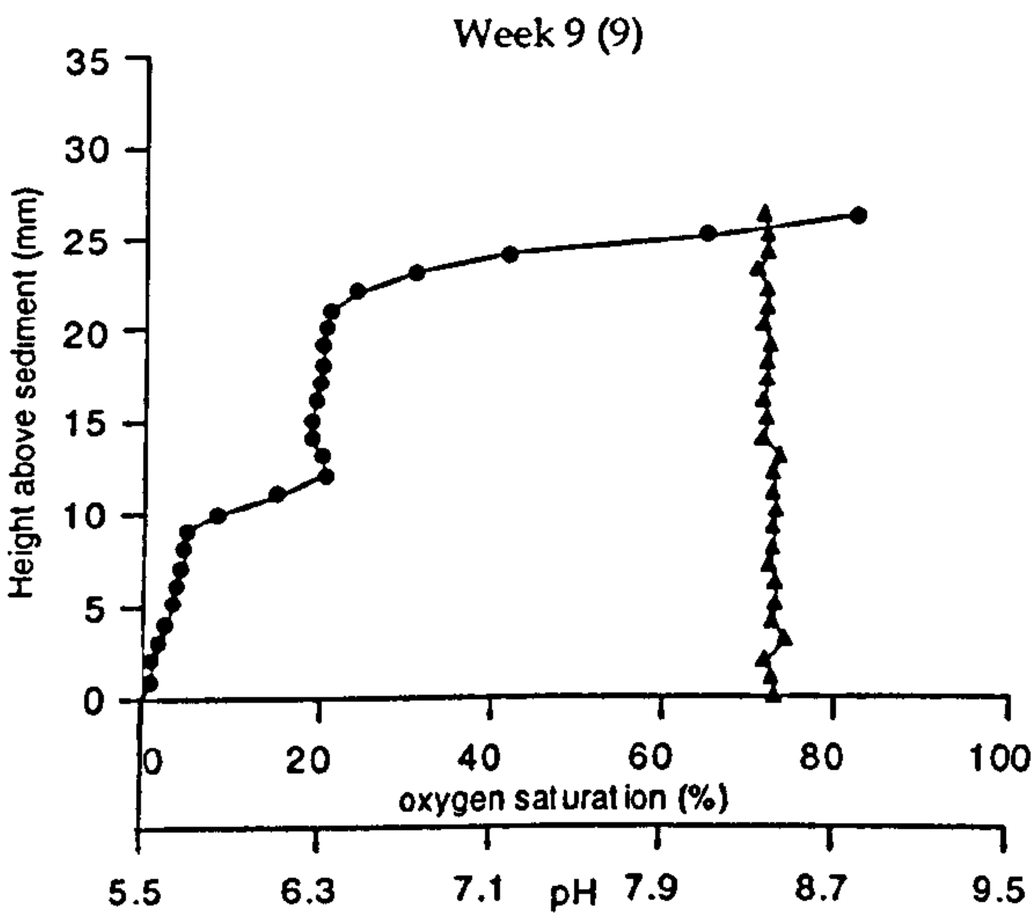

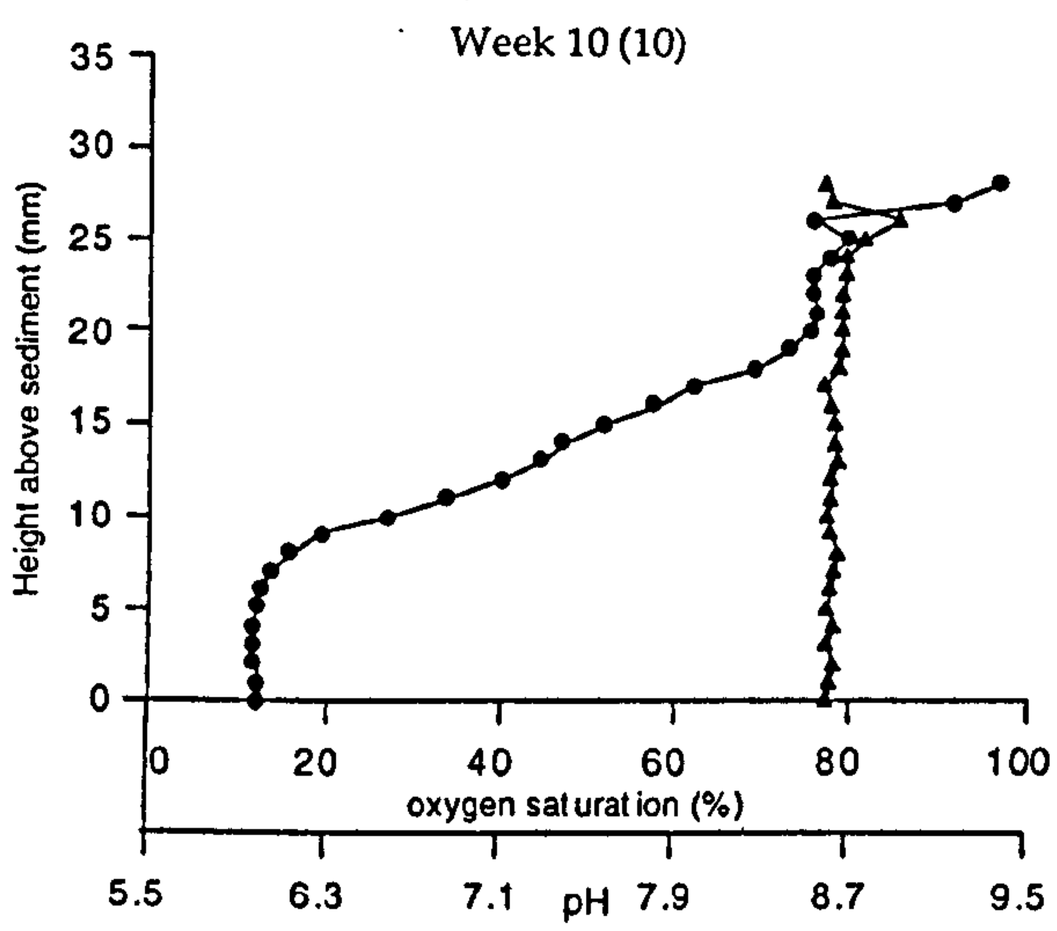

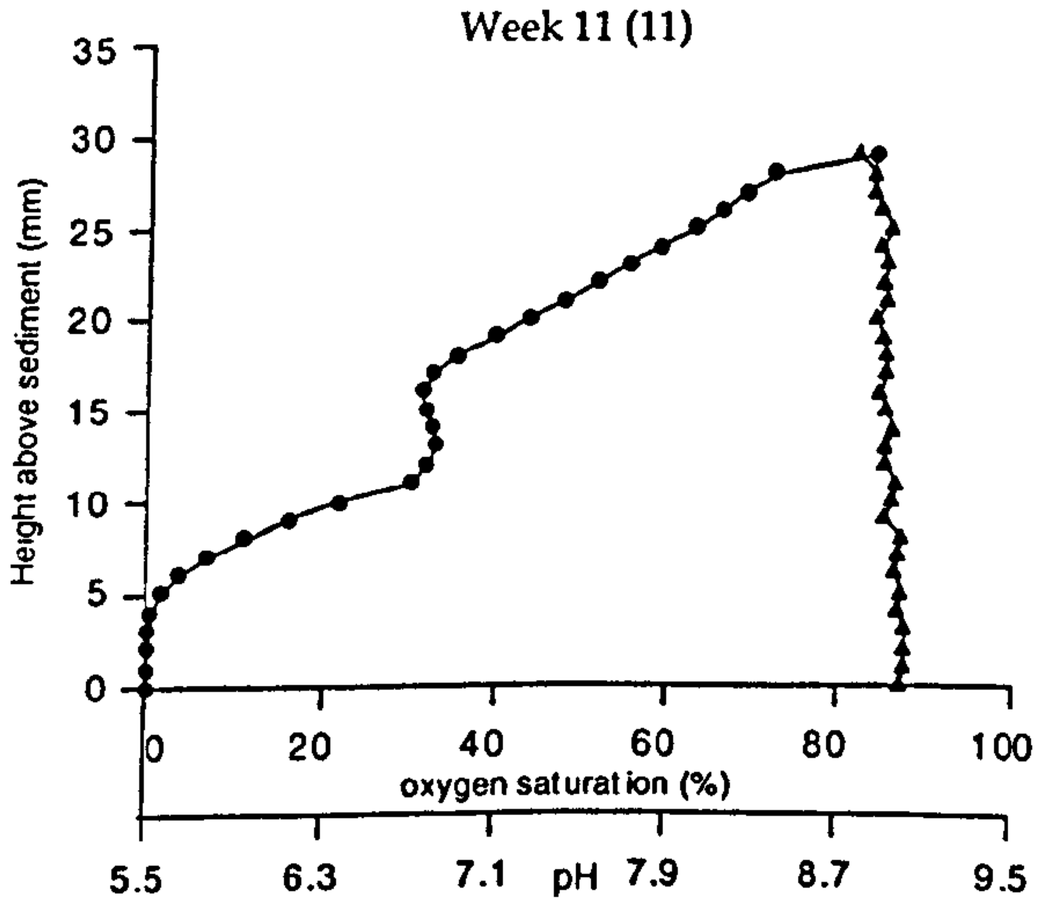

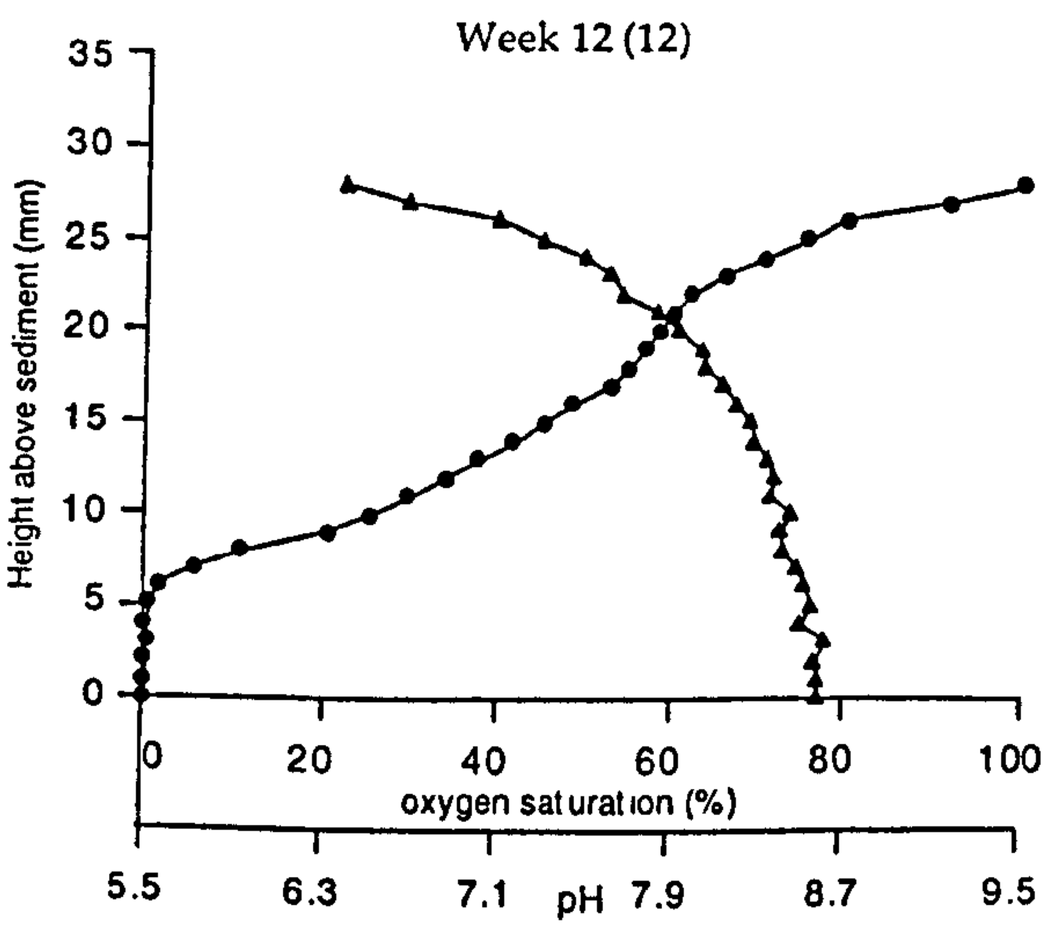

Oxygen and pH depth profiles for weeks 7 to 12 of the standard open marine time series. Infilled circles represent oxygen data points. Infilled triangles represent pH data points. The highest data points above the sediment represent the air-medium interface.

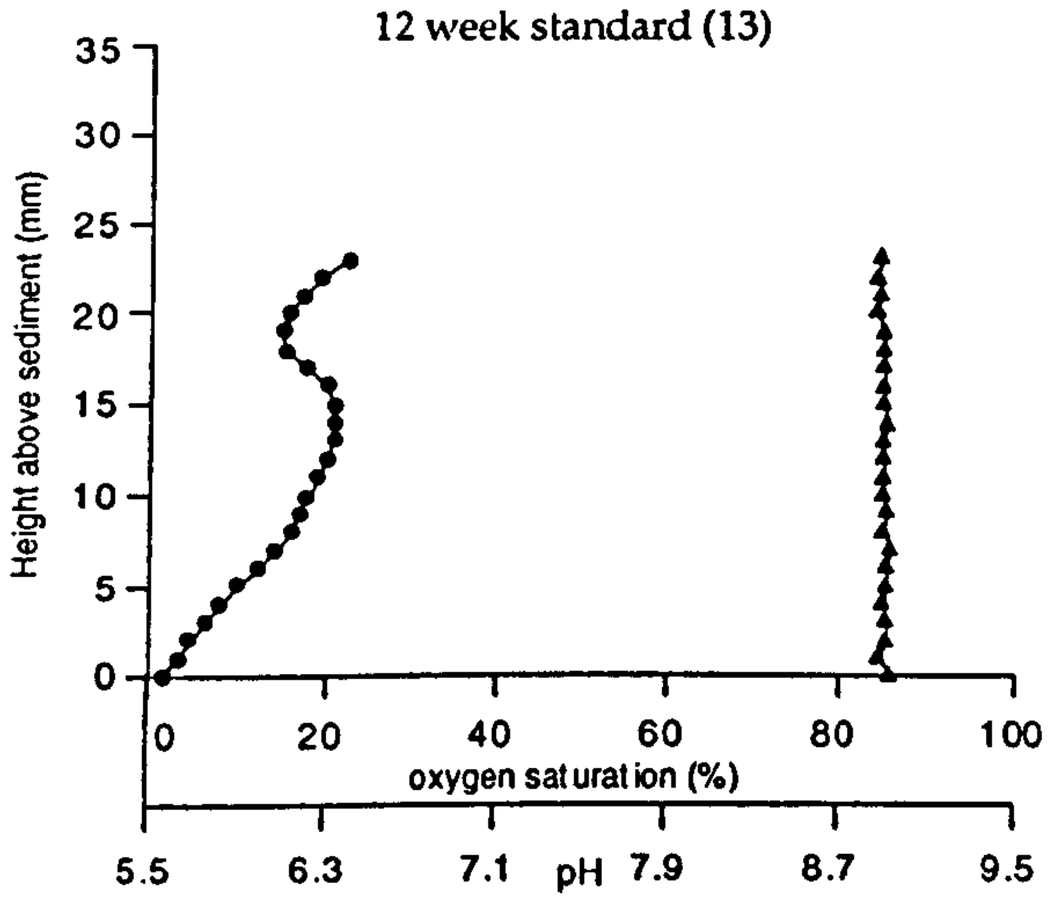

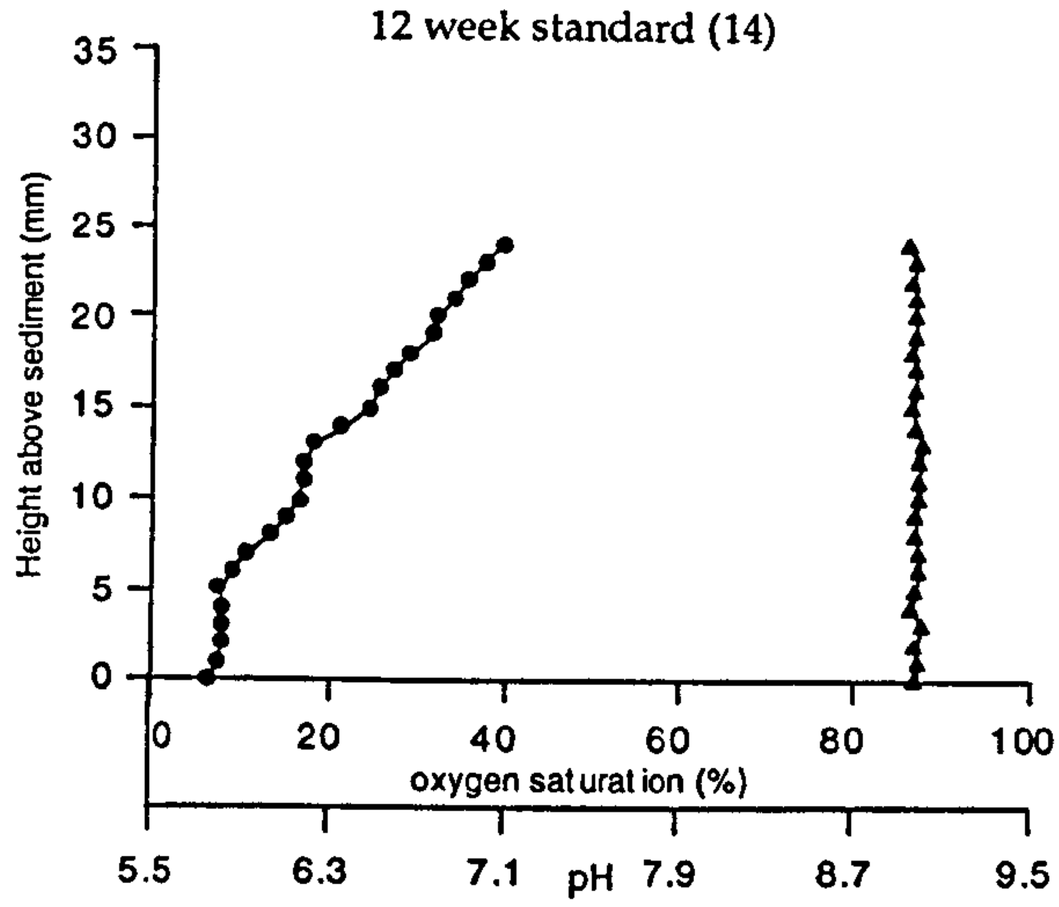

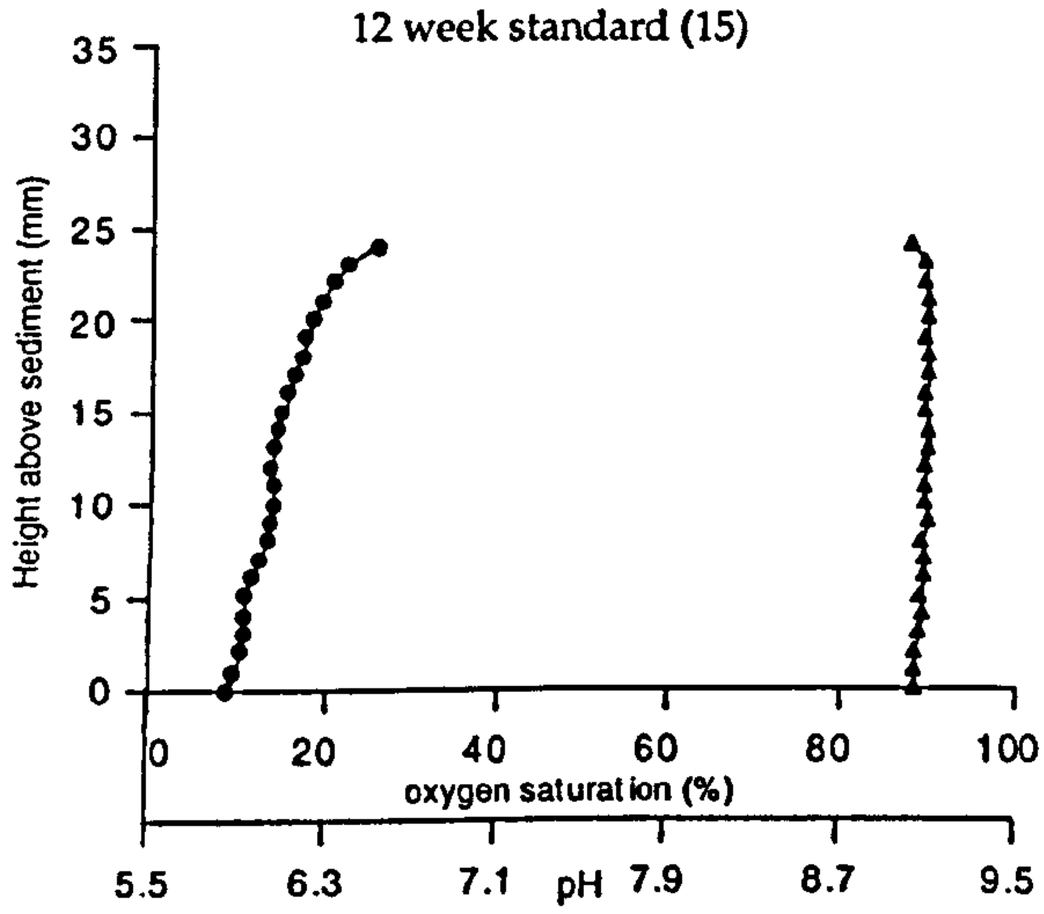

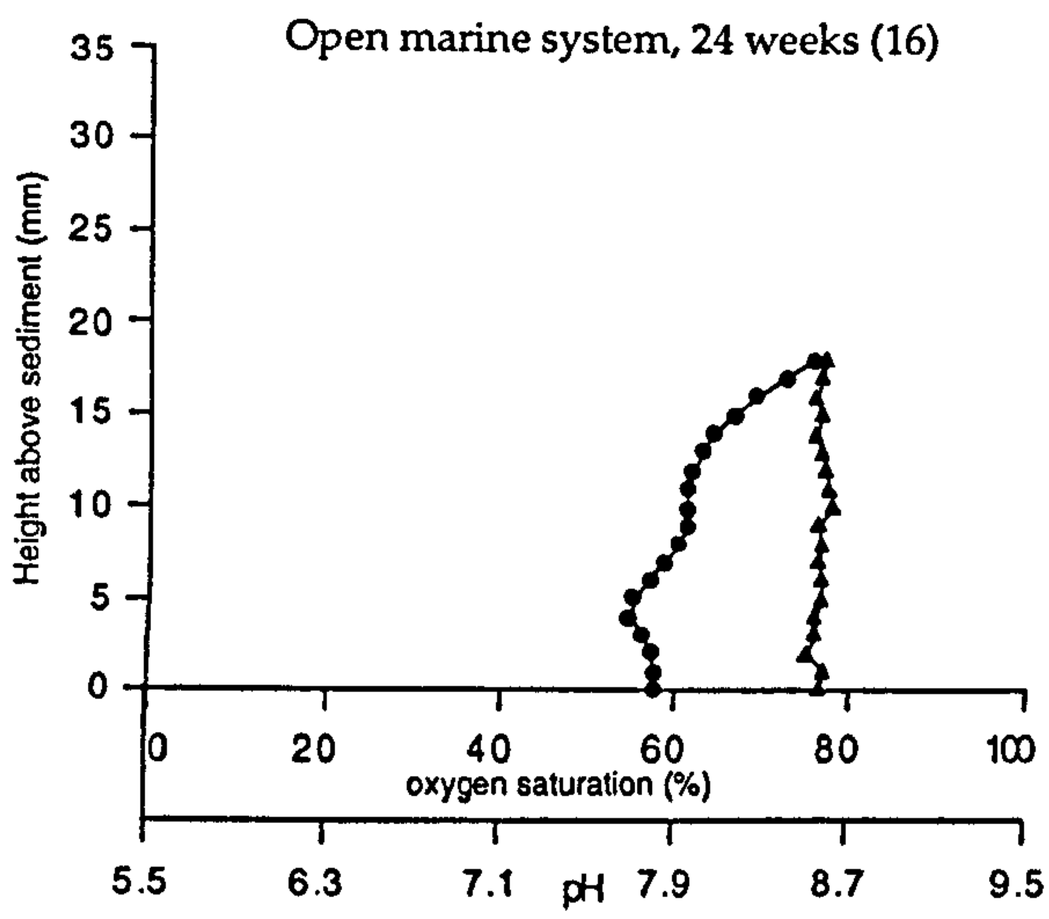

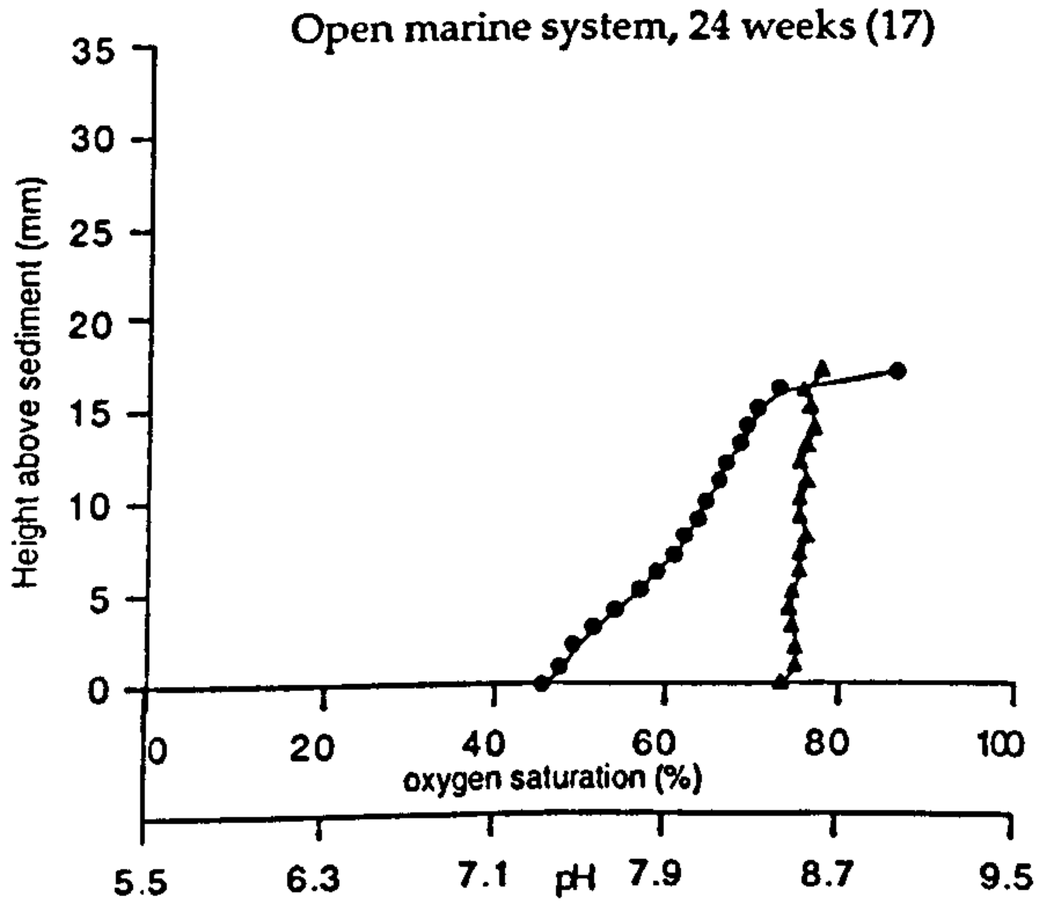

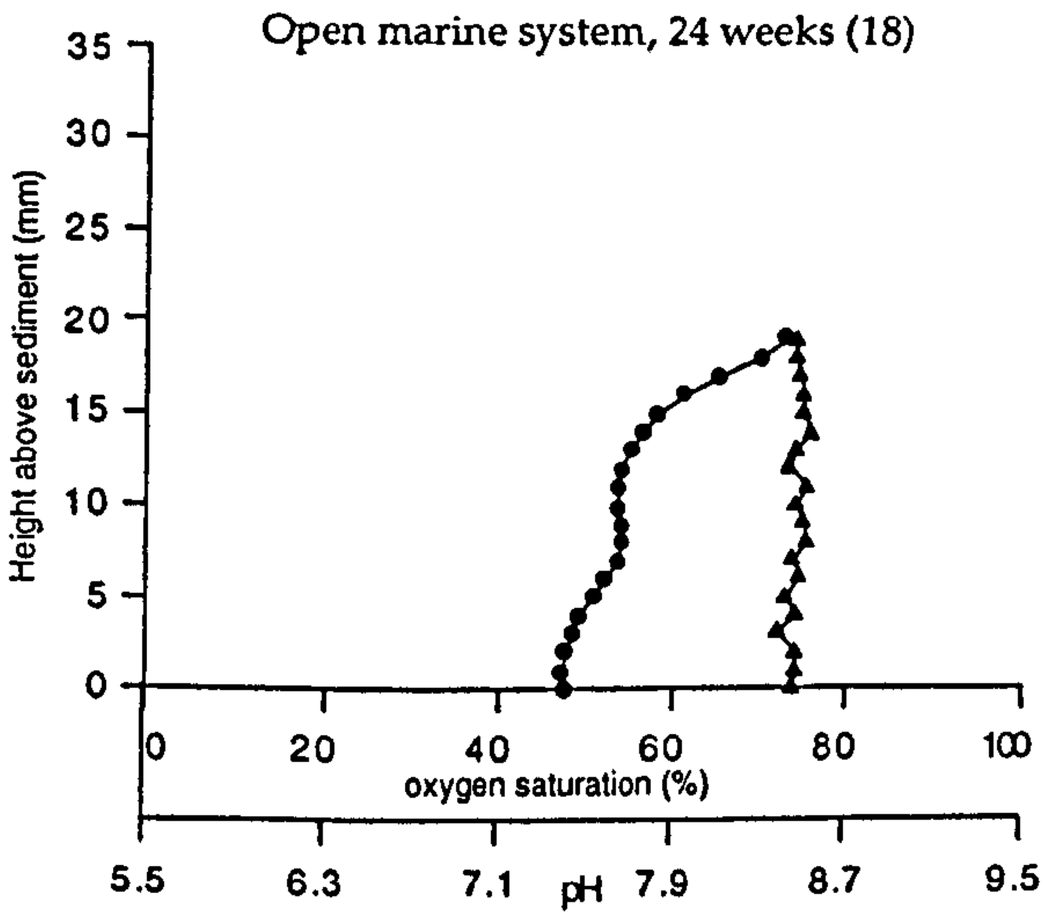

Oxygen and pH depth profiles for the open marine extended time series. Infilled circles represent oxygen data points. Infilled triangles represent pH data points. The highest data points above the sediment represent the air-medium interface.

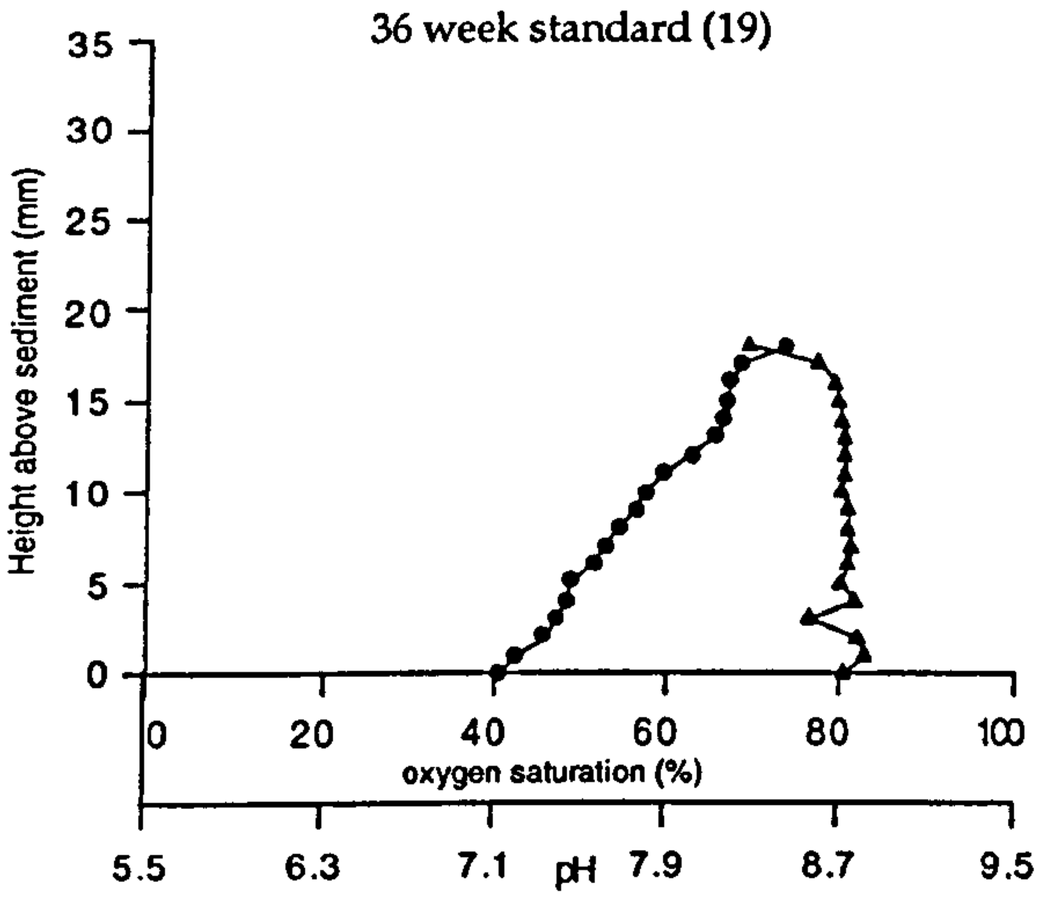

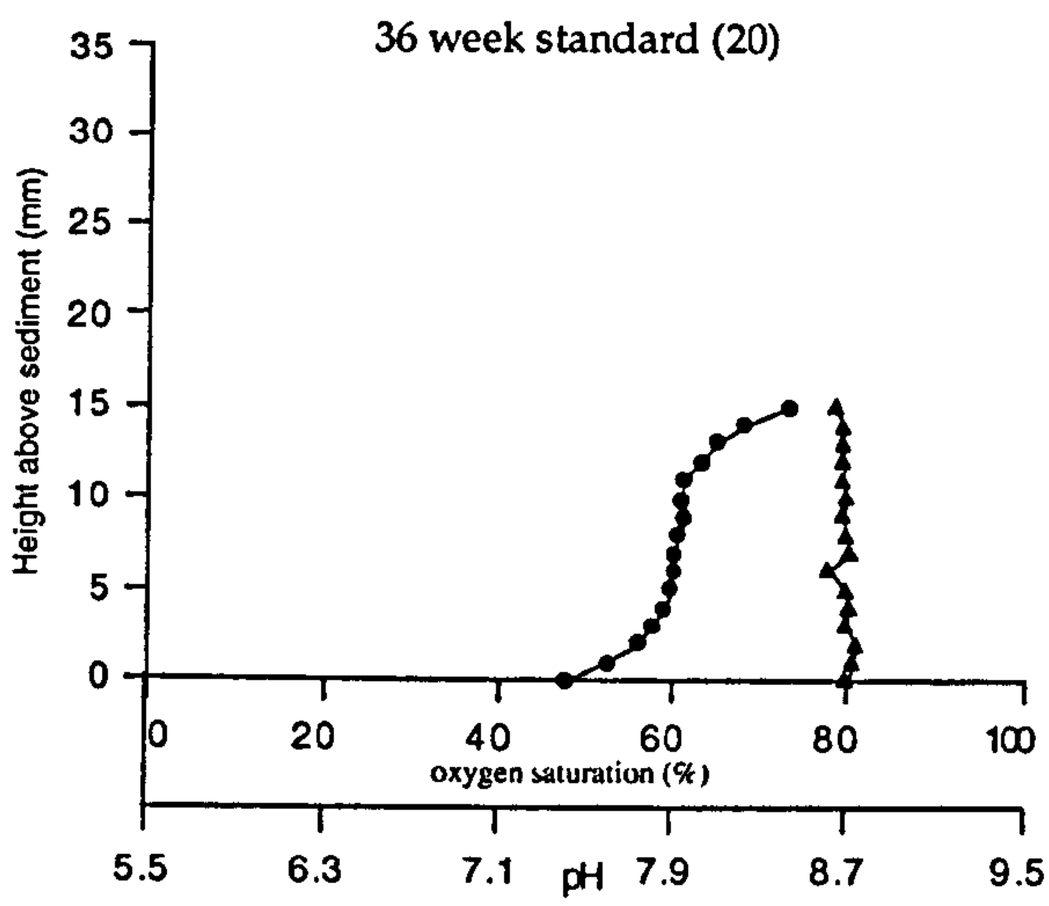

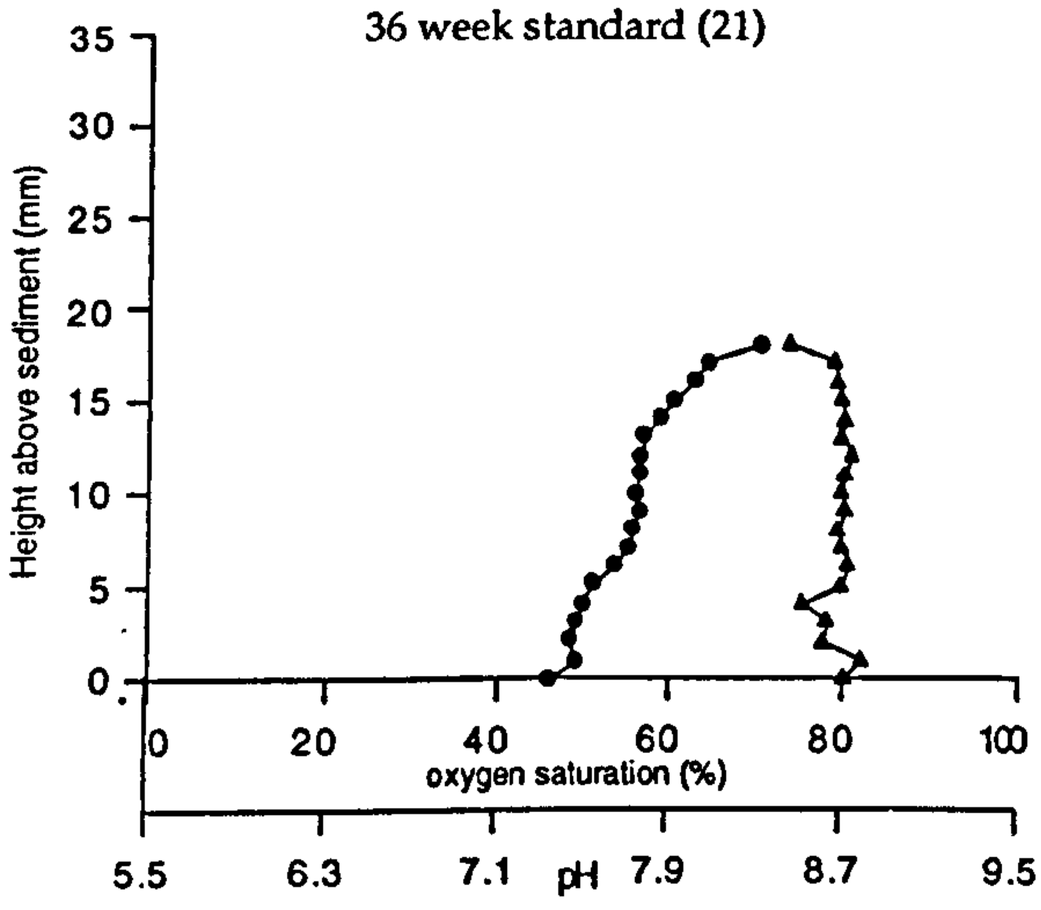

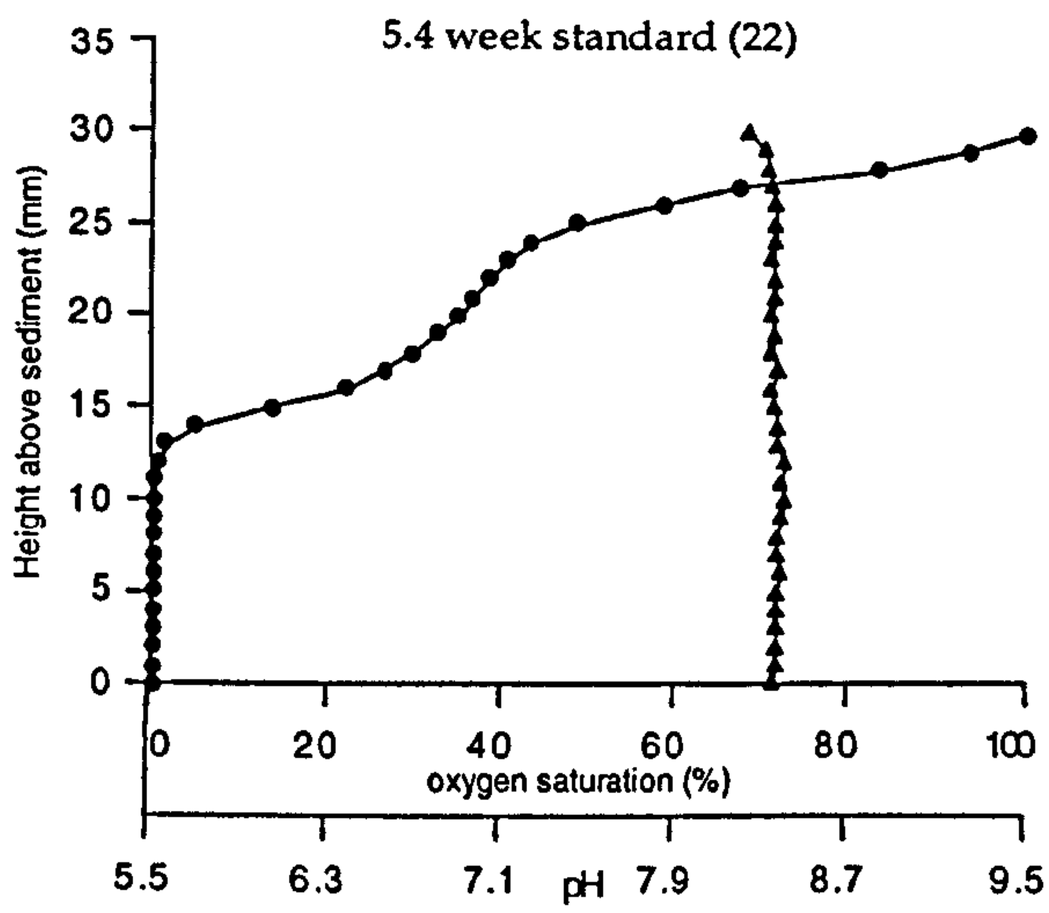

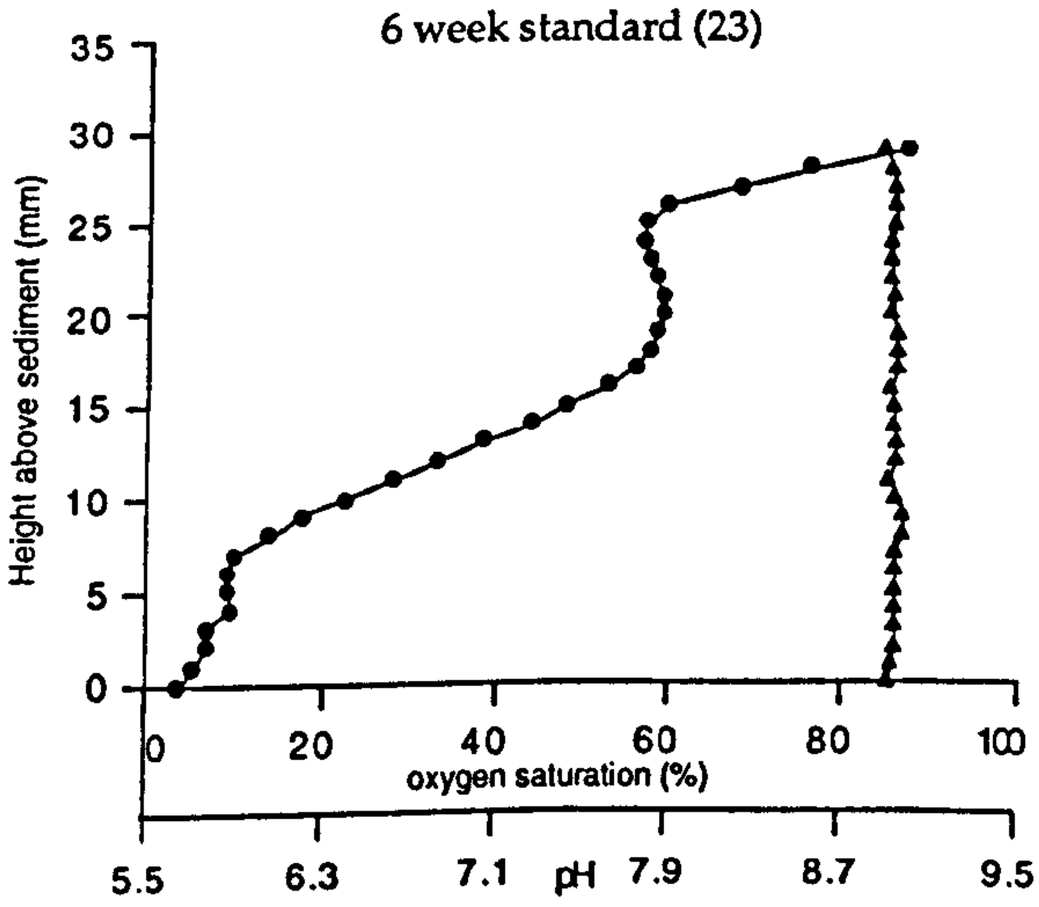

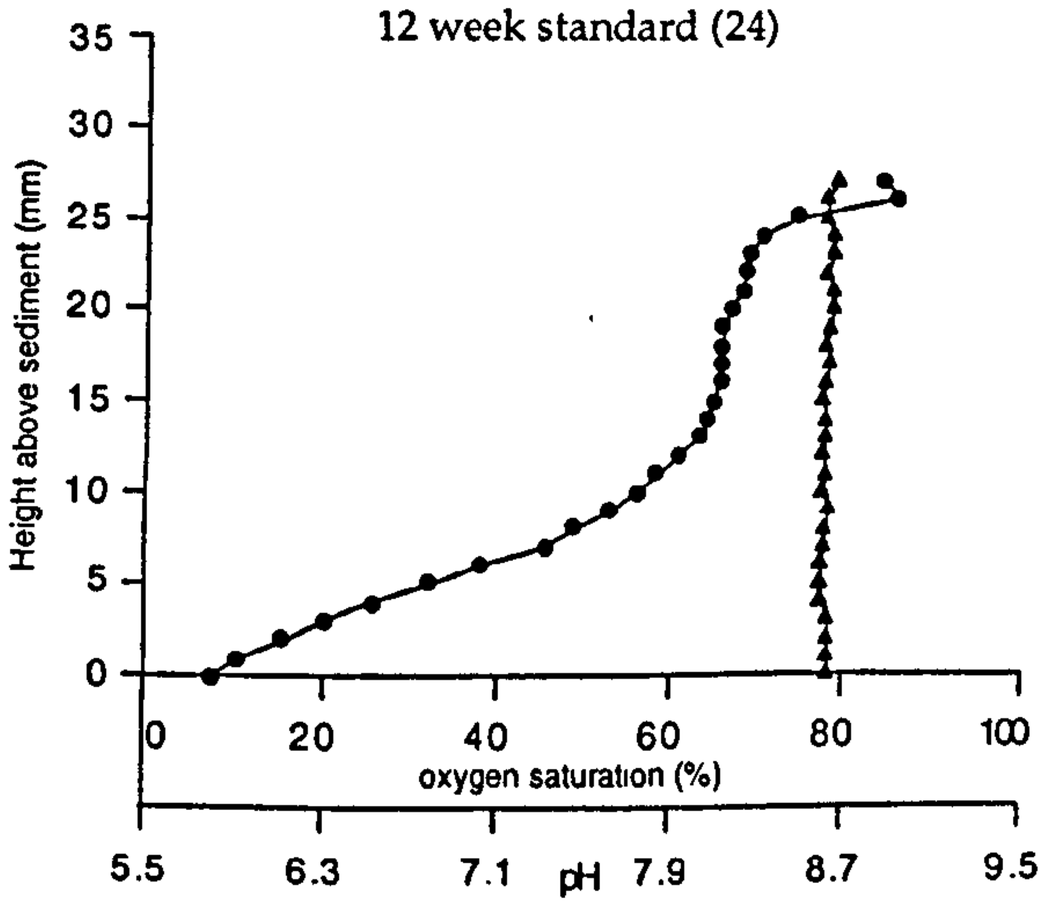

Oxygen and pH depth profiles for the open marine extended time series after 36 weeks and standard open marine systems. Infilled circles represent oxygen data points. Infilled triangles represent pH data points. The highest data points above the sediment represent the air-medium interface.

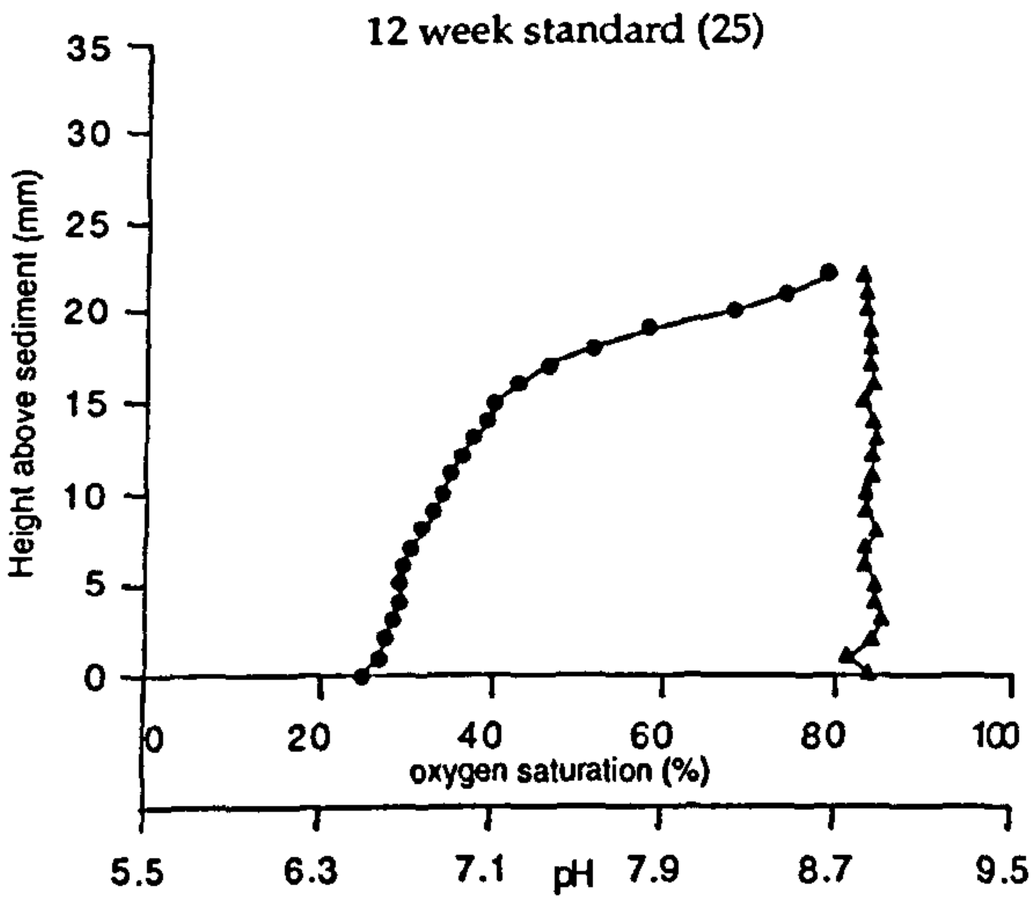

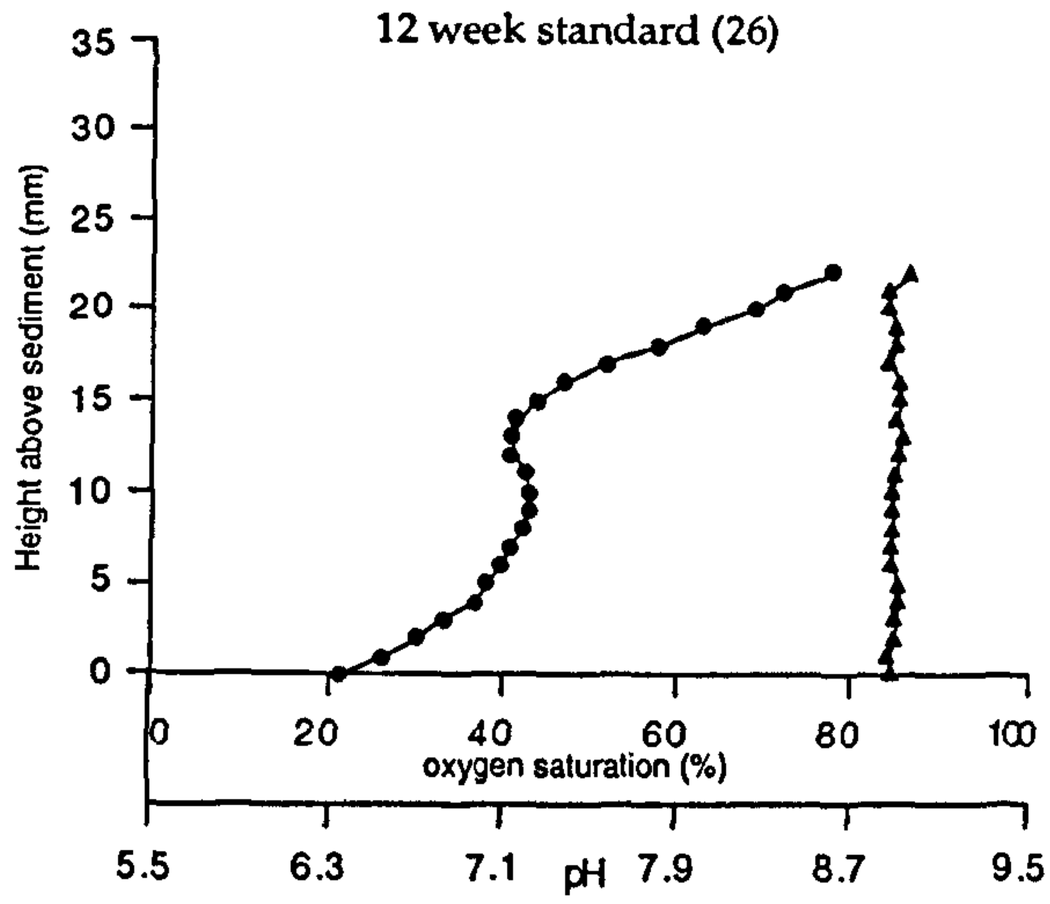

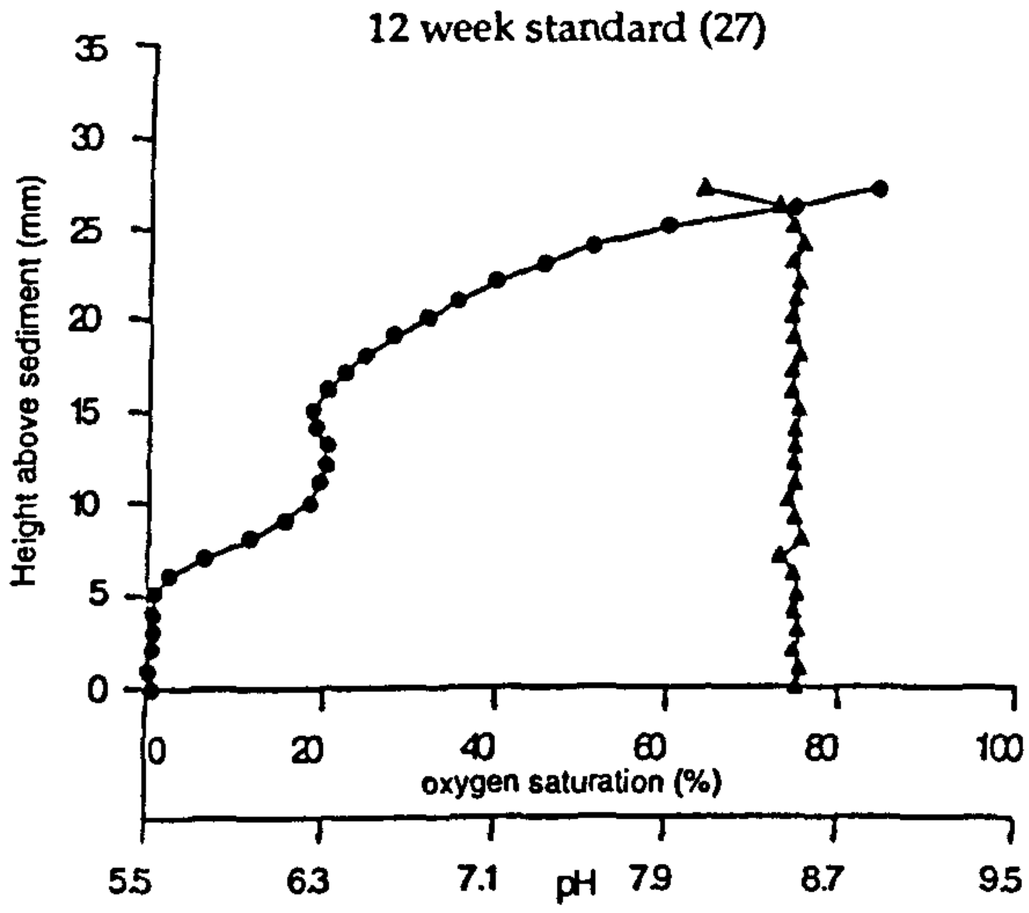

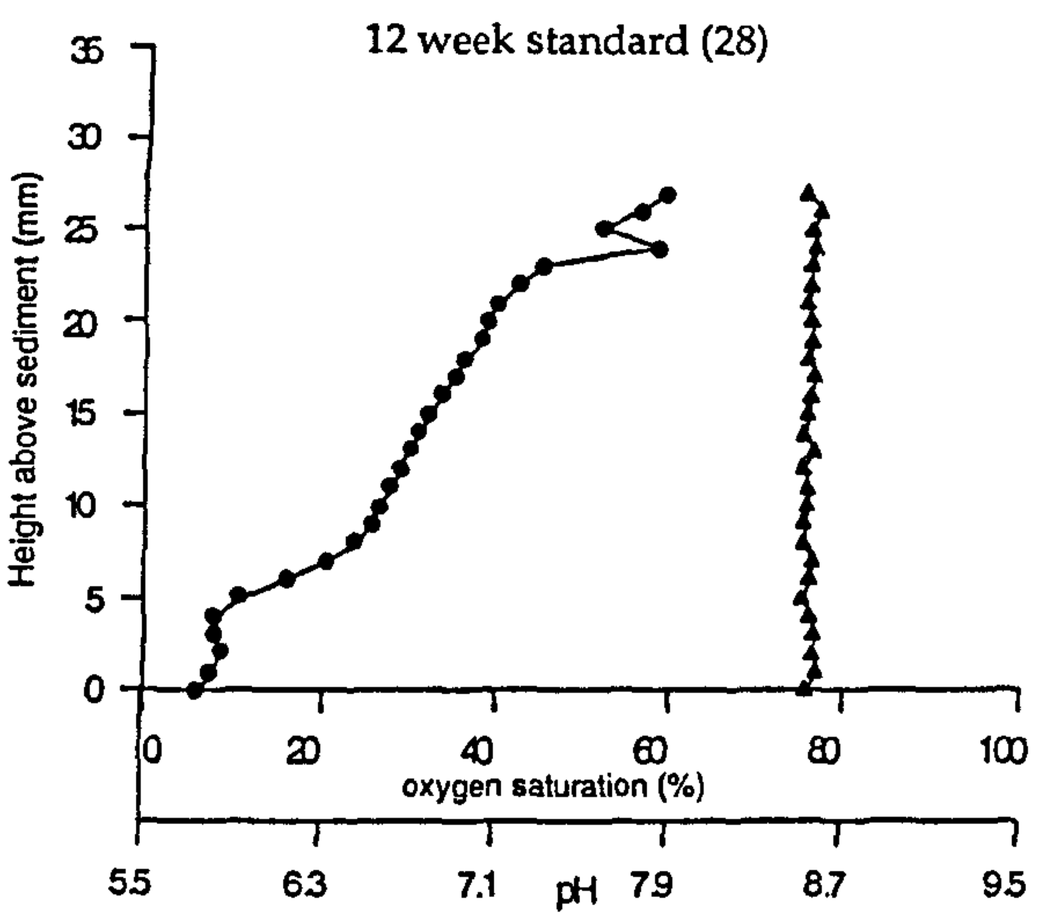

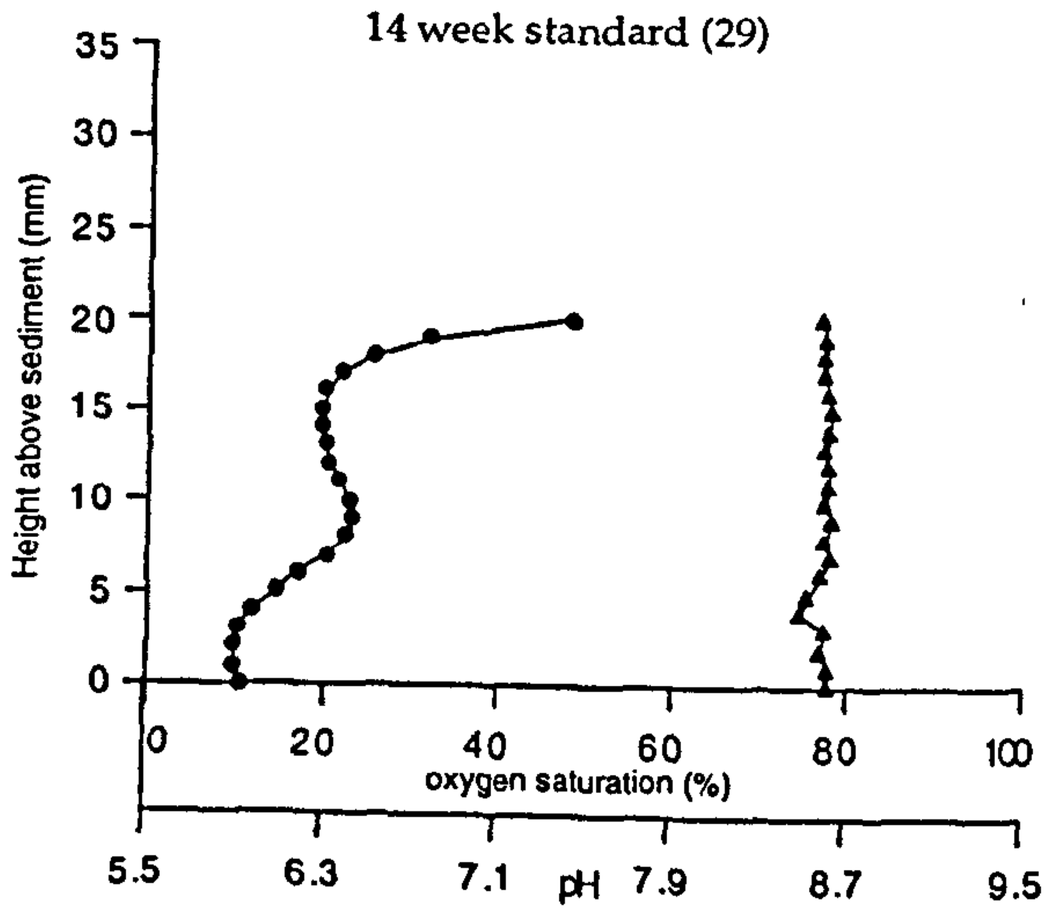

Oxygen and pH depth profiles for standard open marine systems. Infilled circles represent oxygen data points. Infilled triangles represent pH data points. The highest data points above the sediment represent the air-medium interface.

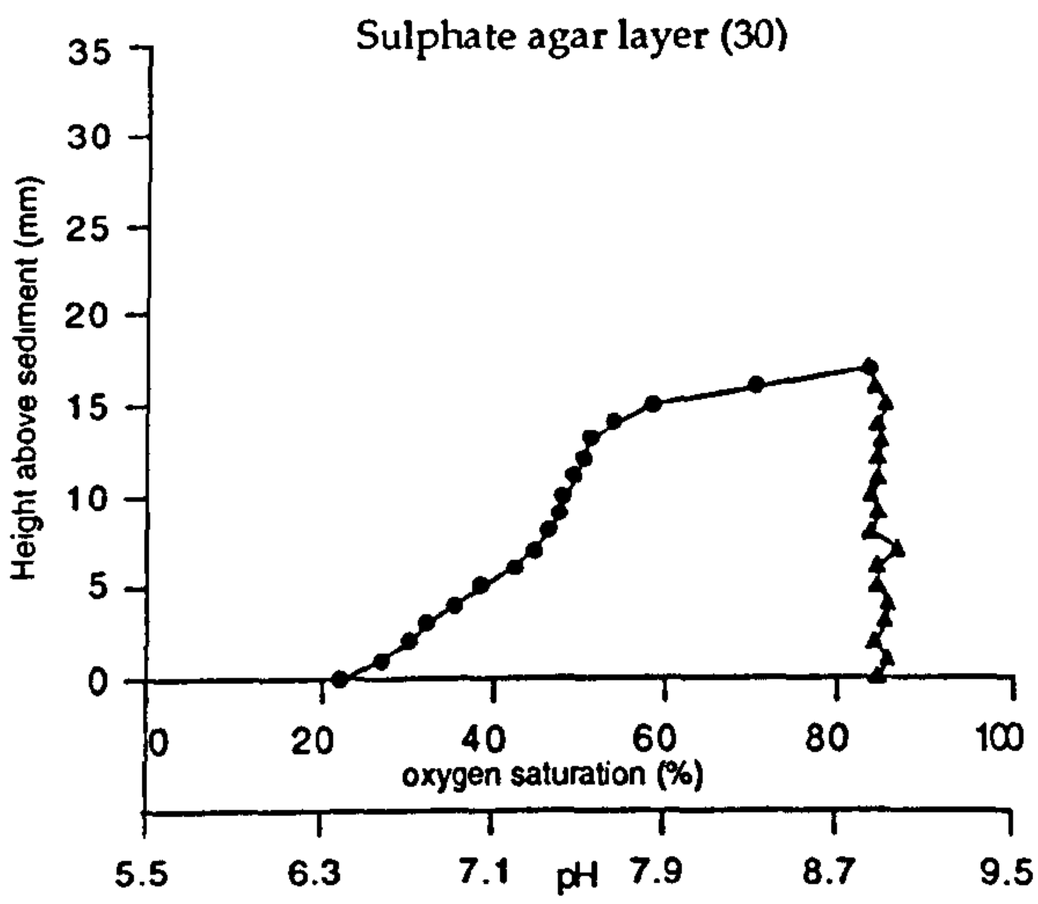

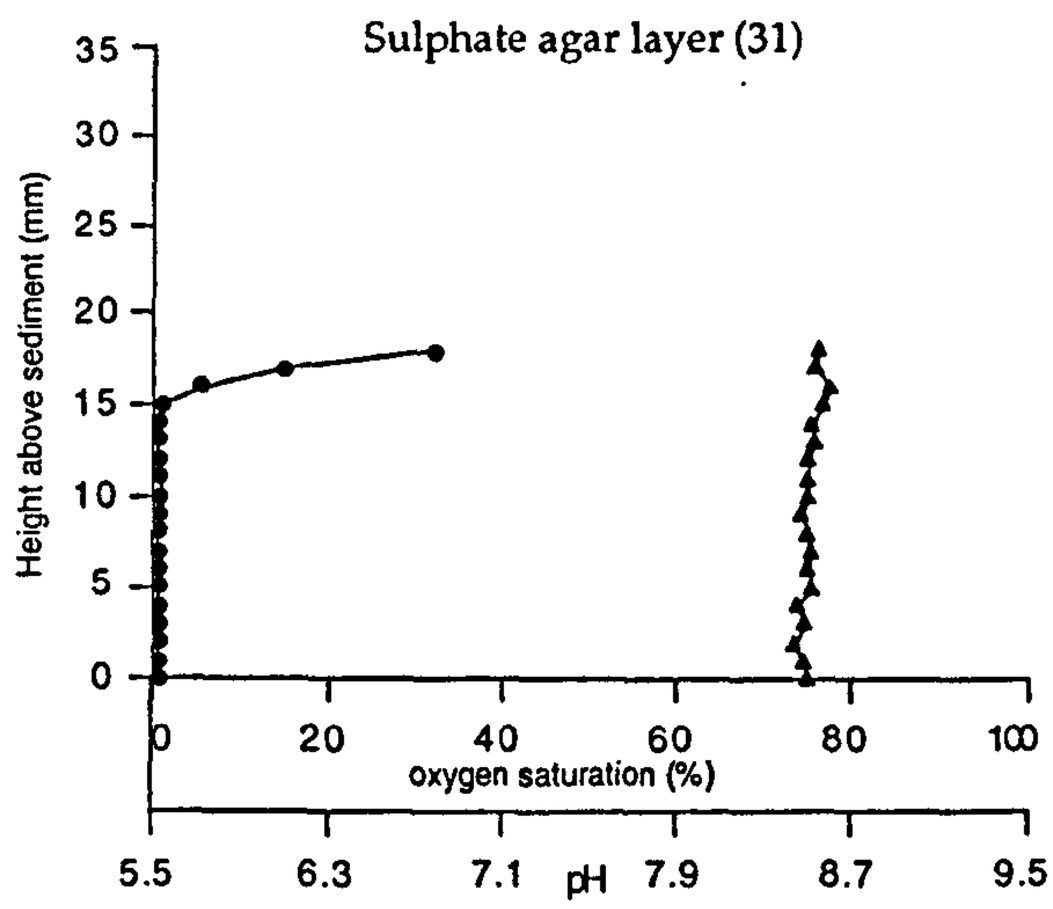

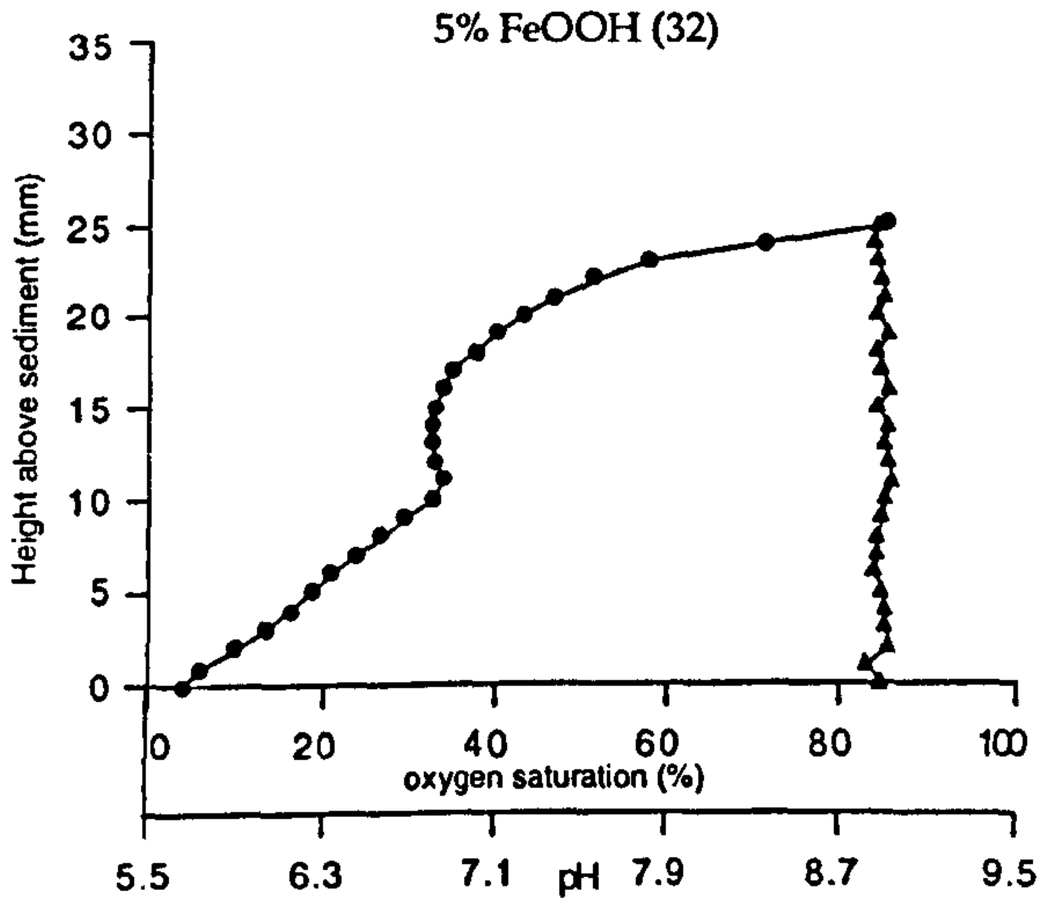

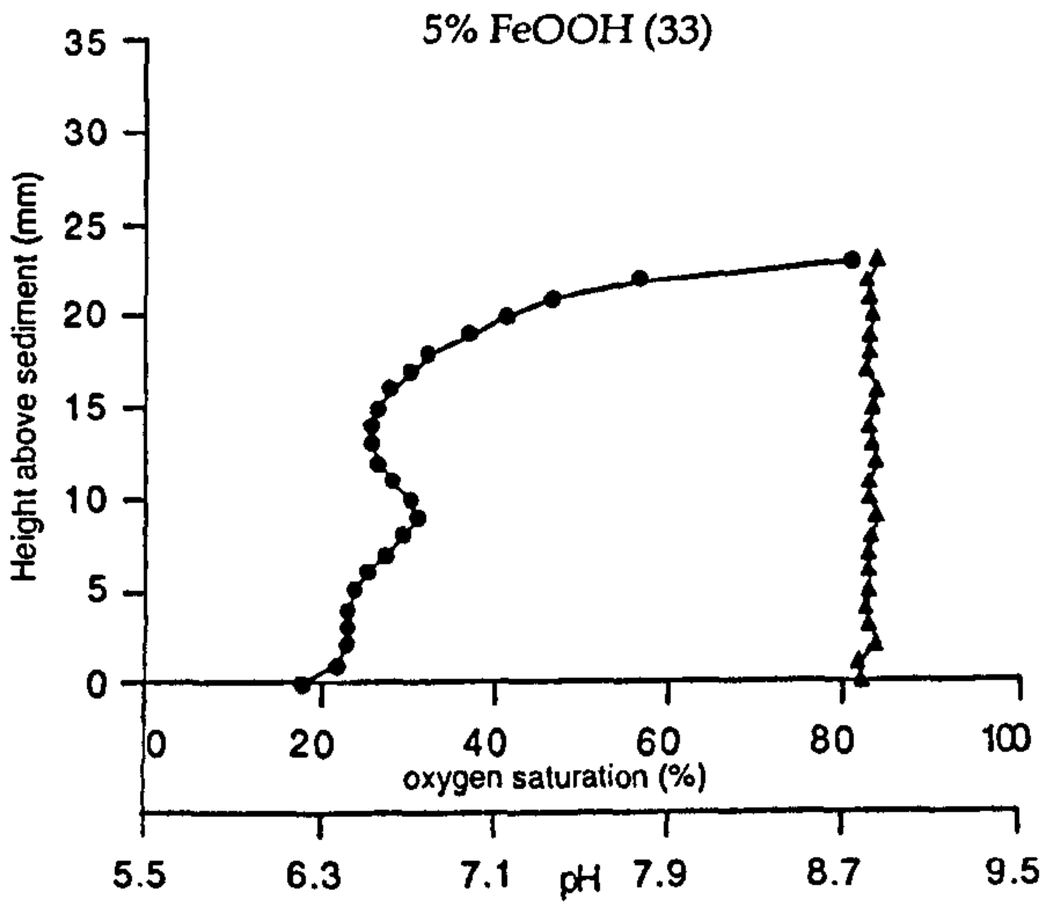

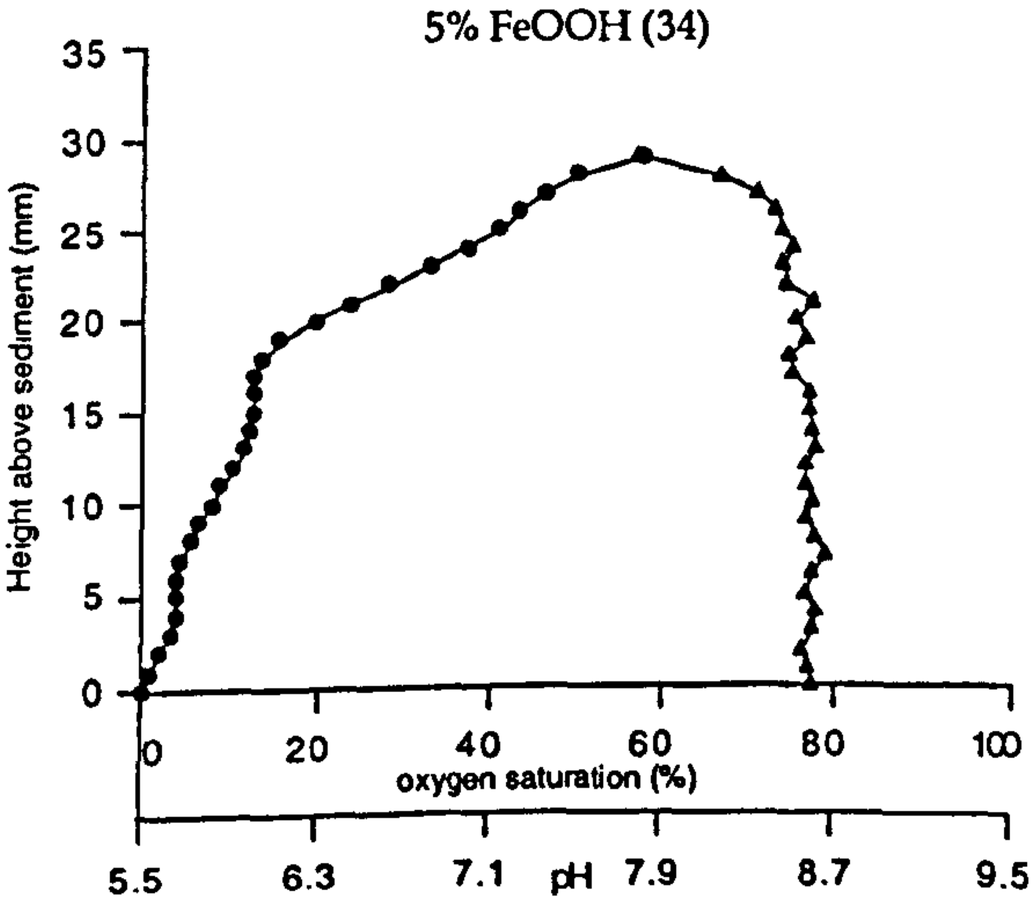

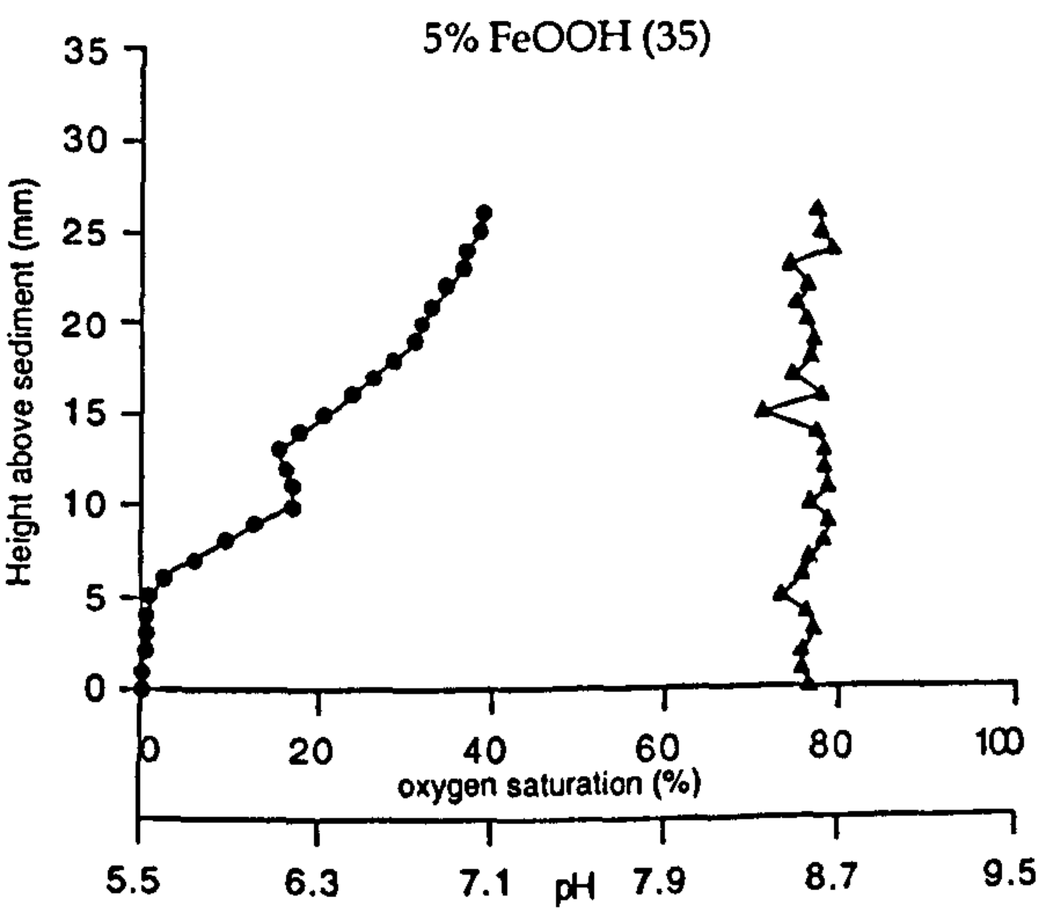

Oxygen and pH depth profiles for open marine systems after 12 weeks. Infilled circles represent oxygen data points. Infilled triangles represent pH data points. The highest data points above the sediment represent the air-medium interface.

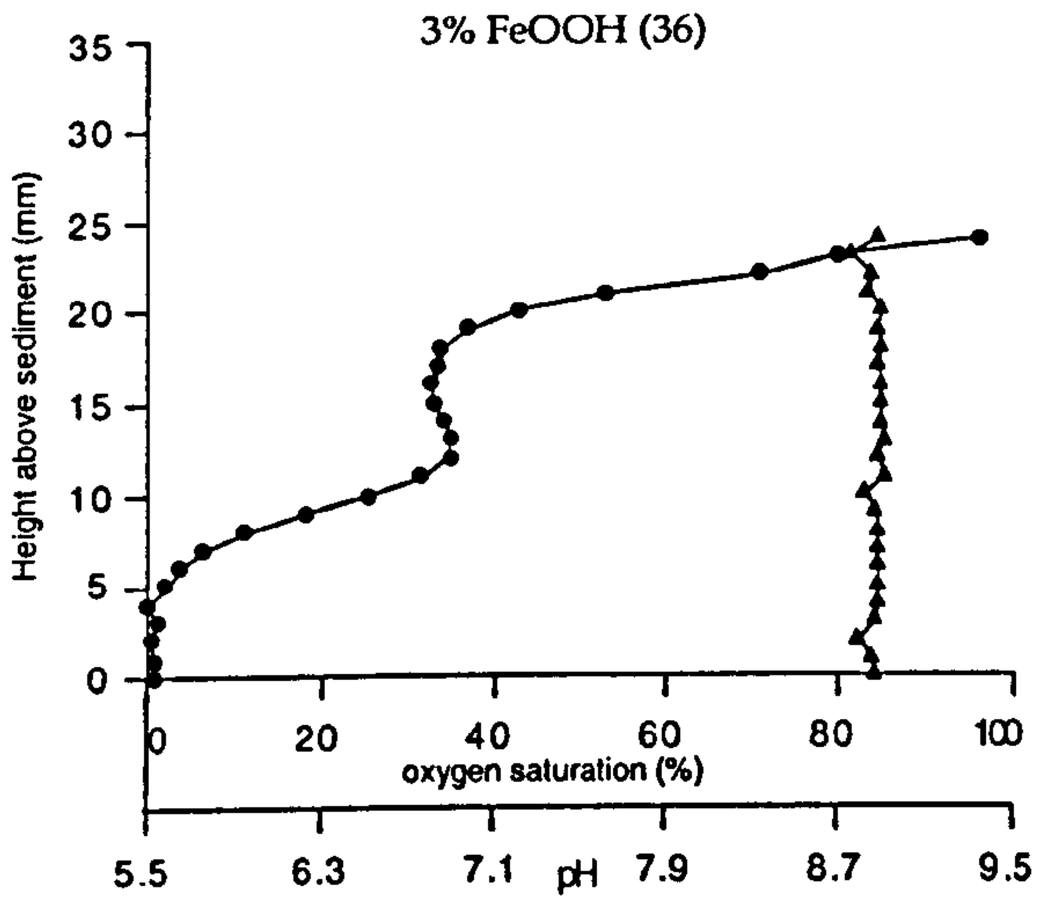

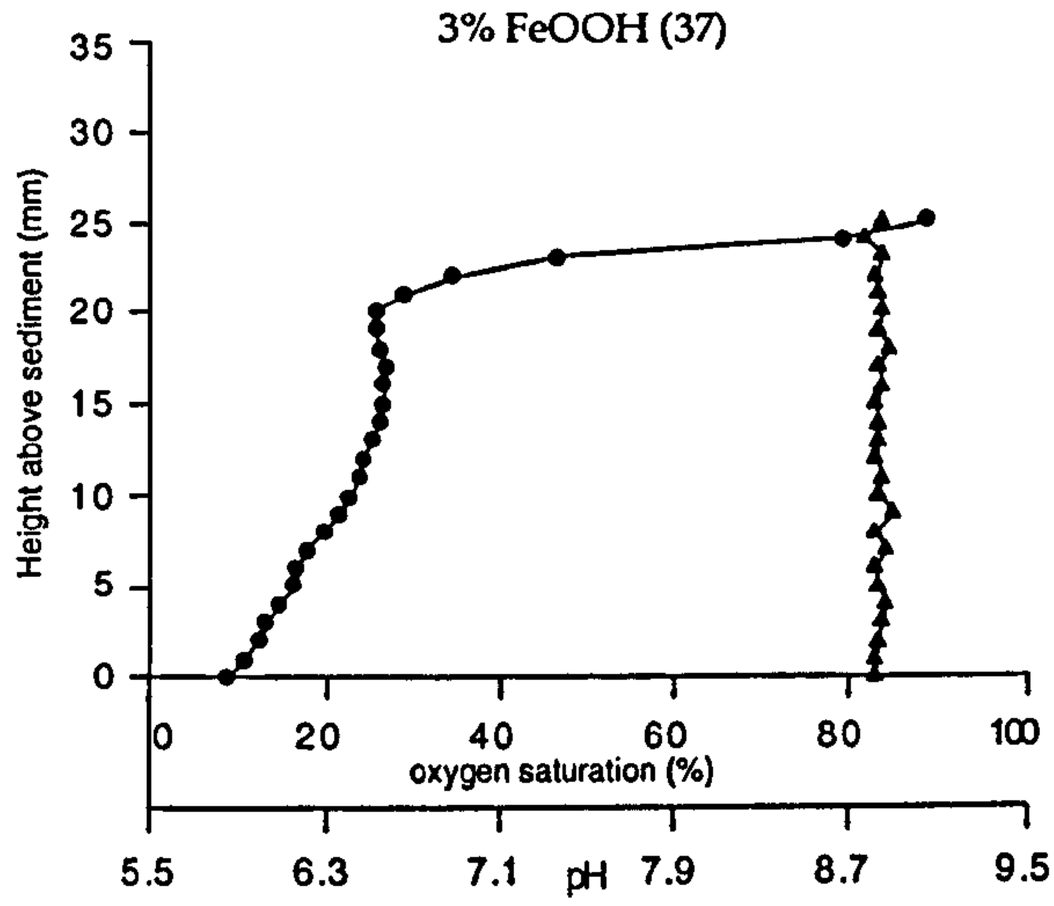

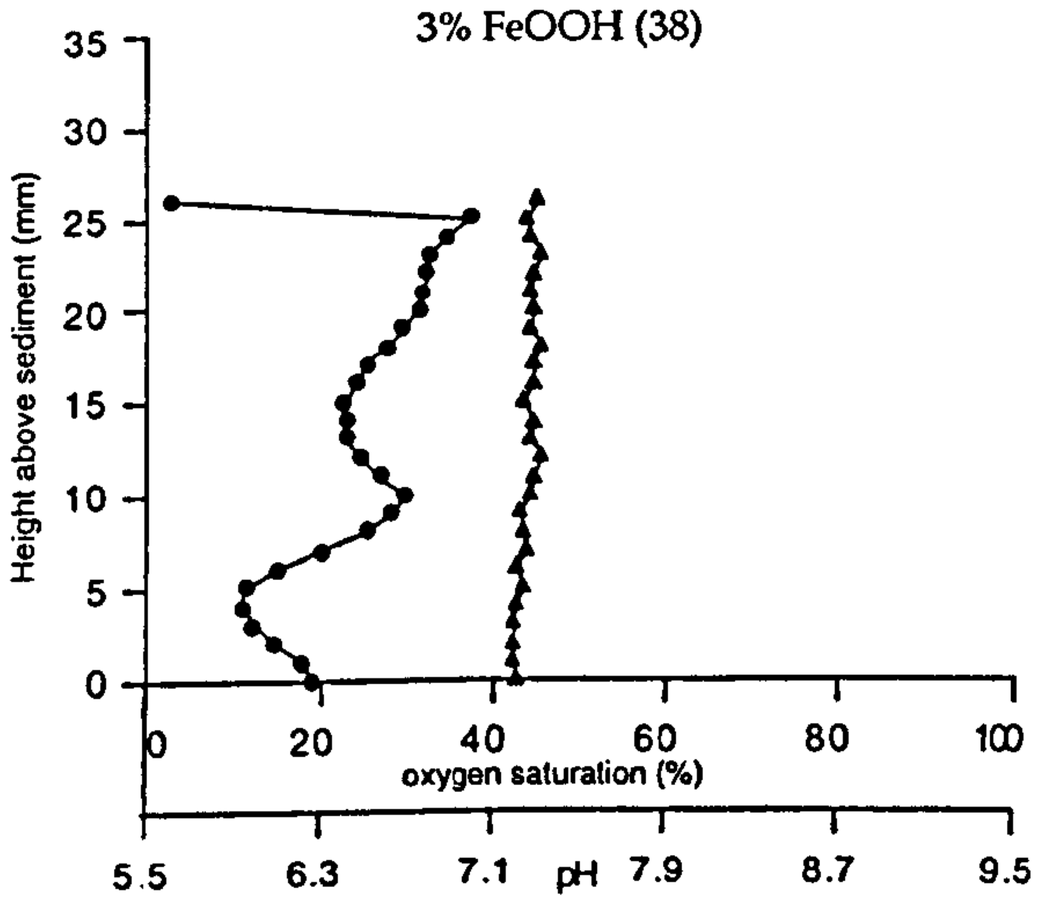

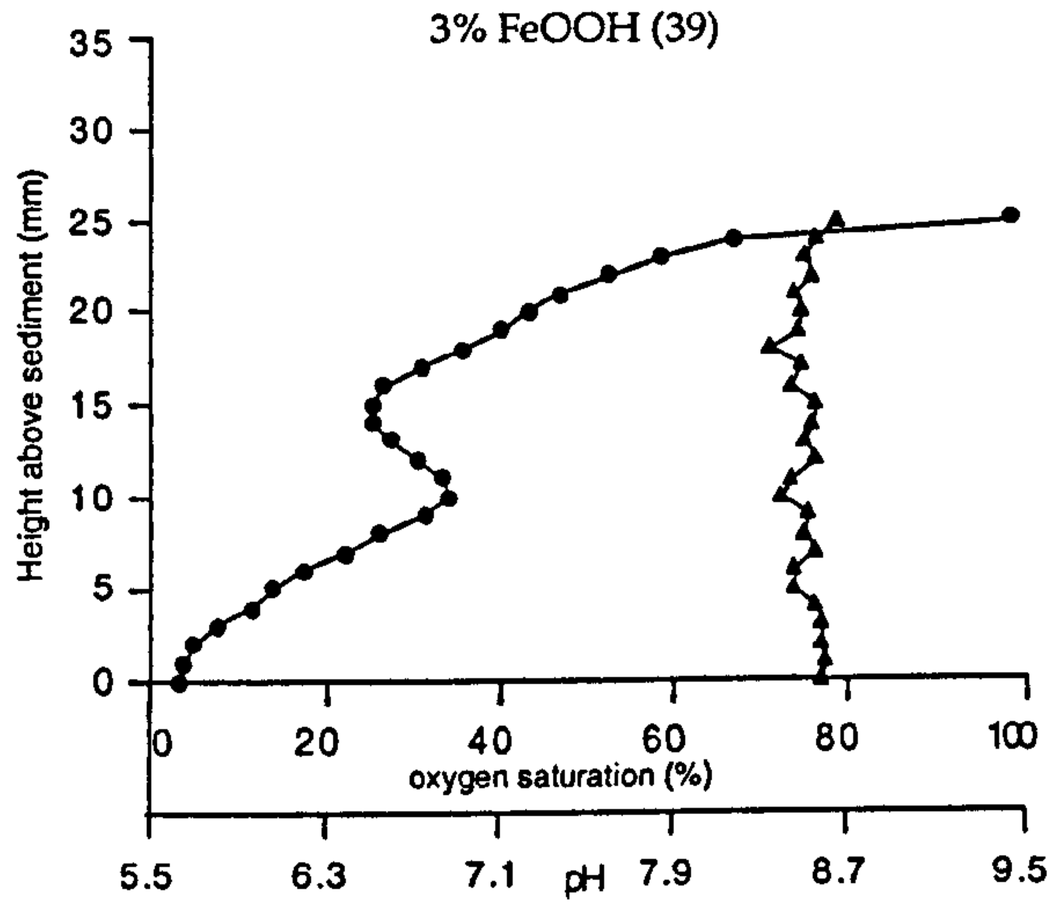

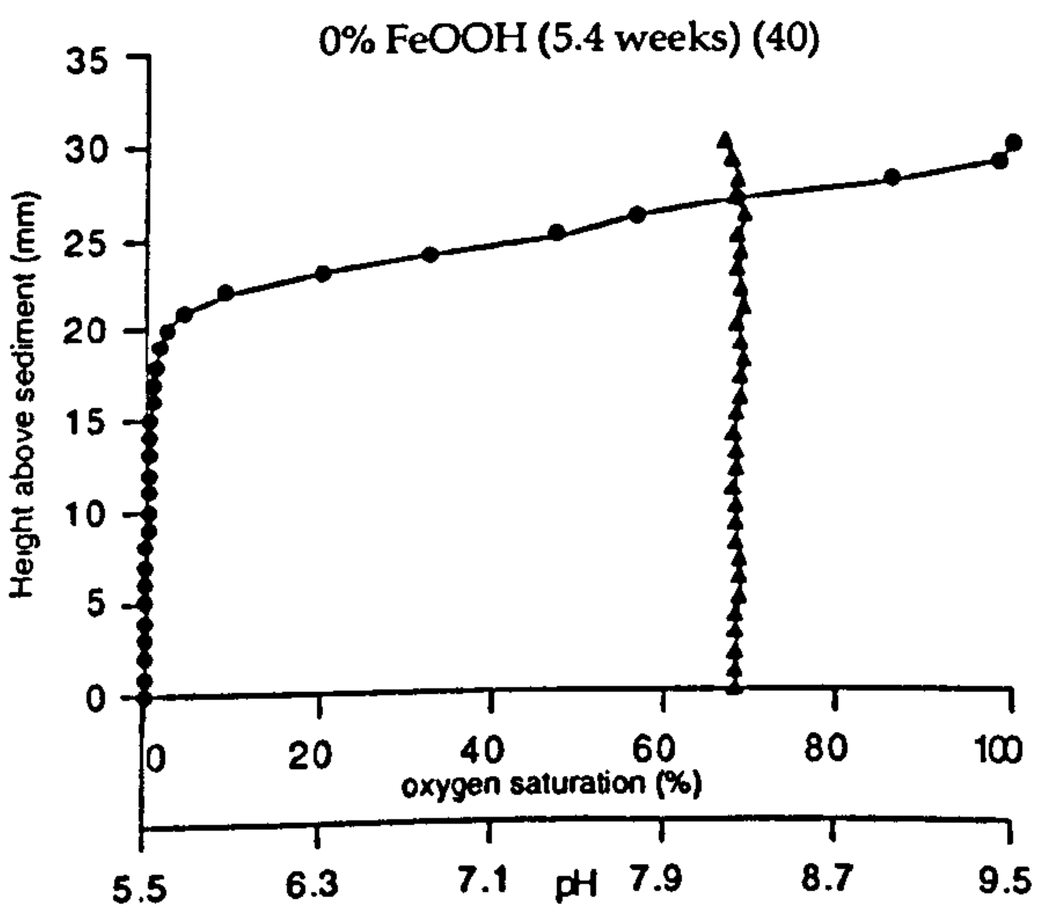

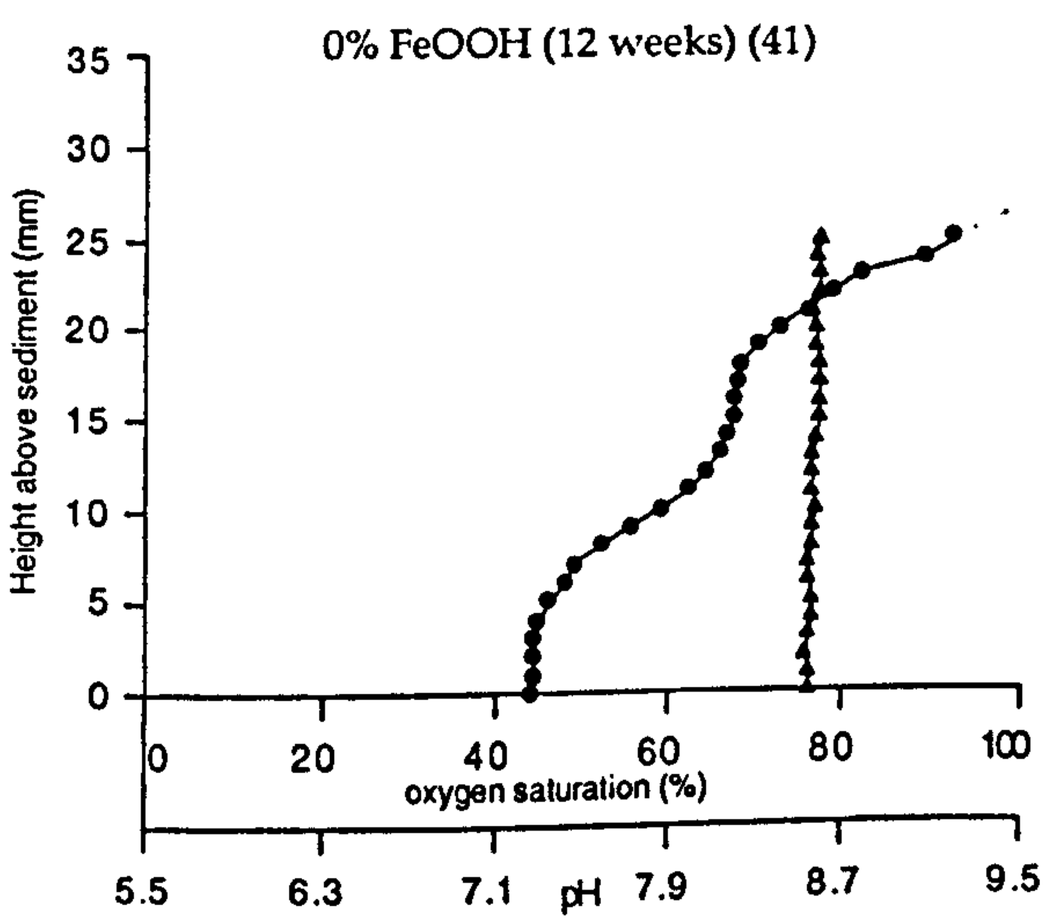

Oxygen and pH depth profiles for open marine systems after 12 weeks. Infilled circles represent oxygen data points. Infilled triangles represent pH data points. The highest data points above the sediment represent the air-medium interface.

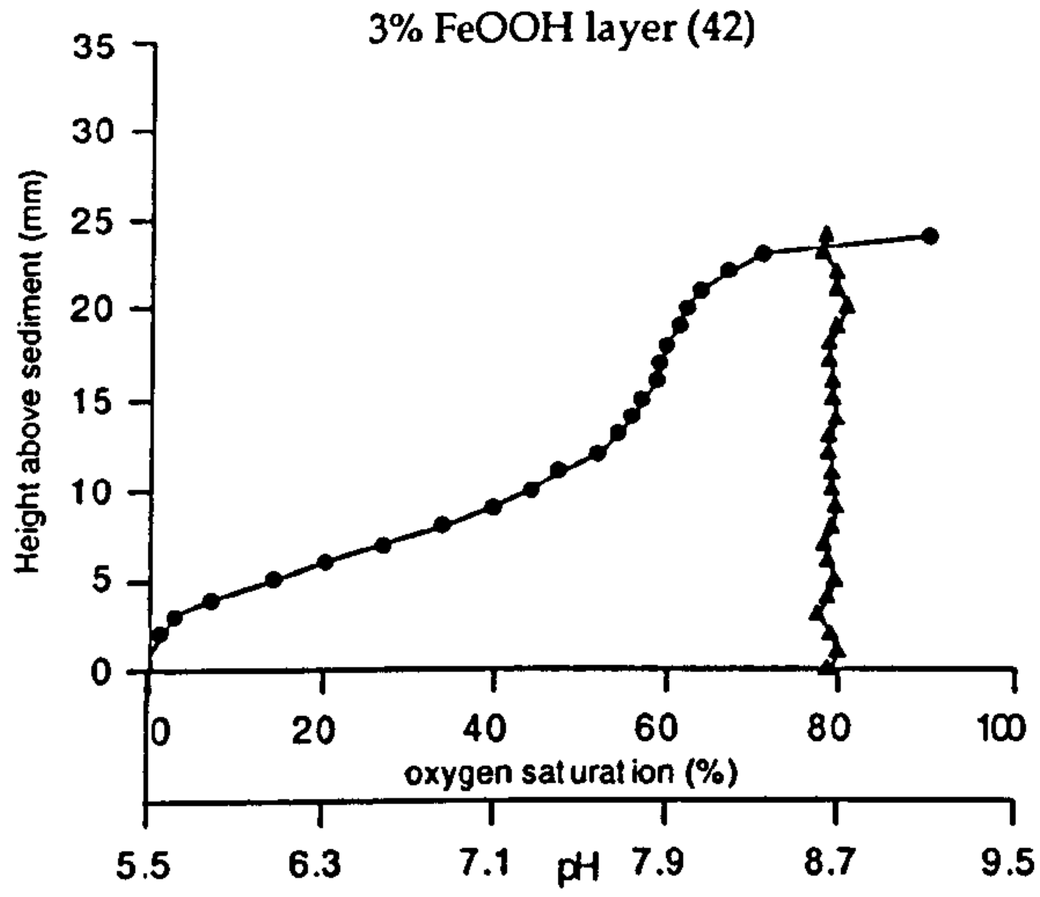

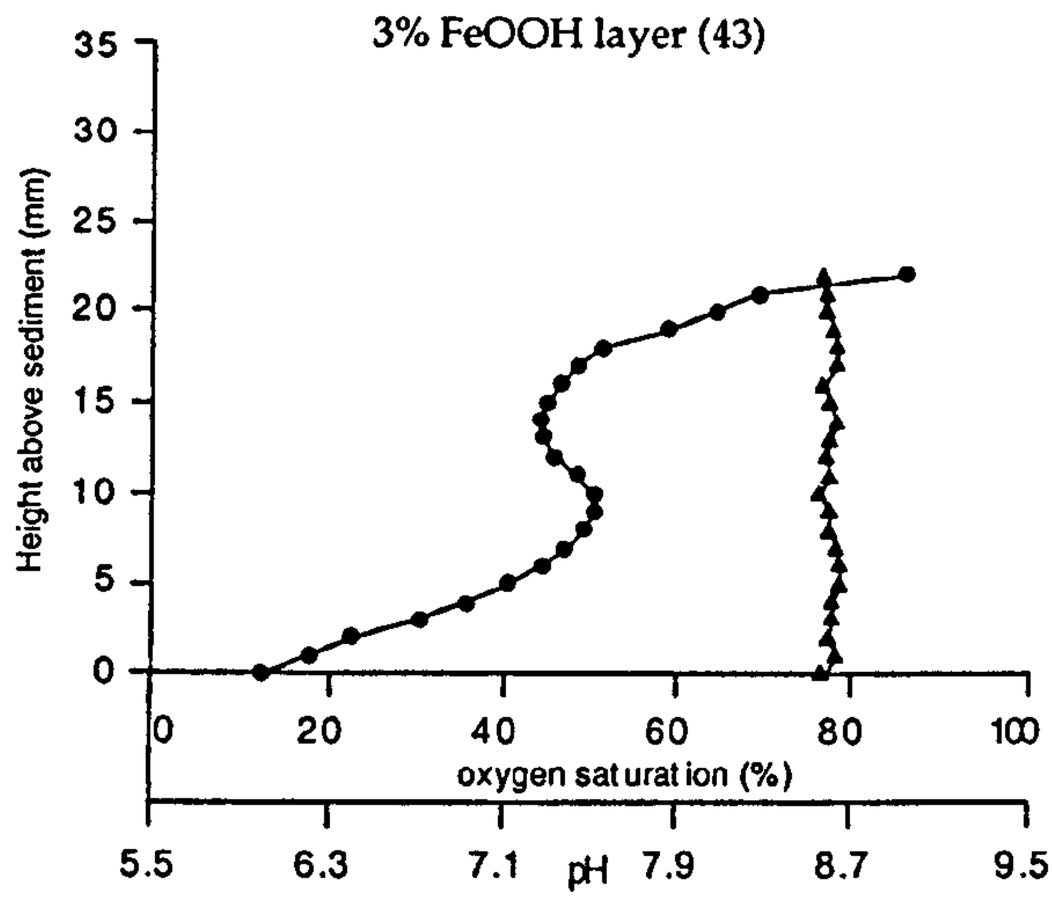

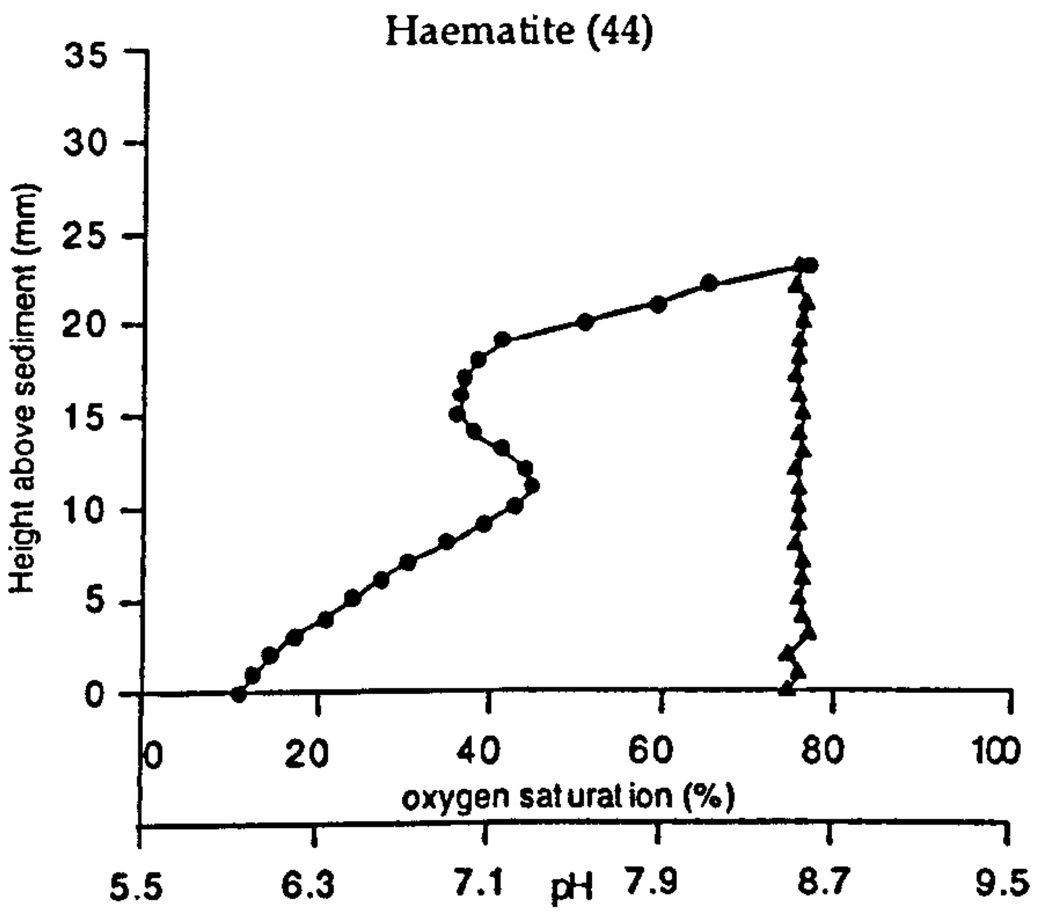

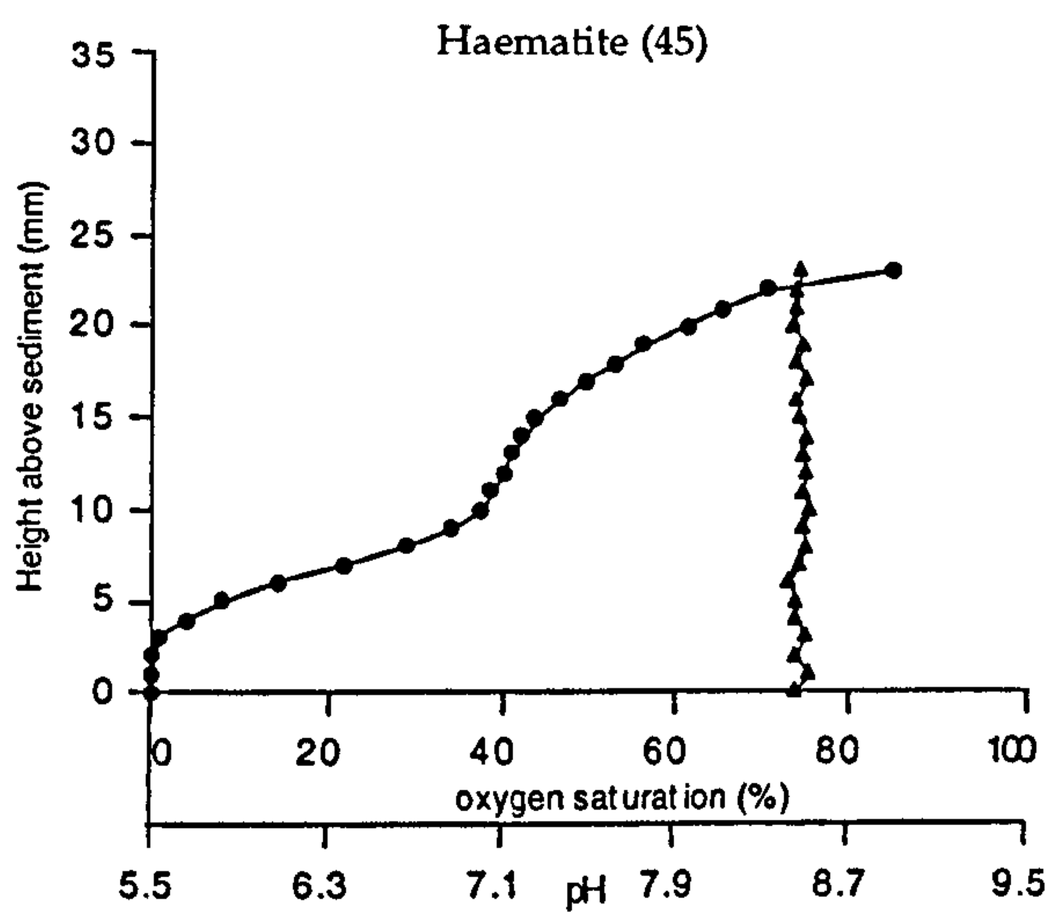

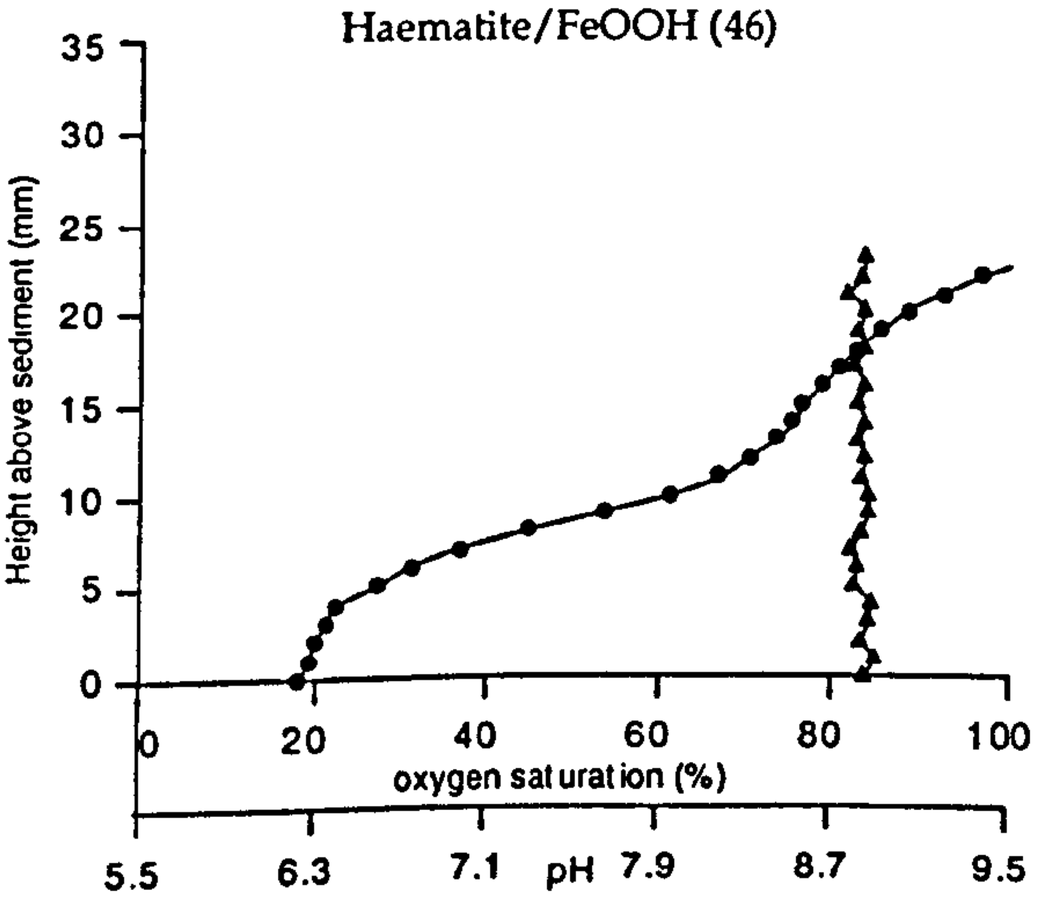

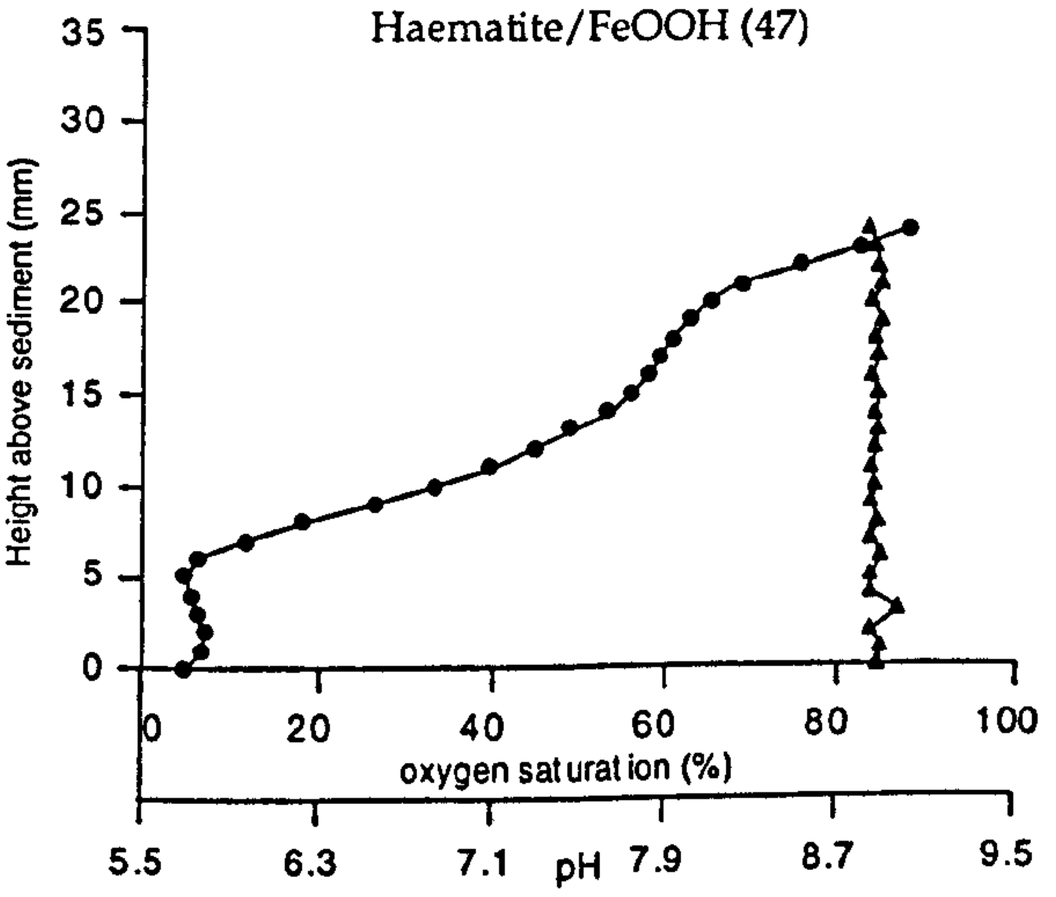

Oxygen and pH depth profiles for open marine systems after 12 weeks. Infilled circles represent oxygen data points. Infilled triangles represent pH data points. The highest data points above the sediment represent the air-medium interface.

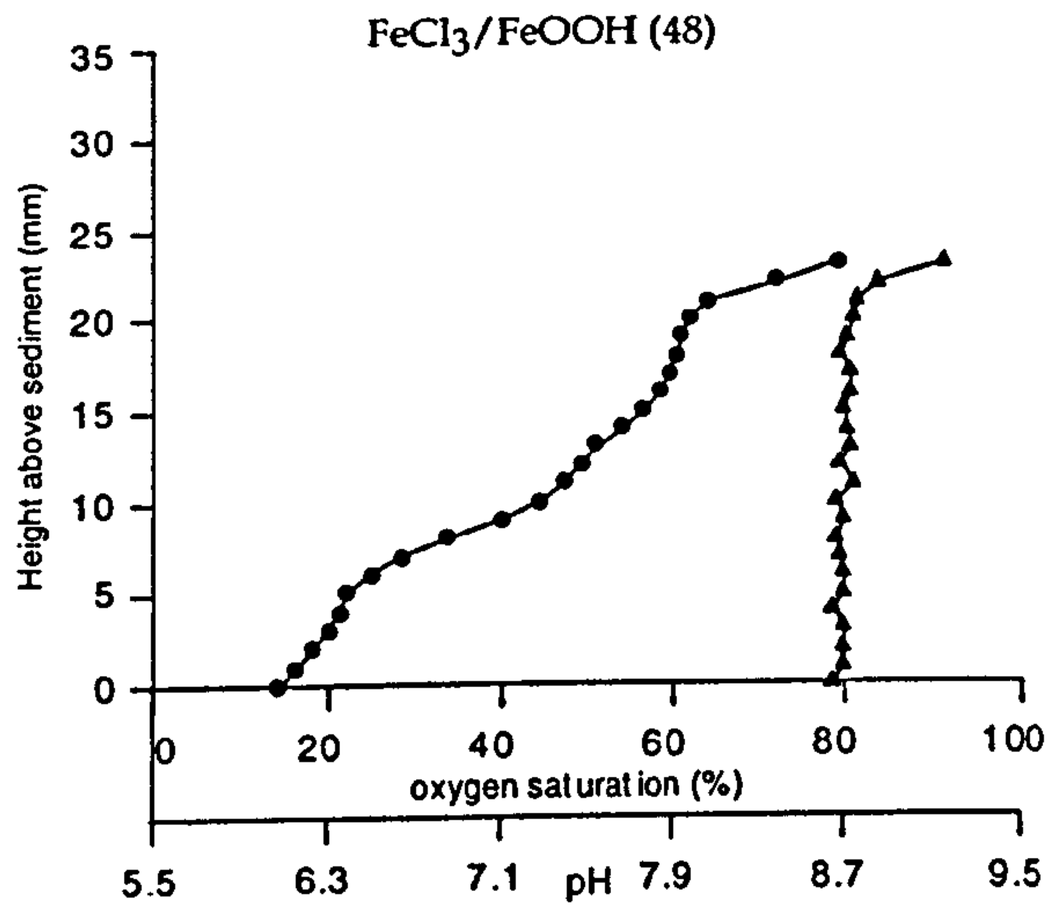

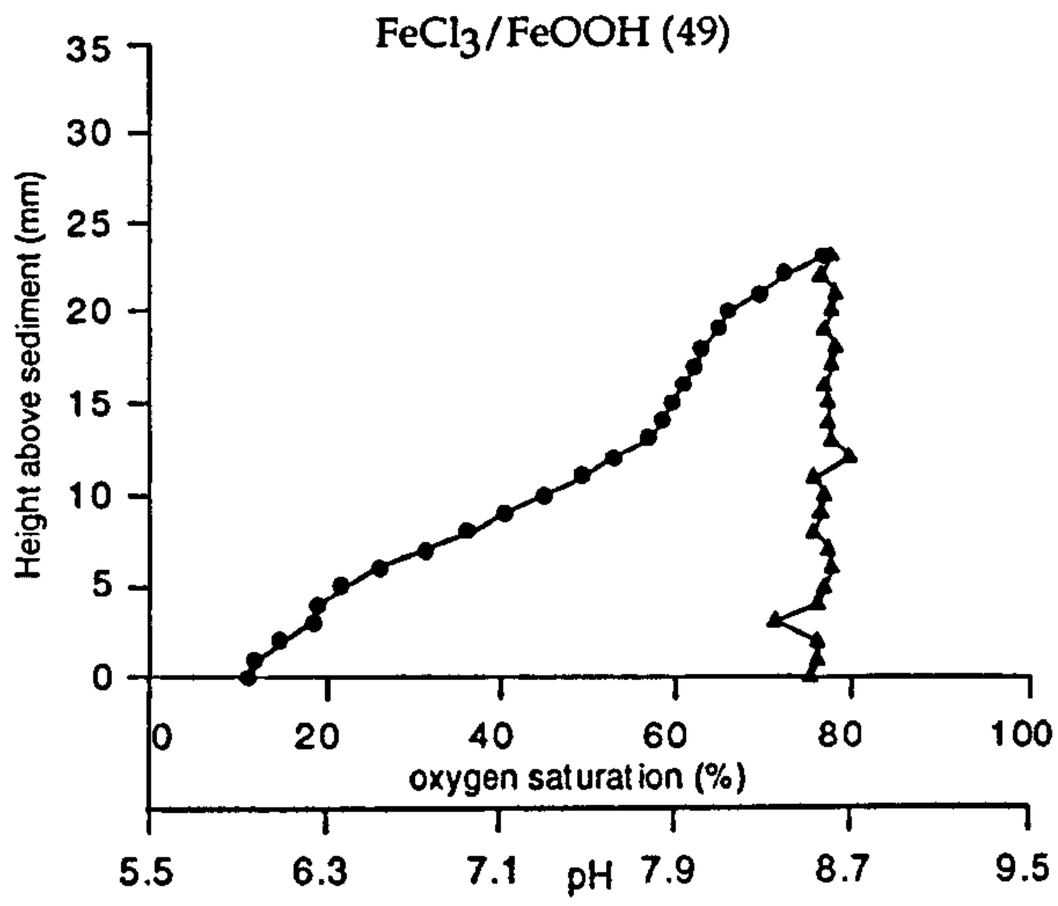

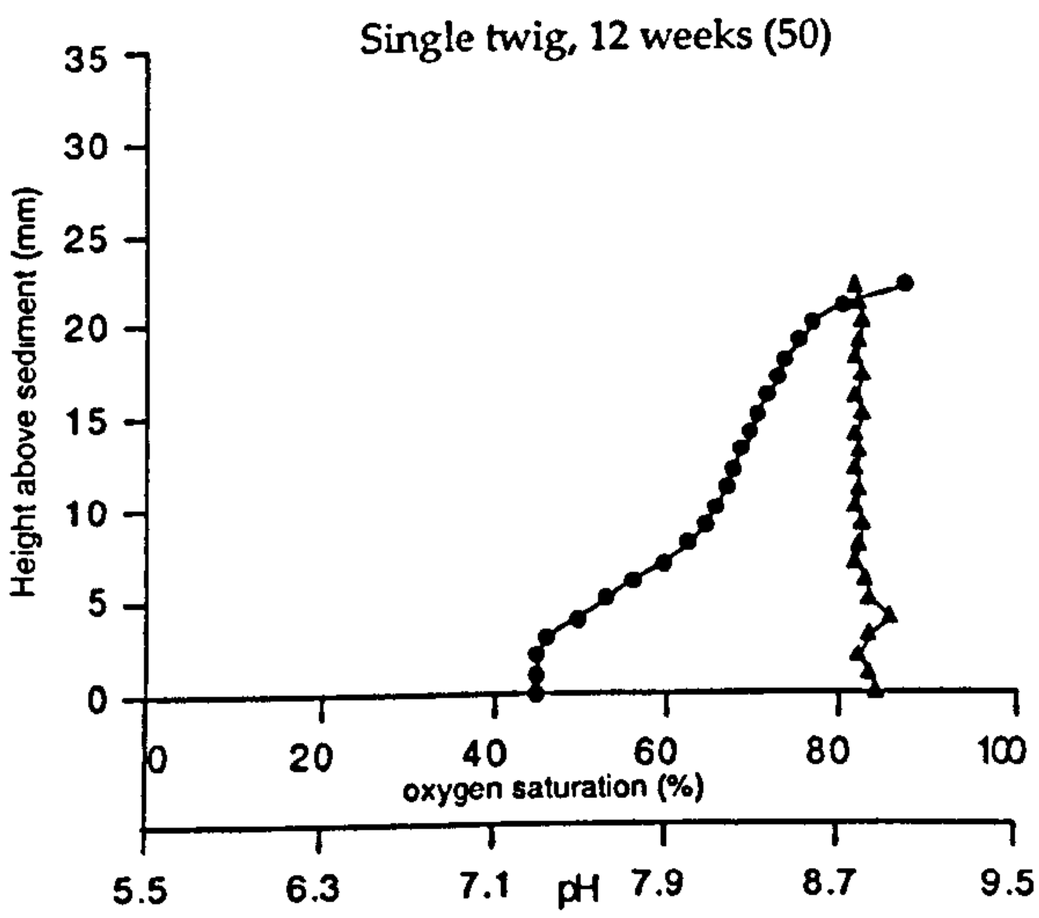

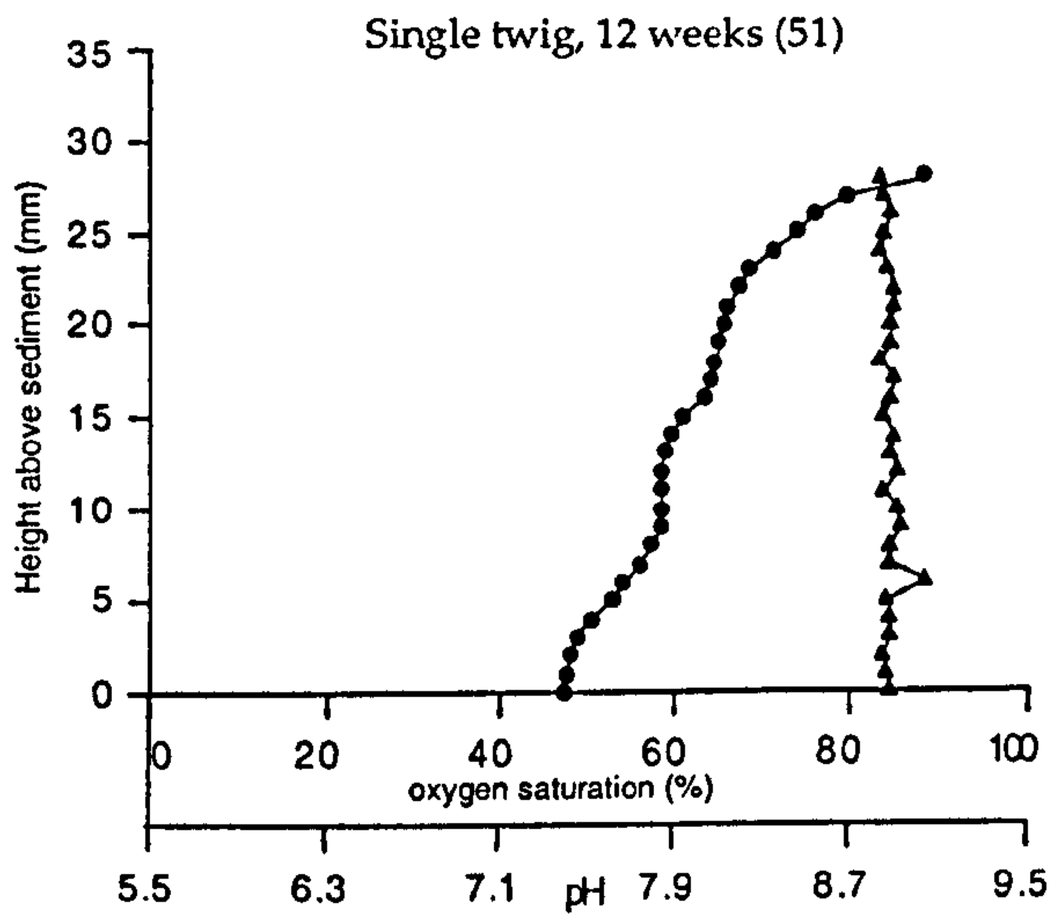

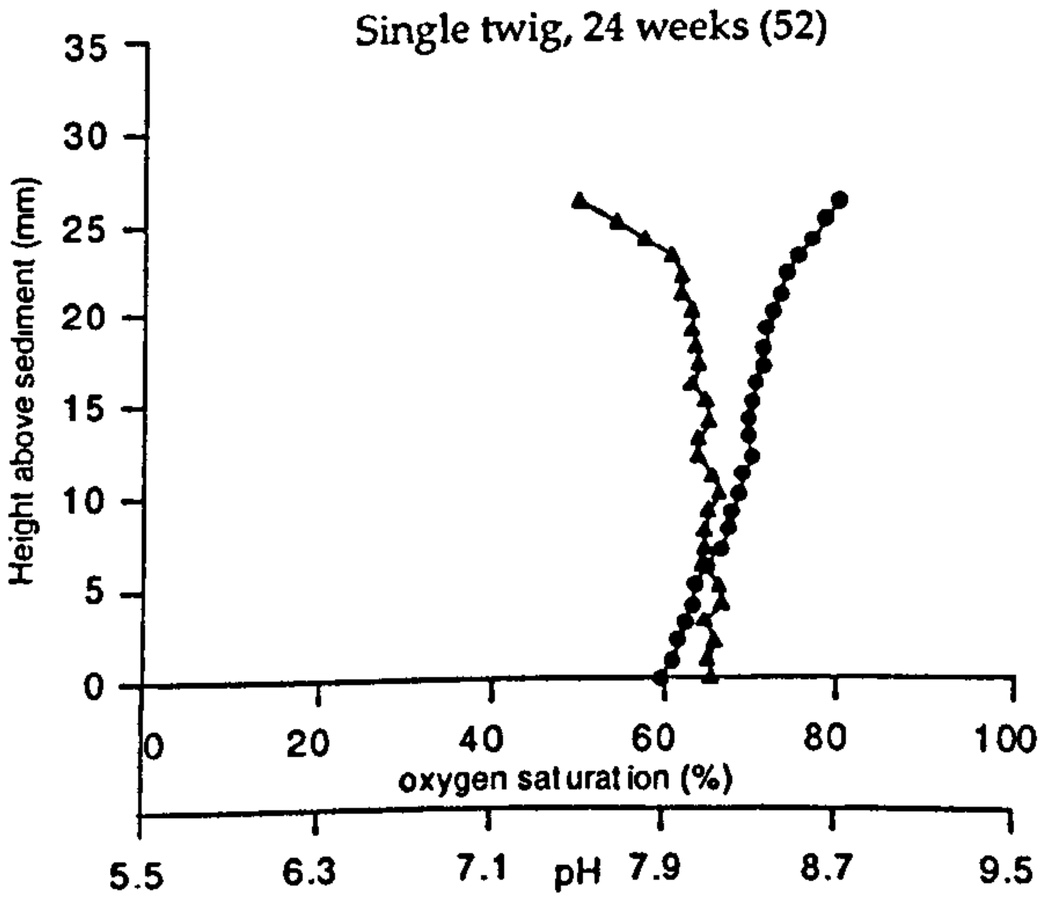

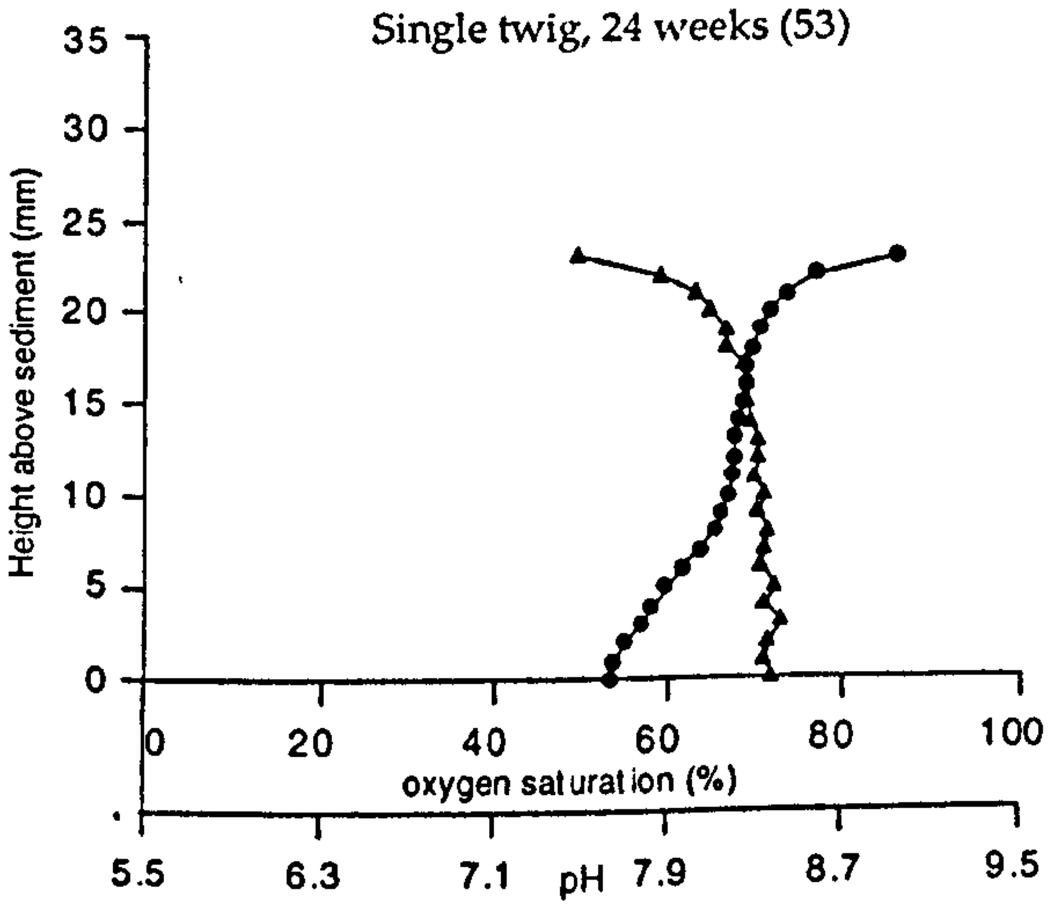

Oxygen and pH depth profiles for open marine systems after 12 weeks unless otherwise stated. Infilled circles represent oxygen data points. Infilled triangles represent pH data points. The highest data points above the sediment represent the air-medium interface.

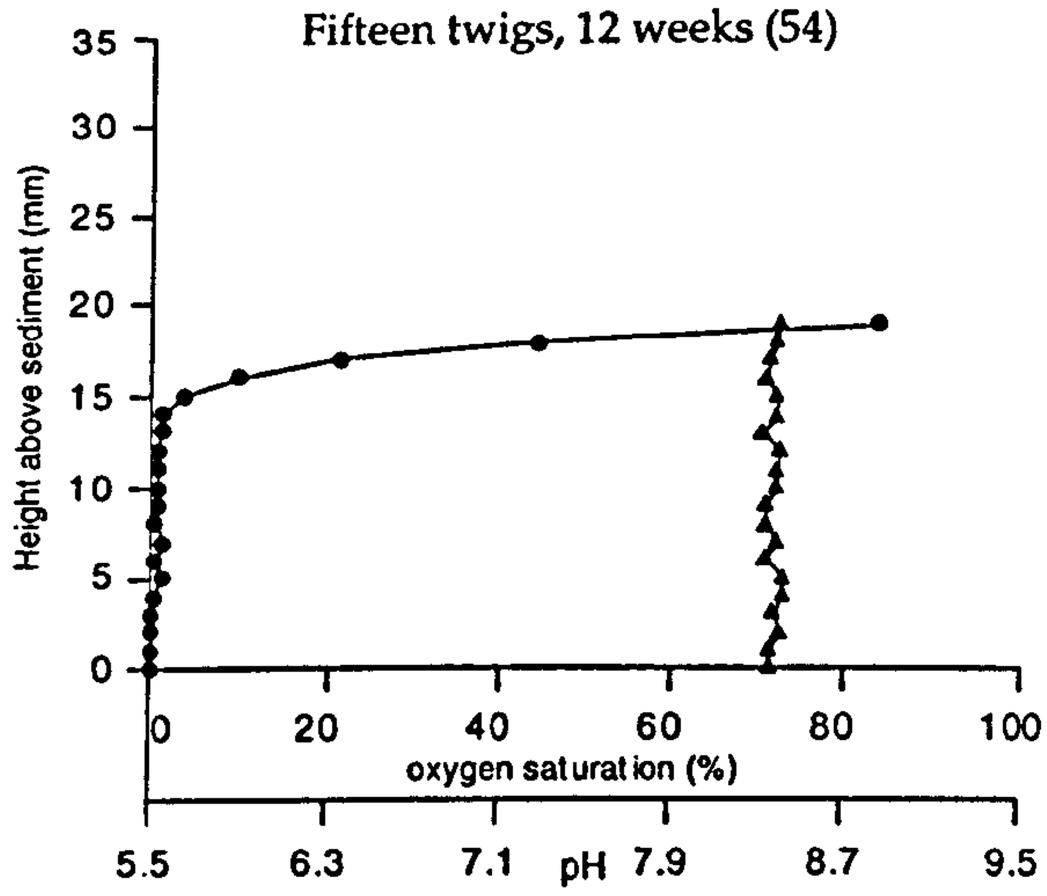

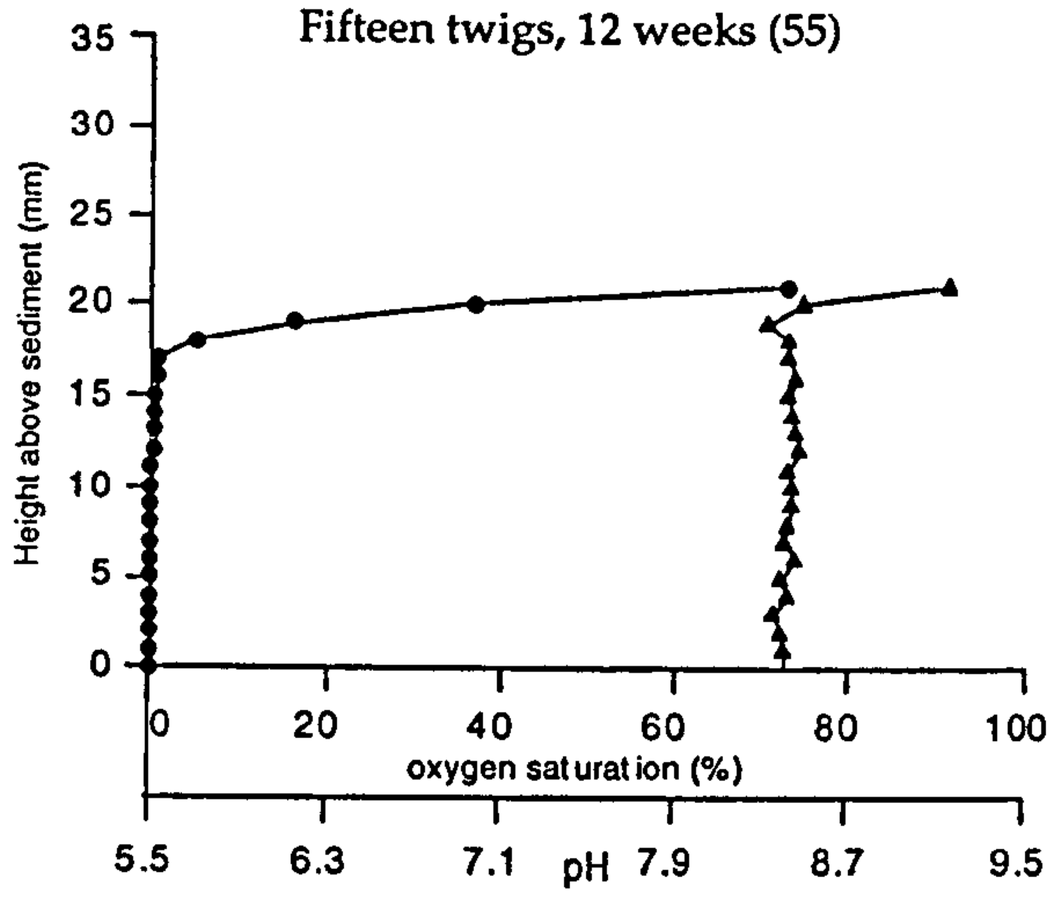

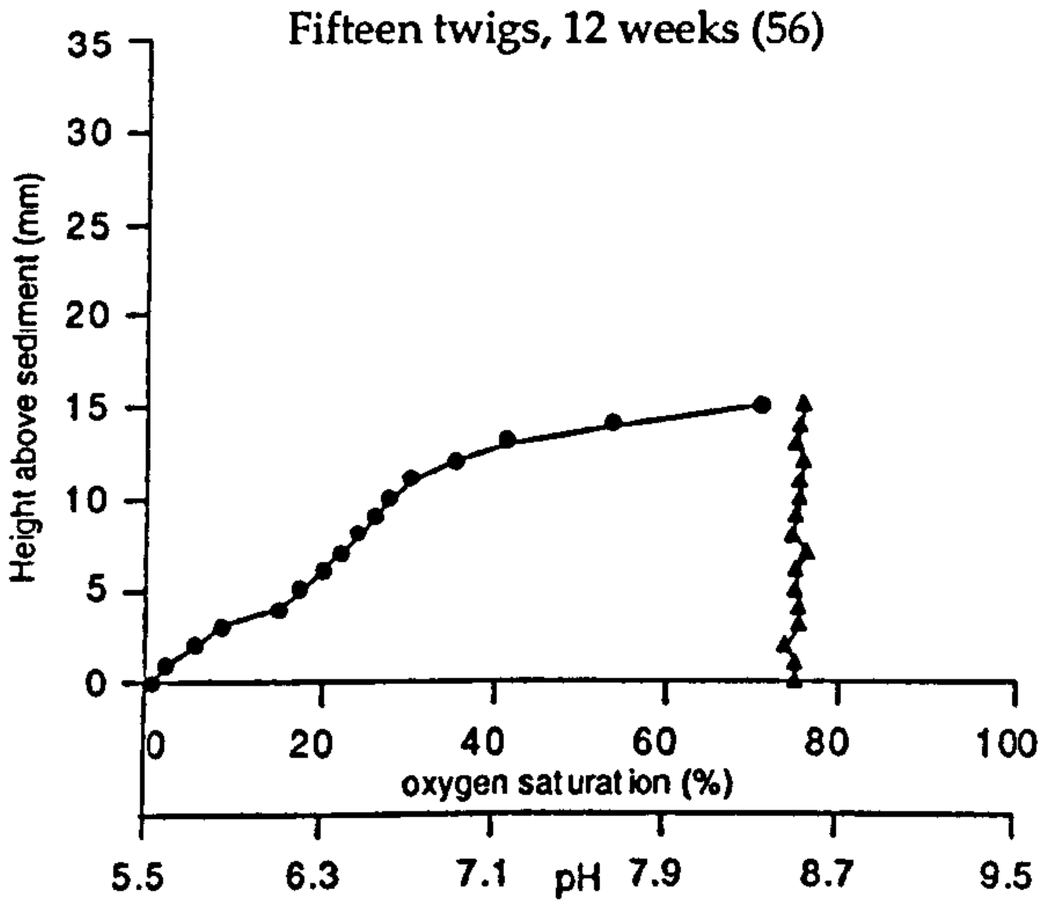

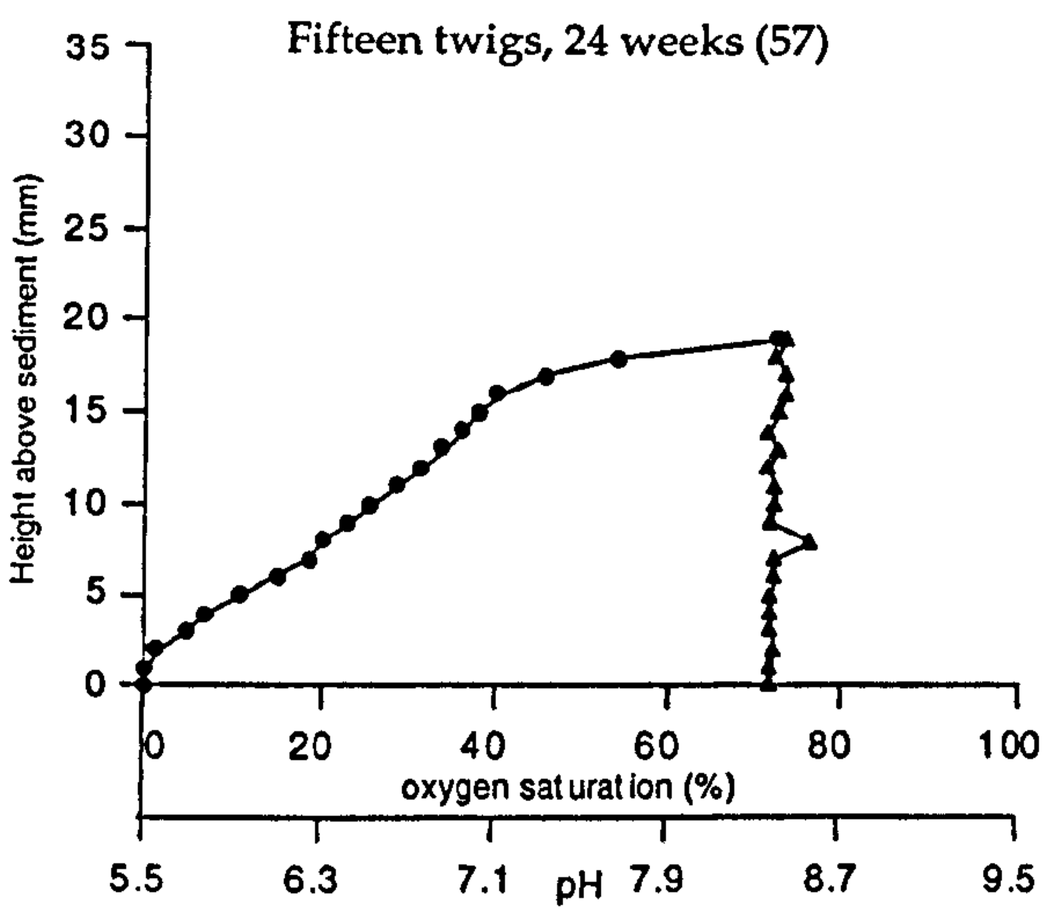

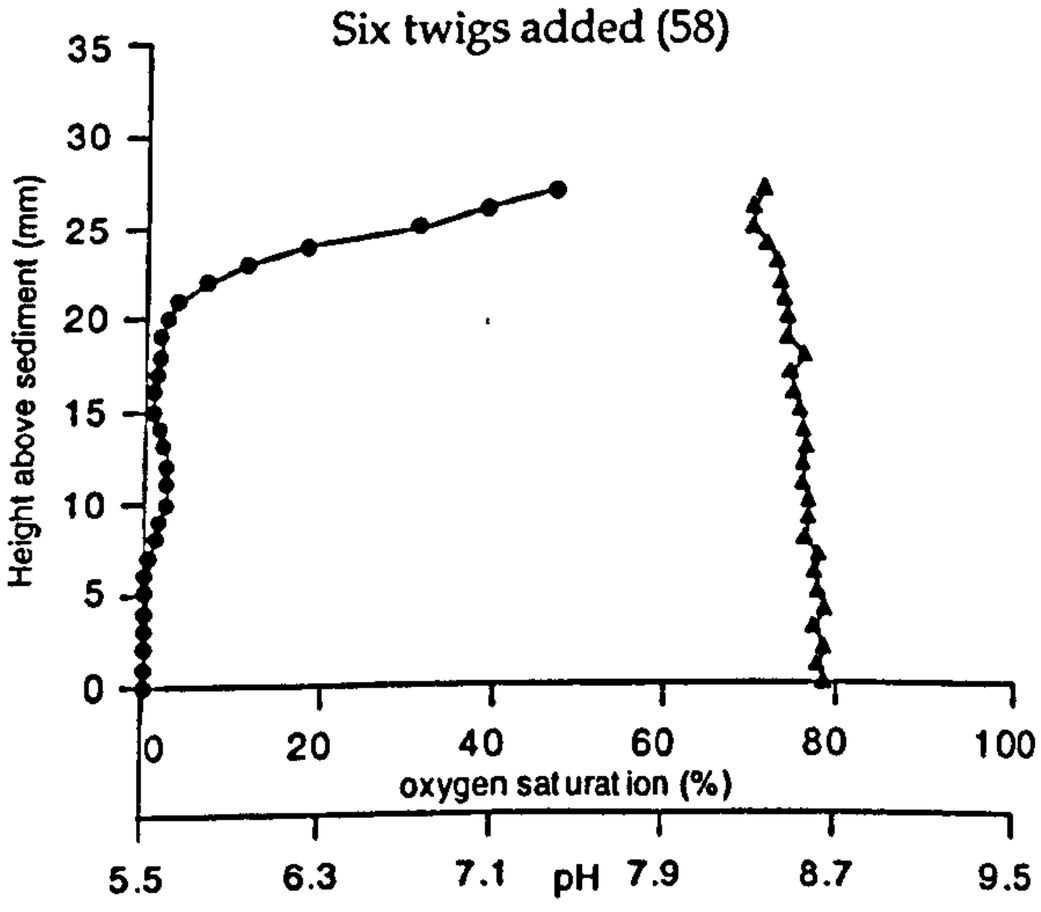

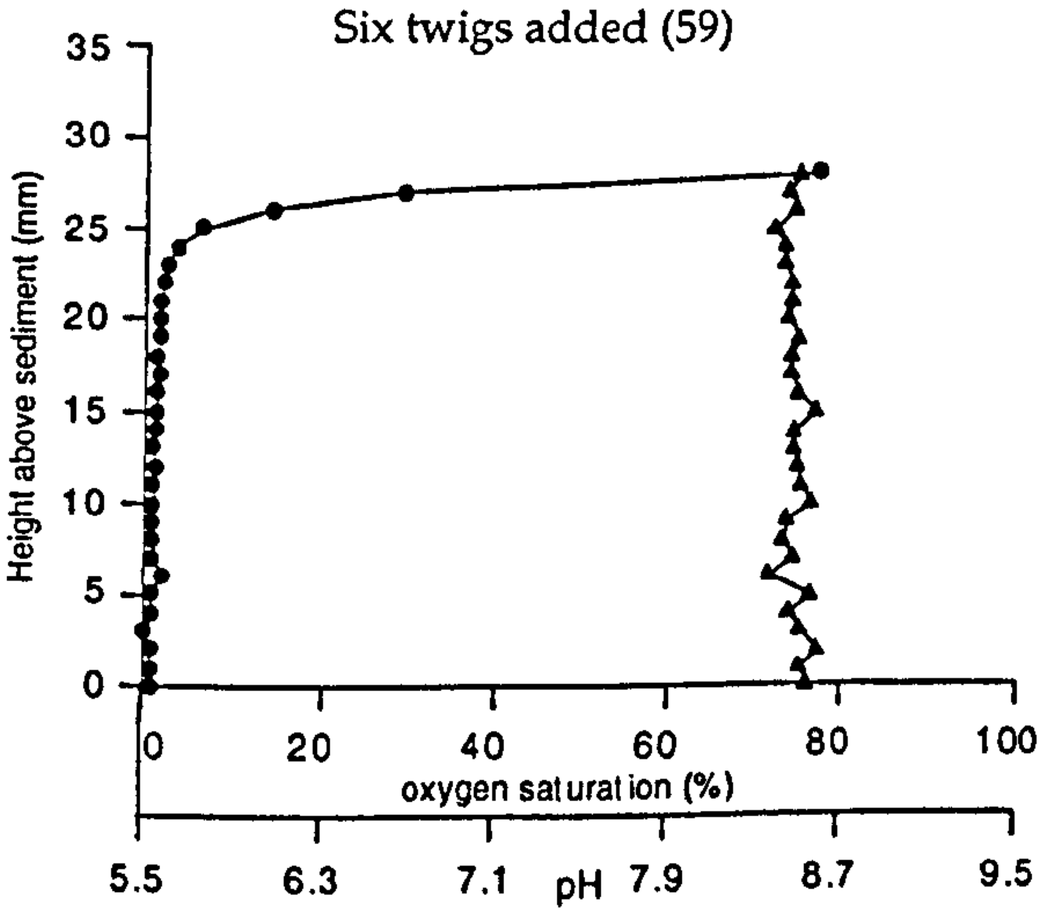

Oxygen and pH depth profiles for open marine systems after 12 weeks unless otherwise stated. Infilled circles represent oxygen data points. Infilled triangles represent pH data points. The highest data points above the sediment represent the air-medium interface.

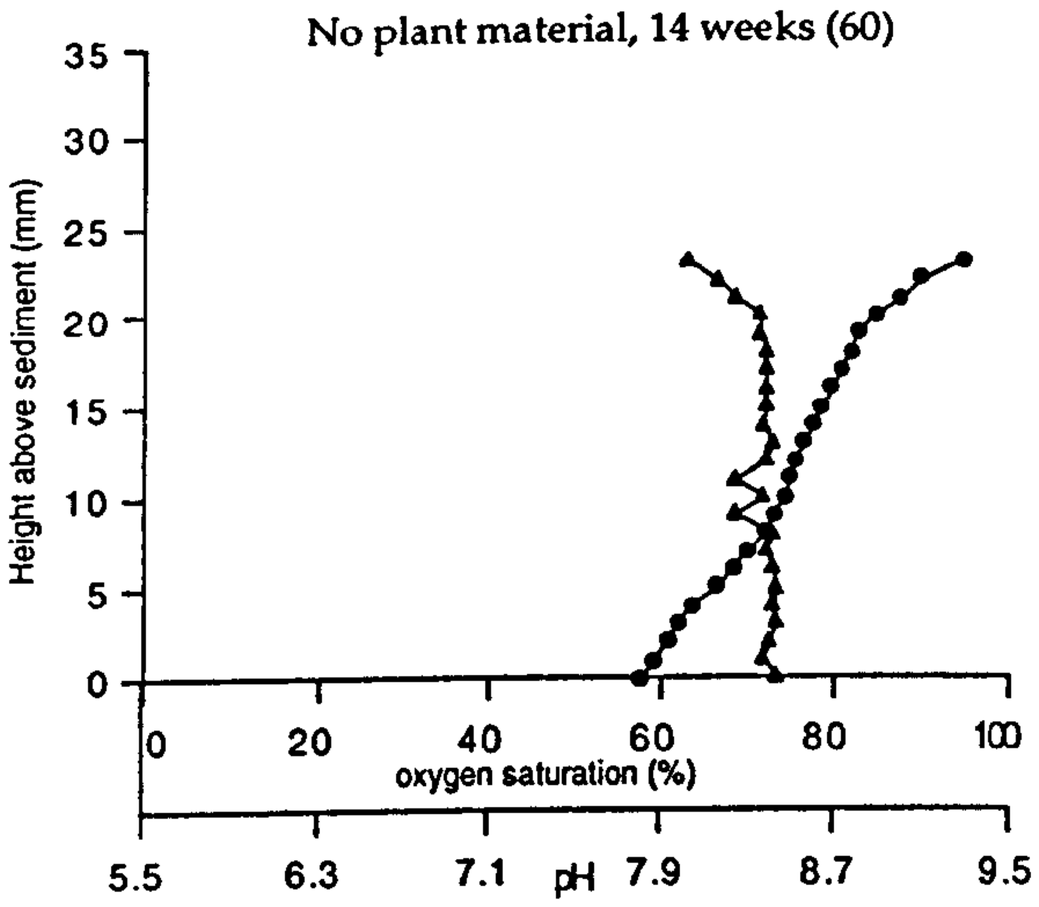

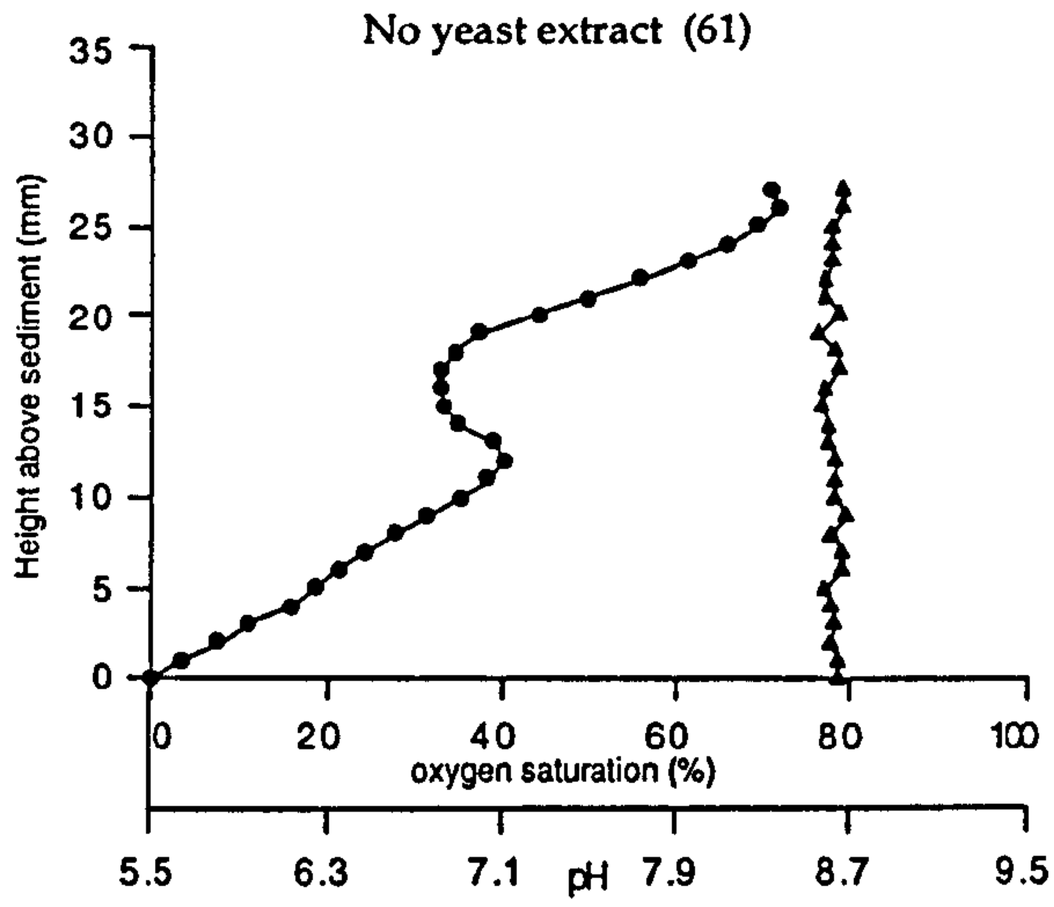

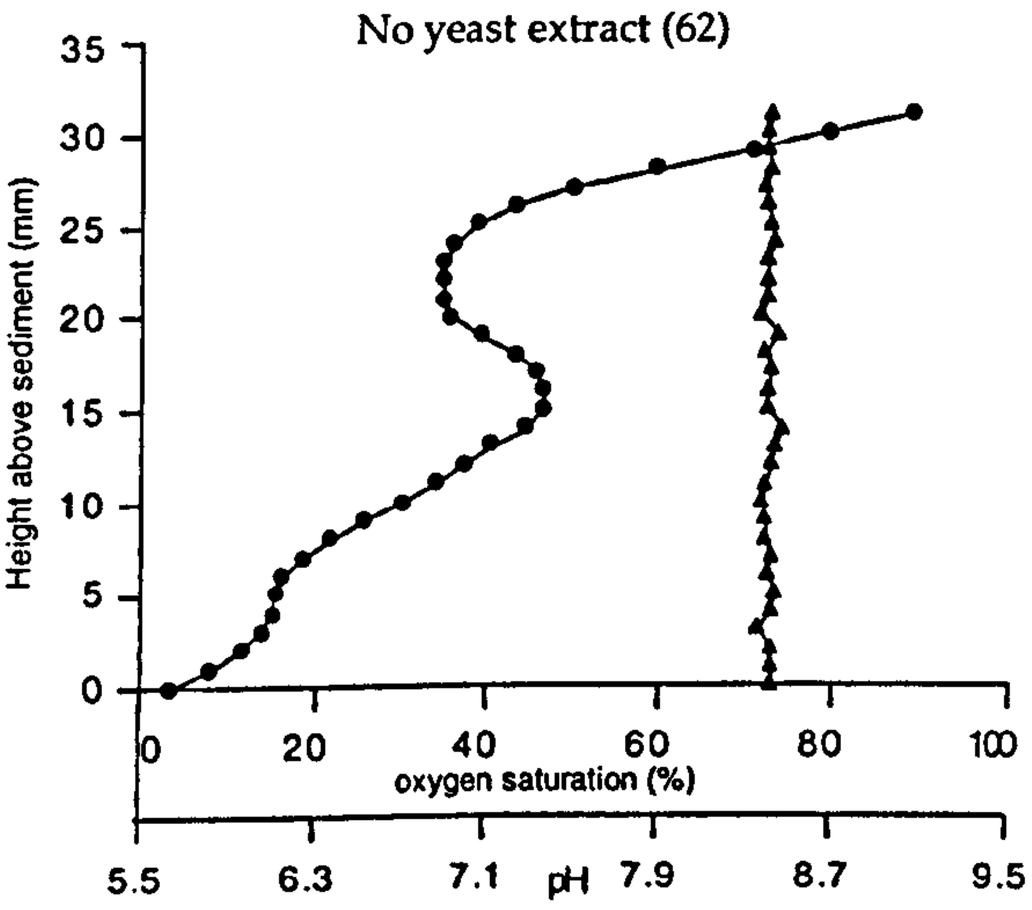

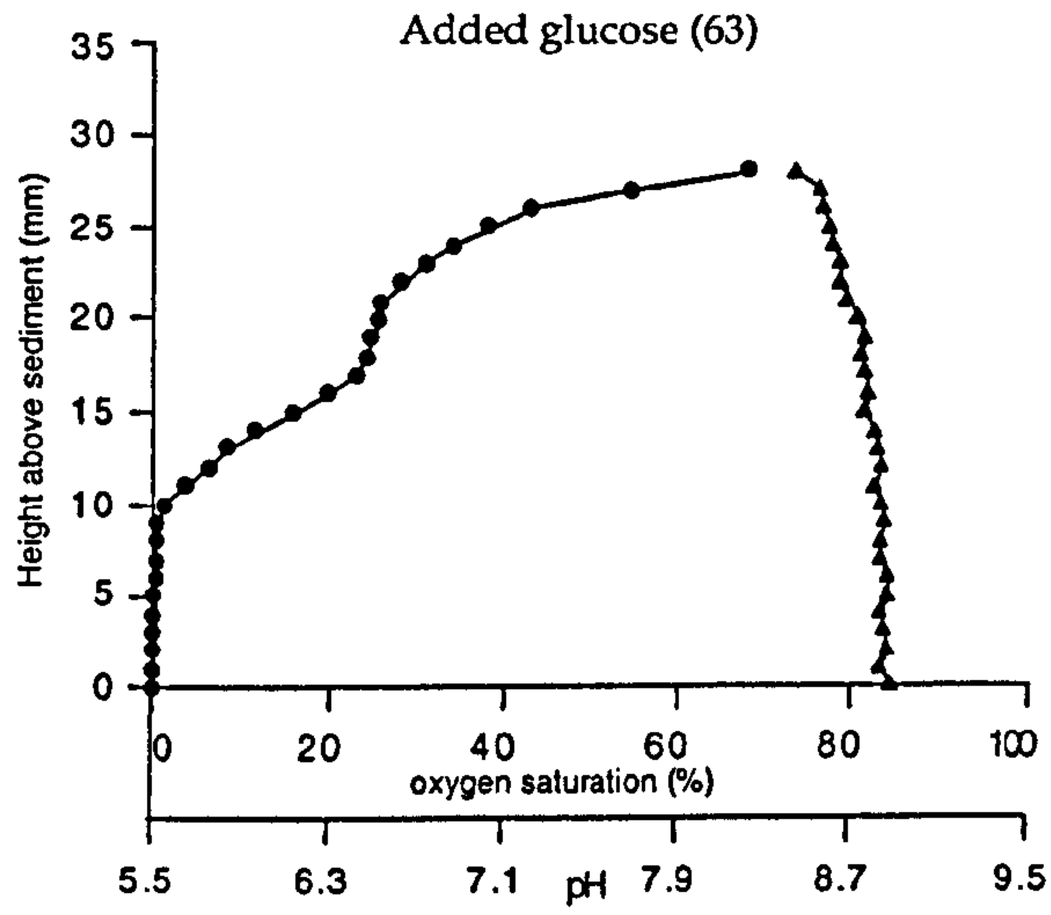

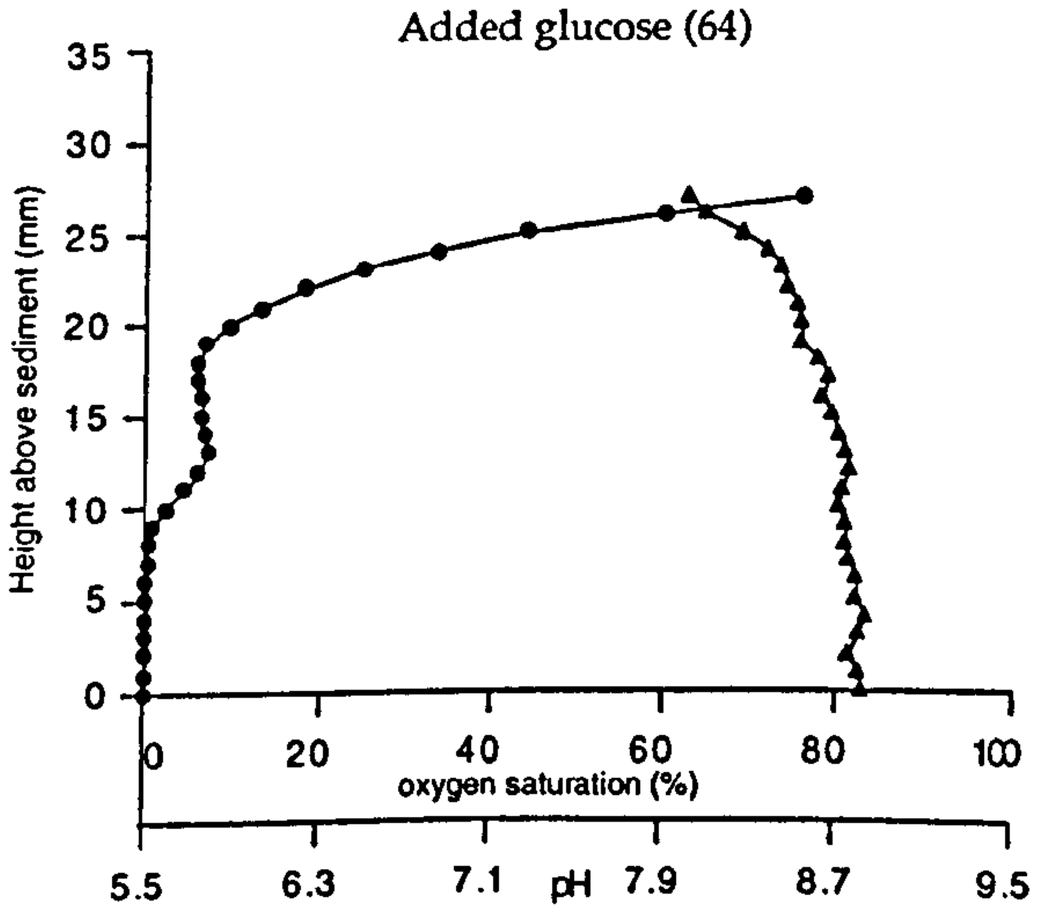

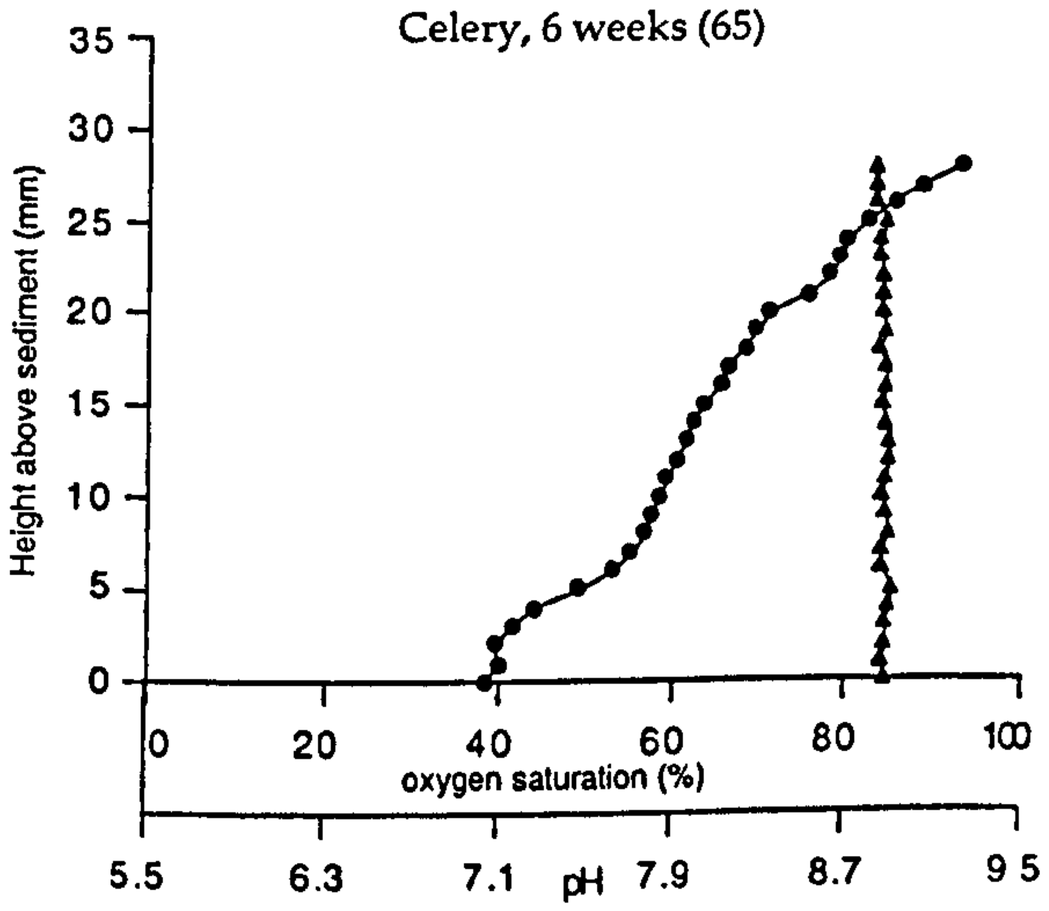

Oxygen and pH depth profiles for open marine systems after 12 weeks unless otherwise stated. Infilled circles represent oxygen data points. Infilled triangles represent pH data points. The highest data points above the sediment represent the air-medium interface.

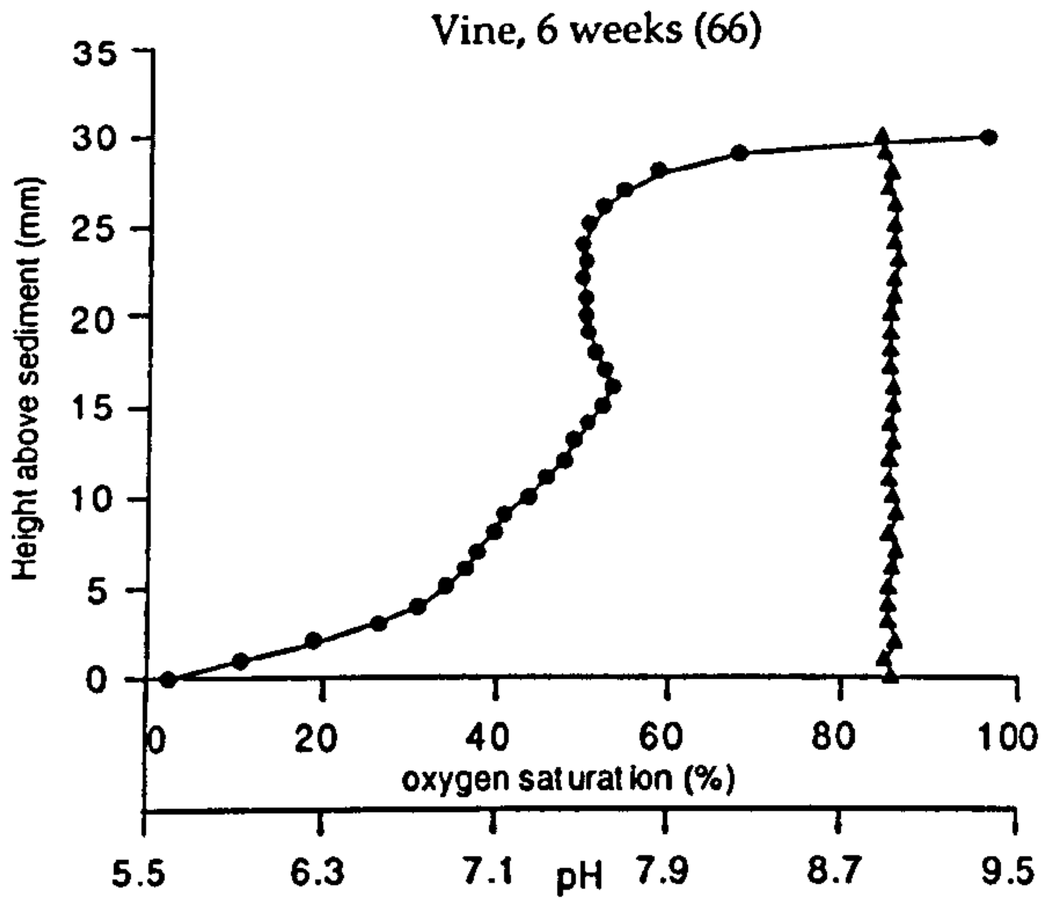

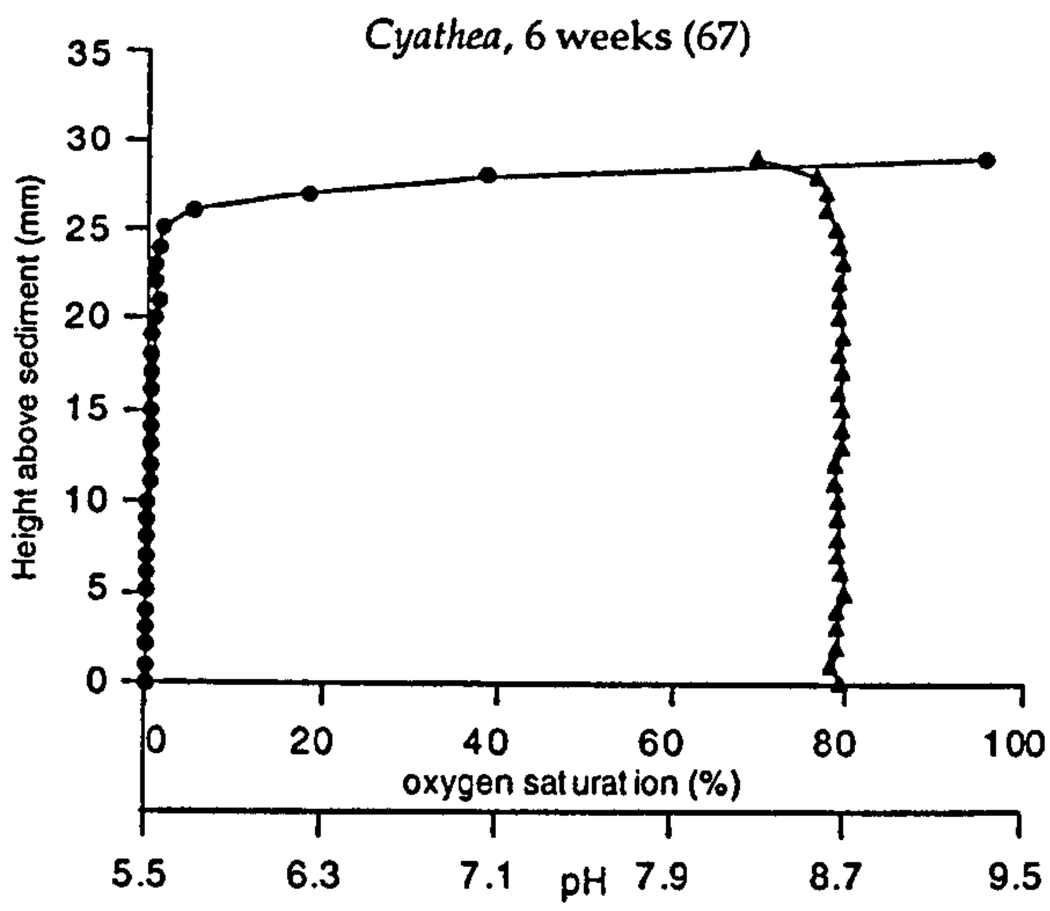

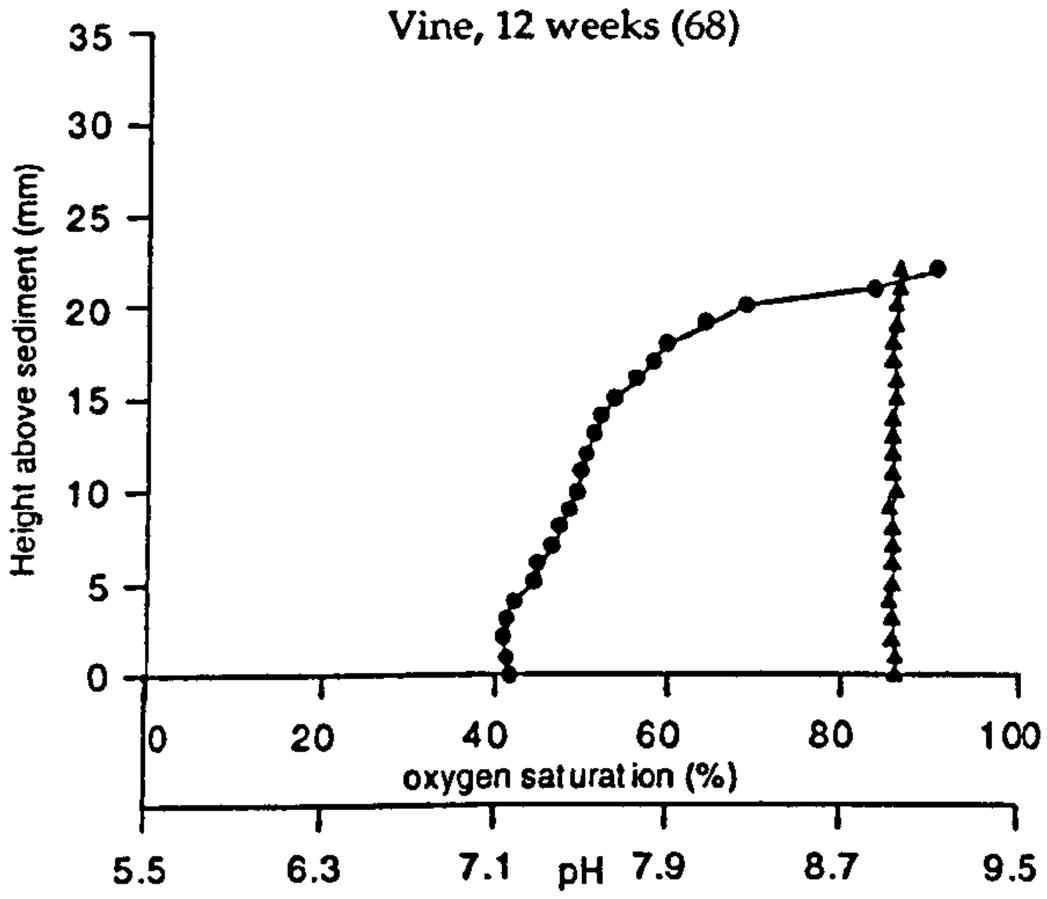

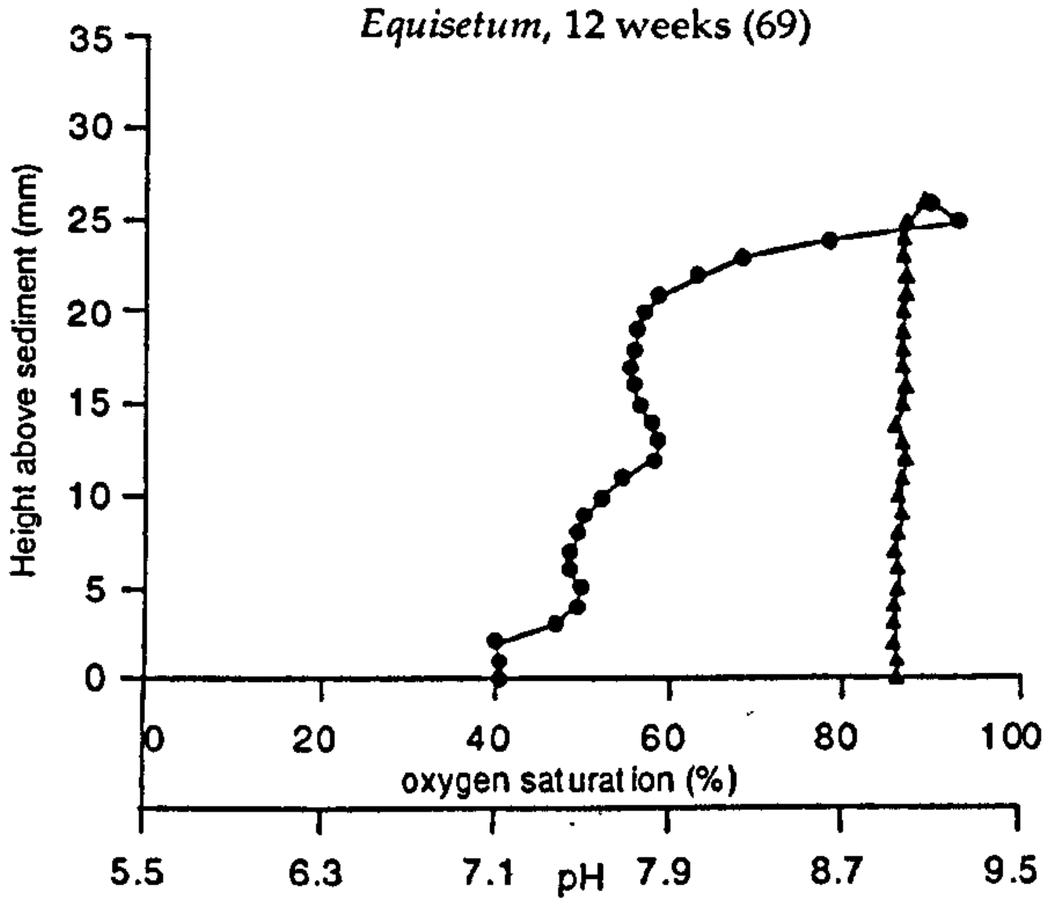

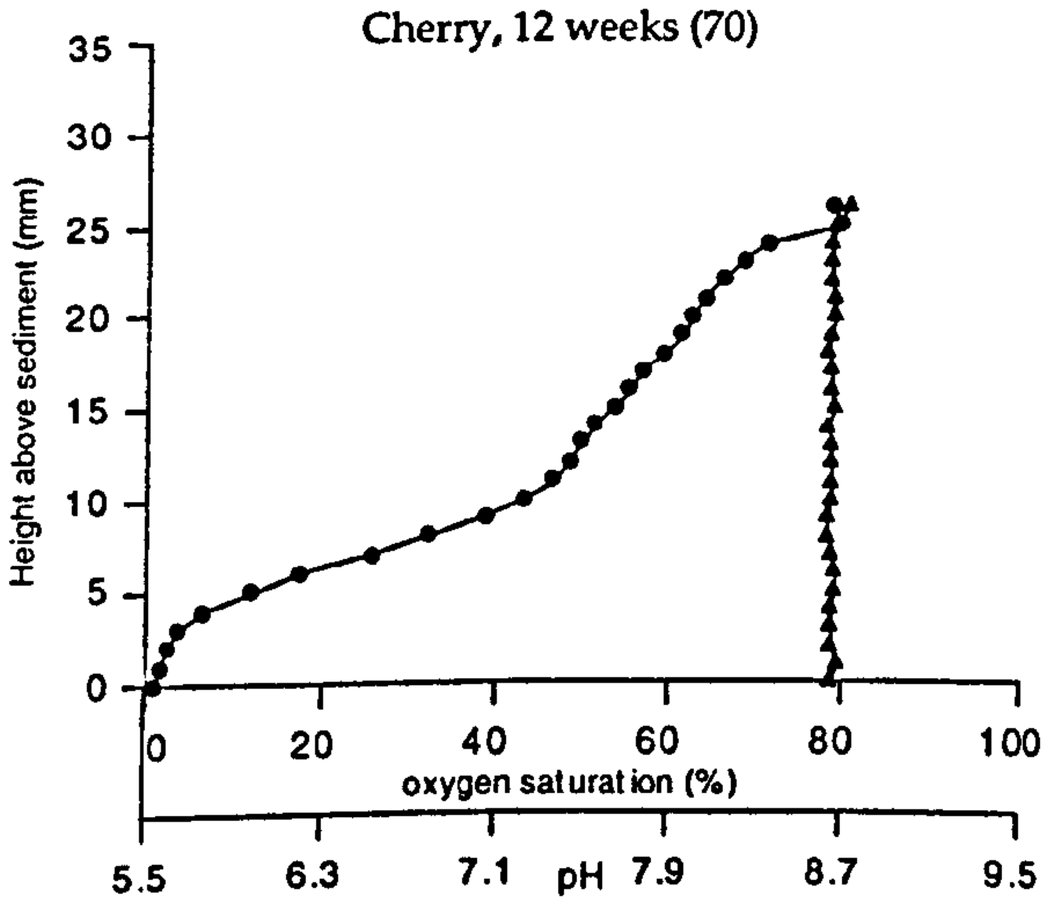

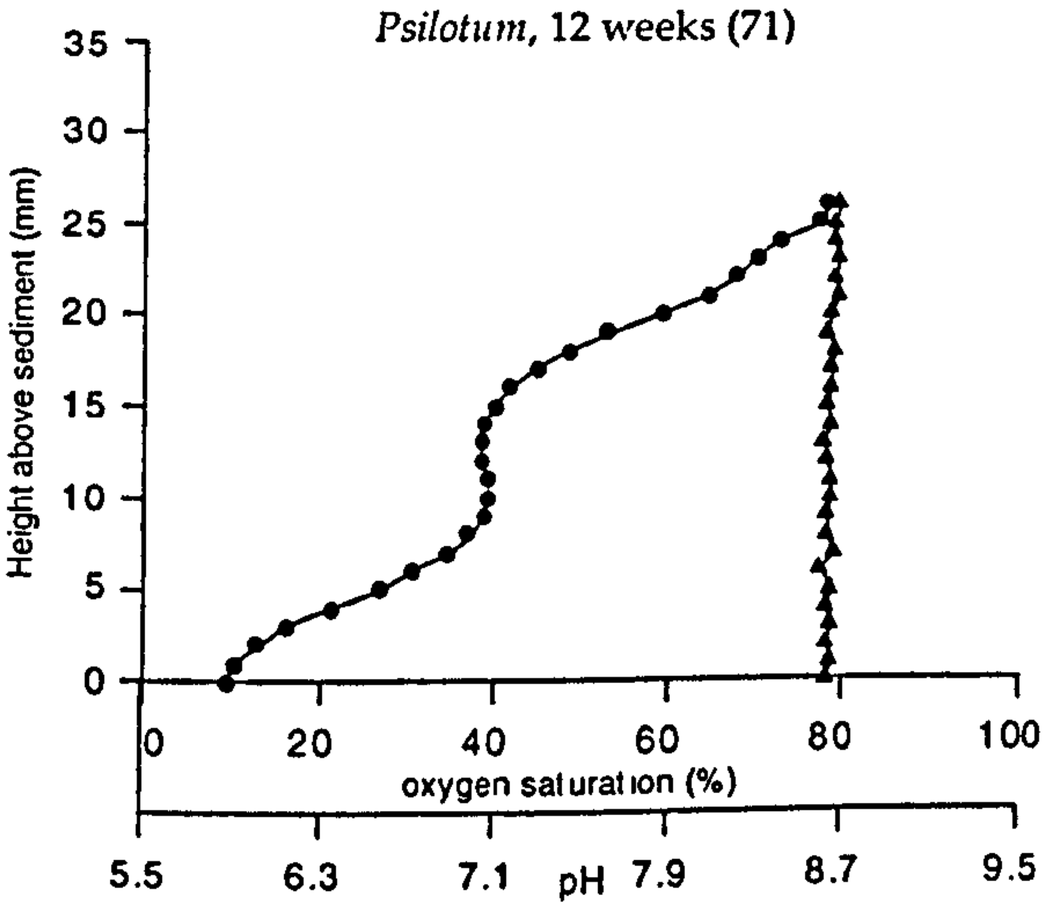

Oxygen and pH depth profiles for open marine systems. Infilled circles represent oxygen data points. Infilled triangles represent pH data points. The highest data points above the sediment represent the air-medium interface.

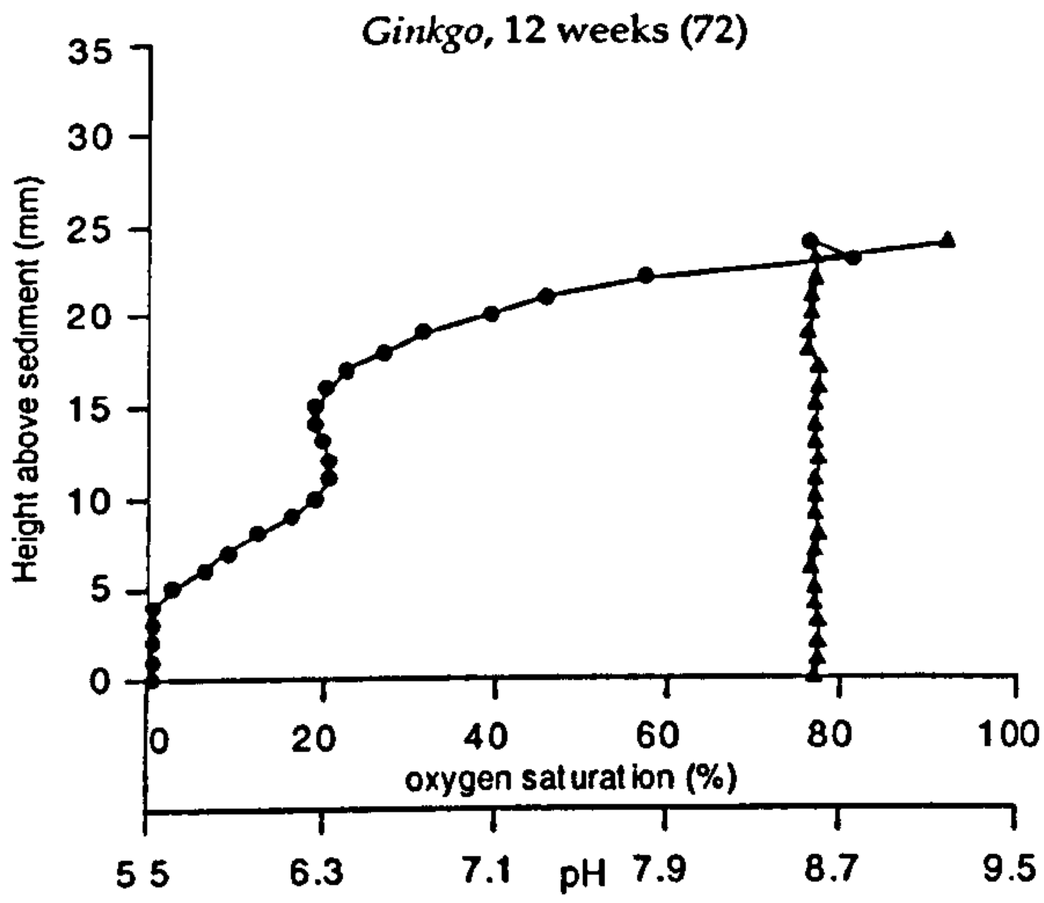

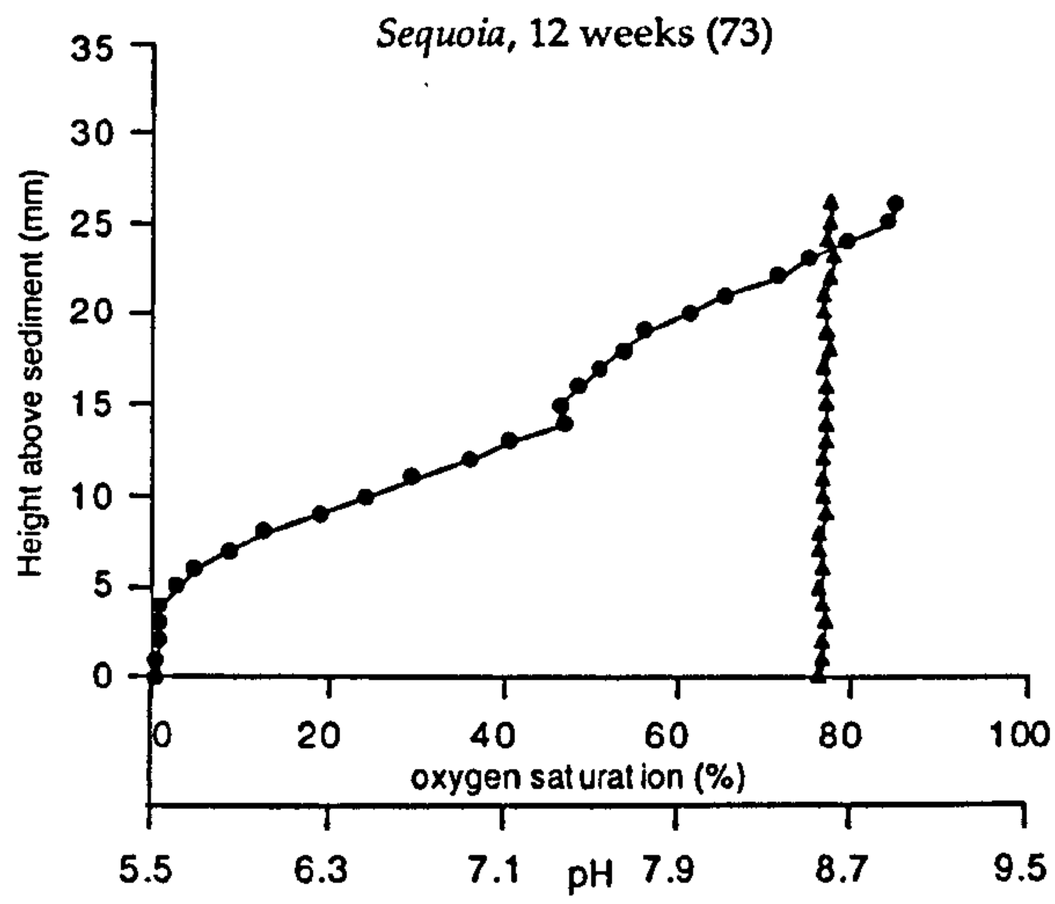

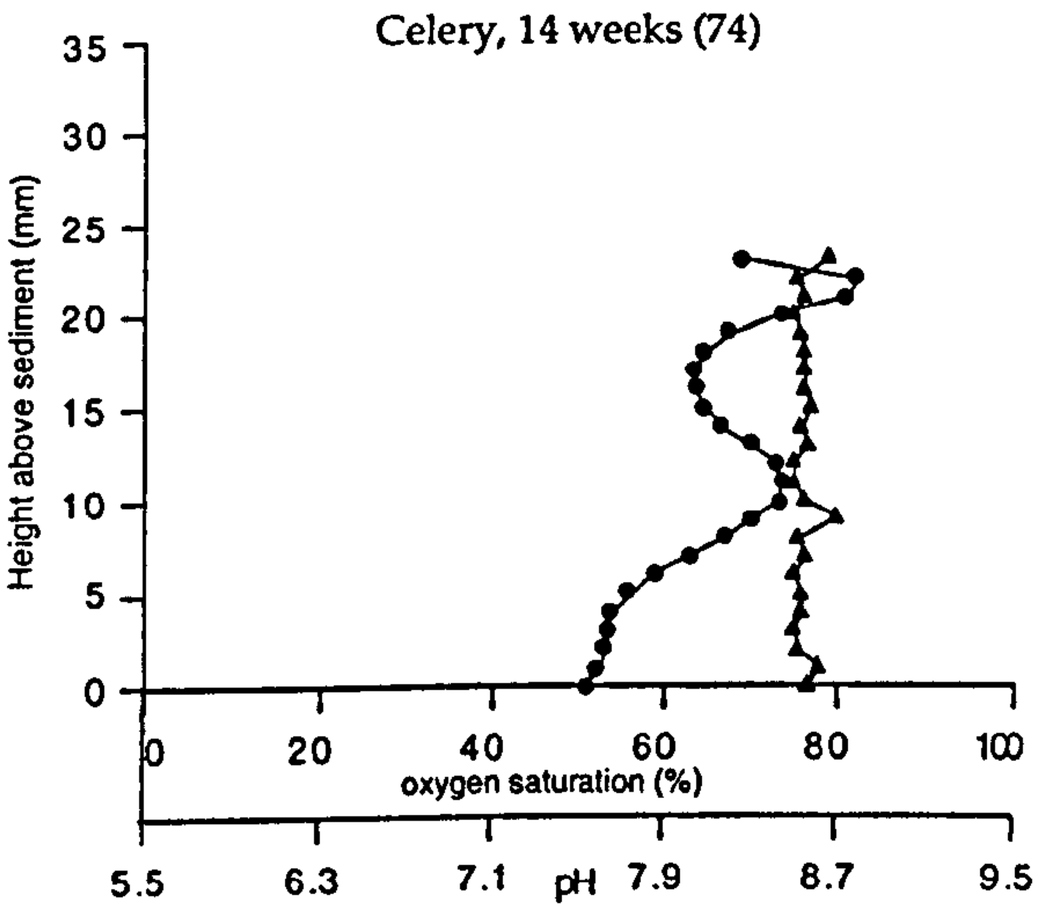

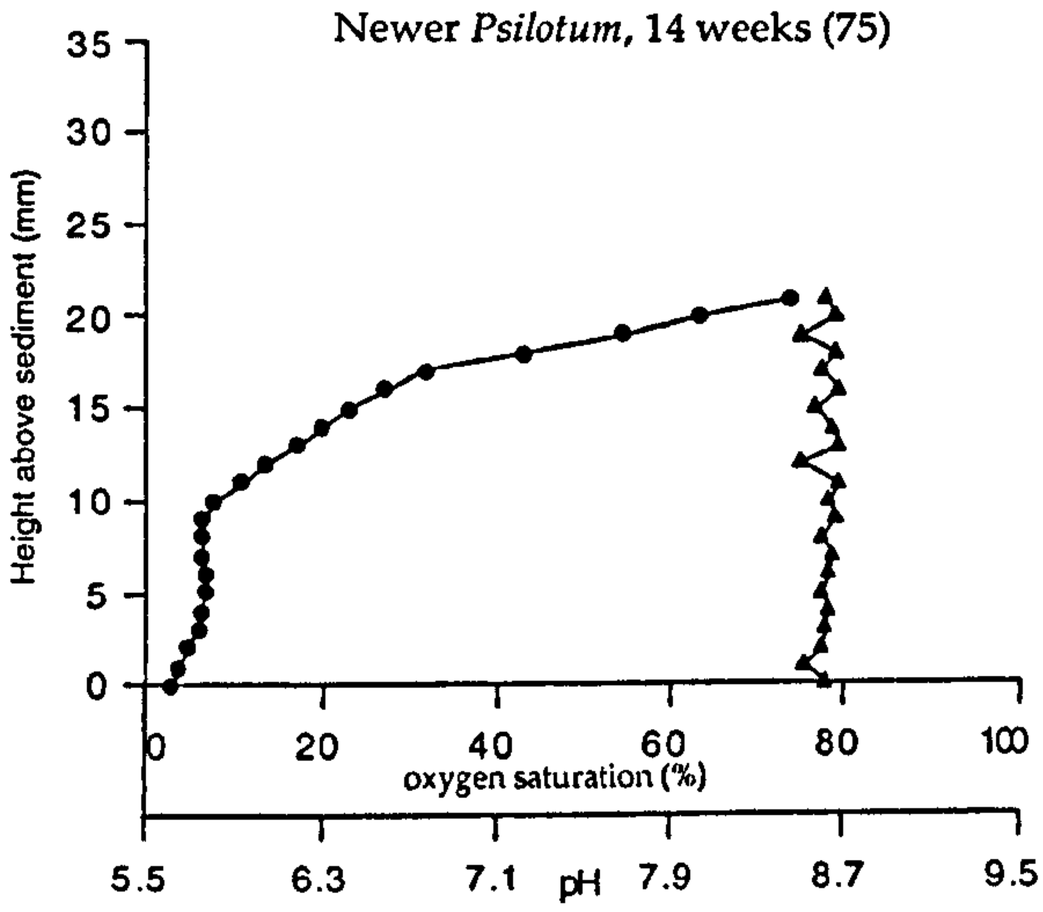

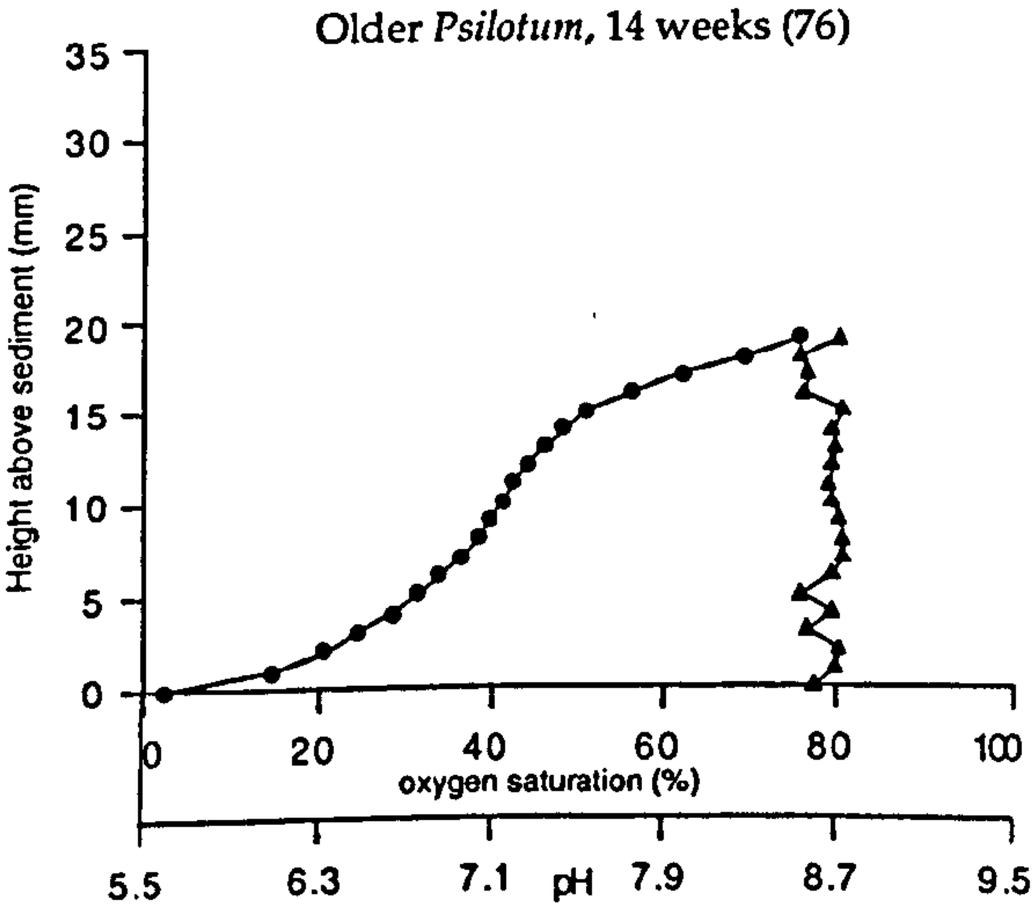

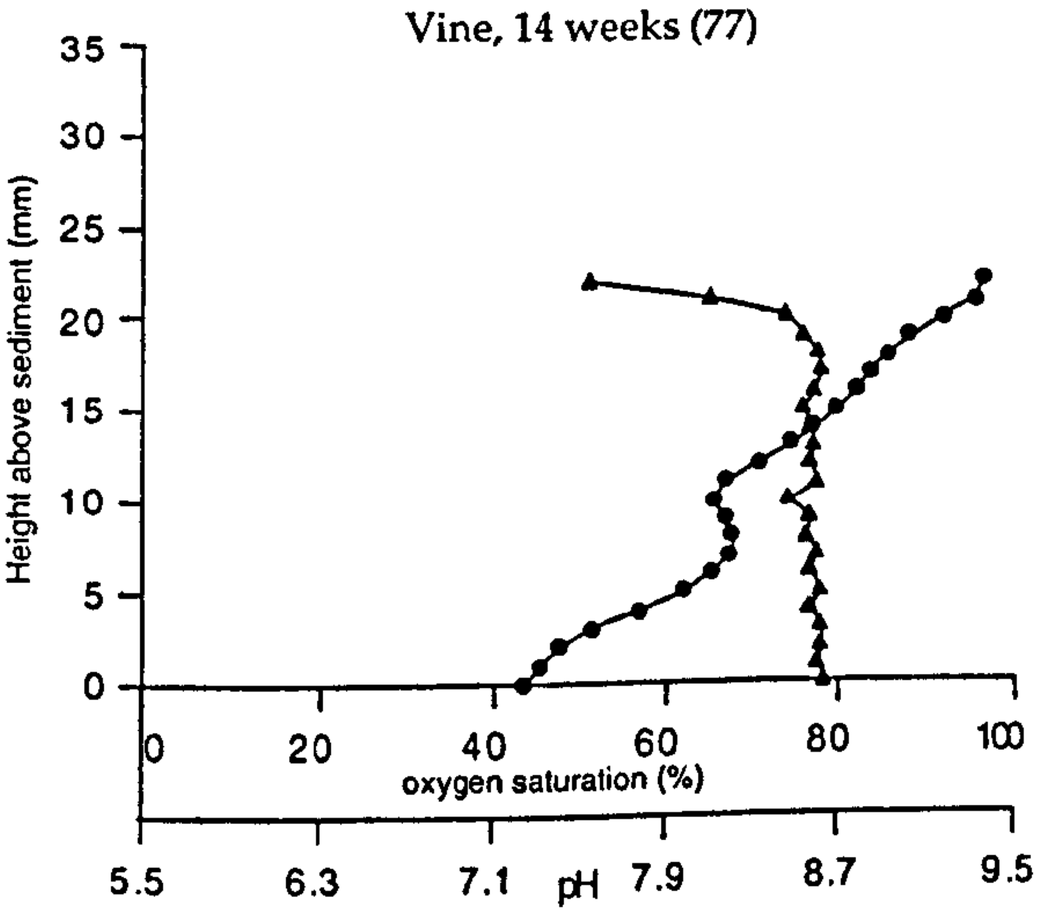

Oxygen and pH depth profiles for open marine systems. Infilled circles represent oxygen data points. Infilled triangles represent pH data points. The highest data points above the sediment represent the air-medium interface.

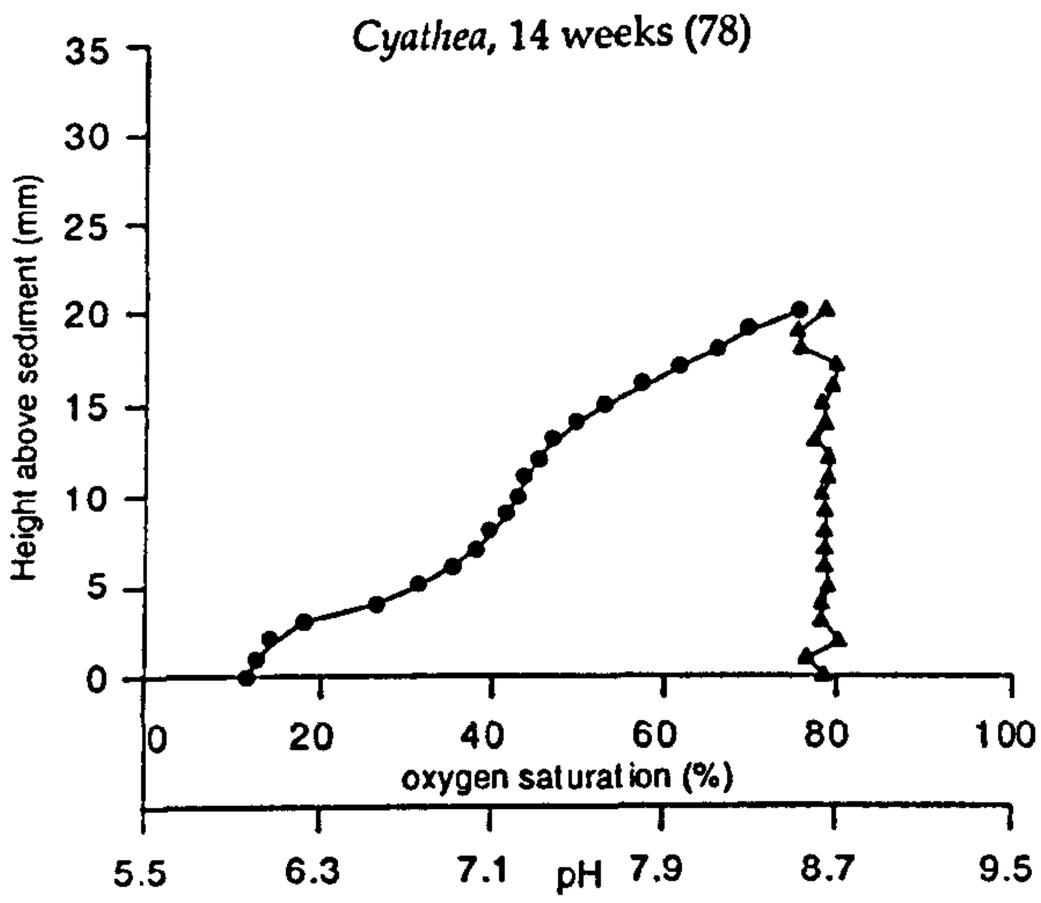

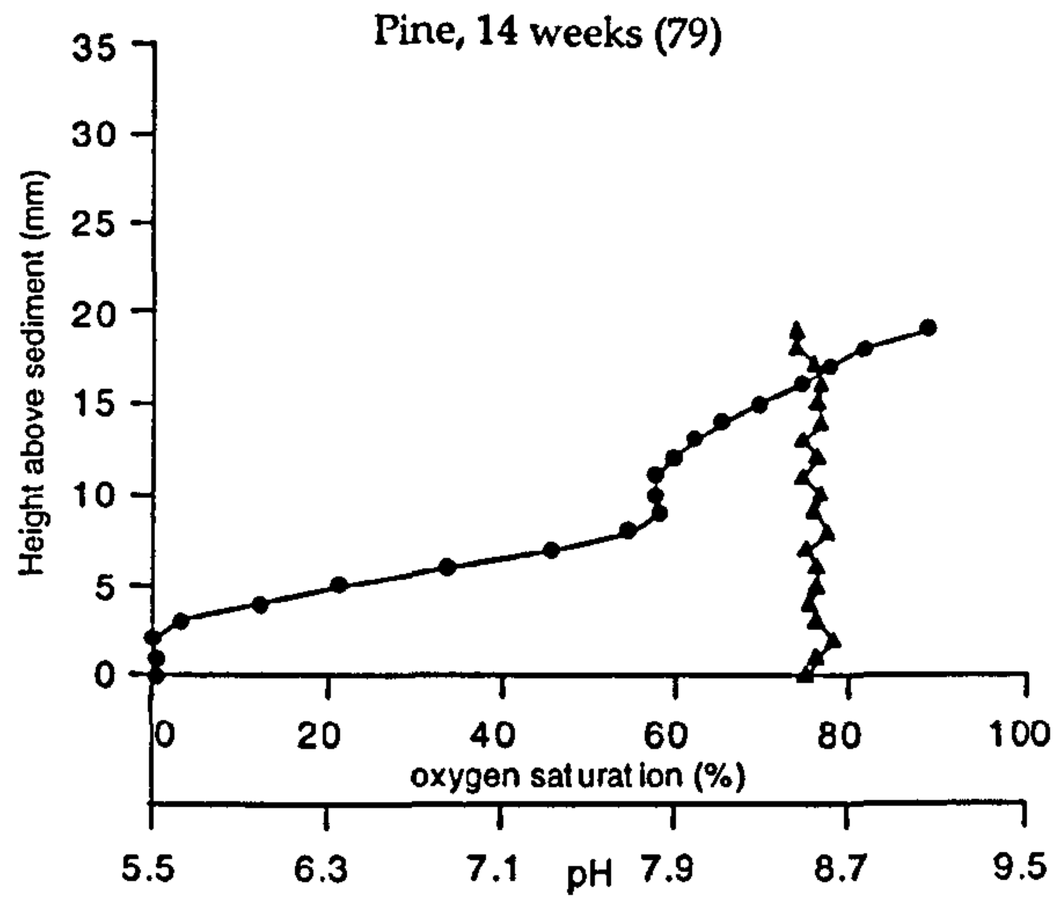

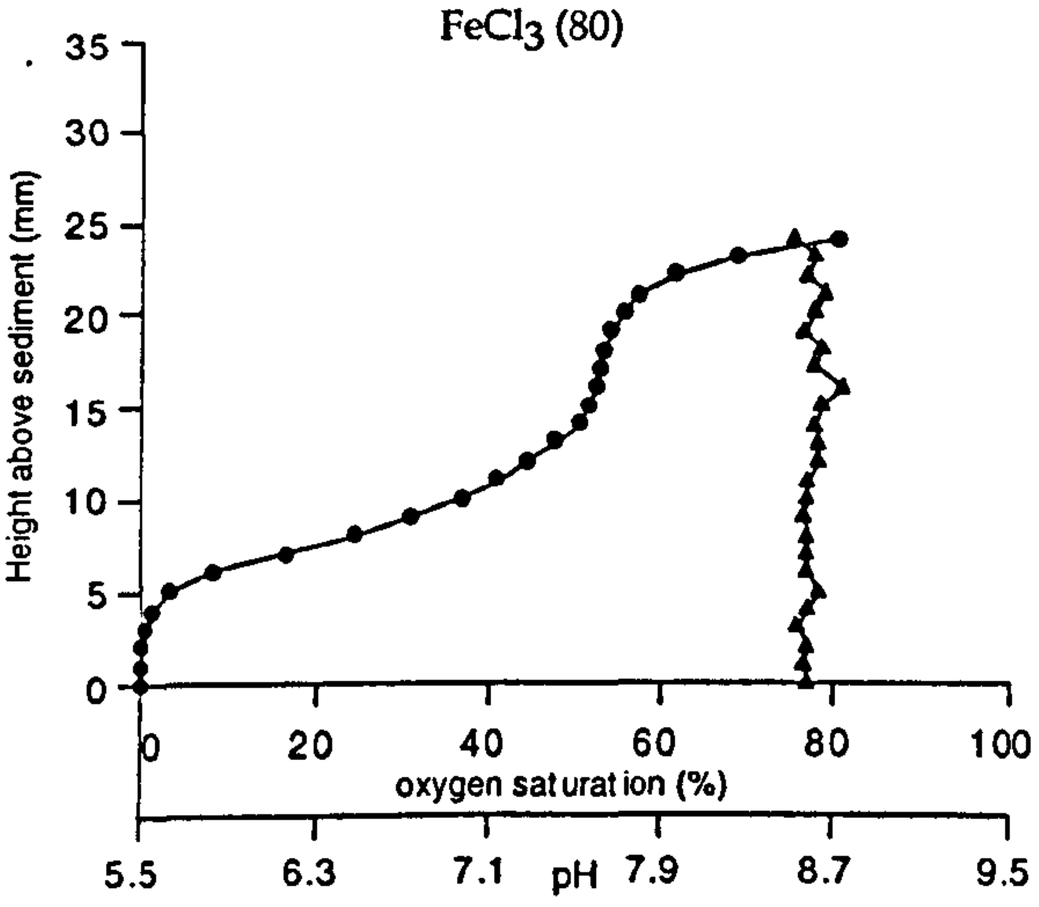

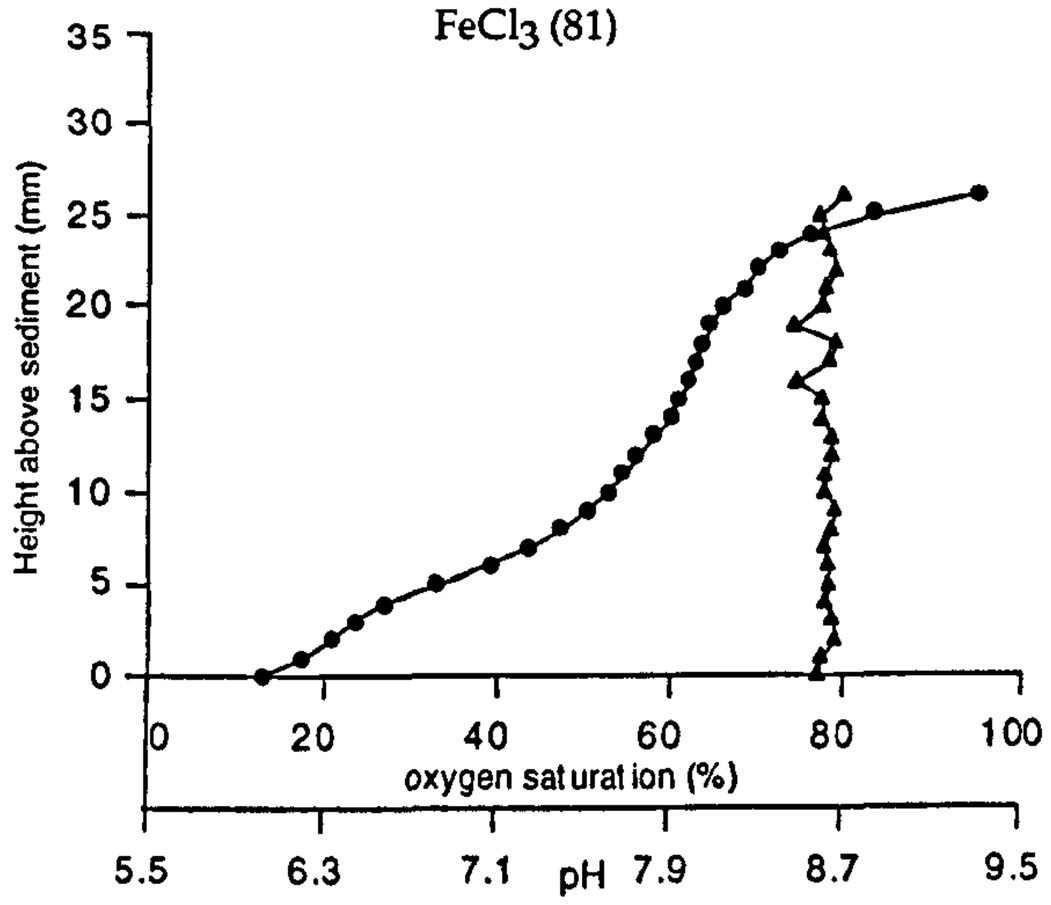

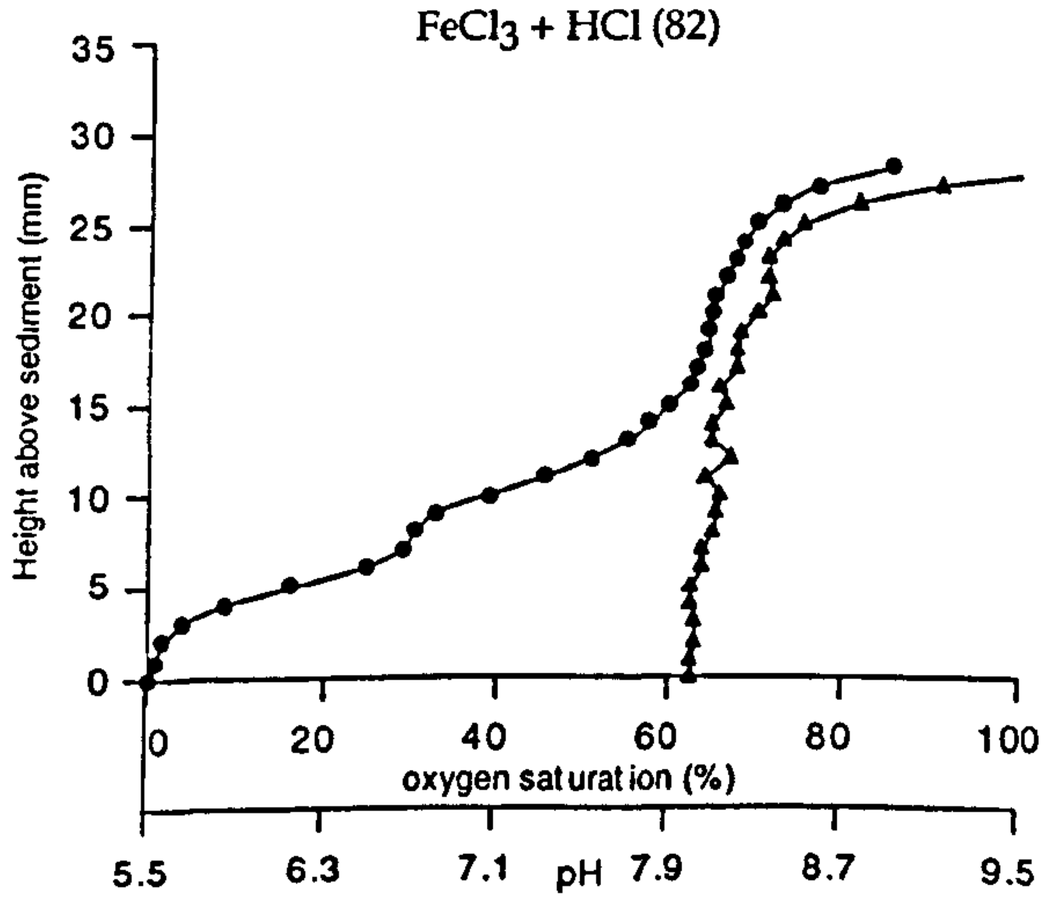

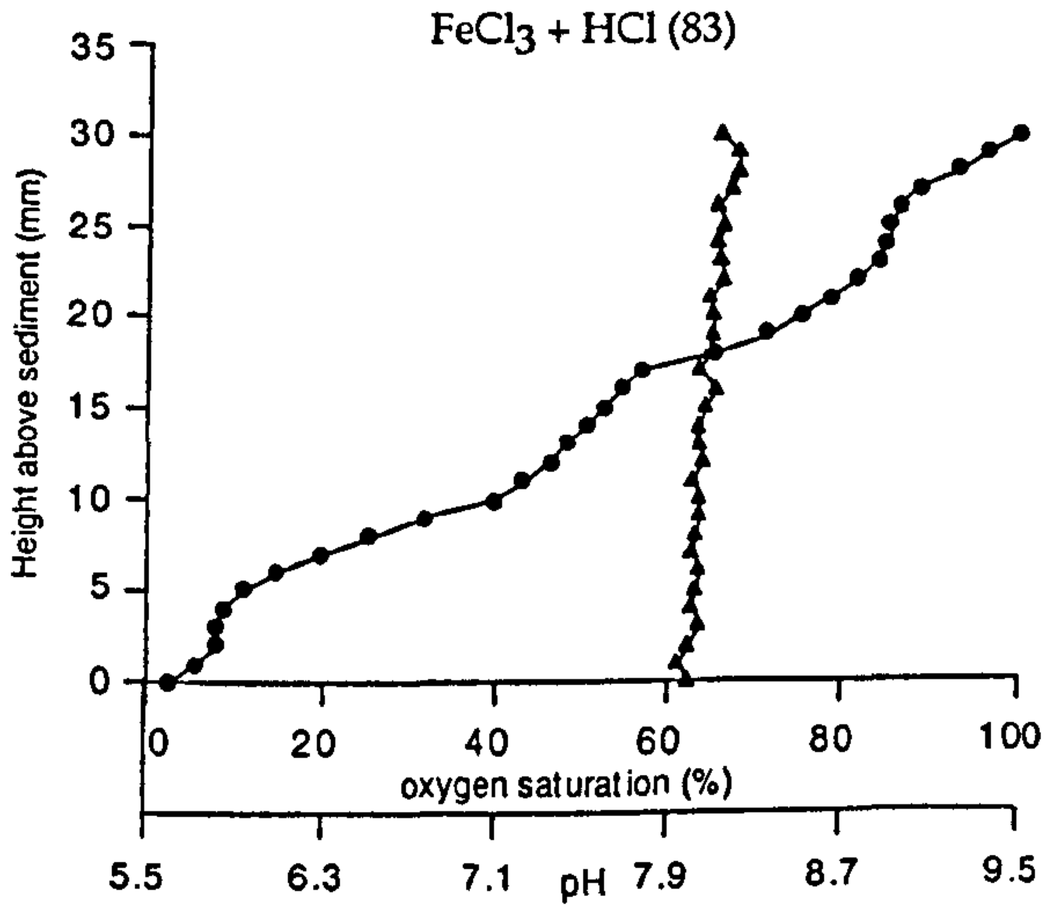

Oxygen and pH depth profiles for open marine systems after 12 weeks unless otherwise stated. Infilled circles represent oxygen data points. Infilled triangles represent pH data points. The highest data points above the sediment represent the air-medium interface.

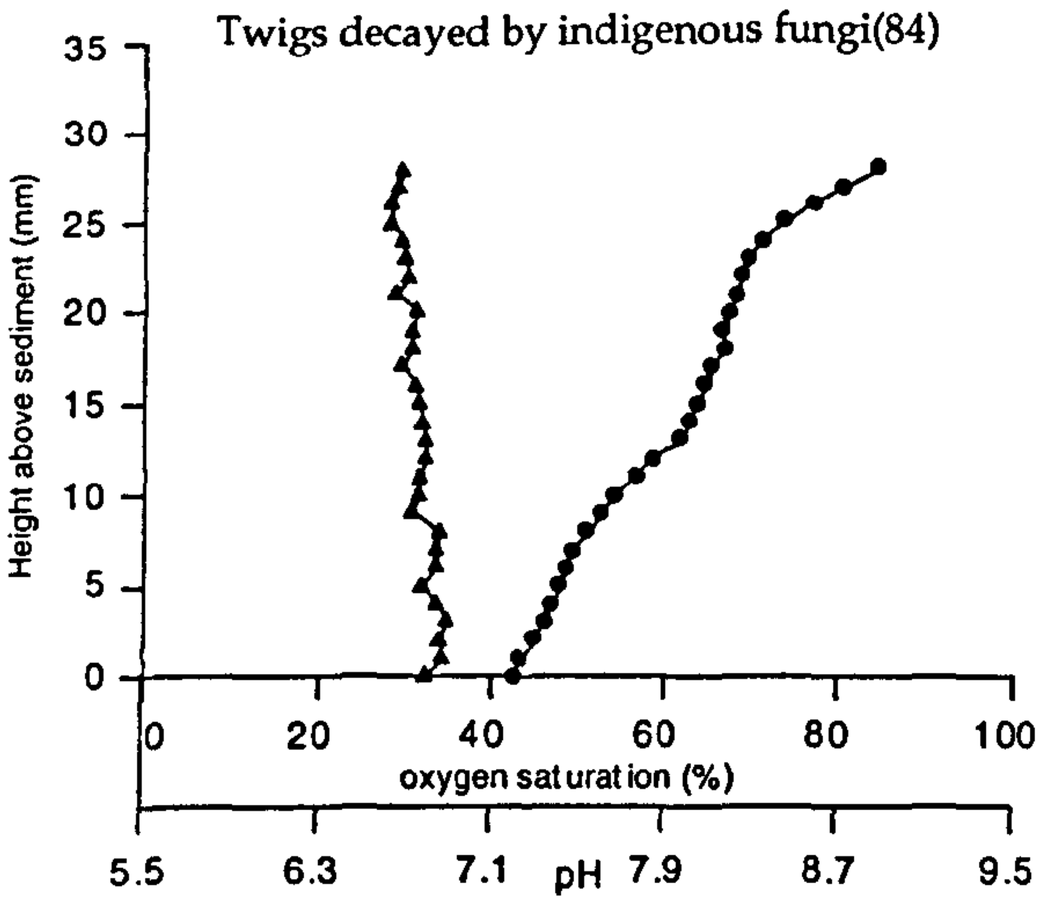

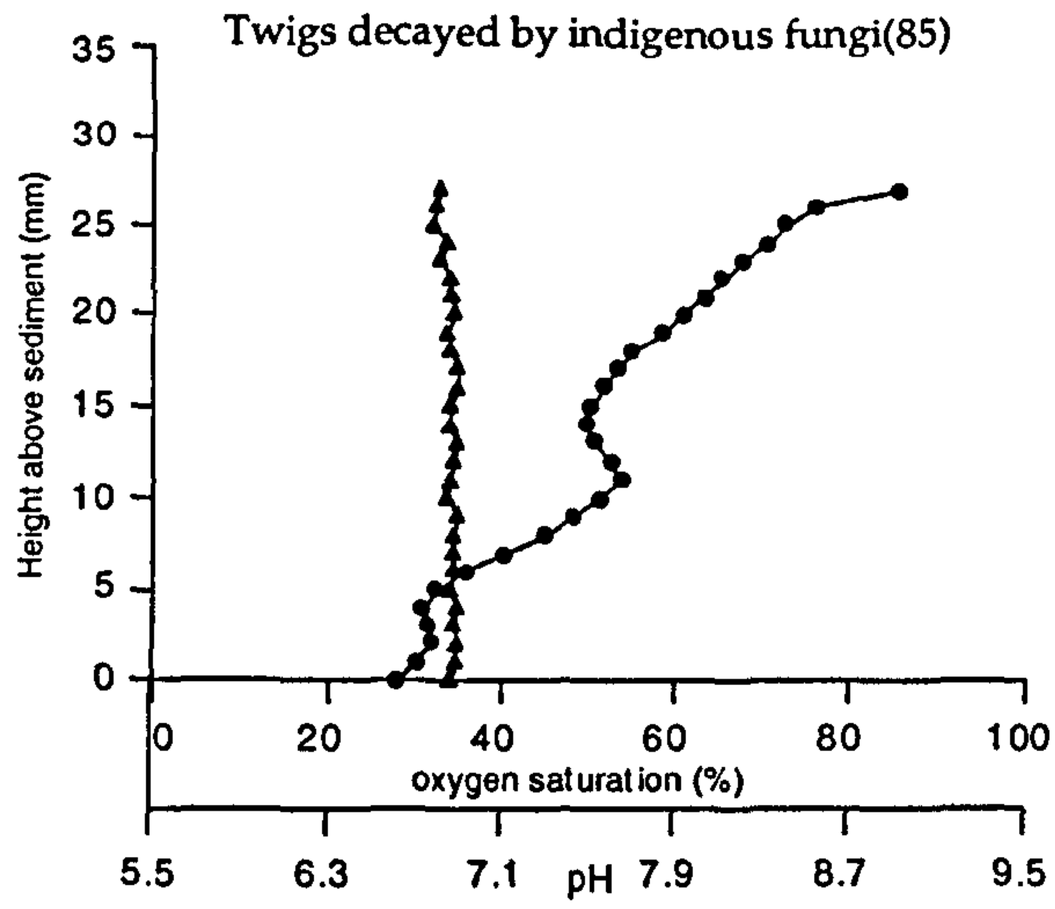

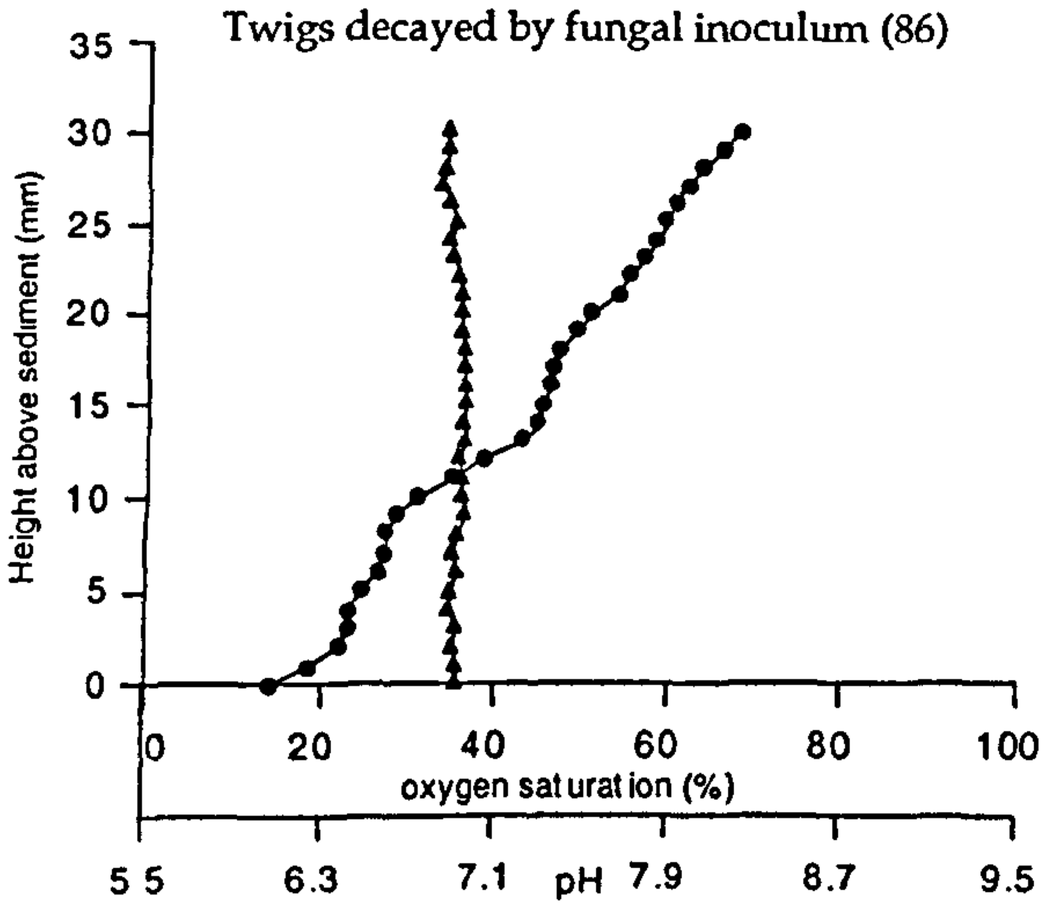

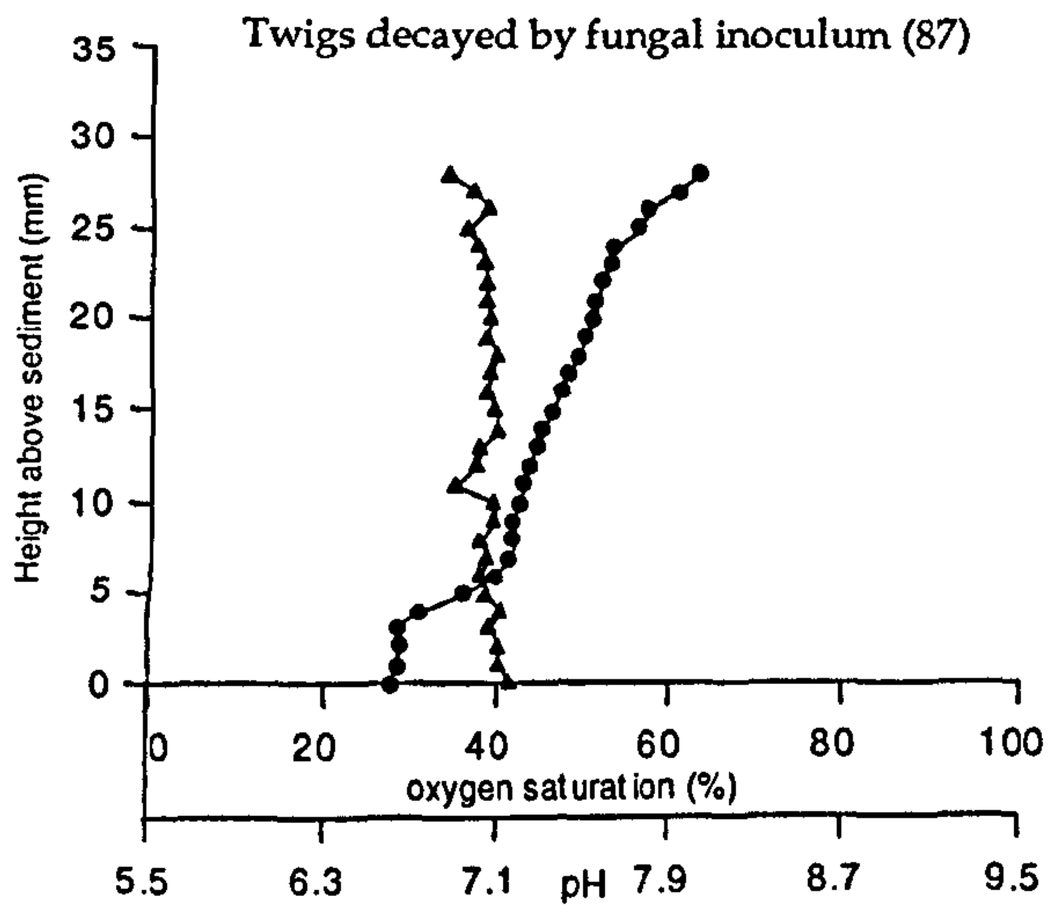

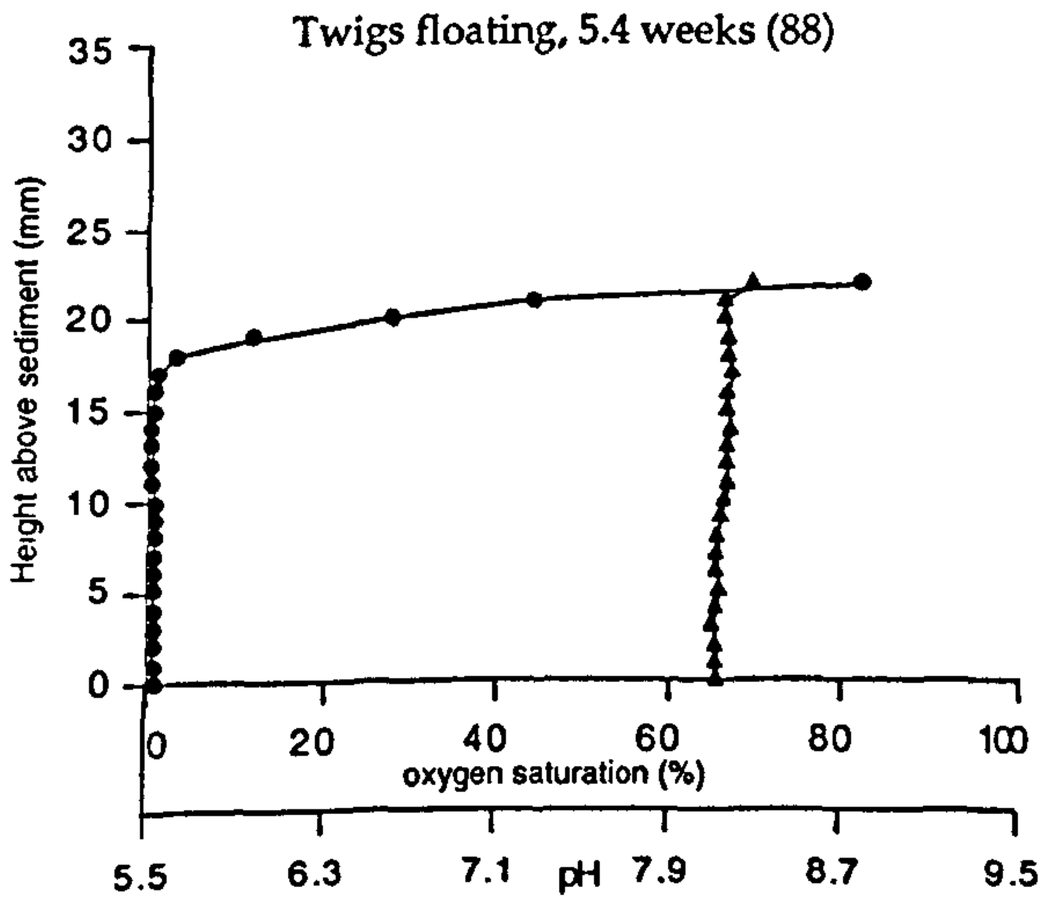

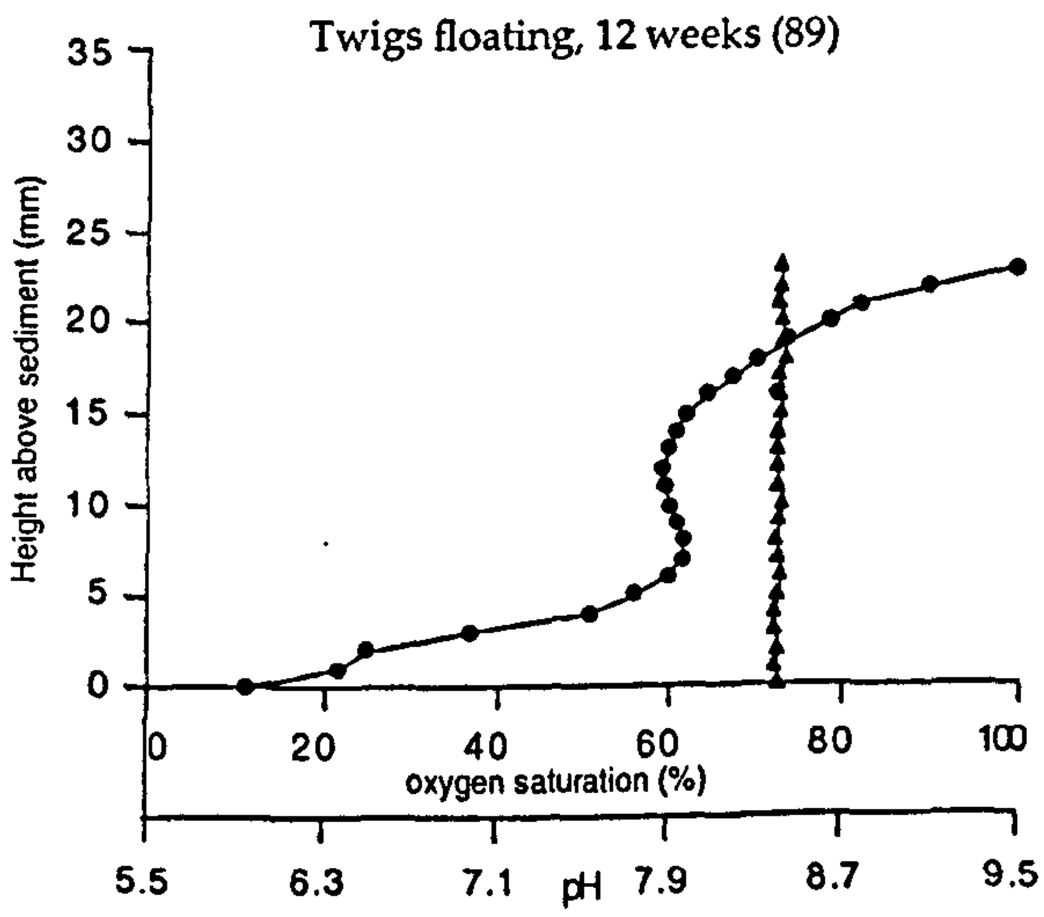

Oxygen and pH depth profiles for open marine systems after 12 weeks unless otherwise stated. Infilled circles represent oxygen data points. Infilled triangles represent pH data points. The highest data points above the sediment represent the air-medium interface.

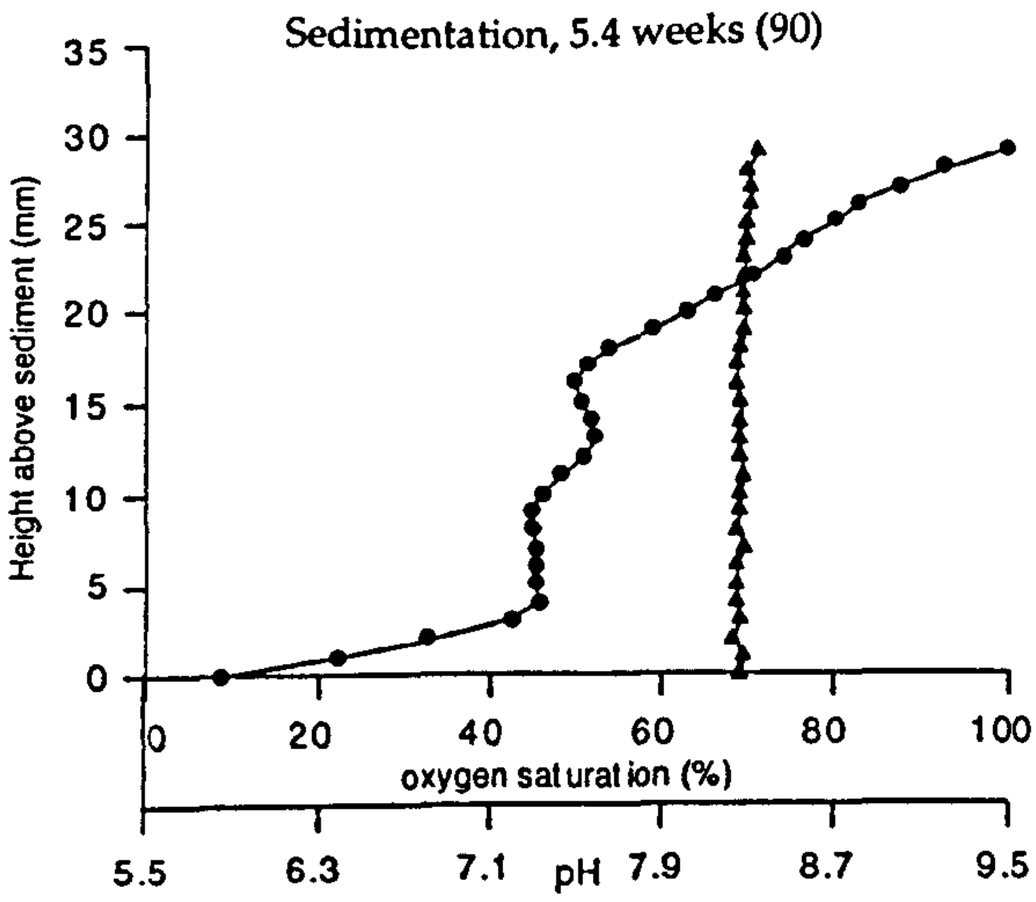

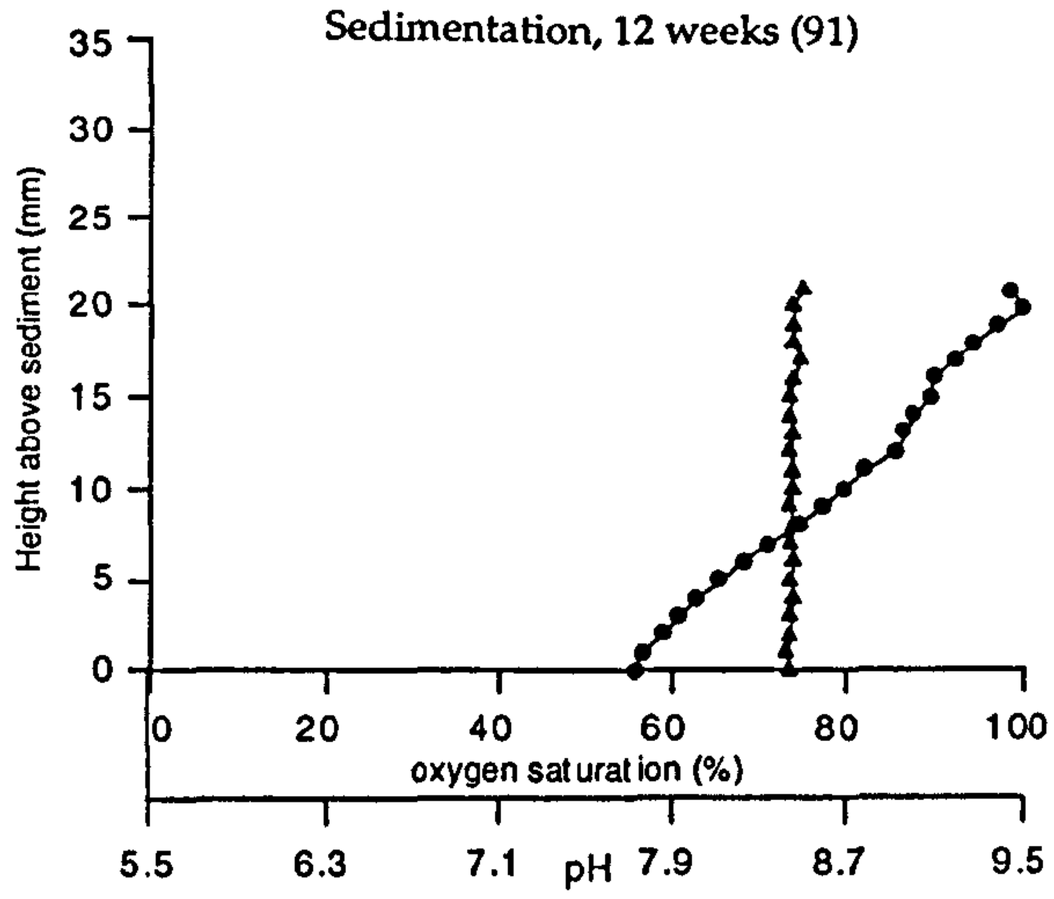

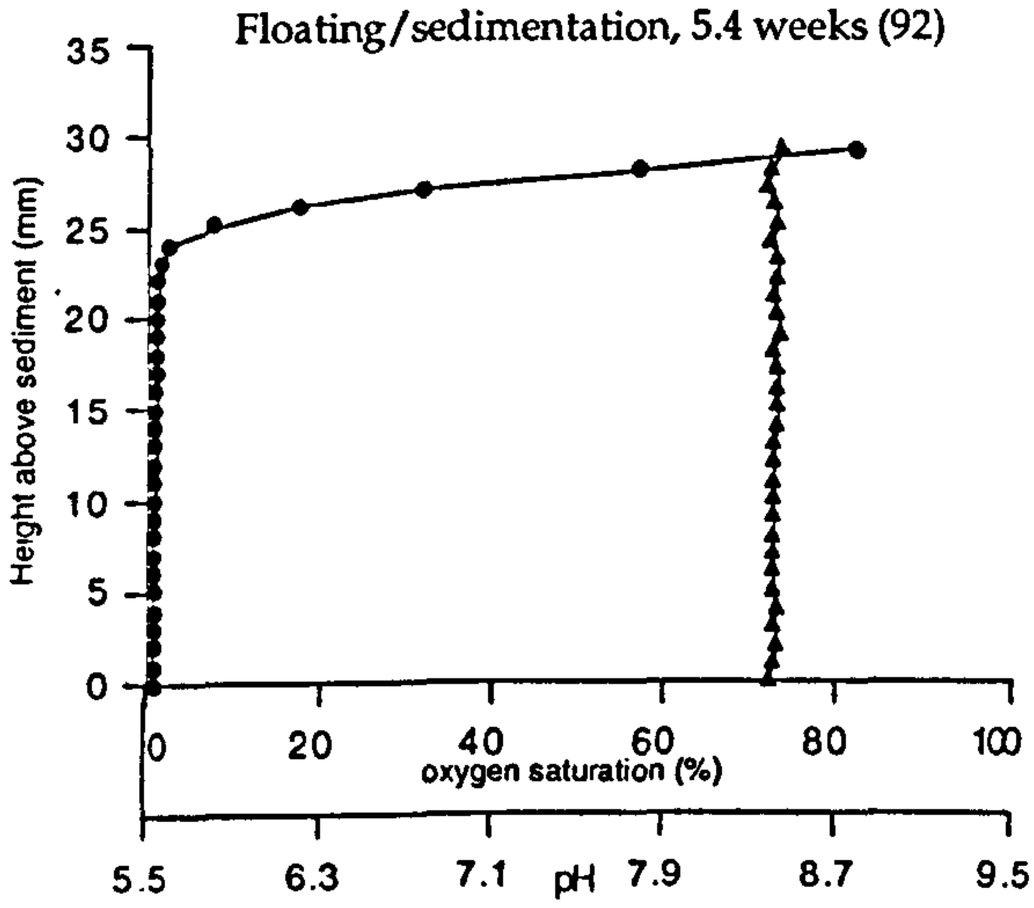

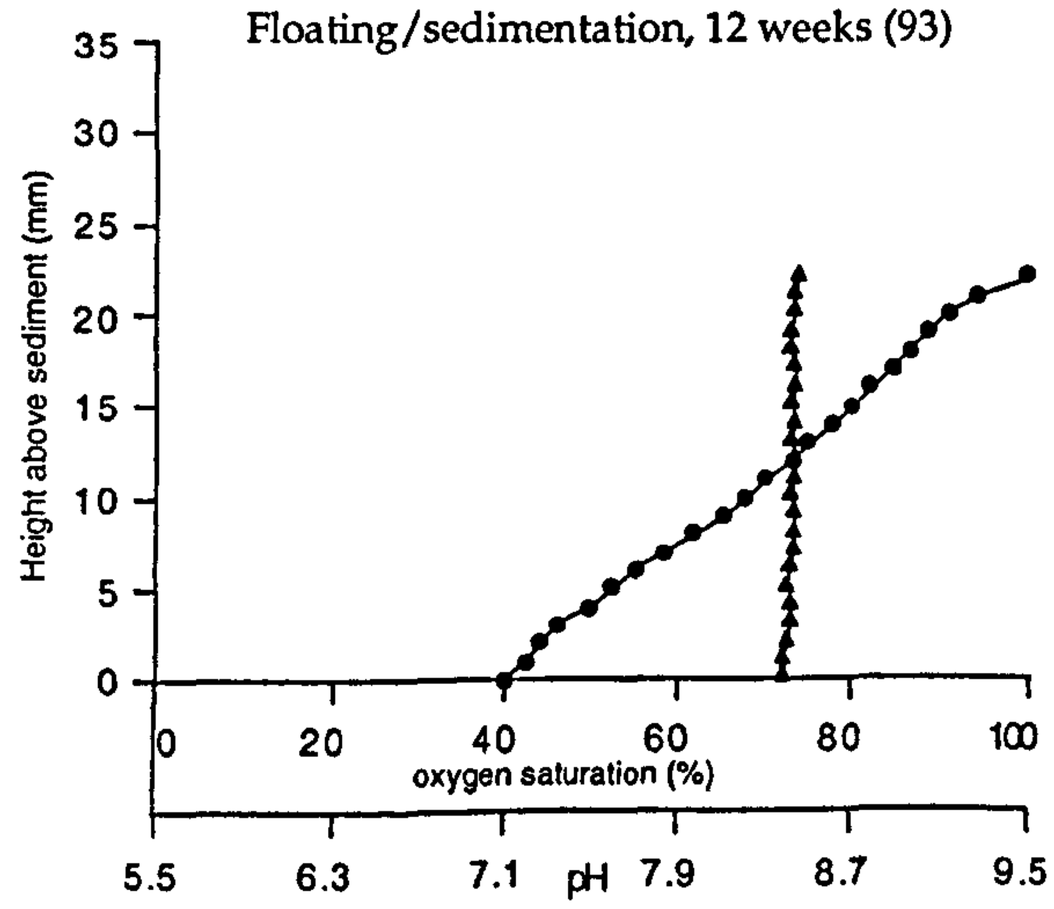

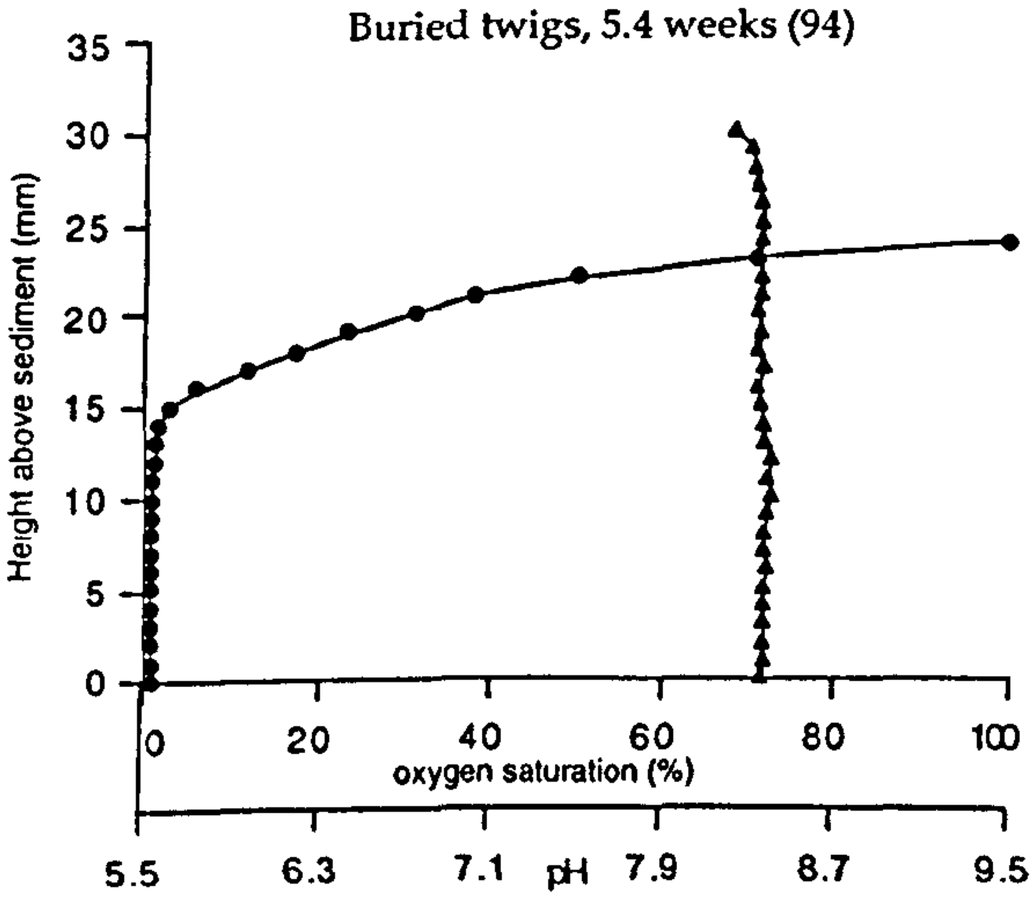

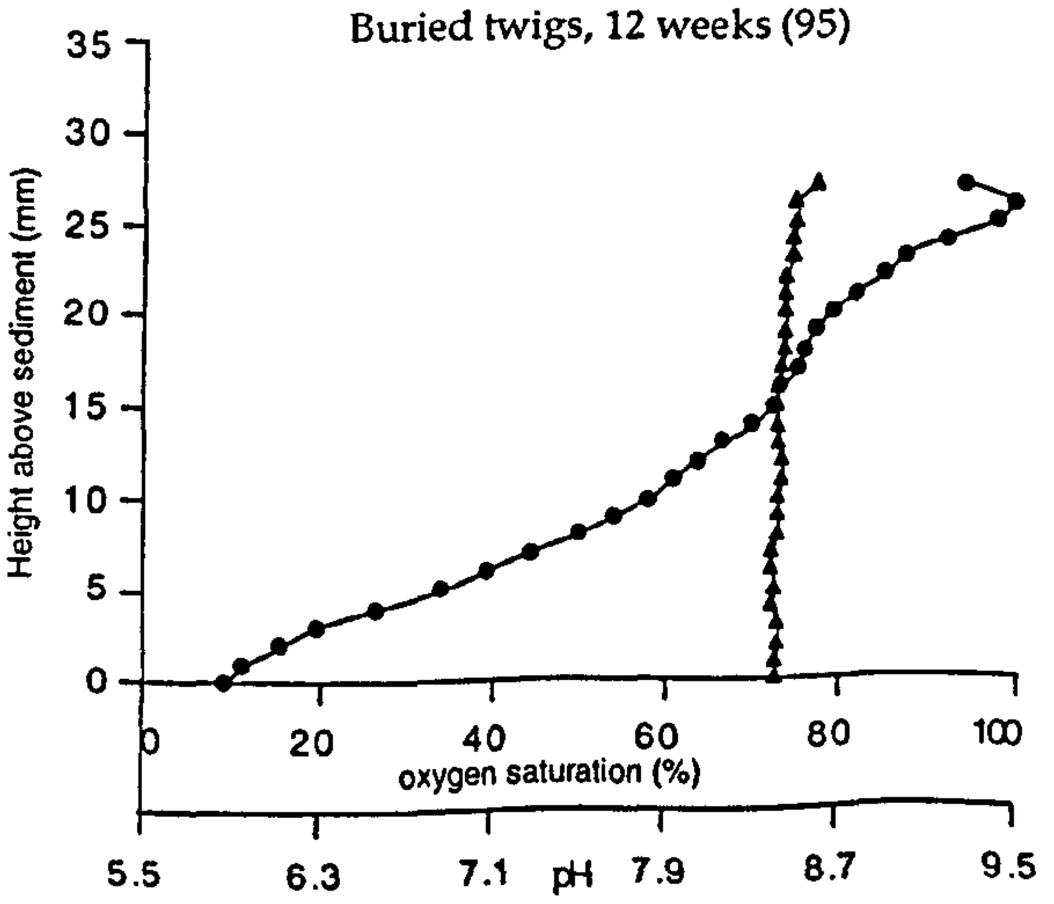

Oxygen and pH depth profiles for open marine systems. Infilled circles represent oxygen data points. Infilled triangles represent pH data points. The highest data points above the sediment represent the air-medium interface.

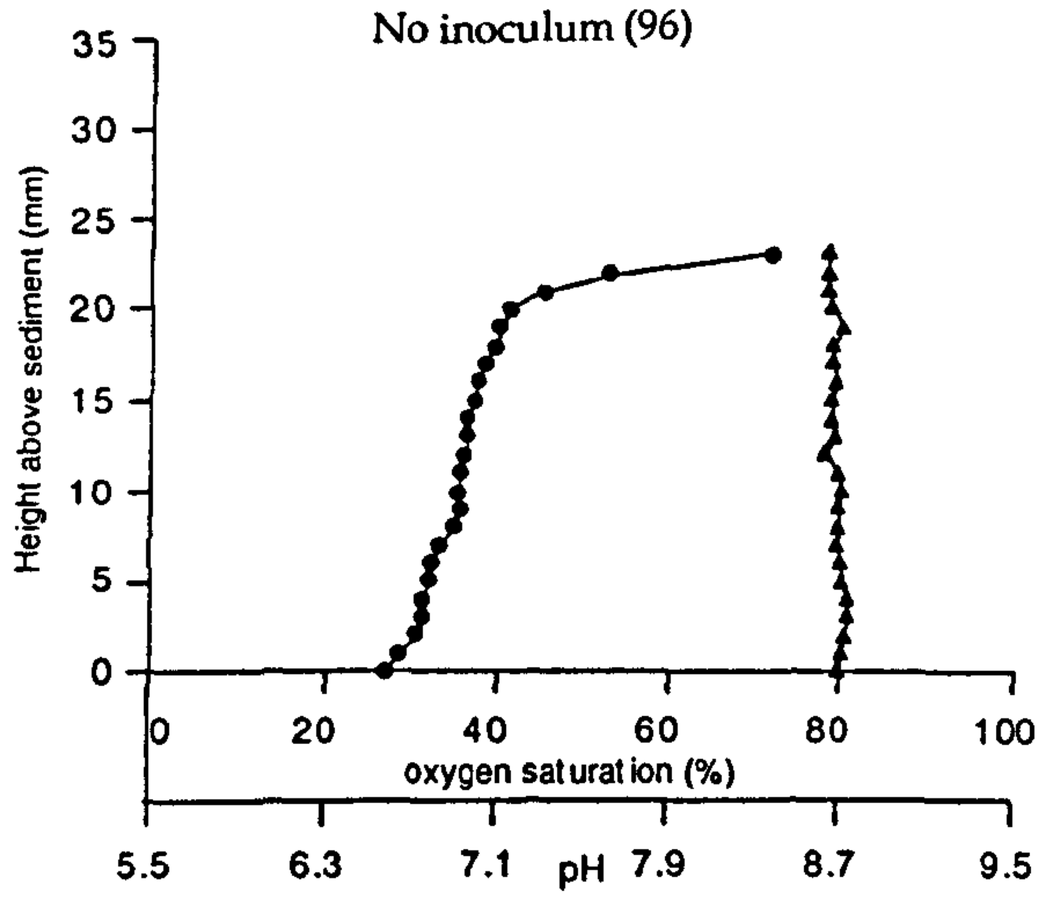

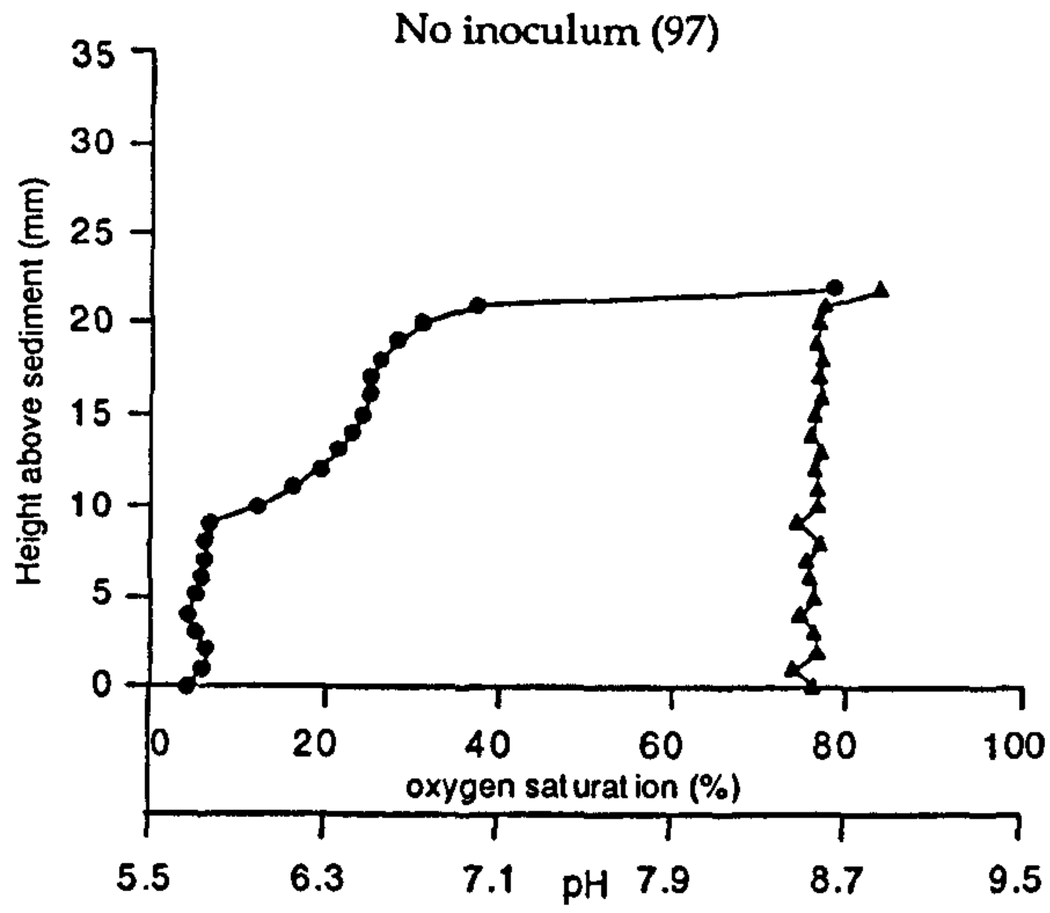

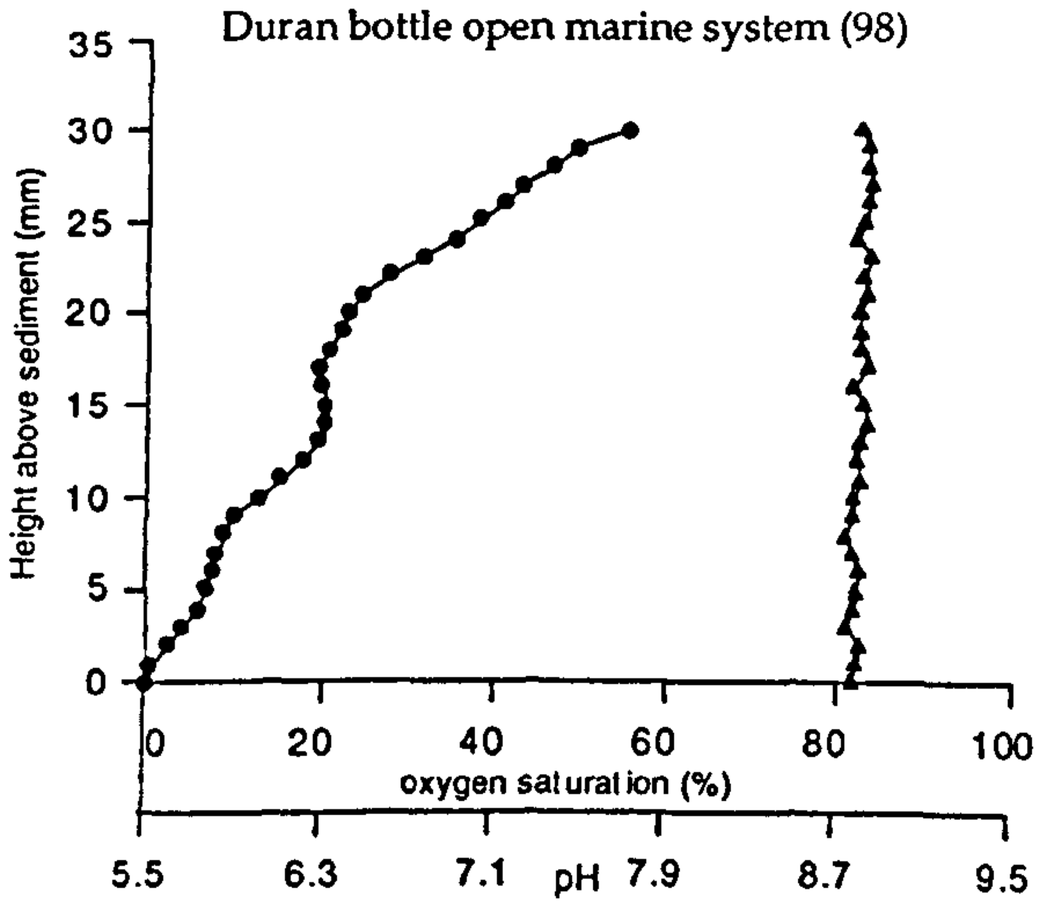

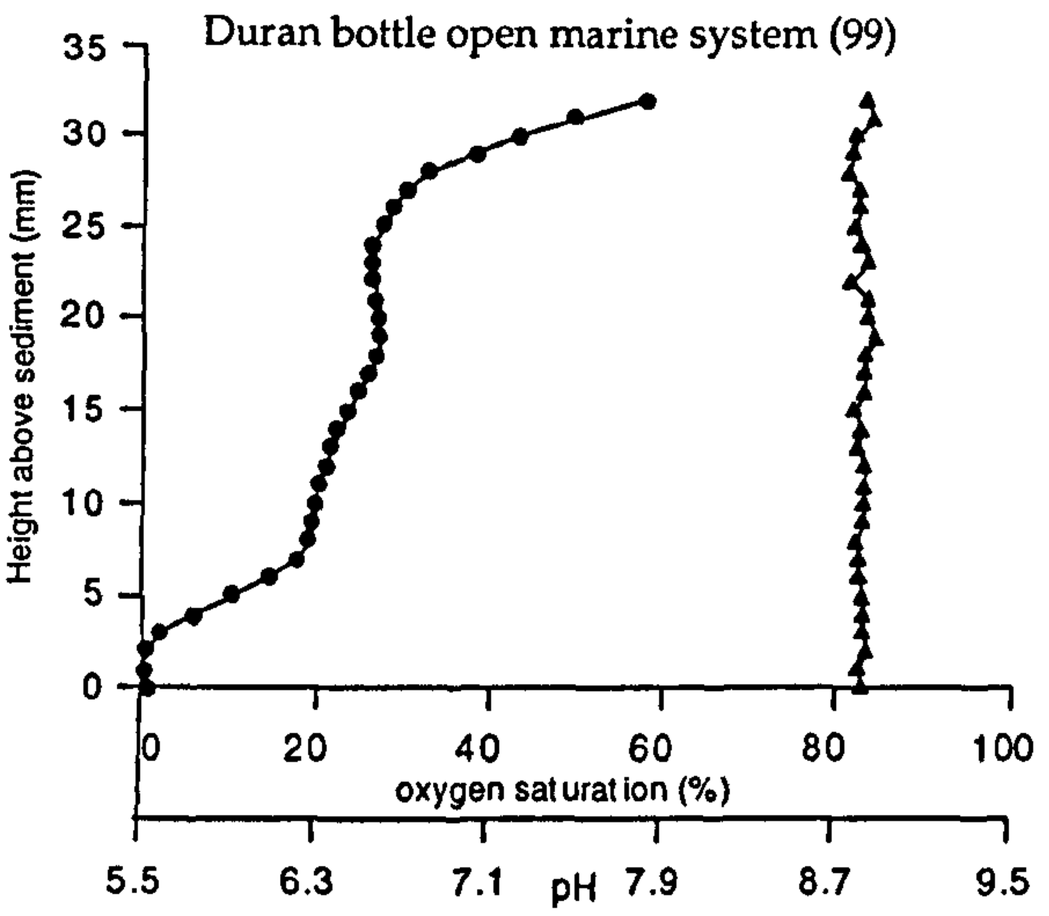

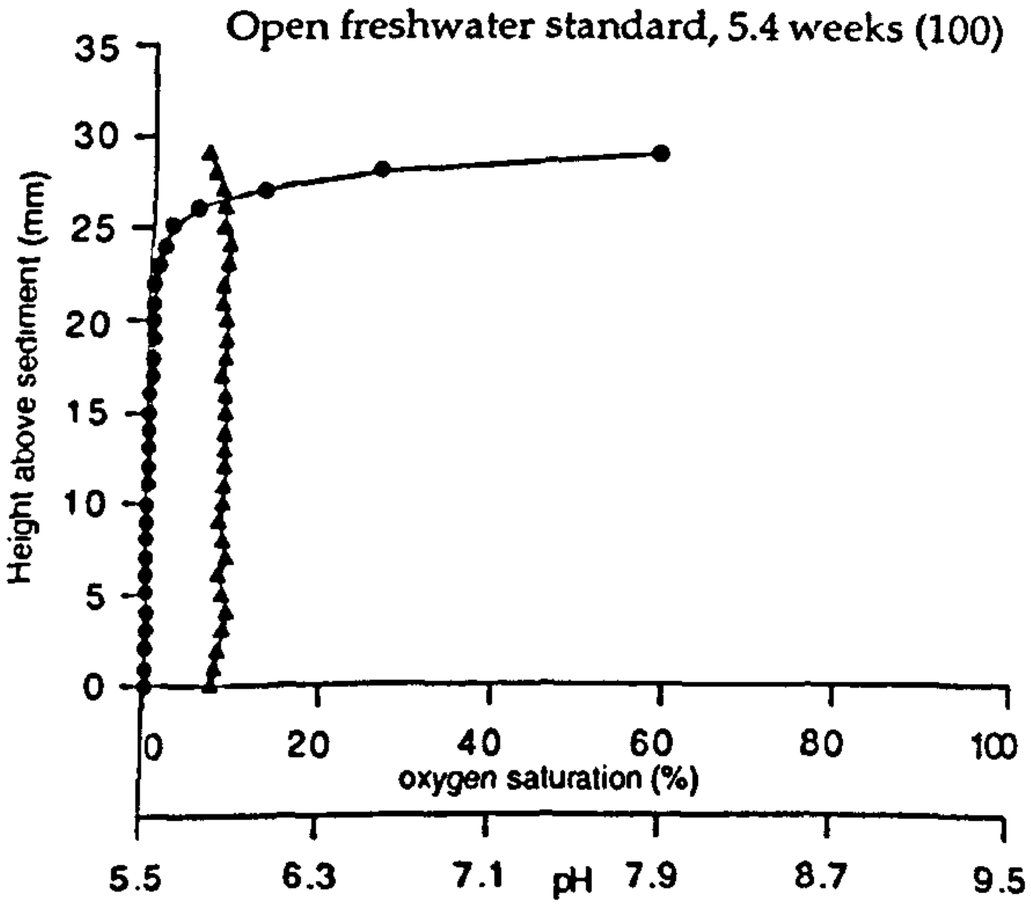

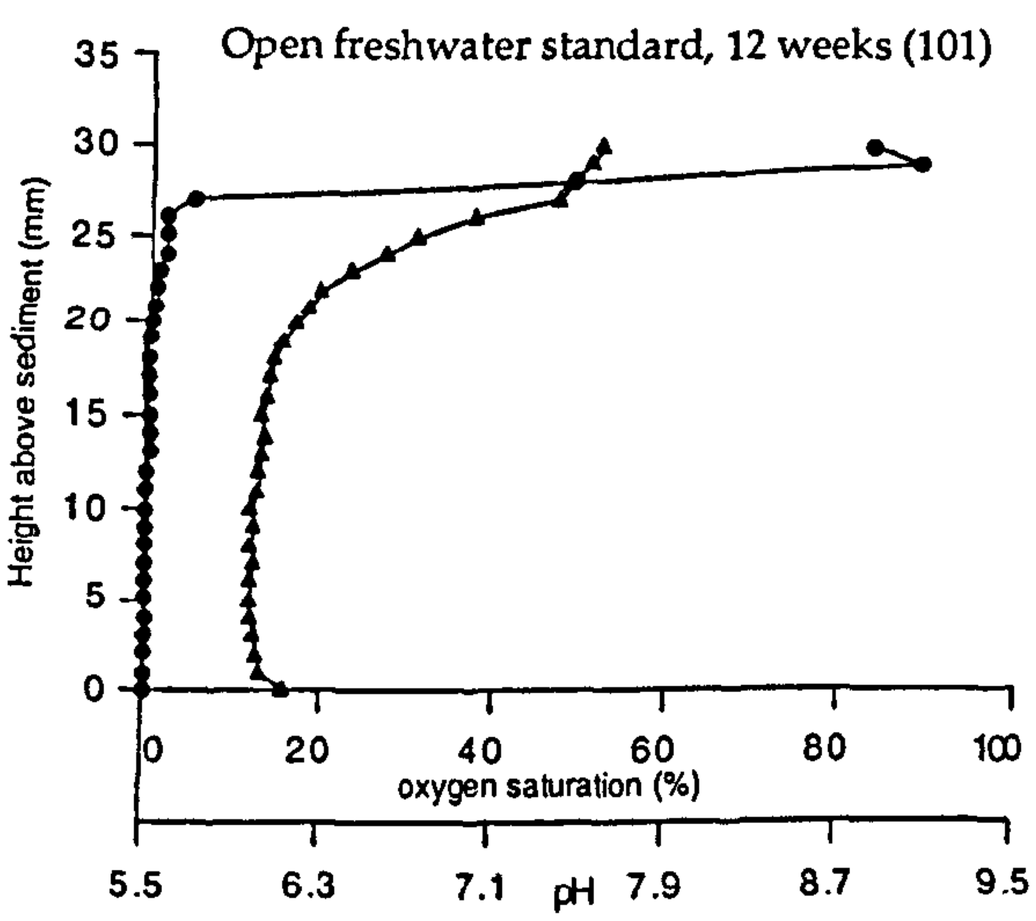

Oxygen and pH depth profiles for open systems after 12 weeks unless otherwise stated. Infilled circles represent oxygen data points. Infilled triangles represent pH data points. The highest data points above the sediment represent the air-medium interface.

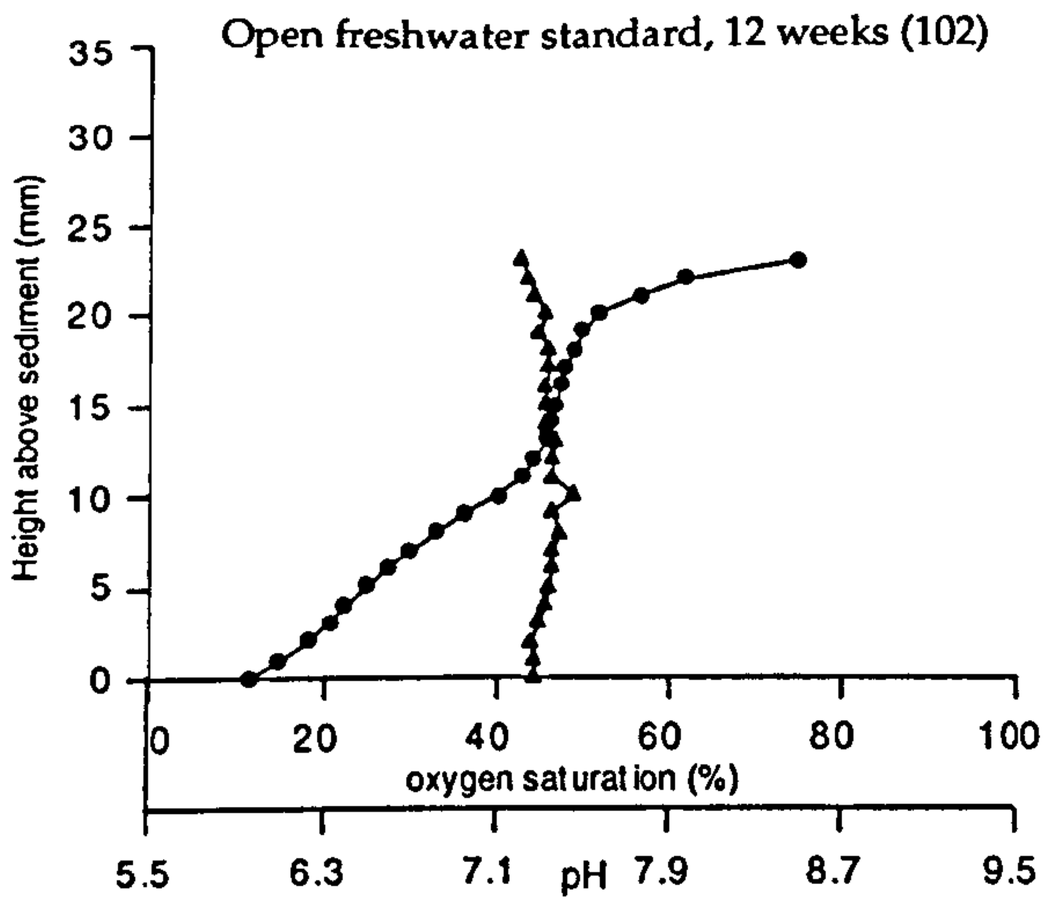

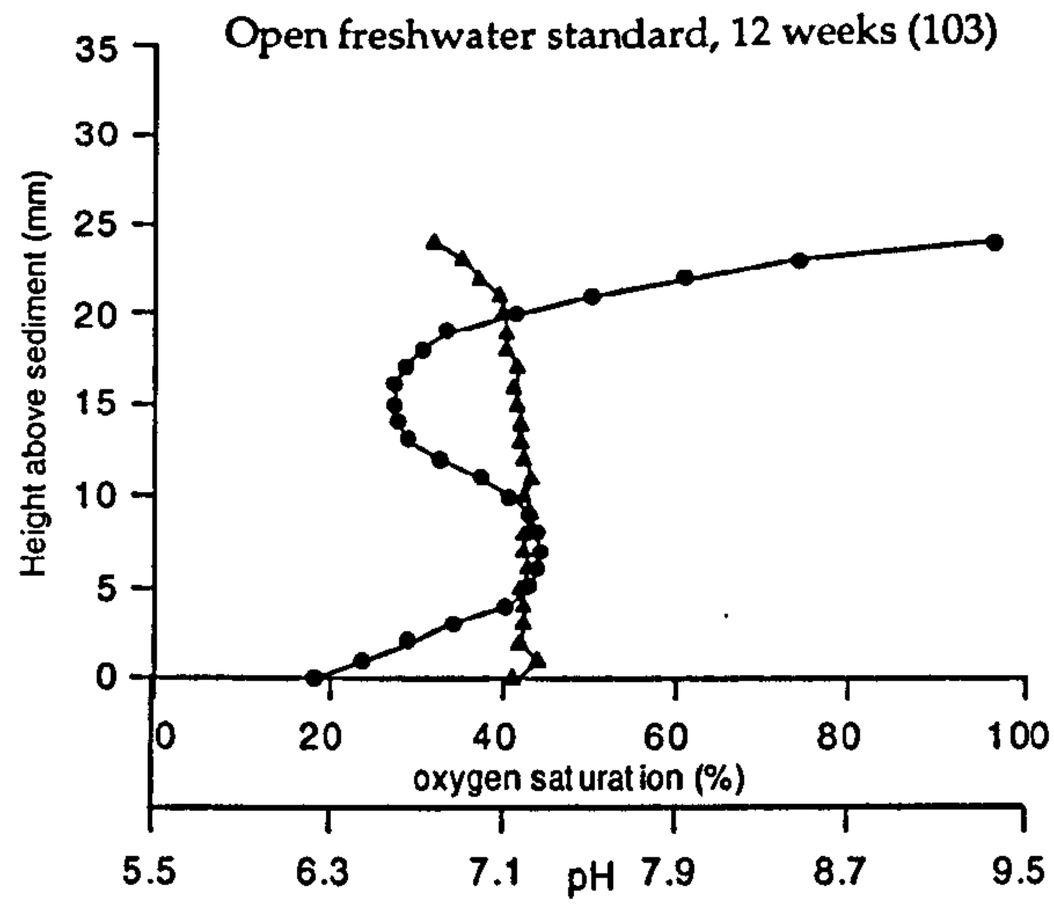

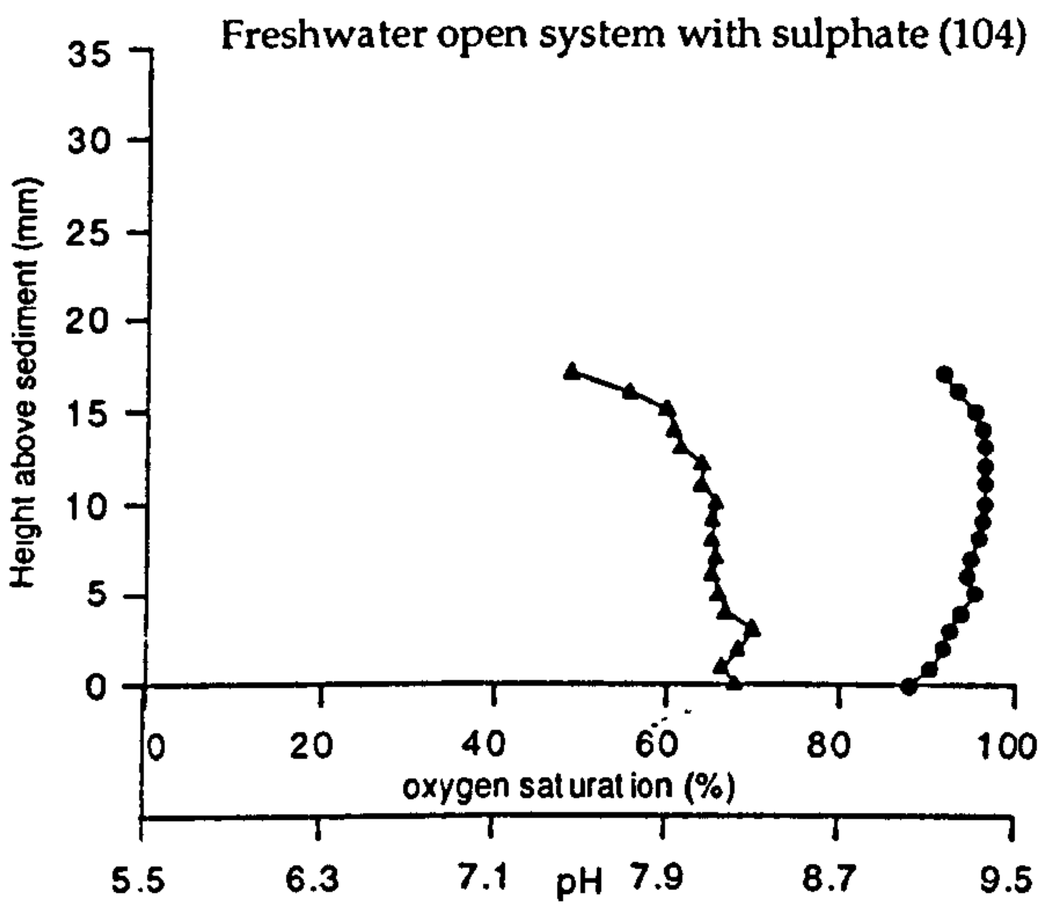

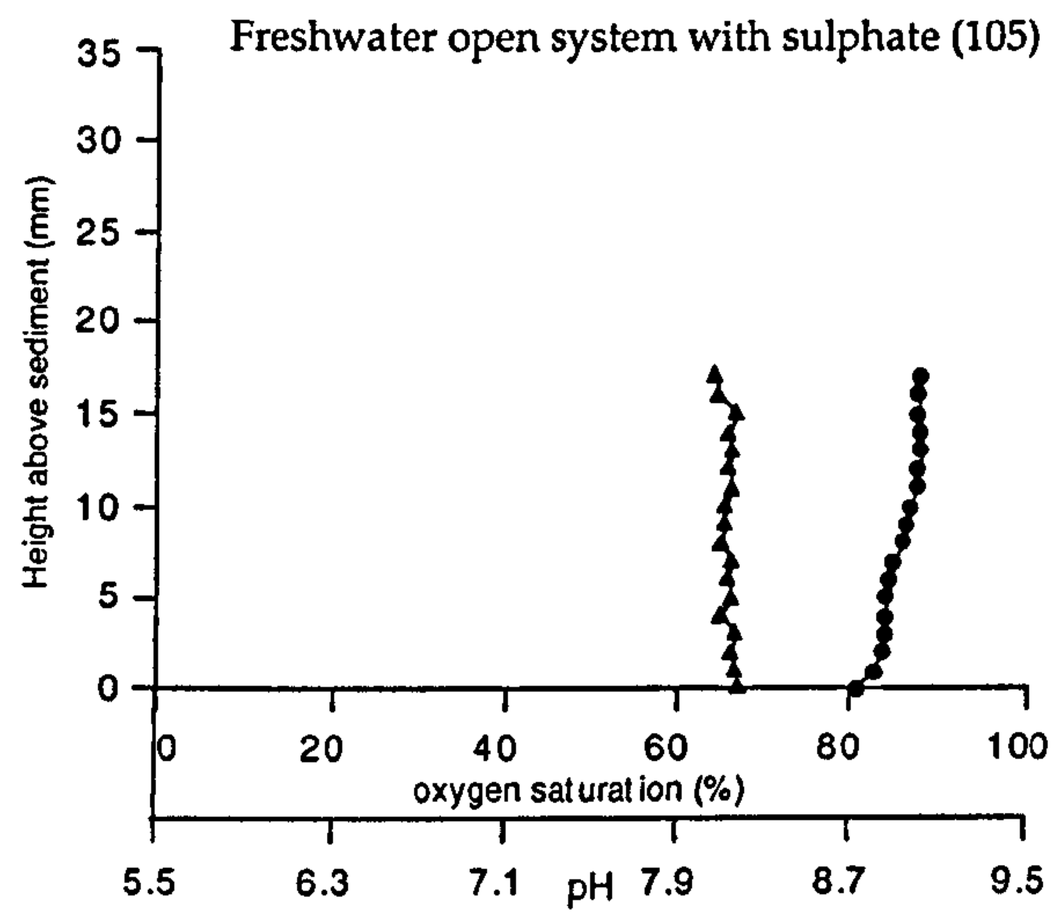

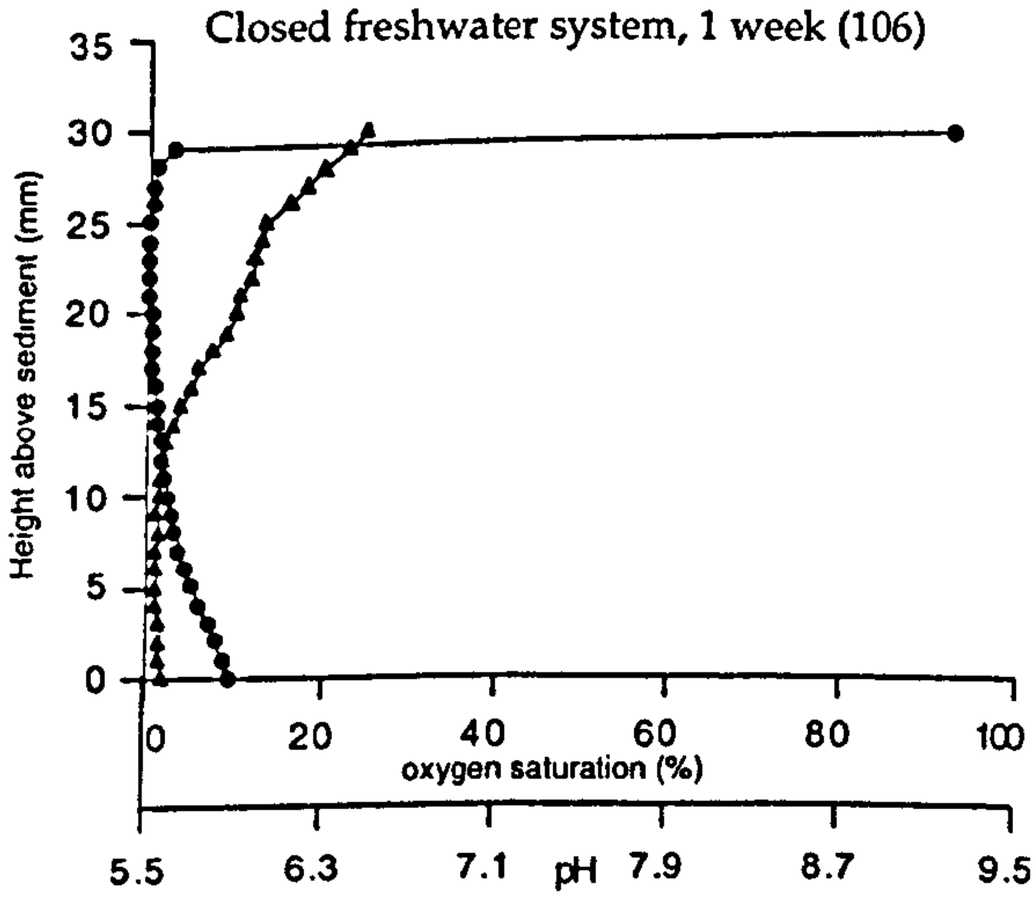

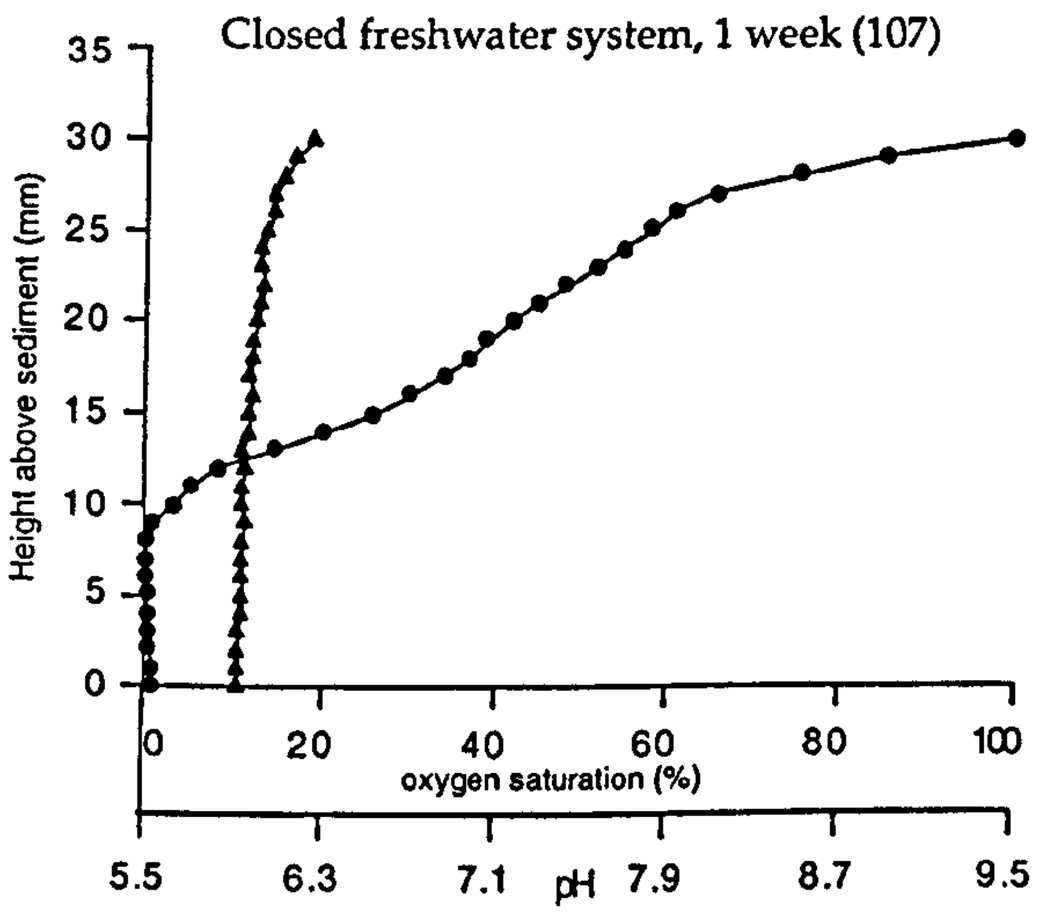

Oxygen and pH depth profiles for freshwater systems after 12 weeks. Infilled circles represent oxygen data points. Infilled triangles represent pH data points. The highest data points above the sediment represent the air-medium interface.

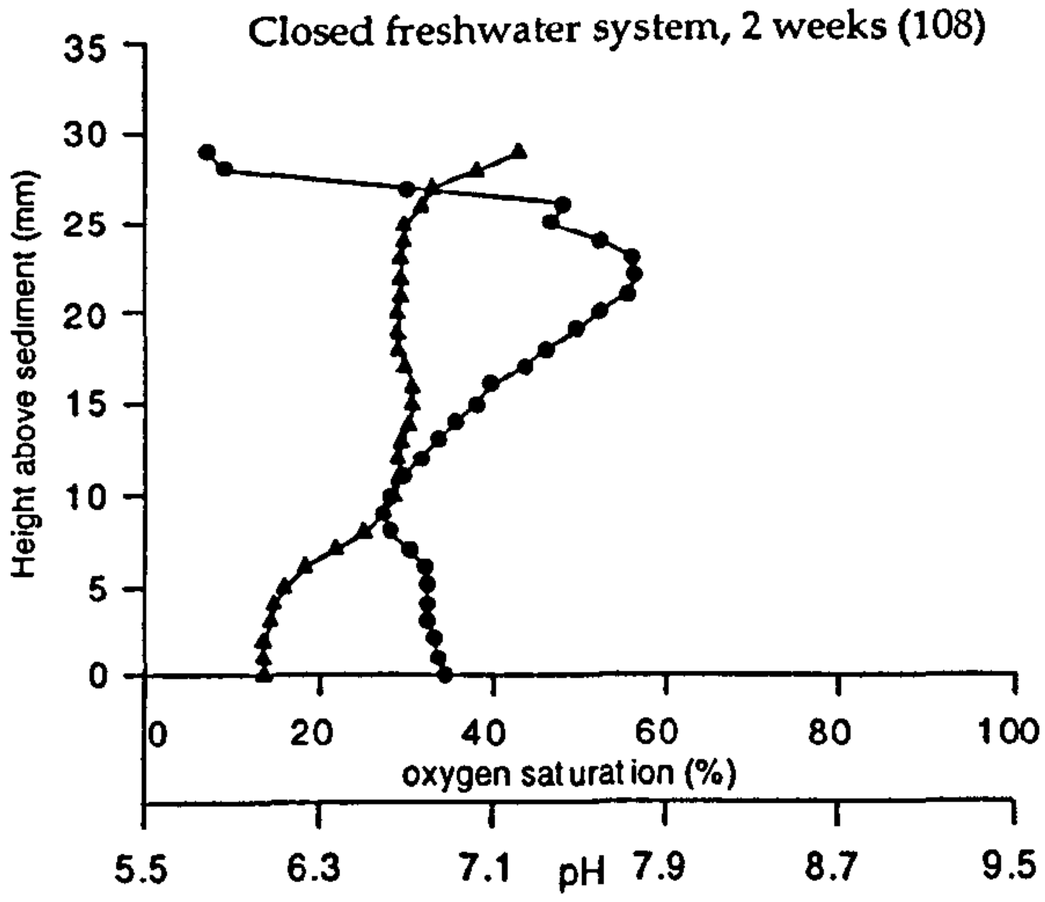

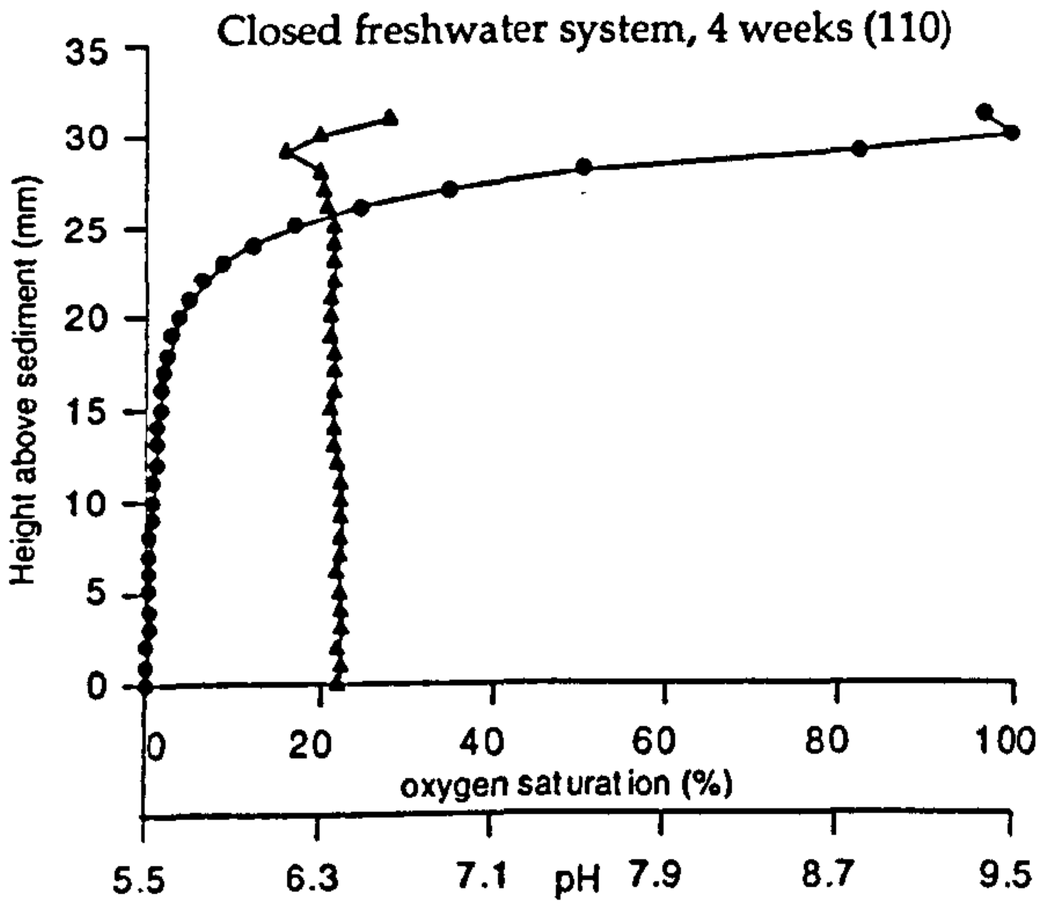

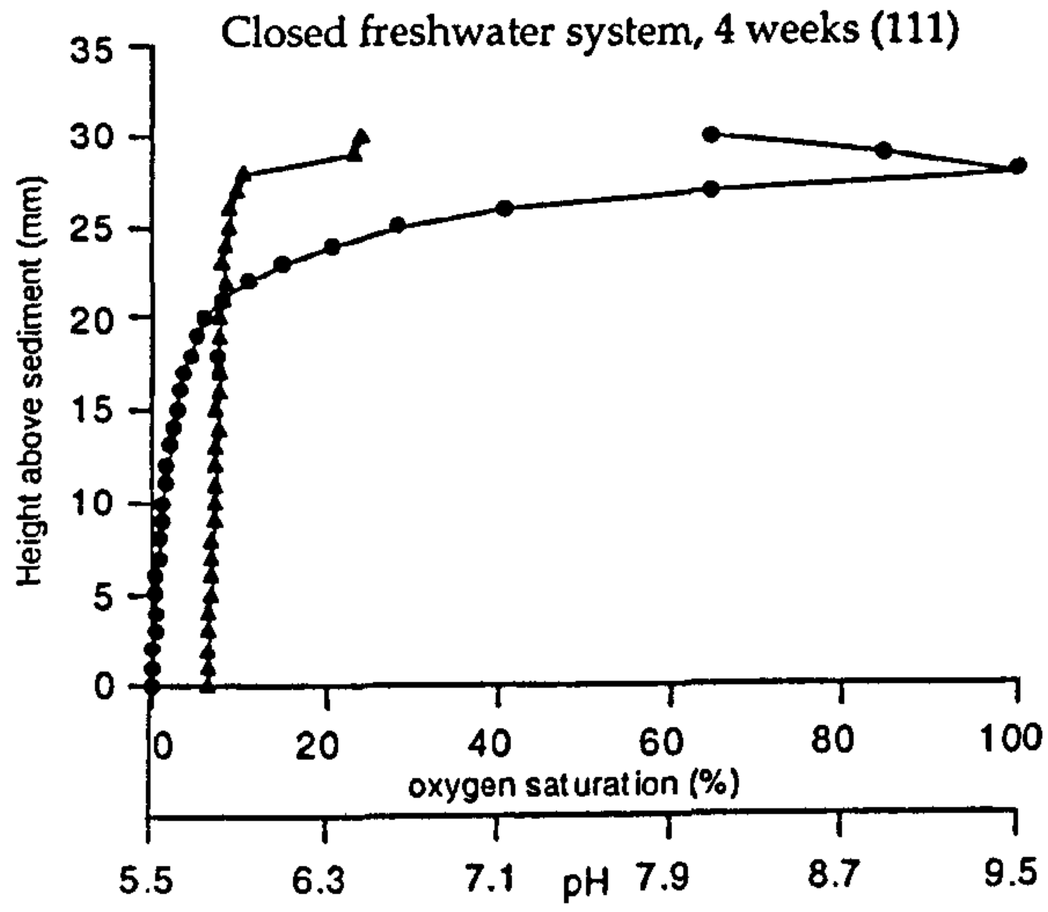

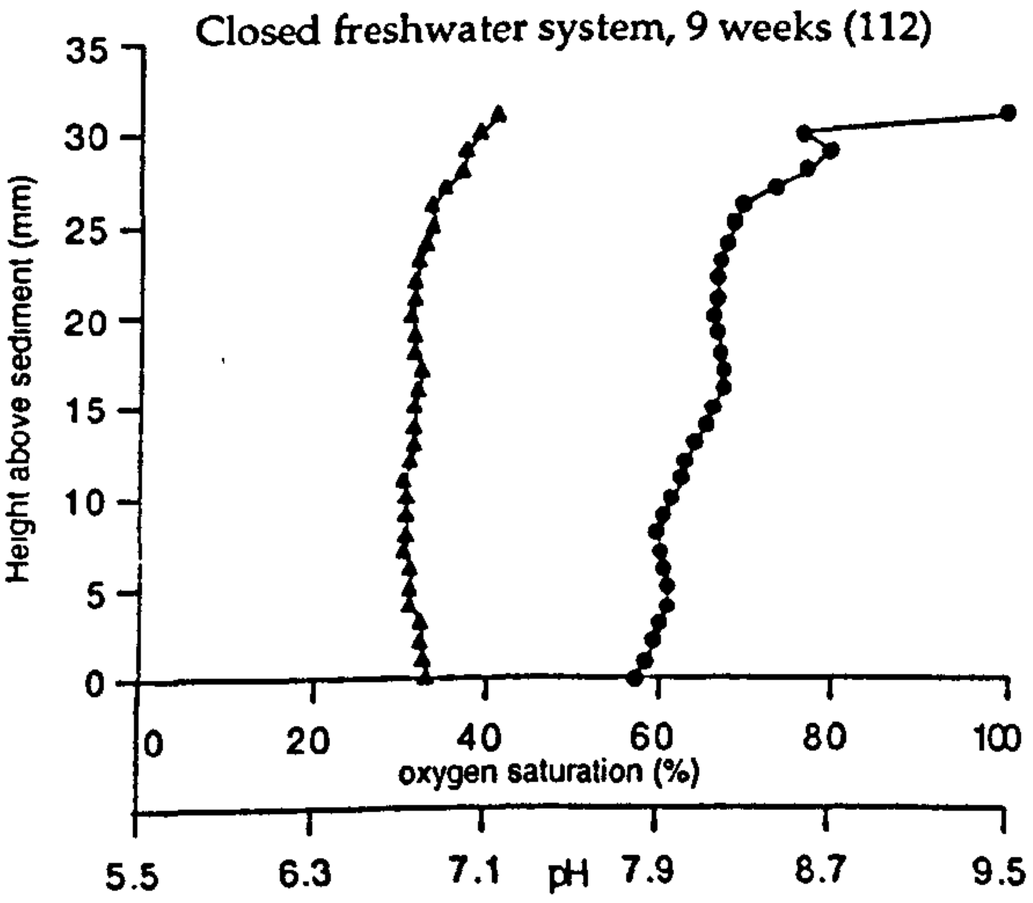

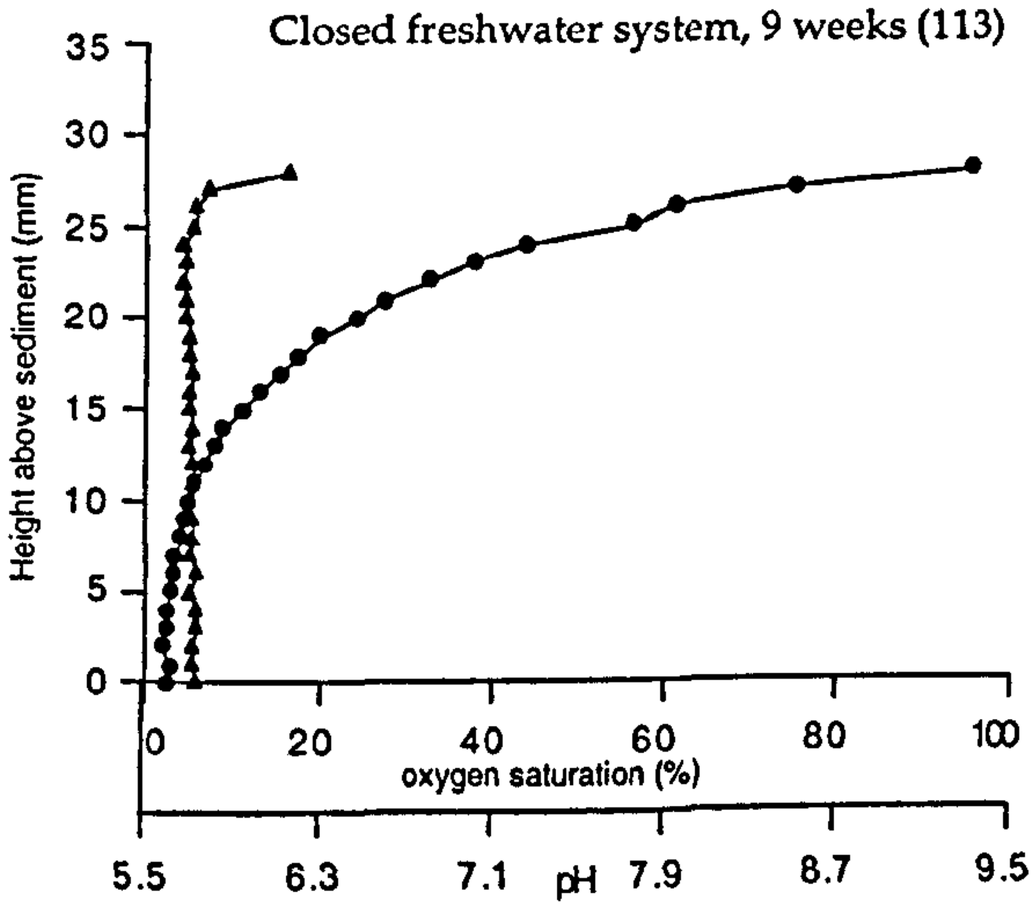

Oxygen and pH depth profiles for closed freshwater systems. Infilled circles represent oxygen data points. Infilled triangles represent pH data points. The highest data points above the sediment represent the air-medium interface.

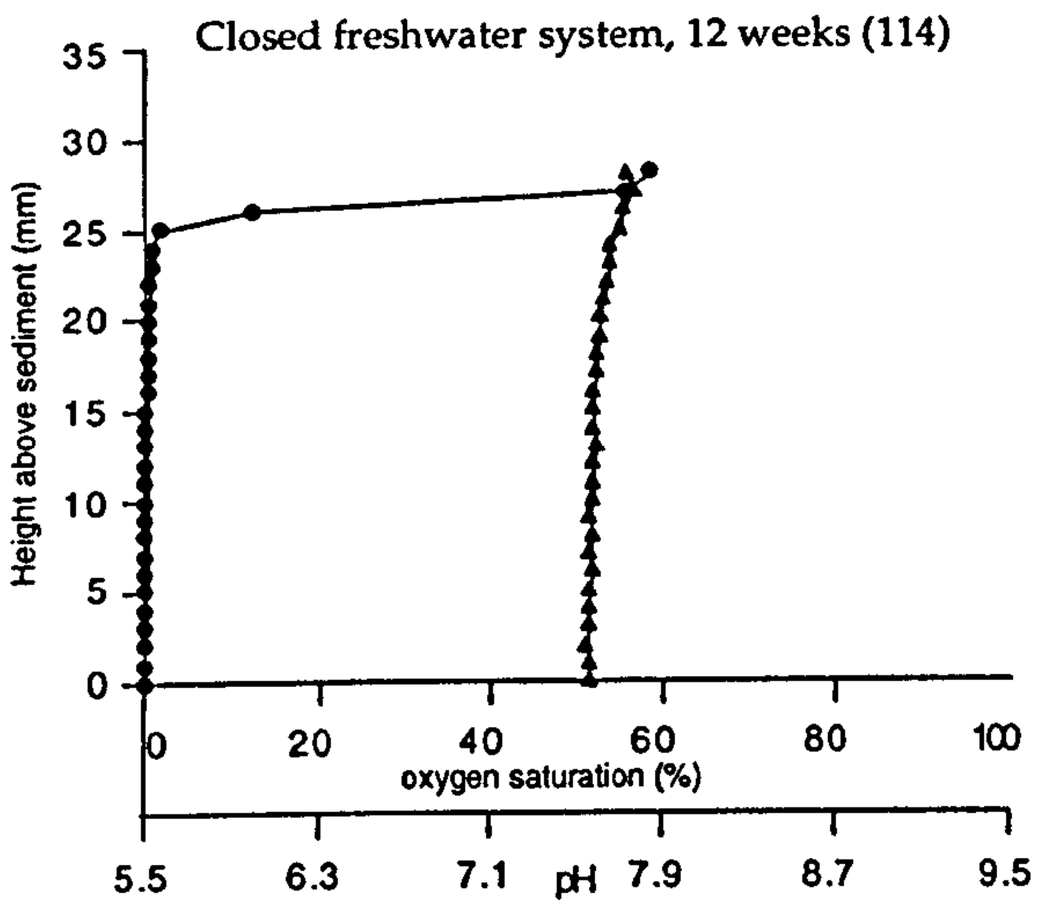

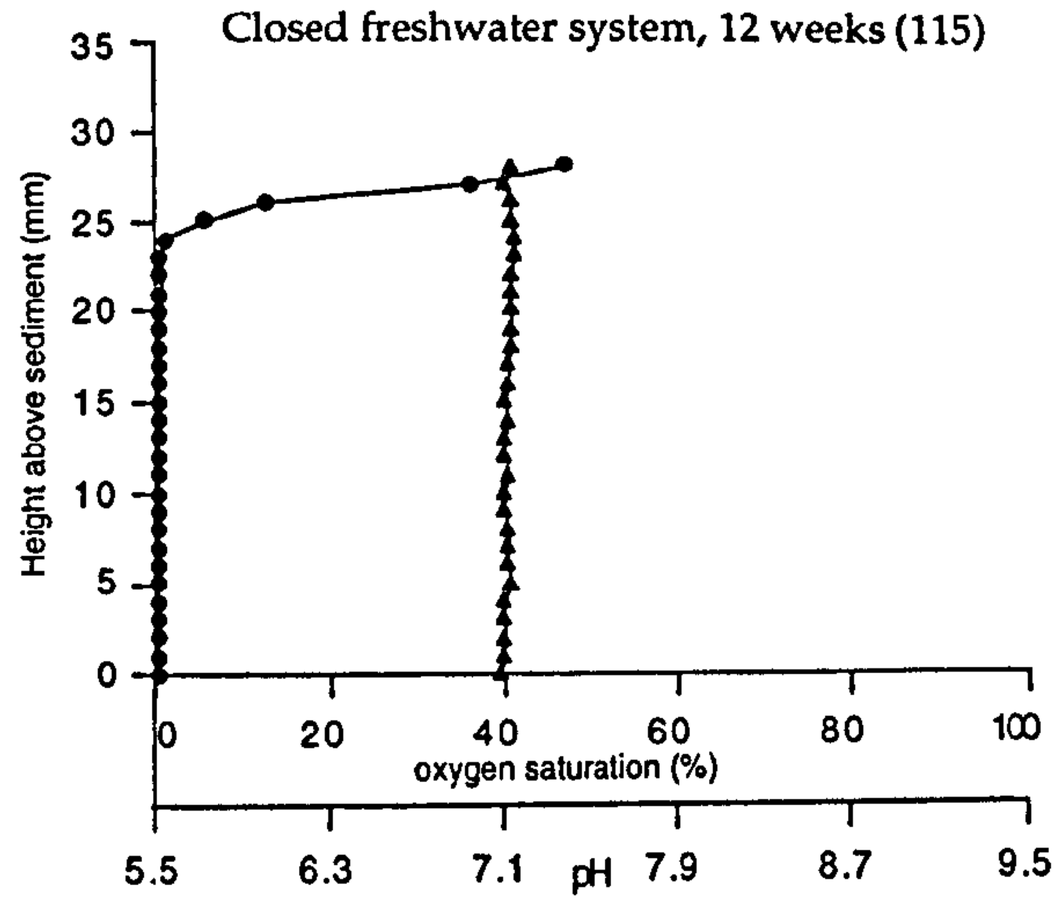

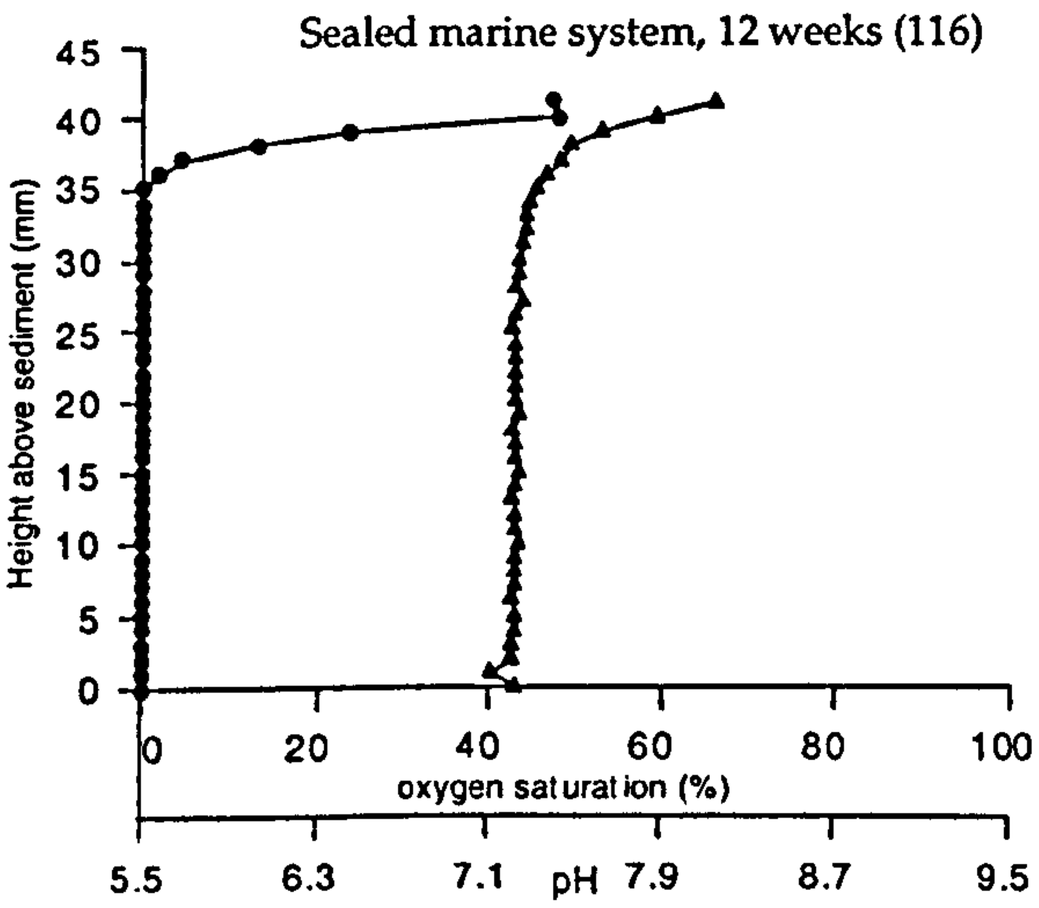

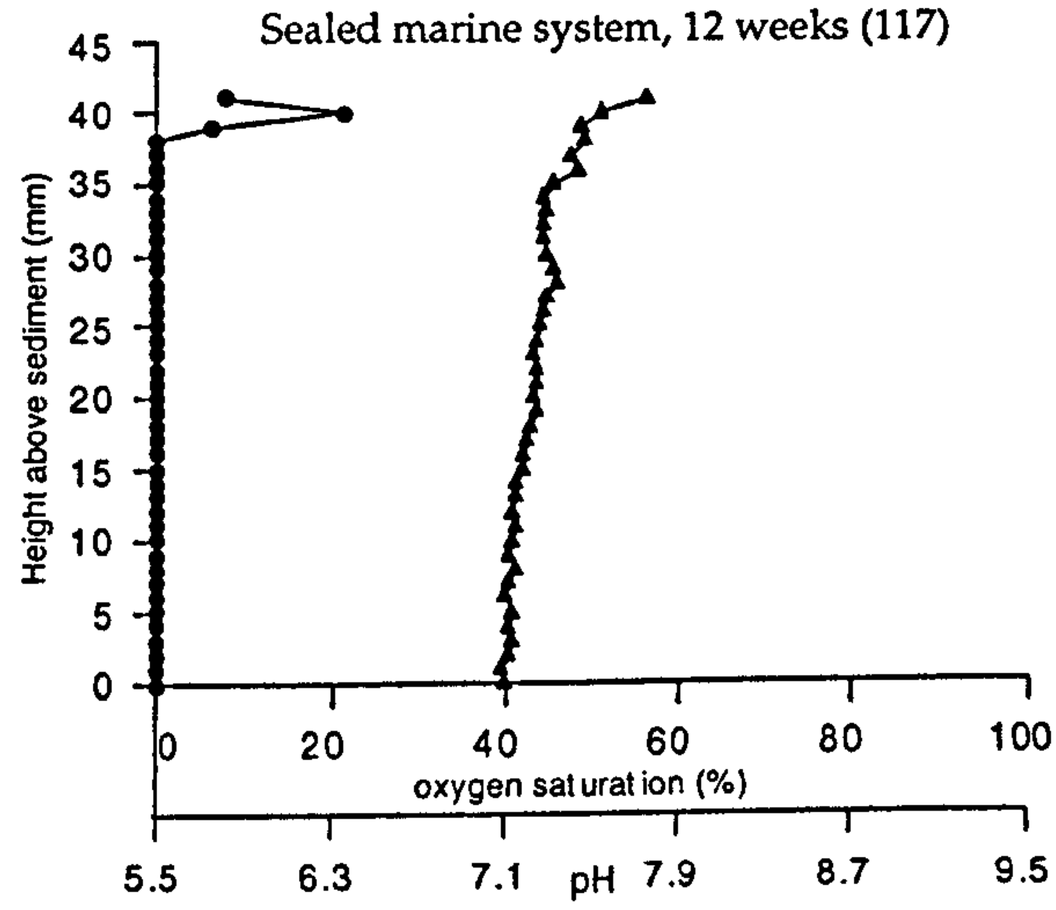

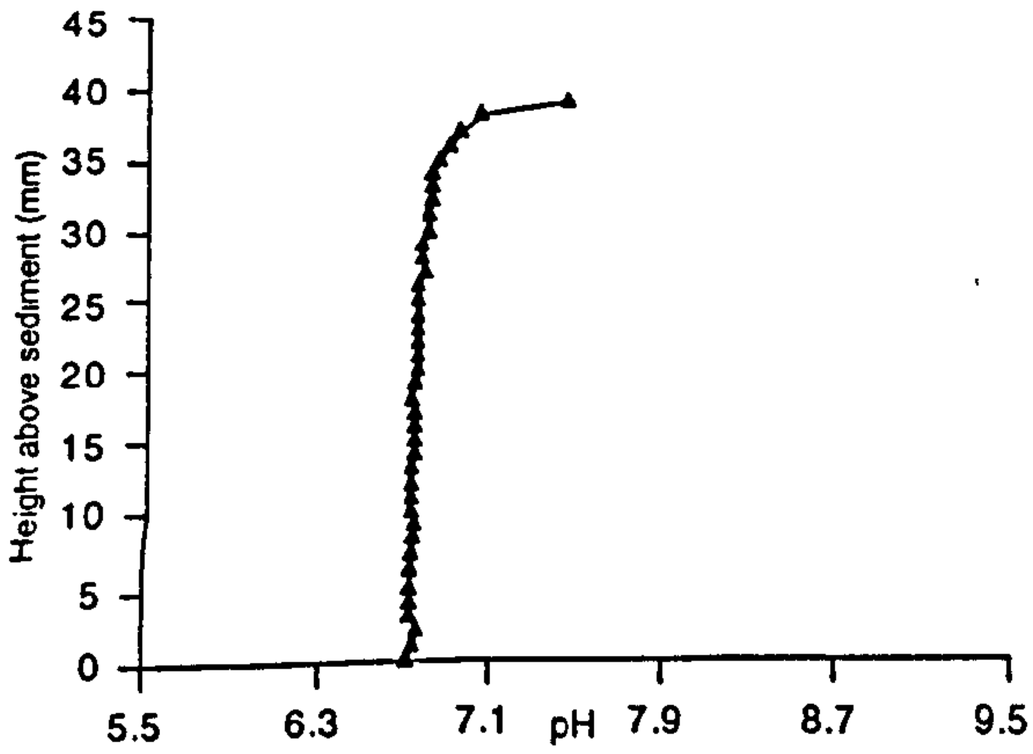

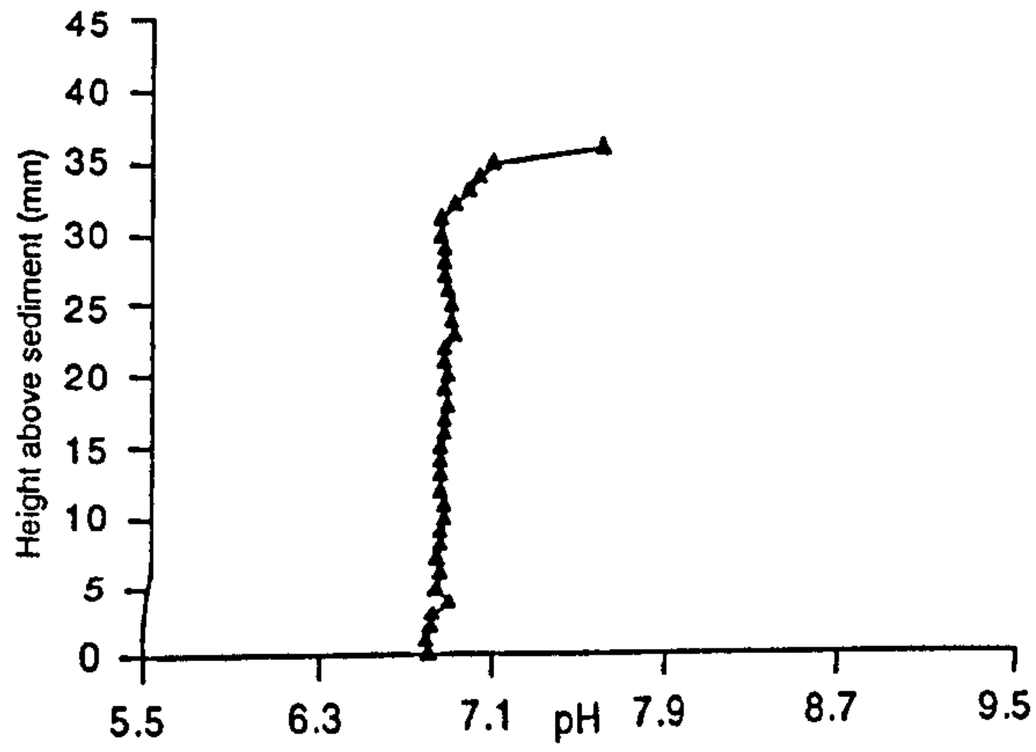

Oxygen and pH depth profiles. Sealed systems are anoxic (no oxygen profiles). Infilled circles represent oxygen data points. Infilled triangles represent pH data points. The highest data points above the sediment represent the air-medium interface.

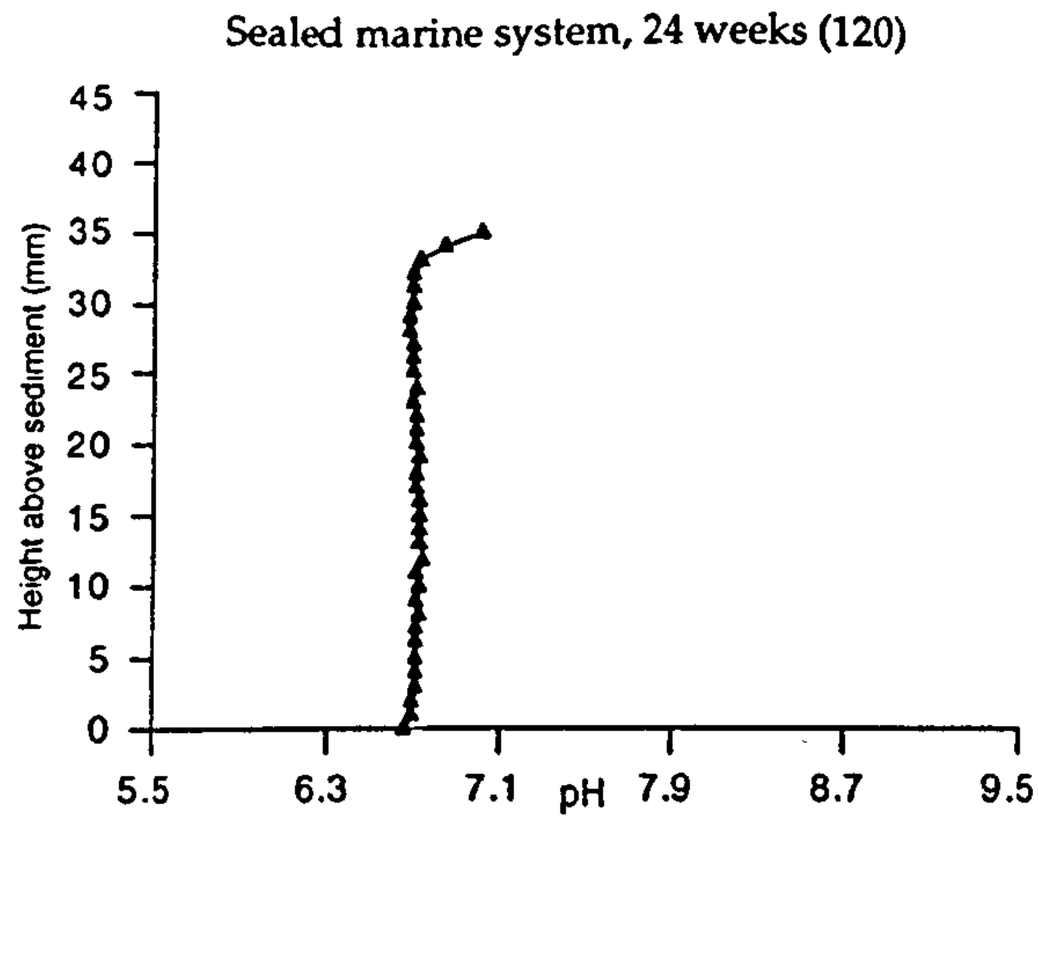

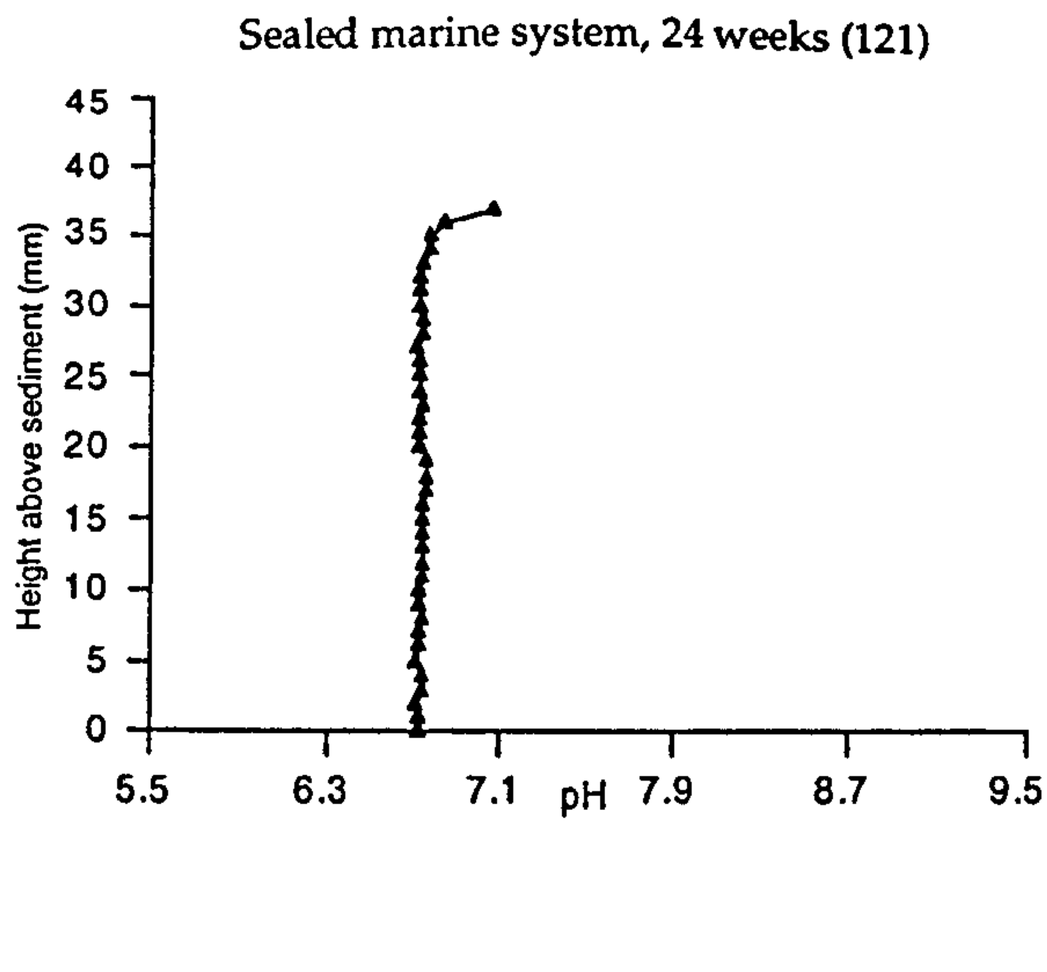

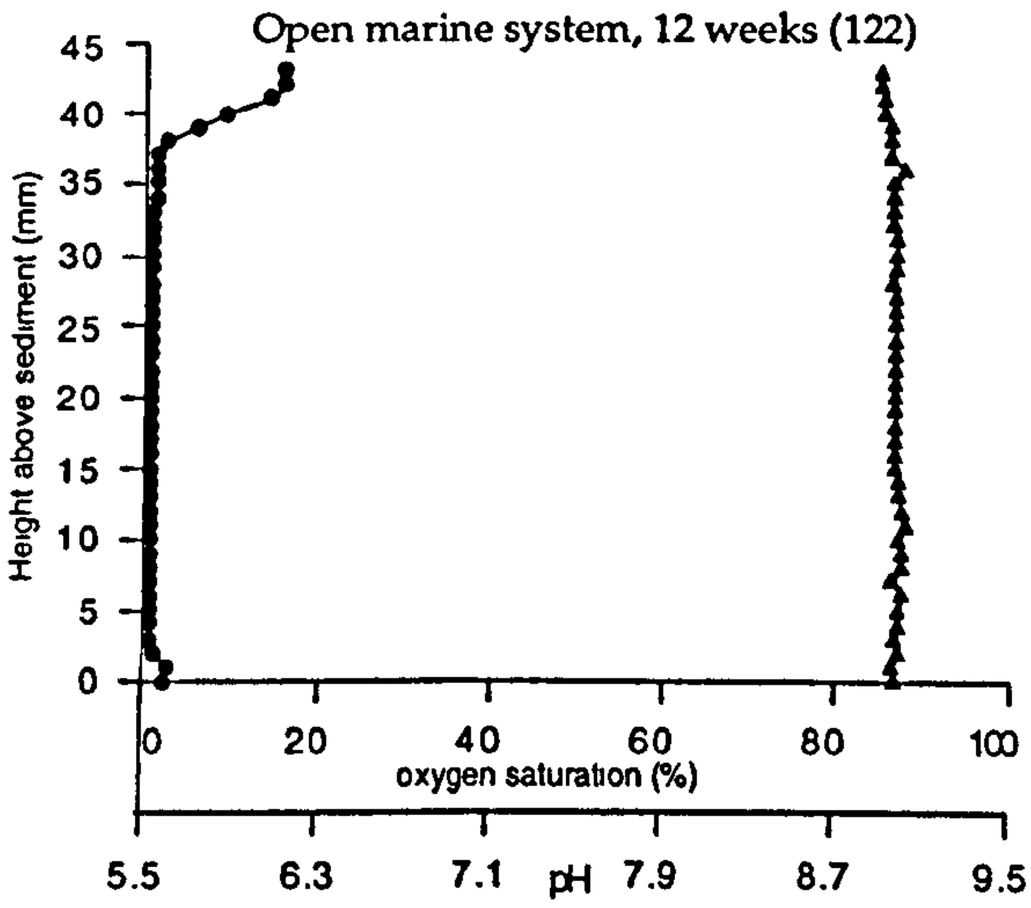

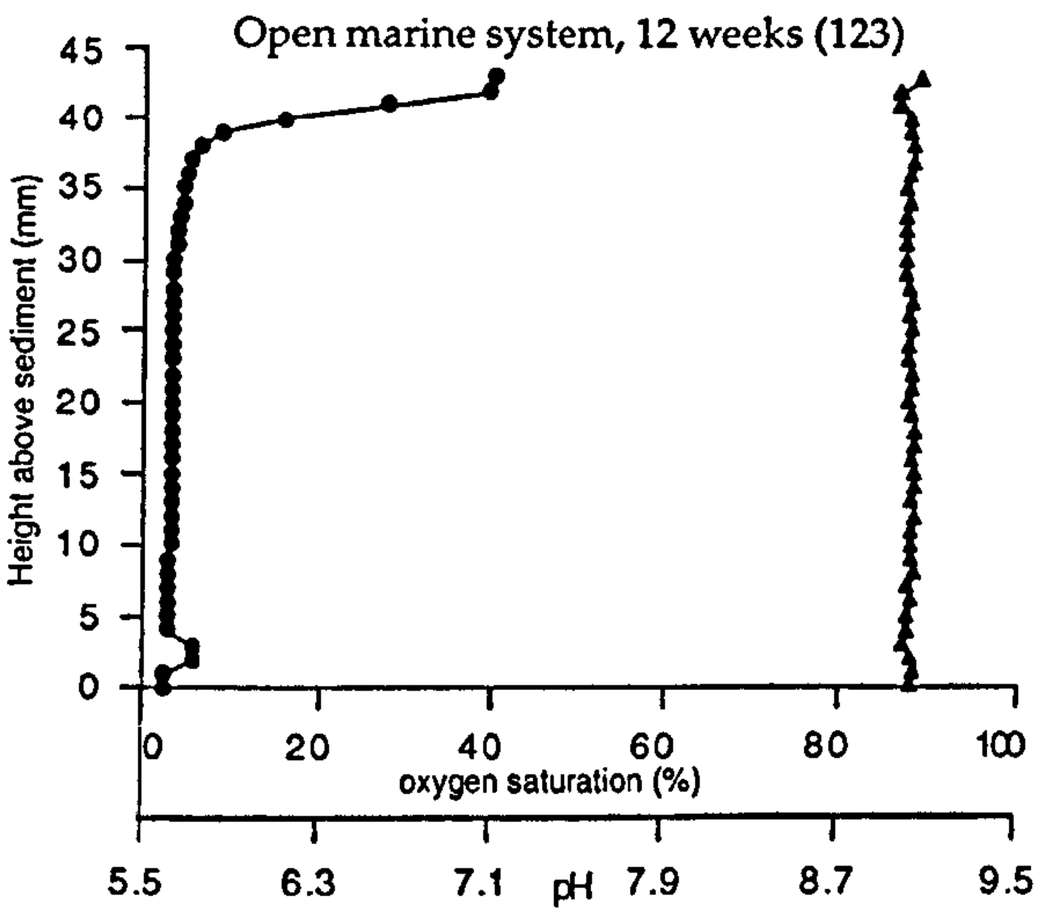

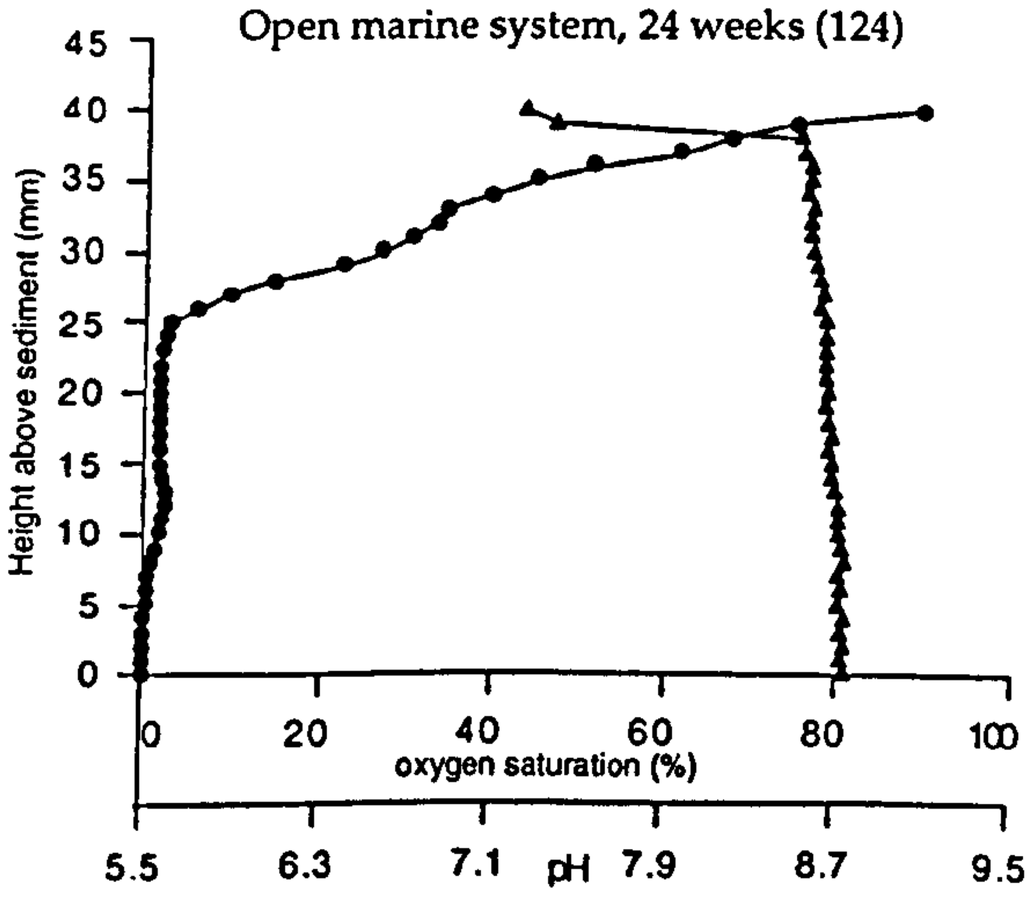

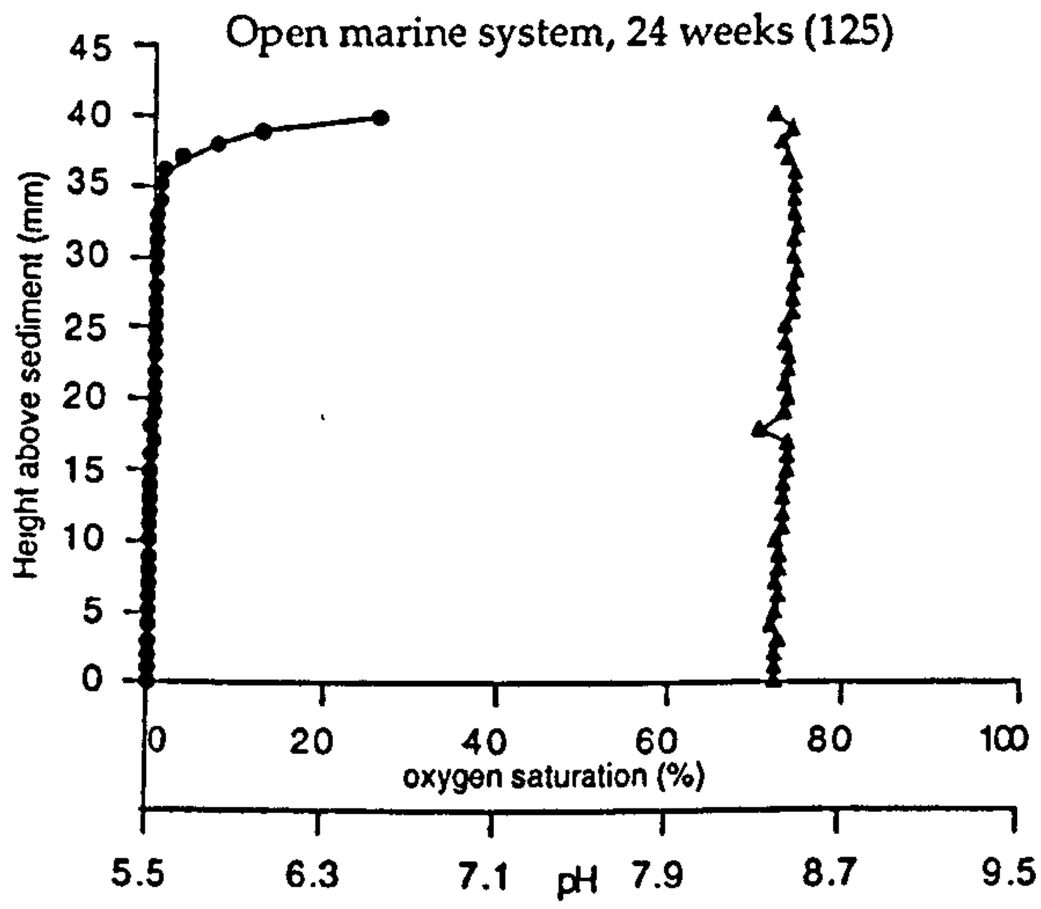

Oxygen and pH depth profiles for marine systems. Infilled circles represent oxygen data points. Infilled triangles represent pH data points. The highest data points above the sediment represent the air-medium interface.

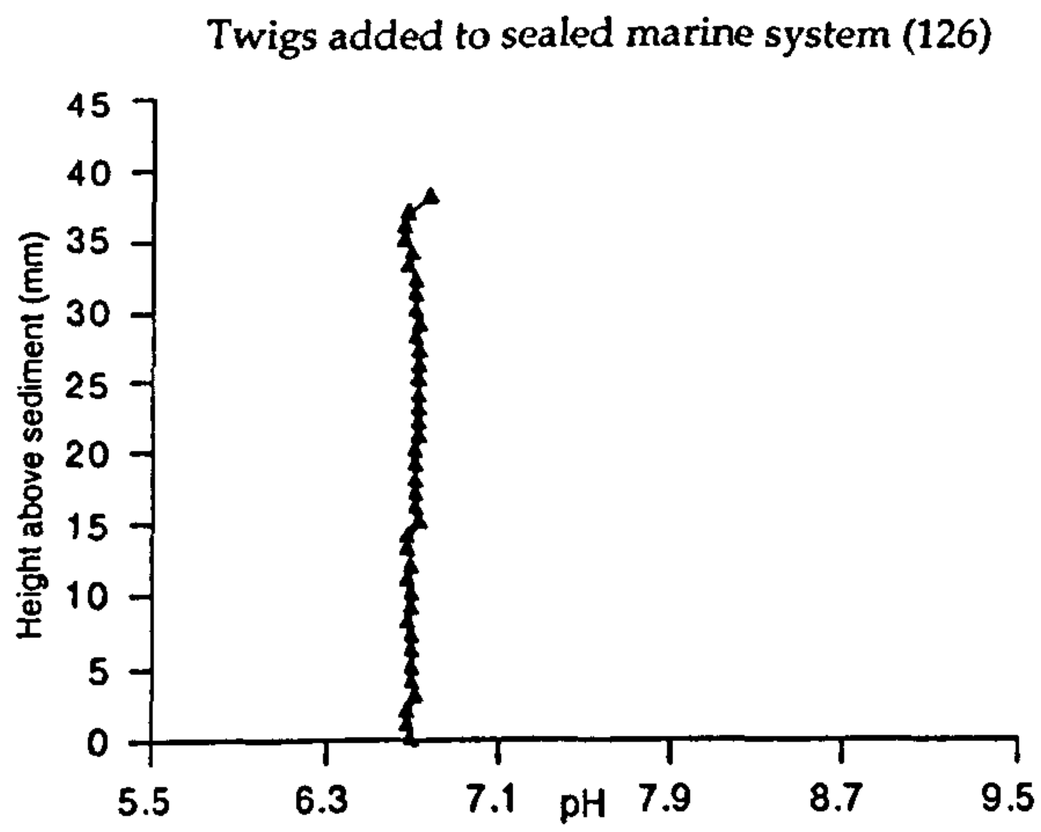

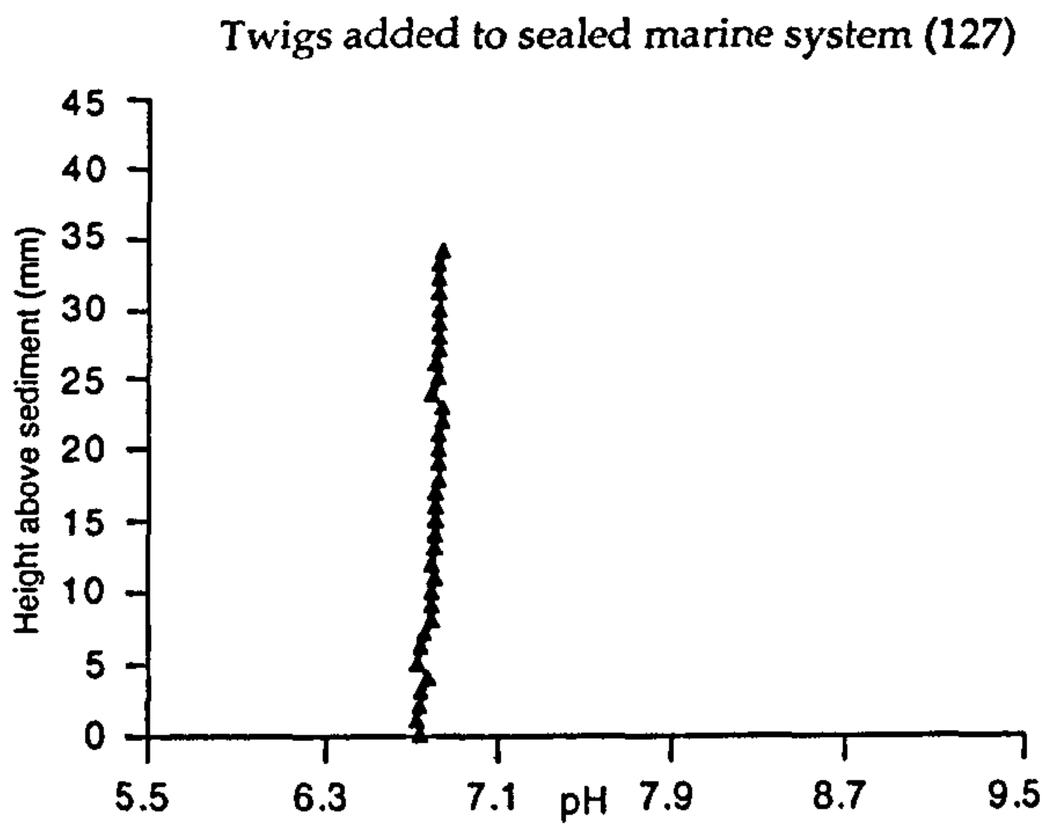

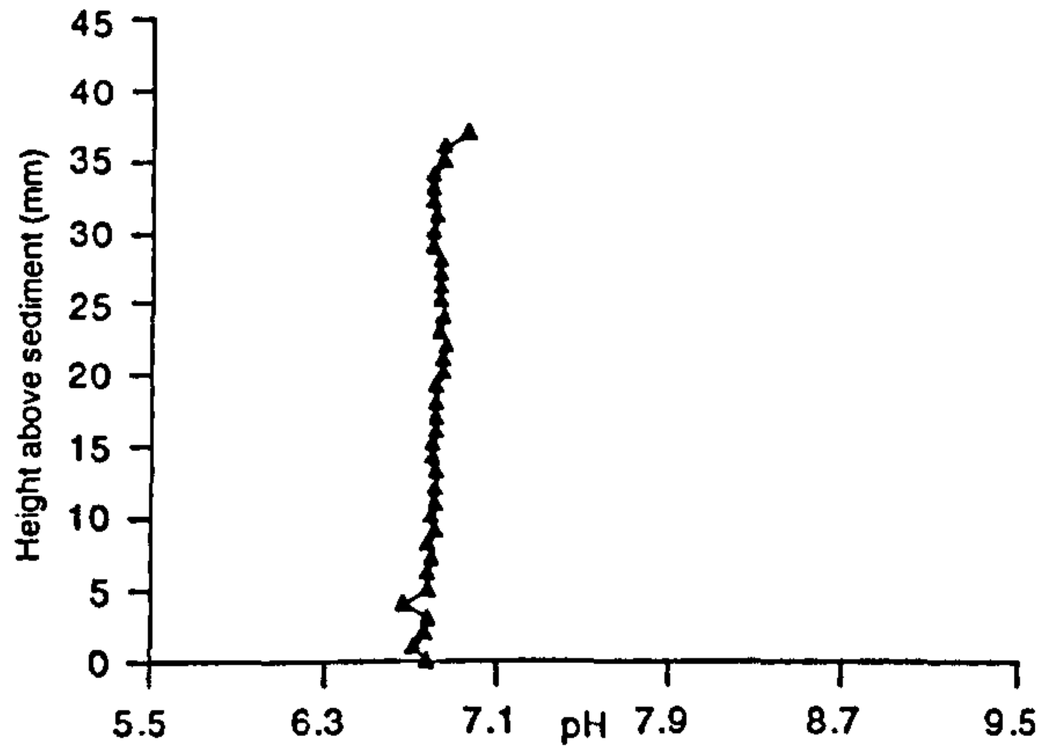

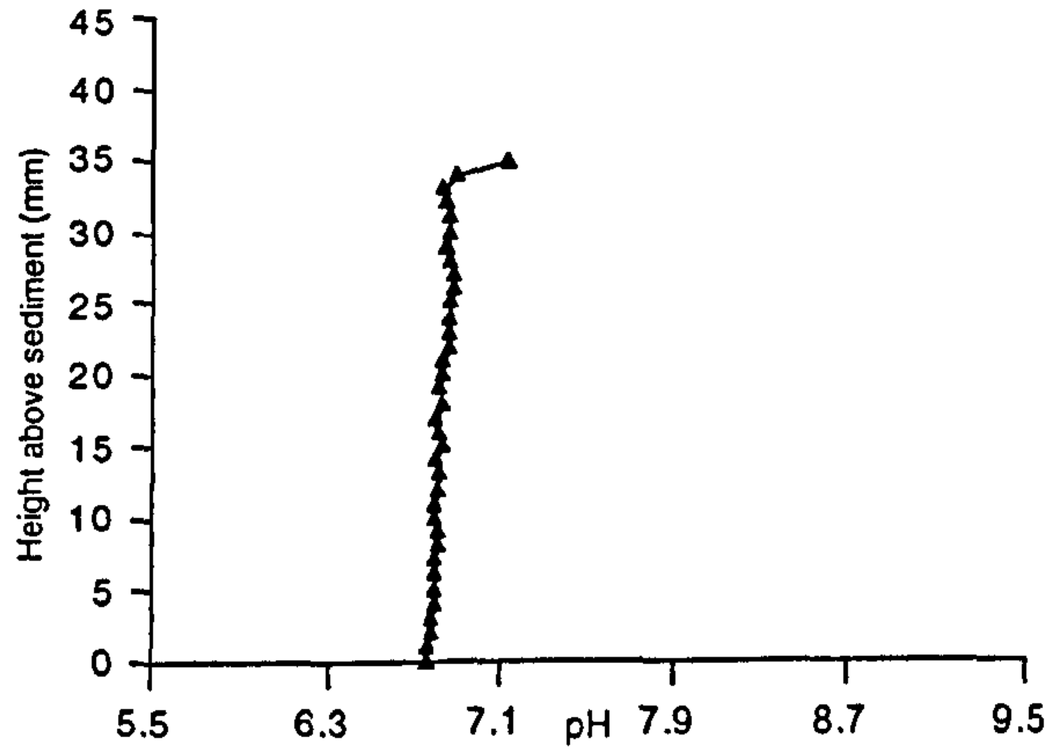

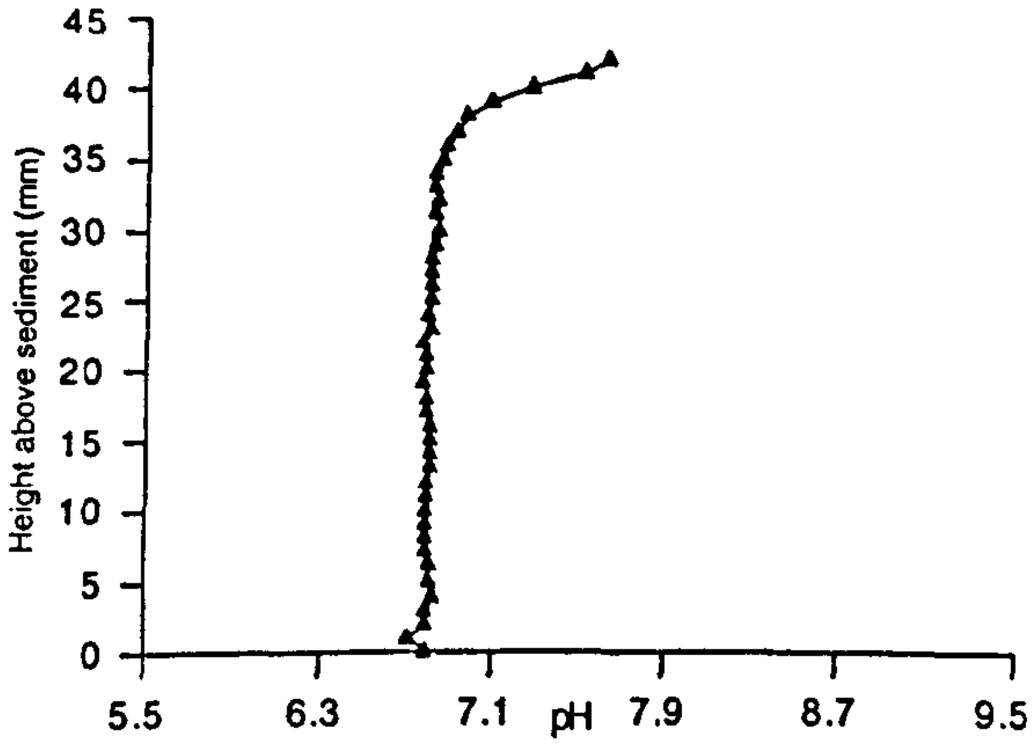

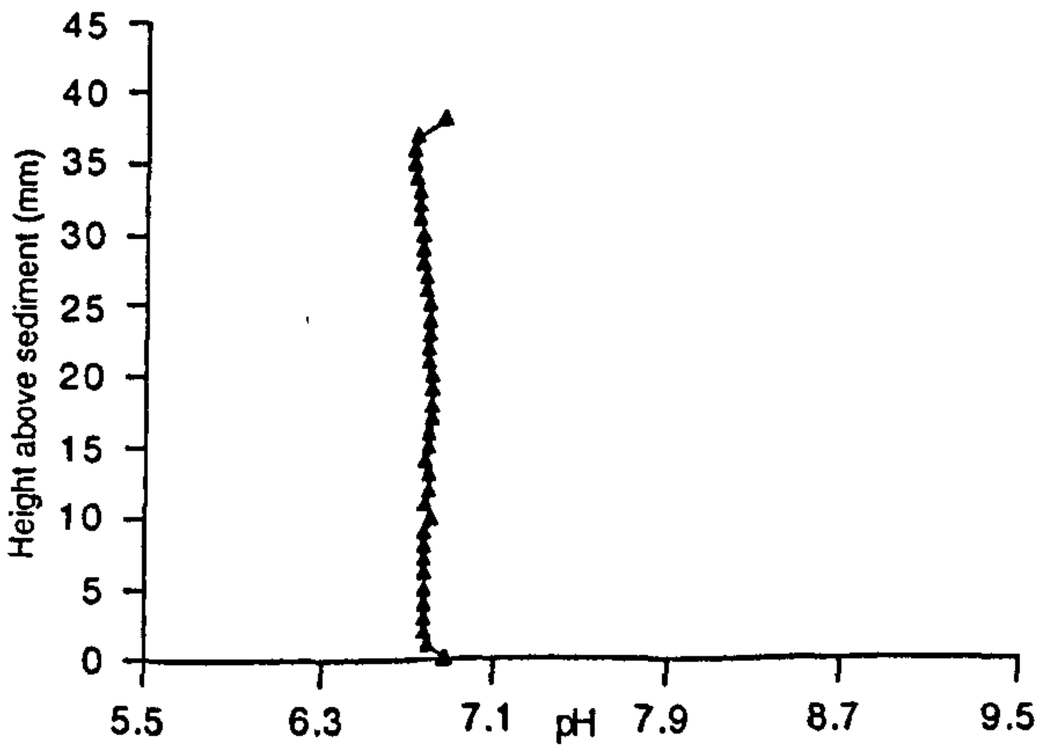

Oxygen and pH depth profiles for sealed marine systems after 24 weeks. Infilled circles represent oxygen data points. Infilled triangles represent pH data points. The highest data points above the sediment represent the air-medium interface.

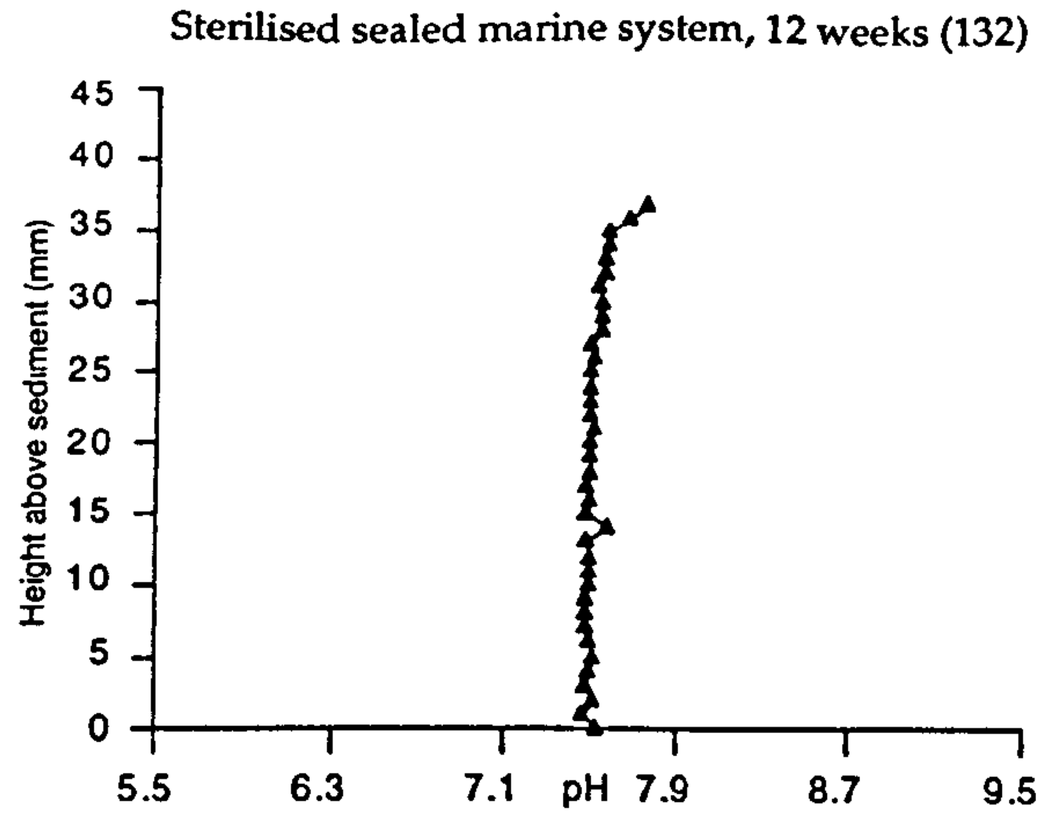

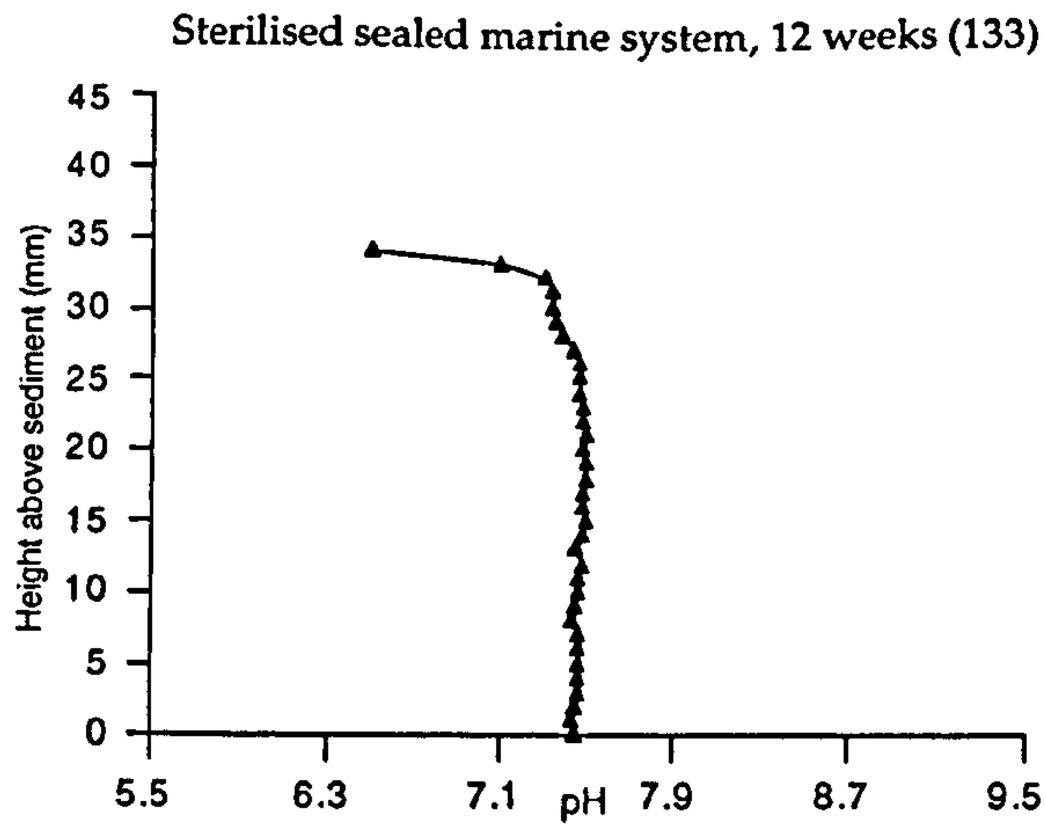

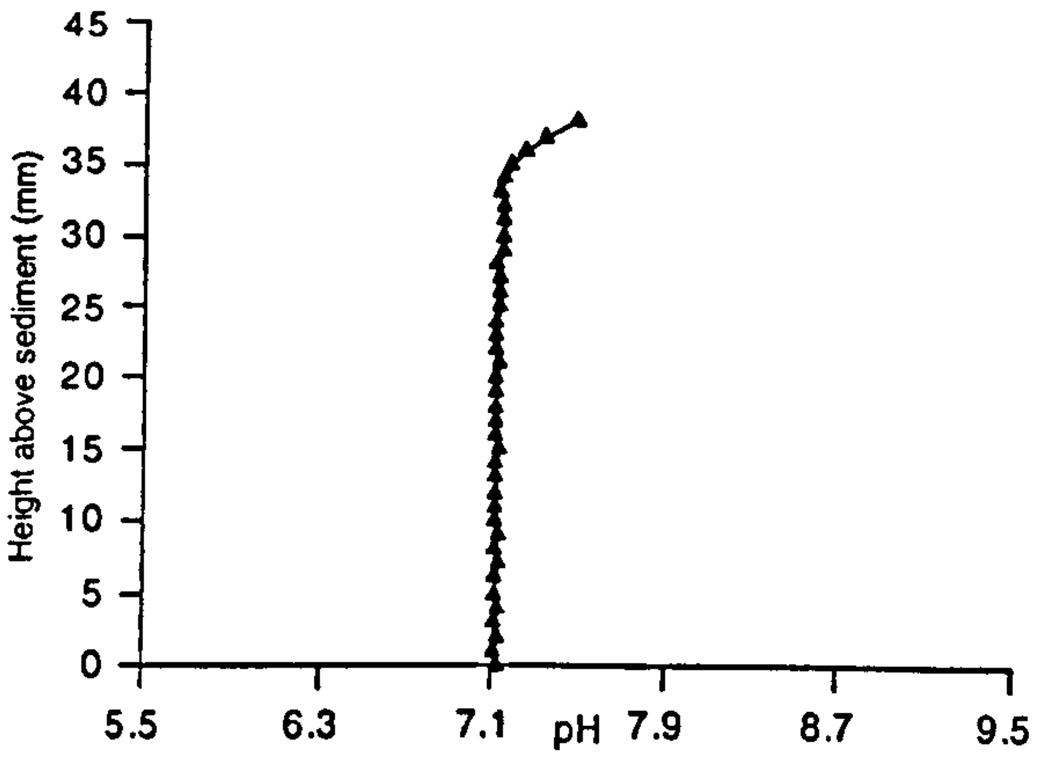

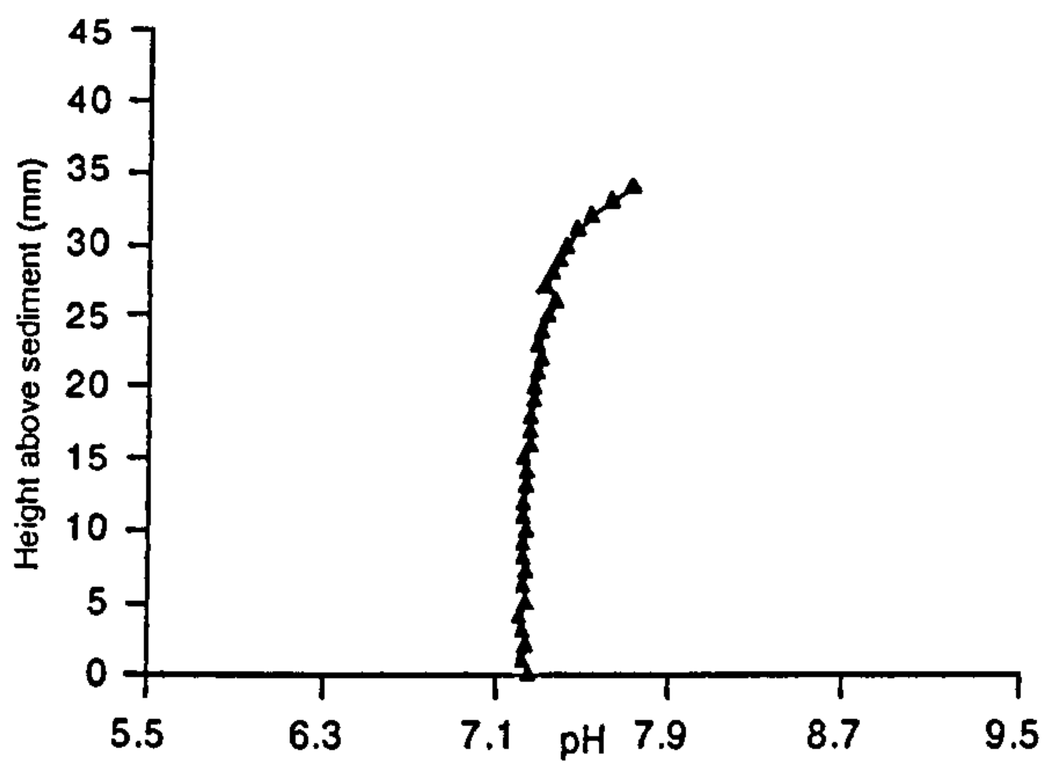

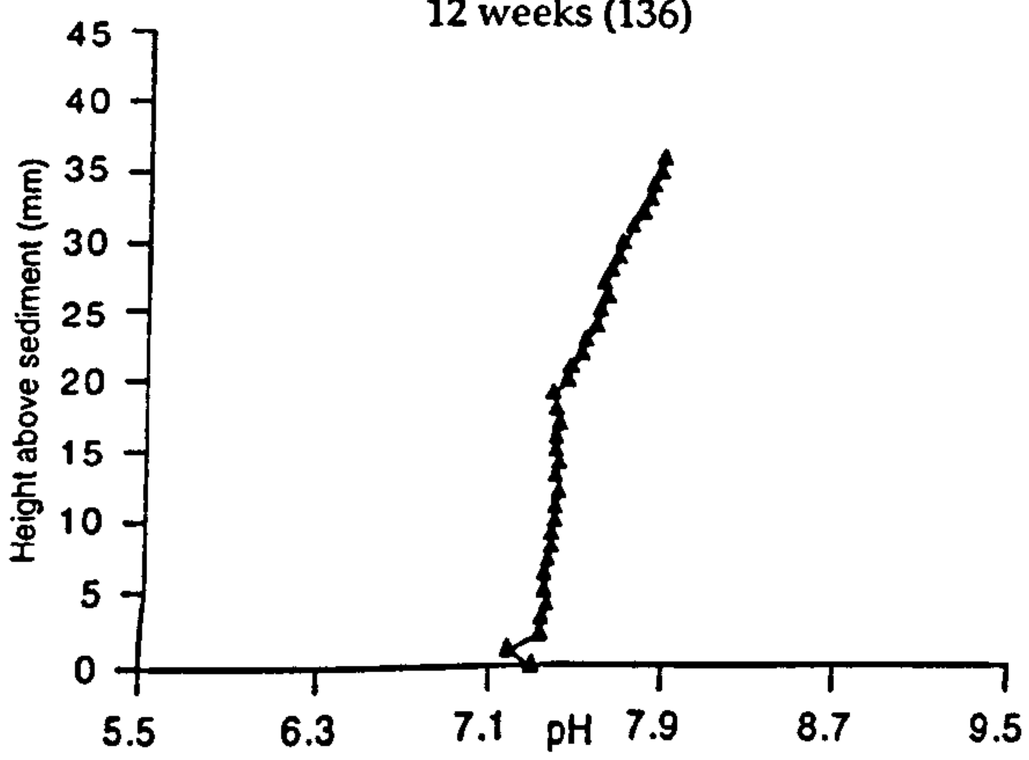

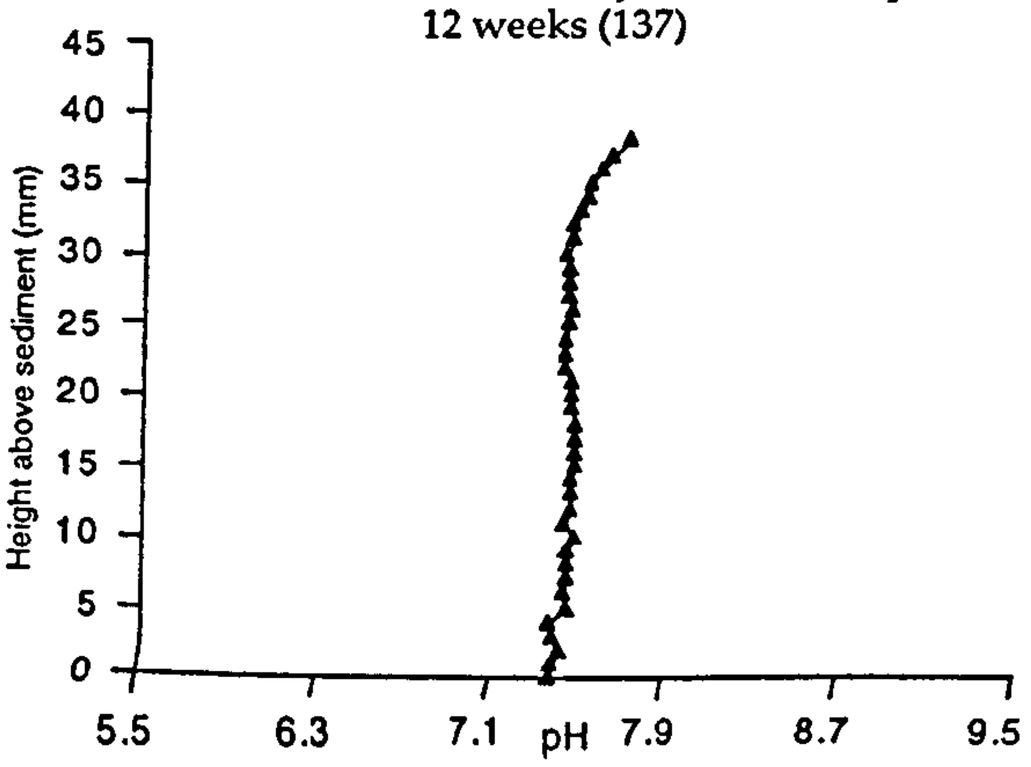

Oxygen and pH depth profiles for sealed sterilised marine systems. Infilled circles represent oxygen data points. Infilled triangles represent pH data points. The highest data points above the sediment represent the air-medium interface.

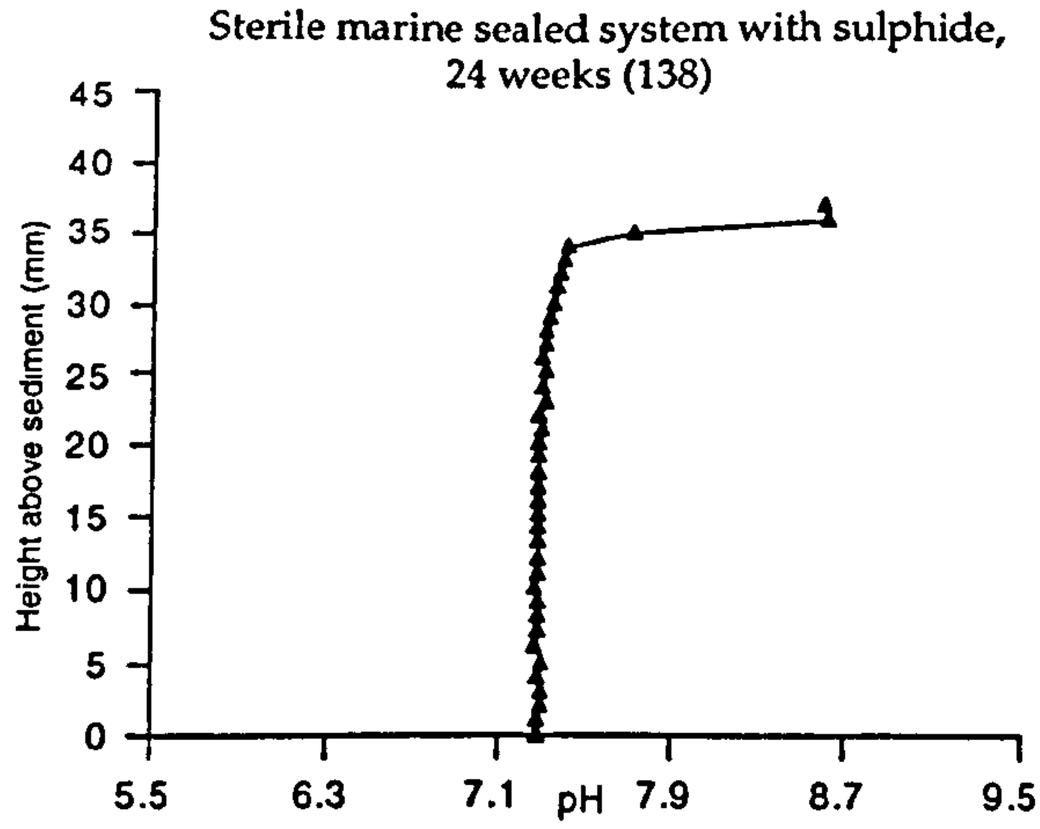

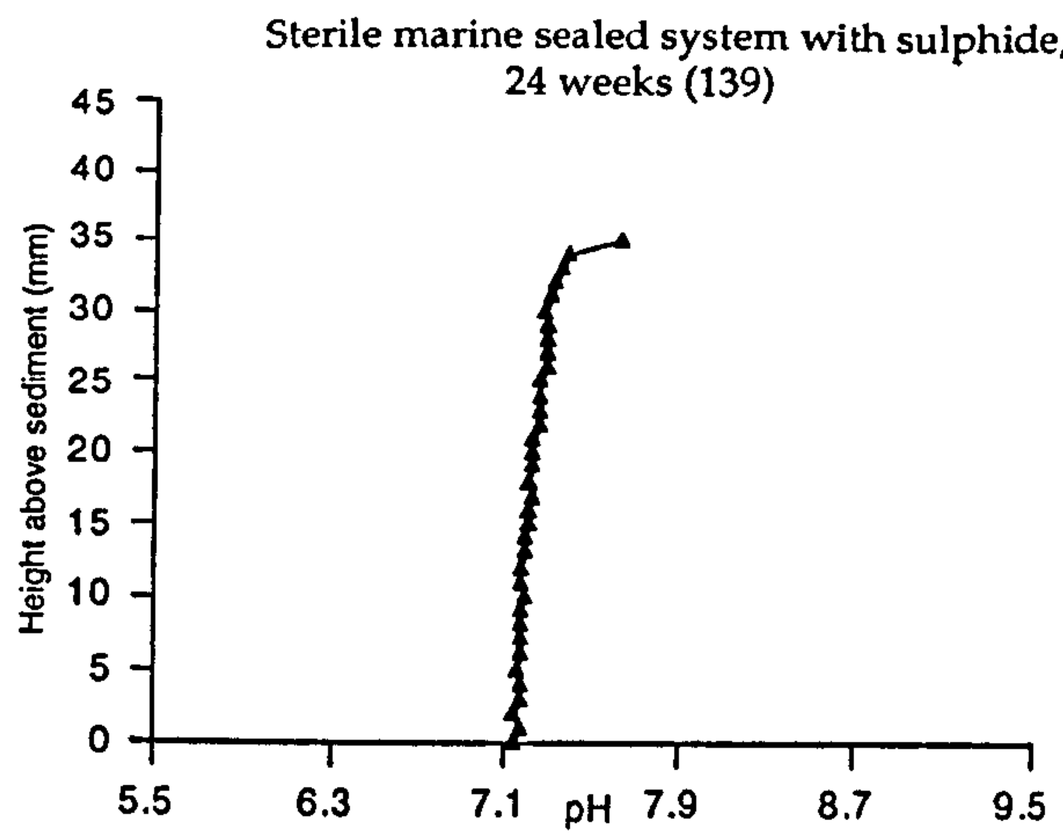

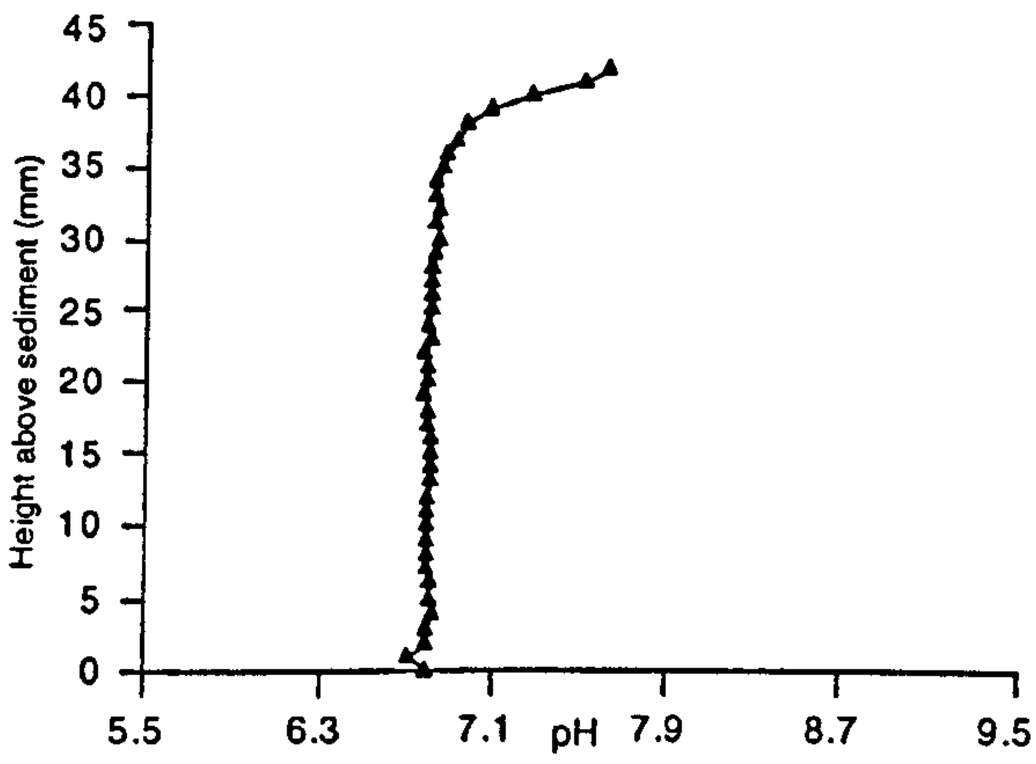

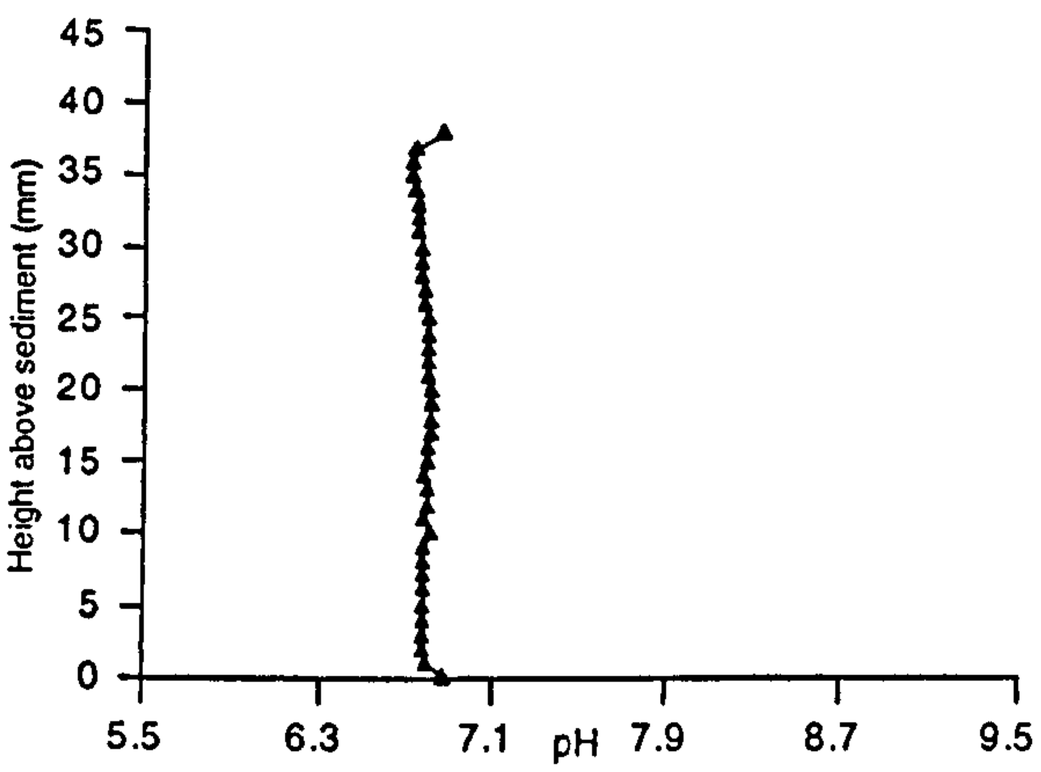

Oxygen and pH depth profiles. Infilled circles represent oxygen data points. Infilled triangles represent pH data points. The highest data points above the sediment represent the air-medium interface.

Experimental conditions	time	sulphate (mM)		sulphide (mM)		ferrous iron (mM)		AVS	pyritic	S°	TRIS	i.d. no.
		top	base	top	base	top	base	sediment sulphur (M)				
standard marine conditions	0 wks	29.5		0		0.01		0	0.6	0.1	0.7	0
	1 wk	23.0	22.1	0.06	0.15	0.08	0.20	0.2	0.8	0.3	1.3	1
	2 wks	18.7	17.4	0.22	0.40	0.01	0.05	1.2	1.5	0.4	3.0	2
	3 wks	16.4	16.7	0.20	0.28	0	0	0.9	1.4	0.9	3.2	3
	4 wks	16.4	14.7	0.22	0.30	0.01	0	1.0	1.5	0.4	2.8	4
	5 wks	14.2	8.9	0.03	0.01	0	0.02	1.2	1.6	0.4	3.3	5
	6 wks	15.3	15.7	0.01	0.02	0.02	0.01	1.3	1.7	0.5	3.5	6
	7 wks	14.5	12.9	0.02	0.02	0.01	0.01	1.1	1.6	0.4	3.1	7
	8 wks	12.0	16.4	0	0	0	0	1.1	1.7	1.0	3.7	8
	9 wks	14.7	11.0	0	0.05	0	0	1.8	1.6	1.1	4.6	9
	10 wks	15.9	16.8	0	0	0	0	1.3	1.7	0.5	3.4	10
	11 wks	15.8	10.6	0	0	0	0	1.3	1.0	0.9	3.1	11
	12 wks	18.6	14.2	0	0	0	0	1.0	1.5	0.9	3.4	12
	12 wks	15.6	15.6	0	0	0	0	-	-	-	-	13
	12 wks	13.9	17.3	0	0	0	0	-	-	-	-	14
	12 wks	15.5	14.8	0	0	0	0	-	-	-	-	15
	24 wks	19.8	20.9	0	0	0	0	-	-	-	-	16
	24 wks	18.1	18.1	0	0	0	0	-	-	-	-	17
	24 wks	21.5	22.9	0	0	0	0	-	-	-	-	18
	36 wks	27.1	27.4	0	0	0.01	0.01	-	-	-	-	19
	36 wks	33.4	31.5	0	0	0.01	0.01	-	-	-	-	20
	36 wks	31.9	29.9	0	0	0.01	0.01	-	-	-	-	21
	5.4 wks	14.2	13.9	0.03	0.31	0.04	0.04	-	-	-	-	22
	6 wks	22.6	22.4	0	0	0	0.03	-	-	-	-	23
	12 wks	13.3	14.1	0	0	0.02	0.03	-	-	-	-	24
(no inoculum)	12 wks	21.4	21.2	0	0	0.02	0.02	1.3	1.0	0.6	2.9	25
(no inoculum)	12 wks	22.5	21.0	0	0.01	0.03	0.04	0.5	1.4	0.3	2.2	26
	12 wks	15.8	15.9	0.02	0	0	0	1.4	2.0	0.3	3.7	27
	12 wks	18.7	18.0	0	0.04	0	0	1.1	2.2	0.3	3.6	28
	14 wks	21.5	21.0	0	0.01	0	0	-	-	-	-	29

Experimental conditions	time	sulphate (mM)		sulphide (mM)		ferrous iron (mM)		AVS	pyritic	S°	TRIS	i.d. no.
		top	base	top	base	top	base	sediment sulphur (M)				
Sulphate availability	12 wks	15.1	14.4	0	0.01	0.02	0.05	1.6	1.8	0.7	4.1	30
	12 wks	9.9	8.4	0.49	0.46	0.02	0.02	1.1	1.5	0.8	3.4	31
Iron availability: 5% FeOOH	12 wks	15.1	15.1	0	0	0.02	0.02	-	-	-	-	32
	12 wks	15.3	13.4	0	0	0.02	0.02	2.2	1.2	0.6	4.0	33
	12 wks	15.1	17.4	0.02	0.03	0	0	1.3	1.8	0.6	3.6	34
	12 wks	13.4	12.5	0.09	0.08	0	0	1.2	1.6	0.4	3.2	35
Iron availability: 3% FeOOH (mixed)	12 wks	12.4	12.2	0	0	0.02	0.03	1.9	0.9	0.7	3.5	36
	12 wks	12.2	11.9	0	0	3.12	0.02	2.8	1.8	0.5	5.1	37
	12 wks	11.3	8.0	0.09	0.04	0	0	1.4	1.7	0.5	3.7	38
	12 wks	10.4	14.2	0.06	0.09	0	0	1.0	1.1	0.7	2.8	39
Iron availabiliy: 0% FeOOH	5.4 wks	10.6	14.9	0.04	0.06	0.04	0.18	-	-	-	-	40
	12 wks	15.2	11.4	0	0	0.01	0.01	-	-	-	-	41
Iron availability: 3% FeOOH (layer)	12 wks	15.8	16.0	0	0	0.02	0.07	2.0	1.7	0.9	4.6	42
	12 wks	18.2	17.8	0	0	0.01	0.01	1.8	1.8	0.4	4.1	43
Iron source: 1% haematite	12 wks	21.9	21.1	0	0	0.01	0.01	1.7	1.6	0.4	3.6	44
	12 wks	22.4	22.4	0	0	0.01	0.02	1.3	1.1	0.4	2.8	45
Iron source: 0.5% haematite/0.5% FeOOH	12 wks	21.7	21.9	0	0	0.01	0.01	-	-	-	-	46
	12 wks	19.7	19.8	0	0	0.01	0.01	1.2	1.3	0.6	3.1	47
Iron source: 0.5% FeCl3 / 0.5% FeOOH	12 wks	15.7	17.8	0	0	0.01	0.01	2.6	2.3	0.5	5.3	48
	12 wks	17.4	17.5	0	0	0	0.02	1.4	1.3	0.4	3.1	49
Organic matter: single twig	12 wks	27.0	26.0	0	0	0.01	0.01	0.1	0.4	0.3	0.8	50
	12 wks	25.3	25.3	0	0	0	0	0.4	0.6	0.3	1.3	51
	24 wks	26.0	26.5	0	0	0	0	0	0.3	0.1	0.4	52
	24 wks	25.5	27.7	0	0	0	0	0.1	0.2	0.1	0.4	53
Organic matter: fifteen twigs	12 wks	4.5	4.6	0	0.13	0.05	0.04	2.3	1.6	0.4	4.3	54
	12 wks	10.1	10.2	0.07	0.15	0.03	0.03	2.2	1.3	0.9	4.4	55
	24 wks	12.6	13.7	0	0.03	0.01	0.02	1.6	1.9	0.2	3.7	56
	24 wks	10.8	11.0	0.02	0.03	0.01	0.01	1.4	1.2	0.4	2.9	57
Six extra twigs added after 6 weeks	12 wks	12.6	13.5	0	0	0	0	1.2	1.6	0.9	3.8	58
	12 wks	12.5	12.2	0	0	0	0	2.1	0.8	0.5	3.3	59

Experimental conditions	time	sulphate (mM)		sulphide (mM)		ferrous iron (mM)		AVS	pyritic	S°	TRIS	i.d. no.
		top	base	top	base	top	base	sediment sulphur (M)				
No plant material	14 wks	27.4	28.9	0	0	0	0	-	-	-	-	60
No added yeast extract	12 wks	16.5	18.0	0.05	0.02	0	0	1.3	1.7	0.3	3.2	61
	12 wks	20.8	21.7	0.01	0	0	0	0.8	1.2	0.3	2.3	62
Added glucose	12 wks	10.6	10.7	0	0	0	0	2.1	1.6	0.7	4.4	63
	12 wks	7.3	7.1	0	0	0	0	1.6	1.9	0.7	4.2	64
Celery	6 wks	19.2	19.1	0	0	0.05	0.02	-	-	-	-	65
Vitis vinifera	6 wks	20.8	21.4	0	0	0.02	0.01	-	-	-	-	66
Cyathea chinensis	6 wks	14.8	14.8	0	0.03	0.03	0.04	-	-	-	-	67
Vine	12 wks	14.4	14.9	0	0	0.01	0.01	-	-	-	-	68
Equisetum	12 wks	11.1	11.2	0	0	0.01	0	-	-	-	-	69
Cherry	12 wks	12.3	13.0	0	0	0.01	0.01	-	-	-	-	70
Psilotum	12 wks	5.9	7.9	0	0	0.01	0.01	-	-	-	-	71
Ginkgo	12 wks	15.8	8.1	0	0	0.02	0.02	-	-	-	-	72
Sequoia	12 wks	10.0	9.5	0	0	0.01	0.06	-	-	-	-	73
Celery	14 wks	22.4	23.4	0	0	0	0	-	-	-	-	74
Psilotum (newer, green material)	14 wks	19.4	19.4	0	0.08	0.05	0.26	-	-	-	-	75
Psilotum (older, orange brown)	14 wks	16.1	16.0	0	0.02	0.06	0.11	-	-	-	-	76
Vitis vinifera	14 wks	22.6	22.4	0	0	0	0.03	-	-	-	-	77
Cyathea chinensis	14 wks	16.9	16.5	0	0.05	0	0.12	-	-	-	-	78
Pine	14 wks	18.1	17.9	0	0	0.02	0.04	-	-	-	-	79
pH: 1% FeCl3 as iron source	12 wks	13.6	13.1	0	0	0.01	0.02	1.8	1.9	1.0	4.7	80
	12 wks	14.6	14.6	0	0	0	0.01	2.1	1.7	1.0	4.8	81
pH: 1% FeCl3 and 50% HCl added	12 wks	2.1	2.5	0	0	0	0	1.5	1.5	0.7	3.7	82
	12 wks	3.0	3.2	0	0	0	0	1.7	1.1	1.0	3.8	83
Fungal decay: indigenous fungi	12 wks	23.7	22.0	0	0	0	0	0.1	1.1	0.3	1.5	84
	12 wks	18.5	22.4	0	0	0	0	0.2	1.1	0.3	1.6	85
Fungal decay: fungal inoculum	12 wks	19.3	21.9	0	0	0	0	0.3	1.3	0.5	2.0	86
	12 wks	23.3	22.3	0.04	0.06	0	0	0.2	1.1	0.4	1.6	87
Twigs floating	5.4 wks	16.3	14.7	0.25	0.53	0.39	0	-	-	-	-	88
	12 wks	15.7	15.9	0	0	0	0.01	-	-	-	-	89

Experimental conditions	time	sulphate (mM)		sulphide (mM)		ferrous iron (mM)		AVS	pyritic	S°	TRIS	i.d. no.
		top	base	top	base	top	base	sediment sulphur (M)				
Sedimentation	5.4 wks	13.7	12.9	0	0	0	0	-	-	-	-	90
	12 wks	12.2	13.1	0	0	0	0	-	-	-	-	91
Twigs floating / sedimentation	5.4 wks	7.5	12.6	0.04	0.07	0.04	0	-	-	-	-	92
	12 wks	7.9	9.1	0	0	0	0	-	-	-	-	93
Burial	5.4 wks	8.0	9.6	0	0.25	0.13	0.01	-	-	-	-	94
	12 wks	14.3	12.6	0	0	0	0.01	-	-	-	-	95
Comparisons with no inoculum	12 wks	15.7	15.4	0	0	0.01	0.01	2.3	1.0	0.7	3.9	96
	12 wks	17.0	16.3	0	0	0.02	0.02	1.2	0.9	0.8	2.9	97
Standard marine systems: Duran bottle	12 wks	19.4	19.0	0	0.02	0.01	0.01	0.6	0.8	0.6	2.1	98
	12 wks	16.0	16.3	0	0	0.01	0.04	0.8	1.6	0.7	3.1	99
Freshwater standards	5.4 wks	0	0	0.28	0.08	2.4	2.3	-	-	-	-	100
	12 wks	0	0	0.08	0.06	1.7	1.7	-	-	-	-	101
	12 wks	1.3	1.3	0	0	0.02	0.02	0.3	0.5	0.2	0.9	102
	12 wks	1.3	1.3	0	0	0.02	0.02	0.2	0.3	0.1	0.6	103
Freshwater with sulphate agar layer	12 wks	1.2	1.3	0	0	0.02	0.02	0.1	0.1	0.2	0.4	104
	12 wks	1.2	1.3	0	0	0.02	0.02	0.3	0.3	0.4	1.0	105
Closed freshwater systems	1 wk	0	0	0	0.04	0.80	1.6	-	-	-	-	106
	1 wk	0	0.10	0	0	0.26	1.1	-	-	-	-	107
	2 wks	0	0	0.06	0.10	0.74	2.3	-	-	-	-	108
	2 wks	0	0	0.04	0.06	0.49	1.8	-	-	-	-	109
	4 wks	0.20	0	0	0	1.2	1.2	-	-	-	-	110
	4 wks	0	0	0.03	0.10	3.5	3.2	-	-	-	-	111
	9 wks	0.1	0.20	0	0	0.01	0	-	-	-	-	112
	9 wks	0	0	0	0	2.4	2.4	-	-	-	-	113
	12 wks	0	0	0	0.01	0.35	0.29	-	-	-	-	114
	12 wks	0	0	0	0	0.67	0.68	-	-	-	-	115

Experimental conditions	time	sulphate (mM)		sulphide (mM)		ferrous iron (mM)		AVS	pyritic	S°	TRIS	i.d. no.
		top	base	top	base	top	base	sediment sulphur (M)				
Sealed marine standards	12 wks	0	0	7.7	4.3	0.04	0	-	-	-	-	116
	12 wks	0	0	6.9	6.9	0	0	-	-	-	-	117
	18 wks	0	0	3.7	3.8	0	0	-	-	-	-	118
	18 wks	0	0	1.2	1.1	0	0	-	-	-	-	119
	24 wks	0	0	0.3	0.2	0	0	-	-	-	-	120
	24 wks	0	0	1.6	3.5	0	0	-	-	-	-	121
Open marine standards: Durans	12 wks	12.3	11.7	0.62	0.94	0	0	-	-	-	-	122
	12 wks	12.8	12.3	0.37	1.3	0	0	-	-	-	-	123
	24 wks	10.3	10.1	0.04	0.06	0	0	-	-	-	-	124
	24 wks	6.9	7.1	0.10	0.19	0	0	-	-	-	-	125
Twigs added to sealed marine standards	24 wks	0	0	0.69	0.10	0.08	0	-	-	-	-	126
	24 wks	0	-	0.08	-	0.22	-	-	-	-	-	127
Sealed marine standards opened briefly	24 wks	0	0	1.7	1.4	0	0.04	-	-	-	-	128
	24 wks	0	0	1.5	0.69	0	0.01	-	-	-	-	129
Cyathea in sealed marine system	12 wks	0	0	5.7	4.3	0.03	0	-	-	-	-	130
	12 wks	0	0	6.5	6.7	0.01	0	-	-	-	-	131
Sterilised sealed marine systems	12 wks	27.3	29.6	0	0	0.01	0.01	-	-	-	-	132
	12 wks	36.2	28.7	0	0	0	0	-	-	-	-	133
	24 wks	36.9	36.7	0	0	0.01	0	-	-	-	-	134
	24 wks	30.0	28.1	0	0	0	0	-	-	-	-	135
Sterilised systems with sulphide	12 wks	27.2	27.6	0	0	0.05	0.04	-	-	-	-	136
	12 wks	21.8	26.2	0	0	0.03	0.03	-	-	-	-	137
	24 wks	19.9	23.2	0	0	0.05	0.04	-	-	-	-	138
	24 wks	25.0	27.3	0	0	0.04	0.05	-	-	-	-	139
Sealed freshwater systems: Durans	12 wks	0	0	0.09	0.03	0.95	0.77	-	-	-	-	140
	12 wks	0	0	0.04	0.03	0.48	0.44	-	-	-	-	141
Effect of light (sealed f'water systems)	9 wks	-	-	0.04	0.03	-	-	-	-	-	-	142
	9 wks	-	-	0	0.07	-	-	-	-	-	-	143
Effect of dark (sealed f'water systems)	9 wks	-	-	0.02	0.08	-	-	-	-	-	-	144
	9 wks	-	-	0.01	0.03	-	-	-	-	-	-	145

	time	P (mM)		Al (mM)		Fe (mM)		Mn (mM)		Mg (mM)		Ca (mM)		i.d. no.
		top	base	top	base	top	base	top	base	top	base	top	base	
Standard marine conditions	0 wks	1.44		0.02		0		0		15.1		1.0		0
	1 wk	0.72	0.89	0	0	0.14	0.25	0.03	0.01	16.0	16.8	3.4	3.6	1
	2 wks	0.86	0.78	0	0	0	0	0	0.03	14.8	14.9	3.1	3.2	2
	3 wks	0.77	0.70	0	0	0	0	0	0	15.1	14.2	2.9	2.5	3
	4 wks	0.77	0.68	0	0	0	0	0	0	16.3	14.3	3.0	2.5	4
	5 wks	0.68	0.74	0	0	0	0	0	0	13.7	14.6	2.2	2.2	5
	6 wks	0.54	0.57	0	0	0	0	0	0	14.9	14.9	2.3	2.3	6
	7 wks	0.39	0.36	0	0	0	0	0	0	15.4	14.0	2.1	1.7	7
	8 wks	0.38	0.39	0	0	0	0	0	0	13.3	13.7	1.6	1.6	8
	9 wks	0.40	0.33	0	0	0	0	0	0	13.5	11.5	2.4	1.7	9
	10 wks	0.36	0.41	0	0	0	0	0.01	0	11.6	12.9	1.3	1.6	10
	11 wks	0.60	0.18	0	0	0	0	0	0	13.0	11.4	2.2	1.7	11
	12 wks	0.12	0.11	0	0	0	0	0	0	12.1	12.0	2.0	2.0	12
	12 wks	0.24	0.20	0	0	0.01	0	0.01	0	15.3	14.4	0.2	0	13
	12 wks	0.05	0.19	0	0.01	0	0.01	0	0.01	14.5	13.0	0	0.2	14
	12 wks	0.14	0.14	0	0	0	0	0	0	14.2	14.4	0	0	15
	24 wks	0.01	0.03	0	0	0	0	0	0	7.2	6.7	0	0	16
	24 wks	0.06	0.11	0	0	0	0	0	0	6.0	6.2	0	0	17
	24 wks	0.03	0.03	0	0	0	0	0	0	6.5	6.5	0	0	18
	36 wks	0.10	0.09	0	0	0	0	0	0	13.1	12.5	2.2	2.0	19
	36 wks	0.09	0.08	0	0	0	0	0	0	14.3	14.7	2.4	2.4	20
	36 wks	0.06	0.04	0	0	0	0	0	0	14.2	14.2	2.0	2.0	21
	5.4 wks	0.34	0.56	0.06	0	0.19	0.05	0.05	0.03	11.7	12.2	2.1	2.0	22
	6 wks	0.18	0.27	0	0	0	0	0	0	12.9	13.1	0.7	0.8	23
	12 wks	0.67	0.71	0	0	0	0	0	0	11.3	13.0	0.01	1.1	24
(no inoculum)	12 wks	0.13	0	0	0	0	0	0	0	12.7	13.0	1.6	0	25
(no inoculum)	12 wks	0.20	0.20	0	0	0	0	0	0	13.1	13.4	1.9	1.9	26
	12 wks	0.20	0.21	0	0	0	0	0	0	10.1	10.7	0.2	0.3	27
	12 wks	0.15	0.16	0	0	0	0	0	0	10.0	10.3	0	0	28
	14 wks	0.07	0.08	0	0	0	0	0	0	5.7	6.0	0	0	29

Experimental conditions	time	P (mM)		Al (mM)		Fe (mM)		Mn (mM)		Mg (mM)		Ca (mM)		i.d. no.
		top	base	top	base	top	base	top	base	top	base	top	base	
Sulphate availability	12 wks	0.18	0.18	0	0	0	0	0	0	11.1	11.2	1.4	1.5	30
	12 wks	0.04	0.52	0	0	0	0	0	0	12.8	12.7	1.7	1.7	31
Iron availability: 5% FeOOH	12 wks	0.13	0.12	0.01	0.01	0	0	0	0	11.6	11.4	1.7	1.6	32
	12 wks	0.17	0.15	0.03	0.01	0	0	0	0	12.5	11.2	1.9	1.7	33
	12 wks	0.09	0.09	0	0	0	0	0	0	9.8	9.6	0	0	34
	12 wks	0.27	0.21	0	0	0	0	0	0	10.1	11.1	0	0	35
Iron availability: 3% FeOOH (mixed)	12 wks	0.07	0.07	0.01	0	0	0	0	0	10.9	10.5	0.9	0.8	36
	12 wks	0.13	0.10	0	0	0	0	0	0	11.8	11.5	1.5	1.5	37
	12 wks	0.12	0.11	0	0	0	0	0	0	9.4	9.3	0	0	38
	12 wks	0.11	0.15	0	0	0	0	0	0	10.1	15.8	0	0.04	39
Iron availability: 0% FeOOH	5.4 wks	0.25	0.51	0.08	0.09	0.33	0.17	0.04	0.04	13.3	12.5	2.5	2.6	40
	12 wks	0.68	0.70	0	0	0.09	0	0.01	0	14.4	14.2	2.1	1.6	41
Iron availability: 3% FeOOH (layer)	12 wks	0.10	0.28	0.01	0.01	0	0.09	0	0	11.9	11.9	1.6	1.8	42
	12 wks	0.11	0.09	0.01	0.01	0	0	0	0	11.5	11.5	1.5	1.6	43
Iron source: 1% haematite	12 wks	0.05	0.11	0.01	0	0	0	0	0	11.6	12.2	1.6	1.7	44
	12 wks	0.13	0.14	0.01	0.01	0	0	0	0	12.1	12.3	1.8	1.8	45
Iron source: 0.5% haematite/ 0.5% FeOOH	12 wks	0.08	0.08	0.02	0.02	0	0	0.01	0.01	11.5	11.6	1.7	1.7	46
	12 wks	0.11	0.09	0.02	0.03	0	0	0.01	0.01	12.3	11.5	1.8	1.7	47
Iron source: 0.5% FeCl3 / 0.5% FeOOH	12 wks	0.13	0.14	0.03	0.03	0.01	0	0.01	0.01	13.5	13.1	3.3	3.2	48
	12 wks	0.07	0.10	0.03	0.03	0	0.02	0.01	0.01	11.7	12.3	2.0	2.1	49
Organic matter: single twig	12 wks	0.10	0.10	0.04	0.03	0.01	0	0.01	0.01	12.9	12.4	1.4	1.4	50
	12 wks	0.11	0.10	0.04	0.04	0	0	0.02	0.01	12.0	12.2	1.3	1.3	51
	24 wks	0.04	0.04	0	0	0	0	0	0	14.1	14.9	0.4	0.4	52
	24 wks	0.10	-	0	-	0	-	0	-	15.1	-	0.4	-	53
Organic matter: fifteen twigs	12 wks	0.46	0.46	0.04	0.04	0	0.01	0.01	0.01	12.5	12.3	2.4	2.3	54
	12 wks	0.38	0.37	0.04	0.04	0.02	0.02	0.01	0.01	12.7	12.6	2.6	2.5	55
	24 wks	0.30	0.23	0	0	0	0	0	0	15.9	14.7	1.9	1.5	56
	24 wks	0.10	0.10	0	0	0	0	0	0	11.2	12.0	0.1	0.2	57
Six extra twigs added after 6 weeks	12 wks	0.24	0.24	0	0	0	0	0	0	11.9	11.9	2.5	2.5	58
	12 wks	0.45	0.46	0	0	0	0	0	0	12.9	13.2	2.5	2.7	59

Experimental conditions	time	P (mM)		Al (mM)		Fe (mM)		Mn (mM)		Mg (mM)		Ca (mM)		i.d. no.
		top	base	top	base	top	base	top	base	top	base	top	base	
No plant material	14 wks	0.15	0.14	0	0	0	0	0	0	7.2	7.6	0	0	60
No added yeast extract	12 wks	0.25	0.26	0	0	0	0	0	0	11.3	11.6	0	0	61
	12 wks	0.36	0.36	0	0	0	0	0	0	12.1	12.6	0	0	62
Added glucose	12 wks	0.38	0.41	0	0	0	0	0	0	12.1	12.7	1.9	2.1	63
	12 wks	0.27	0.27	0	0	0	0	0	0	12.6	12.8	1.7	1.7	64
Celery	6 wks	0.35	0.40	0	0	0	0	0	0	11.8	12.2	1.5	1.3	65
Vitis vinifera	6 wks	0.18	0.16	0	0	0	0	0	0	11.5	12.0	1.0	0.9	66
Cyathea chinensis	6 wks	1.12	1.18	0	0	0	0	0	0	13.0	14.0	0.6	0.5	67
Vine	12 wks	0.37	0.32	0	0.11	0	0	0	0.02	15.2	16.0	2.4	2.5	68
Equisetum sp.	12 wks	0.62	0.52	0.23	0.23	0.26	0.21	0.30	0.24	12.7	12.5	2.0	2.0	69
Cherry	12 wks	0.78	0.80	0.04	0	0.20	0	0.19	0	13.7	11.1	1.8	0	70
Psilotum nudum	12 wks	0.59	0.67	0.11	0.14	0.11	0.17	0.13	0.19	13.5	13.7	3.0	3.0	71
Ginkgo biloba	12 wks	0.29	0.28	0.09	0.09	0	0	0.01	0.01	14.1	14.0	2.1	2.1	72
Sequoia sp.	12 wks	0.42	0.96	0.10	0	0	0	0.02	0	15.3	13.1	2.6	0	73
Celery	14 wks	0.23	0.27	0.01	0	0	0.01	0	0	7.4	7.2	0.8	0.8	74
Psilotum (newer, green material)	14 wks	0.22	0.32	0	0.11	0	0.14	0	0	6.6	7.0	0	1.3	75
Psilotum (older, orange/brown)	14 wks	0.09	0.14	0	0	0	0	0	0	7.5	6.8	0.7	0.7	76
Vitis vinifera	14 wks	0.33	0.37	0	0.02	0	0.03	0	0	7.2	7.0	0.8	0.8	77
Cyathea chinensis	14 wks	0.27	0.26	0	0	0	0	0	0	6.6	6.4	0	0.2	78
Pine	14 wks	0.28	0.27	0	0	0	0	0	0	6.9	7.3	0	0	79
pH: 1% FeCl3 as iron source	12 wks	0.15	0.14	0.01	0.02	0	0	0	0	13.6	13.6	3.4	3.4	80
	12 wks	0.08	0.11	0.02	0.02	0	0	0.01	0.01	13.0	12.8	3.2	3.1	81
pH: FeCl3 and 50% HCl added	12 wks	0.95	0.87	0	0	0	0	0.06	0.05	16.3	14.2	10.6	9.3	82
	12 wks	0.33	0.30	0	0	0	0	0	0	14.6	14.2	8.8	8.7	83
Fungal decay : indigenous fungi	12 wks	0.70	0.74	0	0	0	0	0	0	11.4	12.0	0.5	0.6	84
	12 wks	0.74	0.77	0	0	0	0	0	0	11.5	11.3	0.5	0.5	85
Fungal decay: fungal inoculum	12 wks	0.69	0.67	0	0	0	0	0	0	11.1	10.7	1.2	1.1	86
	12 wks	0.27	0.26	0	0	0	0	0	0	10.8	10.9	0.5	0.5	87
Twigs floating	5.4 wks	0.53	0.59	0.33	0.25	0.53	0.47	0.09	0.07	12.6	12.6	3.0	2.9	88
	12 wks	0.20	0.20	0.08	0.13	0	0	0.02	0.02	14.3	14.6	2.4	2.7	89

Experimental conditions	time	P (mM)		Al (mM)		Fe (mM)		Mn (mM)		Mg (mM)		Ca (mM)		i.d. no.
		top	base	top	base	top	base	top	base	top	base	top	base	
Sedimentation	5.4 wks	0.50	0.46	0.04	0.09	0.18	0.22	0.03	0.03	14.4	13.2	2.5	2.3	90
	12 wks	0.60	0.59	0.13	0.13	0	0	0.02	0.02	16.3	16.5	2.1	2.1	91
Twigs floating /sedimentation	5.4 wks	0	0.12	0.34	0.36	0.54	0.61	0.10	0.09	13.5	12.7	2.6	2.9	92
	12 wks	0.36	0.42	0	0	0	0	0	0	14.0	13.9	1.9	1.9	93
Burial	5.4 wks	0.67	0.59	0.23	0.14	0.45	0.42	0.08	0.05	12.8	12.4	2.5	2.4	94
	12 wks	0.14	0.10	0	0	0	0	0	0	12.5	12.4	1.9	2.0	95
Comparisons with no inoculum	12 wks	0.13	0.14	0	0	0	0	0	0	11.5	12.1	1.5	1.3	96
	12 wks	0.20	0.22	0	0	0	0	0	0	12.9	12.8	1.6	1.7	97
Standard marine systems: Duran bottle	12 wks	0.13	0.13	0	0	0	0	0	0.01	11.2	12.2	1.5	1.7	98
	12 wks	0.16	0.21	0	0	0	0	0.01	0.01	11.8	12.5	1.5	1.7	99
Freshwater standards	5.4 wks	0.53	0.46	0.04	0	1.79	1.64	0.11	0.10	5.0	4.3	16.3	14.0	100
	12 wks	0.63	0.66	0	0	1.72	1.46	0	0	5.3	4.2	22.4	21.2	101
	12 wks	0	0	00	0	0	0	0	0	0.7	0.7	1.5	1.5	102
	12 wks	0	0	0	0	0.8	0	0.01	0.01	0.6	0.6	1.7	1.4	103
Freshwater with sulphate agar layer	12 wks	0	0	0	0	0	0	0	0	0.6	0.6	2.1	2.1	104
	12 wks	0	0	0	0	0	0	0	0	0.6	0.6	1.9	2.0	105
Closed freshwater systems	1 wk	0.44	1.37	0.09	0.01	0.60	1.16	0.05	0.09	3.4	4.6	5.4	9.0	106
	1 wk	0.96	0.84	0.16	0.18	0.60	1.18	0.07	0.10	3.2	3.2	5.2	6.2	107
	2 wks	0.33	0.80	0.04	0.13	0.57	1.61	0.06	0.09	3.3	4.1	6.9	9.5	108
	2 wks	0.07	0.58	0.30	0.15	0.83	1.49	0.11	0.10	3.3	3.5	7.2	8.3	109
	4 wks	0.76	0.73	0.21	0.26	1.17	1.17	0.10	0.11	3.3	3.2	6.2	6.1	110
	4 wks	0.72	0.70	0.07	0.11	2.24	2.45	0.12	0.12	4.3	4.1	13.3	12.7	111
	9 wks	0	0	0.10	0.07	0	0	0.02	0.02	3.1	3.2	6.8	6.3	112
	9 wks	1.18	1.68	0.12	0	2.76	2.04	0.10	0	4.8	1.6	13.6	10.0	113
	12 wks	0.23	0.36	0.10	0.12	0.36	0.38	0.04	0.09	3.3	3.5	6.3	6.8	114
	12 wks	0.75	0.78	0	0	0.21	0	0	0	1.6	0.3	6.5	5.8	115

Experimental conditions	time	P (mM)		Al (mM)		Fe (mM)		Mn (mM)		Mg (mM)		Ca (mM)		i.d. no.
		top	base	top	base	top	base	top	base	top	base	top	base	
Sealed marine standards	12 wks	1.84	1.99	0.02	0.01	0	0	0.04	0.03	15.3	15.6	2.3	2.1	116
	12 wks	1.92	1.95	0	0.01	0	0	0	0.01	14.9	14.9	1.6	1.8	117
	18 wks	1.42	1.57	0.01	0	0	0	0.05	0	13.5	14.9	0.2	0	118
	18 wks	1.56	1.57	0	0.01	0	0	0	0.07	15.3	14.7	0	0.2	119
	24 wks	1.57	1.73	0.01	0.01	0.02	0.01	0.06	0.07	14.3	15.2	0.3	0.3	120
	24 wks	1.60	1.64	0	0	0.01	0.01	0.05	0.06	13.0	14.7	0.02	0.3	121
Open marine standards: Durans	12 wks	0.32	0.29	0	0.03	0	0.01	0	0.02	12.4	12.2	2.0	2.0	122
	12 wks	0.27	0.36	0.03	0	0	0	0	0	12.4	13.7	1.7	2.0	123
	24 wks	0.22	0.25	0.01	0.01	0	0	0.01	0.01	10.4	10.5	0.2	0.2	124
	24 wks	0.22	0.47	0	0.01	0	0	0	0.02	13.5	15.0	0	0.4	125
Twigs added to sealed marine standards	24 wks	2.23	2.32	0.03	0	0.06	0	0.08	0.07	15.4	17.0	0.4	0	126
	24 wks	2.00	-	0.06	-	0.19	-	0.10	-	14.9	-	0.4	-	127
Sealed marine standards opened briefly	24 wks	1.71	1.66	0	0.04	0.01	0.07	0.05	0.09	15.1	16.8	0.3	0.6	128
	24 wks	1.72	1.62	0	0	0.01	0.01	0.05	0.06	14.9	14.3	0.3	0.2	129
Cyathea chinensis in sealed systems	12 wks	1.67	1.54	0.08	0.03	0	0	0.04	0.03	15.6	15.0	2.9	2.7	130
	12 wks	1.55	1.49	0.03	0	0	0	0.02	0.01	14.4	13.9	2.8	2.6	131
Sterilised sealed marine systems	12 wks	0.89	0.86	0	0	0	0	0.07	0.06	13.3	13.9	3.4	3.4	132
	12 wks	0.93	0.99	0	0	0	0	0.02	0.03	12.8	13.7	2.9	3.1	133
	24 wks	1.55	0.78	0	0.02	0	0.02	0.06	0.08	14.5	13.6	0	0.3	134
	24 wks	0.74	0.72	0	0	0	0.01	0	0.05	14.7	12.5	0	0.3	135
Sterilised systems with sulphide	12 wks	0.93	0.90	0	0	0.05	0.01	0.06	0.04	11.7	11.5	2.5	2.5	136
	12 wks	0.97	0.92	0	0.06	0.02	0	0.05	0.03	12.2	12.3	2.3	1.4	137
	24 wks	0.80	0.86	0	0	0.04	0	0.07	0.05	11.6	13.2	0.2	0	138
	24 wks	0.70	0.68	0	0.01	0.04	0.04	0.09	0.09	11.8	11.7	0.3	0.3	139
Sealed freshwater systems	12 wks	1.03	0.98	0.03	0.13	0.98	0.80	0.03	0.02	3.2	2.9	5.9	5.1	140
	12 wks	1.50	1.60	0	0	0.40	0.41	0	0	2.2	2.2	4.2	4.1	141
Effect of light (freshwater)	9 wks	-	-	-	-	-	-	-	-	-	-	-	-	142
	9 wks	-	-	-	-	-	-	-	-	-	-	-	-	143
Effect of dark (freshwater)	9 wks	-	-	-	-	-	-	-	-	-	-	-	-	144
	9 wks	-	-	-	-	-	-	-	-	-	-	-	-	145